Forschungszentrum Jülich
in der Helmholtz-Gemeinschaft

Neutron Scattering at FRJ-2

Experimental Reports 2002

Editors: Th. Brückel, D. Richter, R. Zorn

Persistent Identifier: urn:nbn:de:0001-00021
http://nbn-resolving.de/urn/resolver.pl?urn=urn:nbn:de:0001-00021

Published by Forschungszentrum Jülich GmbH
D-52425 Jülich, Germany
Phone: +49 2461 61-0

Editors: R. Zorn, D. Richter, Th. Brückel

Summary

Forschungszentrum Jülich is operating the research reactor FRJ-2 which, at a thermal power of 23 MW, delivers a neutron flux of 2.2×10^{14} neutrons/cm^{2}s. It is equipped with a cold source which supplies an external neutron guide laboratory. A broad spectrum of instruments is operated which use either thermal or cold neutrons to study elastic and inelastic neutron scattering.

The reactor was in operation for 185 days in the year 2002 and 190 individual experiments were performed. The focus of the experimental work was the study of soft matter systems but also the "hard matter" topics magnetism, structure determination, and phonons were strongly represented. The majority of the experiments were done by external user groups. In this regard, we acknowledge the support of European user groups by the EC funded programme "Jülich Neutrons for Europe".

This documentation contains the experimental reports of the experiments completed during the year 2002. We thank all external users, local users, and instrument responsibles who contributed by their efforts to write the reports to this overview.

Contents

Introduction

With the FRJ-2 research reactor and the ELLA external neutron guide laboratory, the Research Centre Jülich is operating a powerful neutron source with a special priority in the field of cold neutrons. At a thermal power of 23 MW, the FRJ-2 reaches a thermal neutron flux of 2.2×10^{14} neutrons/cm^{2}s in the heavy water moderator. The cold source operated with liquid hydrogen is close to the maximum flux and supplies the ELLA external neutron guide laboratory with cold neutrons via three neutron guides. By operating this neutron source and making it available to a multidisciplinary scientific public, the Research Centre Jülich is fulfilling a task typical of national research centres in the Helmholtz Association, namely of providing large-scale research equipment for a wide range of scientific applications in the university and non-university sector far beyond the Research Centre itself.

The total number of operating days for the reactor was 185 days in this year. This was the largest yearly number since the re-commissioning of the reactor in 1996. 190 experiments were done during this year. Among these 108 were proposed by external users. Fig. 1 shows the distribution of the experiments over the instruments. It can be seen that the largest number of experiments is done by small-angle scattering, SANS (KWS-2). This trend would be even more pronounced if it is considered that one of the SANS cameras, KWS-1, was under repair for a considerable time in 2002. Another instrument with a high throughput is SV-7, a twin diffractometer (powder and four-circle). In both cases the instruments provide the possibility to execute large numbers of experiments in a short time (a few days) because of their high flux and routine operation. Naturally, instruments for inelastic scattering (e.g. backscattering and neutron spin echo) have smaller numbers of experiments because the individual experiments often take weeks for their completion.

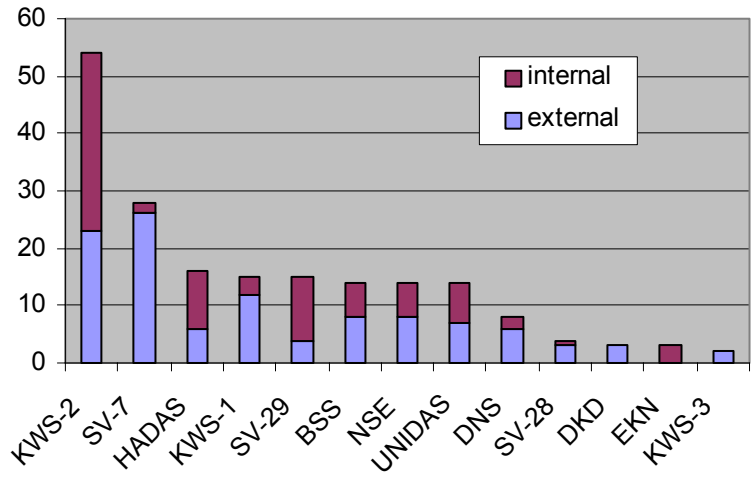

Figure 1: Experiments performed in the year 2002 on the neutron scattering instruments at FRJ-2.

As in the last five years more than 50% of the experiments were done by researchers which came from outside Forschungszentrum Jülich. Fig. 2 shows the geographical and institutional distribution of the user groups visiting Jülich. It can be seen that the largest number comes from universities. This stresses the importance of the facility in the academic community. Also it can be seen that two thirds of the user groups are not from Germany. 15 countries are represented of which nine do not have own neutron scattering installations. This shows that

Jülich also contributes strongly to the formation of the international neutron scattering science landscape.

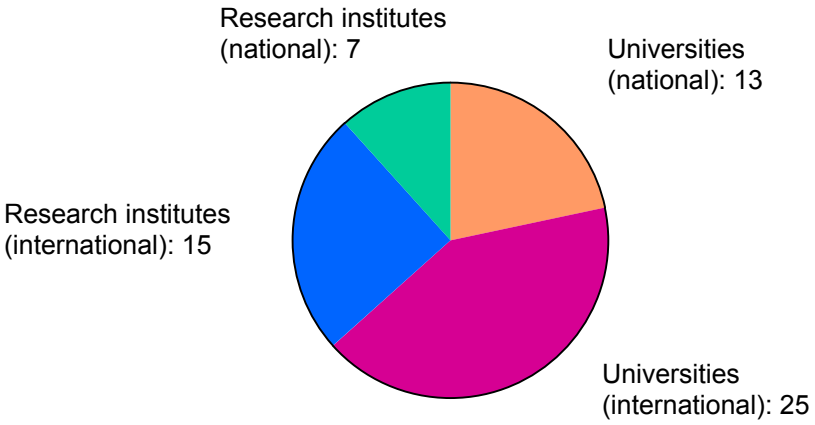

Figure 2: Geographical and institutional breakdown of user groups visiting Forschungszentrum Jülich in 2002 for neutron scattering experiments.

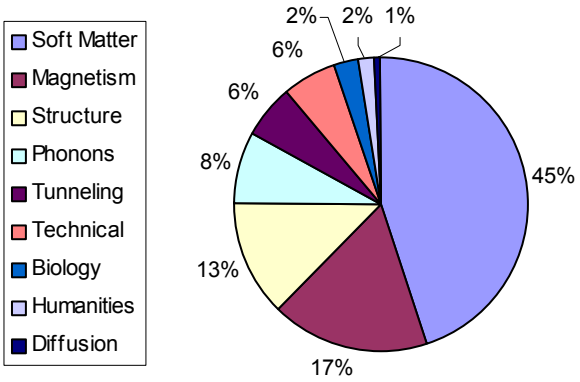

Figure 3: Distribution of topics of the experiments included in this report for the year 2002. "Technical" refers to experiments done to test equipment for other instruments often for external facilities, "humanities" denotes three experiments with the purpose of studying archaeological artefacts.

From the distribution of topics of the experiments done in 2002 it can be seen that the distinctive strength of the Jülich instrumentation (SANS, NSE, BSS) clearly applies to soft matter problems preferentially. Nevertheless, also the "classical" topics of neutron scattering are strongly represented: Studies on magnetic materials were done on DNS, HADAS, and SV-7. The diffractometer SV-7 was mainly used to study structure and texture of "hard matter" samples. Phonons and tunnelling excitations were studied on the various inelastic scattering instruments, UNIDAS, SV-29, DNS, and BSS.

In order to provide the increased number of external users with optimal support during their experiments a dedicated User Office has been founded in 2002. Details about its work and the user access possibilities are summarised at the end of this report.

At this place it should only be noted that the support of non-German European users is possible by the European Union Transnational Access to Infrastructure project "Jülich Neutrons for Europe" since November 2001. Proposals accepted under this programme benefit from funding by the European Commission (travel expenses for users). Of course, the already existing support for German university users is continued. A contractual minimum of 133 instrument-days has to be allocated to this programme. Because the demand is always significantly higher (346 days in 2002) and most proposals are of high quality usually experiments for a larger time (203 days in 2002) are accepted.

In the year 2002 several instrumental developments have opened new experimental possibilities, among them

- The new high resolution small angle scattering camera KWS-3 with focussing mirror could be successfully commissioned. With this world-unique instrument a momentum space resolution down to 2×10^{-4} Å^{-1} can be achieved. For the first experimental results see report KW3-01-901.
- A novel technique of inelastic fixed window scans on the backscattering instrument (BSS) has led to first results (see report BSS-01-008).
- A new instrument (LAP-ND) for spherical neutron polarimetry in transmission was installed and taken into operation.
- The refurbishment of the two small angle scattering instruments KWS-1 and KWS-2 was in full swing. The new electronics and the new detector for KWS-1 are completed and are now being commissioned. Large parts of the new detector for KWS-2 have been built in 2002.

Finally, in 2002 the 6th International Neutron Laboratory Course took place in Jülich. This training course for students was supported by the European Neutron Round Table. As in previous years the number of applicants (89) surpassed largely the available places. Among the 45 selected participants 20 came from outside Germany.

The present document comprises the experimental reports from experiments done at FRJ-2 in the year 2002 and publications from earlier experiments during the last five years. The experimental reports are grouped by instrument[1] and preceded by a tabular description of the instrument parameters. Detailed descriptions of the instruments can be found in the instrument handbook "Neutron Scattering Experiments at the Research Reactor in Jülich" or the web site www.neutronscattering.de .

Reiner Zorn

[1] The SANS proposals are labelled by the instrument they originally applied for. Some experiments were transferred between KWS-1 and KWS-2 because of better feasibility or availability. The instruments SV-30, EKN, LAP-ND, β-NMR are not represented here because they are under construction, only used for test purposes, or not demanded during 2002. Nevertheless, their specifications can be found in the instruments handbook and on the web site.

Twin Diffractometer (SV7)

Instrument Parameters

Monochromators ***- standard:*** ***- optional:***	 Ni (220), PG (002) Ni (200), Cu (111), Pb (311), Ge (111)/(311)
Monochromator angles:	52° and 40°
Wavelengths:	1.0 Å $\leq \lambda \leq$ 2.3 Å
Collimators ***- primary beam:*** ***- scattered beam (optional):***	 Soller: 12 min radially oscillating
Max. beam size:	25 × 40 mm^2
Mean sample volume (cylinder):	10 mm ∅, 30 mm high
Scattering region:	$0° \leq 2\Theta \leq 90°$
Detectors:	linear JULIOS units
Max. neutron flux at sample:	10^6 n/cm^2 s
d-spacings:	0.7 Å $\leq d \leq$ 35 Å
Mean resolution Δd/d:	10^{-2}
Sample environment:	Closed cycle He-cryostat: 4 ... 293 K; He-bath cryostat: 1.5 ... 4.2 K; He-3 cryostat: 0.3 ... 293 K; Split coil magnet cryostat: 0 ... 7 T, 4 … 293 K; cryofurnace 4 ... 400 K; Full circle goniometer with external ω-rotation: 293 K; Flow cryostat containing full circle goniometer: 4 ... 293 K

Instrument Responsible

Dr. Wolfgang Schäfer Tel. +49-(0)2461-61-6024 Email: w.schaefer@fz-juelich.de
DP Ekkehard Jansen Tel. +49-(0)2461-61-4054 Email: e.jansen@fz-juelich.de

Institut für Festkörperforschung
Forschungszentrum Jülich GmbH
D-52425 Jülich

Experimental Report of Neutron Scattering Experiments at the FRJ-2 Reactor

Proposal number:	SV7-01-013		
Experiment title:	**Correlated behaviour of the magnetic order parameter for T→0 and T→T_c**		
Dates of experiment:	29.4.-5.5. u. 23.-31.10.02	Date of report:	5.3.2003
Experimental team: Names	Addresses		
U. Köbler R. Skowronek	Institut für Festkörperforschung FZ Jülich 52425 Jülich MIN/ZFR (Univ. of Bonn)		
Local Contact:	W. Schäfer, Univ. of Bonn		

Experimental report text body

T=0 has long been known as a (quantum) critical point [1]. On approaching T→0 by lowering the temperature the typical critical thermodynamics can be expected. In fact, in contrast to the classical spin wave theory, the thermal decrease of the magnetic order parameter is given to a good approximation by a single power function of the absolute temperature. This law normally holds up to the (thermal) critical range at about $0.85T_c$.
The general validity of a critical power law for T→0 has been confirmed in systematic experimental investigations of many transition metal compounds with a quenched orbital moment and a well defined spin quantum number [2]. Six empirical universality classes for T→0, characterized by the associated critical exponent ε, are now well established. Table I compiles the critical power laws with exponents ε for T→0.
It should be noted that the critical exponents ε are independent of the spin order type and independent of the lattice symmetry, provided the relevant interactions have the same dimensionality.

Table I

exchange interactions	integer spin	half - integer spin
3D	$T^{\frac{9}{2}}$	T^{2}
2D 3D aniso tropic	T^{2}	$T^{\frac{3}{2}}$
1D 2D anisotropic	T^{3}	$T^{\frac{5}{2}}$

Table II

exchange interactions	integer spin	half - integer spin
3D	$\beta = \frac{4}{11}$	$\beta = \frac{1}{2}$
2D	$\beta = \frac{1}{8}$	$\beta = \frac{1}{8}$
1D	$\beta = \frac{1}{3}$	$\beta = \frac{1}{3}$

tabellenaut.cdj

Curiously, the critical exponents ε for $T \rightarrow 0$ are now better known than the conjugated critical exponents β for $T \rightarrow T_c$. The reason for this is that the critical behaviour of real magnetic materials deviates frequently from the predictions of the well known model calculations for continuous phase transitions. One problem is the often not recognized fact that the order parameter can rise discontinuously. At such a phase transition the paramagnetic susceptibility diverges but often with an insignificant critical exponent γ. In other words, the critical behaviour for $T \rightarrow T_c$ is difficult to classify in general considering that the scaling relations can be violated.
The critical exponent β can, however, be used to classify the critical behaviour even if the order parameter behaves discontinuously. Table II displays the conjugated universality scheme to that one of Table I but for the critical exponent β. The proposed universality scheme of Table II is, again, the result of numerous experimental investigations. Note that all β values are assumed to be like the exponents ε rational numbers. Only for isotropic 3D interactions is the critical exponent β different for integer and half-integer spin quantum number.

In order to further test the correspondence between the two universality schemes of Table I and Table II we have measured the temperature dependence of the antiferromagnetic order parameter of a powder sample of $MnCO_3$ with S=5/2 due to the Mn^{2+} ion (Fig. 1 and 2).

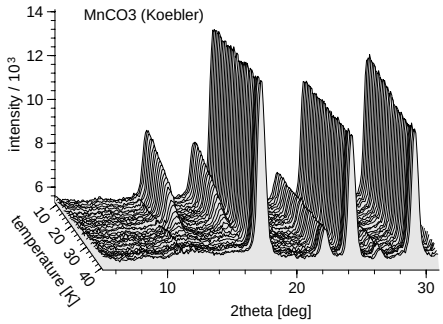

Fig. 1: Sequence of temperature dependent diffraction patterns on $MnCO_3$

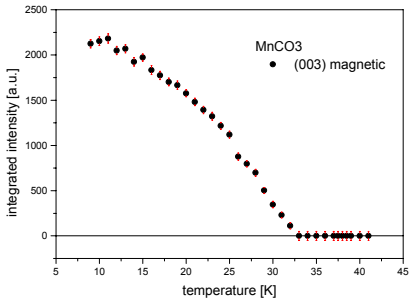

Fig. 2: Temperature dependence of the strongest magnetic peak intensity

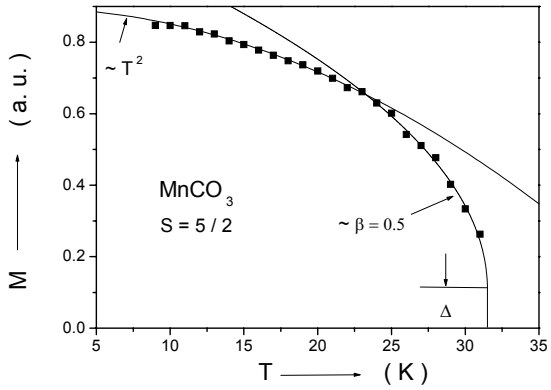

Fig. 3: Magnetization, i.e. square root of the observed integrated magnetic intensity (dots), vs. temperature; fits (solid lines) with T^2 dependence (low T-range) and $\beta = 0.5$ power law (high T-range)

Fig. 3 shows the sublattice magnetization as a function of temperature. A clear crossover between a T^2 dependence as is typical for a half-integer spin and isotropic 3D interactions and a critical power law with $\beta=1/2$ is seen. Moreover, the order parameter is discontinuous at T_N. The two observed exponents conform to the upper right universality classes of Table I and TableII and confirm the correspondence of the two schemes. Since $MnCO_3$ has a rhombohedral lattice symmetry the observed T^2 law shows that the exchange anisotropy is too small to become thermodynamically relevant. Otherwise a $T^{3/2}$ law should be observed.

[1] J.A.Hertz: Phys. Rev. B **14** (1976) 1165.
[2] U.Köbler, A.Hoser, J.Englich, A.Snezhko, M.Kawakami, M.Beyss and K.Fischer: J. Phys. Soc. Japan **70** (2001) 3089.

Institut für Festkörperforschung
Forschungszentrum Jülich GmbH
D-52425 Jülich

Experimental Report
of Neutron Scattering Experiments
at the FRJ-2 Reactor

Proposal number:	SV7-01-015		
Experiment title:	**Longtime stability of copper rolling and recrystallization textures**		
Dates of experiment:	8 Tage, Sept 01; May 02	Date of report:	17.03.2003
Experimental team: Names	Addresses		
J. Palacios	Escula Superior de Fisica y Mathematicas I.P.N. 07300 Mexico		
E. Jansen W. Schäfer A. Kirfel	Mineralogisch-Petrologisches Institut Universität Bonn Poppelsdorfer Schloss 53115 Bonn		
Local Contact:	W. Schäfer		

Experimental report text body

Motivation

Texture transfers structure-related anisotropies from the tiny single crystal into macroscopic properties of the bulk material, e.g. elasticity, hardness, thermal expansion, thermal and electric conductivity, magnetization or corrosion resistance. Thus, texture is an important characteristic of industrial materials like metals, alloys or ceramics, and the longtime stability of textures is expected to ensure stability and reproducibility of material specifications. In continuation of a previous study of the longtime stability of textures in two copper specimens having covered a period of about six years we have monitored the same specimens, a 'rolled' and a 'recrystallized' one, over further six years in order to obtain a longtime experimental control of the texture development.

The initial sample preparation in 1990 had been performed by cold rolling a high purity copper sheet to a final thickness reduction of 95 %. This sheet was cut into platelets of 10x10x1 mm^3, half of which were annealed for 20 min at 300 °C for subsequent recrystallization. Equally oriented platelets were then glued on top of each other yielding two cubes of rolled and rolled plus recrystallized material, resp. No further treatment has taken place since then.

Metal textures can be described by superposition of a small number of texture components starting from ideal crystallite orientations. The texture of cold rolled copper is descibed by three main components: {112}<111>, {110}<112>, and {123}<634> usually denoted as copper, brass and S-shape components, resp. The recrystallized copper texture is dominated by a {001)<100> cube and an additional {122}<212> component (compare Fig. 1).

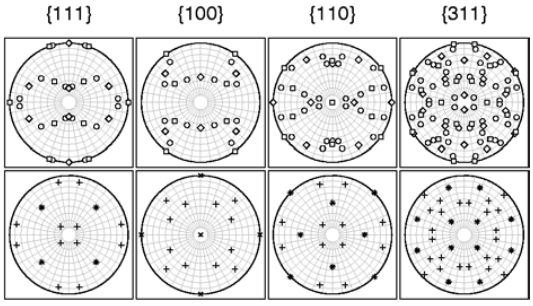

Fig. 1: *Ideal pole figures of planes (top line) modelled by the copper (□) , brass (~), and S-shape (◊) rolling components (top row) and by the cube (×) and {122}<212> (+) recrystallization components (bottom row).*

Experimental

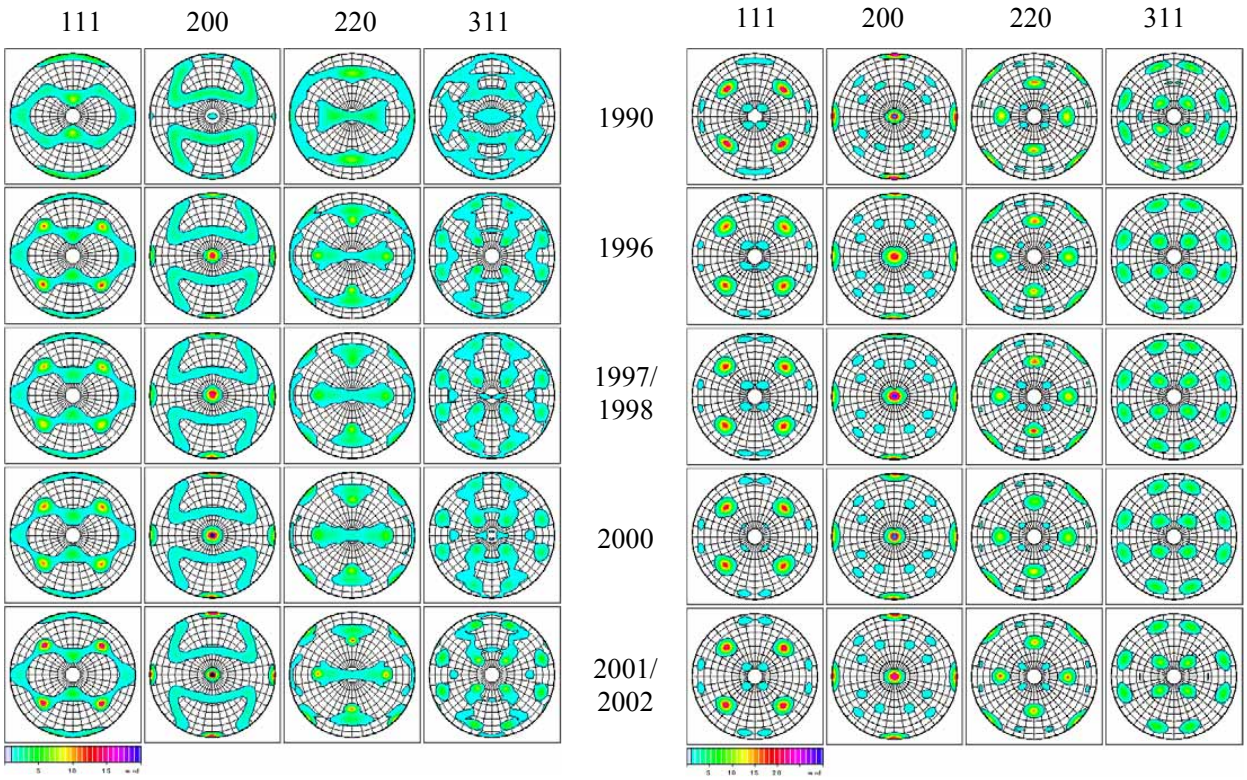

***Fig. 2**: Experimental pole figures of the 'rolled' (left) and 'recrystallized' (right) copper specimens in chronological sequence: 1990, 1996, 1997(8), 2000, and 2001(2) (top to bottom)*

Results

The longtime stability of the Cu textures is shown by the refined volume texture components of the 'rolled' and the 'recrystallized' specimen in Fig. 3 and Fig. 4 resp.

(1) The almost continuous decrease of the rolling texture in favour of recrystallization ends after a period of about 8 years. Then a kind of regeneration occurs and simultaneously recrystallization enhances at the expense of random orientations.

(2) Most probably caused by relaxation the volume shares of the two main recrystallization components show a continuous decrease over a period of about 6 years. Since then, however, this trend ends and even partly reverses

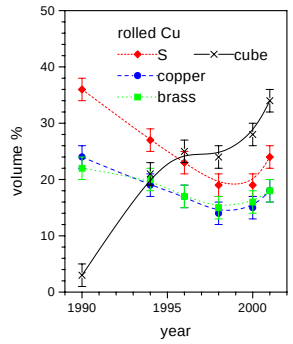

***Fig. 3**: Development of volume texture components of the **'rolled'** specimen*

Conclusions

Metal textures have proven remarkably instable over more than a decade. Changes are continuously ongoing and longtime trends of texture evolution may even be reversed.

Findings of longtime relaxation and subsequent reorientation effects enrich the knowledge of texture transformations which, so far, have mainly been studied on short time scales, e.g. during intermediate stages of deformation and/or annealing.

Reference

E. Jansen, W. Schäfer, A. Kirfel, J. Palacios, Proc. of EPDID-8 in Uppsala (Mater. Science Forum, in print)

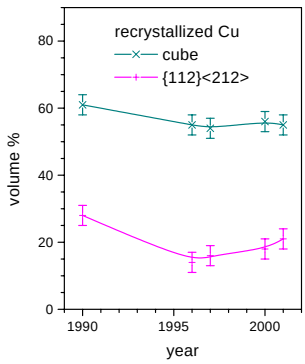

***Fig. 4**: Development of volume texture components of the **'recrystallized'** specimen*

Institut für Festkörperforschung
Forschungszentrum Jülich GmbH
D-52425 Jülich

Experimental Report
of Neutron Scattering Experiments
at the FRJ-2 Reactor

Proposal number:	SV7-01-018		
Experiment title:	**Hydrogen bonds and octahedra distortion in chloroantimonates with organic cations**		
Dates of experiment:	17 days: Jan, May, Nov, Dez	Date of report:	30-12-2002
Experimental team: Names	Addresses		
M. Bujak (J. Zaleski)	Institute of Chemistry, University of Opole, Oleska 48 45-052 Opole, Poland		
R. Skowronek	MIN/ZFR (Univ. of Bonn) Forschungszentrum Jülich 52425 Jülich, Germany		
Local Contact:	W. Schäfer, Univ. of Bonn		

Experimental report text body

Chloroantimonates(III) with organic cations have recently attracted considerable attention with regard to (a) the elucidation of the deformation of inorganic polyhedra, (b) mechanisms of phase transitions and (c) correlations between structure and physical properties. The anionic sublattices of chloroantimonates(III) defined by the general formula $R_aSb_bCl_c$ (R-organic cation; a, b, c-stoichiometric coefficients (c=a+3b)) are composed of almost always deformed $[SbCl_6]^{3-}$ octahedra and/or $[SbCl_5]^{2-}$ square pyramids which may exist as isolated or connected with each other by corners, edges or faces polyanionic units. The cavities between inorganic moieties are filled by organic cations. The organic cations are bound to anionic sublattices through the hydrogen bonds and/or electrostatic interactions. The distortion of single $[SbCl_6]^{3-}$ and $[SbCl_5]^{2-}$ inorganic units in the structures of chloroantimonates(III) is due:

(1) *primary deformation;* the tendency of the $[SbCl_6]^{3-}$ octahedra and $[SbCl_5]^{2-}$ square pyramids to share Cl-atoms with each other resulting in the formation of polyanionic units,

(2) *secondary deformation;* the presence of asymmetric surroundings caused by the N-H…Cl (and C-H…Cl) hydrogen bond system additionally distorts inorganic polyhedra by shifting Cl atoms in the direction of positive charges located on organic cations.

Complementary to previous X-ray measurements neutron diffraction experiments have been performed on polycrystaline $[ND_2(CD_3)]_2\ SbCl_5$ using both (1) the powder diffractometer SV7-a (wavelength $\lambda = 1.0957$ Å) and (2) the texture diffractometer SV7-b ($\lambda = 2.332$ Å). Both instruments are equipped with linear position-sensitive scintillation detectors. The sample material was contained in a cylindrical vanadium can. Diffraction patterns on SV7-a have been collected at temperatures T = 293K, 250K, 150K, 100K and 2K using an orange-type He-cryostat (see Fig. 1 and Fig. 2).

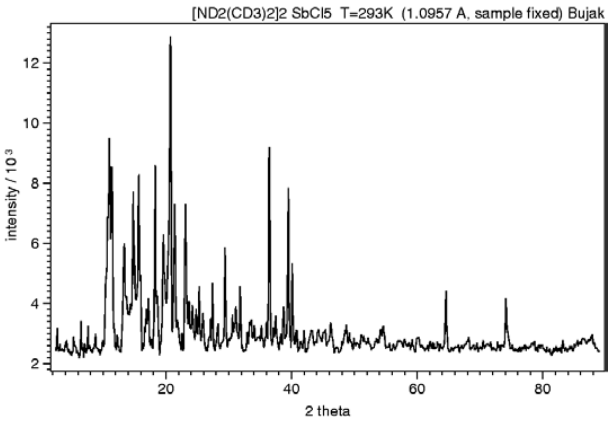

Fig. 1: Room temperature diffraction pattern

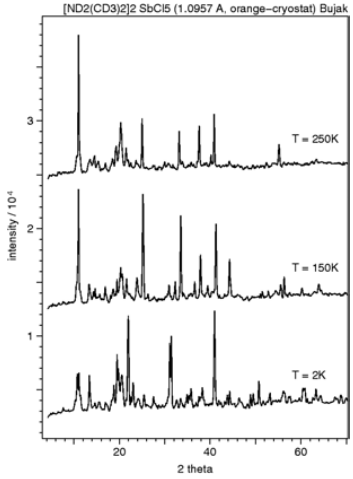

Fig. 2: Temperature dependent diffraction patterns

Table: Basic structural model (space group Pnma)

Atom	site	x	y	x
Sb	4c	0.8066	0.7500	0.6043
Cl(1)	8d	0.8135	0.9679	0.5960
Cl(2)	4c	0.0099	0.7500	0.4932
Cl(3)	4c	0.6096	0.7500	0.4828
Cl(4)	4c	0.0661	0.7500	0.7262
N	8d	0.8020	0.0223	0.3805
C(1)	8d	0.8256	0.9292	0.3164
C(2)	8d	0.6444	0.0626	0.3880
D(11)	8d	0.8924	0.1186	0.4006
D(12)	8d	0.7878	0.9291	0.4674
D(13)	8d	0.0341	0.9616	0.3162
D(14)	8d	0.8379	0.8226	0.3359
D(15)	8d	0.7905	0.9684	0.2620
D(21)	8d	0.6308	0.1100	0.4355
D(22)	8d	0.5954	0.0787	0.3314
D(23)	8d	0.5791	0.0045	0.4097

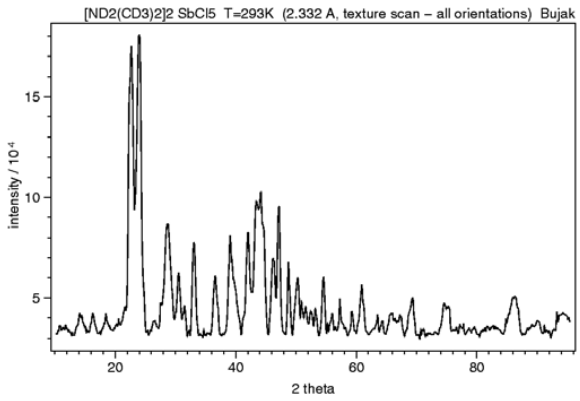

Fig. 3: Sum diagram over all sample orientations

Rietveld refinements (FULLPROF) of the 293 K pattern based on the existing structural model (see Table) and first inspections of the temperature dependent patterns revealed the existence of strong preferred orientations within the moderately hygroscopic poly-crystalline material. In order to experimentally overcome the preferred orientation effects the sample has been remeasured on the texture diffractometer with its full-circle Eulerian cradle. A pole figure scan of about 500 different sample orientations resulted in the sum diffraction pattern shown in Fig. 3. In this pattern, however, reflections of a new (so far unknown) phase appeared which probably is a reaction product of the sample material with the vanadium container where it was stored. Therefore it was decided to prepare a new charge of sample material. Neutron diffraction measurememts on the new material have been performed in late 2002.

Institut für Festkörperforschung
Forschungszentrum Jülich GmbH
D-52425 Jülich

Experimental Report
of Neutron Scattering Experiments
at the FRJ-2 Reactor

Proposal number:	SV7-01-019		
Experiment title:	**Characterisation of coins using neutron texture and phase analysis**		
Dates of experiment:	22-24 Apr 2002	Date of report:	19-02-2003
Experimental team: Names	Addresses		
W. Kockelmann* E. Jansen A. Kirfel (R. Linke) (M. Schreiner)	Mineralogisch-Petrologisches Institut Universität Bonn Poppelsdorfer Schloss 53115 Bonn Academy of Fine Arts Institute of Science and Technologies in Art Vienna, Austria	* at ISIS Facility (ROTAX) Rutherford Appleton Laboratory Chilton, U.K.	
Local Contact:	E. Jansen		

Experimental report text body

Motivation

On the University of Bonn operated ROTAX instrument at the spallation source ISIS of the Rutherford Appleton Lab, TOF neutron diffraction has been successfully applied to non-destructive mineral phase analysis of archaeological objects for the classification, e.g. firing conditions, of ceramics [1, 2]. These activities have attracted a novel class of neutron users working in the fields of archaeometry and archaeology (compare [3]). Further characteristic information on making processes is expected from microstructure analysis by mapping grain orientation distributions to determine the deformation history of e.g. ancient bronzes and coins.

In the course of an ISIS project (proposal RB 12301) submitted to ROTAX by Dr. R. Linke and Prof. M. Schreiner, Institute of Science and Technologies in Art, Vienna, Austria, dealing with a feasibility study on contemporary Ag/Cu coins and test experiments on ancient and medieval coins, supplementary measurements have been performed on the angle-dispersive neutron texture diffractometer SV7-b in Jülich in order to construct experimental pole figures from well-established conventional monochromatic diffraction measurements and to evaluate reliable correction factors in view of the plate-like form of coins.

References

[1] W. Kockelmann, E. Pantos, A. Kirfel, in *Radiation in Art and Archaeometry* (ed. D.C. Creagh and D.A. Bradley) Elsevier Science, 2000, p. 247-277.
[2] W. Kockelmann, A. Kirfel, E. Hähnel, J. Archaeological Science 28 (2001) 213.
[3] S. Siano, W. Kockelmann, U. Bafile, M. Celli, M. Iozzo, M. Miccio, R, Pini, R. Salimbeni, M. Zoppi, Appl. Phys. A 74 (2002), S1139.

Measurements and Results

Pole figure measurements have been performed in the standard SV7-b scan mode on an Austrian 25 Schilling coin consisting of 80 % silver and 20 % copper (Fig. 1). The Ag and Cu pole figures are shown in Fig. 2.

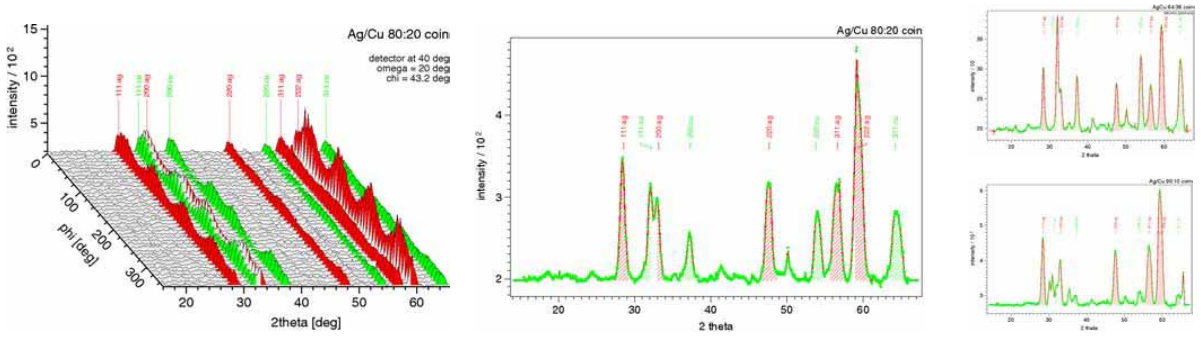

Fig. 1 (left): Sequence of diffraction patterns of the coin as funtion of the rotation angle φ in fixed χ-orientation showing the texture dependent intensity variations of Ag- and Cu-diffraction peaks measured simultaneously with the large linear JULIOS detector on SV7-b; (middle) sum diagram over all sample orientations showing Ag- and Cu-reflections reflecting the 80:20 Ag/Cu composition; (right) comparative diffraction patterns of 10 Schilling (top) and 50 Schilling (bottom) coins of 64:36 and 90:10 composition relations, respectively.

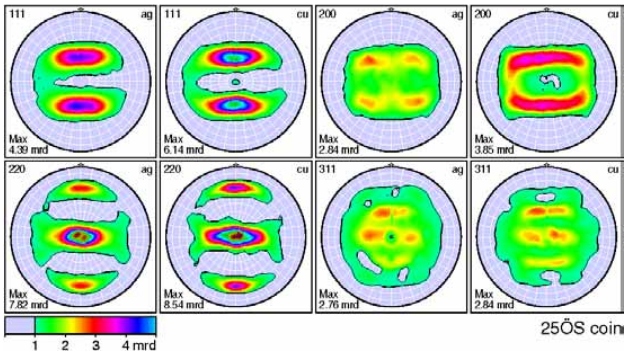

Fig. 2: Experimental pole figures of fcc reflections of both the silver and copper components of Ag and Cu of the 25 Schilling coin; (right) (111), (200) and (220) pole figures of the Ag and Cu components after performing the above mentioned absorption correction

Experimental absorption corrections have been performed on the basis of a comparative pole figure measurement on a ball-shaped Cu-specimen (Fig. 3). The correction factor (Fig. 3) is defined by fac_i = {sum(ball[i,j])} / {sum(coin[i,j])} with the number i of small-circle starting in the center of the pole figure, the points j on the small-circle, and sum being the sum over all points j. Application of this absorption correction on the pole figures of the 25 Schilling coin is shown in Fig. 4.

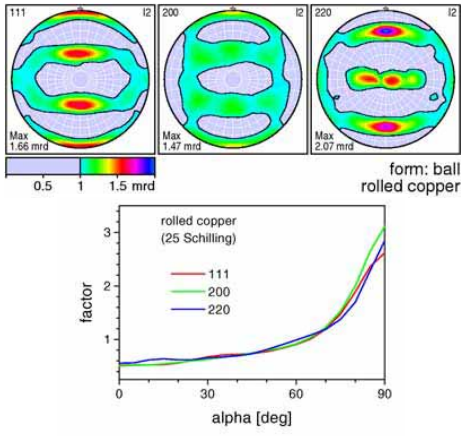

Fig. 3: Experimental pole figures of a ball-shaped copper specimen (top) and experimentally determined absorption corrrection factor for the pole figure coordinate alpha (pole distance)

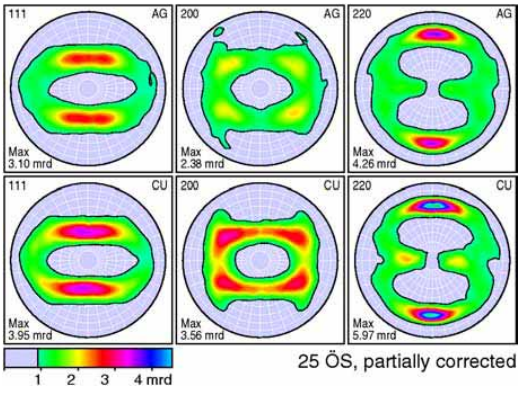

Fig. 4: Appearance of the pole figures of the 25 Schilling coin (top: Ag reflections, bottom: Cu reflections) after application of the absoprtion correction.

Institut für Festkörperforschung
Forschungszentrum Jülich GmbH
D-52425 Jülich

Experimental Report
of Neutron Scattering Experiments
at the FRJ-2 Reactor

Proposal number:	SV7-01-021		
Experiment title:	**Magnetic order and phase transitions in intermetallic R_2CuIn_3 (R=Tb, Ho, Er)**		
Dates of experiment:	Jan 14-18, 2002	Date of report:	14-02-2003
Experimental team: Names	Addresses		
I.M. Siouris (I.P. Semitelou) (J.K. Yakinthos R. Skowronek	Electrical and Computer Engineering Department Physics Laboratory Democritos University of Thrace 671 00 Xanthi, Greece MIN/ZFR (Univ. of Bonn)		
Local Contact:	W. Schäfer		

Experimental report text body

Introduction and previous meassurements

Neutron diffraction and magnetization measurements have been performed to study competing ferro- and antiferromagnetism in AlB_2-type intermetallics (Fig. 1) . The hexagonal AlB_2-type family collects a plethora of intermetallic ternary rare earth(R) – transition metal compounds combined to the metals and metalloids of the IIIa group elements of the periodic table in various chemical compositions. However, the crystallization of such compounds in 'binary-type' structures may set a state of structural disorder imposed by the statistical occupation of the boron site by two different atoms as in R_2CuIn_3 where the hexagonal unit cell contains one formula unit with R on site 1a (0,0,0) and the (Cu, In) atoms statistically distributed over the site 2d (⅓,⅔,½) stacked on layers, alternating with layers of R, normal to the c-axis (see Fig. 1). This may result in an inhomogenous distribution of the surrounding electric charges, leading to a variant electric field seen by the rare earth atoms and consequnetly displaying unusual magnetic properties.

According to low-temperature susceptibility the Tb and Ho compounds Exhibit antiferromagnetic behaviour (T_N = 33 K and 9 K, resp.), while the Er-compound reveals peculiar almost re-entrant spin glass characteristics. Previous neutron diffraction on SV7, however, revelead the absence of any long range magnetic order in the Ho and Er compounds, but confirmed collinear antiferro-magnetic order in Tb_2CuIn_3 [1] and indicated also the presence of a spin glass state.

The coexistence of ordered and spin glass states has been anticipated by mean field theory. Clear evidence was provided in a study of the dilute antiferromag-netic $Fe_{0.55}Mg_{0.45}Cl_2$ [2]. $TbCu_2In_3$ is probably a further example. Therefore, we performed futher low-temperature neutron diffraction on Tb_2CuIn_3 with and without the exposure in external magnetic fields using a cryomagnet on SV7.

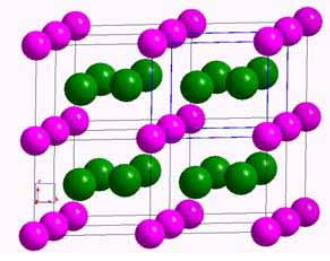

Fig. 1: Structural unit cell of AlB_2-type binary R_2CuIn_3 intermetallics showing a statistical distribution of Cu and In atoms on 2d-sites (green)

Neutron diffraction measurements and data analysis

a) Establishing the collinear antiferromagnetic structure of Tb_2CuIn_3 below 33 K

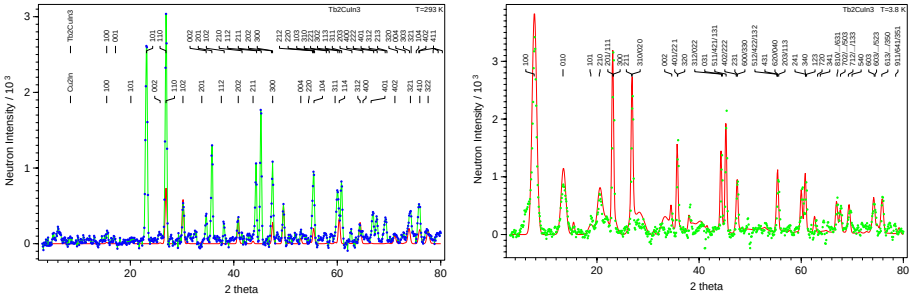

Fig. 2: Rietveld analysed diffraction patterns at 293 K (left) and 4.2 K (right)

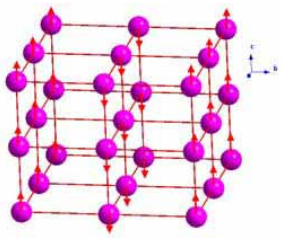

Fig. 3: Collinear antiferro-magnetic structure with spin orientations along c

b) Establishing the presence of a spin glass state

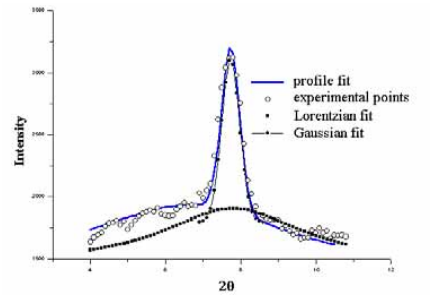

Fig. 4: Broad Lorentzian-type diffuse magnetic peak beyond the Gaussian-type magnetic (100) Bragg-peak

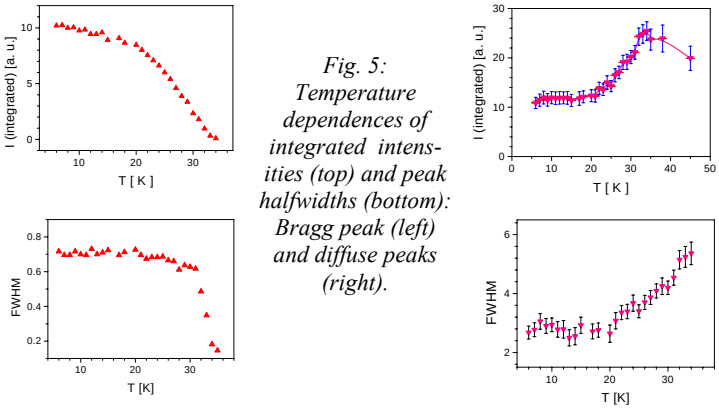

Fig. 5: Temperature dependences of integrated intens-ities (top) and peak halfwidths (bottom): Bragg peak (left) and diffuse peaks (right).

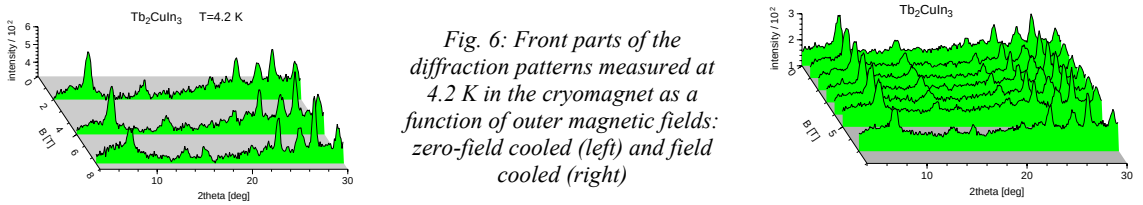

Fig. 6: Front parts of the diffraction patterns measured at 4.2 K in the cryomagnet as a function of outer magnetic fields: zero-field cooled (left) and field cooled (right)

Results and Conclusions

Tb_2CuIn_3 is an antiferromagnet (Fig. 2 and 3) with competing exchange interactions ($J_1 > 0$ for nearest neighbours and $J_2 < 0$ for next nearest neighbours) and an ordering temperature $T_N = 33 \pm 1$ K. Powder diffraction measurements reveal a broad diffuse peak - due to short-range magnetic order - underneath the (100) long-range order magnetic Bragg peak (Fig. 4 and 5). Neither the long range magnetic order nor the short range order are destroyed by outer magnetic fields up to 7.5 T, under both field-cooled and zero-field-cooled conditions (Fig. 6). The almost field independent behaviour of the magnetic intensities is explained by the existence of a spin glass state. Support on the simultaneous presence of antiferromagnetic and spin glass states is given by recent ac-dc magnetic measurements. The infinite range model for spin glasses with strong uniaxial anisotropy has predicted this kind of magnetic behaviour.

Full paper: I.M. Siouris, I.P. Semitelou, J.K. Yakinthos, W. Schäfer, Mat. Sci. Forum (EPDIC-8) in press

Results presented: ESS-Conference, 15-17 may 2002 in Bonn; EPDIC-8 Conference 23-26 May in Uppsala

References

[1] P.Z. Wong, S.V. Molnar, T.T. Palstra, J.A. Mydosh, H. Yoshizawa, S.M. Shapiro, A. Ito, Phys. Rev. Letters 55 (1985) 2043

[2] I.M. Siouris, I.P. Semitelou, J.K. Yakinthos, W. Schäfer, R.R. Arons, J. Alloys Comp. 314 (2001) 1 and J. Magn. Magn. Mater. 226-230 (2001) 1128

Institut für Festkörperforschung
Forschungszentrum Jülich GmbH
D-52425 Jülich

Experimental Report
of Neutron Scattering Experiments
at the FRJ-2 Reactor

Proposal number:	SV7-02-001		
Experiment title:	**Structure and magnetism of nanocrystalline ferrihydrite**		
Dates of experiment:	Jan 18-21, 2002	Date of report:	13-02-2003
Experimental team: Names	Addresses		
A. Kyek	Physik-Department E15 Technische Universität München 85747 Garching, Germany		
U. Schwertmann	Lehrstuhl für Bodenkunde Technische Universität München 85350 Freising, Germany		
E. Jansen	MIN/ZFR, (Univ. of Bonn)		
Local Contact:	W. Schäfer, Univ. of Bonn		

Experimental report text body

What are ferrihydrites and why neutron diffraction?

Ferrihydrite is an Fe(III)-oxyhydroxide (bulk formula: 5 Fe_2O_3 · 9 H_2O) of considerable importance in mineralogy and metallurgical processing (see [1]). Natural ferrihydrite occurs in waters and sediments, soils, weathering crusts and mine wastes; it is commonly formed by rapid oxidation of Fe^{2+}-containing solutions followed by hydrolysis in the presence of crystallization inhibitors. In iron and steel industries, ferrihydrite occurs as a corrosion product of iron and steel.

Ferrihydrite is characterized by high dispersion, small particle size, and poor cristallinity. Therefore, X-ray diffraction patterns consist of only a few broad peaks the number of which varies between 2 and 6-7. The structure was first described by Towe and Bradley in 1967 [2]. Since then, a variety of structure models has been suggested. Drits et al. [3] reported on disagreements between X-ray diffractograms and the existing models. They suggested a new structure model consisting of a mixture of essentially two phases: (1) a defect-free phase (space group P-31c) of anionic ABACA... close packing in which Fe atoms occupy only octrahedral sites and (2) a defective phase being composed of two structural fragments of the defect-free phase completely randomly distributed within a hexagonal super-cell. In addition, they suggested an admixture of hematite. The magnetic properties of ferrihydrite are also controversially discussed. According to Murad [4] natural ferrihydrite is superparamagnetic at RT and remains so to temperatures as low as 23 K. Ferrimagnetic and antiferromagnetic states are attributed to the 2-line and 6-line species, respectively (Pankhurst and Pollard [5]).

Neutron diffraction with its electron-independent nuclear scattering and its unique magnetic scattering is considered as a useful tool in obtaining complementary information with respect to both structural and magnetic properties of ferrihydrite (compare Fig. 1).

Neutron diffraction results

The crystal structure of ferrihydrite can be best described by a superposition of two components as proposed by Drits et al. and being referred to as defect-free (f) and defective (d) phases, respectively, and being described in the trigonal space groups P –31c and P 3, respectively. The room temperature lattice constants are a_0 = 0.2955(4) nm and c_0 = 0.937(2) nm. The corresponding values at the measuring temperatures of 5 K and 343 K are a_0 = 0.2942(1) nm, c_0 = 0.9361(9) nm and a_0 = 0.2957(3) nm, c_0 = 0.946(2) nm, respectively. The layered structure of ferrihydrite is depicted in Fig. 2 indicating an ABAC sequence of OH and O for the f-phase.

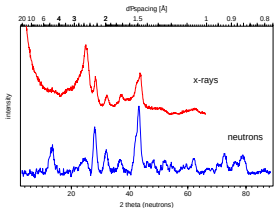

Fig. 1: Comparison of X-ray and neutron diffractograms of ferrihydrate at 293K

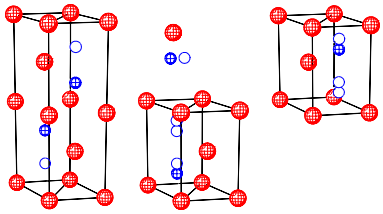

Fig. 2: The layered structure of ferrihydrate composed of a random sequence of a detect-free ABACA and two defective ABA, ACA phases

The d-phase which consists of a subunit ($c_d = c_f/2$) of the f-phase, originates by a symmetry reduction (P-31c $\rightarrow$ P 3) which involves atomic site splittings and consequently a higher degree of disorder due to varying occupancies and additional vacancies in the structure. Fig. 3 depicts the Rietveld refined diffraction pattern. The Bragg scattering contributions of the f- and d-phase are separately extracted.

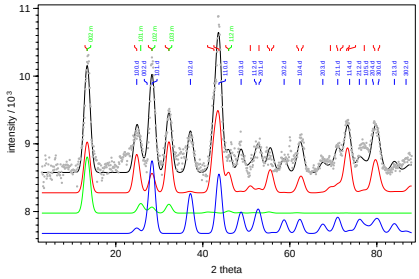

Fig. 3: Rietveld analysed diffraction pattern at 5 K with 3 phases: magnetic (dashed), defect-free (dash-dotted), defective (dotted)

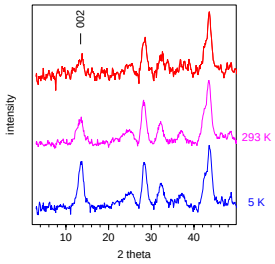

Fig. 4: Sections of diffraction patterns at 323 K, 293 K and 5 K

The nuclear Bragg scattering in the diffraction patterns is superimposed by coherent magnetic scattering due to an order of the magnetic iron spins. This is clearly visible by the first strong (002) peak when comparing the temperature dependent neutron diffraction patterns (Fig. 4) and the 5 K Rietveld refinement (Fig. 3). The determination of the magnetic structure has been performed by a comparison of different spin configurations considering the octrahedrally coordinated iron atoms on the 4f sites. The neutron measurements are in accordance with a collinear antiferromagnetic structure; the magnetic moments orientated perpendicular to the trigonal axis. Intensity refinements reveal a magnetic moment of 3.2(3) μ_B per Fe-ion at 5 K.

The nanocrystalline nature of the ferrihydrite specimen is evident from significant broadenings of all diffraction peaks. The quantitative analysis of the mean particle size s is based on the the Scherrer formula $s = \lambda / (B \cos \Theta)$ containing the experimental, specimen-specific peak halfwidth B. Accordingly, a mean particle size of 2.7(8) nm is obtained for the actual ferrihydrite specimen.

Neutron measurement reference: E. Jansen, A. Kyek, W. Schäfer, U. Schwertmann, Appl. Phys. A 74 (2002) S1004.

Literature

[1] U. Schwertmann, in Iron in Soils and Clay Minerals, NATO ASI Ser. 217 (1988) 267.
[2] K.M. Towe, W.F. Bradley, J. Colloid Interface Sci. 24 (1967) 384.
[3] V.A. Drits, B.A. Sakharov, A.L. Salyn, A. Manceau, Clay Miner. 28 (1993) 185.
[4] E. Murad, in Iron in Soils and Clay Minerals, NATO ASI Ser. 217 (1988) 309.
[5] Q.A. Pankhurst, R.J. Pollard, Clays Clay Miner. 40 (1992) 268.

Institut für Festkörperforschung
Forschungszentrum Jülich GmbH
D-52425 Jülich

Experimental Report
of Neutron Scattering Experiments
at the FRJ-2 Reactor

Proposal number:	SV7-02-002		
Experiment title:	**A neutron powder diffraction study of the magnetic structure of several $RFe_{12-x}Mo_x$ Compounds**		
Dates of experiment:	25.-29.3.2002	Date of report:	27.2.2003
Experimental team: Names	Addresses		
R. Hermann F. Grandjean G.J. Long	Département de Physique – Bat B5 Université de Liège B-4000 LIEGE BELGIQUE		
R. Skowronek	MIN/ZFR (Univ. of Bonn)		
Local Contact:	W. Schäfer, Univ. of Bonn		

Experimental report text body

Motivation

Permanent magnets are a major commercial field for the electronic industry and research for new materials with improved magnetic properties for permanent magnet applications has been very active for the past twenty years after the discovery[1,2] of $Nd_2Fe_{14}B$ and of the $R_2Fe_{17}N_3$ interstitial nitrides, where R is a rare-earth atom. In the search for better materials, another series of compounds, $RFe_{12-x}M_x$, where R is a rare-earth atom, M is a metal such as Ti, V, or Mo, and x is less than three, has also been investigated[3-6] by various techniques, such as x-ray and neutron diffraction, magnetic measurements, Mössbauer spectroscopy, and x-ray absorption spectroscopies. We have recently undertaken detailed iron-57 Mössbauer spectral studies of the $RFe_{12-x}Mo_x$ compounds, where R is Y, Ce, Ho, and Tb, and $0 < x \leq 3$.
The Mössbauer spectra obtained from $CeFe_9Mo_3$ and $YFe_{11.5}Mo_{0.5}$ at 295 and 90 K are very complex because the iron atoms occupy three different crystallographic sites, the 8*f*, 8*i*, and 8*j* sites, and have a distribution of near-neighbor environments due to the partial occupation of one or more of these three crystallographic sites by molybdenum. The analysis of these spectra will be both greatly facilitated and much more meaningful if the specific Mo site occupancies and the orientation of the iron and rare-earth magnetic moments are known from powder neutron diffraction studies.

Experimental

Within this starting project, a series of five $YFe_{12-x}Mo_x$ compounds has been investigated by room temperature neutron powder diffraction using a wavelength of 1.096 Å on SV7:

$YFe_{11.5}Mo_{0.5}$ $YFe_{11.0}Mo_{1.0}$ $YFe_{10.8}Mo_{1.2}$ $YFe_{10.0}Mo_{2.0}$ $YFe_{9.0}Mo_{3.0}$

Data analysis

So far, data analysis was concentrated on structure information in view of the (Fe, Mo)-concentration dependent cell parameters and fractional atomic position parameters on 8i and 8j sites the knowledge of which is essential for the analysis of the hyperfine field splittings of the Mössbauer spectra (compare Fig. 1). The room temperature diffraction patterns have been analysed by full-pattern Rietveld refinements using Fullprof (Fig. 2).

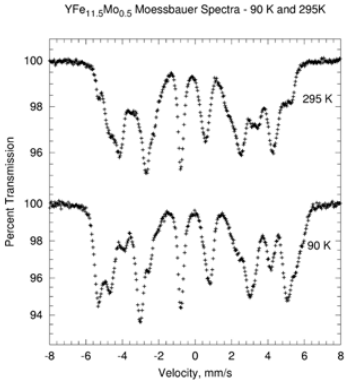

Fig. 1: Mössbauer spectra of $YFe_{11.5}Mo_{0.5}$

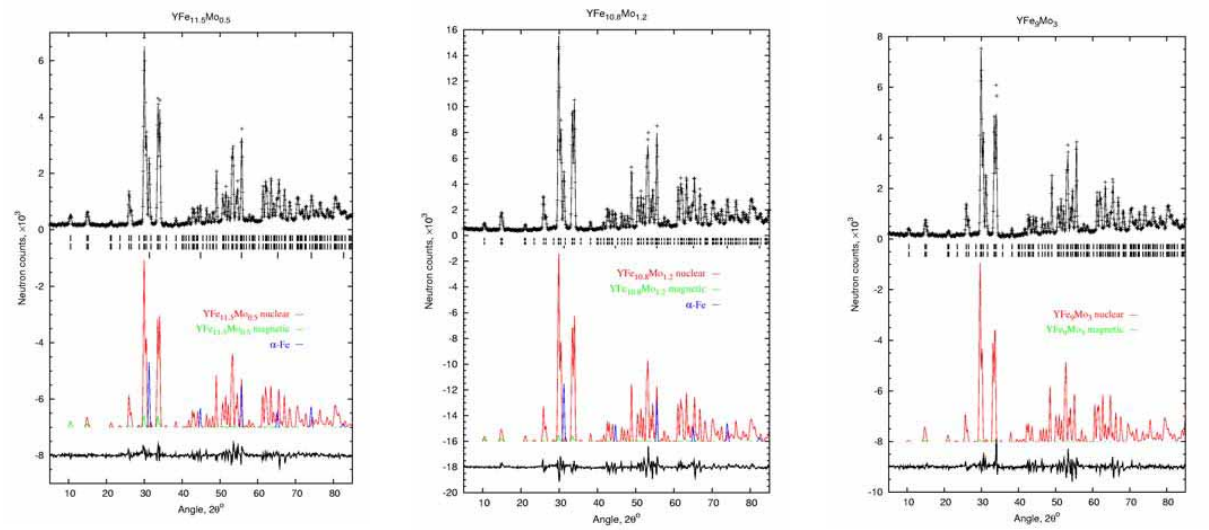

Fig. 2: Rietveld analysed room temperature diffraction patterns of $YFe_{12-x}Mo_x$ compounds:
top: experimental points (+) and fit (line)
below: calculated pattern composed of nuclear and magnetic parts as well as a α-Fe phase contamination
bottom: differences between experimental and fit curve

Structure results

The observed linear and non-linear dependences of the lattice parameters a and c, resp. (Fig. 3) from the Mo-concentration x are structure specific, because a strongly depends on Y and c only on Fe and Mo. Hypothesis: A linear isotropic dilatation is superimposed by a repulsive extension of the c-axis. This is consistent with the variation of the fractional position parameters (Fig. 4) leading to an anisotropic dilatation.

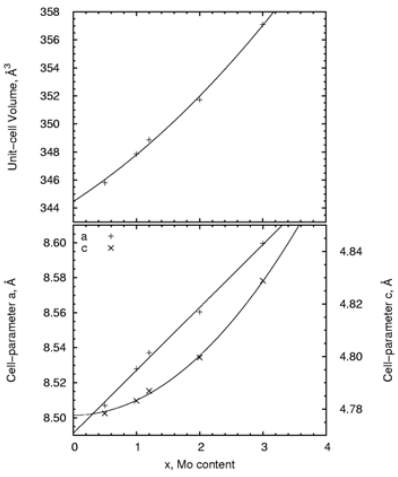

Fig. 3: Mo-concentration dependent cell parameters and unit cell volume

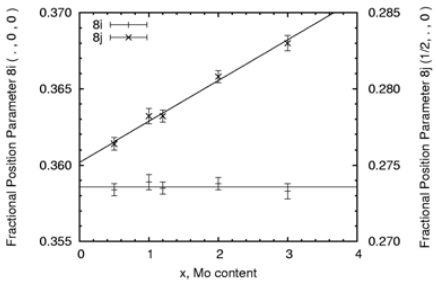

Fig. 4: Mo-concentration dependent fractional atomic position parameters

Institut für Festkörperforschung
Forschungszentrum Jülich GmbH
D-52425 Jülich

Experimental Report
of Neutron Scattering Experiments
at the FRJ-2 Reactor

Proposal number:	SV7-02-003		
Experiment title:	**Magnetic structures of three compounds of the brownmillerite series $Ca_2(Fe_{2-x}Al_x)O_5$**		
Dates of experiment:	10d, Jan 2002	Date of report:	6.3.2003
Experimental team: Names	Addresses		
G. Redhammer (G. Roth) R. Skowronek	Institut für Kristallographie RWTH Aachen Jägerstr. 17-19 52056 Aachen MIN/ZFR (Univ. Bonn)		
Local Contact:	W. Schäfer		

Experimental report text body

On the structure

Brownmillerite, chemical formula $Ca_2(FeAl)O_5$ is one of the four main components of Portland cement clinkers. Brownmillerite itself is one composition of the solid solution series $Ca_2Fe_2O_5$ - $Ca_2Al_2O_5$. Under ambient conditions, there is a complete solid solution series for compositions $Ca_2Fe_{2-x}Al_xO_5$ up to x = 1.4. Pure $Ca_2Fe_2O_5$, also known under its mineral name srebrodoskite, is orthorhombic and crystallizes in space group *Pnma* at 25°C, lattice parameters are a = 5.4260(1) Å, b = 14.7631(1) Å and c = 5.5969(1) Å (from powder X-ray diffraction).

The crystal structure of $Ca_2Fe_2O_5$ at room temperature was first determined by Bertaut et al. (Acta Cryst. 12 (1959) 149) and then refined several times, e.g. by Coville (Acta Cryst. B25 (1970) 1469) and very recently by Redhammer et al. (Acta Cryst. B, in preparation). The structure consists of alternate layers of $Fe^{3+}O_6$ octahedra sharing corners and $Fe^{3+}O_4$ tetrahedra sharing corners interleaved by Ca^{2+} iones surrounded by eight O^{2-} ions. Each octahedron shares two corners with tetrahedra in adjacent layers.

The Fe^{3+}-ions are equally distributed on two a-c planes which contain either octrahedrally or tetrahedrally coordinated sites and which are alternatively stacked along the b-direction.

On the magnetic order

According to Geller et al. (Progr. Sol. State Chem. 5 (1971) 1-26) $Ca_2Fe_2O_5$ is antiferromagnetically ordered below 720 K. The magnetic structure has been determined by crystal - chemical considerations in analogy to $Sr_2Fe_2O_5$. The spins lie in a plane perpendicular to the *b* axis and parallel to the *a* - axis. The magnetic space group Pcm´n´ was proposed. Even if the principal magnetic structure of $Ca_2Fe_2O_5$ is known, no detailed information concerning spin arrangements, on variation of the intensity of magnetic Bragg - reflections as a function of temperature, and concerning the magnetic (and crystallographic) structure at 295 K and very low temperatures (4 K) is known.

Mößbauer measurements on $Ca_2Fe_2O_5$ at 295 K reveal well ordered magnetic subspectra for both, the octahedral and tetrahedral site in this compound. ^{57}Fe hyperfine parameters are in the typically range for high spin Fe^{3+} in octahedral and tetrahedral coordination, area ratio of both subspectra is 1:1.

The situation - however - becomes much more complicated when Fe^{3+} is replaced by Al^{3+}. Line broadening and appearance of a second Fe^{3+} component for the tetrahedral site are observed in the Mößbauer spectra of the Al^{3+} substituted compounds. This is indicated in Figure 2 for the most evident parts in the Mößbauer spectrum by arrows. To our opinion, these effects are due to magnetically different environments around the Fe^{3+} probe nucleus. In literature there are no clear information concerning the magnetic structure of Al^{3+} substituted $Ca_2Fe_2O_5$. Knowledge of the magnetic structure - however - is the key in interpreting the Mößbauer spectra of the samples along the brownmillerite solid solution. Thus, powder neutron diffraction experiments are needed.

Neutron measurements

We have synthesized a total of 16 polycrystalline samples along the $Ca_2Fe_{2-x}Al_xO_5$ solid solution series up to x = 1.4 at 1673 K. Out of these samples, three compositions were synthesized in larger amounts as 15 g batches suitable for neutron powder diffraction measurements (x = 0.0, 0.5 and 1.0). So far, diffraction patterns have been collected on SV7 at 293 K and 4.2 K using wavelengths of 1.095 Å and 2.332 Å (Fig. 1).

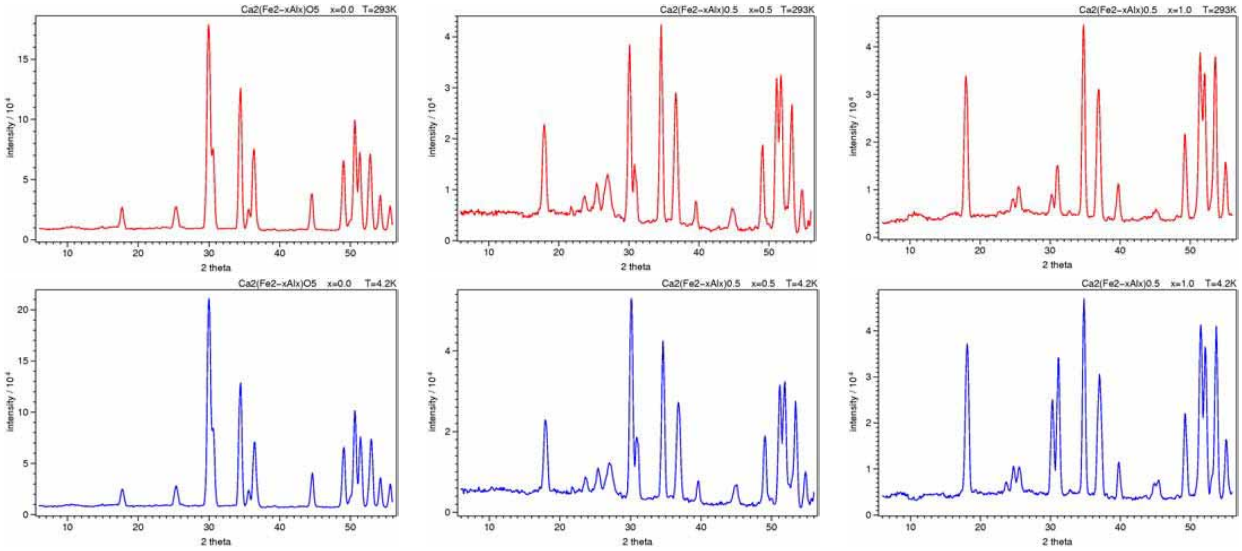

Fig. 1: Neutron diffraction patterns (2.332 Å) collected at 293K (top) and 4.2K (below) on $Ca_2Fe_{2-x}Al_xO_5$ with x=0.0 (left), x=0.5 (middle), x=1.0 (right). The spectra contain both nuclear and magnetic reflections.

Additional measurements at about 800 K, i.e. above the magnetic phase transitions are planned, using the new furnace which has been constructed for SV7.
Data evaluation using full-pattern Rietveld refinements has been started on the pure $Ca_2Fe_2O_5$ compound (see Fig. 2). The magnetic structure is antiferromagnetic for both the tetrahedral and octahedral planes. The spins are oriented along a and perpendicular to b with moment values of $\mu = 4.5(1)\ \mu_B$ and $3.3(1)\ \mu_B$ in the terahedral and octahedral sublattices, respectively.
The partial substitution of Fe by Al results in significant changes of the magnetic structure as becomes obvious by a comparison of the diffraction patterns in Fig. 1. The changes concern both spin directions and moment values. So far, however, the structures are not finally solved.

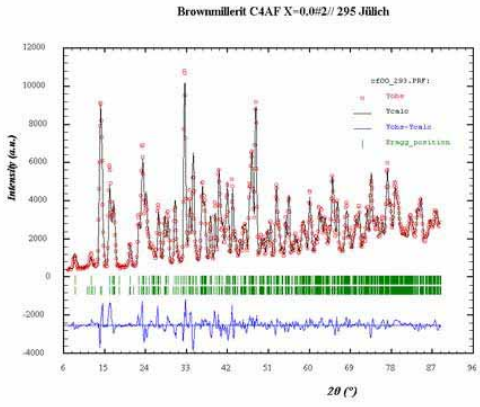

Fig. 2: Rietveld-plot of the room-temperature pattern (x=0.0) and wavelength of 1.095 Å

Institut für Festkörperforschung
Forschungszentrum Jülich GmbH
D-52425 Jülich

Experimental Report
of Neutron Scattering Experiments
at the FRJ-2 Reactor

Proposal number:	SV7-02-005		
Experiment title:	**Experimentelle Bestimmung der Gleitsysteme von Hämatit bei Temperaturen über 400°C (hier: bei 600°C verformte Einkristalle)**		
Dates of experiment:	18 Tage: Jan, Feb 2002	Date of report:	26.2.2003
Experimental team: Names	Addresses		
H. Siemes* B. Klingenberg	Institut für Mineralogie und Lagerstättenlehre RWTH Aachen Bunsenstr. 8 52056 Aachen	*Förderung: DFG Si 209/32-1	
(E. Rybacki) (M. Naumann)	Geoforschungszentrum Potsdam Projektbereich 3.2: Rheologie und Tectonophysics Telegrafenberg D429 14474 Potsdam		
Local Contact:	E. Jansen, Univ. Bonn		

Experimental report text body

Motivation

Experimentelle Bestimmungen der Gleitsysteme an Einkristallen von Hämatit unter definierten Bedingungen der Temperatur (25°C, 200°C, 400°C), Manteldruck (400 MPa) und Verformungsrate (~$10^{-5}s^{-1}$) und der Bestimmung der Zwillingspannungen bzw. kritischen Schubspannungen liegen bisher nur von Hennig-Michaeli & Siemes (1982) [1] vor. In Verformungsversuchen an Einkristallen soll die Kenntnis der Gleitsysteme von Hämatit auf Temperaturen von 600°C bis 800°C ausgedehnt werden.

Ausgangsmaterial und Verformungsversuche

Als Ausgangsmaterial wurden natürliche Einkristalle von verschiedenen Fundpunkten in Minas Gerais, Brasilien verwendet. Diese Kristalle wurden orientiert geschnitten und zu prismatischen Probenkörpern von etwa 7 mm * 7 mm Querschnitt und 13 mm Länge verarbeitet; bzgl Orientierungen siehe Abb. 1 und Tabelle. Die Versuche wurden in einer Paterson-Apparatur [2, 3] mit Argongas als Manteldruckmedium ausgeführt. Vom Gasmedium werden die in der Regel zylinderförmigen Proben durch eine Eisenhülle, die im Bereich der Probe 15 mm Durchmesser und 0,34 mm Wandstärke hat, getrennt. Die prismatischen Proben wurden in einen Kupferzylinder von 15 mm Durchmesser mit einem passenden zentralen prismatischen Ausschnitt eingepasst. Zur Vermeidung einer Reaktion zwischen Kupfer und Hämatit wurden noch dünne Folien von Silber und Palladium bzw. eine Silber(70)-Palladium(30)-Legierung zwischen Probe und Kupfer eingebracht, vgl. [6].

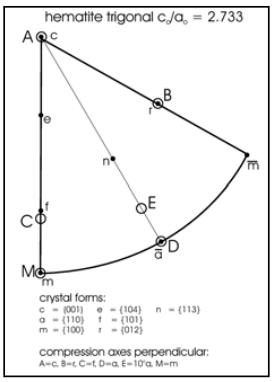

Abb. 1: Orientierungen der Kristallachsen

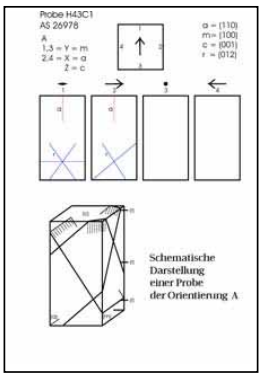

Abb. 2: Orientierung der Probe H43C1

Tabelle 1: Verformungsversuche an vier im Jahr 2002 innerhalb dieses Projektes mit Neutronenbeugung untersuchten prismatischen Hämatit-Einkristallen (7x7x13 mm^3)

Probenbe-zeichnung	*Probenoberflächen Z X Y* *Stauchachse ⊥ Z*	*Verformung Datum*	*Temperatur °C*	*Rate s^{-1}*	*Mantel-druck MPa*
H91R B	r a 5°e	12.2001	600	10^{-5}	300
H42M3 M	m a c	12.2001	600	10^{-5}	300
H43C1 A	c a m	12.2001	600	10^{-5}	300
HS230 DD	a 3°r 9°e	12.2001	600	10^{-5}	300

Berichtet wird hier über die experimentellen Ergebnisse an Probe H43C1 (Orientierung in Abb. 2 dargestellt).

Neutronen-Texturmessungen

Die Neutronen-Texturmessung von 5 Reflexen (Abb. 3 a, c-f) zeigt jeweils die Ausgangsorientierung und drei Zwillingsorientierungen in fast gleicher Intensität. Abb.4 b gibt die theoretischen Positionen der Ausgangsorientierung A mit den 3 Zwillingsorientierungen wieder. Man erkennt, daß die Pole der Zwillingskristalle z. T. dicht beieinander liegen (z.B. a), z. T. aufeinander liegen (z.B. f, a) und mit den Polen des Ausgangskristalls zusammenfallen (r). Die kleineren Zwillingsmaxima in der (003)-Polfigur (Abb. 3a) sind auf ein Teilvolumen der Hämatitprobe mit einer geringfügig versetzten Ausgangsorientierung zurückzuführen. Im Zentrum der f=(101)-Polfigur entstehen durch die Verzwillingung drei nahe beieinander liegende Maxima, diese entsprechen der Orientierung C der Abb. 1.

Die (110)- und die (003)-Polfigur wurden so gewälzt, daß das (110)-Hauptmaximum im Zentrum der Polfigurder Abb. 4(oben) liegt. Wenn man annimmt, daß diese Längung in ähnlicher Weise erzeugt wird wie der Asterismus in Laueaufnahmen von verformten Kristallen [4, 5], dann zeigt das zentrale, stark ausgelängte Maximum eine Gleitung auf der (110)-Fläche an. Das würde bedeuten, daß die Normale zur langen Achse Biegungsachse ist, die senkrecht zur Gleitrichtung steht. In Abb. 4(unten) sind die wichtigsten Hämatitpole in einer Projektion wie in Abb. 4(oben) dargestellt. Daraus kann man ablesen, daß das Gleitsystem {a}<m> nicht die Ursache sein kann, da in diesem Fall die c-Achse Biegungsachse sein müßte. Möglicherweise erhält man aus der Analyse der anderen Proben eine Lösung für dieses Problem.

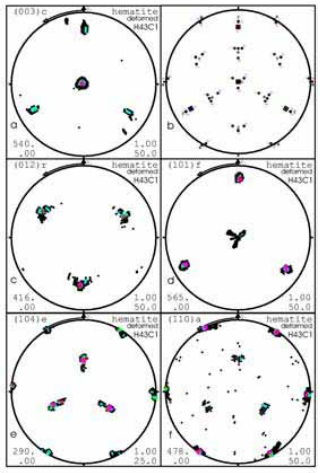

Abb. 3: Gemessene Polfiguren

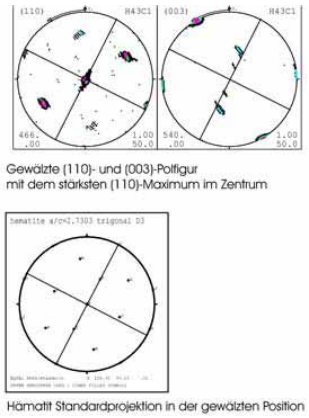

Abb. 4: Gewälzte Polfiguren

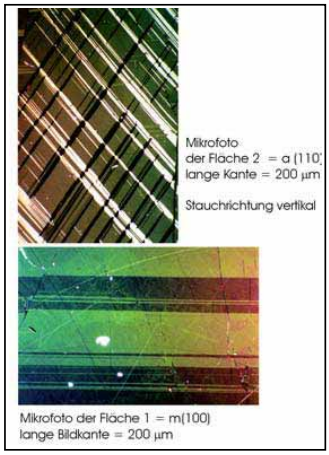

Fig. 5: Mikrofotos der Flächen 1 und 2 (siehe Abb. 2)

Die Neutronenbeugungsmessungen und optische Untersuchungen (vgl. Abb. 5) ergänzen sich hervorragend zur Bestimmung der Bildung der Deformationszwillingsbildung und sind sehr hilfreich bei der Bestimmung der Slipsysteme. Ob noch ergänzende Untersuchungen mit elektronenmikroskopischen Methoden (EBSD) notwendig sind, wird zur Zeit untersucht. Die in dem verformten Einkristall sehr intensiv auftretenden Zwillingslamellen werden bei gleicher Versuchstemperatur in experimentell verformtem polykristallinen Hämatit nur spärlich gefunden [6].

Literaturangaben

[1] Hennig-Michaeli, Ch. & Siemes, H.: In: High Pressure Research in Geoscience, Schweizerbart'sche Verlagsbuchhandlung, Stuttgart (1982) 133-150.

[2] Paterson, M.S., 1970. Intern. J. Rock Mechanics and Mining Sciences 7 (1970) 517-526.

[3] Paterson, M.S., 1990: In: The Brittle-Ductile Transition in Rocks. The Heard Volume American Geophysical Union Geophysical Monograph 56 (1990) 187-194.

[4] Maddin, R., Chen, N.K., Progress in Metal Physics 5 (1954) 53-95.

[5] Siemes, H., Saynisch, H.J., Borges, B., N. Jb. Miner. Abh. 119 (1973) 65-82.

[6] Siemes, H., Klingenberg, B., Rybacki, E., Naumann, M., Schäfer, W., Jansen, E., Rosière, C.A., J. Struct. Geology (2003).

Institut für Festkörperforschung
Forschungszentrum Jülich GmbH
D-52425 Jülich

Experimental Report
of Neutron Scattering Experiments
at the FRJ-2 Reactor

Proposal number:	SV7-02-007		
Experiment title:	**Hämatittexturen von Eisenerzlagerstätten Südafrikas**		
Dates of experiment:	17d, mar, sep, oct 2002	Date of report:	5.3.2003
Experimental team: Names	Addresses		
H. Siemes B. Klingenberg	Institut für Mineralogie und Lagerstättenlehre RWTH Aachen Bunsenstr. 8 52056 Aachen		
C. Rosière	Instituto de Geosciencas Universidade Federal de Minas Gerais Av. Antonio Carlos, 6627 CEP 31270-901 Belo Horizonte, MG, Brasilia		
Local Contact:	E. Jansen, Univ. Bonn		

Experimental report text body

Einführung

Textur und Mikrogefüge von Hämatiterzen der Sishen Mine in Südafrika wurden aus zwei Gründen untersucht:
(1) In einem gemeinsamen Projekt von Geowissenschaftlern aus Belo Horizonte, Clausthal und Aachen sind in den vergangenen Jahren die Hämatitlagerstätten des Eisernen Vierecks des Bundesstaates Minas Gerais, Brasilien intensiv beprobt und untersucht worden (s. z.B. [1, 2]). Die Ergebnisse waren der Anlaß, die Untersuchungen auf weitere Erzgebiete auf der Südhalbkugel der Erde auszudehnen. Die hier vorliegenden Messungen sind ein Teil dieses Projektes.
(2) In einem kürzlich abgeschlossenen Projekt über experimentelle Verformungen an Hämatiterzen [3], wurde ein Hämatiterz aus Südafrika für die Herstellung der Probenkörper verwendet. Der nähere Fundpunkt des Erzes war unbekannt, aber es war zu vermuten, daß das Erz aus der Sishen Mine war.

Probenfundpunkte

Die Sishen Mine liegt in Northern Cape, Südafrika, etwa 220 km nordwestlich von Kimberley. Die Hämatiterze werden in einem Tagebau von etwa 11 km Länge, 1,5 km Breite und bis 400 m Tiefe abgebaut. Die Erzformation enthält fein gebänderte (laminated) Erze, massive Erze und konglomeratische Erze (vgl. Abb. 1). Unterlagert wird der Erzhorizont von der Banded Iron Formation (BIF).
Die Erzenerzgrube Thabazimbi liegt in der Northern Province ca. 180 km nord-nordwestlich von Pretoria.

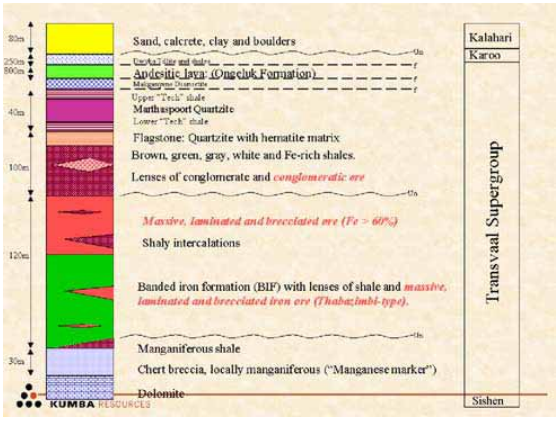

Abb. 1: Profil durch den Lagerstättenbereich

Neutronenmessungen

Für Polfigurmessungen an SV7 standen folgende Proben zur Verfügung:

S05, North Mine, laminated ore, 06.08.2002 (Siemes)
S07, South Mine, specularite, 06.08.2002 (Siemes)
S09, Bohrkern, Banded Iron Formation, 06.08.2002 (Siemes)
Th1, massive ore, 05.12.2001 (Rosière)

Von bis zu 7 gemessenen Hämatit-Polfiguren sind im Folgenden die jeweils 3 aussagefähigsten abgebildet; außerdem je 3 Quarzpolfiguren des Bänderzes S09 und des Hämatit/Quarzerzes Th1 aus der Grube Thabazimbi

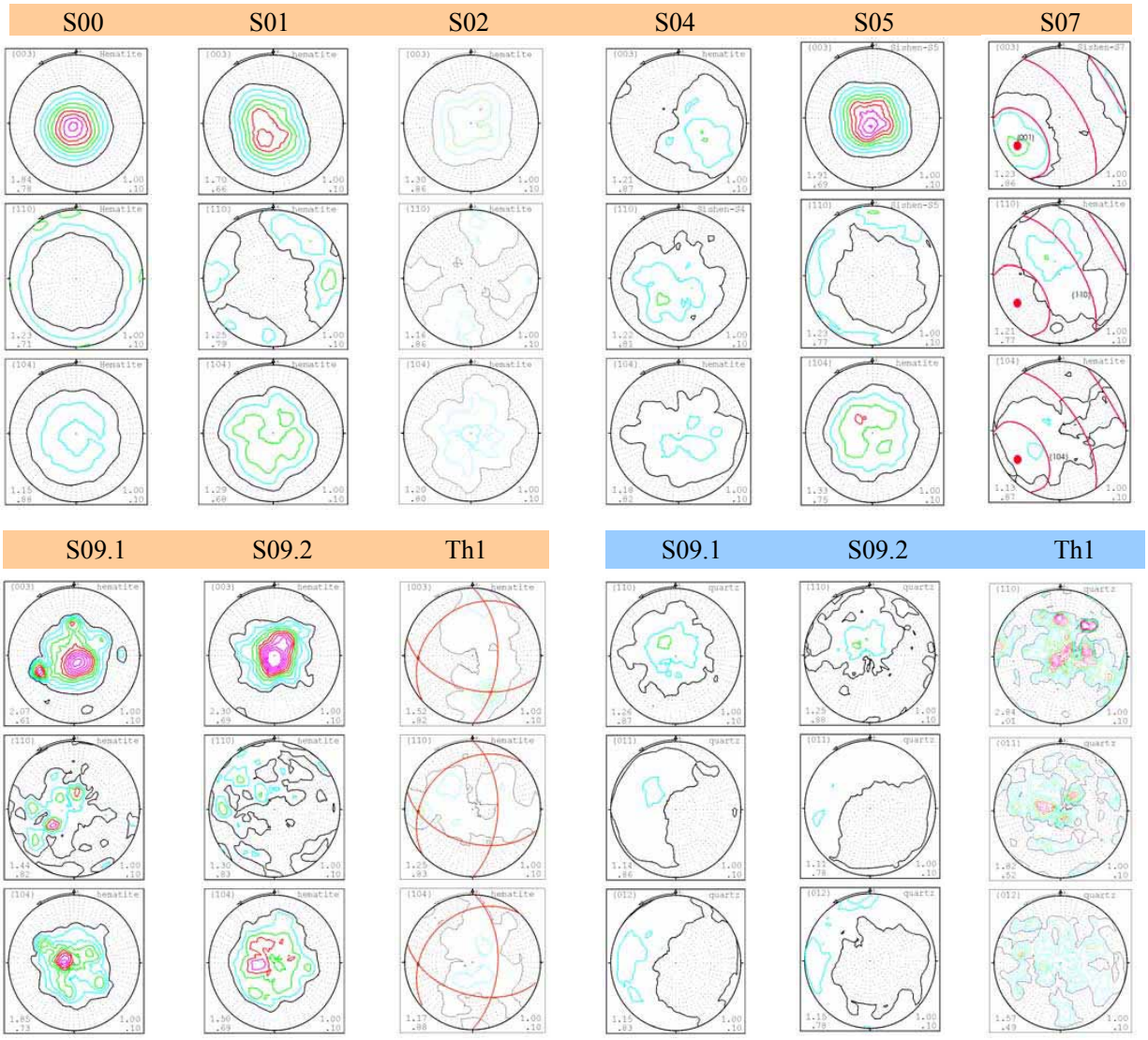

Die Sishenerze sind gewissermaßen durch zwei Texturendglieder gekennzeichnet. Die laminierten Erze weisen eine axialsymmetrische Textur (vgl. Probe S05) auf. Die massiven Erze haben keine Vorzugsorientierung. Alle anderen bisher gemessenen Texturen sind Abwandlungen dieser beiden Typen. Die vergleichenden Textur- und Mikrostrukturuntersuchen an den Proben aus Sishen bestätigten die Herkunft des Erzes der Probe S00 (1971), wenn auch die Korngrößen des S00-Erzes größer als die der neueren Proben sind.

Ref. [1] Quade, Rosière, Siemes, Brokmeier, Zeitschr. f. angewandte Geowissenschaftem, SH1 (2000) 155-162.
[2] Rosière, Siemes, Quade, Brokmeier, Jansen, J. Struct. Geol. 23 (2001) 1429-1440.
[3] Siemes, Kligenberg, Rybacki, Naumann, Schäfer, Jansen, J. Struct. Geol. (2003) in print.

Institut für Festkörperforschung
Forschungszentrum Jülich GmbH
D-52425 Jülich

Experimental Report
of Neutron Scattering Experiments
at the FRJ-2 Reactor

Proposal number:	SV7-02-008.a		
Experiment title:	**Structure and magnetic order of rare earth – magnesium intermetallics (Part I: Tm_5Mg_{24} and Er_5Mg_{24})**		
Dates of experiment:	18-27 Feb 2002	Date of report:	17-02-2003
Experimental team: Names	Addresses		
W. Schäfer	Mineralogisches Institut University of Bonn 53115 Bonn, Germany		
K.H.J. Buschow	Van der Waals-Zeeman Institute University of Amsterdam NL-1018 XE Amsterdam, The Netherlands		
R. Skowronek	MIN/ZFR (Univ. of Bonn)		
Local Contact:	W. Schäfer		

Experimental report text body

Introduction

Rare earth – magnesium compounds are of interest in view of their high-temperature technological properties, e.g. their ability to improve casting characteristics, and in view of their magnetic behaviour. Investigations on the magnetic properties including both light and heavy rare earths have been reported on RMg, RMg_2 and RMg_3. The series of R-Mg compounds is accomplished by several intermediate stoichiometries, such as R_5Mg_{24} corresponding to 82.8 atomic % of Mg, i.e. slightly below that of RMg_3. The stability range of R_5Mg_{24} is restricted to the heavy rare earths only; for details of the Er-Mg and Tm-Mg phase diagrams see.

For the RMg series a sign change of the asymptotic Curie temperature has been observed between the light and heavy rare earth compounds, thus pointing to antiferromagnetism for the former and to ferromagnetic for the latter compounds. While most of the RMg_2 compounds order ferromagnetically at temperatures well below 100 K, RMg_3 compounds exhibit antiferromagnetic behaviour for the light rare earth elements and both ferro- and antiferromagnetic interactions for the heavy rare earths.

Neutron diffraction on Er_5Mg_{24} and Tm_5Mg_{24} is aimed at both crystal structure refinements and magnetic structure determinations.

Experimental

Specimens: Sample preparation by sealing high purity R and Mg into Mo-containers, heating to 1000 - 1100°C for several hours and then quenching in water.

Neutron diffraction: Powder diffractometer SV7-a at the FRJ-2 reactor in Jülich; λ = 1.095 Å; V-container; diffraction at room and low temperatures; orange cryostat

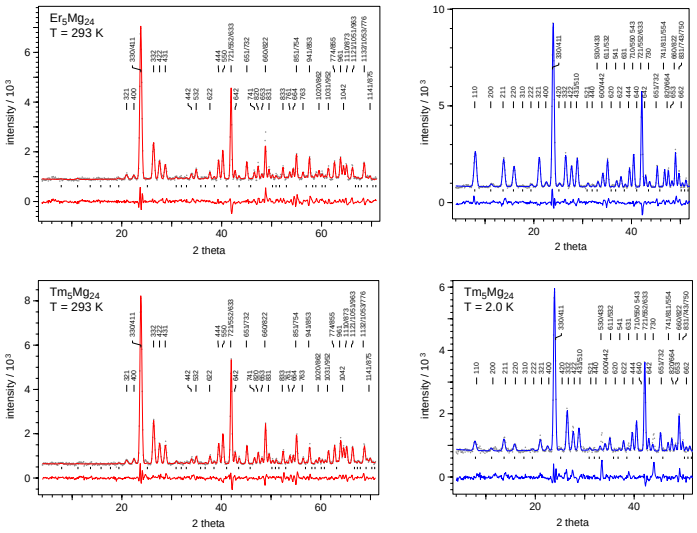

Fig. 1: Rietveld analysed room and low-temperature diffraction patterns of Er_5Mg_{24} (top) and Tm_5Mg_{24} (bottom)

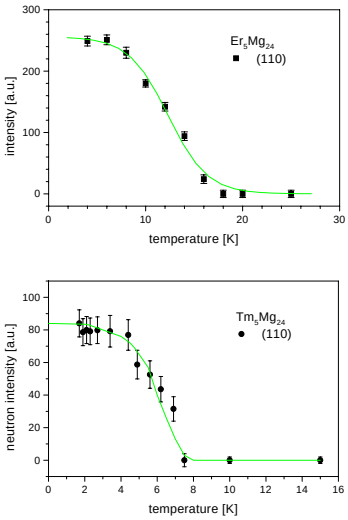

Fig. 2: Temperature dependences of the magnetic (110) peak intensities

Crystal structure

Ti_5Re_{24}-type [7]
space group I $\bar{4}$3m
R1 in 2a (0,0,0)
R2 in 8c (x,x,x)
Mg1 in 24g (x,x,z)
Mg2 in 24g (x,x,z)

a(Er) = 11.263(2) Å
a(Tm) = 11.215(1) Å

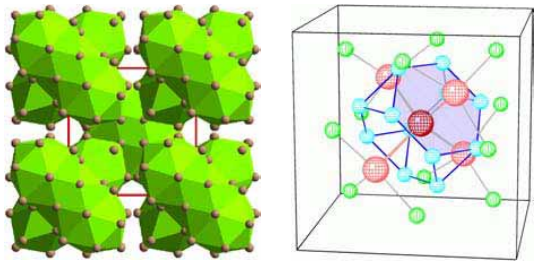

Fig. 3: Tetragonal unit cell, left: CRYSTMET representation; right: central R1-surrounding

Table: Atomic position parameters (top) and interatomic distances (bottom)

	Er_5Mg_{24}	Tm_5Mg_{24}
x(R)	0.3126(6)	0.3152(5)
x(Mg1)	0.3557(9)	0.3568(4)
z(Mg1)	0.0324(16)	0.0342(7)
x(Mg2)	0.0927(10)	0.0915(4)
z(Mg2)	0.2791(12)	0.2778(4)

	Er_5Mg_{24}	Tm_5Mg_{24}
R1-Mg1 12x	3.47(1)	3.44(1)
R2-Mg1 3x	3.23(1)	3.22(1)
3x	3.65(1)	3.67(1)
R2-Mg2 6x	3.49(1)	3.43(1)
3x	3.52(1)	3.57(1)

Ferromagnetic Order

Magnetic Bragg intensities on nuclear reflection positions

⇒ ferromagnetic order

Er_5Mg_{24}
T_C = 17.5(5) K
Tm_5Mg_{24}
T_C = 7.5(5) K

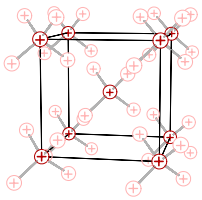

Magnetic moment refinements

Er_5Mg_{24} at T = 4.2 K
$\mu(Er1) = 7.5(2)\ \mu_B$
$\mu(Er2) = 4.4(2)\ \mu_B$
Tm_5Mg_{24} at T = 2.0 K
$\mu(Tm1) = 3.0(3)\ \mu_B$
$\mu(Tm2) = 2.8(2)\ \mu_B$

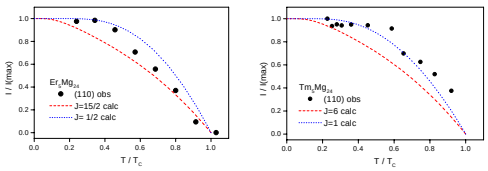

Fig. 5: Deviations of spontaneous magnetization from Brillouin curves J=15/2 (Er) and J=6 (Tm)

Conclusions

- The ferromagnetic structures of Er_5Mg_{24} and Tm_5Mg_{24} confirm the reported preference for ferromagnetic exchange in heavy rare earth – magnesium compounds.
- The rare earth moments which are considerably reduced from the free ion values and the observed temperature dependences of the spontaneous magnetization are indications of substancial influences of the crystalline electric fields or may point to a more complex ordering behaviour.
- This corroborates earlier findings of complex magnetic ordering processes in other intermetallic rare earth - magnesium compounds.

Full paper: W. Schäfer, K.H.J. Buschow, Mater. Sc. Forum (EPDIC-8) in press

Institut für Festkörperforschung
Forschungszentrum Jülich GmbH
D-52425 Jülich

Experimental Report
of Neutron Scattering Experiments
at the FRJ-2 Reactor

Proposal number:	SV7-02-008.b		
Experiment title:	**Structure and magnetic order of rare earth – magnesium intermetallics (Part II: RMg_3 R = La, Ce, Pr, Nd)**		
Dates of experiment:	3-7 Mar 2002	Date of report:	14-02-2003
Experimental team: Names	Addresses		
W. Schäfer	Mineralogisches Institut University of Bonn 53115 Bonn, Germany		
K.H.J. Buschow	Van der Waals-Zeeman Institute University of Amsterdam NL-1018 XE Amsterdam, The Netherlands		
R. Skowronek	MIN/ZFR (Univ. of Bonn)		
Local Contact:	W. Schäfer		

Experimental report text body

On RMg_3 intermetallics

RMg_3 intermetallics (R = La, Ce, Pr, Nd, Sm, Gd, Tb, Dy) crystallize in the BiF_3-type structure. According to magnetization measurements [2] the asymptotic Curie temperature was found to be negative for $CeMg_3$, $PrMg_3$ and $NdMg_3$, but positive for $GdMg_3$ and $TbMg_3$.

According to a study of magnetization, electric resistivity, and crystal field excitations based on inelastic neutron scattering [3] $CeMg_3$ and $NdMg_3$ should antiferromagnetically order at 3.5 K and 6.5 K, resp., whereas no magnetic order should occur in $PrMg_3$.

According to neutron diffraction [4, 5] $TbMg_3$ undergoes ferromagnetic or antiferromagnetic ordering below 26 K depending on sample preparation. Molecular field calculations show that in both $GdMg_3$ and $TbMg_3$ ferro- and antiferromagnetic interactions are in the same order of magnitude. Slight changes in the composition or in the Tb-Mg order-disorder parameter will therefore shift this ratio of interactions significantly and can therefore effect the type of magnetic ordering and the transition temperature.

The present neutron diffraction study is about the binary and pseudobinary light rare earth compounds $LaMg_3$, $CeMg_3$, and $PrMg_3$ as well as $La_{0.9}Pr_{0.1}Mg_3$, $La_{0.9}Nd_{0.1}Mg_3$.

Experimental

Specimens: Sample preparation by sealing high purity R and Mg into Mo-containers, heating to 1000 - 1100°C for several hours and then quenching in water.

Neutron diffraction: Powder diffractometer SV7-a at the FRJ-2 reactor in Jülich; λ = 1.095 Å; V-container; measuring temperatures 293 K and 1.8(2) K; orange cryostat

Diffraction patterns

T=293 K | T = 1.8 K | T-difference

$LaMg_3$

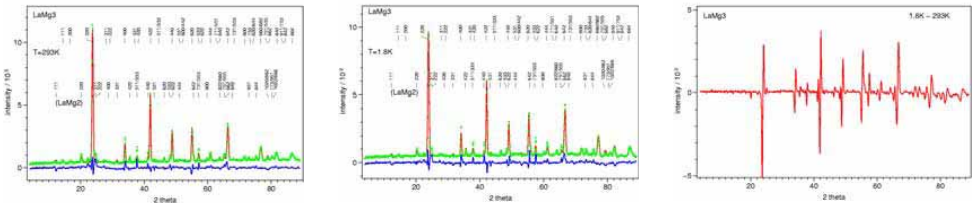

$CeMg_3$

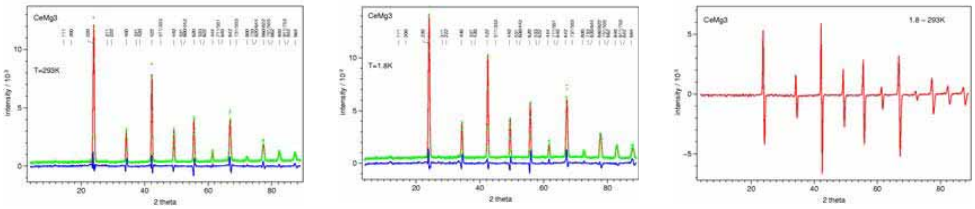

$PrMg_3$

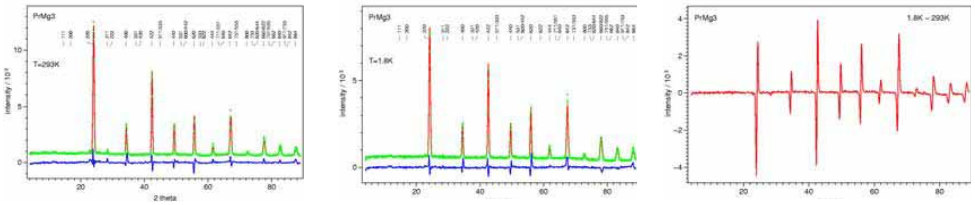

No magnetic Bragg intensities visible in the difference patterns

Exclusion of any kind of long-range magnetic order in these compounds

Structure Results

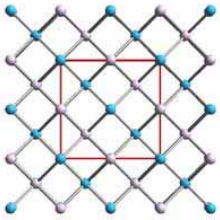

Space group Fm3m
(Z = 4)
R: 4a (0,0,0)
Mg_1: 8c (¼,¼,¼)
Mg_2: 4b (½,½,½)

Table: Lattice constants and isotropic atomic thermal displacements in RMg_3 from Fullprof refinements of the 293 K (1. line) and 1.8 K data (2. line)

R	**La**	**$La_{0.9}Pr_{0.1}$**	**$La_{0.9}Nd_{0.13}$**	**Ce**	**Pr**
a [Å]	7.4776(1)	7.4813(3)	7.4765(3)	7.4242(3)	7.4037(3)
	7.4473(4)	7.4498(3)	7.4443(3)	7.3923(3)	7.3704(3)
B_R	1.40(1)	1.29(14)	1.31(13)	0.67(36)	0.47(45)
	0.66(16)	0.44(11)	0.61(13)	0.09(34)	0.15(41)
B_{Mg1}	1.46(12)	1.37(12)	1.53(11)	1.66(36)	1.76(52)
	0.74(16)	0.62(9)	0.77(10)	0.89(35)	0.99(27)
B_{Mg2}	1.30(23)	1.04(20)	1.00(18)	1.72(60)	1.65(80)
	0.59(27)	0.32(16)	0.21(19)	0.98(58)	0.55(64)

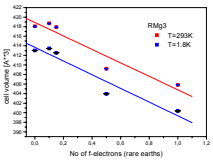

Volume changes

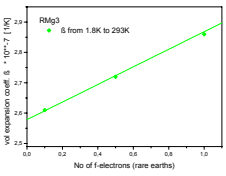

The results are presented on the 11. Jahrestagung der Deutschen Gesellschaft für Kristallographie, 10-13 march 2003 in Berlin: *W. Schäfer and K.H.J. Buschow, Neutron diffraction on binary and pseudobinary RMg_3 intermetallics (R = La, Ce, Pr, Nd)*

References

[1] A. Iandelli, A. Palenzona, in Handbook on the Physics and Chemistry of the Rare Earths, North-Holland Publ. Comp. 1979.
[2] K.H.J. Buschow, J. Less-Common Metals 44 (1976) 301.
[3] R.M. Galera, A.P. Murani, J. Pierre, J. Magn. Magn. Mater. 23 (1981) 317.
[4] G. Will, M.O. Bargouth, K.H.J. Buschow, J. Magn. Magn. Mater. 6 (1977) 131 and Inst. Phys. Conf. Series 37 (1978) 273.

Institut für Festkörperforschung
Forschungszentrum Jülich GmbH
D-52425 Jülich

Experimental Report
of Neutron Scattering Experiments
at the FRJ-2 Reactor

Proposal number:	SV7-02-009		
Experiment title:	**Short range order in fast ionic conductors $ATi_{0,85}Fe_{0,15}O_{2,925}$ (A=Ca, Sr)**		
Dates of experiment:	26-28 Apr, 11-12 May 02	Date of report:	17-02-2003
Experimental team: Names	Addresses		
Mashkina, Elena	Lehrstuhl für Kristallographie & Strukturphysik Universität Erlangen-Nürnberg Bismarckstr. 10 91054 Erlangen		
Magerl, Andreas	Lehrstuhl für Kristallographie & Strukturphysik Universität Erlangen-Nürnberg Bismarckstr. 10 91054 Erlangen		
Local Contact:	W. Schäfer, Univ. of Bonn		

Experimental report text body

Perovskites belonging to the system $CaFe_xTi_{1-x}O_{3-x/2}$ ($0<x<1$) shows a continuous variation of oxygen defect concentrations, from zero in $CaTiO_3$ to 0.5 per formula unit in $CaFeO_{2.5}$. The $CaFeO_{2.5}$ end-member exhibits a structure with alternating layers of octahedral and tetrahedral coordinated Fe, the latter due to the clustering of oxygen vacancies into defect chains. However, the degree of ordering depends on the annealing temperature and vacancy concentration. Several papers describe the detailed mechanism and the type of oxygen vacancy ordering in this system from short- and long-range order [1]. X-ray diffraction which has been used extensively for structural investigations and refinements may not be well suited to look for these correlations on the oxygen sublattice whereas they should be well observable with neutrons.

In this work we concentrate on low content members of the system $CaFe_xTi_{1-x}O_{3-x/2}$ (x=0.15, 0.3) annealed at temperatures such the oxygen vacancies are randomly distributed (for x=0.15, 0.3; $T=1200^0C$) and partially ordered (for x=0.3, $T=1000^0C$), according to the earlier reported phase diagram [1].

The data are shown on a fig.1. Rietveld refinement had been done for the composition of x=0.15 based on the space group Pnma and the result is summarized in Table 1. The evaluated lattice parameters are: a≈5.442(9)Å, b≈7.661(1) Å, c≈5.400(1) Å. The data are consistent with the previously published X-ray data.

The refinement of composition x=0.3 annealed at $T=1000^0C$ and $T=1200^0C$ is in a progress now. Composition annealed at $T=1200^0C$ belongs to the disordered part of the phase diagram [1]. Both high intensity peaks and most of weak reflections can be successfully fitted to an orthorhombic Pnma space group.

The composition annealed at T=1000^{0}C belongs to the partially ordered part of the phase diagram [1]. Based on a model proposed by Grenier [2] for the distribution of the oxygen vacancies, the TO sequence for the composition with x=0.3 is n=5.6, i.e. approximately six octahedral sheets per tetrahedral sheet (TO6). Starting from the TOO model proposed by Rodriguez-Carvajal [3] the space group was chosen $Pcm2_1$ with $b=na_c$, where n is the number of T and O per unit cell. A model with six octahedral sheets (i.e. TO6) fit the strong peaks, however, the match between the intensities of the experimental and theoretical peaks is still poor.

Thus, it is obvious that there is a strong influence of trivalent iron and the temperature on structural changes of $CaTiO_3$ perovskite.

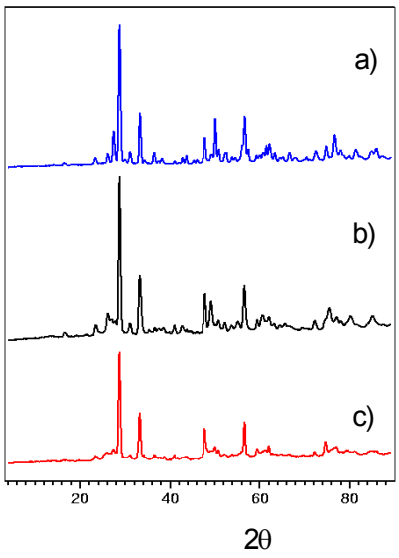

Fig.1. Diffraction patterns of $CaFe_xTi_{1-x}O_{3-x/2}$
a) x=0.15, annealed at T=1200^{0}C
b) x=0.3, annealed at T=1000^{0}C
c) x=0.3, annealed at T=1200^{0}C

Table1. Structural refinement for $CaFe_xTi_{1-x}O_{3-x/2}$ (x=0.15). R_f = 6.28%

	x	y	z	Occ	B_{iso}
Ca	-0.0308 (±0.0012)	0.25	-0.008 (±0.002)	3.92276	0.26011
Ti	0.0	0.0	0.5	3.49967	0.16545
Fe	0.0	0.0	0.5	0.50033	0.16545
O1	0.0149 (±0.001)	0.25	0.429 (±0.001)	3.96658	0.66679
O2	-0.2106(±0.0007)	-0.0357(±0.0006)	0.2113(±0.0007)	7.87484	0.58955

[1] Ana I. Becerro, F. Langenhorst, R. J. Angel, S.Marion, C. McCammon, F.Seifert, Phys. Chem. Chem. Phys. 2, 3933-3941, 2000
[2] J.C. Grenier, M.Darriet, M.Pouchard, P. Hagenmuller, Mater. Res. Bull., 1976, 11, 1219
[3] J. Rodriguez-Carvajal, M.Vallet-Regi, J.M.Gonzalez Calbet, Mater. Res. Bull., 1989, 24, 423

Institut für Festkörperforschung
Forschungszentrum Jülich GmbH
D-52425 Jülich

Experimental Report
of Neutron Scattering Experiments
at the FRJ-2 Reactor

Proposal number:	SV7-02-010		
Experiment title:	**Determination of the crystallographic orientation for a trichloromesitylene single-crystal**		
Dates of experiment:	25-28 Apr, 8-11 Dec 2002	Date of report: 28.02.03	19-02-2003
Experimental team: Names	Addresses		
J. Meinnel H. Grimm	Groupe Matière Condensée et Matériaux, UMR 6626 CNRS-Université de Rennes 1, Campus de Beaulieu, Bât. 22, F-35042 Rennes Cedex , France Institut für Festkörperforschung Forschungszentrum Jülich 52425 Jülich, Germany		
Local Contact:	E. Jansen , Univ. of Bonn		

Experimental report text body

Motivation

The crystal structure of the 1,3,5-Trichloro-2,4,6-trimethylbenzene (trichloromesitylene or TCM) has been solved at 297 and 150 K by X-ray diffraction [1]. The symmetry is triclinic, space group *P*-1, with two molecules within the unit cell, related by a symmetry center. TCM is an orientationally disordered crystal insofar as molecules are jumping in their plane by 120°. Quantum mechanical calculations establish that the isolated TCM molecule has a three-fold symmetry. Nevertheless, in a previous INS experiment at ILL with a polycrystalline sample, it was observed that each of the three methyl (Me) groups has its own tunnelling excitation energy [2]. An INS experiment at the FRJ-2 in Jülich on BSS – resolution about 1μeV – with a TCM single-crystal revealed that not only the energy of the tunnelling excitations is confirmed but also the original possibility to assign each excitation to a specific Me group in the crystal and also to study its Q-dependence [3]. But the first of these goals can be achieved only if the orientation of the crystallographic axes with regard to the neutron beam is known.

Experimental

The incident wavelength chosen was 2.332Å. The eulerian cradle was positioned at ω=15° together with a setting of the center of the linear detector at 2Θ=30°, thereby covering the range 5° ≤ 2Θ ≤ 55°. The single crystal (blue, see fig to the right) with dimensions of 30x4x1.5 mm^3 was wrapped into Al-foil and mounted via an Al-holder (red). The figure shows both the initial and the central final wave vectors k_i,f together with the crystal oriented at φ=0° (azimuth) and χ=0° (pole distance), thereby bisecting the two wave vectors.

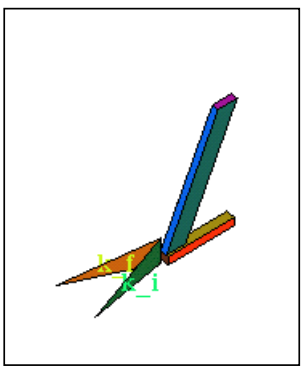

Because of the low symmetry and the similar lengths of the cell parameters, the most decisive information about the cell orientation originates from the low indexed Bragg-reflections According to the structure analysis [1] there are 4 reflections which can contribute to the scattering range $2\Theta \leq 20°$, i.e. the (010), (001), (011), and (100) at 17.68°, 18.37°,19.06°, and 19.04°, respectively. However, the latter one can be discarded because of its nearly vanishing structure factor whereas the former 3 reflections should be of similar intensity. The four obtained pole figures (χ,φ-maps) shown below correspond to the ranges $16° \leq 2\Theta \leq 18°$, $17° \leq 2\Theta \leq 19°$,$18° \leq 2\Theta \leq 20°$, and $16° \leq 2\Theta \leq 20°$ (from left to right).

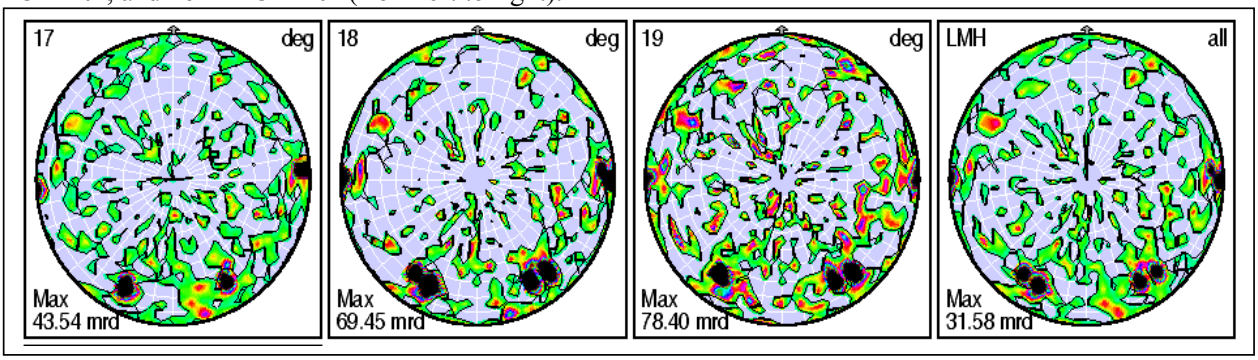

Results

The latter pole figure (LMH) exhibits 6 strong peaks (black dots), i.e. one each at the 'east' and 'west' location and pairs in 'south-west' and 'south-east'. Comparing that figure with the narrower 'slice' around $2\Theta=17°$ (left) identifies the most 'southern' peaks uniquely as (010). Similarly, one can identify 'east' and 'west' as (001) and the remaining 2 reflections as (011). In addition, it follows, (i) that the crystal is twinned with about 50:50 volume fraction, (ii) that the $\pm c^*$-axis is perpendicular to the large face and (iii) that the $\pm$a-axis is along the large edge of the crystal. The labels of the four choices follow from the representation of the long edge and the large face in the right-handed cartesian crystal-system. Its x-axis is defined as pointing from the fixation point of the xtal to the free end of the supporting bar (red), its z-axis points from the crystal along the M8 screw used for fixation. Then the a-axis is created by rotating [±a,0,0] around the y-axis by about 70°. The c*-axis is then [0,±c*,0]. Selecting either equal (fig. 'e-twins' below) or different signs (fig. 'd-twins' below) delivers the shown orientation of the six relevant lattice vectors relative to the shape of the crystal. The 'e-twins' can be discarded since the six Bragg spot would show up in the 'northern' hemisphere of the above pole figures.

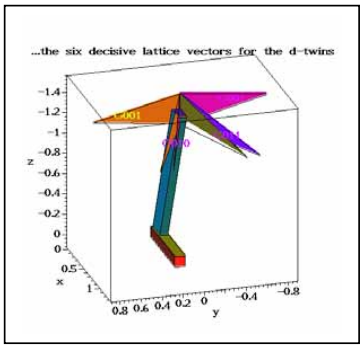

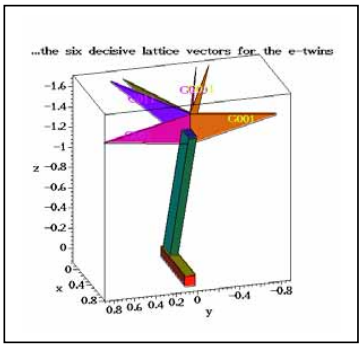

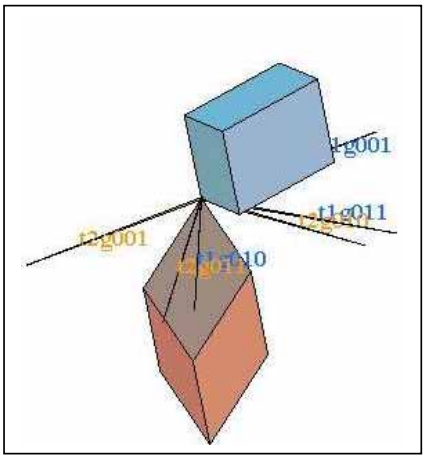

The resulting orientation of the unit cells of the 'twins' is shown in the figure to the right together with the decisive lattice vectors (001), (010, and (011).

[1] M. Tazi, J. Meinnel, M. Sanquer, M. Nusimovici, F. Tonnard, R. Carrié. *Acta Cryst. B*51, 838-847 (1995).

[2] J. Meinnel, W. Häusler, M. Mani, M. Tazi, M. Nusimovici, M. Sanquer, B. Wyncke, A. Heidemann, C. Carlile, J. Tomkinson and B. Hennion. *Physica B,* 180 & 181, 711-713 (1992).

[3] J. Meinnel, C.J. Carlile, K.S. Knight and J. Godard. *Physica B,* 226, 238-240 (1996).

Institut für Festkörperforschung
Forschungszentrum Jülich GmbH
D-52425 Jülich

Experimental Report
of Neutron Scattering Experiments
at the FRJ-2 Reactor

Proposal number:	SV7-02-011		
Experiment title:	**Powder diffraction investigation of Melilith-type compounds $La_{1+x}Sr_{1-x}Ga_3O_{7-\square}$**		
Dates of experiment:	18 days: May, Jun, Jul	Date of report:	11-02-2003
Experimental team: Names	Addresses		
M. Rozumek (P. Majewski) (F. Aldinger) R. Skowronek	MPI für Metallforschung, Heisenbergstr. 3, 70569 Stuttgart, Germany MIN/ZFR (Univ. of Bonn) FZJ 52425 Jülich		
Local Contact:	W. Schäfer, Univ. of Bonn		

Experimental report text body

Following the plan as described in our proposal, we performed powder neutron diffraction studies of two selected samples of Daltonian as well as of a La-rich composition at room and at elevated temperatures. Rietveld-analysis was subsequently carried out, in order to obtain detailed information on the structure of the two materials.

A major restriction, when performing Rietveld analysis of powder x-ray diffraction data, is that oxygen signals are much too weak to allow for the refinement of the occupation of the oxygen sub-lattice sites. The method of choice instead is powder neutron diffraction, as the scattering lengths of oxygen is much larger for neutrons than that for x-rays. For this reason, powder neutron diffraction was performed on two melilite samples (x=0.00 and 0.45). In this study, wavelengths of λ=1.0959 Å and, to increase resolution, of λ=2.332 Å were used. Data collection was performed at ambient (T=24 °C) and elevated temperatures (T=250 °, 500 °C) in a static air atmosphere. Powder diffraction data obtained were analysed with respect to structure refinemnets using the FullProf.. Sample preparation involved moderate grinding of a polycrystalline precursor material in an agate mortar, in order to yield a coarse powder with an approximate volume of two cubic centimetres.

We investigated two $La_{1+x}Sr_{1-x}Ga_3O_7$ samples (x=0.00 and x=0.45). As the results obtained with neutrons of both energies are to a large extent consistent, only results based on the smaller wave-length (λ=1.0959 Å) are reported (figure 1). Lattice parameters of $LaSrGa_3O_7$ were refined to be a=8.0656(4) Å and c=5.3411(4) Å, and the ones of $La_{1.45}Sr_{0.55}Ga_3O_7$ to be a=8.0540(4) Å and c=5.2917(5) Å (table 1). It is evident that both lattice parameters decrease with increasing La content, whereby the shrinkage in c axis is much more pronounced.

This behaviour is in good agreement with the results obtained by Rietveld analysis of XRD data. Another finding is that the relative atom positions in the structure do not significantly change with compositional variation. For the Dalton composition, these are identical with the ones reported by Steins et al. for a single crystal sample. No new reflections in the neutron diffraction pattern are observed for the La rich sample, indicating the structural stability of this compound within the homogeneity region. This is in good agreement with the conclusions drawn from electron diffraction data.

Isotropic Debye-Waller coefficients (a relative measure of the vibrational motion of atoms) do differ to a certain degree between the two compositions. However, it is difficult to assess the possible implications this may have. The quality indicator for Rietveld analysis (*i.e.*, R value) differs substantially between the two samples. For the Dalton composition it is 5.8 %, meaning a good quality refinement of the scattering data, while for the La rich composition it is much poorer being 8.6 %. This difference can be attributed to a significant appearance of diffuse scattering in the La rich sample which can hardly be taken into account in Rietveld analysis. Generally, diffuse scattering is an indicator of structural disorder on an atomic level. The nature of this disordering remains to be investigated.

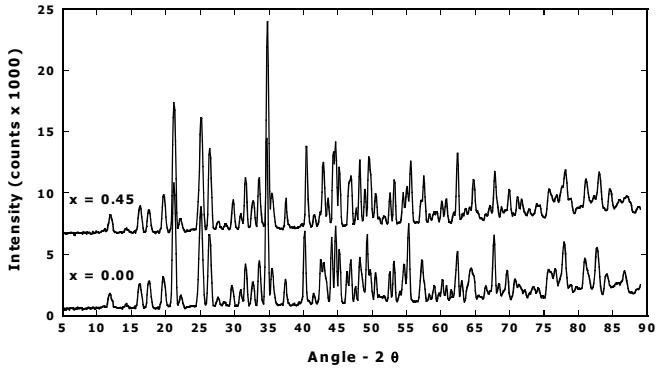

Fig. 1: *Neutron diffraction patterns of $LaSrGa_3O_7$ (x=0.00) and $La_{1.45}Sr_{0.55}Ga_3O_7$ (x=0.45) powders at 293 K in air atmosphere*

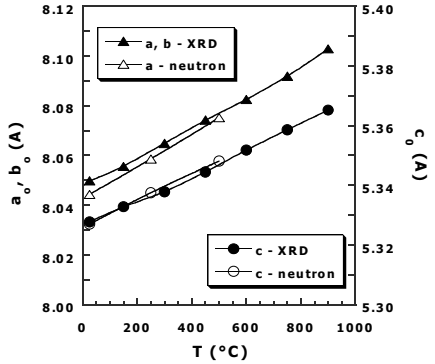

Fig. 2: Thermal expansion of lattice parameters, as determined by XRD and neutron diffraction for $LaSrGa_3O_7$ (x=0.00).

Neutron diffraction experiments of a sample of Daltonian composition at elevated temperatures revealed a thermal expansion of the lattice parameters (figure 2), quite comparable to the findings by intermediate-temperature x-ray diffraction analysis. At elevated temperatures, no new reflections are found, indicating the structural stability of the melilite compound. Relative lattice positions of the constituent elements in the unit cell remain constant for temperatures up to 500 °C. As expected, isotropic Debye-Waller factors do increase with increasing temperature.

Eventually, it may stated that the investigation performed in the present project was exceedingly helpful in obtaining a consistent structural data set of the melilite-type compound $La_{1+x}Sr_{1-x}Ga_3O_{7-\delta}$ for variable composition and temperature. The results obtained, however, were not able to explain the increase in ion conductivity when the compound is tuned for high-La contents.

Tab. 1: Structural data of $La_{1+x}Sr_{1-x}Ga_3O_{7-\delta}$ samples, as determined by Rietveld analysis of neutron diffraction data (T=293 K).

Gitterkonstante		a = 8.0656(4) [Å]		c = 5.3411(4) [Å]	
Atomlagen	***Occ***	***x***	***y***	***z***	***B(iso)***
4e(1)	Sr: 2.0 La: 2.0	0.6615(5)	0.8386(5)	0.4906(11)	0.47(8)
2a	Ga(1): 2.0	0.0	0.0	0.0	0.05(10)
4e(2)	Ga(2): 4.0	0.8570(5)	0.6430(5)	0.0355(10)	0.29(8)
2c	O(1): 2.01(7)	0.5	0.0	0.8102(17)	0.26(21)
4e(3)	O(2): 4.09(8)	0.8608(7)	0.6392(7)	0.6957(13)	1.04(17)
8f	O(3): 7.75(13)	0.9146(7)	0.8372(7)	0.2018(10)	0.83(13)

The results of this study have been submitted for publication:

M. Rozumek, P. Majewski, and F. Aldinger, **Preparation, Constitution, and Structure of Melilite-Type $La_{1+x}Sr_{1-x}Ga_3O_{7-\delta}$**, submitted to *J. Am. Ceram. Soc.* The support by the Forschungszentrum Jülich was duefully mentioned in the text.

Everything considered, the present study was extremely useful, and the collaborative work together with the project partner at the Forschungszentrum Jülich (Dr. W. Schäfer) was pleasant, cooperative and fruitful along the full duration of the project.

Institut für Festkörperforschung
Forschungszentrum Jülich GmbH
D-52425 Jülich

Experimental Report
of Neutron Scattering Experiments
at the FRJ-2 Reactor

Proposal number:	SV7-02-012		
Experiment title:	**Neutron powder diffraction on magnetic $ThMn_{12}$-type compounds $YFe_{12-x}Mo_x$ and $TbFe_{12-x}Mo_x$**		
Dates of experiment:	30.3.-4.4. u. 22.-24.4.2002	Date of report:	4.3.2003
Experimental team: Names	Addresses		
R. Hermann F. Grandjean G.J. Long	Département de Physique – Bat B5 Université de Liège B-4000 LIEGE BELGIQUE		
R. Skowronek	MIN/ZFR (Univ. of Bonn)		
Local Contact:	W. Schäfer, Univ. of Bonn		

Experimental report text body

Motivation

A large variety of binary and ternary intermetallic compounds AB_{12} and $AB_{12-x}C_x$, respectively, crystallize in the tetragonal $ThMn_{12}$ - type structure (Fig. 1). This structure is characterized by 2a sites occupied by the A atom and three non-equivalent sites 8f, 8i and 8j to accomodate the B and C atoms according to special site preferences. Members of a subgroup of this family of intermetallics with A being a rare earth (R) and B being the 3d transition element Fe are of special interest in view of their potential use as permanent magnets. R-Fe intermetallics are assumed to combine strong magnetization anisotropy and high Curie temperatures which are associated with the rare earth ions and high iron concentrations, respectively. Binary RFe_{12} compounds, however, do not exist. The $ThMn_{12}$ structure has to be stabilized by an additional element C, e.g. Mo to form $RFe_{12-x}Mo_x$ compounds.

This project represents a continuation of project SV7-02-002 (see Experimental Report belonging to it) which was restricted to a measuring time of 5 days to be spent for the series of $YFe_{12-x}Mo_x$ compounds. This report documents the neutron diffraction measurements on the series of $TbFe_{12}$-xMo_x compounds.

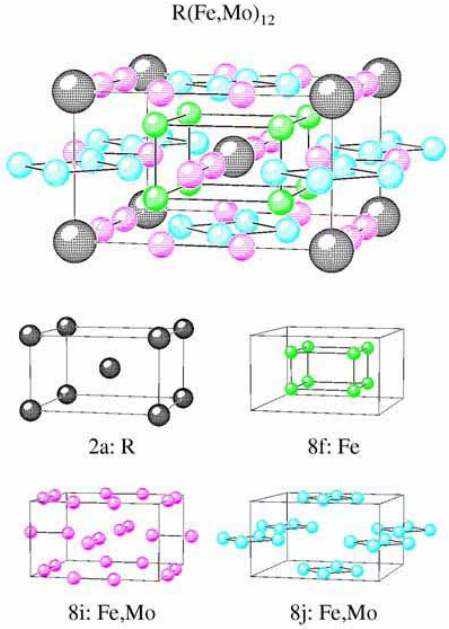

Fig. 1: $ThMn_{12}$-type structure: tetragonal unit cell and sublattices

Experimental

We have recently undertaken detailed iron-57 Mössbauer spectral studies of the RFe$_{12-x}$Mo$_x$ compounds, where R is Y, Ce, Ho, and Tb, and $0<x\leq3$. The Mössbauer spectra obtained e.g. from CeFe$_9$Mo$_3$ (Fig. 2) at 295 and 90 K are very complex because the iron atoms occupy three different crystallographic sites, the 8*f*, 8*i*, and 8*j* sites, and have a distribution of near-neighbor environments due to the partial occupation of one or more of these three crystallographic sites by molybdenum. The analysis of these spectra will be both greatly facilitated and much more meaningful if the specific Mo site occupancies and the orientation of the iron and rare-earth magnetic moments are known from powder neutron diffraction studies.

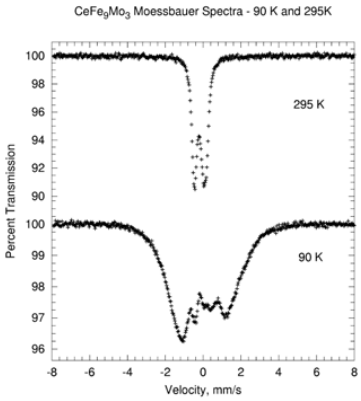

Fig. 1: Mössbauer spectra of CeFe$_9$Mo$_3$

Within this project, a series of five TbFe$_{12-x}$Mo$_x$ compounds has been investigated by room temperature neutron powder diffraction using a wavelength of 1.096 Å on SV7:

TbFe$_{10.5}$Mo$_{1.5}$ TbFe$_{10.0}$Mo$_{2.0}$ TbFe$_{9.5}$Mo$_{2.5}$ TbFe$_{9.0}$Mo$_{3.0}$ TbFe$_{8.5}$Mo$_{3.5}$

Experimental Data

Fe : Mo 10.5 : 1.5

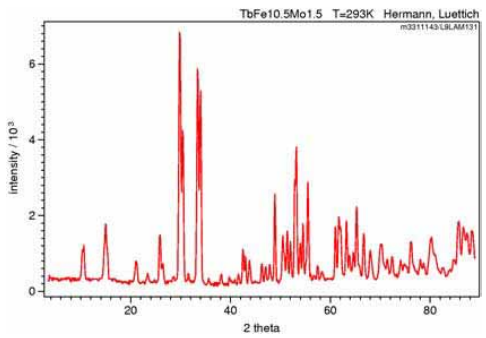

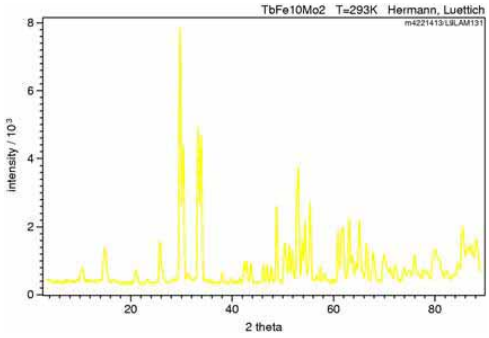

Fe : Mo 10.0 : 2.0

Fe : Mo 9.5 : 2.5

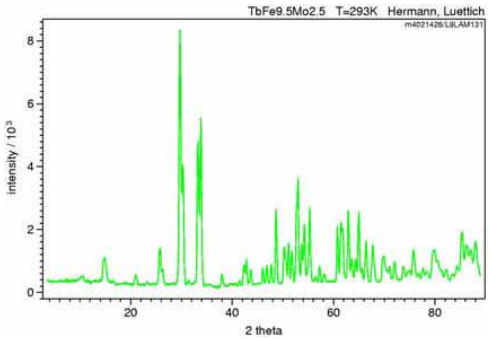

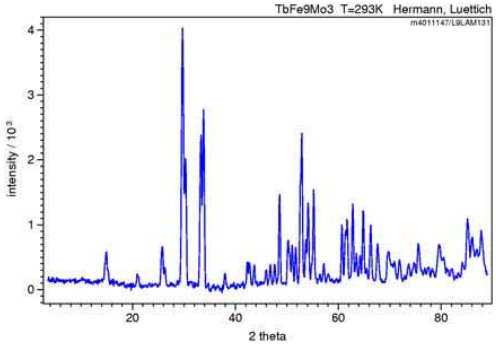

Fe : Mo 9.0 : 3.0

Fe : Mo 8.5 : 3.5

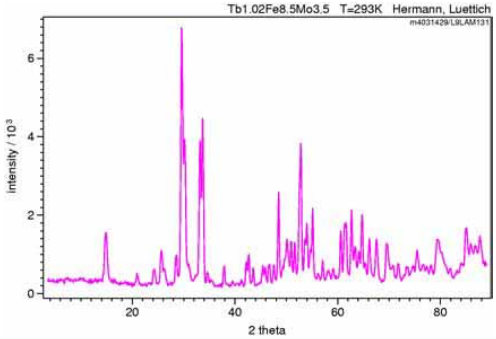

Figs. 2: Room temperature diffraction patterns of TbFe$_{12-x}$Mo$_x$ compounds;

Rietveld analyses of the diffraction patterns in view of unit cell parameters, atomic site occupancies and magnetic Tb and Fe moments as function of the Mo-concentration are in progress.

Institut für Festkörperforschung
Forschungszentrum Jülich GmbH
D-52425 Jülich

Experimental Report
of Neutron Scattering Experiments
at the FRJ-2 Reactor

Proposal number:	SV7-02-013 (including SV7-02-004)		
Experiment title:	**Magnetic structure of $NdNi_4Al$ and $TbNi_4Al$ (RNi_4B) alloys studied by neutron diffraction**		
Dates of experiment:	17 days, Jan, Oct, Nov	Date of report:	13-02-2003
Experimental team: Names	Addresses		
T. Tolinski (A. Kowalczyk) R. Skowronek	Institute of Molecular Physics Polish Academy of Sciences Smoluchowskiego 17 60-179 Poznan, Poland MIN/ZFR (Univ. of Bonn)		
Local Contact:	W. Schäfer, Univ. of Bonn		

Experimental report text body

Basic Information

The interest in the RNi_4Al compounds with R = Y or rare earth, crystallizing in the hexagonal $CaCu_5$-type structure, originates from the successful commercial use of the $LaNi_5$ alloys by reason of their large hydrogen absorption [1]. Applications in batteries and for hydrogen storage have been performed [2]. Magnetic, electronic, structural and thermodynamic properties of $TbNi_{5-x}Al_x$ and $LaNi_{5-x}Al_x$ hydrogen systems have already been carefully studied. The case of R = Gd, Dy and Er was also addressed. Our interest in the RNi_4Al series is a consequence of our previous wide research on RNi_4B compounds [3-5].

The RNi_4Al system possesses advantages compared with the B-based compounds. The substitution of B by Al opens the possibility to carry out detailed analysis using neutron scattering and the mentioned applications of these materials make them an important object for investigations. The RNi_4B compounds, like those of the RNi_4Al series, are characterized by zero or negligible magnetism of the Ni atoms, which simplifies the interpretation of the magnetic, transport or electronic properties of these materials which have been studied already by measurements of the dc magnetization, of the ac susceptibility and of the electrical resistivity.

First neutron test measurements on RNi_4B specimens, prepared by induction melting, but using natural boron, revealed the prospected too high absorption when using the standard thermal neutron wavelength of 1.096 Å on SV7. The project was therefore concentrated on the RNi_4Al system.

In 2002, powder diffraction measurements were performed on $NdNi_4Al$ at 293 K and 4.2 K using a refrigerator cryostat and in outer magnetic fields up to 5 T using a cryomagnet with the magnetic field directed perpendicular to the scattering plane of the diffractometer.

Results

Fig. 1 presents the neutron diffraction pattern of $NdNi_4Al$ recorded at 293 K. Full-pattern Rietveld refinements using Fullprof have been performed on the 293K and the 4.2K data. The refined lattice constants are a = 5.0103(13) Å, c = 4.0601(7) Å at room temperature and a = 4.9955(14) Å and c = 4.0551(7) Å at 4.2K. The structure is described in the hexagonal space group P6/mmm. Nd occupies the 1a site (0,0,0) and Ni(1) the 2c site (⅓,⅔,0). Ni(2) and Al are statistically distributed on the 3g site (½,0,½). The Al atoms are found exclusively on the 3g positions and are absent on 2c sites.

The 4.2 K diffraction pattern does not show any detectable long-range magnetic order, i.e., neither new magnetic reflections nor noticeble enhancements of intensities on nuclear reflection positions. Therefore, the neutron diffraction experiments have been extended to meaurements in outer outer magnetic fields. Fig. 2 shows the neutron diffraction patterns at 4.2 K for *H* in the range from zero to 5 T providing a strong evidence of ferromagnetic order by additional magnetic intensities.

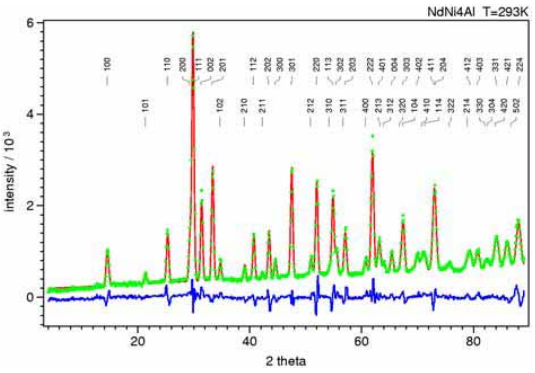

Fig. 1: Rietveld analysed room emperature diffraction pattern of $NdNi_4Al$

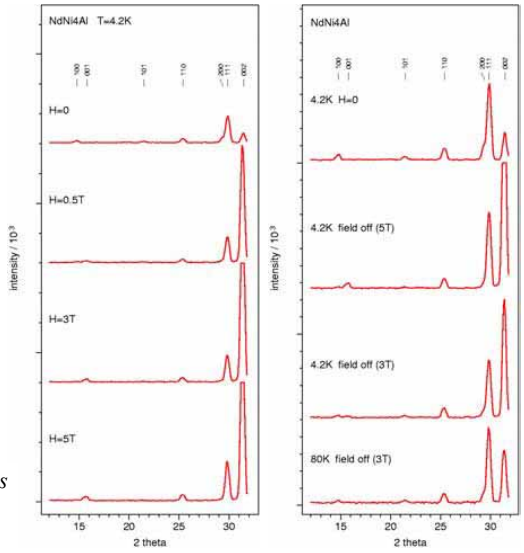

Fig. 2: Low angle part of the diffraction patterns collected at various external magnetic fields (left)and after switching off various field (right)

As becomes visible from the appearance of the (001) and the very strong increase of the (002) and the disappearance of the (100) and the (200) peaks, the ferromagnetic alignment must be perpendicular to the hexagonal axis, i.e. the moments are ordered in the hexagonal basis plane. The field dependence of the (001) and (002) reflection intensities reveals the typical magnetization curves approaching saturation with increasing field and those of (100) and (200) approaching zero (Fig. 3). This behaviour is in good agreement with the magnetization curve of $NdNi_4Al$.

The ferromagnetic order is partly maintained even after switching off the external magnetic field of (see Fig. 2). The fact that in the virgin state, i.e. before the treatment with the magnetic field, the magnetic moment is zero or negligible yields an important prove that the Ni atoms are nonmagnetic in $NdNi_4Al$.

Full Paper: "***Neutron diffraction, magnetic and transport studies of $NdNi_4Al$***" by T. Tolinski, W. Schäfer, A. Kowalczyk, A. Hoser in preparation

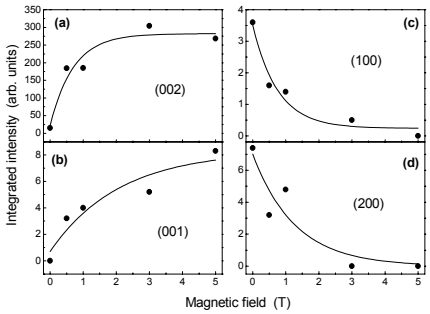

Fig. 3: Magnetic field dependences of the (001), (002), (100) and (200) peak intensities

References
[1] E.L. Houston and G.D. Sandrock, J. Less-Common Met. 74 (1980) 435.
[2] M. Wada, Sci. Technol. Japan 51 (1994) 54.
[3] T. Toliński, G. Chełkowska and A. Kowalczyk, Solid State Commun. 122 (2002) 145.
[4] T. Toliński, A. Kowalczyk, A. Szlaferek, M. Timko and J. Kováč, Solid State Commun. 122 (2002) 363.
[5] T. Toliński, A. Kowalczyk and G. Chełkowska, Physics Letters A (2003), in press.

Institut für Festkörperforschung
Forschungszentrum Jülich GmbH
D-52425 Jülich

Experimental Report
of Neutron Scattering Experiments
at the FRJ-2 Reactor

Proposal number:	SV7-02-014		
Experiment title:	**Hämatittexturen von Proben aus Eisenerzlagerstätten Indiens**		
Dates of experiment:	7.-12.5. und 27.-31.5 2002	Date of report:	26.2.2003
Experimental team: Names	Addresses		
C. Rosière	Instituto de Geosciencas Universidade Federal de Minas Gerais Av. Antonio Carlos, 6627 CEP 31270-901 Belo Horizonte, MG, Brasilia		
H. Siemes B. Klingenberg	Institut für Mineralogie und Lagerstättenlehre RWTH Aachen Bunsenstr. 8 52056 Aachen		
Local Contact:	E. Jansen, Univ. Bonn		

Experimental report text body

Motivation

Dieses Projekt ist Teil einer umfassenderen Studie, die einen systematischen Vergleich von Hämatittexturen aus Eisenerzlagerstätten verschiedener Kontinente zum Ziel hat. Dazu werden Proben aus Lagerstätten Brasiliens, Südafrikas, Australiens und Indiens am Texturdiffraktometer in Jülich untersucht. Diese vergleichenden Texturuntersuchungen an Hämatiterzen verfolgen (1) ein grundlagen- und (2) ein anwendungsorientiertes Ziel:

(1) Erkundung der natürlichen Deformationsprozesse hinsichtlich Art, Ablauf und Stärke auf den verschiedenen Kontinenten
(2) Praxisrelevante Vor- und Nachteile bei der Verhüttung der Eisenerze auf Grund unterschiedlicher Texturen.

Experimentelles

Im Jahr 2002 standen folgende 5 Proben aus Indien für Texturmessungen an SV7 zur Verfügung:

AD2	Hämatit, Magnetit
RJ01	Hämatit, Quarz, Magnetit
RJ02	Hämatit
RJ11	Hämatit, Quarz
RJ03	Hämatit

Von bis zu 7 extrahierten Hämatitpolfiguren sind im Bericht die wichtigsten und aussagekräftigsten wiedergegeben. Soweit makroskopisch eine Foliation S erkennbar war, wurden die Proben so geschnitten und gemessen, daß der Pol von S im Zentrum der Polfigur liegt. Bei erkennbarer Lineation sollte diese nahe 0° in der Polfigur liegen. Von allen Proben liegen Anschliffe und Mikrofotos vor, bearbeitet von Birgit Klingenberg (vgl. Abb. 1)

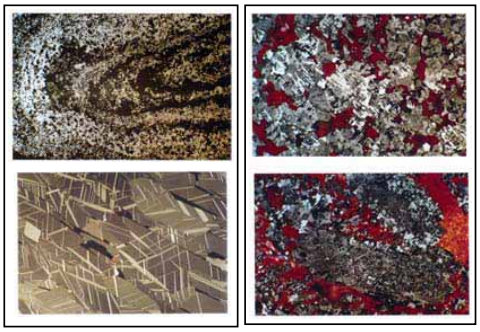

Abb. 1: Mikrofotos von RJ11(o.li), AD2(u.li) und RJ03(re) mit unterschiedlichem Korngefüge

Auswahl experimenteller Polfiguren

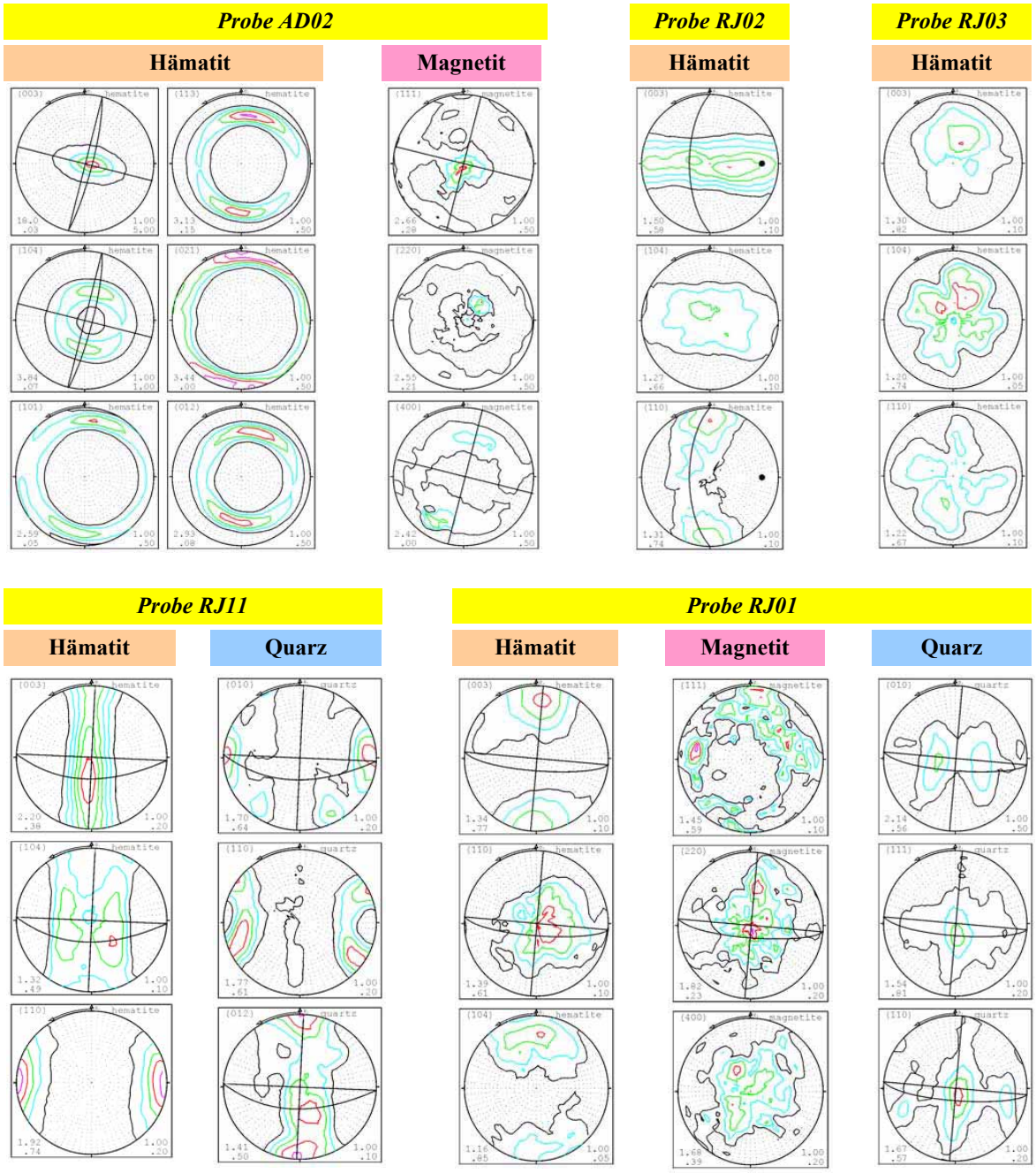

Interpretationen der Hämatit-Polfiguren

AD02: Klassische Hämatit-Textur mit starkem, elliptischen (003)-Maximum; Prismen-Maximum in Lineation.

RJ01: Nur schwache Regelung; wenig elliptisches (003)-Maximum nahe am Grundkreis; (110)-Maximum nahe dem Zentrum der Polfigur; Umkehrung der Hämatitregelung ist noch erklärungsbedürftig..

RJ02: (003) und (110) gürtelförmig; (110)-Maximum am Grundkreis bei 0°; Foliation ist gefaltet (gebogen) mit der Faltenachse = Lineation.

RJ03: praktisch ohne Vorzugsorientierung; Polfiguren spiegeln evtl. würfelförmige Probenform wider.

RJ11: Bekannter klassischer Texturtyp mit gelängtem (003)-Maximum im Pol von S auf Großkreisbesetzung; (104)-Schmetterlingsform; (110)-Prismen-Maximum in Lineation = Faltungsachse der Foliation.

Institut für Festkörperforschung
Forschungszentrum Jülich GmbH
D-52425 Jülich

Experimental Report
of Neutron Scattering Experiments
at the FRJ-2 Reactor

Proposal number:	SV7-02-015		
Experiment title:	**Textures of subduced and exhumated eclogite rocks from the Tauern window and the Koralm Complex (Eastern Alps)**		
Dates of experiment:	52days in Jan, Feb, May, Jun, Jul, Sep	Date of report:	12-02-2003
Experimental team: Names	Addresses		
W. Kurz .	Institut für Technische Geologie und Angewandte Mineralogie Technische Universität Graz Rechbauerstr. 12 A-8010 Graz, Austria		
N. Froitzheim	Geologisches Institut Universität Bonn Nussallee 8 D-53115 Bonn, Germany		
Local Contact:	E. Jansen, Univ. Bonn		

Experimental report text body

Microstructures and Crystallographic Preferred Orientations (CPOs, textures) of omphacite within eclogites from distinct (ultra-) high-pressure units of the Alps were analyzed in order to constrain the deformation conditions during and after high-pressure metamorphism.

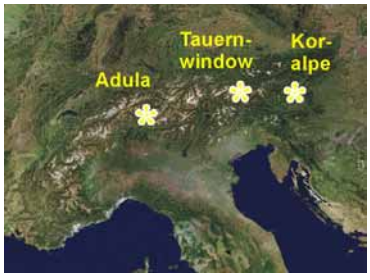

Eclogite zones in the Alps

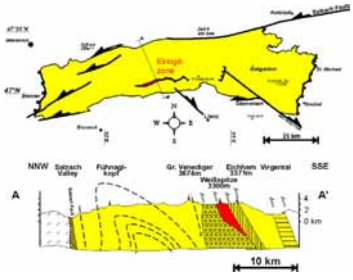

Geological map of the Tauern window

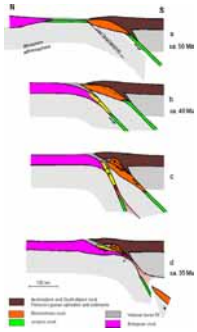

Subduction/exhumation history of eclogites

Especially the omphacite CPOs bear significant details for the reconstruction of the deformational evolution of several units. CPOs from the Austroalpine Koralm-Saualm Complex (WK20-97, WK51-97, WK17-98a, WK3-99, WK7-97, WK8-97) correspond to S- type fabrics (with a girdle distributuon of c [001] within the X-Y-plane, and b [010] clusters near Z), related to a deformation geometry within the flattening field. This geometry is documented by the shape fabrics, too.

Textures described from the Dora Maira Massif (WK70-01, WK72-01, WK73-01) show L>S- and L- type CPO fabrics, indicating a plane strain to constrictional deformation geometry. The CPOs from the Adula Nappe (WK147-01, WK151-01, WK153-01, WK154-01, R54, R56, B14, WK159-01, WK160-01, WK144-01) may all be described in terms of very well developed L- type fabrics (with c [001] clusters near Z, and a girdle distribution of b [010] axes within the Y-Z- plane) formed within the constrictional field. Constrictional strain (axial elongation) is interpreted to have started at the peak of high-pressure metamorphic conditions and was continued along the retrograde path. Omphacite CPOs from the Eclogite Zone of the Tauern Window (WKOA01-1, WK109-97, WK108-97, WK46-98, WK50-98, WK48-98, WK110-97, WK526, WK527) show a continuous transition from S- to L- type fabrics, corresponding to the transition from coarse-grained eclogites to fine-grained eclogite mylonites. This evolution is related to the final phases of the prograde evolution unit and coincides with a transition from a flattening to a constrictional deformation geometry. This is indicated by the shape fabrics, too. The constrictional geometry prevailed along the retrograde section of the PT path.

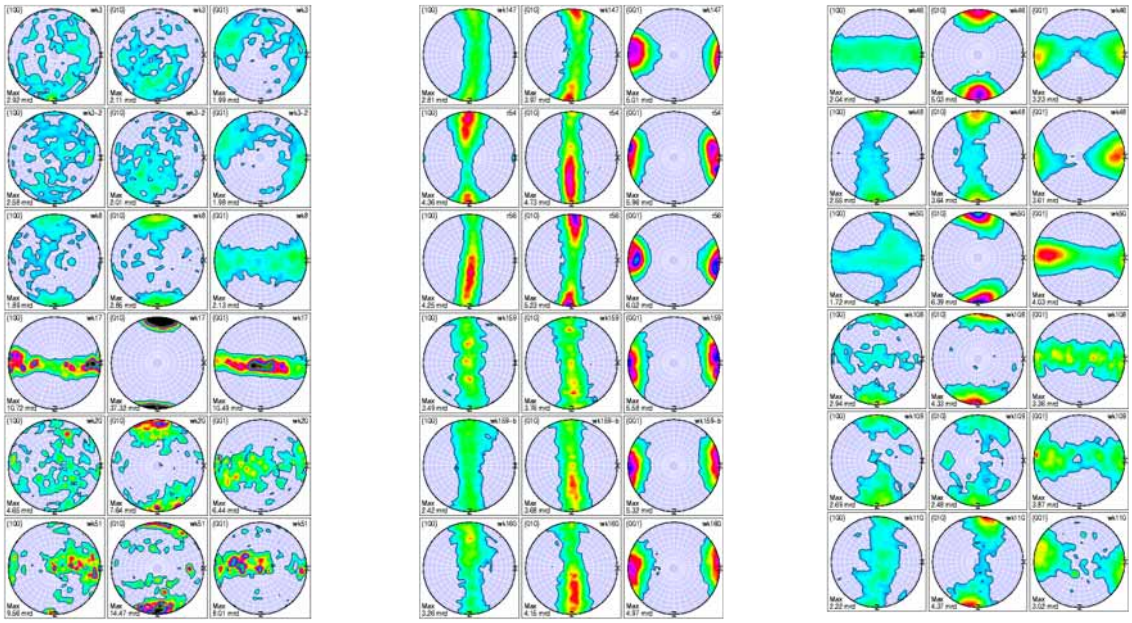

Experimental pole figures (100), (010) and (001) of the monoclinic omphacite phase of various elogite rocks from different tectonic regions in the Alpes: Koralm (left), Adula nappe (middle) and Tauern window (right). This is a selection of results obtained from a total of 28 specimens measured on SV7.

The evolution of microstructures and CPOs is assumed to correlate with the deformation geometry, which is directly linked with the mechanisms of exhumation. S- type fabrics predominantely occur within eclogites exhumed by crustal extension, in particular the Koralm-Saualm Complex. L>S- and L- type fabrics predominantely occur within eclogites exhumed by extrusion within a low-angle corner ("subduction channel"), in particular the Dora Maira Massif, the Adula nappe, and the Eclogite Zone. S- type CPOs from the Eclogite Zone were formed along the prograde path and are assumed to indicate compressional deformation related to the burial of this unit.

Institut für Festkörperforschung
Forschungszentrum Jülich GmbH
D-52425 Jülich

Experimental Report
of Neutron Scattering Experiments
at the FRJ-2 Reactor

Proposal number:	SV7-02-016		
Experiment title:	**Strukturelle Änderungen an Co- und Mn-Ferriten in Abhängigkeit von Präparationsbedingungen (Sauerstoffgehalt, Wärmebehandlung)**		
Dates of experiment:	29.6.-7.7. u. 10.12.2002	Date of report:	25.2.2003
Experimental team: Names	Addresses		
F. Sauerwald K. Wacker	Wissenschaftliches Zentrum für Materialwissenschaften (Mineralogie, Petrologie, Kristallographie) Philipps-Universität Marburg Hans-Meerwein-Str. 35032 Marburg		
R. Skowronek	MIN/ZFR (Univ. of Bonn)		
Local Contact:	W. Schäfer, Univ. of Bonn		

Experimental report text body

Problemstellung

Im Rahmen der Fortführung des DFG-Forschungsprojektes (Univ. Marburg) "Impedanzspektroskopie im System $CoFe_2O_4$ – $MnFe_2O_4$" geht es um die Untersuchung der Veränderungen von magnetischen, elektrischen und mechanischen Eigenschaften von Co- und Fe-Ferriten als Funktion der Materialsynthese. Die in Marburg erhaltenen impedanzspektroskopischen Ergebnisse sollen mit strukturellen Daten aus Neutronenbeugung korreliert werden.
Aus Neutronenbeugung sind zu bestimmen:
(a) Kationenverteilung auf Tetraeder- und Oktaederlagen, exakte Besetzungszahlen
(b) Besetzung der Sauerstofflagen (evtl. Leerstellen) und Besetzung von Zwischengitterpositionen mit Sauerstoff.
Komplementäre Untersuchungen erfolgen in Salzburg (Mössbauerspektroskopie) und in Marburg (Magnetisierung und Suszeptibilität).
Zunächst sollen zwei Co-Ferrite, später dann zwei Mn-Ferrite, untersucht werden. Das Projekt stellt eine Fortsetzung der in den Jahren 2000 und 2001 an SV7 durchgeführten Untersuchungen an Spinellmischkristallen dar (vgl. Experimental Reports SV7-01-010 und SV7-01-016). Die Messungen erfolgen im Rahmen der Doktorarbeit von F. Sauerwald.

Experimentelles

Zwei Co-Ferrit-Verbindungen wurden aus den Oxiden Fe_2O_3, Mn_2O_3 und Co_3O_4 durch Sinterreaktionen in einem Rohrofen bei 1200 °C bzw. 778 °C hergestellt. Seit 2002 besteht in Marburg die Möglichkeit, in einer Gasmischanlage mittels Masseflussreglern und Druckreglern wohl definierte Ofenatmosphären mit kleinen Sauerstoffpartialdrucken reproduzierbar einzustellen und so reproduzierbare Proben herzustellen. Je nach Sauerstoffgehalt erhält man hochohmige oder recht gut elektrisch leitende Ferrite.

Die Neutronenmessungen (λ = 1.096 Å; Vanadium-Pobenhalter) liefen - für beide Proben gleich - wie folgt ab:
(1) Messung bei Raumtemperatur (Ausgangszustand der Probe),
(2) Aufheizung auf 540 °C, d.h. oberhalb der magnetischen Ordnungstemperatur
(3) Messung bei 540 °C
(4) Abkühlung auf Raumtemperatur
(5) Messung bei Raumtemperatur zwecks Kontrolle der strukturellen Reversibilität.
Hinzu kamen Referenzmessungen mit leerem Probenhalter unter ansonsten identischen Messbedingungen und Messungen der Temperaturabhängigkeit während einer späteren Aufheizphase einer Probe.

Messdaten und erste Ergebnisse

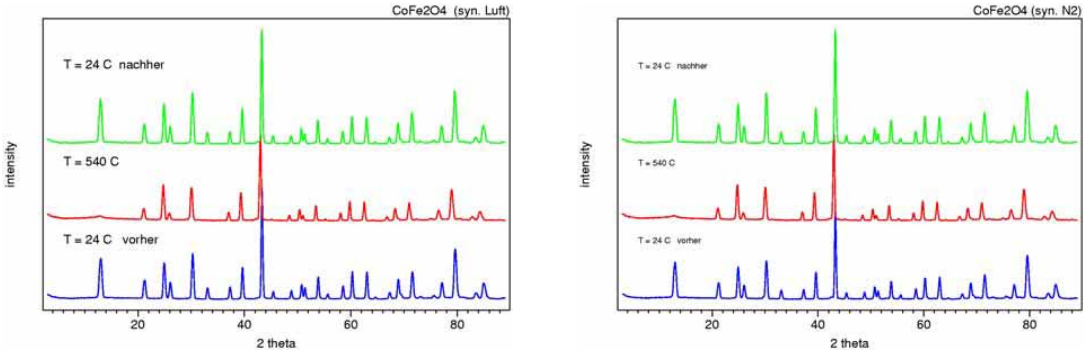

Neutronendiagramme vor, während und nach der Heizphase der unter Luft (links) und N_2 (rechts) synthetisierten Co-Ferritproben

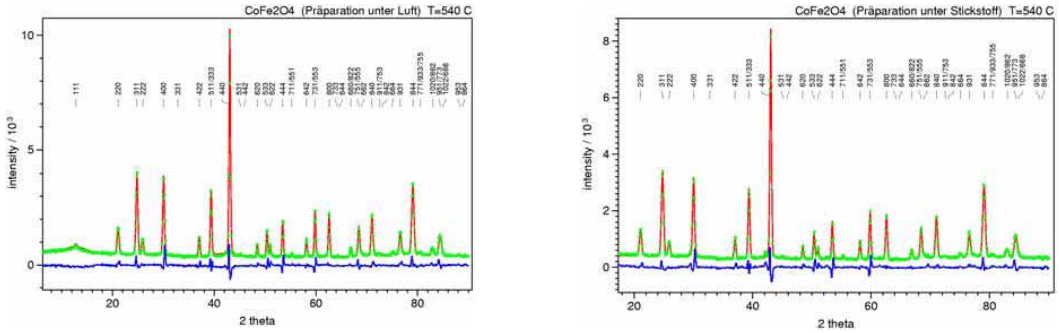

Rietveld-Verfeinerungen der Kristallstruktur aus den Beugungsdiagrammen bei 540 °C oberhalb der magnetischen Ordnung

Aus den Verfeinerungen der Hochtemperaturmessungen ergeben sich nahezu identische Besetzungsverhältnisse in der Spinellstruktur bei den beiden unterschiedlich synthetisierten Proben. Co Atome besetzen ausschließlich die Oktaederplätze, währen sich Fe Atome auf Oktaeder- und Tetraederlage finden. Dieser Befund ist erstaunlich, da sich die physikalischen Eigenschaften beider Proben stark unterscheiden, z.B. der spez. elektrische Widerstand beträgt 10^7 Ohm cm bei der unter Luft synthetisierten Probe und nur weinige Ohm cm dei der unter N_2 synthetisierten Substanz.
Die temperaurabhängige Beugungsmessungen (Abb. links) bestätigen die magnetische Ordnungstemperatur von 520 °C.

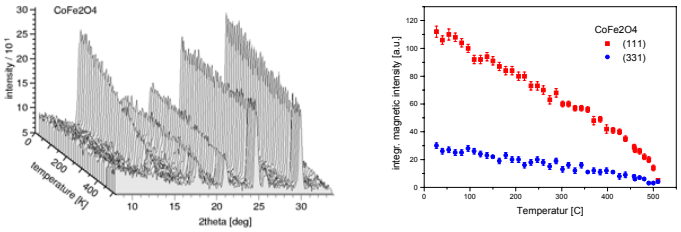

Sequenz von Beugungsdiagrammen als Funktion der Temperatur und Temperaturabhängigkeit der Magnetreflexe (111) und (331).

Referenzen

[1] Jimenez Mateos et al. : J. Solid State Chem. 93 (1991) 443, Composition and cation-vacancy distribution of cation-deficient Mn/Fe spinel oxides.

[2] F. Sauerwald, K. Wacker, P. Buck, W. Schäfer: Z. Krist, Suppl. 18 (2001) 94, Neutronenbeugungsuntersuchungen an (2,3)-(□,3)-Spinellmischkristallen $MnFe_2O_{4+\delta}$.

Institut für Festkörperforschung
Forschungszentrum Jülich GmbH
D-52425 Jülich

Experimental Report
of Neutron Scattering Experiments
at the FRJ-2 Reactor

Proposal number:	SV7-02-017		
Experiment title:	**Texture reference measurements on rolled and rolled+pressed copper and silver specimens**		
Dates of experiment:	14 d: jan mar, jun jul 2002	Date of report:	24-02-2003
Experimental team: Names	Addresses		
E. Jansen W. Kockelmann* A. Kirfel	Mineralogisch-Petrologisches Institut Universität Bonn Poppelsdorfer Schloss 53115 Bonn	* at ISIS Facility (ROTAX) Rutherford Appleton Laboratory Chilton, U.K.	
Local Contact:	E. Jansen		

Experimental report text body

Motivation

Neutron phase analysis and texture measurements are being performed on the ROTAX instrument at ISIS for the characterisation of ancient and medieval coins. These activities are performed in continuation and extension of the non-destructive neutron diffraction investigations on archaeological objects on ROTAX (for references see Experimental Report SV7-01-019). Texture reference measurements in conventional monochromatic diffraction technique are considered crucial in order to control, detect and avoid systematic errors which may arise from different and newly developed scan techniques and pole figure constructions using time-of-flight neutron data. Aims of the present study on SV7 are:

(i) to evaluate reliable correction factors of experimental pole figures in view of the plate-like form of the coins by using ball- and coin-shaped specimens (compare SV7-01-019),

(ii) to analyse both copper and silver specimens with regard to the two metal composition of the coins investigated, and

(iii) to distinguish different making processes of coins by using differently treated material:
  (a) rolled material and
  (b) rolled + pressed material.

Final aim is to determine whether a coin is authentic or a fake.

Experimental

Pole figure measurements have been performed on ball- and coin-shaped specimens formed from commercial copper and silver metal sheets produced after rolling. Additionally, coin-shaped (rolled) specimens have been pressed to simulate mechanical coin treatment.

Experimetal data and pole figure construction

Copper | Silver

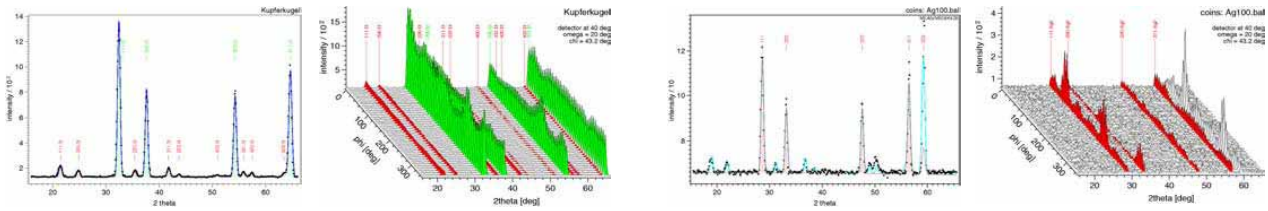

Neutron diffraction patterns (fcc indexing) and orientation dependent intensity variations of ball-shaped rolled metals (λ=2.332 Å)

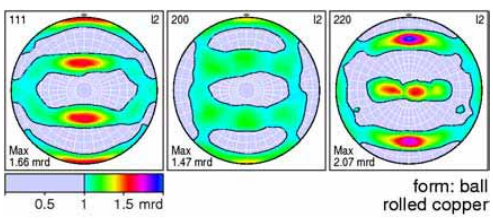

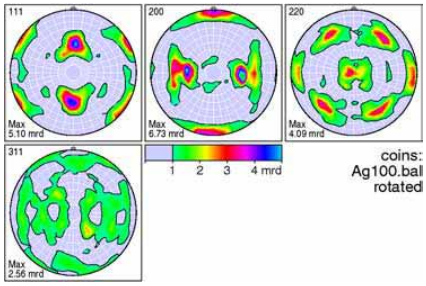

↑ *Experimental pole figures of **ball-shaped** **rolled** metal specimens* →

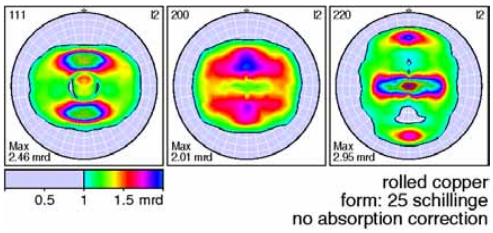

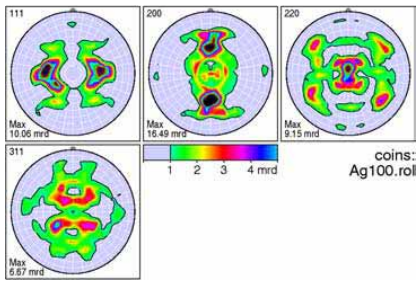

↑ *Experimental pole figures of **coin-shaped** **rolled** metal specimens* →

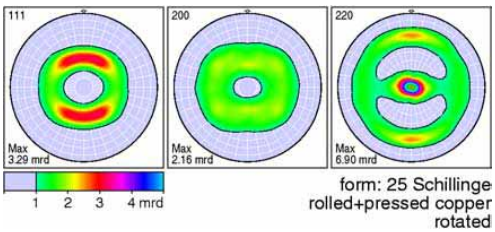

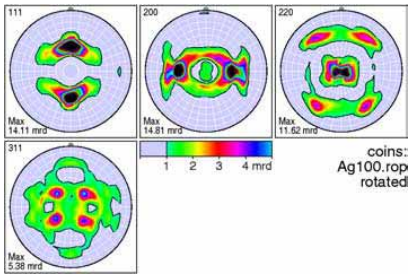

↑ *Experimental pole figures of **coin-shaped** **rolled+pressed** metal specimens* →

Results and Conclusions

The coin-shaped experimental pole figures have been corrected for absorption by calculating experimental absorption factors using the ball-shaped measurements (compare Experimental Report SV7-01-019). This absorption correction has been applied for both the rolled and the rolled+pressed specimens. The latter ones proved to be similar to those of a simulated fcc model texture produced by rolling and compression (see Fig below).

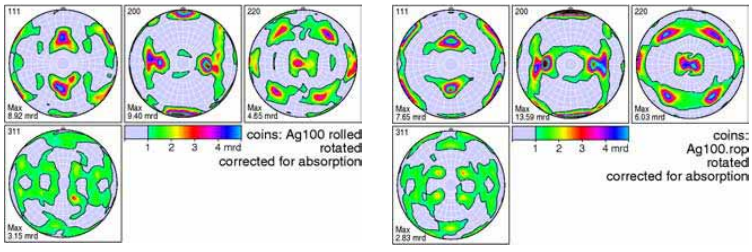

Absorption corrected rolled (left) and rolled+pressed (right) silver pole figures

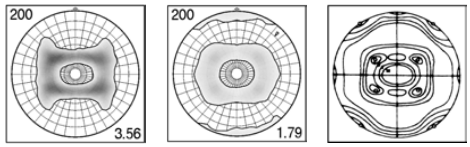

Experimental 200 pole figure of an Austrian 25 Shilling coin (left) compared to that from the rolled+ pressed Cu material (center) and to that of a fcc model texture (right) developed by rolling and compression

Institut für Festkörperforschung
Forschungszentrum Jülich GmbH
D-52425 Jülich

Experimental Report
of Neutron Scattering Experiments
at the FRJ-2 Reactor

Proposal number:	SV7-02-018		
Experiment title:	**Coexistence of one- and three-dimensional magnetic order in Ca_3CoRhO_6**		
Dates of experiment:	14 days, may, june	Date of report:	12-02-2003
Experimental team: Names	Addresses		
M. Loewenhaupt	Institut für Angewandte Physik (IAPD) Technische Universität Dresden 01062 Dresden, Germany		
E.V. Sampathkumaran	Tata Institute of Fundamental Research Homi Bhabha Road Mumbai-400 005, India		
R. Skowronek	MIN/ZFR (Univ. of Bonn)		
Local Contact:	W. Schäfer, Univ. of Bonn		

Experimental report text body

Motivation for new diffraction measurements

The pseudo low dimensional insulators have been of constant interest among physicists and chemists for the past few decades as the interplay between intrachain and interchain interactions has been found to result in novel magnetic anomalies. Till todate, in all such compounds, the presence of weak interchain magnetic coupling results in eventual loss of the identity of the chains, thereby paving the way for three dimensional magnetic ordering at low temperatures. Ca_3CoRhO_6 apparently has the signatures of the correlations within a chain coexisting with long range magnetic order, thereby providing a novel situation in this direction of research.

Ca_3CoRhO_6 crystallizes in the K_4CdCl_6-type rhombohedral structure (space group $R\bar{3}c$) belonging to the class of compounds, $(Sr,Ca)_3MXO_6$ (M, X = a metallic ion, magnetic or non-magnetic) having spin-chains (M-X) separated by Sr/Ca and the magnetic chains form a triangular lattice. In this structure, there is face-sharing of octa trigonal prisms of M ions (Fig. 1). On the basis of previous neutron diffraction data on Ca_3CoRhO_6 [1] it was inferred that this compound can be classified a "Partially Disordered Antiferromagnet (PDA)"- a novel magnetic structure. In the temperature range below the paramagnetic state the chains at the apices of the hexagon are anti-ferromagnetically coupled to each other, whereas the one at the centre of the hexagon is left incoherent; as the temperature is lowered further, the incoherent chains can undergo spin-glass freezing or couple ferrimagnetically with other chains.

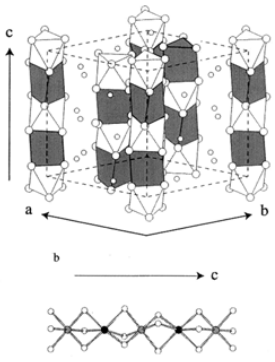

Fig. 1: Chain structure of Ca_3CoRhO_6 [1]

Dc magnetic susceptibililty (χ) reflects these different temperature regions by: (1) by a broad maximum of χ versus T around 100 to150 K, (2) a highly non-linear magnetization between 40 and 90K, but (3) tending to a constant χ at still lower temperatures. However, ac

susceptibililty exhibits a broad feature in the range 40-70 K with an unusually strong frequency dependence, implying more exotic magnetic behavior of this compound [2]. Motivated by this situation, we have subjected this compound to more careful neutron diffraction investigations on SV7 by more precise investigations of the temperature regime between 4 K and 150 K (Fig. 2).

Results

A careful look at Fig. 2 indicated that there is a broad weak peak superimposed ("magnetic short-range-order-like") over the magnetic peak present at all investigated temperatures, both above and below long-range magnetic ordering temperature. The strongest magnetic reflection (100) is superimposed by a broad diffuse share as obtained by peak profile fits using two Gaussian-type curves shown in Fig. 3 in expanded scale.

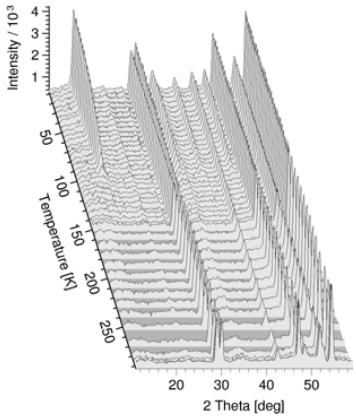

Fig. 2: Temperature dependent patterns showing (100) at 16.5 deg (λ = 2.332 Å)

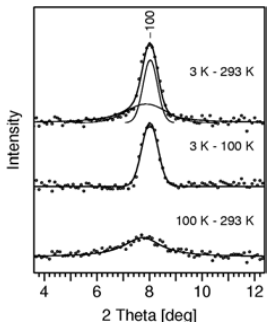

Fig. 3: Gaussian profile fits of the (100) peak at 3K (here at 8 deg, λ=1.096 Å) show the composition of the Bragg peak with a diffuse share which also exists at 100 K.

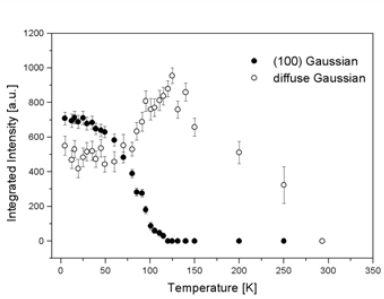

Fig. 4: Temperature dependence of the integrated (100) magnetic Bragg intensity and of the diffuse intensity of Ca_3CoRhO_6 after subtraction of a constant background assuming Gaussian line shapes for both lines.

In order to highlight the features due to the diffuse part, we have fitted the (100) peak region by a superimposition of two Gaussians with different widths. In Fig. 4, we present the temperature dependence of the relevant intensity of the diffuse peak, apart from showing the temperature dependence of the intensity related to the long-range magnetic order. The most remarkable feature is that the diffuse peak intensity persists in the entire temperature range of investigation, as though the magnetic ions responsible for this peak are essentially decoupled from those undergoing long range magnetic ordering.

The diffuse peak intensity increases as the temperature is lowered below 300 K, interestingly attaining a maximum around 100 to 150 K, followed by a decrease at lower temperatures. This qualitatively mimics the behaviour of χ expected for antiferromagnetic correlations in one-dimensional chains and observed in the mentioned χ data. The reader may see in Ref. 2 the tendency for the flattening of χ in the range 100 – 150 K as though there is a Bonner-Fischer-type peak and the fall of χ below 100 K is presumably intercepted by the enhancement of χ due to the onset of long range magnetic order. Thus, the present neutron data is able to distinctly delineate the features due to long range magnetic ordering and the intrachain effects. We therefore believe that the "so-called" incoherent chains described above retain their individuality ("isolated intrachain interactions") down to low temperatures.

The width of the broad diffuse peak has been used for an estimation of the correlation length at 4 K. The estimation is based on the reciprocal relation between cluster size and peak half width broadening. The calculation results in a characteristic value of 23 Å for the linear extension of the antiferromagnetic chain segments. In the region without long-range order, i.e. above 100 K, the diffuse peak is somewhat broader, hence the characteristic length for the one-dimensional cluster size is correspondingly smaller (16 Å).

Full paper: M. Loewenhaupt, W. Schäfer, A. Niazi, E.V. Sampathkumaran, Europhysics Letters (submitted)

References

[1] S. Nitaka et al. J. Phys. Soc. Jpn, 70 (2001) 1222 and Phys. Rev. Lett. 87 (2001) 177202
[2] E.V. Sampathkumaran, A. Niazi, Phys. Rev. B 65 (2002) 1800401

Institut für Festkörperforschung
Forschungszentrum Jülich GmbH
D-52425 Jülich

Experimental Report
of Neutron Scattering Experiments
at the FRJ-2 Reactor

Proposal number:	SV7-02-019		
Experiment title:	**Metastable Ferromagnetic fcc Fe-Cu Alloys: A New Invar System?**		
Dates of experiment:	16-20 December 2002, 13-18 January 2003	Date of report:	4 March 2003
Experimental team: Names	Addresses		
A. Orecchini	Istituto Nazionale per la Fisica della Materia – Group OGG-Grenoble at Institut Laue-Langevin 6, rue Jules Horowitz B.P. 156 F-38042 Grenoble Cedex 9 – FRANCE		
D. Finarelli (C. Petrillo)	Politecnico di Milano – Dipartimento di Fisica Piazza Leonardo da Vinci, 32 I-20133 Milano – ITALY		
R. Skowronek	MIN/ZFR (Univ. of Bonn)		
Local Contact:	W. Schäfer, Univ. of Bonn		

Experimental report text body

For more than a century, the Invar effect, namely the anomalously low thermal expansion of magnetic alloys like $Fe_{65}Ni_{35}$, attracted considerable scientific and technological interest. Other than in $Fe_{65}Ni_{35}$, this effect was found in several fcc Fe alloys, all of them magnetic. A host of other magnetic anomalies indicated that magnetism is deeply involved in the Invar effect. Among the proposed theoretical models, the most popular ascribes the Invar behaviour to the coexistence of two electronic states of Fe, with different magnetic moments: a high moment ferromagnetic state and a low moment antiferromagnetic state [1].
Quite recently we undertook the investigation of metastable Fe-Cu alloys produced by high energy ball milling. As Cu does not contribute to the magnetic moment of the system, Fe-Cu alloys allow the study of electronic and magnetic properties of iron in the fcc phase. Indeed, pure fcc Fe is stable only at high temperature, where no spontaneous magnetic ordering is observed. Thus the magnetic properties of fcc Fe can only be studied in systems where Fe is forced into an fcc environment, like alloys, solid solutions or Fe films grown on fcc substrates. The high-energy ball milling technique is very effective in producing fcc Fe-Cu alloys in the Fe concentration range from 0 to 60 at.%. All these samples were found to be ferromagnetic and single fcc phase, as resulting from bulk magnetisation, hard X-ray diffraction and spin density distribution measurements. These experimental results allowed for a description of the magnetic state of fcc Fe which is compatible with the two-state model [2]. In addition, very recent X-ray diffraction measurements we performed on the $Fe_{50}Cu_{50}$ powder revealed an Invar-like temperature behaviour of the lattice parameter [3]. Indeed, similar to what observed in Fe-Ni alloys, the linear expansion coefficient displays an anomalous *plateau* at about 200 K, and the 0.2% observed variation of the lattice parameter over the temperature range 25 – 300 K is smaller than what an extrapolation from structural data of pure elements and parent compounds would yield, namely 0.35%.
In such scenario, we performed a neutron diffraction experiment to determine the lattice parameter thermal dependence of the whole series of Fe_xCu_{100-x} alloys, with x = 20, 40, 50, 60. Indeed, the neutron technique has the advantage of enabling the investigation of a bulk sample without suffering of the large X-ray absorption. This is particularly important in our case of nanocrystalline powder alloys with quite different grain sizes,

which would affect the X-ray measurements in different ways. The experiment was carried out at the diffractometer SV-7a in the FRJ-2 Reactor in Jülich, with an incident neutron wavelength of 1.0959 Å and within the angular range 4 – 89°. The diffraction patterns of the Fe-Cu alloys at the four iron concentrations were collected at 10 different temperatures in the range 4 – 300 K. As an example, the diffraction pattern of the $Fe_{50}Cu_{50}$ alloy at 293 K, is shown in Fig. 1. A preliminary data analysis was carried out by means of a standard Rietveld refinement and the resulting assignment of the visible reflections is indicated in Fig. 1. The most intense and defined peaks belong to an fcc crystallographic phase, with a lattice parameter of 3.6336 Å at 293 K. The further, weaker, visible peaks arise from a small bcc phase contamination, with a 2.874 Å lattice parameter. The presence of such bcc phase depends on the Fe concentration: the bcc peaks are indeed well visible in the $Fe_{60}Cu_{40}$ spectra too, whereas their intensity is weakened in $Fe_{40}Cu_{60}$ and disappears completely in $Fe_{20}Cu_{80}$. Therefore, with increasing Fe concentration, the alloy tends to partly recover the bcc configuration of pure iron [4].

The temperature trend of the fcc lattice parameter, expected to display an Invar-like behaviour, is shown in Fig. 2. The dependence upon the Fe concentration is also reported in the inset, and is found to be in good qualitative agreement with what expected for this kind of systems [4]. As to the temperature dependence, the relative variation of the lattice parameter can be evaluated from the reported data. For the four Fe concentrations x = 20, 40, 50, 60, it turns out that the relative expansion of the lattice parameter, in the range 4 – 300 K, is respectively 0.31%, 0.24%, 0.21%, 0.20%. In agreement with X-ray data [3], all these variations are lower than the 0.35% variation expected for parent compounds over the same temperature interval. In addition, such relative expansion becomes smaller and smaller with increasing iron content, i.e. upon moving toward compounds where the Invar behaviour is expected to be more and more evident. All these indications are actually consistent with the presence of an Invar effect in the studied alloys. On the other hand, the present data do not unambiguously show an anomalous *plateau* in the lattice parameter temperature dependence, as instead observed by X-rays at 200 K. However, it should be remarked that the lattice parameter obtained by this very preliminary analysis is affected by larger statistical errors with respect to that deduced by X-ray data. Therefore, an attempt of pushing the presented neutron data analysis to a higher level of accuracy is strictly necessary to unambiguously understand whether the two sets of measurements are contrasting, or whether the neutron diffraction patterns should be collected with better statistics for a proper comparison with X-ray data.

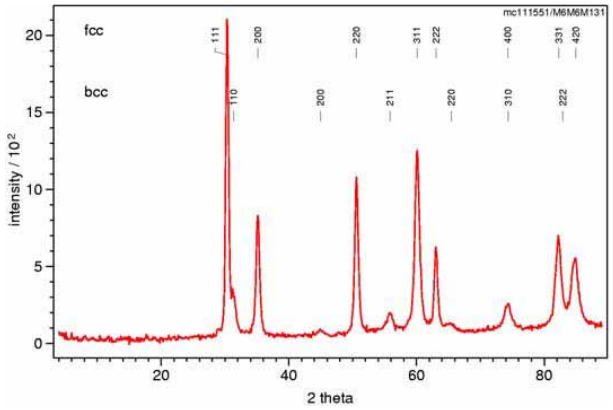

Fig. 1. Neutron diffraction pattern of the $Fe_{50}C_{50}$ alloy at 293 K. The assignment of the detected reflections is indicated, for both the fcc and bcc observed structures.

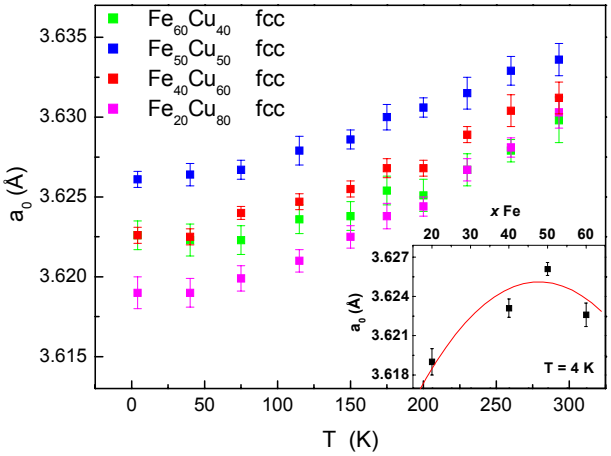

Fig. 2. Temperature behaviour of the lattice parameter of the Fe_xCu_{1-x} alloys, for x = 20, 40, 50, 60, obtained by neutron diffraction. *Inset*: Fe concenctration dependence of the lattice parameter at 4 K. The red line is a guide to the eye.

References

[1] R. J. Weiss, Proc. Roy. Soc. London **A82**, 281 (1963).
[2] L. E. Bove, C. Petrillo and F. Sacchetti, G. Mazzone, Phys. Rev. B **61**, 9457 (2000).
[3] F. Sacchetti and C. Petrillo, unpublished results.
[4] E. Maa, M. Atzmon, F. E. Pinkerton, J. Appl. Phys.. **74**, 955 (1993).

Institut für Festkörperforschung
Forschungszentrum Jülich GmbH
D-52425 Jülich

Experimental Report
of Neutron Scattering Experiments
at the FRJ-2 Reactor

Proposal number:	SV7-02-020		
Experiment title:	**Structural correlations and magnetic structures of the double perovskite Ba_2MnWO_6**		
Dates of experiment:	9-15 Sep 2002	Date of report:	21-02-2003
Experimental team: Names	Addresses		
(S.A. Ivanov)	Karpov Institute of Physical Chemistry Vorontsovo pole 10 103064 Moscow, Russia		
(A.K. Azad) (S.-G. Eriksson)	Dep. of Inorganic Chemistry Univ. of Gothenburg 412 96 Göteborg, Sweden	Studsvik Neutron Research Lab. Uppsala University 611 82 Nyköping, Sweden	
R. Skowronek	MIN/ZFR (Univ. of Bonn)		
Local Contact:	W. Schäfer, Univ. of Bonn		

Experimental report text body

Introduction

The discovery of high-temperature superconductivity in cuprates [1] and of colossal magnetoresistance (CMR) in manganites [2,3] have during the last years raised a strong interest in complex transition metal oxides containing mixed valence ions. Perovskite oxides have the general formula ABO_3 where the A- cation can be an alkaline metal, an alkaline earth metal or a lanthanide. The B-site is often occupied by transition metals, and can accommodate two or more different metal ions. Complex metal oxides with the general formula $A_2B'B''O_6$, where B' and B'' sites are occupied alternately by different cations, depending on their valences and relative ionic radii, are known as double perovskites or elpasolites [4]. A continued interest in their synthesis and physical properties, especially their magnetic behaviour, can be seen [5-6]. These compounds are also characterised by a two-dimensional antiferromagnetic behaviour, because of the *ab*-plane superexchange interaction between the magnetic ions via an array of non-magnetic ions. When double perovskites include transition metal ions within the B sublattice, the magnetic properties are strongly influenced by the ordering of the cations within this sublattice. Barium perovskites have revealed a variety of magnetic structures, such as antiferromagnetic in Ba_2CoWO_6 and Ba_2NiWO_6 [7,8], ferrimagnetic in Ba_2MnReO_6 [9,10], Ba_2FeMoO_6 [11], and Ba_2FeReO_6 [12], and a spin spiral arrangement has been found in Ba_2CoReO_6 [13]. Moreover, the double perovskites Ba_2CoNbO_6, Sr_2FeRuO_6, $BaLaNiBiO_6$ and Ba_2LnNbO_6 [14-15] have been suggested to exhibit spin-glass like behaviour at low temperature. The structures are face-centered cubic and the perovskite cell is doubled along all three axes.

Experimental and preliminary data analysis

Polycrystalline Ba_2MnWO_6 was prepared by a traditional solid-state reaction from stoichiometric amounts of $BaCO_3$, MnO and WO_3, in order to give the desired composition, i.e. the 2:1:1 cation ratio. All the starting materials were mixed in an agate mortar and as a grinding aid ethanol was added. The ground powder was

placed in an Al_2O_3 crucible and calcined at 1223K for 15 hours. The sample was reground and pressed into a pellet, thereafter fired at 1373K for 48 hours, 1473K for 72 hours and 1523K for 48 hours. Between each sintering step the pellets were ground to a fine powder and new pellets formed before the consecutive heat treatment. All the heat treatments were performed under a controlled N_2 atmosphere, and heating as well as cooling rates were 4^0/min. In between each sintering step phase purity was checked by X-ray diffraction. When no impurity phases could be detected the reaction was considered to be complete.

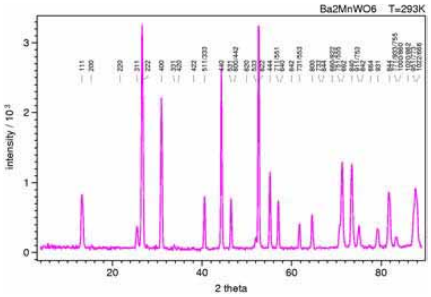

Fig. 1: Room temperature diffraction pattern of Ba_2MnWO_6 indexed by the perovskite-type structural unit cell

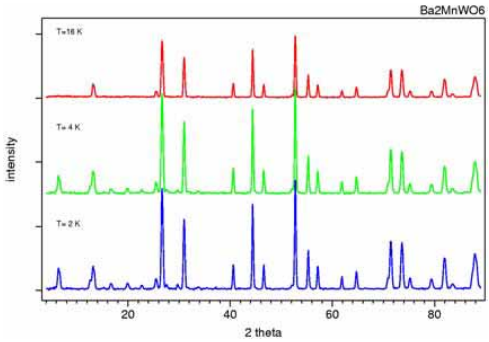

Fig. 2: Diffraction patterns at 2 K, 4 K and 16 K

Room temperature (Fig. 1) and low temperature powder diffraction patterns (at 2 K, 4 K, and 16 K, see Fig. 2) were collected at SV7 in Jülich, Germany. A vanadium can was used as sample holder. The NPD data sets earlier collected at Studsvik at 293 K and 16 K were refined by the Rietveld method. The lattice parameter, *a*, at 16 K is found to be 8.1788(2) Å. The *x* coordinate of oxygen is varied during the refinement and determined to be 0.2657(1).

Additional data were collected at 8 intermediate temperatures between 4K and 16 K (Fig. 3). NPD patterns below about 10 K show additional peaks the strongest of which is found at $2\theta \sim 8^0$. We attribute this peak to be of magnetic origin. The extra magnetic peaks could be indexed on the basis of a doubling of the chemical unit cell in all three directions. The antiferromagnetic structure is most likely of G-type. Fig. 4 depicts the temperature dependence of the strongest magnetic peak. The magnetic structure will be analysed and published later.

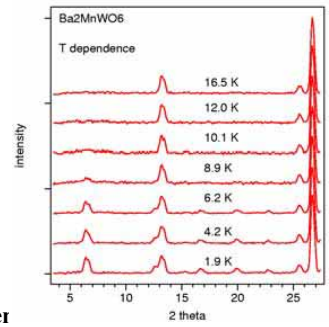

Fig. 3: Small angle section of temperature dependent patterns

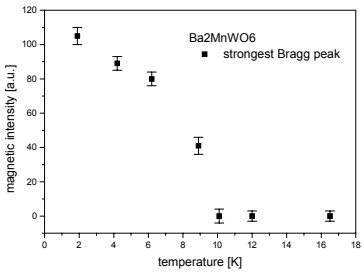

Fig. 4: Temperature dependence of the integrated intensities of the strongest magnetic reflection

Referer

1. J.G. Bednorz, K.A. Müller, Z.Phys. B 64 (1986) 189.
2. S.Jin, T.H. Tiefel, M. McCormack, R.A. Fastncht, R. Ramesh, L.H. Chen, Science 264 (1994) 413.
3. R.Von Hemlholt, J. Wecker, B. Holzapfel, L.Shultz, K. Samwer, Phys, Rev. Lett. 71 (1994) 2331.
4. M. T. Anderson, K. B. Greenwood, G. A. Taylor, K. R. Poppelmeier, Prog. Solid State Chemistry, 22 (1993) 197.
5. K.I.Kobayashi, T.Kimura, H.Sawada, K.Terakura, Y.Tokura Nature, 395 (1998) 677.
6. K.Ueda, H.Tabata, T.Kawai Science 280 (1998) 1064.
7. D.E. Cox, G. Shirane, B.C. Frazer, J. Appl. Phys. 38 (1967) 1459.
8. C.P. Khattak, D.E. Cox, F.F.Y. Wang, J. Solid State Chem. 13 (1975) 77.
9. A.W. Sleight, J.F. Weiher, J. Phys. Chem. Solids, 33 (1972) 679.
10. C. Ritter, M.R. Ibara, L. Morellon, J. Blasco, J. Garcia, J.M. De Teresa, J. Phys.:Conds. Matter, 12 (2000) 8295.
11. W. Prellier, V. Smolyaninova, A. Biswas, C. Galley, R.L. Greene, K. Romesa, J. Gopalkrisnan, J. Phys C, 12 (2000) 965.
12. C.P. Khattak, D.E. Cox, F.F.Y. Wang, A.I.P. Conf. Proc. No. 10 (1972) 674.
13. F.K. Patterson, C.W. Moeller, R. Ward, Inorg. Chem. 2 (1963) 196.
14. P.D. Battle, T.C. Gibb, A.J. Herod, S.H. Kim, P.H. Hunns, J. Mater. Chem. 5 (1995) 75.
15. P.D. Battle, T.C. Gibb, A.J. Herod, J.P. Hodges, J. Mater. Chem. 5 (1995) 865.

Institut für Festkörperforschung
Forschungszentrum Jülich GmbH
D-52425 Jülich

Experimental Report
of Neutron Scattering Experiments
at the FRJ-2 Reactor

Proposal number:	SV7-02-023		
Experiment title:	**Construction and neutronic tests of a low-cost furnace on the powder diffractometer**		
Dates of experiment:	1.-9.12.2002	Date of report:	25.2.2003
Experimental team: Names	Addresses		
H. Phiesel R. Skowronek A. Kirfel	Mineralogisch-Petrologisches Institut Universität Bonn Poppelsdorfer Schloss 53115 Bonn		
Local Contact:	W. Schäfer, Univ. of Bonn		

Experimental report text body

Motivation and requirements

So far, the powder diffractometer SV7 is well equipped with additional sample environment for low-temperature diffraction (refrigerators, orange-cryostat, He-3-cryostat, cryomagnet), but not for measurements at high temperatures. Paying regard to the increasing number of project proposals in recent years requiring diffraction measurements at elevated temperatures we have decided to construct a new furnace. This device should

(i) fit into the large evacuated sample chamber (Fig 1) which is centered on the diffractometer table and is equippped with a standardized top-flange for insertion and adjustment of the low-temperature cryostats,
(ii) should take advantage (considering diffraction) from the large oscillating radial collimator for suppression of unwanted secondary radiation in the two linear position-sensitive JULIOS detectors;
(iii) cover the temperature range from room temperature to about 1200 °C;
(iv) not be a commercial one (cost factor), but a cost-effective construction to be built in the workshop of our institute.

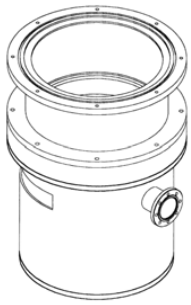

Fig. 1: Sample chamber on SV7

Construction

Core pieces of the new furnace are two commercial U-shaped $MoSi_2$ based electric heating elements 'Kanthal Super 1700' leaving a free space of about 60 mm around the standard cylindrical Vanadium sample can which is mounted on a central sample stick. Both, heating elements and sample stick are mechanically fixed to a ceramic plate. The whole unit is surrounded by a graphite cylinder of about 200 mm diameter to ensure both heat shielding and uniform heat reflection onto the sample (see Fig. 2).

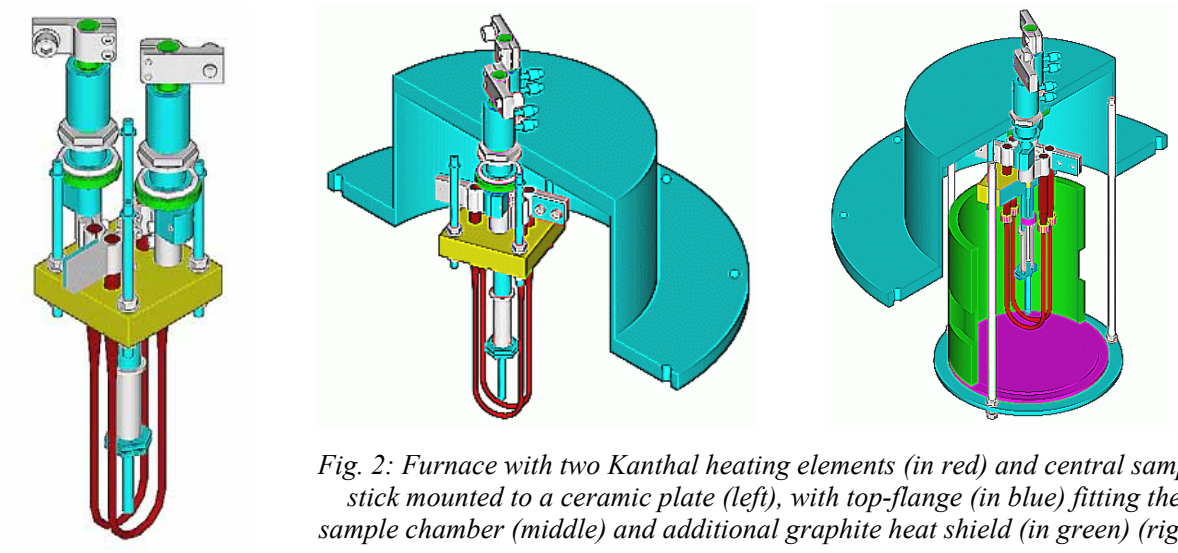

Fig. 2: Furnace with two Kanthal heating elements (in red) and central sample stick mounted to a ceramic plate (left), with top-flange (in blue) fitting the sample chamber (middle) and additional graphite heat shield (in green) (right)

Performance tests

Neutronic tests have been performed with the furnace inserted in the evacated sample chamber and under normal operation conditions with the oscillating radial collimator before the linear detector. No contaminating peaks from the furnace are visible (Fig. 3) as is also confirmed by a Rietveld refinement of a quartz diffraction pattern (Fig. 4).

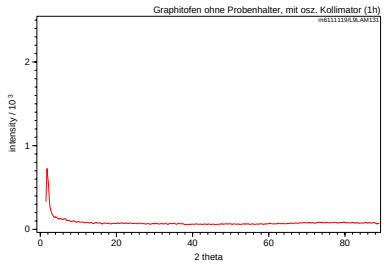

Fig. 3: Diffraction pattern of the furnace without sample

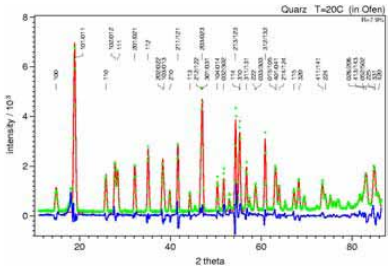

Fig. 4: Rietveld refined diffraction pattern of SiO_2

Temperature control is achieved by a commercial EUROTHERM unit using two thermocouples positioned on top and besides the sample. The performance is illustrated by the α-β phase transition of quartz at 573°C. Fig. 5 depicts a sequence of diffraction patterns of quartz measured in the furnace between 20°C and 630°C. Rietveld fits of the diffraction patterns revealed the temperature dependence of the unit cell volume shown in Fig. 6. The phase transition from trigonal α-quartz (SG $P3_121$) to hexagonal β-quartz (SG $P6_222$) is clearly visible by the discontinuous slope at 573°C.

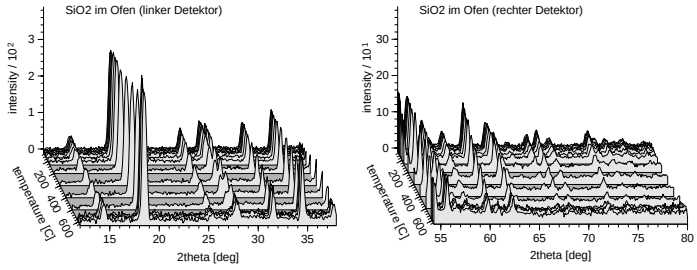

Fig. 5: Sequences of temperature dependent quartz diffraction patterns collected in the furnace; low-angle detector (left) and high-angle detector (right)

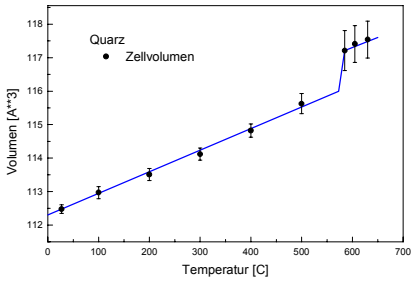

Fig. 6: Jumpf of the unit cell volume of quartz at the α-β phase transition

Institut für Festkörperforschung
Forschungszentrum Jülich GmbH
D-52425 Jülich

Experimental Report
of Neutron Scattering Experiments
at the FRJ-2 Reactor

Proposal number:	SV7-02-024		
Experiment title:	**Beziehungen zwischen texturell/mikrostrukturellen Eigenschaften und Anreicherungsverfahren (Flotation) von Itabiriten**		
Dates of experiment:	1.-4.12. u. 8.-19.12.2002	Date of report:	6.3.2003
Experimental team: Names	Addresses		
P. Hackspacher V. Teodore de Oliveira	Dep. de Petrologia e Metalogenia IGCE, Univ. Rio Claro C. Postal 178 13 506-610 Rio Claro-SP, Brasilien		
H. Siemes	Institut für Mineralogie und Lagerstättenlehre RWTH Aachen 52056 Aachen		
Local Contact:	W. Schäfer		

Experimental report text body

Hintergrund und Problemstellung

Die Reicheisenerz-Vorräte im Eisernen Viereck (Gebiet von Erzlager- und Erzabbaustätten in Brasilien) haben in den 80er Jahren stark abgenommen. Das führte zu einem verstärkten Abbau von Armerzen (Itabiriten) mit rund 32 % Fe-Gehalt. Itabirite sind Bändererze mit den wesentlichen Mineralbestandteilen Hämatit und Quarz. Die Umstellung auf Armerze brachte große Probleme bei der Erzaufbereitung, da jede Eisenerzgrube unterschiedliche Itabiritarten abbaut. Eines dieser Probleme ergibt sich bei der Anreicherung der Itabirite durch Flotation. Es ist bekannt, daß das Flotationsergebnis stark von der Mikrostruktur (Korngrösse, Kornformen) und Textur der unterschiedlichen Erze abhängt.
Zur Zeit wird eine Mischung verschiedener Erzarten verarbeitet, um die Flotationsverluste niedrig zu halten. Die Mischung erfolgt nach empirischen Erkenntnissen und derzeit ohne fundierten wissenschaftlichen Hintergrund.

Untersuchungen

In dieser Arbeit sollen die mikrostrukturelle und texturellen Eigenschaften der Itabirite (Armerze) mit Ergebnissen der verschiedenen Flotationsverfahren verglichen werden. Dazu wurden verschiedene Eisenerzbergbaue des Eisernen Vierecks beprobt und auf Flotationseigenschaften und Mikrogefüge untersucht. Vierzig Proben werden in Brasilien auf ihre Hämatit- und Quarzregelungen untersucht. Dazu werden das Röntgen-Textur-Goniometer und der optische U-Tisch verwendet.
Wegen der im Vergleich zu den Röntgen- und optischen Texturanalysen weitaus höheren Aussagekraft von Neutronentexturanalysen durch Ausmessung großer Probenvolumina mit wirklich aussagefähiger Kornverteilungsstatistik erfolgen komplementäre Texturanalysen an diesen 40 Proben am Neutronentexturdiffraktometer in Jülich.

Neutronenmessungen

Bisher befinden sich 19 Itabiriterz-Proben aus Brasilien in Jülich, von denen nach Start des Projektes im Dezember 2002 sechs Proben (im Berichtsjahr 2002) vermessen werden konnten. Dieser Bericht kann daher lediglich als eine erste experimentelle Zwischendokumentation ohne eingehende Datenanalyse und Interpretation angesehen werden.

Die Proben sind würfelförmig geschnitten mit Kantenlängen von 15 mm. Untersucht wurden:

Probe AL.1 (Foliation 346/40)
Probe AL.12 (Foliation 353/40)
Probe AL.46 (Foliation 188/70)
Probe AL.58 (Foliation 174/65)
Probe AL.90 (Foliation 136/43)
Probe AL.103 (Foliation 118/55)

Abb. 1 zeigt beispielhaft die Zusammensetzung der Itabirite aus mehreren Mineralkomponenten.

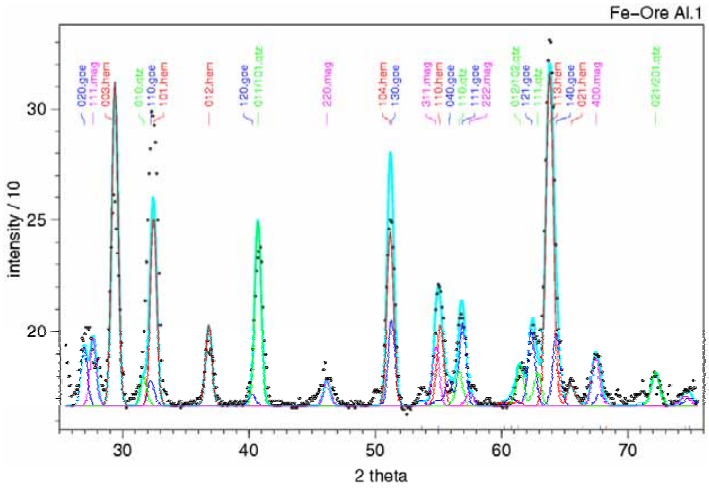

Abb. 1: Beugungsdiagramm im Rahmen eines Polfigurscans an SV7 (λ = 2.332 Å). Die Reflexe (Messdaten als Punkte) werden mittels einer full-pattern Modellrechnung auf vier Mineralanteile separiert: Hämatit (hem), Magnetit (mag), Goethit (goe) und Quarz (qtz).

Experimentelle Polfiguren

Aus den Messdaten konstruierte experimentelle Polfiguren, jeweils von drei Mineralkomponenten, sind in den folgenden Abbildungen vergleichsweise für zwei Proben dargestellt.

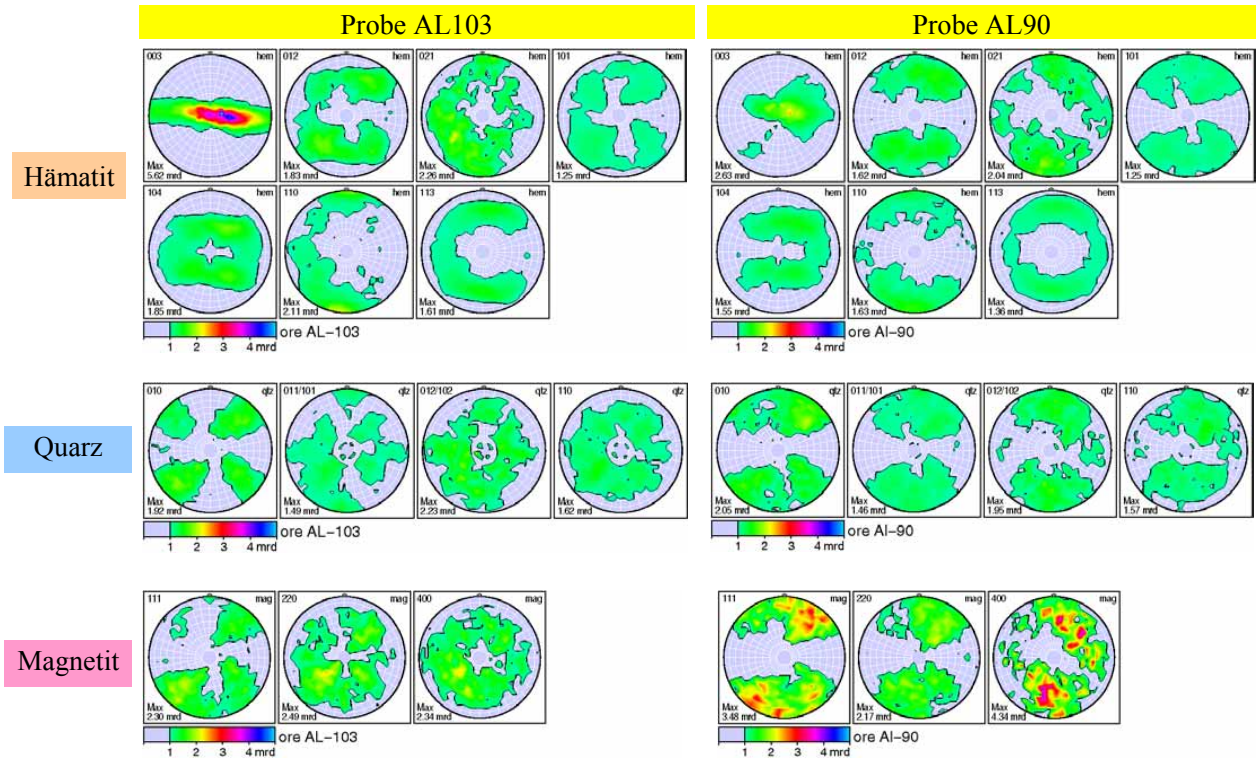

Die Texturanalysen erfolgen im Rahmen einer Doktorarbeit von V. de Oliveira.

Institut für Festkörperforschung
Forschungszentrum Jülich GmbH
D-52425 Jülich

Experimental Report
of Neutron Scattering Experiments
at the FRJ-2 Reactor

Proposal number:	SV7-02-025		
Experiment title:	**Bestimmung der Wasserstoffpositionen von $(NH_4)[NbOBr_4]$**		
Dates of experiment:	18.-26.10.2002	Date of report:	5.3.2003
Experimental team: Names	Addresses		
Ch. Kusterer J. Beck R. Skowronek	Institut für Anorganische Chemie Universität Bonn Gerhard-Domagk-Straße 1 53121 Bonn MIN/ZFR (Univ. Bonn)		
Local Contact:	W. Schäfer, Univ. Bonn		

Experimental report text body

Grundlagen: Polare, polymere Anionenteilstrukturen $[MOX_4^-]_n$

Wenn die Oxidtrihalogenide der Elemente Molybdän, Wolfram und Niob ($MoOCl_3$, $MoOBr_3$, $WOCl_3$, $WOBr_3$, $NbOCl_3$ und $NbOBr_3$) im Sinne von Lewis-Säure-Base-Reaktionen Halogenid-Ionen aufnehmen, entstehen Oxotetrahalogenometallat-Anionen der allgemeinen Formel $[MOX_4]^-$, die allesamt eine quadratisch-pyramidale und damit polare Struktur haben. In bestimmten Strukturen sind diese Anionen zu Strängen asoziiert, in denen kurze und lange M-O-Abstände alternieren. Abb. 1 zeigt einen solchen Anionenstrang als Beispiel aus der Struktur von $Te_7^{2+}[WOBr_4]^-Br^-$. In dieser zentrosymmetrischen Struktur kommen beide Strangrichtungen zu gleichen Anteilen vor [1].

Eine weitere Struktur mit einem solchen polaren Anionenstrang findet sich in der Literatur in Form des $(NH_4)[NbOBr_4]$ [2]. Allerdings zeigen die thermischen Auslenkungsellipsoide einige physikalisch sinnlose Formen, die ansonsten - und in unseren Strukturen stets so angetroffen - pyramidalen MOX_4-Gruppen sind hier planar (Abb. 2). Wir begannen daher eine Neuuntersuchung dieser Substanz und eine Neubestimmung der Struktur. Hierbei stellte sich heraus, dass die Struktur fälschlicherweise in einer zentrosymmetrischen Raumgruppe beschrieben war. Geht man von *C*2/*m* zu *Cm* lässt sich die Struktur in gewohnter Weise verfeinern, die $[NbOBr_4^-]_n$-Stränge sind pyramidal und polar, die Auslenkungsellipsoide normal. Durch den Nachweis nichtlinearer optischer Effekte durch ein SHG-Experiment ist die Nichtzentrosymmetrie dieser Struktur gesichert.

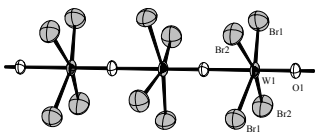

Abb. 1: Der polare Anionenstrang $[WOBr_4^-]_n$ in $Te_7[WOBr_4]Br$

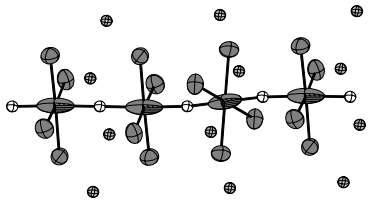

Abb. 2: Der $[NbOBr_4^-]$-Strang und die umgebenden N-Atome, welche die NH_4^+-Ionen repräsentieren, in der Struktur von $(NH_4)[NbOBr_4]$ mit Auslenkungen der thermischen Schwingungen der Atome gemäß [2].

Zur Vervollständigung des Strukturmodells bestand der Wunsch, auch die Positionen der H-Atome der NH_4^+-Ionen zu kennen. Im Röntgenbeugungsexperiment gelang die Zuordnung von Differenz-Fourier-Maxima zu H-Atomen, die an N gebunden sind, nicht. Wir stellten daher eine ausreichende Menge an deuteriertem $(ND_4)[NbOBr_4]$ für Neutronenpulverdiffraktometrie her.

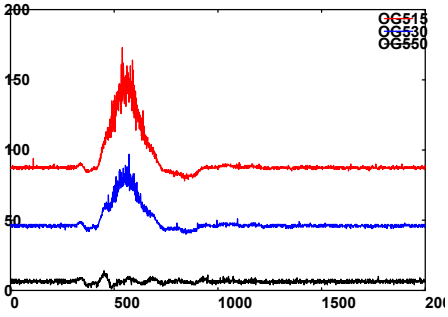

Abb. 3: Pulver-SHG-Messungen an $(NH_4)[NbOBr_4]$. Anregung bei 1064 nm, Response bei 532 nm. Aufge tragen sind die Pulsintensitäten (aufintegriert über jeweils 250 Laserpulse) mit unterschiedlichen Kantenfiltern [3].

Neutronenmessungen

Die Messungen erfolgten an SV7 in einem gekapselten Vanadiumzylinder von 8 mm Durchmesser. Beugungsdiagramme wurden bei 293 K und 123 K mit einer Neutronenwellenlänge von 1.096 Å aufgenommen; eine zusätzliche Raumtemperaturmessung erfolgte bei höherer Auflösung mit 2.332 Å.

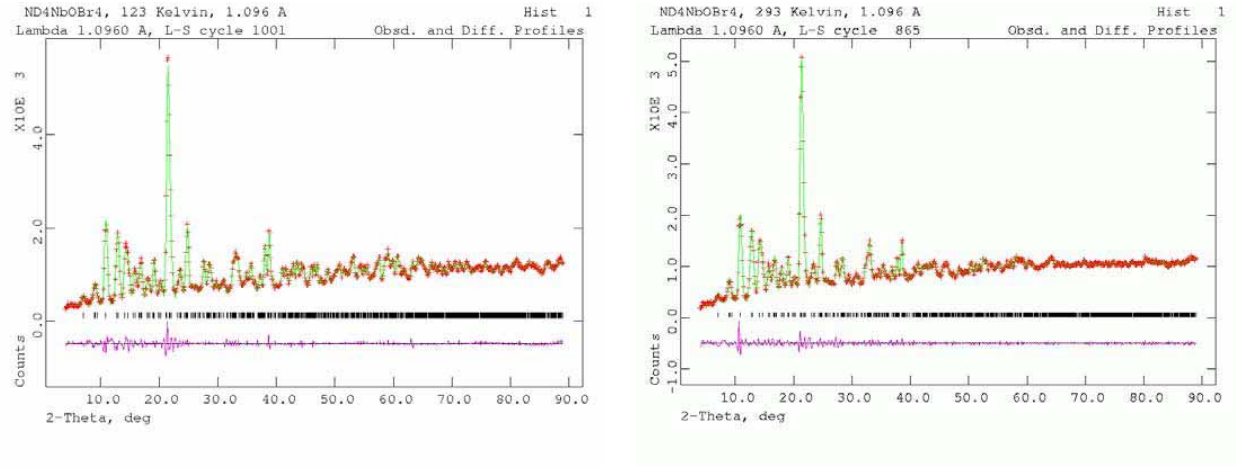

Abb. 4: Neutronenbeugungsdiagramme von $(ND_4)[NbOBr_4]$, gemessen mit λ = 1.096 Å bei 123 K (links) und 293 K (rechts); vgl. Text

Datenanalyse

Die Abb. 4 und 5 zeigen die zur Verfeinerung von Gittermetrik und Instrumentparametern nach dem Le Bail - Verfahren, d.h. noch ohne Strukturmodell, unter Verwendung von GSAS analysierten Beugungsdiagramme. Aus den Messungen mit λ = 1.096 Å wurden folgende monoklinen Zellparameter bestimmt:

T = 132 K	T = 293 K
a = 7.739(1)	a = 7.742(2)
b = 13.776(2)	b = 13.854(2)
c = 11.778(1)	c = 11.823(2)
β = 101.95(1)°	β = 102.01(1)°

Die Strukturbestimmung zur Lokalisation der D-Atompositionen ist derzeit in Arbeit.

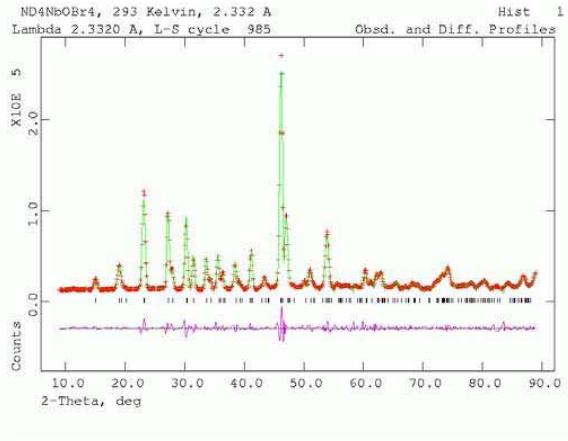

Abb. 5: Raumtemperaturdiagramm gemessen mit λ=2.332 Å

Referenzen: [1] Beck, J., *Angewandte Chemie (German Edition)* **1991**, *102*, 1149-1151.
[2] Hoerner, M., Hiller, W., Straehle, J., *Zeitschr. für Naturforschung, Teil B*, **1988**, *43*, 981-984.
[3] Wir danken Herrn Prof. Klaus Betzler, U. Osnabrück, FB Physik, für die Messung der SHG-Intensitäten.

Neutron Diffractometer (SV28)

Instrument Parameters

	Diffractometer 1	*Diffractometer 2*
Monochromator (reflection):	Cu (220)	Cu (200)
Wavelength:	0.087 nm	0.124 nm
Neutron flux density:	2.5×10^6 n/cm^{2}s	2.55×10^6 n/cm^{2}s
Mean FWHM of the Bragg reflections:	0.5°	0.5°
Detector, monitor:	^{3}He tubes, fission chambers	
Inner diameter of the Eulerian cradle:	40 cm	25 cm
Diffractometer control:	PC 486 Linux, interface type Stoe, stepping motor drive (steps of 0.005°), angle encoders with a resolution of 0.005°.	

Instrument Responsible

DP Stefan Mattauch Tel. +49-(0)-2461-61-3140 Email: s.mattauch@fz-juelich.de
Chunhua Hu Tel. +49-(0)-2461-61-3140 Email: c.hu@fz-juelich.de

Institut für Festkörperforschung
Forschungszentrum Jülich GmbH
D-52425 Jülich

Experimental Report
of Neutron Scattering Experiments
at the FRJ-2 Reactor

Proposal number:	S28-02-002		
Experiment title:	**The neutron beam size at the centre of four-circle diffractometer in SV28**		
Dates of experiment:	18.10.02 — 24.10.02 09.12.02 — 13.12.02	Date of report:	23.02.2003
Experimental team: Names	Addresses		
Chunhua, Hu	Institut für Festkörperforschung Forschungszentrum Jülich GmbH D-52425 Jülich		
Local Contact:	Chunhua, Hu		

Experimental report text body

(Please use 12 pt letters here !)

Motive

Why do we want to know the neutron beam size at the centre of four-circle diffractometer in SV28, i.e. the sample position?

First, like X-ray method, for a single crystal with a certain size the beam size should fit with the crystal size: a. If the largest edge of the crystal is much bigger than the beam size, the diffracted beam is contributed from the part of the crystal, so that its intensity cannot give the information of the entity of the crystal; b. *Vice versa*, if the beam size is too big, the background will rise. The best choice is that let the beam size equal to or slightly bigger than the crystal to ascertain the minimum lose of the intensity.

Second, the beam size is adjustable by changing the slit lying at the end of the collimating tube, but this size is not equal to that at the sample position. The neutron intensity from the reactor is rather limited. With respect to the intensity, the beam with the certain range of wavelength is chosen to be monochromated. So the beam after the monochromator and the collimating tube is not a parallel wave with a single wavelength. It will have a distribution, i.e. so-called beam divergence. It is important to know the relationship between the slit size and the effective beam size at the sample position.

Method

A metal plate of about $5\times5\times2$ mm^3 made from cadmium with a small hole in the middle (its diameter is about 1 mm) can be used as the checking material. First, align the hole into the center of the diffractometer optically. Then find such a position that the Cd plate can face to the neutron beam, and put the detector (2θ circle) to zero position so that it can record the signal through the Cd plate. After recording the first signal at the starting position, more can be done by moving the Cd plate in the horizontal and vertical directions step by step. When the hole moves out of the strongest part of the beam, weaker signals will be found. According to the signal changing, the beam diameters in two directions can be drawn out, i.e. the neutron beam size at the sample position.

Result

We got the typical diagrams like the following figure. For example, for the 10mm primary slit the effective beam size is about 5mm in the horizontal direction and 4mm in the vertical one, which means that the intensity distribution of the beam is like a disk, not a circle.

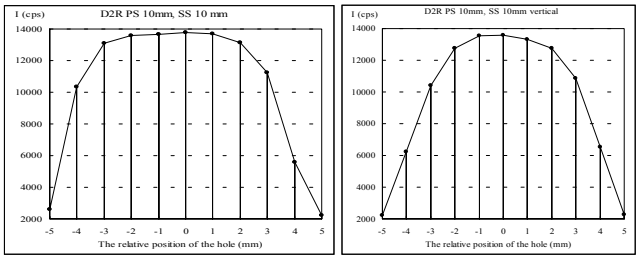

Finally we can know an approximate relationship between the slit and beam size at the sample position (see the table).

Slit size (mm)	Beam size (mm)		Max. crystal size (mm)
	horizontal	vertical	
5	2	1	1
7	3	2	2
10	5	4	4
15	8	7	7
20	11	10	10
25	12	10	10
30	13	12	12

Institut für Festkörperforschung
Forschungszentrum Jülich GmbH
D-52425 Jülich

Experimental Report
of Neutron Scattering Experiments
at the FRJ-2 Reactor

Proposal number:	S28-02-003		
Experiment title:	**Transmission and performance of metal foil collimators**		
Dates of experiment:	27.-28.11.2002	Date of report:	20.1.2003
Experimental team: Names	Addresses		
Dr. Martin Meven	ZWE FRM-II, TU München Lichtenbergstraße 1 85747 Garching		
Local Contact:	Dr. Stefan Mattauch		

Experimental report text body

Two metal foil collimators (60' and 30') were tested at the SV28-links. The collimators were made at the HMI/Berlin. They are supposed to be used as collimators for the primary beam of the single crystal diffractometer at the hot source of FRM-II, HEiDi.

To determine the quality of the collimators two parameters were investigated:

1. Divergence:
   The collimator hole was centered horizontally and vertically to the primary beam on the Euler cradle. Then the collimator was rotated around the omega-(or phi-)axis corresponding to a rocking scan with the detector centered in the primary beam. The measurements were repeated with the collimators upside down and with the front side and back side switched.
2. Homogeneity of transmission:
   Again the collimator hole was centered horizontally and vertically to the primary beam on the Euler cradle. This time the collimator was translated horizontally and perpendicular to the primary beam. This way inhomogeneous transmission caused by varying foil distances and coating could be observed.

Summary: The results from data analysis show the following properties:

1. Divergence:
   Both collimators show almost perfect triangular transmission profiles with FWHMs of 1.11° for the 60' and with FWHMs of 0.63° for the 30' collimator. The enlargement of the FWHMs in comparison to the ideal values of 1.0° and 0.5° are caused simply by the fact that the real maximum intensities are reduced of by the nonzero thicknesses of the foils. The intensities follow a homogeneous distribution of the radiation by giving a factor of two between the values of the 30' collimator (2105 cps) in comparison to the 60' collimator (4125 cps).

2. Homogeneity of transmission:
   The intensities are very homogeneous along the total widths of both collimators. The noticeable oscillation of the intensities is caused by the proximity of the detector to the collimator window of about 200 mm and has no influence for the intended purpose.

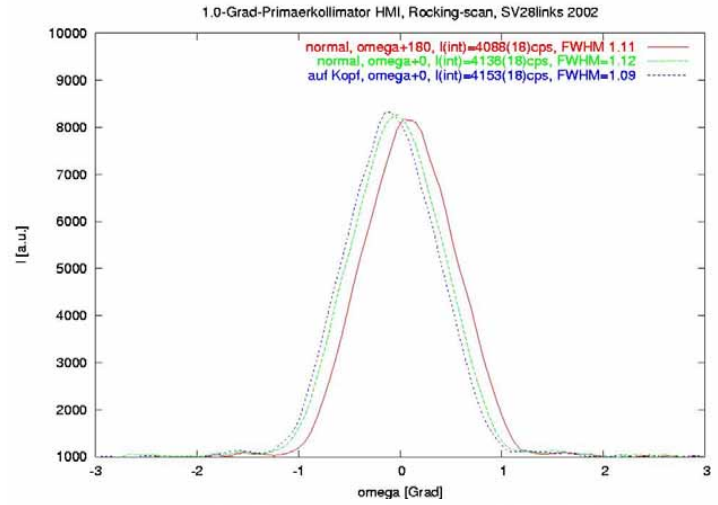

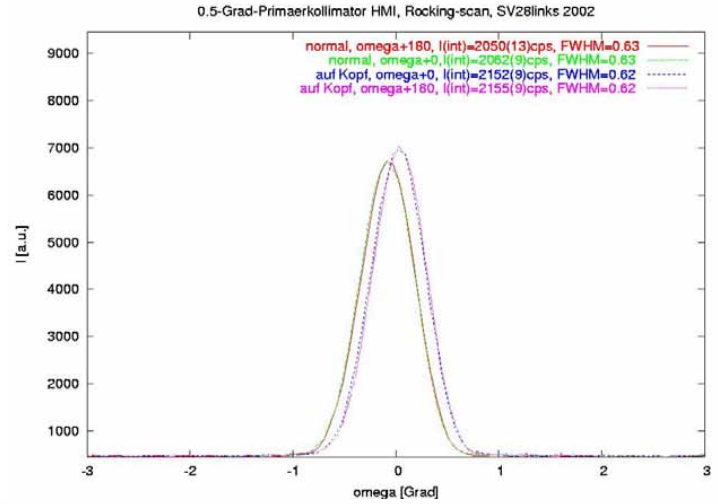

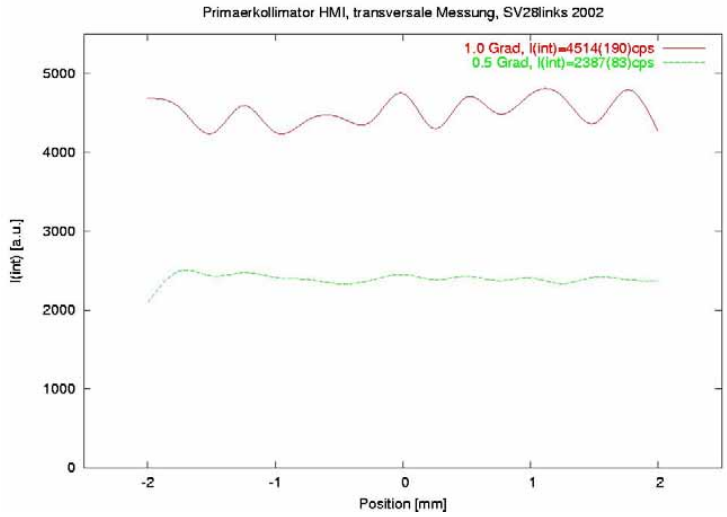

Institut für Festkörperforschung
Forschungszentrum Jülich GmbH
D-52425 Jülich

Experimental Report
of Neutron Scattering Experiments
at the FRJ-2 Reactor

Proposal number:	S28-02-005		
Experiment title:	**Calibration of diffractometer d2r by Ge test crystals**		
Dates of experiment:	25.10.02 — 30.11.02 26.11.02 — 27.11.02 28.11.02 — 04.12.02	Date of report:	23.02.2003
Experimental team: Names	Addresses		
Chunhua, Hu	Institut für Festkörperforschung Forschungszentrum Jülich GmbH D-52425 Jülich		
Local Contact:	Chunhua, Hu		

Experimental report text body

(Please use 12 pt letters here !)

1. What kinds of information can we obtain by this measurement?
   a) Make a complete measurement: from orientation matrix and unit cell determination to data collection; from data reduction to structure solving and refinement;
   b) According to Bragg law ($2d_{hkl} \sin\theta_{hkl} = \lambda$), calculate averaged diffracted wavelength λ, i.e. monochromatic wavelength by Cu(200) monochromator, with its deviation.
   c) Calculate the relationship between FWHM (full width of half maximum of reflection profile) and diffracted angle θ according to the formula:
   FWHM (hkl) $= \sqrt{u + v\tan\theta + w\tan^2\theta}$;
   d) Establish the reflection profile standards. Making a comparison between these standards and profiles from other samples, we can know the approximate quality of samples;
   e) Others: crystal faces reading, extinction correction by psi scan, and alignment of diffractometer center, etc.
2. Known information about Ge crystals:
   Ge: atomic number 32, atomic weight 72.59, density 5.32 g.cm^{-3}; fcc packing, space group F$\bar{4}$3m (no. 216), atom numbers in a unit cell Z = 8, unit cell a = 5.6575 Å, V = 181 Å^3; neutron scattering length *b* = 8.185 barns; independent atom positions and occupancies in the unit cell: 0,0,0; $\frac{1}{24}$ and ¼,¼,¼; $\frac{1}{24}$.

Result

1. Crystal data from my measurement: unit cell: a = 5.6607(7) Å, V = 181.39(3) $Å^3$;
2. The wavelength calculation by Bragg law ($2d_{hkl} \sin\theta_{hkl} = \lambda$):

Indices	d (Å)	$2\theta_{exp}$ (°)	λ_{calc} (Å)	$\overline{\lambda}$ (Å)	σ	$\overline{\sigma}$	λ (Å)
111	3.266	21.904	1.24099	1.24052	0.00047	0.00053	1.2405(5)
220	2.000	36.146	1.24091		0.00039		
311	1.706	42.657	1.24099		0.00047		
422	1.155	64.930	1.23997		-0.00055		
440	1.000	76.613	1.23974		-0.00078		

3. From three given different reflections, *u*, *v* and *w* are calculated to be 6.1, -14.6, 18.4, so the minimal scan width can be known that it is about 1.80° at 2θ = 43.32.
4. Profile analysis: ($\Delta\omega$ is about 1.0°)

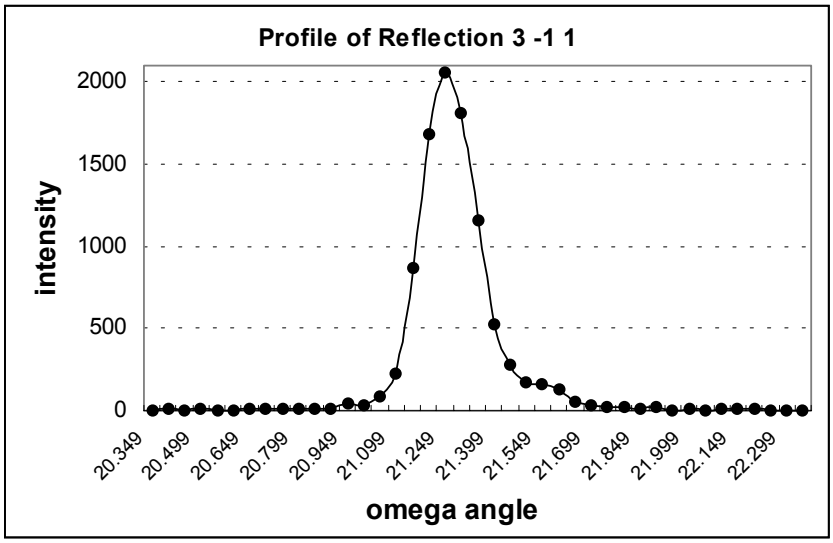

5. Crystal faces:

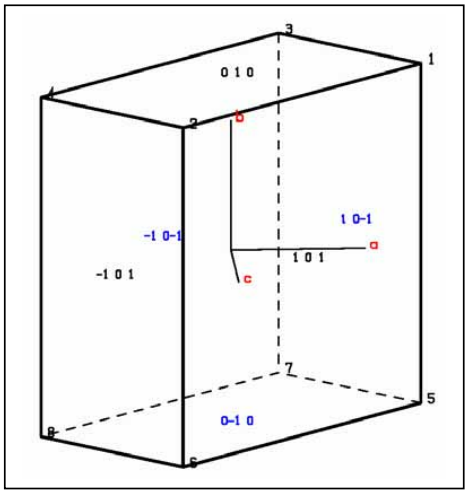


```
 0  1  0: 1.525mm
 0 -1  0: 1.525mm
 1  0  1: 0.875mm
-1  0 -1: 0.875mm
 1  0 -1: 1.550mm
-1  0  1: 1.550mm
```

Institut für Festkörperforschung
Forschungszentrum Jülich GmbH
D-52425 Jülich

Experimental Report
of Neutron Scattering Experiments
at the FRJ-2 Reactor

Proposal number:	S28-02-007		
Experiment title:	**H bonds and disorder in potassium trisoxalatochromate(III) trihydrate**		
Dates of experiment:	11.12.02 — 20.12.02	Date of report:	23.02.2003
Experimental team: Names	Addresses		
Englert, Ulli Kalf, Irmgard	Institut für Anorganische Chemie RWTH Aachen Professor Pirlet Strasse 1 D-52056 Aachen		
Local Contact:	Chunhua, Hu		

Experimental report text body

(Please use 12 pt letters here !)

Facts prior to our jobs

The X-ray diffraction experiments on single crystals of the title compound published to date [1-4] agreed with respect to lattice constants and the correct space group $P2_1/c$. In 1951 van Niekerk and Schoening observed that the experimental intensities almost match the integral extinction condition required for the supergroup $C2/c$ [1]. In the following year the same authors solved the structure in the supergroup [2]. Stoichiometry, lattice constants, and space group but no atomic coordinates were published by Gillard and coworkers [3]. The most recent study by Taylor [4] stated that both a potassium countercation and a water molecule are cooperatively disordered. The results were based on room temperature data and involved one surprisingly short K...O contact of 2.35 Å. No H positions were included in this latter structure model.

Our result by XN method

We have performed a neutron diffraction experiment and located all hydrogen atoms. Their positions clearly indicate that the structure model developped in [4] must be modified: A hydrogen atom of the water molecule involved in the alleged 2.35 Å potassium-oxygen contact points in the direction of the cation. It leads to a prohibitevely short H-K intersite distance of 1.3 Å and requires that water and cation positions cannot be occupied at the same time. A partial occupancy is therefore ascribed to the water molecule under discussion, and the resulting model completely avoids unusual interatomic distances.

The disorder model we propose is in full agreement with tentative occupancy refinements based on X-ray data collected in our laboratory. Neither neutron nor X-ray data suggest additional water sites. We therefore conclude that the title compound is not a trihydrate; the molar ratio of between tris(oxalato)chromate anions and water is expected to be around 1:2.7. The alternative stoichiometry is confirmed by thermogravimetric results.

Molecular Picture

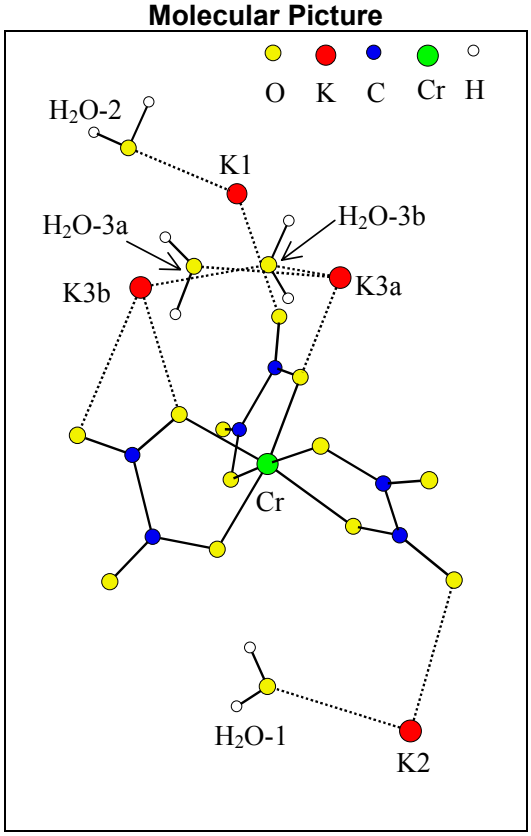

1) K3 and H_2O-3 are disordered in two positions with the radio of about 7:3;
2) H_2O-2 is cooperatively disordered with K3a, and occupies about 70%.

References

1. J. van Niekerk & F. R. L. Schoening (1951) *Acta Crystallogr.* **4**, 381-382.
2. J. van Niekerk & F. R. L. Schoening (1952) *Acta Crystallogr.* **5**, 196-206.
3. R. D. Gillard, S. H. Laurie & P. R. Mitchell (1969) *J. Chem. Soc. A*, 3006-3011.
4. D. Taylor (1973) *Aust. J. Chem.* **31**, 1455-1462.

Time-of-Flight Spectrometer (SV29)

Instrument Parameters

Beam line:	4H2 (radial beam tube)
Monochromator:	matrix of 75 PG002/PG004, vertical+horizontal focusing
Incident wavelengths:	$1.0 \le \lambda \le 4.0$ Å
Take-off angle:	$35 \le 2\Phi_M \le 75°$
Momentum transfer:	$\approx 1 \ldots 10$ Å^{-1}
Energy resolution:	$3\% \le \Delta E/E \le 8\%$
2 phased choppers:	≤ 21000 rpm
Collimation:	0.8°
Duty cycle:	4×10^{-3}
Neutron flux at sample:	$\approx 10^5$ n/cm^2 s
Beam size at sample:	3×8 cm^2
Flight path:	1.91 m
Detectors:	500 ^{3}He counters in 90 units
Solid angle covered:	≈ 0.05 srad
Range of scattering angles:	$10° \le \Theta_S \le 130°$
Sample environment: ***- Cryostats:*** ***- Top-loading cryofurnace:*** ***- Furnaces:*** ***- Low-T pressure cell:***	 $1.5 \le T \le 310$ K $1.5 \le T \le 600$ K $50 \le T \le 1400$ °C $p \le 3.5$ kbar at $T \ge 4.5$ K

Instrument Responsible

Dr. Michael Prager Tel. +49-(0)-2461-61-6759 Email: m.prager@fz-juelich.de

Institut für Festkörperforschung
Forschungszentrum Jülich GmbH
D-52425 Jülich

Experimental Report
of Neutron Scattering Experiments
at the FRJ-2 Reactor

Proposal number:	S29-01-001		
Experiment title:	**Inelastic Neutron Scattering from CH_4 - clathrate, THF- clathrate, acetone - clathrate and Ice**		
Dates of experiment:	18.1. - 24.1., 31.1. - 4. 2. und 26.4. - 29.4. 2002	Date of report:	19.9.2002
Experimental team: Names	Addresses		
M. Prager H. Conrad H. Soltner W. Kuhs	FZ-Jülich FZ-Jülich FZ-Jülich Universität Göttingen		
Local Contact:	M. Prager		

Experimental report text body

Inelastic neutron scattering with emphasis on energetically low lying modes has been performed on four prospective advanced cold moderator materials. Employing the time-of-flight instrument SV29 at the Jülich FRJ-2 reactor, spectra have been obtained from synthetic methane clathrate, tetrahydrofurane (THF) clathrate, acetone clathrate and light water ice at several temperatures between 2 K and 70 K. Clearly separated excitations at energy transfers of ±1 meV, +2 meV and +3 meV have been observed with synthetic methane clathrate. In hexagonal ice at T = 2 K up to now unreported low lying energy levels were found at energy transfers of 1.8 meV and 2.8 meV. An additional line at about 10 meV could be detected in the THF clathrate, which is most likely due to the embedded THF molecule.

The motivation for the investigations described here is the development of advanced cold neutron moderators in particular with respect to pulsed spallation sources. Solid methane at low temperatures, e.g. T = 20 K, is generally considered the best moderator medium for cold neutron sources. In contrast to liquid hydrogen at the same temperature it experimentally exhibits a Maxwellian spectrum with a “neutronic” temperature of about 23 K. The observation that neutrons are virtually in thermal equilibrium with methane at this temperature is attributed to the low lying energy levels, which in turn are believed to be due to the free rotations of a limited number of methane molecules in the solid phase. In addition, methane yields an intensity gain of a factor of 3 to 4 at neutron energies around 2 meV as compared to liquid hydrogen.

A not quite as perfect cold spectrum is observed with water ice at 20 K. On the other hand, ice shows an extended slowing down spectrum covering the so-called thermal neutron energy range (ambient temperature regime). This would entail narrower neutron pulse widths (better resolution for time-of-flight spectrometers) than those obtainable from common ambient temperature water moderators.

Therefore, a combination of methane and water at low temperatures could be the ideal moderator over a broad energy range from 2 meV up to, say, 100 meV. Indeed, there are inclusion compounds of gases or other molecules in water, the clathrates, which might exactly serve this purpose.

A well-known example is methane clathrate, a substance, which even occurs naturally on the deep sea floor. Unfortunately, it is only stable under these conditions (high pressure and/or low temperature). On the other hand, inelastic neutron scattering on a few samples of natural deep sea methane clathrates revealed nearly the same low energy levels, which have been discovered long ago with pure solid methane [1].
Since the proper composition of natural methane clathrate is not predictable, we investigated the spectral properties of synthetic material with the correct stoichiometric ratio of one methane molecule per six water molecules. The results of the experiments are shown in Figure 1.
Due to the technical difficulties with the synthesis of methane clathrate (30 bars at 70 K), it seems worthwhile to search for a compound easier to produce, such as tetrahydrofurane (THF) clathrate. The room temperature liquid THF (C_4H_8O) and water mix easily and form an inclusion compound at 6°C. This hydrate composed of one THF per 17 water molecules can thereafter easily be cooled down to cryogenic temperatures. Inelastic neutron data are shown in Figure 2. In order to complete our studies with respect to searching for low lying excitations in solid cryogenic moderator media we also did some measurements with water ice, which is still a candidate for pulsed sources due to reasons described above.
The peaks at the lowest energy transfers in Fig.2 we have observed in ice as well. To our knowledge there is no report in the literature about a similar observation. The physical origin of these excitations is not understood yet.

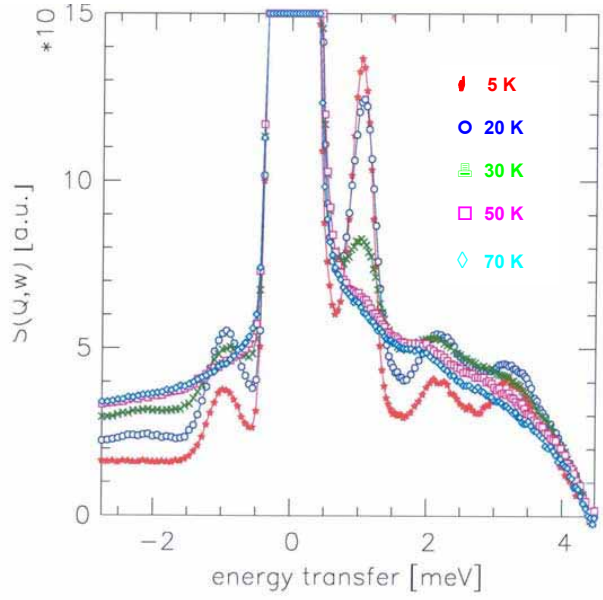

FIG. 1: Inelastic spectrum from synthetic methane clathrate at 5 different temperatures (E_0 = 7 meV, δE = 0.4 meV; Q_o = 2.9 Å^{-1}).

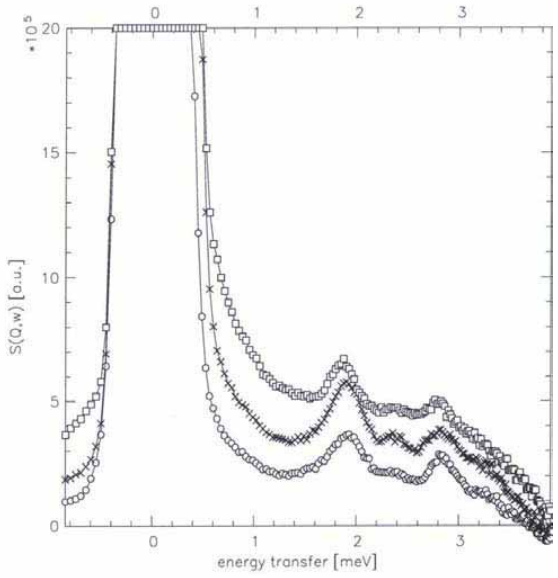

FIG. 2: Inelastic spectrum from THF clathrate at T = 2 K and three different scattering angles. (E_0 = 7 meV, δE = 0.4 meV; Q_o = 1.5; 1.9 and 2.9 Å^{-1} resp.).

The measurements have been performed with three different incoming energies, 7 meV, 26 meV and 41 meV. A distinct separation of the expected lowest rotational levels (±1 meV, +2 meV and +3 meV) from the elastic line was possible with 7 meV, as can be seen in Fig. 1. It should be noted that at the highest temperature of 70 K the discrete lines of the free rotations are smeared out to a quasi-elastic line due to diffusional motions. The energies of the observed lines at the lowest temperature corresponds perfectly to the lines found with natural deep sea methane clathrate [2].

REFERENCES

[1] H. Kapulla and W. Gläser; Neutron Inelastic Scattering IAEA-SM-155/G3; p 841 - 849 (1972)
[2] C. Gutt, B. Asmussen, W. Press, C. Merkl, H. Casalta, J. Greinert, G. Bohrmann, J.S. Tse and A. Hüller; Europhys. Lett., 48 (3), 269 (1999)

Institut für Festkörperforschung
Forschungszentrum Jülich GmbH
D-52425 Jülich

Experimental Report
of Neutron Scattering Experiments
at the FRJ-2 Reactor

Proposal number:	S29-01-002		
Experiment title:	**The methyl rotational potentials of Ga(CH3)3 derived by neutron spectroscopy**		
Dates of experiment:	28.2.02 – 5.3.02	Date of report:	18.2.2003
Experimental team: Names	Addresses		
Michael Prager	Forschungszentrum Jülich		
Local Contact:	M. Prager		

Experimental report text body

The results are published in J. Phys.: Condens. Matter 14 (2002) 10145 - 10157

The methyl rotational potentials of $Ga(CH_3)_3$ derived by neutron Spectroscopy

M. Prager[1], J. Combet[2], S. F. Parker[3], A. Desmedt[4], R. E. Lechner[4]

[1]Institut fuer Festkoerperforschung, Forschungszentrum Juelich D-52425 Juelich, Germany
[2]Institut Laue Langevin, 156X, F-38042 Grenoble Cedex9, France
[3]ISIS Facility, Rutherford Appleton Laboratory, Chilton, Oxon OX11 0QX, UK
[4]Hahn-Meitner Institut, Glienickerstr. 100, D-14109 Berlin, Germany

Abstract
High resolution neutron spectra of $Ga(CH_3)_3$ show tunneling transitions between 4.5 and 19 μeV. The spectrum can be explained within the single particle model on the basis of the monoclinic C2/c(Z=16) low temperature crystal structure of $Ga(CH_3)_3$ with 6 inequivalent methyl groups in the unit cell. The overlapping tunneling lines prevent the extraction of temperature dependent line widths which would allow us to assign the librational energies measured in the phonon density of states. Classical rotational motion is studied by quasielastic neutron scattering. Three activation energies could be extracted. Methyl librations, tunneling energies and barrier heights are combined with consistent intensities into rotational potentials. Only the concerted application of all spectroscopic techniques yields a conclusive description.

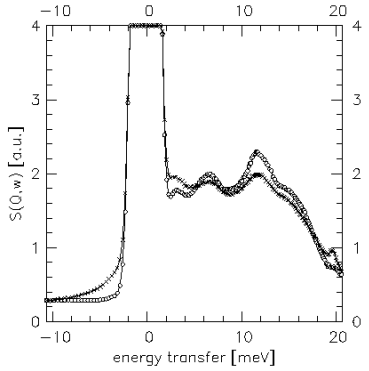

Figure: Spectra of $Ga(CH_3)_3$ obtained at sample temperatures of 2.5K (oooo) and 30K (xxxx).
Spectrometer: SV29, λ=1.76A

The thermal time-of-flight spectrometer SV2 was used with λ=1.76A to determine the excitations of $Ga(CH_3)_3$ in the regime of lattice modes below 21meV. The elastic energy resolution was δE=2.0meV. The figure shows two spectra measured at sample temperatures T=2.5K (open circles) and T=30K(crosses). The low temperature spectrum shows several maxima of the density of states at energies 3.0, 6.4, 11.8, 15.1 and 21 meV. An additional peak at 27meV is weakly seen in the 3rd order spectrum with λ=1.07A. The interpretation of the bands is not straightforward. At first, the finite energy resolution most likely hides fine structure. Secondly methyl librational modes coinciding with other phonon energies loose their Einstein character and – due to coupling – become affected by dispersion. At T=30K all bands beside of the lowest one are strongly damped which makes them candidates for methyl librational excitations. At T=60K any inelastic fine structure is lost.

A consistent description requires to include more experimental information. By combining librational energies with activation energies from quasielastic spectra (not shown here) and measured tunneling transitions (not shown here) with the observed intensities a convincing set of methyl rotational potentials could be derived which may serve for future ab-initio calculations if the low temperature crystal structure will be quantitatively solved.

For more details see the publication.

Institut für Festkörperforschung
Forschungszentrum Jülich GmbH
D-52425 Jülich

Experimental Report
of Neutron Scattering Experiments
at the FRJ-2 Reactor

Proposal number:	S29-01-003		
Experiment title:	**The methyl rotational potentials of In(CH3)3 derived by neutron spectroscopy**		
Dates of experiment:	22.4.02 – 26.4.02	Date of report:	18.2.2003
Experimental team: Names	Addresses		
Michael Prager	Forschungszentrum Jülich		
Local Contact:	M. Prager		

Experimental report text body

Trimethyl indium is used to dope Si or GaAs semiconductors with In. The investigation of the In-compound is a natural extension of the so far studied homologuous materials $Al(CH_3)_3$ and $Ga(CH_3)_3$. While $Al(CH_3)_3$ shows a low temperature crystal structure with space group C2/c and dimers $Al_2(CH_3)_6$ with 3 inequivalent methyl groups as the molecular units [1], the $Ga(CH_3)_3$ appears in the same space group but as monomers. A loss of symmetry leads to 6 inequivalent methyl rotors [2]. According to literature [3] $In(CH_3)_3$ is built up at room temperature by layers consisting of 2-dimensional molecular networks of tetramers. Like in trimethyl aluminum there are 3 inequivalent methyl groups of which one acts as weak bridge to another molecule. The corresponding bond is elongated by about 1%. A recent X-ray crystallographic study has shown that the system undergoes a phase transition around 70K. The low temperature unit cell contains 6 inequivalent methyl groups like in $Ga(CH_3)_3$. This complexity is confirmed by tunneling spectroscopy (see the corresponding experimental report). The density of states measured on SV29 contains information on the librational excitations of all these methyl groups. Using a wavelength of 1.76A with a corresponding energy resolution of 2.2meV a number of bands is clearly resolved in the energy range below 20meV and at a sample temperature of 2.5K (figure). All bands beside the lowest are strongly damped with increasing the temperature to 50K. This information is used in combination with tunneling transitions and a set of activation energies derived from quasielastic neutron spectra, to get the most likely assignment of all observables consistent with occurrence probabilities to individual methyl groups. As final result six rotational potentials of the shape

$$V(\varphi) = \sum_1^2 V_{3n}(1-\cos(3n\varphi))/2$$

are obtained (table) which will form the basis for a test of future ab-initio calculations. Only the obtained consistency of all spectroscopic information –rotational tunneling, quasielastic scattering and the phonon density of states - gives confidence in the outlined interpretation of a complex dynamic system.

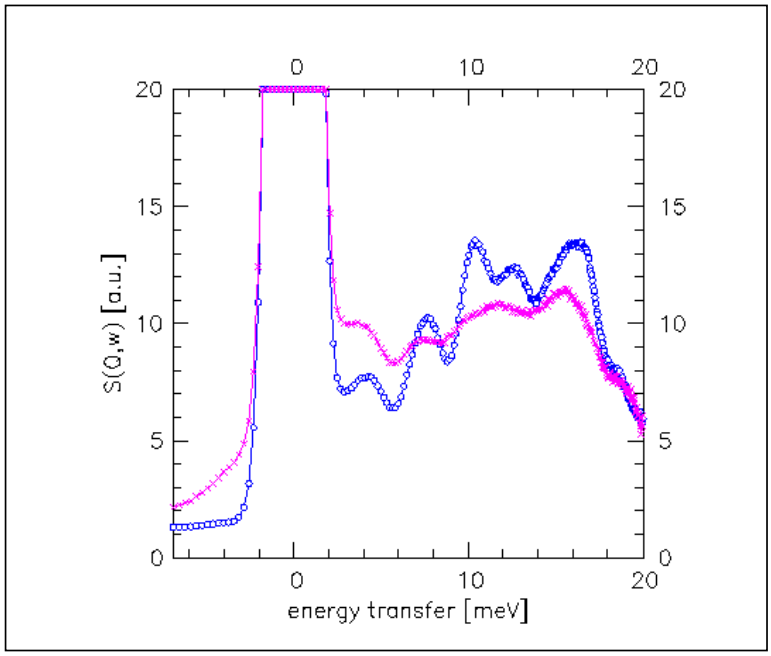

Figure: Sum of the detectors between 60 and 120 degree. Wavelength: 1.76A. Energy resolution: 2.2meV. Sample temperatures: 2.5K (blue symbol) and 50K (pink symbol)

Tunnel splitting [μeV]	Relative intensity	Libration E_{01} [meV]	Activation energy E_a [K]	Threefold term V3 [meV]	Sixfold term V6 [meV]	Calculated E_{01} [meV]	Calculated E_a [K]
1.7	1/2	16.2	305	37.8	10.7	17.2	320
4.7	1/6	12.7	305	34.8	1.8	13.3	310
8.7	1/6	10.9	305	36.7	---	10.3	310
15.9	1/6	10.9	210	25.8	1.7	11.2	220

Table: Tunnel splittings together with ist relative line intensities, librational transition energies and activation energies from quasielastic experiments again with its relative intensities are used to determine methyl rotational potentials. These potentials reproduce the tunnel splittings exactly. For comparison the calculated librational and activation energies are shown.

[1] S McGrady, JFC Turner, RM Ibberson, M Prager, Organometallics 19,4398(2000)
[2] R Boese, D Blaeser, to be published
[3] AJ Blake, S Cradock, J. Chem. Soc. Dalton Trans. 1990,2393

Institut für Festkörperforschung
Forschungszentrum Jülich GmbH
D-52425 Jülich

Experimental Report
of Neutron Scattering Experiments
at the FRJ-2 Reactor

Proposal number:	S29-01-004		
Experiment title:	**Investigation of CH3 librations in the charge transfer complex tetracyanoethylen/hexamethylbenzene (TCE/HMB)**		
Dates of experiment:	29.1. – 31.1.2002	Date of report:	18.2.2003
Experimental team: Names	Addresses		
A.Pawlukojc M. Prager	Institute of nuclear chemistry and technology, Warsaw (proposer only) Forschungszentrum Jülich		
Local Contact:	M. Prager		

Experimental report text body

Molecular complexes of the charge transfer type (EDA complexes) attract considerable interest, since many of them exhibit interesting physical and chemical properties from the point of view of their potential applications. Recently, besides already widely known photoconducting phases, the possible existence of phases with superconducting and photoelectric properties has been shown.
We shall trace the changes of structural and dynamic transformations of electron donor systems when a second component with rising electron acceptor properties will be added. Hexachlorobenzene, hexabromobenzene, trinitrochlorobenzene, tetrachlorobenzoquinone, tetracyanoethylene, tetracyanoquinodimethane and hexacyanobenzene are proposed to be used. In all these cases one may expect the formation of column lattices with alternating donor and acceptor molecules. Hexamethylbenzene has been chosen because of its symmetry properties and the presence of six methyl groups, which enhance the electrodonor properties of the system.
The tetracyanoethylene hexamethylbenzene complex under study consists of sheets of molecules which overlap in such a way that the C=C bond of the „acceptor“ molecules TCE lie parallel to the aromatic rings of the HMB „donor“ molecules in the manner characteristic of π– charge transfer complexes (fig.1).

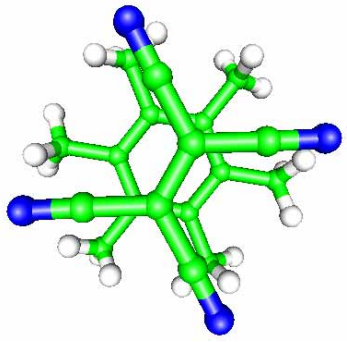

Fig. 1: Tetracyanoethzylene-hexamethylbenzene complex

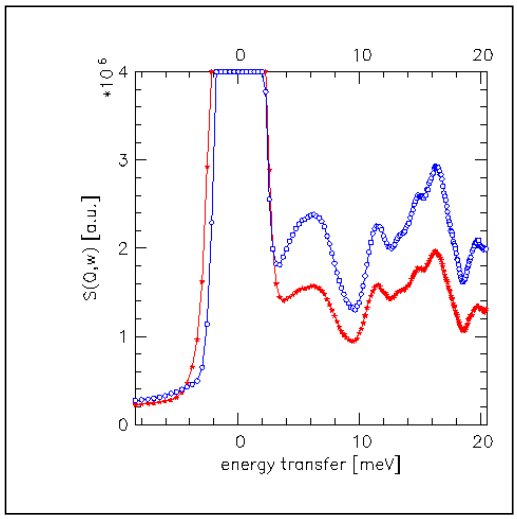

Fig. 2: Spectra of the hexamethylbenzene-tetracyanoethylene complex. Sample temperature 2.1K. Wavelength 1.76A. Scattering angles 50°(*) and 120° (□).

The inelastic neutron scattering experiment in the regime of phonon energies aimed to detect the changes in the dynamics of the methyl groups, in particular those of their torsional modes. Above the low energy acoustic phonons fig. 2 shows an intense broad and structured band extending from ~11 to ~19meV which may contain the torsional modes. To our knowledge the density of states of pure hexamethylbenzene is not known. Therefore we guess librational energies from an NMR relaxation experiment [1] which has obtained a tunnel splitting of 0.04μeV. For a pure cos(3φ) potential this is related with a torsional energy of 21meV. Thus the lower torsional bands show that the rotational potentials are reduced in the charge transfer complex. To which extent this is due to the structural and chemical change of the nearest neighbours and to which extent to the interesting charge transfer between the two constituents requires the use of ab-initio calculations. A basic ingredient for such calculations is the precise low temperature crystal structure. Corresponding x-ray and neutron structural studies are under way.

In a forthcoming experiment the torsional modes of hexamethylbenzene shall be measured directly.

To complement the above experiment, standard infra red spectra, Raman spectra and the photoconcuctivity will be measured to characterize the complexes as potential new materials of technological significance.

[1] S. Takeda, G. Soda, H. Chihara, Sol. State Comm. 36,445(1980)

Institut für Festkörperforschung
Forschungszentrum Jülich GmbH
D-52425 Jülich

Experimental Report of Neutron Scattering Experiments at the FRJ-2 Reactor

Proposal number:	S29-02-001		
Experiment title:	Crystalline electric field excitations in CeBiPt		
Dates of experiment:	03.2002 06.2002	Date of report:	4.3.2003
Experimental team: Names:	Addresses:		
M. Prager O. Stockert	Institut für Festkörperforschung, Forschungszentrum Jülich, D-52425 Jülich Max-Planck-Institut CPfS, Nöthnitzer Straße 40, D-01187 Dresden		
Local contact:	M. Prager		

Investigations of ternary rare earth compounds continue to be an active topic of research because of their intriguing magnetic properties. The equiatomic ternary RBiPt intermetallic compounds (R = rare-earth elements) crystallize in the cubic MgAgAs-type structure (space group $F\bar{4}3m$) and show a variety of low temperature properties ranging from semiconductor or semimetal-like behavior of NdBiPt to magnetism and heavy fermion-like behavior in YbBiPt with one of the highest measured specific heat coefficients $\gamma = C/T = 8\,\mathrm{J/molK^2}$ [1,2,3].
In particular CeBiPt, first characterized by Canfield et al. [1] with a lattice constant a = 6.811 Å, shows antiferromagnetic order at $T_\mathrm{N} \approx 1\,\mathrm{K}$ as evidenced by sharp maxima in specific heat, susceptibility and magnetization measurements [4]. Neutron diffraction on the diffractometer D23 at the ILL/Grenoble on a CeBiPt single crystal [5] have revealed that the antiferromagnetic structure is an AF-type I structure with a propagation vector τ = (1 0 0) and moments also along [1 0 0]. A crude analysis of the magnetic intensity (major extinction effects are observed) yields an ordered moment of $\mu \approx 0.5\,\mu_\mathrm{B}$. We determined a Neel temperature $T_\mathrm{N} = 1.15\,\mathrm{K}$ in good agreement with thermodynamic measurements.
To shed more light on the magnetic ground state properties of CeBiPt we performed inelastic neutron scattering on CeBiPt powder ($m \approx 12\,\mathrm{g}$) using the time-of-flight spectrometer SV29 at FRJ-2/Jülich with a fixed energy of the incident neutrons $E_i = 30\,\mathrm{meV}$ at temperatures between $T = 2\,\mathrm{K}$ and $T = 100\,\mathrm{K}$. In particular, we investigated the crystalline electric field (CEF) excitations in CeBiPt. As a nonmagnetic reference compound we used LaBiPt.
Since the spectrometer was running with a preliminary setup, i.e. the final choppers have not yet been installed, we had to cope with the problem of higher harmonics in the incident beam. However, these parasitic effects can be well separated at low temperatures. Therefore we will focus on the data taken at $T = 2\,\mathrm{K}$.

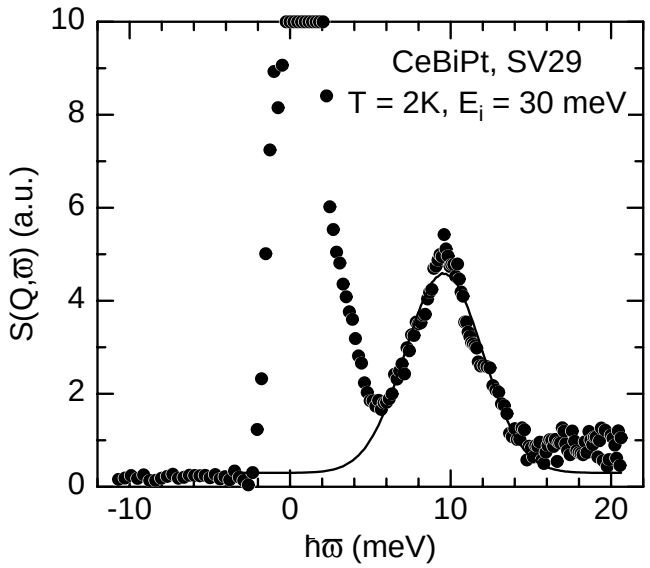

Fig. 1: Magnetic excitation spectrum of CeBiPt powder at $T = 2\,\mathrm{K}$.

The neutron spectra were normalized to vanadium and the nonmagnetic phononic contribution was taken out by properly subtracting the LaBiPt data from the CeBiPt spectra. Fig. 1 displays the magnetic scattering of CeBiPt derived in this way for scattering angles $43° \leq 2\Theta \leq 57°$. Beside a strong incoherent elastic and quasielastic contribution there is clearly visible an inelastic excitation at $\hbar\omega \approx 9.5\,\mathrm{meV}$. This excitation is identified as a CEF excitation since it is independent of $\vec{q}$. In addition, its intensity decreases with increasing momentum transfer $|q|$ (scattering angle) as is expected for a magnetic excitation due to the $|q|$-dependence of the magnetic form factor of Ce^{3+}. No further inelastic excitations have been observed.
For Ce with $J = 5/2$ there exist six crystal field levels which split into a doublet and a quartet due to the cubic fcc symmetry of the Ce sublattice. One should therefore either have a twofold or a fourfold degeneracy of the crystal field ground state of CeBiPt. The entropy S of the ground state is hence $R\ln 2$ or $R\ln 4$. Integration of C/T vs. T in zero magnetic field yields the entropy S which already reaches a value of $R\ln 2$ at $\approx 2.7\,\mathrm{K}$ [6]. However, the entropy S continues to increase much further to higher temperature. Together with the large CEF splitting this yields the ground state to be the Γ_8 quartet and the excited state to be the Γ_7 doublet with a splitting of $\Delta \approx 110\,\mathrm{K}$.

References:

[1] P. C. Canfield et al., J. Appl. Phys. 70 (1991) 5800.
[2] R. A. Robinson et al., Phys. Rev. B 50 (1994) 9595.
[3] D. T. Morelli, P. C. Canfield, P. Drymiotis, Phys. Rev. B 53 (1996) 12896.
[4] T. Pietrus et al., Physica B 281–282 (2000) 745.
[5] O. Stockert et al., unpublished results.
[6] T. Pietrus, PhD thesis, Cuvillier Verlag Göttingen (1999).

Institut für Festkörperforschung
Forschungszentrum Jülich GmbH
D-52425 Jülich

Experimental Report
of Neutron Scattering Experiments
at the FRJ-2 Reactor

Proposal number:	S29-02-002		
Experiment title:	**Investigation of CH3 librations in 1,3,5-trimetoxybenzene and tetramethylpyrazine**		
Dates of experiment:	2.5. – 3.5. and 28.5 – 30.5.2002	Date of report:	18.2.2003
Experimental team: Names	Addresses		
A.Pawlukojc M. Prager	Institute of nuclear chemistry and technology, Warsaw (proposer only) Forschungszentrum Jülich		
Local Contact:	M. Prager		

Experimental report text body

Our research is devoted to the problem of charge-transfer (CT) interaction in molecular systems. The CT molecular complexes evoke increasing interest in connection with discovering in molecular materials such phenomena like electric conductivity (and even superconductivity) and ferroelectricity. The properties of such materials depend on ionisation potential and electron affinity of interacting components as well as on structural parameters especially in case of π - π donor – acceptor complexes.
The goal of our studies is to gather new information on those systems based on low frequency transitions reflected in INS spectra. Just low frequency transitions can well be recorded by using this technique. For instance the tunnelling splitting and librational motion of CH_3 groups present in donor molecules can be a sensitive parameter of the CT interaction. To our knowledge there are no reports in the literature related to this problem.
As a first step in our searches is to find proper electron donors containing CH_3 groups which could be complexed with various acceptors. We suggest that at beginning most convenient could be 1,3,5-trimethoxybenzene $C_6H_3(OCH_3)_3$ (fig.3) and tetramethylpyrazine $C_4N_2(CH_3)_4$.
Using a wavelength of 1.76A spectra of these materials could be recorded in the energy regime below 20meV. Tetramethylpyrazin shows two sharp and strong bands at 15 and 20meV of guessed relative intensities 1:3 (fig.1) which may be assigned to methyl librations. A safe assignment could be based on the isotopic shift of these lines. Unfortunately a deuterated sample was not available. No further strong transitions were found up to energy transfers of 32 meV. Lacking the knowledge of the crystal structure any further guesses are absed on the molecular structure: 3 methyl groups seem to feel a rather similar rotational potential which is significantly stronger than that of the remaining 4^{th} group.

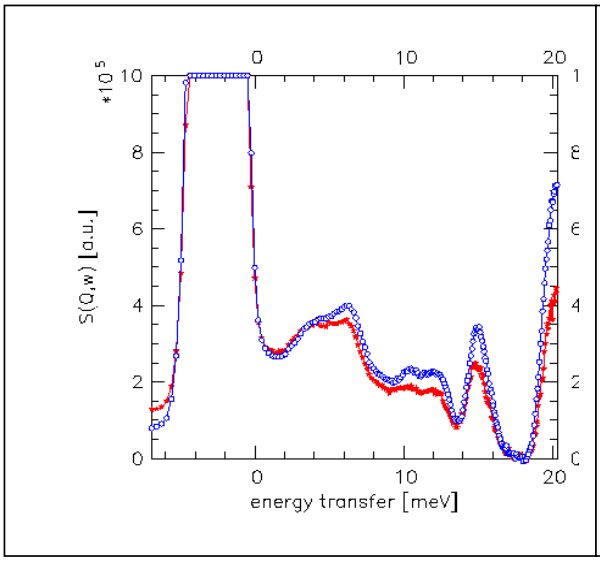

Fig. 1: Spectra of tetramethylpyrazin at sample temperatures 2.2K and 50K

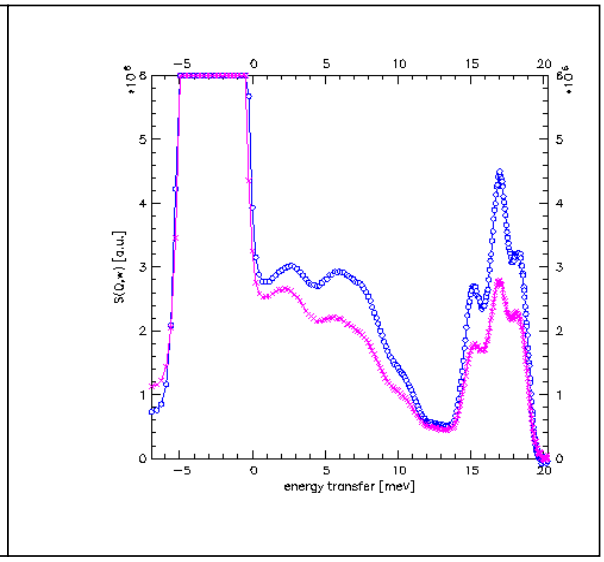

Fig. 2: Spectra of trimethoxy benzene at two scattering angles 50° and 110°

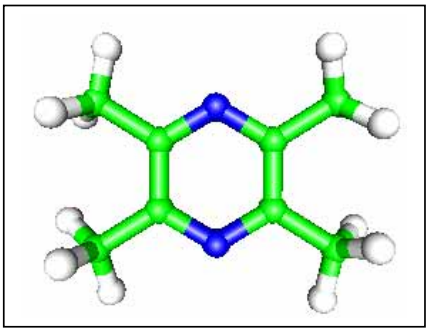

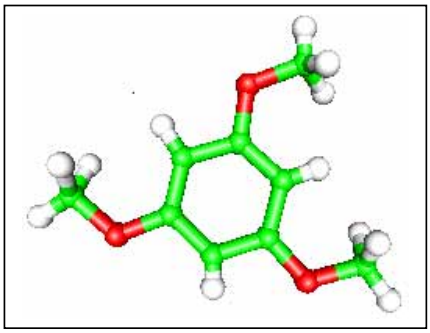

Fig. 3: The molecules tetramethylpyrazine and trimethoxy benzene

Trimethoxy benzene shows above a clear gap three about equally strong bands at 17, 26 and 33meV. (The two higher bands are found using the 3rd order of diffraction with a wavelength of 1.17A). It is tempting to assign each band to librations of each of the methoxy groups within one molecule. All bands are to high in energy to be related with a resolvable tunnel splitting of the methyl librational ground state. The spectrum measured with the 2nd order of diffraction (fig. 2) shows that the low energy band – and thus likely the unresolved higher ones too – show fine structure which is possibly due to phonon dispersion. In this example, too, the low temperature crystal structure must be known and the deuterated material should be available to make further progress.

Institut für Festkörperforschung
Forschungszentrum Jülich GmbH
D-52425 Jülich

Experimental Report
of Neutron Scattering Experiments
at the FRJ-2 Reactor

Proposal number:	S29-02-003		
Experiment title:	**Phonon density of states of $NdAl_2$ and YAl_2**		
Dates of experiment:	1.6.2002 - 16.6.2002	Date of report:	06.03.2003
Experimental team: Names	Addresses		
Prof. Dr. Ernst Gratz Christian Anzur	1040 Wien, Wiedner Hauptstraße 8-10 1040 Wien, Wiedner Hauptstraße 8-10		
Local Contact:	Dr. M. Prager		

Experimental report text body

The aim of our time of flight experiment was twofolded: On the one hand we wanted to study the crystal field excitations of NdAl2 and on the other hand the nature of two specific excitations, found in earlier measurements at the UNIDAS spectrometer at the FZ Jülich.
We performed measurements on powdered sample material of NdAl2 and the non-magnetic isostructural compound YAl2 in order to separate the crystal field exctitations from the phonons. The measurements were done at various temperatures to identify those peaks which were of crystal field nature. In Figure 1 one is able to see the rather strong temperature dependence of the phonon density of states of NdAl2 caused by the CEF whereas in Figure 2 there is nearly no temperature dependence in YAl2.
We also investigated the PDOS at different scattering angles to improve our presumptions and to emphasize the magnetic origin of the excitations. An example of such an experiment is shown in Figure 3.
Finally we were able to compare the two compounds and got good data to fix the CEF excitations at specific energies.
The second, and maybe more interesting problem was to clarify the nature of two very sharp peaks of high intensity at energies of 30,8 and 25,5 meV. The first discoveries of these excitations were made in an experiment, with the aim to study the lattice dynamic of NdAl2, performed by us at the UNIDAS-triple-axes-spectrometer. Those measurements were done at different temperatures, and we observed very strong temperature-dependencies of those peaks, like the behaviour of phonons should be. On the other hand the very high intensity (up to 200 000 counts at some directions) and the sharpness as well as the non dispersivity is contrary to the assumption, that those peaks were of phononic origin.

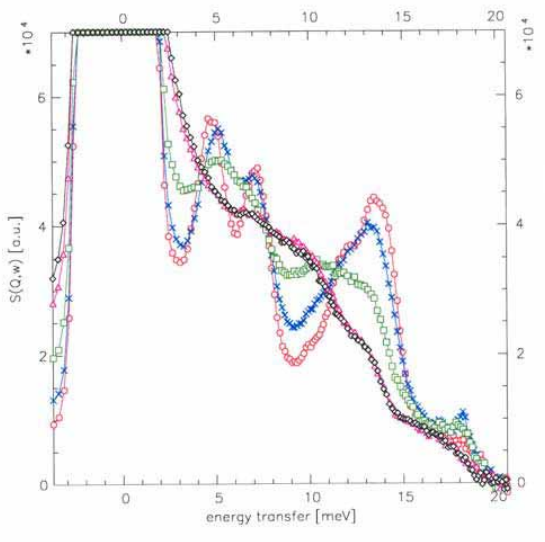

Fig. 1: PDOS from NdAl2 at the temperatures: 2,5 K (red), 40 K (blue), 60 K (green), 80 K (pink) and 100 K (black)

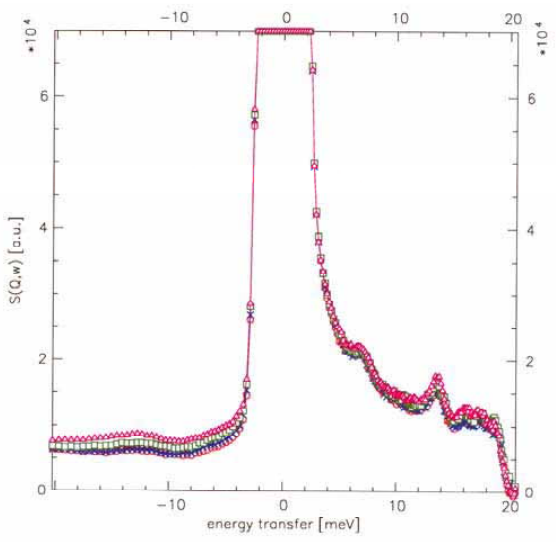

Fig. 2 PDOS from YAl_2 at the temperatures 2.5 K (red), 40 K (blue) 70 K (green) and 100 K (pink)

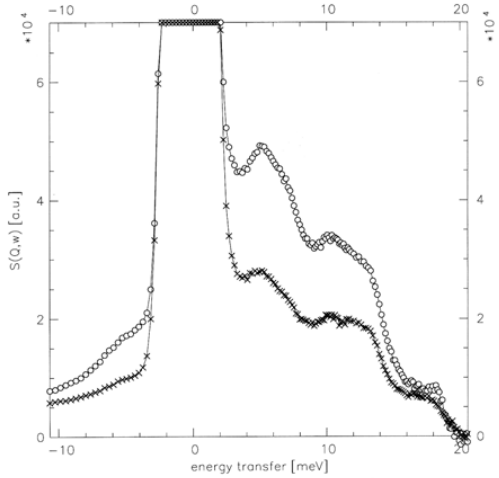

Fig. 3 PDOS from NdAl2 at the scattering angles 65,2 (circles) and 108,4 (crosses)

To minimize exogen effects we also studied those peaks at various Gamma Points in the Brillouin zone, what strengthened the suspicion, that our observations were of physical origin of the bulk material.
Because of the non dispersive behaviour of those excitations they should have been seen very clearly in the phonon density of state measurements. Unfortunable it was not possible to perform useful TOF experiments at energies higher than round about 20 meV. So further measurements will contribute to our studies.

Institut für Festkörperforschung
Forschungszentrum Jülich GmbH
D-52425 Jülich

Experimental Report
of Neutron Scattering Experiments
at the FRJ-2 Reactor

Proposal number:	S29-02-004		
Experiment title:	**Inelastic neutron scattering study of methyl group librations in 2,3- and 2,5-dimethylpyrazine**		
Dates of experiment:	14.1. – 19.1.2002	Date of report:	18.2.2003
Experimental team: Names	 Addresses		
O. Kirstein M. Prager	Forschungszentrum Jülich Forschungszentrum Jülich		
Local Contact:	O. Kirstein, M. Prager		

Experimental report text body

The combined measurement of librations and rotational tunneling frequencies are very sensitive probes for the local rotational potential experienced by by rotors like methyl groups in molecular crystals [1]. CH3 groups attached to aromatic rings of benzene and pyridine have been extensively studied [2]. Recently 2,6-dimethylpyrazine out of the class of di-nitrogen-substituted benzenes was investigated. The observed tunneling spectrum shows two tunneling lines at 20 and 29 μeV and librational transitions at 8 and 10 meV [3]. The low temperature structure of 2,6-dimethylpyrazine has been solved [4] and in agreement with the spectroscopic results the two CH3 groups of the molecule were found to be inequivalent. Dimethylpyrazine exhibits two other isomers 2,3- and 2,5-dimethylpyrazine. The study aims to establish systematic changes with structural differences of the isomers at identical atom-atom potentials similar to earlier studies on the xylene family [5]. For completeness the study was extended to include 2,3,5-trimethylpyrazine and 2,3,5,6-tetramethylpyrazine.

The spectrometer SV29 was used with a wavelength of incoming neutrons of 1.76A and the second order of diffraction of the graphite monochromator. The elastic energy resolution was 2.2meV. The figure shows 3 of the 4 spectra measured each at a sample temperature T=2.1K. A tentative assignment is based on the fact that the strongest peaks are due to hydrogen with its strong scattering cross section there with methyl librations due to the large amplitude of this motion. The strongest bands are just at the edge of the accessible energy range for all materials. In 2,3-di-, 2,5-di- and 2,3,5-tri-methylpyrazin this peaks are in the regime 18-22meV and are followed by a second peak around 24-27meV. In tetramethylpyrazin such a second peak is not observed. In the lattice regime the 2,3-di- and the tetra-methylpyrazin spectra look rather similar. Librational energies of 20(26)mev are related with rotational potentials of ~80(130)meV amplitude. Corresponding tunnel splittings are much below the energy resolution of backscattering instruments.

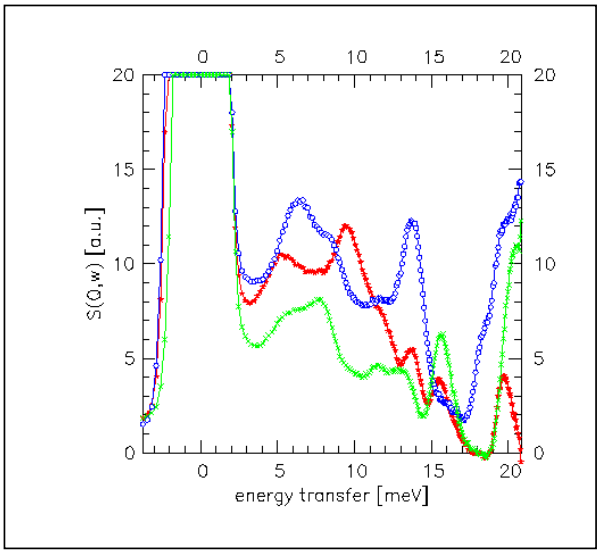

Fig.: spectra of some methyl pyrazines.
Sample temperatures 2.1K
scattering angle ~60°
2,3-dimethylpyrazine(∗)
2,5-dimethylpyrazine(o)
2,3,5,6-tetramethylpyrazine(x)

For further the exploitation of the isotope effect is necessary to get a unique assignment. A determination of the crystal structures could make the start for a computational approach on the basis of molecular interactions.

[1] W. Press, Springer Tracts Modern Phys. 92 (1981) 1
[2] M. Prager and A. Heidemann, Chem. Rev. 97,2933(1997)
[3] B. Nicolaii, E. Kaiser, F. Fillaux, G.J. Kearley, A. Cousson, W. Paulus, Chemical Physics 226 (1998) 1-13
[4] E. Kaiser, B. Nicolaii, W. Paulus, A. Cousson, F. Fillaux, G. Heger, G.J. Kearley, O. Randl, Acta. Cryst. E 57 o1113-o1115, 2001
[5] O. Kirstein, M. Prager, Applied Physics A74,1236(2002)

Institut für Festkörperforschung
Forschungszentrum Jülich GmbH
D-52425 Jülich

Experimental Report
of Neutron Scattering Experiments
at the FRJ-2 Reactor

Proposal number:	S29-02-005		
Experiment title:	**Rotational tunneling in amorphous acetamide: the potential distribution function in a biological material**		
Dates of experiment:	29.4. – 1.5. and 8.7. – 11.7.2002	Date of report:	18.2.2003
Experimental team: Names	Addresses		
M. Prager	Forschungszentrum Jülich		
Local Contact:	M. Prager		

Experimental report text body

Rotational tunnelling is the most sensitive probe for weak changes of rotational potentials. This property is used in recent times to explore the potential distribution function of polymers [1] and other amorphous or disordered materials [2,3]. Similarly the librational bands are modified by disorder.

All systems studied so far suffer from the problem that the potential distribution function is either spoiled by overlap with another component [3] or that only a wing of the potential distribution function scatters into the energy window accessible by the spectrometer [1,2]. A convincing independent proof whether amorphous materials see generally a Gaussian potential distribution function requires a system where a main part of the related distribution of tunneling energies including the maximum are found in the energy regime of the used spectrometer. The existing experience seems to show that the suited material has to have a significant intramolecular hindering barrier like the polymers where the mean potential is little changed with amorphisation. At the same time the potential must be weak enough to show large tunnel splittings. Toluene [2] did not fulfill the first condition and amorphisation led to a huge increase of the rotational barrier.

A recent publication shows [4] that acetamide can be prepared as amorphous material if condensed from the gas directly onto a cold surface. The x-ray structural study [4] claims further that the neighborhood of molecules is very similar to that of the crystalline material. Crystalline acetamide shows a large tunnel splitting of 32 ueV which is mainly intramolecular [5]. On this basis one can expect that the barrier height for methyl rotation does not change drastically. Acetamide as one of the simplest molecules showing the biologically important peptide bond is by itself an interesting subject to study.

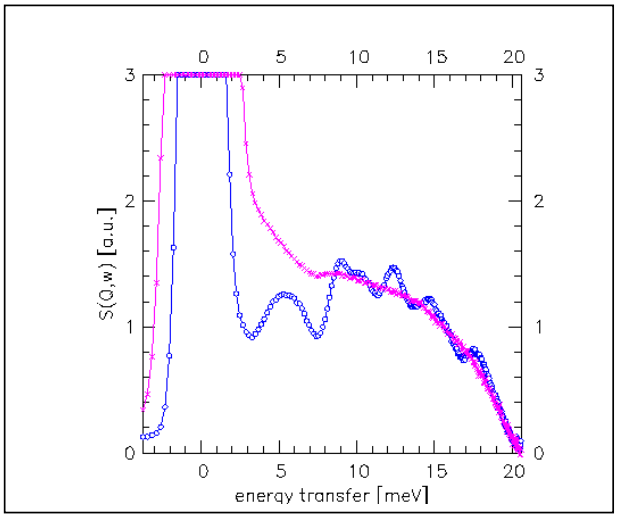

Figure: crystalline acetamide(□), T=4.5K
quenched acetamide(*), T=4.5K

The proposed condensation is successfully repeated using our matrix condensation sample stick. The figure shows the spectrum of the amorphous material (figure,*) in comparison to the crystalline one (figure, □). The phonon density of states of the amorphous material has lost the fine structure of the crystalline one but retains the overall shape. This points towards the claimed [4] microscopic similarity of the two states.

A corresponding expected distribution of tunnel splittings centered around that of crystalline acetamide is not observed, however. Instead – as often [1,2] – an unresolved wing of inelastic intensity is present in the backscattering spectrum (see the corresponding experimental report in this volume). This shows that disorder strengthens the rotational barriers significantly.

[1] J. Colmenero, R. Mukhopadhyay, A. Alegria, B. Frick, Phys. Rev. Lett. 80,2350(1998)
[2] A. Moreno, A. Alegria, J. Colmenero, M. Prager, H. Grimm, B. Frick, J. Chem. Phys. 115,8958(2001)
[3] M. Prager, P. Schiebel, J. Combet, Chem. Phys. 276,69 (2002)
[4] S. Nasr, J. Chem. Phys. 115,6569(2001)
[5] M. Prager, N. Wakabayashi, M. Monkenbusch, Z. Phys. B: Condens. Matter 94,69(1994)

Institut für Festkörperforschung
Forschungszentrum Jülich GmbH
D-52425 Jülich

Experimental Report
of Neutron Scattering Experiments
at the FRJ-2 Reactor

Proposal number:	S29-02-007		
Experiment title:	**Methyl iodide clathrate: probing internal absorption sites by tunneling spectroscopy**		
Dates of experiment:	5.7. – 8.7. and 10.9. – 22.9.2003	Date of report:	18.2.2003
Experimental team: Names	Addresses		
M. Prager	Forschungszentrum Jülich		
Local Contact:	M. Prager		

Experimental report text body

Clathrates are a fascinating class of materials: a framework of matrix molecules forms cages which allow to incorporate simple molecules in identical environments and thus experience the same matrix effect. Therefore spectral lines are usually rather sharp and contain clear information. The combination of different host and guest molecules allows a huge variety of clathrates to be produced. Water clathrates with water soluble guest molecules like tetrahydrofuran can be prepared easily. A recently grown interest concentrates on the methane clathrates [1] which are only stable in a certain pressure-temperature regime. This 'burnable ice' exists in nature and may form one of the largest energy reservoirs on earth. From a fundamental point of view methane represents a prototype of a non polar guest molecule.

CH_3I is an interesting and different probe of the clathrate cages compared to methane because it interacts with the host surface via dipolar interaction. It is not straightforward to incorporate this non water-soluble molecule to form the clathrate. A special preparation technique was developed to make CH_3I x $17H_2O$ [2].The system crystallizes in the cubic II structure with only the large cages filled. We have prepared a new sample by this technique. The formation of the clathrate is controlled by the transformation into a transition gel state and an increase of the melting point of the new material to T_m~4C. Finally, neutron diffraction was applied. All observed Bragg peaks can be indexed according to the cubic II structure.

Different isotopic mixtures of the material were studied by spectroscopy. In the following, results involving a protonated matrix and both, protonated or deuterated guests, are presented. The thermal neutron TOF spectrometer SV29 allows in its actual setup to measure simultaneously with all diffraction orders. With an incoming wavelength λ=1.76A a characteristic double peak (figure 1) in the regime of lattice modes confirms the formation of the clathrate structure. An additional mode characteristic of the methyl iodide is found around 4meV with protonated guest molecules. The spectrum from the first order neutrons (λ=3.52A) shows a shoulder

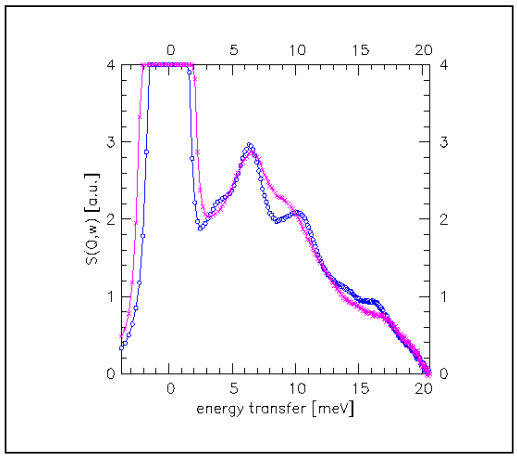

Figure 1: spectra of CH_3I x $17H_2O$ and CD_3I x $17H_2O$. Sample temperature T=4.5K. δE=2.2meV.

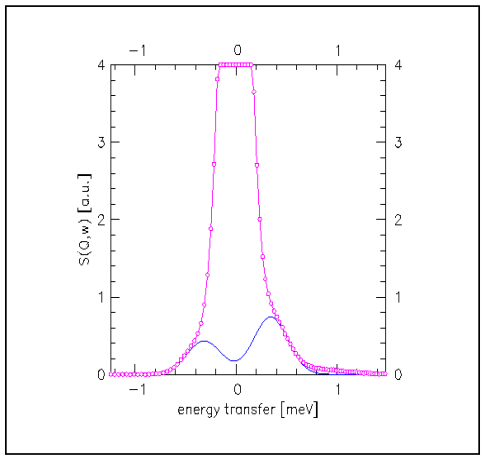

Figure 2: The inelastic wings observed with the 1. order of diffraction. δE=0.33meV.

of the elastic line at 0.36meV (figure 2) which represents almost free rotation of the methyl iodide in the cage. The width of this unresolved lines is clearly larger than the energy resolution of the spectrometer. This indicates either fine structure or disorder.

The tunneling aspect of this material will be further studied in detail using an appropriate cold time-of-flight spectrometer.

[1] C. Gutt, W. Press, A. Hüller, J. Tse, H. Casalta, J. Chem. Phys. **114**,4160(2001)
[2] C. Albayrak, Dissertation, Aachen 1988

Triple-Axis Spectrometer (UNIDAS)

Instrument Parameters

Beam tube:	4H4 radial ∅ 4"
Monochromators:	pyrolytic graphite (002), vertical focusing
Analyzers:	pyrolytic graphite (002), focusing germanium (111)
Filter:	pyrolytic graphite, for incident and/or final beam
Collimators:	15' ... 60' (Rutherford collimators)
Angular range ***- Monochromator:*** ***- Scattering angle:*** ***- Analyzer:*** ***- Sample:***	 $12.5° \le \Theta_M \le 60°$ $-90° \le \Phi \le 130°$ $-75 \le \Theta_A \le 75°$ (with different configurations) $-180° \le \psi \le 180°$ $-180° \le \chi \le 180°$ (with $-180° \le \varphi \le 180°$ Eulerian cradle)
Beam size at specimen:	35 x 90 mm^2
Neutron flux at sample position:	typically 5×10^6 n/cm^2 s
Incident:	$0.8 Å \le \lambda \le 4 Å$
Energy transfer:	$0.02 meV \le \hbar\omega \le 80 meV$
Momentum transfer:	$0.05 Å^{-1} \le Q \le 10 Å^{-1}$
Detector:	^{3}He (8 bar)
Background:	≤ 2 cnts/min
Time resolution for stroboscopic experiments:	$2 ms \le \Delta t \le 200 s$
Sample environment:	goniometer, ±20° tilt; Eulerian cradle; 2 closed-cycle cryostats (10 K ≤ *T* ≤ 300 K); 2 bath cryostats (4 K ≤ *T* ≤ 300 K); 2 standard furnaces (300 K ≤ *T* ≤ 1100 K); 1 special furnace (500 K ≤ *T* ≤ 1800 K); 2 four-circle furnaces (300 K ≤ *T* ≤ 1300 K) ; furnace for uniaxial (periodic) pressure; automatic temperature control

Instrument Responsible

Dr. Andreas Hoser Tel. +49-(0)2461-61-4762 Email: a.hoser@fz-juelich.de

Institut für Festkörperforschung
Forschungszentrum Jülich GmbH
D-52425 Jülich

Experimental Report
of Neutron Scattering Experiments
at the FRJ-2 Reactor

Proposal number:	UDS-01-007		
Experiment title:	**Dimensionality crossover in $KNiF_3$**		
Dates of experiment:	30.01. – 03.02.	Date of report:	26.02.2003
Experimental team: Names	Addresses		
U. Köbler A. Hoser	IFF		
Local Contact:	A. Hoser		

Experimental report text body

The standard behaviour for the temperature dependence of the (normalized) magnetic order parameter, $m_s(T)$, consists in a crossover from the $T \rightarrow 0$ critical power function

$$m_s(T) = 1 - c * T^{\varepsilon} \qquad (1)$$

to the $T \rightarrow T_c$ critical power function

$$m_s(T) \sim (T-T_c)^{\beta} \qquad (2)$$

at the intersection of the two functions which is normally at about $0.85T_c$ [1].
The empirical values for the critical exponents ε for $T \rightarrow 0$ are now well known [2]. Table I illustrates how the exponent ε depends on the spin quantum number and on the dimensionality of the relevant interactions.

Table I

exchange interactions		integer spin	half - integer spin
3D		$T^{\frac{9}{2}}$	T^{2}
2D	3D anisotropic	T^{2}	$T^{\frac{3}{2}}$
1D	2D anisotropic	T^{3}	$T^{\frac{5}{2}}$

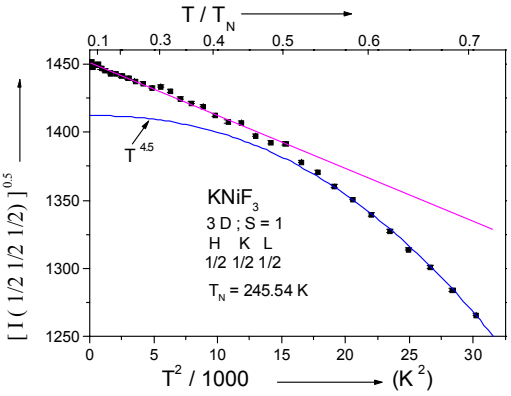

It should be noted that the critical exponents ε and β are independent of the spin order type.

There can be more crossover events than only that one between eq.(1) and eq.(2). In materials with a strong exchange anisotropy a lattice distortion can occur. Many cubic materials are known to undergo a trigonal lattice distortion due to an anisotropic exchange striction. NiO is one well known example for this [3]. An anisotropic exchange striction can change the interactions from isotropic to anisotropic and can induce a change of the universality class, i.e. an exponent crossover to the next lower line in Table I. Since lattice distortions are continuous processes [3] a threshold value must exist for a thermodynamic crossover to occur.
$KNiF_3$ with S=1 due to the Ni^{2+} ion belongs to the class of materials showing an exponent crossover. We have measured the antiferromagnetic order parameter on account of the 1/2,1/2,1/2 superstructure reflection intensity. Fig.1 shows the results for the antiferromagnetic order parameter on a T^2 scale. It can be seen that the $T^{9/2}$ law for isotropic interactions holds over a large temperature range but that at about 130 K a crossover to a T^2 law is noticed. The T^2 law is typical for anisotropic 3D interactions and integer spin value. We must, hence, assume that in $KNiF_3$ a magnetostrictive lattice distortion occurs similar as for NiO. Those lattice distortions are small effects and difficult to detect but they change the exchange interactions appreciably.

[1] U.Köbler, A.Hoser and D.Hupfeld: Physica B (2003) in press.
[2] U.Köbler, A.Hoser, J.Englich, A.Snezhko, M.Kawakami, M.Beyss and K.Fischer: J. Phys. Soc. Japan **70** (2001) 3089.
[3] L.C.Bartel and B.Morosin: Phys. Rev. B **3** (1971) 1039.

Institut für Festkörperforschung
Forschungszentrum Jülich GmbH
D-52425 Jülich

Experimental Report
of Neutron Scattering Experiments
at the FRJ-2 Reactor

Proposal number:	UDS-01-010		
Experiment title:	**CEF-phonon interaction in the orthorhombic compound NdCu2**		
Dates of experiment:	14.01.2002 – 20.01.2002	Date of report:	06. 03. 2003
Experimental team: Names	K. Hense Addresses		
	[1)]Inst. f. Festkörperphysik, TU Wien, Wiedner Hauptstr. 8-10 A 1040 Wien		
Local Contact:	A. Hoser		

Experimental report text body

(Please use 12 pt letters here !)
Investigations of the lattice dynamic as well as of the crystal electric field (CF) excitations have been studied in many details in the last decades for a quite large number of rare earth intermetallics. These results are discussed in most of the cases based on the assumption that the interaction among the lattice dynamic and the crystal electric field is negligible small.
The arguments given are: The CF-phenomena typically one particle excitations, whereas in the case of phonons, there are some 10^{20} particles participating one is speaking of a collective phenomena. Furthermore according to Born - Oppenheimer approximation electronic transitions are much faster than the lattice vibrations.

However, in the orthorhombic RCu_2 compounds with light rare earth elements (e.g. Ce, Nd) both phenomena (lattice dynamic and CF) show anomalous properties which can hardly be understood unless assuming an interplay of the lattice vibrations and the CF excitations [1]. As an example: It has been observed that in case of $CeCu_2$ one of the three CF excitations is missing in the experiment although from theoretical point of few the intensity of these interaction should be easily measurable [2]. In $NdCu_2$ phonons with a special symmetry (capable to couple to the crystal electric field) show an unexpected strong softening when increasing the temperature. A closer inspection of these phenomena revealed that both observations can be explained when assuming an accordingly strong interaction of the lattice dynamic and the CF excitations in these group of compounds [3].

In order to study whether the softening of these phonon branches in $NdCu_2$ is driven by an interaction of the phonons with the CF, we studied the temperature dependence of the corresponding phonon branches in the isostructural, nonmagnetic YCu_2, where no CF exits, since that Y has no 4f electrons.
All these investigations of the lattice dynamic and the CF excitations have been performed using the UNIDAS spectrometer at FZ Jülich.

The figure shows a comparison of the temperature dependence of the lowest optical phonon mode (A_g mode) at the centre of the Brillouin Zone of $NdCu_2$ and YCu_2. As can be seen a much stronger temperature dependence in of $NdCu_2$ .This is why we assume that in $NdCu_2$ phonon - CF interaction is strong enough to be seen in the experiment and that the phonon softening in this kind of substances is driven by an interaction of the phonons with the CF.

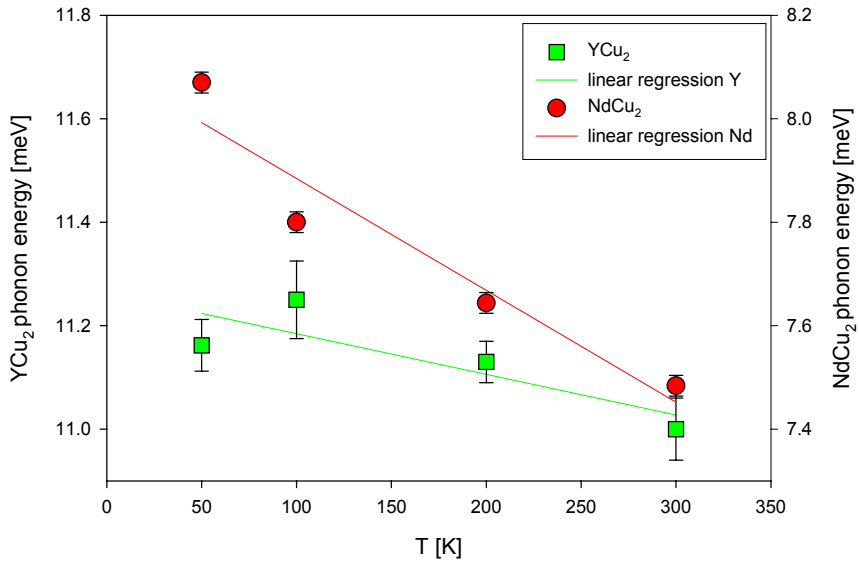

Comparison of the temperature dependence of the lowest optical phonon branch (A_g-mode) in YCu_2 and $NdCu_2$.

[1] Hense K, Gratz E, Nowotny H, Hoser A, Witte U, Löwenhaupt M, in *Crystal Field-Phonon interaction in $NdCu_2$*; to be published
[2] Loewenhaupt M, Prager M, Gratz E, Frick B in *Magnetic Excitations in $CeCu_2$*
J. Magn. Magn. Mat. **76 - 77** (1988) 415 – 416
[3] Hense K, PhD Thesis, TU Wien 2002
[4] Gratz E, Loewenhaupt M, Divis M, Steiner W, Bauer E, Pillmayr N, Müller H, Nowotny H, Frick B in *Structural, Magnetic, Electronic and Transport Properties of $NdCu_2$*
J. Phys. Cond. Matter **3** (1991) 9297 - 9318

Institut für Festkörperforschung
Forschungszentrum Jülich GmbH
D-52425 Jülich

Experimental Report
of Neutron Scattering Experiments
at the FRJ-2 Reactor

Proposal number:	UDS-01-011		
Experiment title:	**Phonon Dispersion in YCu_2**		
Dates of experiment:	March 2002	Date of report:	March 2003
Experimental team: Names	K. Hense, E. Gratz Addresses		
	Inst. f. Festkörperphysik, TU Wien, Wiedner Hauptstr. 8-10 A 1040 Wien		
Local Contact:			

Experimental report text body

(Please use 12 pt letters here !)
The intermetallic RT_2 compounds with R=rare earth and T=transition metals (Mn, Fe, Co, and Ni) or Al crystallize in the cubic Laves phase type structure (space group Fd3m), with a few exceptions in the RMn_2 series (R=Dy, Ho, Er, Tm) which crystallize in the hexagonal Laves phase type structure.
The physical properties of these Laves phase compounds have been studied in the last four decades in many details, mainly because of the large variety of magnetic phenomena for which these intermetallics are known.
When proceeding in the periodic table, the compounds with Cu do not show the Laves phase structure, but crystallize in the orthorhombic $CeCu_2$-type structure (space group Imma). Recently a number of investigations have been published concerning the properties of the RCu_2 series. Mainly investigations of the magnetic properties, such as magnetic phase diagram studies have been done.
In contrast to the cubic 1:2 intermetallics, a systematic study oft the lattice dynamics for the low symmetric orthorhombic 1:2 compounds does not exist, at least to our knowledge.

The phonon dispersion relation of YCu_2 has been studied in the scope of the diploma thesis of K. Hense (TU Vienna[1]). These investigations of the lattice dynamic have been performed using the UNIDAS spectrometer at FZ Jülich.

The spectrometer was used in the 'zig zag' configuration having optimal condition for measurements of the transverse acoustic phonons. For the low energy part of the acoustic phonons, constant energy scans were made, otherwise constant Q-scans. For the low lying optical phonon branches k_i=2.66 $Å^{-1}$ was used, for the higher optical phonon branches k_i=3.62 $Å^{-1}$ has been chosen. The quality of the YCu_2 crystal used for these sort

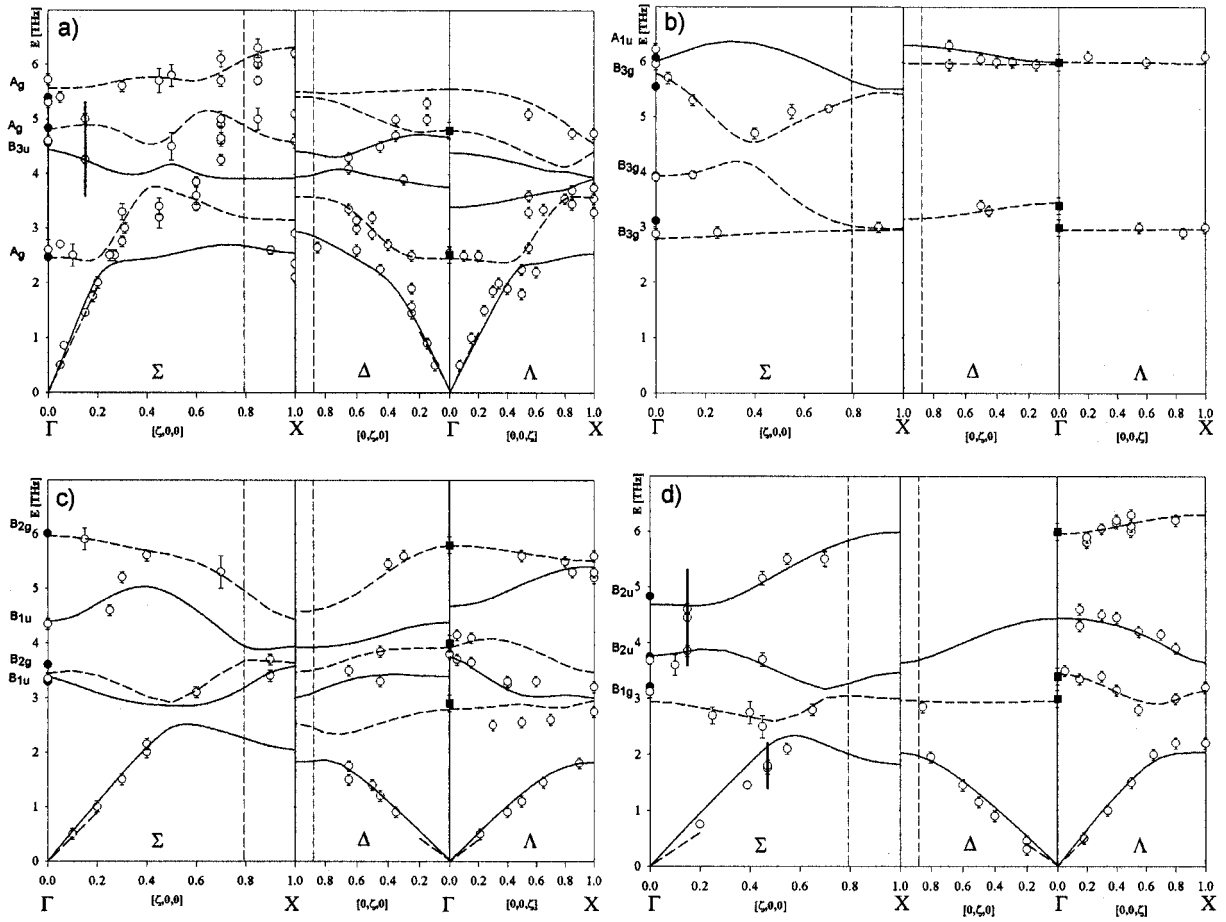

of experiments was checked by measuring the Rocking curves on the(200) - and (002)-Bragg reflections. A weak shoulder on the flank of the (200) peak has been found which is obviously caused by a twinning of a small part in the sample material, whereas the Rocking curve on the (002) Bragg reflection was ideal.

The measured phonon dispersion relation, as well as the Born - von Karman fit (line through the data points) are shown in the figure.
These investigations served as a kind of a pre-experiment for our study of the lattice dynamic in the magnetic $NdCu_2$ compound and the study of the phonon – crystal field interaction in this compound.

Phonon dispersion of YCu_2

[1] Hense K; diploma thesis, TU Wien (1999)
[2] Hense K, Gratz E, Lindbaum A, Michor H, Nowotny H, Güthoff F, Hoser A, Knoll P, in: *Lattice dynamics of YCu_2,* J. Alloys and Compounds 349 (2003) 28-36

Institut für Festkörperforschung
Forschungszentrum Jülich GmbH
D-52425 Jülich

Experimental Report of Neutron Scattering Experiments at the FRJ-2 Reactor

Proposal number:	UDS-02-002		
Experiment title:	Quality check and adjustment of mosaic spread for highly oriented pyrolytic graphite crystals for the backscattering spectrometer RSSM for the FRM-II		
Dates of experiment:	09.09. - 21.09. 18.10 - 27.10.	Date of report:	19.02.03
Experimental team: Names	Addresses		
M. Prager, P. Rottländer, O. Kirstein, T. Kozielewski	Forschungszentrum Jülich GmbH IFF 52425 Jülich Germany		
Local Contact:	A. Hoser		

Experimental report text body

The thermal triple-axis spectrometer (UNIDAS) at the Jülich FRJ-2 reactor was used for quality check and adjustment of the mosaic spread of 220 highly oriented pyrolytic graphite crystals (PG002) which are needed for the phase-space-transformation-chopper [1] of the backscattering spectrometer RSSM [2] for the FRM-II reactor. The crystals used should exhibit a mosaic spread of 2.5(±0.5) deg (FWHM). Since it seems to be difficult to obtain the desired mosaic spread (due to manufacturing processes) we characterised not only the quality of the delivered 340 crystals but also we adjusted crystals which were out of the tolerance required for our purposes in co-operation with Advanced Ceramics Corporation as described in U.S. Patent 5798075. This was a iterative procedure: A crystal had to be characterised first. If this crystal did not fall within the defined mosaic range, it was texturing or smoothing at room temperature using a hand –pumped hydraulic press. Afterwards the crystal had to be checked again. This procedure was repeated until its FWHM fell into the desired range.

The first two days were used to setup the spectrometer as well as getting a “feeling” for the pressing procedure (amount of time, pressure). After that we were able to check and adjust 40 crystals per day.

It was the main goal to raise the mosaic spread of crystals with low mosaic spread into the 2-3°range and preferably above the mean value of 2.5°. For this purpose the quality of crystals was deteriorated by deforming the crystals under load between two metal nets. Most of the work was to press in the second step between smooth dies to bring the mosaic spread back down to the desired range. The force required for this operation had to be varied (300 – 800 kg), generally it was much smaller than that used in texturing (1500 – 4000 kg).

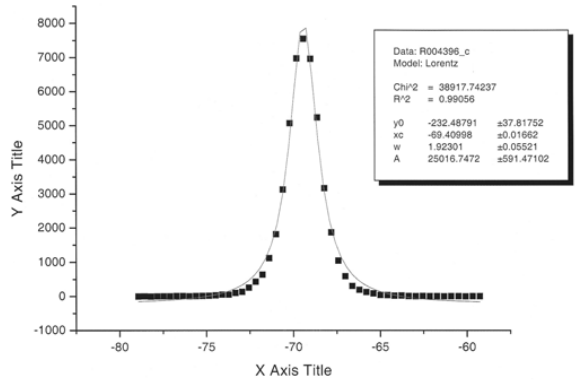

Fig. 1

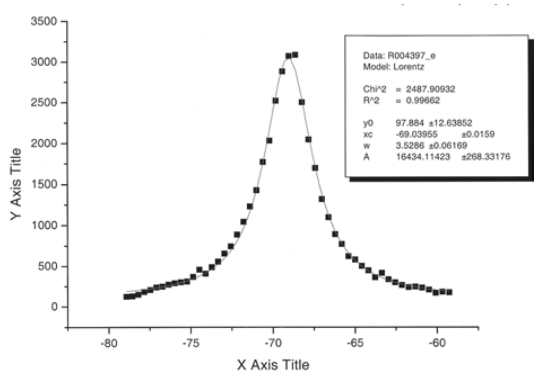

Fig. 2

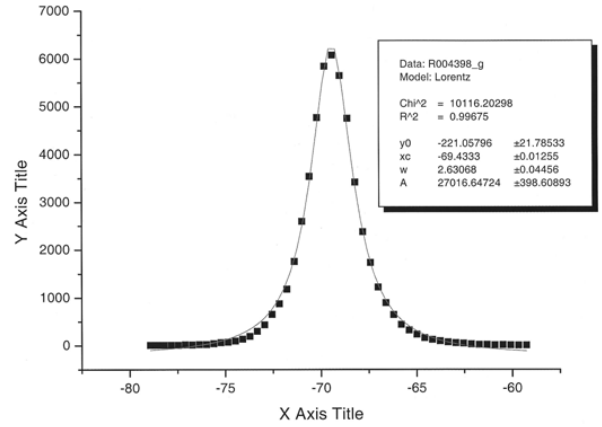

Fig.3

Example: A peace of HOPG with initial neutron mosaic spread of 1.92° (Fig.1) was pressed with pads of wire cloth (24 x 24 mesh) at 3000 kg for a few seconds. After this texturing, the neutron mosaic spread of the HOPG was 3.53° (Fig.2). Finally the HOPG-crystal was smoothed to 2.63° at 600kg (Fig. 3) .

Using the above described procedure we were able to complete the required number of HOPG-crystals for our phase-space-transformation-chopper of the backscattering spectrometer.

[1] http://iffwww.iff.kfa-juelich.de/rssm/
[2] J. Schelten, B. Alefeld, in: R. Scherm, H. H. Stiller (Hrsg.), Proceedings of the Workshop on Neutron Scattering Instrumentation for SNQ, Report Jül-1954, FZ Jülich, 1984

Institut für Festkörperforschung
Forschungszentrum Jülich GmbH
D-52425 Jülich

Experimental Report
of Neutron Scattering Experiments
at the FRJ-2 Reactor

Proposal number:	UDS-02-004		
Experiment title:	**On the temperature dependence of the magnetic excitations in terbium**		
Dates of experiment:	29.10. - 04.11. 10.12. - 18.12.	Date of report:	05.03.2003
Experimental team: Names	Addresses		
A. Hoser U. Köbler	IFF		
Local Contact:	A. Hoser		

Experimental report text body

Classical spin wave theories predict a $T^{3/2}$ dependence for the thermal decrease of the ferromagnetic order parameter and a $T^{5/2}$ dependence for the thermal decrease of the magnetic excitations, i.e. the spin wave stiffness constant D(T), in first approximation. These predictions have never been confirmed experimentally in a convincing way.
The classical spin wave theory does not consider that T=0 is a quantum critical point [1]. Experiments show that on approaching T→0 the temperature dependence of the order parameter is given to a good approximation by a single power function of the absolute temperature. This is the typical behaviour in the vicinity of a singular point. Table I compiles the empirical critical exponents ε for the T^{ε} power law for T→0. It should be noted that the exponents ε are independent of the spin order type and independent of the symmetry of the lattice provided the dimensionality of the relevant interactions is constant [2].

Table 1

exchange interactions	integer spin	half - integer spin
3D	$T^{\frac{9}{2}}$	T^{2}
2D 3D anisotropic	T^{2}	$T^{\frac{3}{2}}$
1D 2D anisotropic	T^{3}	$T^{\frac{5}{2}}$

The power laws of Table I hold also in the presence of a magnon energy gap. Terbium is a typical example for this. Terbium is one of the few ferromagnets with an integer quantum number (J=6) according to the configuration $^7F_6$. Although an appreciable single ion anisotropy (crystal field splitting) is observed in the paramagnetic phase the saturation moment for T→0 conforms to the free ion value. This is because the exchange interactions are five times larger than the crystal field splitting.

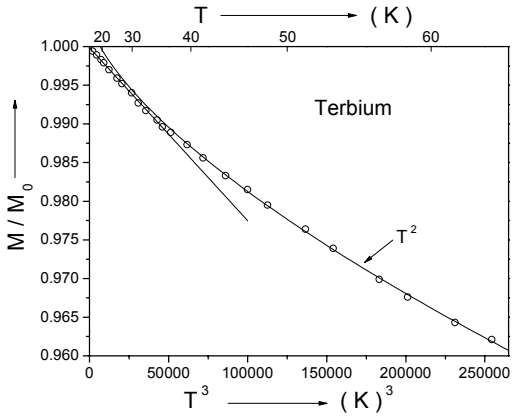

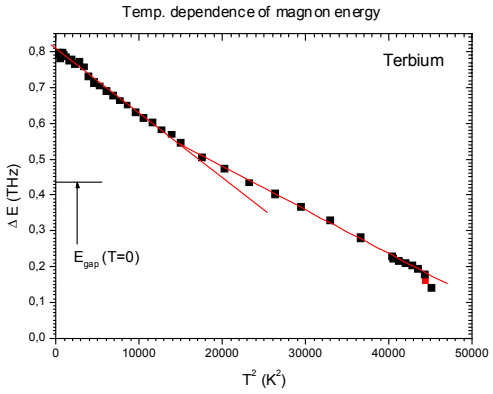

The only effect of the orbital moment is to make the exchange interactions anisotropic. This reveals from measurements of the spontaneous magnetization. Fig.1 shows our normalized spontaneous magnetization data in the temperature range where the crossover from the low temperature T^3 law to the high temperature T^2 law occurs. The magnon energy gap is Eg= 21K for T→0 but nevertheless a pure T^3 law is observed.
Inspection of the literature indicates that the magnetic excitations decrease with the same temperature power function as the order parameter (Table I). In other words, there is only one type of temperature function for all quantities. The shape of the magnon dispersion is therefore unimportant. However, very little detailed experimental information on the temperature dependence of the magnetic excitations is available.
We have therefore performed inelastic neutron scattering measurements on a Terbium single crystal in order to test the hypothesis of an identical temperature dependence. Fig.2 shows preliminary results. These data can be described by two T^2 functions with an amplitude crossover. This crossover is also seen in the spontaneous magnetization. As a conclusion, order parameter and magnetic excitations show the same T^2 dependence.

[1] J.A.Hertz: Phys. Rev.B **14** (1976) 1165.
[2] U.Köbler, A.Hoser, J.Englich, A.Snezhko, M.Kawakami, M.Beyss and K.Fischer: J. Phys. Soc. Japan **70** (2001) 3089.

Institut für Festkörperforschung
Forschungszentrum Jülich GmbH
D-52425 Jülich

Experimental Report
of Neutron Scattering Experiments
at the FRJ-2 Reactor

Proposal number:	UDS-02-005		
Experiment title:	**Reflectivity and Profile Analysis of Cu-(220) monochromator crystals**		
Dates of experiment:	18.-20.12.2002	Date of report:	20.1.2003
Experimental team: Names	Addresses		
Dr. Martin Meven	ZWE FRM-II, TU München Lichtenbergstraße 1 85747 Garching		
Local Contact:	Dr. Andreas Hoser		

Experimental report text body

The reflectivity and reflection profiles of two Cu-(220) plates (thickness 8 mm, about 200 mm height, about 15 mm width) were tested to determine the optimum direction for cutting them into slices of about 14 mm height and 120 mm length for a focussing monochromator. To achieve a suitable bragg angle for the crystals, the lambda/2-radiation of UNIDAS of about 1.18Â was used.

Five data sets were taken (each of 36 data points (36+15) for no. 1):

- Crystal no. 1, side A, mark left, I(int)=80598 cps, FWHM=0.051°
- Crystal no. 1, side A, mark up, I(int)= 105368 cps, FWHM=0.057°
- Crystal no. 1, side B, mark up, I(int)=90829 cps, FWHM=0.057°
- Crystal no. 2, side A, mark left, I(int)=103753 cps, FWHM=0.056°
- Crystal no. 2, side A, mark up, I(int)=104756 cps, FWHM=0.058°

The intensities and FWHM given above are the mean values from the data points taken for each data set. Data analysis shows that the distributions around the mean values are much more inhomogeneous for crystal no. 2. Furthermore, the orientation of the crystal around the bragg-vector is crucial for its diffraction properties as can be seen for the two orientations of crystal no.1, side A. For illustration the figures show the integrated intensities and FWHM's of crystal no. 1, side A, mark up and crystal no. 2 side A, mark left. The figures of crystal no. 2 yield a rather poor correlation between the integrated intensities and FWHMs. This underlines the fact that the description of a high quality monochromator crystal cannot be reduced to the plain value of its intensity or FWHM only.

In summary, crystal no. 1 is the most suitable for a monochromator device if using the orientation "side A, mark up".

Cu-(220)-Kristall 1 Seite A oben, Messung Unidas 2002

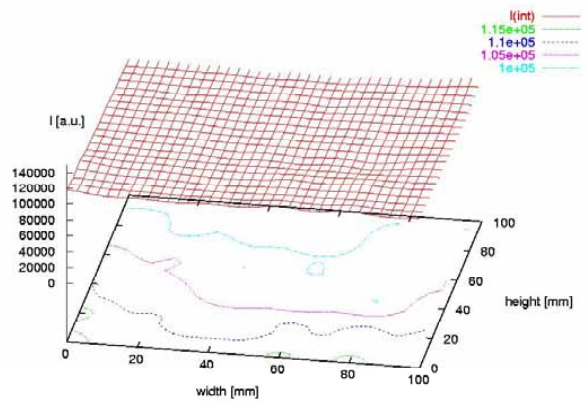

Cu-(220)-Kristall 1 Seite A oben, Messung Unidas 2002

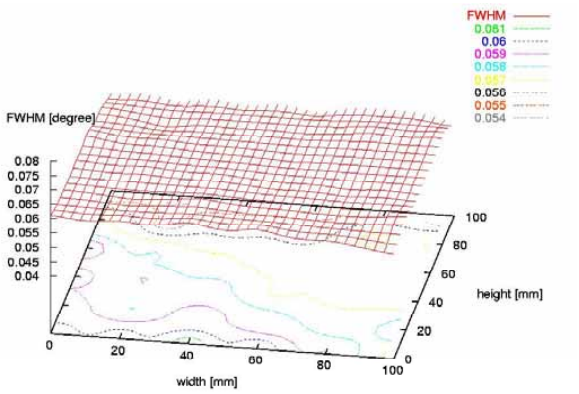

Cu-(220)-Kristall 2 Seite A links, Messung Unidas 2002

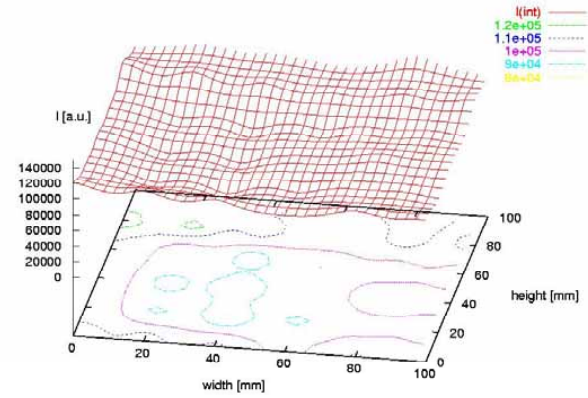

Cu-(220)-Kristall 2 Seite A links, Messung Unidas 2002

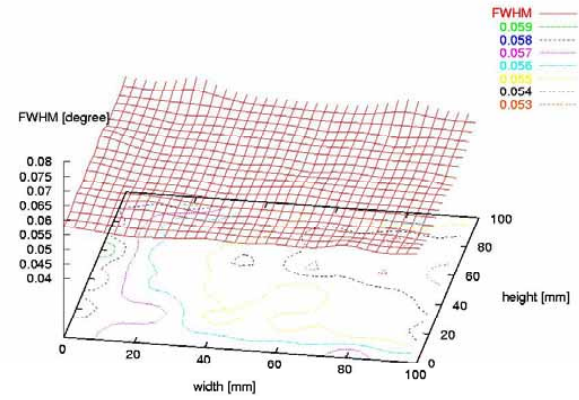

Institut für Festkörperforschung
Forschungszentrum Jülich GmbH
D-52425 Jülich

Experimental Report
of Neutron Scattering Experiments
at the FRJ-2 Reactor

Proposal number:	UDS-02-006		
Experiment title:	Reflectivity and Profile Analysis of four PG analyser crystals		
Dates of experiment:	27.11.2002	Date of report:	20.1.2003
Experimental team: Names	Addresses		
Dr. Martin Meven	ZWE FRM-II, TU München Lichtenbergstraße 1 85747 Garching		
Local Contact:	Dr. Andreas Hoser		

Experimental report text body

Four crystals of pyrolytic graphite (short: PG) with a size of 30*50 mm² of the reflecting (002) plane and a thickness of 2 mm were tested at **k**=2.667/Â. The reflection profiles of the (002) reflection were taken from the front planes of all four crystals and of the back planes of the crystals no. 3 and no. 4. All crystals show a homogeneous gauss-like profile. The integrated intensities vary from 4182(82) cps for crystal no. 1 to 4698(92) cps for crystal no. 4. This yields a mean standard deviation of about 4.7% from the mean value of 4447.5 cps. The FWHM of all four crystals are very similar with a mean value of about 0.66 degree. The differences between front planes and back planes are noticeable only for crystal no. 3. For crystal no. 4 there is no significant difference at all. For further details see figure No. 1.

Summary: The crystals no. 3 and 4 are slightly better concerning reflectivity, all crystals are suitable for the intended application (analyzer crystals).

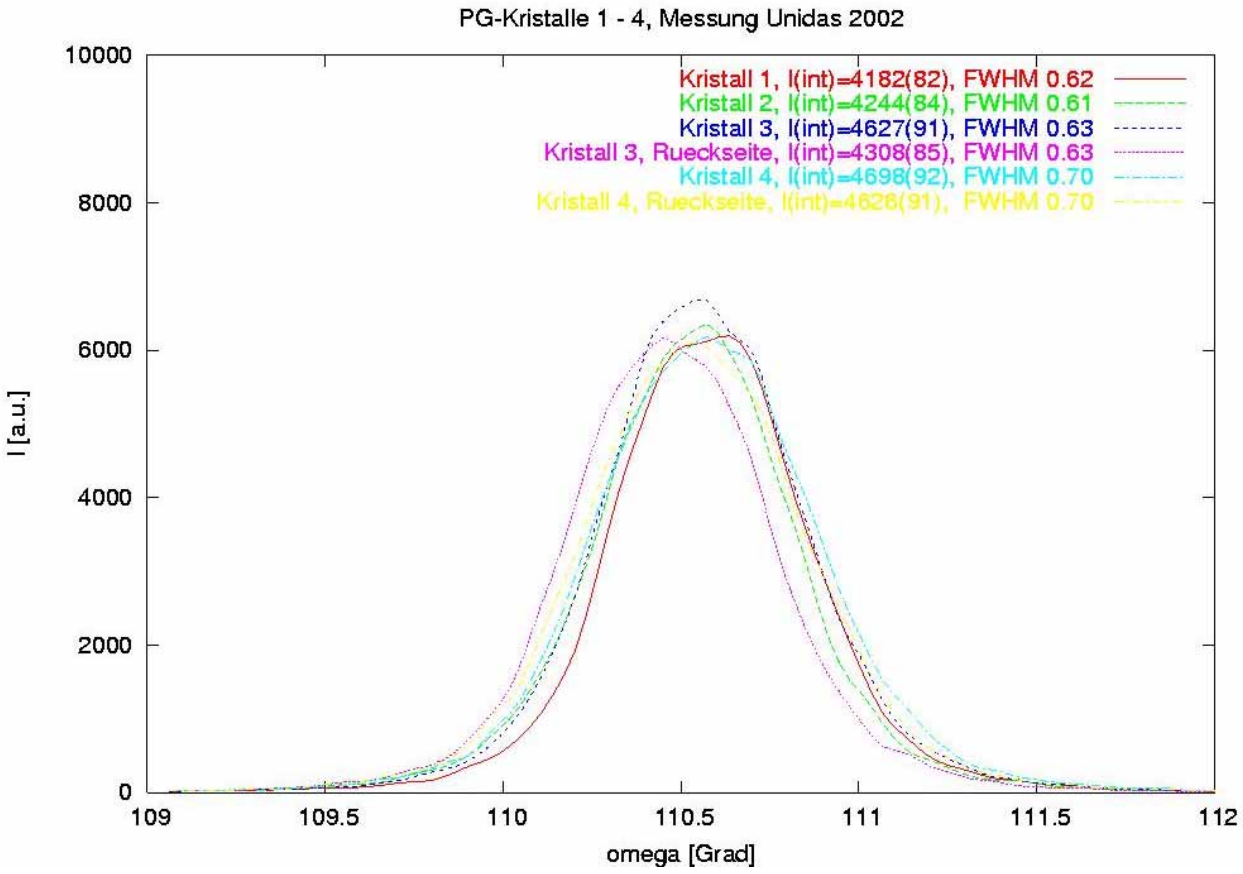
PG-Kristalle 1 - 4, Messung Unidas 2002
Kristall 1, I(int)=4182(82), FWHM 0.62
Kristall 2, I(int)=4244(84), FWHM 0.61
Kristall 3, I(int)=4627(91), FWHM 0.63
Kristall 3, Rueckseite, I(int)=4308(85), FWHM 0.63
Kristall 4, I(int)=4698(92), FWHM 0.70
Kristall 4, Rueckseite, I(int)=4626(91), FWHM 0.70
I [a.u.]
omega [Grad]
10000
8000
6000
4000
2000
0
109
109.5
110
110.5
111
111.5
112

Institut für Festkörperforschung
Forschungszentrum Jülich GmbH
D-52425 Jülich

Experimental Report
of Neutron Scattering Experiments
at the FRJ-2 Reactor

Proposal number:	UDS-02-007		
Experiment title:	**Thermodynamics of the ferromagnetic order parameter of $NdAl_2$**		
Dates of experiment:	04.03 – 10.03.2002	Date of report:	26.02.2003
Experimental team: Names	Addresses		
U. Köbler A. Hoser	IFF		
Local Contact:	A. Hoser		

Experimental report text body

For many transition element compounds with a quenched orbital moment and a well defined spin quantum number it was observed that the thermal decrease of the (normalized) magnetic order parameter is given to a good approximation by a single power function according to:

$$m_s = 1 - c * T^{\varepsilon} \qquad (1)$$

Normally, this power law holds up to the critical range at about $0.85T_c$ where the analytical change (crossover) to the well known critical power law

$$m_s \sim (T_c - T)^{\beta} \qquad (2)$$

occurs. The standard behaviour of the magnetic order parameter is therefore given by the two functions of eqs.(1) and (2) with a crossover at the intersection of these functions.
The fact that a single power function seems to be exact also for $T \rightarrow 0$ conforms to the view that T=0 is a singular point similar as $T=T_c$. In the vicinity of those poins simple power functions hold over a finite temperature range.
Based on systematic studies of many transition element compounds the critical exponents ε for the $T \rightarrow 0$ power law are now all known [1]. Table I compiles the critical exponents ε.

Table I

exchange interactions	integer spin	half - integer spin
3D	$T^{\frac{9}{2}}$	T^{2}
2D 3D anisotropic	T^{2}	$T^{\frac{3}{2}}$
1D 2D anisotropic	T^{3}	$T^{\frac{5}{2}}$

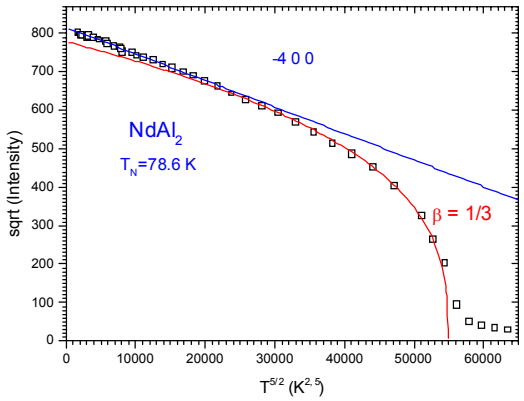

It should be noted that the critical exponents ε are like the conjugated critical exponents β independent of the spin order type. They are different for integer and half-integer spin quantum numbers and, of course, they are different for the different dimensionalities of the relevant interactions.

In order to test whether the universality scheme of Table I applies also for materials with a finite orbital moment we have performed neutron scattering measurements on a single crystal of ferromagnetic $NdAl_2$. Note that in zero field neutron scattering measurements all demagnetization problems are avoided.
In this intermetallic alloy the neodymium can be assumed to be in the Nd^{3+} state with the electronic configuration $^4I_{9/2}$ meaning that S=3/2, L=6 and J=9/2. The resulting moment is therefore half-integer. Due to an orbital moment of L=6 the magnetic interactions can be anisotropic even for this cubic material. Moreover, anisotropic magnetostriction is possible.

Fig.1 shows our results for the temperature dependence of the ferromagnetic order parameter (square root of the 400 scattering intensity after subtraction of the nuclear contribution). These data are plottet vs. $T^{5/2}$. It can be seen that the two fit functions with a critical exponent for $T \rightarrow 0$ of $\varepsilon=5/2$ and a critical exponent for $T \rightarrow T_C$ of $\beta=1/3$ describe the data excellently.

exchange interactions	integer spin	half - integer spin
3D	$\beta = \frac{4}{11}$	$\beta = \frac{1}{2}$
2D	$\beta = \frac{1}{8}$	$\beta = \frac{1}{8}$
1D	$\beta = \frac{1}{3}$	$\beta = \frac{1}{3}$

tabellenurl.opj

Although these two conjugated critical exponent values are consisten with each other as can be seen by a comparison of Table I and Table II a strong uniaxial magnetostriction must be assumed to explain the one-dimensional thermodynamics in this nominally cubic ferromagnet.

[1] U.Köbler, A.Hoser, J.Englich, A.Snezhko, M.Kawakami, M.Beyss and K.Fischer: J. Phys. Soc. Japan **70** (2001) 3089
We thank E.Gratz, TU-Wien for providing us with the $NdAl_2$ single crystal.

High Resolution Backscattering Spectrometer (BSS)

Instrument Parameters

Beam tube:	NLI, cold neutrons, straight guide, 10 cm (height) × 7 cm (width)
Beam size at sample:	3.5 cm × 3.5 cm
Neutron flux at sample:	10^4 n/cm^{2}s
Background:	≈ 8 counts/h
Monochromators:	Si(111), $Si_{0.9}Ge_{0.1}$(111)
Analyser:	Si(111)
Detectors:	nine ^{3}He counters, one ^{3}He monitor
Incident energy:	2.08 meV Si(111), 2.07 meV $Si_{0.9}Ge_{0.1}$ (111)
Incident wavelength:	6.271 Å Si(111), 6.30 Å $Si_{0.9}Ge_{0.1}$ (111)
Energy transfer range:	–15 ... 15 µeV Si(111), –29 ... 1 µeV $Si_{0.9}Ge_{0.1}$ (111)
Energy resolution (FWHM):	1.2 ... 2.4 µeV Si(111), ≈ 2 µeV $Si_{0.9}Ge_{0.1}$ (111)
Elastic Q-range:	0.2 ... 1.9 Å^{-1}
Q-resolution:	0.05 Å^{-1} ... 0.25 Å^{-1}
Sample environment	orange cryostat 1.4 ... 300 K; closed cycle cryostat 12 ... 350 K; cryofurnace 80 ... 750 K; furnace 300 ... 1900 K

Instrument Responsible:

Dr. Hans Grimm Tel. +49-(0)-2461-61-4749 Email: h.grimm@fz-juelich.de
Dr. Stefan Kahle Tel. +49-(0)-2461-61-6394 Email: st.kahle@fz-juelich.de

Institut für Festkörperforschung
Forschungszentrum Jülich GmbH
D-52425 Jülich

Experimental Report
of Neutron Scattering Experiments
at the FRJ-2 Reactor

Proposal number:	BSS-01-007		
Experiment title:	**Methyl group rotation in trimethylindium and dimethylethylamine alane**		
Dates of experiment:	22.4.02 – 26.4.02	Date of report: 3.03.03.03	18.2.2003
Experimental team: Names	Addresses		
Michael Prager Hans Grimm S. Kahle	Forschungszentrum Jülich Forschungszentrum Jülich Forschungszentrum Jülich		
Local Contact:	H. Grimm, S. Kahle		

Experimental report text body

Organometallic compounds represent one of the major classes of materials. Since these materials inherently contain methyl groups, rotational tunneling spectroscopy is a suitable tool for their investigation. Group III trimethyl metal compounds have gained special interest due to their technical applications. The vicinity to the semiconducting elements in the periodic system and the instability of the materials make them an important starting material for doping Si or Ge with B, Al, Ga, In and Tl by thermal decomposition of the respective trimethyl metal molecules at the hot semiconductor surface.
The investigation of the In-compound is an extension of the so far studied homologuous materials $Al(CH_3)_3$ and $Ga(CH_3)_3$. $Al(CH_3)_3$ shows a low temperature crystal structure with space group C2/c and dimers $Al_2(CH_3)_6$ with 3 inequivalent methyl groups as the building units of the molecular crystal [1]. According to literature [2] $In(CH_3)_3$ at room temperature consists of layers of a 2-dimensional molecular networks of tetramers. Like in trimethyl aluminum there are 3 inequivalent methyl groups of which one acts as weak bridge to another molecule. A recent X-ray crystallographic study has shown that the system undergoes a phase transition around 70K. The low temperature unit cell contains 6 inequivalent methyl groups like in the low temperature crystal structure of $Ga(CH_3)_3$ [3].
The backscattering spectrometer was used both in its offset- and centered-configuration. Fig.1 shows the evolution of tunneling spectra in the temperature range 4K....28K for the offset-configuration (monochromator=$Si_{0.9}Ge_{0.1}$, range=,-32μeV....3μeV, resolution=1.8 μeV). Whereas three tunneling bands are well resolved, the existence of a fourth band is indicated by comparison with the resolution curve (Vanadium). In Fig.2 the similar temperature range is investigated in the centered configuration (monochromator=Si, range=,-17μeV....17μeV, resolution=1.3 μeV). The presence of the fourth band is now clearly recognizable as a shoulder. The fourth band represents the remaining three methyl groups, since, at the lowest sample temperature, the four tunneling bands approach intensity ratios of about1:1:1:3.

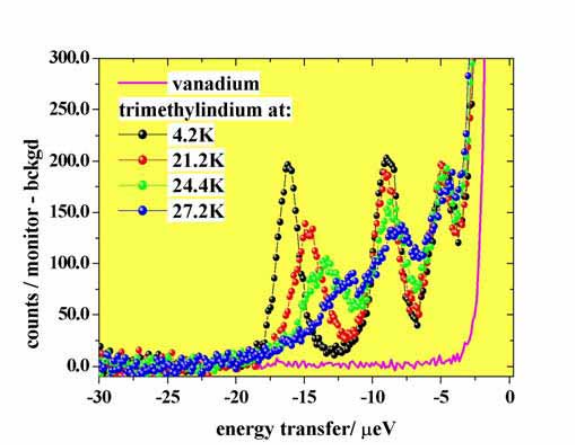

Fig 1 trimethylindium measured with SiGe-monochromator

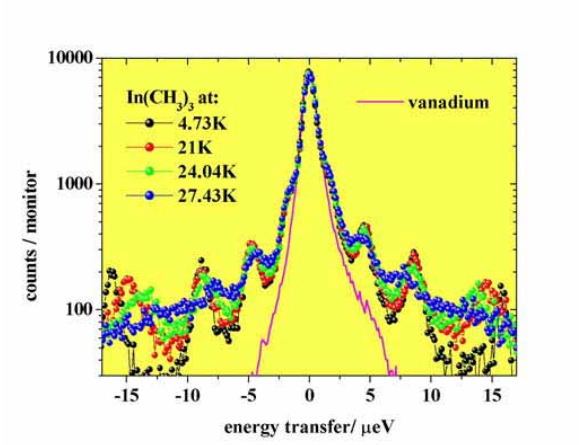

Fig.2 trimethylindium measured with Si-monochromator

Rotational potentials are a link between experiment and the ab-initio understanding of a system. On the one hand they can be calculated from the fundamental intermolecular interaction potentials on the basis of the crystal structure. Experimentally they are derived within the single particle model of rotational tunneling from the measured characteristic rotational energies. To get reliable results in a multi rotor system like $In(CH_3)_3$ tunneling and librational transition energies and barrier heights have to be combined correctly. To avoid as much as possible a wrong combination we proceed according to the following rules:
1) If resolved, the tunnel splitting is used as the most safe and exact information.
2) If possible, librational modes are taken from the broadening of these tunnel lines since this is the only undoubtable link between these two eigenenergies of a given rotor. If not, the density of states is exploited.
3) $h\nu_t$ and E_{01} determine a rotational potential to second order. This potential is connected with a calculated activation energy. Experimental activation energies from QNS closest to the above expectation are assigned to the methyl group under consideration.The final results are contained in the table.

Tunnel splitting [μeV]	Relative intensity	Libration E_{01} [meV]	Activation energy E_a [K]	Threefold term V3 [meV]	Sixfold term V6 [meV]	Calculated E_{01} [meV]	Calculated E_a [K]
1.7	1/2	16.2	305	37.8	10.7	17.2	320
4.7	1/6	12.7	305	34.8	1.8	13.3	310
8.7	1/6	10.9	305	36.7	---	10.3	310
15.9	1/6	10.9	210	25.8	1.7	11.2	220

Table: Tunnel splittings together with its relative line intensities, librational transition energies and activation energies from quasielastic experiments again with its relative intensities are used to determine methyl rotational potentials. These potentials reproduce the tunnel splittings exactly. For comparison the calculated librational and activation energies are shown.

The test of dimethylethylamine alane revealed no tunneling lines within the accessible range (Fig.3).

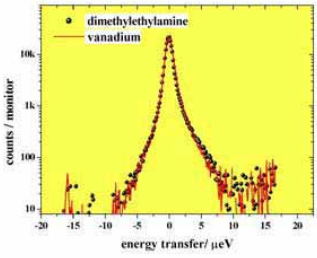

Fig.3 test of dimethylethylamine alane

[1] S McGrady, JFC Turner, RM Ibberson, M Prager, Organometallics 19,4398(2000)
[2] AJ Blake, S Cradock, J. Chem. Soc. Dalton Trans. 1990,2393
[3] A Amann, M Prager, unpublished
[4] R Boese, D Blaeser, to be published

Institut für Festkörperforschung
Forschungszentrum Jülich GmbH
D-52425 Jülich

Experimental Report
of Neutron Scattering Experiments
at the FRJ-2 Reactor

Proposal number:	BSS-01-008		
Experiment title:	**Dynamic Heterogeneities in Polymer Electrolytes**		
Dates of experiment:	Jan/Feb '02	Date of report: 28.02.'03	27.02.2003
Experimental team: Names	Addresses		
TRIOLO, Alessandro AIHARA, Yuichi	Istituto Processi Chimico-Fisici, Sezione di Messina – CNR Via la Farina 237 98123 MESSINA, Italy Yuasa Corp. 4-5-1 Ohgi-cho, Odawara 250-0001, Japan		
Local Contact:	Grimm Hans		

Experimental report text body

The use of Polymer Electrolytes (PE) is presently attracting a great attention from both academic and industrial groups, as a consequence of the large range of applications where these materials could provide an effective alternative to more conventional materials. Today PEs are already used in the development of high performance secondary batteries, electrochromic windows and a large number of further applications are continuously developed.
We have been active in the field of both structural and dynamical characterization of PEs. This class of materials can be exemplified by a mixture of Polyethylene Oxide ($-(CH_2-CH_2-O)_n-$) with inorganic salt, such as $LiClO_4$ etc. Due to the presence of the ether groups in the polyether, a strong complexation of the salt cation can occur, leading to the formation of strong, though transient, bonds between the oxygen atoms and the cation. In the crystalline phase, this phenomenon leads to the formation of new and peculiar crystalline phases which possess strongly different properties as compared to the properties of the pure semicrystalline polymer. In the molten phase, the differences are less strong, but still both the bulk and microscopic properties of the mixtures are different from the pure polymer ones. In particular the relaxation dynamics occurring in the polymer is strongly affected even by minor salt additions. Due to the formation of the chemical complex, a single cation can be directly connected to a number of oxygen atoms (Molecular Dynamics simulation showed that up to four O atoms can concur in complexing a Li+ cation in molten PEO). These ether units may belong either to the same polymer chain of to different, neighboring chains. This implies the formation of transient crosslinks that substantially slow down the relaxational dynamics of the polymer. Accordingly Quasi Elastic Neutron Scattering techniques evidenced the substantial slowing down of the segmental relaxation of the polymer. Moreover, when describing the relaxation in terms of a stretched exponential model, a clear stretching of the relaxation has been observed, as indicated by lower value of the stretching parameter b, as compared to the value for the pure polymer.

We used high resolution backscattering spectroscopy to probe the dynamic behavior of a PE of industrial

interest. In particular the polymer matrix is a randomly mixed PEO-PPO polymer (where PPO corresponds to (-(CH_2-CH(CH_3)-O)$_n$-), whose molecular weight is approx. 8000, with a ratio PEO:PPO=4:1. LiN(SO_2CF_3)$_2$ has been used as doping salt. This mixtures has been used in a prototype of a rechargeable secondary battery capable of up to 300 charge-discharge cycles at 60°C [1].
At present, this system has already been investigated using a conventional Time of Flight spectrometer (NEAT, HMI) and a high resolution backscattering instrument (IRIS, RAL), thus covering a large dynamic range. In order to explore in a more detailed the dynamic features of this system we collected inelastic fixed window scans. These measurements also allowed to characterize the influence of salt addition on the polymer dynamics.

In Fig. 1, a comparison between the temperature dependence of the inelastic fixed window scan from the pure polymer and from a doped sample (ether:Li=20:1) is reported. Both samples show deviations from the Lamb-Moessbauer behavior already at temperatures as low 100 K. This feature can be rationalized considering that at this temperature the hopping process of the PPO side methyl groups enters in the dynamic window accessible to the instrument. Further dynamic events become appreciable above ca. 230 K, where the skeletal relaxation of the polymer enter the dynamic window of the instrument.

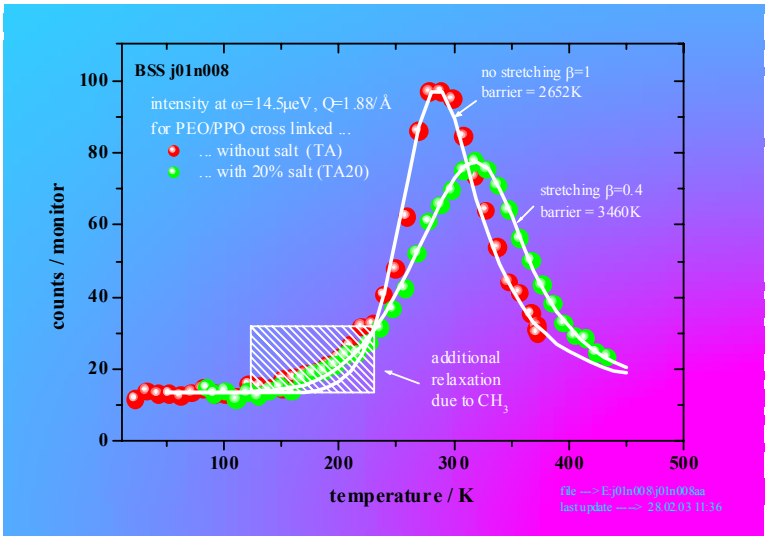

Fig1 Inelastic fixed window scan for pure and doped polymer. The scattering angle is 140° or Q=(1.87±0.06) Å^{-1}

In Fig. 2, the experimental results for energy scans at fixed temperatures are reported for the pure polymer. At this preliminary stage, the reported data allow the characterization of the dynamic events in the pure polymer (both the rapid methyl hopping and the slow skeletal process can be detected in Figure 1 and 2) and some preliminary observation on the effect of salt addition on the matrix dynamics. Though we do not possess energy scan data on the polymer-salt mixture, Figure 1 indicates that only minor, if any, effect is played by salt addition onto the methyl group relaxation. On the other hand, the salt addition leads to a substantial slowing down of the skeletal relaxation of the polymer.

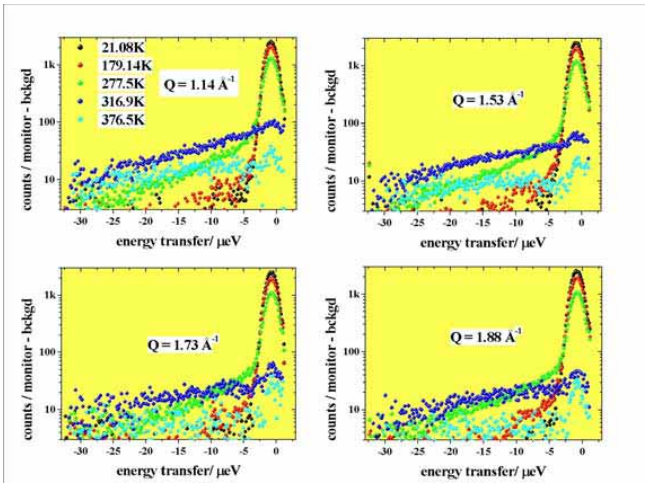

Fig.2 Dependence of the relaxational spectra for the pure polymer on temperature and momentum transfer.

Work is now in progress in order to rationalize the existing, though limited, data set in view of the chemical details of the system and of the information already obtained at complementary dynamic windows.

References

[1] Aihara et al., J. Chem. Phys. 113, 4785 (2000)

Institut für Festkörperforschung
Forschungszentrum Jülich GmbH
D-52425 Jülich

Experimental Report
of Neutron Scattering Experiments
at the FRJ-2 Reactor

Proposal number:	BSS-01-010		
Experiment title:	**Assignment of the 3 methyl tunnelling lines in a trichloromesitylene single crystal**		
Dates of experiment:	Feb/Mar '02	Date of report:	24.02.2003
Experimental team: Names	Addresses		
MEINNEL Jean HERNANDEZ Olivier	Groupe Matiere Condenseede l'Universite de Rennes1 Campus de Beaulieu Bat22 F-35042 Rennes-Cedex FRANCE Laboratoire de Chimie du Solide Campus de Beaulieu Bat10 F-35042 Rennes-Cedex FRANCE		
Local Contact:	Grimm Hans		

Experimental report text body

From quantum mechanics calculations and X-ray structural determinations (150 K) the 1,3,5-trichloro-2,4,6-trimethyl-benzene (also trichloromesitylene or TCM) molecule has the three-fold symmetry. Nevertheless in a crystal of TCM, the three methyl groups are different as their tunnel splittings are found at 4.3, 9.2 and 13.1 micro eV (powder with IN10 at ILL). The goal of the experiment was to assign each excitation to a specific methyl group in the crystal. All molecules are packed in an antiferroelectric parallel way, in the (100) planes, so each "kind"of methyl has a single orientation. The proposed experiment was to rotate a single crystal of TCM around its a* axis perpendicular to the molecular plane and to study , at 4.2 K, the intensities variations of the tunnel lines. To this end, the single crystal (blue, see fig. below) with dimensions of 30x4x1.5 mm^3 was wrapped into Al-foil and fixed to an Al-holder (red) such that the estimated a* axis coincides with the axis of the cryostat (z-axis).

Spectra were measured for 14 values of the rotation around z in steps of 18°. First and last orientations with respect to initial and final wavevectors (green, 140°-detector) are shown to the right. Scattering angles of 62, 81,100, 120 and 140 ±10° were recorded and fitted.

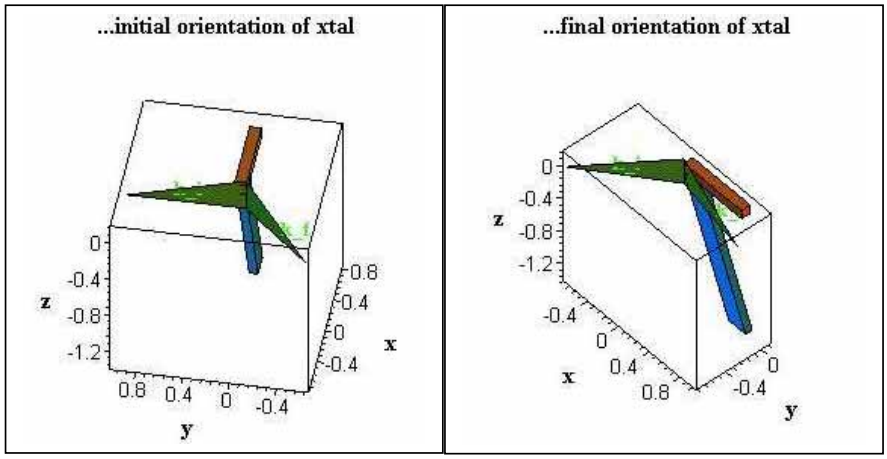

All 70 spectra exhibit three well defined excitations at 4.4, 9.6 and 13.2 μeV as shown e.g. for the detector at 140° and three of the 14 xtal-orientations (fig to the right, initial=green, intermediate=black, final=red). The solid lines represent fits by Gaussians. Before further analysis, possible contaminations of the elastic scattering by Bragg-scattering had to be identified. This was done by comparing the sum of all 4 areas to the relevant effective scattering volume. The latter can be approximated - apart from a common scaling factor - on the basis of the incoherent cross-section and an effective ratio of the xtal dimensions within the scattering plane. (see fig below).

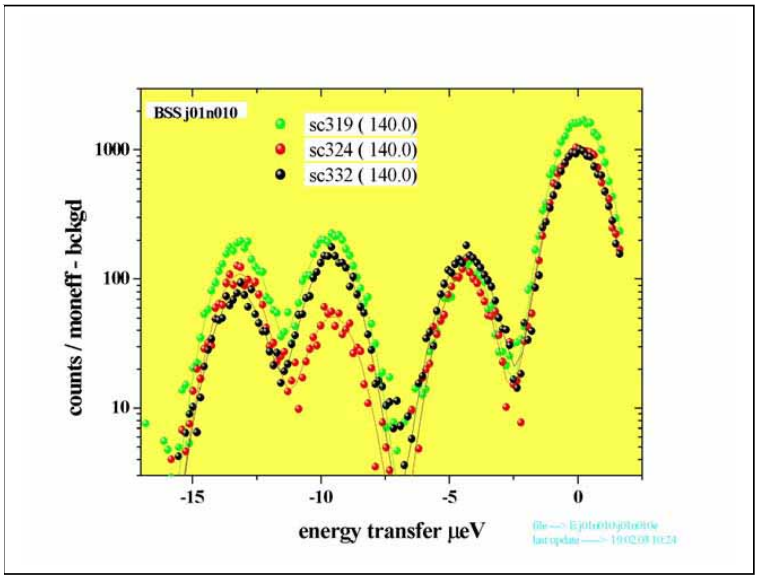

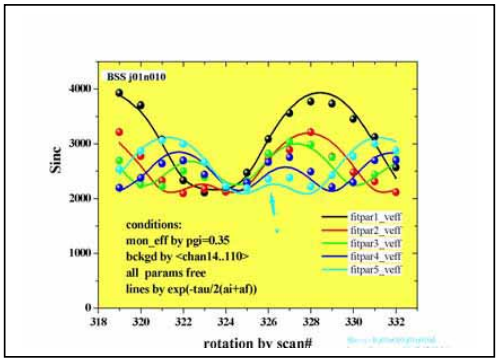

A ratio of 2.2 rather than 4/1.5=2.67 seems to describe the angular variation rather well. This difference seems acceptable in view of the large solid angles of the analyzers involved and the approximation of the xtal cross-section by an ellipsoid. An apparent deviation from this prediction occured for one orientation and one detector, only (marked by arrow). In this case, a coherent 'contamination' of 25% had to be deduced for the elastic peak. No attempt was made to identify the responsible Bragg-peak. The five figures below show the resulting angular variation of the 3 tunnel lines in units of the incoherent scattering for the 5 detectors.

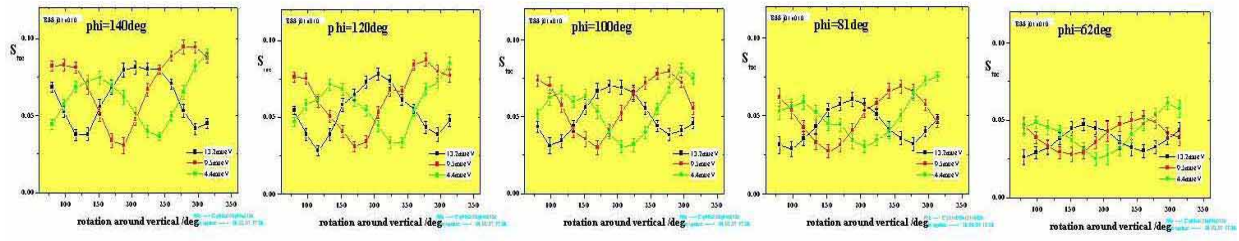

Qualitatively, the angular variation of the tunnel line intensities corresponds to expectation, i.e. an about 60° shift between the three lines and a diminishing amplitude towards smaller scattering angles as expected from the form-factor of the methyl group. However, the quantitative comparison with a model calculation suggests discrepancies between the assumed and underlying crystal orientation. These discrepancies are ascribed to a structural phase transition at 140K. It consists in alternative shifts of the molecules around the a-axis, leaving their orientation unchanged relative to the a^*-axis, but associated with large strain effects. Thus it appears that the assignment may be attained, but it appears that it is necessary to check orientation and possible domain distribution of the crystal on its experimental holder before and after the experiment.

Institut für Festkörperforschung
Forschungszentrum Jülich GmbH
D-52425 Jülich

Experimental Report
of Neutron Scattering Experiments
at the FRJ-2 Reactor

Proposal number:	BSS-01-011		
Experiment title:	**Rotational tunneling of methyl groups studies in tetracyanoethylene hexamethylbenzene complex**		
Dates of experiment:	25-27.01.02	Date of report:	27.02.03
Experimental team: Names	Addresses		
Andrzej Pawlukojc	Pernament: Institute of Nuclear Chemistry and Technology, Dorodna 16 str., 03-195 Warsaw, Poland Temporary: Joint Institute for Nuclear Research, 141980 Dubna, Russia		
Local Contact:	Grimm Hans		

Experimental report text body

Molecular complexes of the charge transfer type (EDA complexes) attract considerable interest, since many of them exhibit interesting physical and chemical properties from the point of view of their potential applications. Recently, besides already widely known photoconducting phases, the possible existence of phases with superconducting and photoelectric properties has been shown.
In the frame of this project we proposed to start a research on a group of crystals in which the electron donor will be represented by hexamethylbenzene. We shall trace the changes of structural and dynamic transformations of the systems when the second component with rising electronacceptor properties will be added. Hexachlorobenzene, hexabromobenzene, trinitrochlorobenzene, tetrachlorobenzoquinone, tetracyanoethylene, tetracyanoquinodimethane and hexacyanobenzene are proposed to be used. In all these cases one may expect the formation of column lattices with alternating donor and acceptor molecules. Hexamethylbenzene has been chosen because of its symmetry properties and the presence of six methyl groups, which enhance the electrodonor properties of the system.

Two basic methods have been used in these studies: the spectroscopy of inelastically scattered neutrons (INS) and X-ray and neutron diffractions. The adoption of the INS method in these studies will be particularly important, since it will permit to detect the changes in the dynamics of the methyl groups, in particular to investigate their torsional modes. The X-ray and neutron structural studies will be also necessary, because the crystal structures of the new complexes are not known. As supplementary, standard infra red, Raman spectra and the photoconductivity measurements will be carried out, if the necessity will arise to characterize the complexes as potential new materials of technological significance.

In the present experiment we have searched for rotational tunneling excitations of the methyl groups in the tetracyanoethylene hexamethylbenzene complex on the backscattering spectrometer BSS. In the structure at 295K the sheets of molecules overlap in such a way that the C=C bond of the „acceptor“ molecules lie parallel to the aromatic rings of the HMB „donor“ molecules in the manner characteristic of π-charge transfer complexes. This molecular overlap is illustrated in Fig.1.

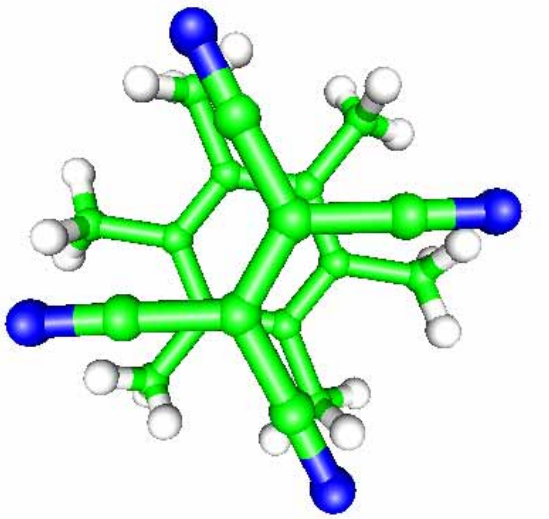

Fig.1. Tetracyanoethylene hexamethylbenzene complex

The sample was sealed in an Al-container and measured at T=4.6K and 25K. The observed spectra are shown in Fig.2 together with that of a Vanadium-sample as reference. The spectra are averaged over 50° < scattering angle < 150° for better statistics, corrected for background, and scaled to equal elastic amplitude. Obviously, neither tunneling lines nor quasielastic scattering is observable for this charge transfer complex.

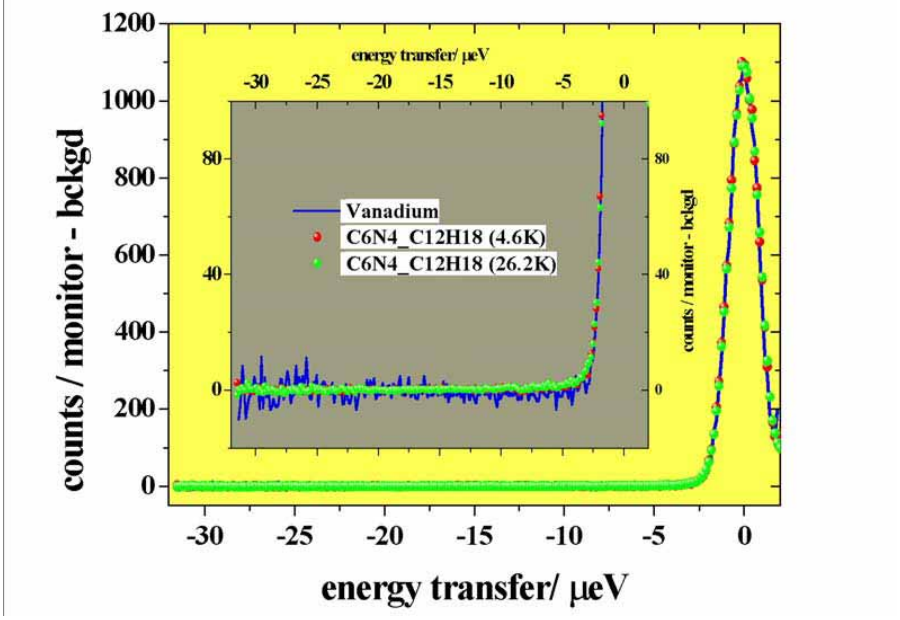

Fig.2 Spectra taken at the back-scattering-spectrometer in offset configuration.

Institut für Festkörperforschung
Forschungszentrum Jülich GmbH
D-52425 Jülich

Experimental Report
of Neutron Scattering Experiments
at the FRJ-2 Reactor

Proposal number:	BSS-01-012		
Experiment title:	**Mobility of water and aqueous electrolyte solutions under confinement**.		
Dates of experiment:	25.04. – 13.05.2002	Date of report:	25.02.2003
Experimental team: Names	Addresses		
Yuri Melnichenko	Solid State Div. Oak Ridge		
Local Contact:	Stefan Kahle		

Experimental report text body

In the 11 days we have measured three different solutions (LiCl, $CaCl_2$, and $NdCl_3$ in water) in bulk and confinement. Further, for background correction, and resolution measurements we have carried out two empty scans (empty Al sample holder, and Al sample holder with unloaded confinement material), and a resolution scan (vanadium), respectively. The aim the investigation was the observations of slow water. To get the best energy resolution of the instrument (~1μeV) we have used perfect Si111 crystals for both monochromator and analyzers. The energy variation of $\Delta E = \pm 17\mu eV$ is performed by moving the monochromator and exploiting the Doppler effect. The corresponding time window was from 170ps up to 2 (3) ns. The Q-range covered by the instrument was from 0.16 to 1.84$Å^{-1}$.

Figure 1 shows backscattering spectra measured at the three different bulk samples. The behavior of the three different salt solutions is similar, i.e. no essential effect in the in the quasi-elastic intensity in spectra is observed. Of course, we observe a small effect in the elastic intensity, however this is the results of the different absorbtions of neutrons of the different ions (Li,Ca,Nd) in the samples. A similar result is observed for the investigation of the samples in confinement (not shown). In contrast, the bulk water measurement is different from the solution measurements, i.e. the ions produce slow water molecules in its environment, but the charge of the ions is not relevant for the dynamics of water molecules.

Figure 2 compare bulk and confinement experiments for the $NdCl_3$/water solution. We observe a distinct quasi-elastic broadening of the confinement measurement. Also included in this figure is the empty sample holder scan (unloaded vycor glass) and the instrument resolution. The scattering of the unloaded vycor material is much higher than the confinement experiment. This is the result of the absorbtion of the Nd ions. Note that due to the principle of Babineè we observe small angle scattering of the vycor material (see Figure3).

However, we observe a clearly slower dynamics in the confinement measurement than in the bulk experiments.

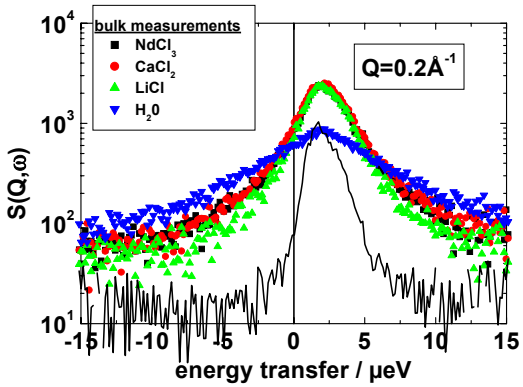

Figure1. Bulk measurements of three different water solutions (see legend), and pure water, respectively, at room temperature and Q=0.2Å^{-1}. The solid line corresponds to the instrument resolution.

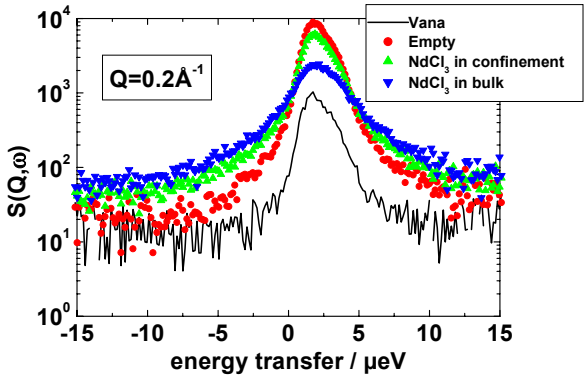

Figure2. Comparison between bulk and confinement measurements of the $NdCl_3$ in water solutions (see legend) at room temperature and Q=0.2Å^{-1}. The solid line corresponds to the instrument resolution. Also included is the empty confinement material

Figure 3 shows the Q dependence of the elastic intensity for empty and filled confinement material. For the lowest Q we observe a higher scattering of the unloaded vycor material, i.e. it is not possible to subtract the this "empty" measurement from the confinement experiments. However, for the background correction we have to consider the absorbtion of the material in confinement.

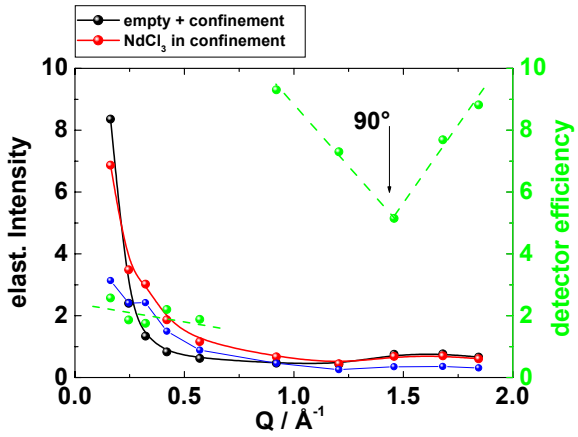

Figure3. Q dependence elastic intensity of empty and filled confinement material (left axis). Additionally, the efficiency of the detectors is shown (right axis). Not that the flat sample holder was perpendicular to the neutron beam (90°).

Institut für Festkörperforschung
Forschungszentrum Jülich GmbH
D-52425 Jülich

Experimental Report
of Neutron Scattering Experiments
at the FRJ-2 Reactor

Proposal number:	BSS-02-001		
Experiment title:	**The microscopic origin of fast ionic conduction in $ATi_{0,7}Fe_{0,3}O_{2,85}$ (A=Ca, Sr) systems**		
Dates of experiment:	27.06.2002-11.07.2002	Date of report:	21.02.2003
Experimental team: Names	Addresses		
Mashkina, Elena	Lehrstuhl für Kristallographie & Strukturphysik Universität Erlangen-Nürnberg Bismarckstr. 10 91054 Erlangen		
Magerl, Andreas	Lehrstuhl für Kristallographie & Strukturphysik Universität Erlangen-Nürnberg Bismarckstr. 10 91054 Erlangen		
Local Contact:	Grimm Hans, Kahle Stefan		

Experimental report text body

The ABO_3 perovskite structure is stable at high temperatures, reducing atmospheres and even at high defect concentration, enabling high electronic and ionic conductivities. This makes such materials interesting as ceramic membranes in high temperature solid-state electrochemical devices. Studies of $SrTiO_3$ doped with Fe have been carried out by several investigators, reporting electrical conductivity and defect structure as a function of composition, temperature and oxygen partial pressure.

Earlier measurements of the electrical properties on $SrTi_{1-x}Fe_xO_{3-x/2}$ with x=0.3 show the value of ionic conductivity of 0.068 S/cm and 0.022 S/cm at T=1000^{0}C and T=900^{0}C respectively. According to published results ionic conductivity has an exponential dependence on the temperature for this composition, thus higher temperatures provoke higher oxygen mobility [1]. However, still there is no information on the microscopic mechanism for the observed high ionic conductivity.

So far no neutron measurements had been done to look into the dynamics of oxygen. A fixed inelastic window scan with the offset of 14.5 μeV was performed on the BSS spectrometer for $SrTi_{1-x}Fe_xO_{3-x/2}$ with x=0.3. A representative fixed window scan is shown in fig.1. The data indicate a slight increase of the intensity at high Q, however the temperature scan was not extended high enough to speculate on the expected quasi elastic line broadings.

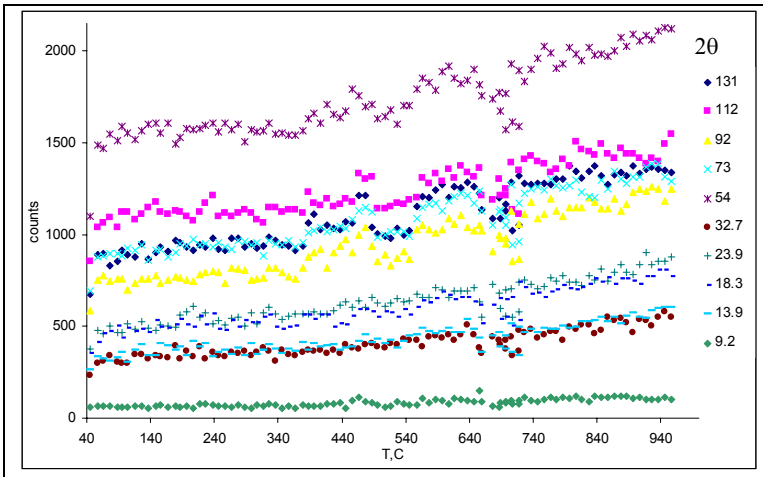

Fig.1. Fixed window temperature scan for $SrTi_{1-x}Fe_xO_{3-x/2}$ with x=0.3.

[1] S.Steinsvik and et., J.Phys.Chem. Solids, Vol.85, N.6, pp 969-976, 1997

Institut für Festkörperforschung
Forschungszentrum Jülich GmbH
D-52425 Jülich

Experimental Report of Neutron Scattering Experiments at the FRJ-2 Reactor

Proposal number:	BSS-02-002		
Experiment title:	**Bound water on the surface of ionic micelles**		
Dates of experiment:	within 28.3.02 –5.5.02	Date of report:	02.03.03
Experimental team: Names	Addresses		
Vass, Szabolcs Gilányi Tíbor	Laboratory of Material Science KFKI Atomic Energy Research Institute 29-33 Konkoly-Thege út, 1121 Budapest, Hungary 1525 Budapest, P.O.Box 49, Hungary Department of Colloid Chemistry Loránd Eötvös University 1A Pázmány sétány, 1117 Budapest, Hungary 1518 Budapest 112, P.O.Box 32, Hungary		
Local Contact:	S.Kahle		

Experimental report text body

A recent SANS study revealed significant differences between the core radius R_c of ionic micelles and $R_0 = D_0/2$, the half-distance of their closest approach D_0. The core radius was calculated by assuming that the micelles are spheroids of axial ratio η which may grow in the axial direction, the distance of their closest approach was obtained from the structure factor of micelles interacting via Deryaguin-Landau-Verwey-Overbeek (DLVO) potential. The results are shown in Table 1:

n_C	N_{agg}	R_c [nm]	η	R_0 [nm]	c_M [M]
9	23.8 ±1.4	1.16 ±0.02	1.00 ±0.08	2.11 ±0.17	0.066
10	33.7 ±1.2	1.31 ±0.03	1.07 ±0.04	2.62 ±0.08	0.033
11	52.5 ±1.4	1.42 ±0.04	1.42 ±0.13	2.95 ±0.25	0.0175
12	69.5 ±1.6	1.57 ±0.03	1.53 ±0.09	3.22 ±0.27	0.0084
13	84.8 ±1.2	1.72 ±0.02	1.52 ±0.05	3.42 ±0.07	0.0043
14	107.3 ±1.9	1.87 ±0.03	1.61 ±0.07	4.23 ±0.24	0.0022
15	129.4 ±1.1	1.98 ±0.03	1.74 ±0.09	4.17 ±0.16	0.0016
16	135.1 ±1.2	2.11 ±0.02	1.60 ±0.04	5.00 ±0.12	0.0006

Table 1. Aggregation number N_{agg}, core radius and axial ratio R_c, and η, respectively; half-distance of the closest approach R_0 of the micelles found at 40 °C in 0.072 mol/dm^3 D_2O solutions of sodium alkyl sulphates of chain length n_C = 9-16. In the last column the critical concentration c_M of micelle formation is listed. Data taken from The Journal of Physical Chemistry B, 2000, vol. 104, pp. 2073-2081.

The difference can be explained in one or both of the following two ways: (i) Many experiments indicate that there is a so-called solvent structural term that must be included in the interaction potential. It arises because of the influence of a surface on adjacent solvent layers with decay length typically of order of 1.0 *nm* (Hunter, R.J.; *Foundations of Colloid Science*, Vols. 1 and 2, Clarendon Press, Oxford, 1989.). (ii) A too close approach of the micelles leads to the deformation of the local electric field. Provided that the double-layers frequently overlap, this deformation may induce energetically unfavorable changes in the core structure of the neighboring micelles, in particular in case of longer chains.

Molecules responsible for the solvent structural term should be bound to the surface of the micellar cores and, consequently, they are expected to move essentially slower than bulk solvent molecules. This is the basis of the proposed neutron backscattering measurments. In the first step 0.07 mol/dm^3 H_2O solutions of sodium nonyl-, dodecyl- and hexadecyl sulphate have been studied at 40 °C; the results versus energy transfer at 9.2° (Q = 0.160 Å^{-1}) are plotted in Figure 1, together with those from a vanadium reference sample. Because the solvent molecules bound to the micellar core surface move together with the micelles, their translational diffusion coefficient should decrease with the micellar size which increases with the number of carbon atoms in the alkyl chain (see Table 1). Although the trend observed in the half widths of the Lorentzians supports this expectation, the incoherent contribution from the H atoms in the alkyl chains and a possible coherent contribution from elastic small-angle scattering may cause serious systematic errors. In order to exclude these sources of error, further neutron backscattering- and small-angle scattering experiments are planned on H_2O solutions of deuterized surfactants.

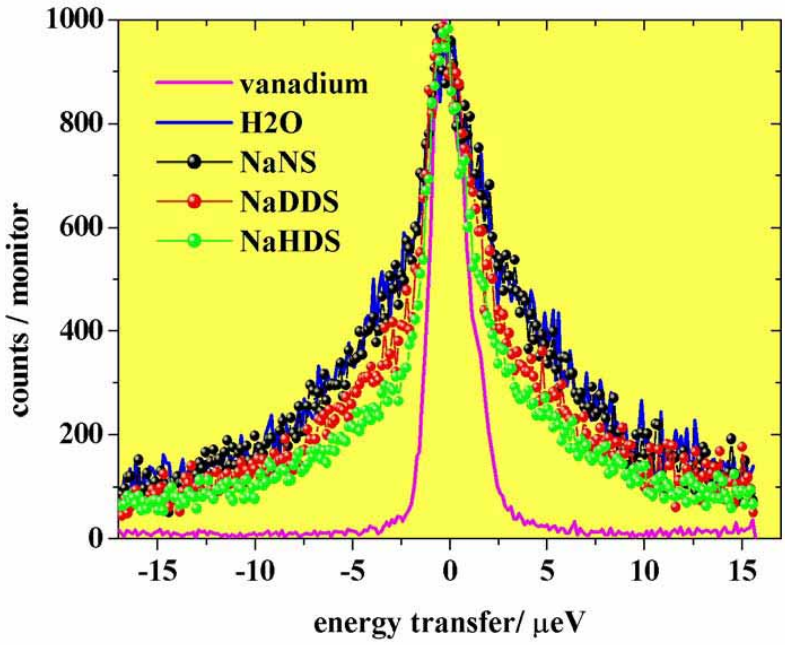

Fig.1: Backscattering spectra at Q=0.16Å^{-1} for 0.07 mol/dm^3 H_2O solutions of sodium nonyl-, dodecyl- and hexadecyl sulphate at 40 °C

Institut für Festkörperforschung
Forschungszentrum Jülich GmbH
D-52425 Jülich

Experimental Report
of Neutron Scattering Experiments
at the FRJ-2 Reactor

Proposal number:	BSS-02-003		
Experiment title:	**Test experiment – methyl groups tunnelling rotational in 1,3,5-trimetoxybenzene and tetramethylpyrazine**		
Dates of experiment:	25-27.09.02	Date of report:	26.02.03
Experimental team: Names	Addresses		
Andrzej Pawlukojc	Pernament: Institute of Nuclear Chemistry and Technology, Dorodna 16 str., 03-195 Warsaw, Poland Temporary: Joint Institute for Nuclear Research, 141980 Dubna, Russia		
Local Contact:	Grimm Hans		

Experimental report text body

Our research is devoted to the problem of charge-transfer (CT) interaction in molecular systems. The CT molecular complexes evoke increasing interest in connection with discovering in molecular materials of such phenomena like electric conductivity (and even superconductivity) and ferroelectricity. The properties of such materials depend on ionisation potential and electron affinity of interacting components as well as on structural parameters especially in case of π - π donor – acceptor complexes.
The goal of our studies is to gather new information on those systems based on low frequency transitions reflected in INS spectra. Just low frequency transitions can well be recorded by using this technique. For instance the tunnelling splitting and librational motion of CH_3 groups present in donor molecules can be a sensitive parameter of the CT interaction. To our knowledge there are no reports in the literature related to this problem.
As a first step in our searches is to find proper electron donors containing CH_3 groups which could be complexed with various acceptors. We suggest that at beginning most convenient could be 1,3,5-trimethoxybenzene (fig.1) and tetramethylpyrazine (fig.2). Therefore our suggestion is to perform experiments tending towards whether those compounds show tunnelling frequencies in the region which could be exploited in further studies with CT complexes containing those components.

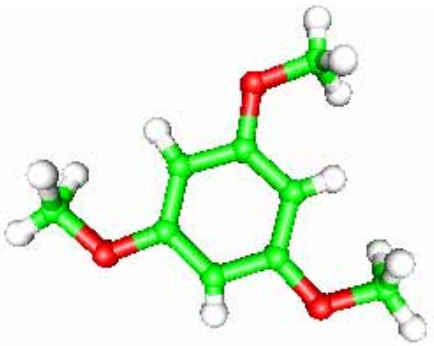

Fig.1. 1,3,5-trimethoxybenzene molecule

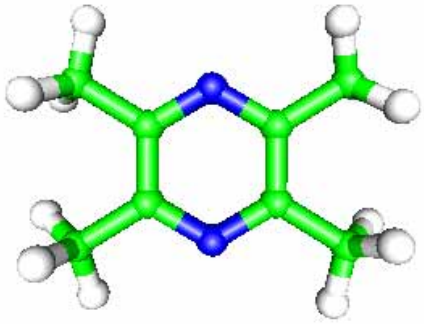

Fig.2. Tetramethylpyrazine molecule

The two molecular complexes were sealed in Al-containers and cooled to T=4.6K. The observed spectra are shown in Fig.3 together with the well known tunneling spectrum of 2-Fluortoluol as reference. The latter was measured just before the two complexes of interest under the same conditions. Obviously, neither tunneling lines nor quasielastic scattering is observable for the two donor molecules within the accessible range of the spectrometer.

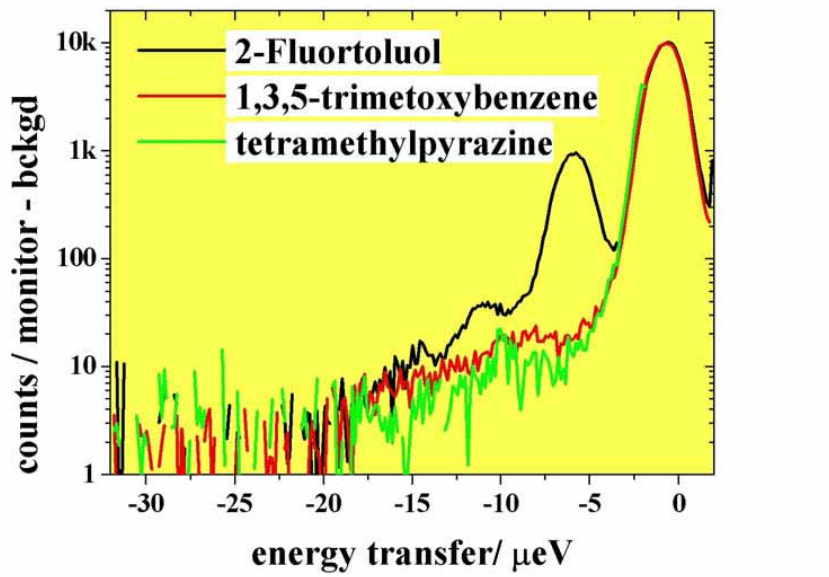

Fig.3 Spectra taken at the back-scattering-spectrometer in offset configuration at T=4.6K

Institut für Festkörperforschung
Forschungszentrum Jülich GmbH
D-52425 Jülich

Experimental Report
of Neutron Scattering Experiments
at the FRJ-2 Reactor

Proposal number:	BSS-02-004		
Experiment title:	**Explore the hydrogen-nitrogen pair interaction potential by studying rotational tunneling of methyl pyrazines**		
Dates of experiment:	11.7.02 to 14.7.02	Date of report:	02.03.03
Experimental team: Names	Addresses		
O. Kirstein M. Prager H. Grimm	Forschungszentrum Jülich Forschungszentrum Jülich Forschungszentrum Jülich		
Local Contact:	H. Grimm		

Experimental report text body

The combined measurement of librations and rotational tunneling frequencies are very sensitive probes for the local rotational potential experienced by by rotors like methyl groups in molecular crystals [1]. CH3 groups attached to aromatic rings of benzene and pyridine have been extensively studied [2]. Recently 2,6-dimethylpyrazine out of the class of di-nitrogen-substituted benzenes was investigated. The observed tunneling spectrum shows two tunneling lines at 20 and 29 μeV and librational transitions at 8 and 10 meV [3]. The low temperature structure of 2,6-dimethylpyrazine has also been solved [4]. In agreement with the spectroscopic results the two CH3 groups of the molecule were found to be inequivalent. Dimethylpyrazine exhibits two other isomers 2,3- and 2,5-dimethylpyrazine. The study aims to establish systematic changes with structural differences of the isomers at identical atom-atom potentials similar to earlier studies on the xylene family.

The backscattering spectrometer was used for energy transfers up to -32μeV. Sample temperatures were 4.6K.In the figures the integrated sample spectrum is compared to the resolution function of the spectrometer (vanadium run). For both samples no indication of a tunnel split librational groundstate is found .

[1] W. Press, Springer Tracts Modern Phys. 92 (1981) 1
[2] M. Prager, A. Heidemann, Chem. Rev. 97,2933(1997)
[3] B. Nicolaii, E. Kaiser, F. Fillaux, G.J. Kearley, A. Cousson, W. Paulus, Chemical Physics 226 (1998) 1-13
[4] E. Kaiser, B. Nicolaii, W. Paulus, A. Cousson, F. Fillaux, G. Heger, G.J. Kearley, O. Randl, Acta. Cryst. E57,1113(2001)

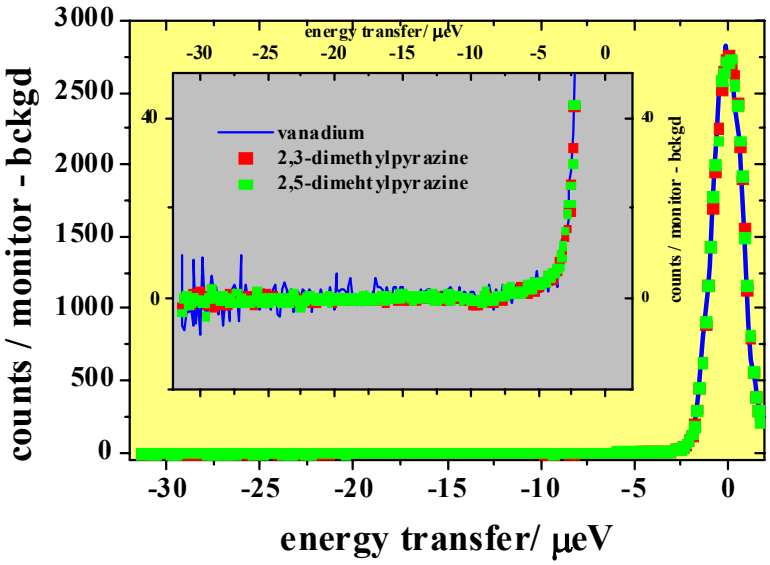

Spectra taken at the back-scattering-spectrometer in offset configuration at T=4.6K. The scattering angle Φ is averaged over 50° < Φ < 150°.

Institut für Festkörperforschung
Forschungszentrum Jülich GmbH
D-52425 Jülich

Experimental Report
of Neutron Scattering Experiments
at the FRJ-2 Reactor

Proposal number:	BSS-02-005		
Experiment title:	**Rotational tunneling in amorphous acetamide: the potential distribution function in a biological material**		
Dates of experiment:	29.4. – 1.5. and 8.7. – 11.7.2002	Date of report:	18.2.2003
Experimental team: Names	Addresses		
M. Prager	Forschungszentrum Jülich		
Local Contact:	M. Prager		

Experimental report text body

Rotational tunneling is the most sensitive probe for weak changes of rotational potentials. This property is used in recent times to explore the potential distribution function of polymers [1] and other amorphous or disordered materials [2,3]. Similarly the librational bands are modified by disorder.

All systems studied so far suffer from the problem that the potential distribution function is either spoiled by overlap with another component [3] or that only a wing of the potential distribution function scatters into the energy window accessible by the spectrometer [1,2]. A convincing independent proof whether amorphous materials see generally a *Gaussian potential distribution function* requires a system where a main part of the related distribution of tunneling energies including the maximum is found in the energy regime of the used spectrometer. The existing experience seems to show that the suited material has to have a significant intramolecular hindering barrier like the polymers where the mean potential is little changed with amorphisation. At the same time the potential must be weak enough to show large tunnel splittings. Toluene [2] did not fulfill the first condition and the glassy material shows a huge increase of the rotational barrier.

A recent publication shows [4] that acetamide can be prepared as amorphous material if condensed from the gas directly onto a cold surface. The x-ray structural study [4] claims further that the neighborhood of molecules is very similar to that of the crystalline material. Crystalline acetamide shows a large tunnel splitting of 32 ueV which is mainly intramolecular [5]. On this basis one can expect that the barrier height for methyl rotation does not change drastically. Acetamide as one of the simplest molecules showing the biologically important peptide bond is by itself an interesting subject to study.

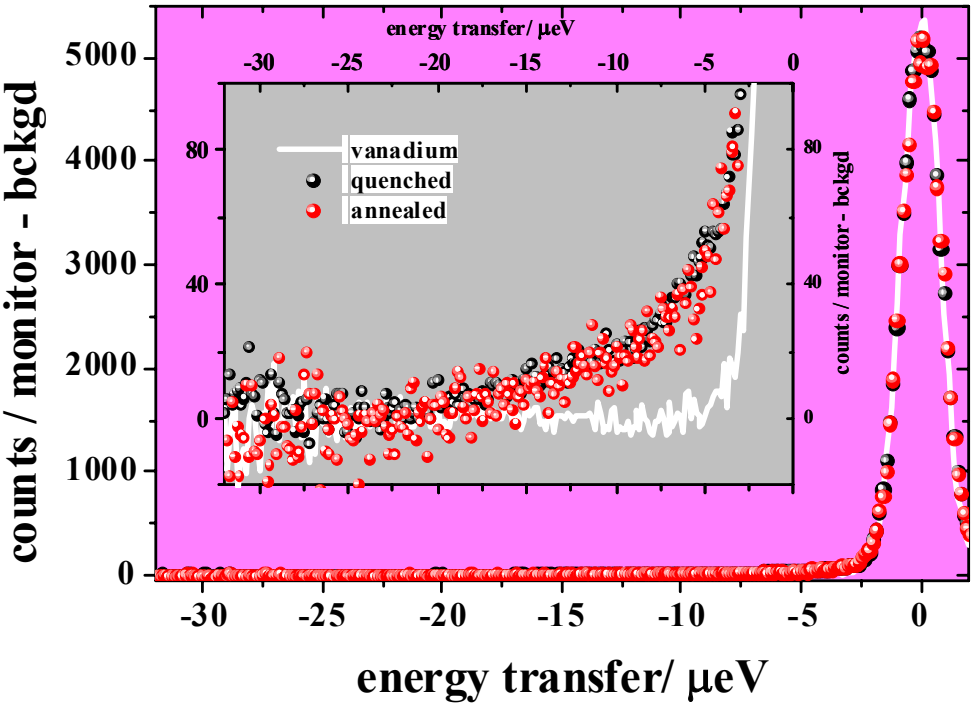

Figure: Backscattering spectra of acetamide in the quenched and annealed state measured at T=6.2K. The larger scatter of the data for the annealed status (4h at 120K) is due to the shorter measuring time (21h vs 5h). The experimental resolution is represented by the scan for Vanadium.

The proposed condensation was successfully performed using our matrix condensation sample stick. The sample was cooled down to 4.5K. The BSS spectrometer was used in the energy regime from –32 to 2µeV. The detectors in the angular range from 45° to 141° were added. The expected distribution of tunnel splittings centered around that of crystalline acetamide is not observed. Instead – as often [1,2] – an unresolved wing of inelastic intensity is present in the backscattering spectrum (figure, inset). This shows that disorder strengthens the rotational barrier significantly. A forthcoming data analysis will extract the mean rotational barrier height and the width of the potential distribution function.

[1] J. Colmenero, R. Mukhopadhyay, A. Alegria, B. Frick, Phys. Rev. Lett. 80,2350(1998)
[2] A. Moreno, A. Alegria, J. Colmenero, M. Prager, H. Grimm, B. Frick, J. Chem. Phys. 115,8958(2001)
[3] M. Prager, P. Schiebel, J. Combet, Chem. Phys. 276,69 (2002)
[4] S. Nasr, J. Chem. Phys. 115,6569(2001)
[5] M. Prager, N. Wakabayashi, M. Monkenbusch, Z. Phys. B: Condens. Matter 94,69(1994)

Institut für Festkörperforschung
Forschungszentrum Jülich GmbH
D-52425 Jülich

Experimental Report
of Neutron Scattering Experiments
at the FRJ-2 Reactor

Proposal number:	BSS-02-006		
Experiment title:	**Investigation of the self correlation of α and β process of poly methylacrylate**		
Dates of experiment:	05.12.—20.12.02	Date of report:	17.02.2003
Experimental team: Names	Addresses		
Stefan Kahle	IFF, FZ-Jülich		
Local Contact:	S. Kahle		

Experimental report text body

(Please use 12 pt letters here !)
In the 14 days we have measured a fully protonated poly methylacrylate sample (PMA) at eleven temperatures between 220 ... 450K. Further, for background correction, and resolution measurements we have carried out an empty sample holder scan, and a resolution scan (sample at 4K), respectively. Additionally, to estimate the detector efficiency we have carried out a vanadium scan. To get the best energy resolution of the instrument (~1μeV) we have used perfect Si111 crystals for both monochromator and analyzers. The energy variation of $\Delta E = \pm 17\mu eV$ is performed by moving the monochromator and exploiting the Doppler effect. The corresponding time window was from 170ps up to 2 (3) ns. The Q-range covered by the instrument was from 0.16 to 1.84$Å^{-1}$.

The aim of this investigations is to observe separate the β relaxation. Figure 1 shows the Arrhenius diagram, measured with dielectric spectroscopy. From this figure we observe that the β process is in the frequency window of the backscattering instrument (log ω_{min} = -9.6) at temperatures higher than 300K. However, the α process comes into the backscattering window at T=350K. I.e. there is a good chance to investigate the β process separately in relativ wide temperarure range.

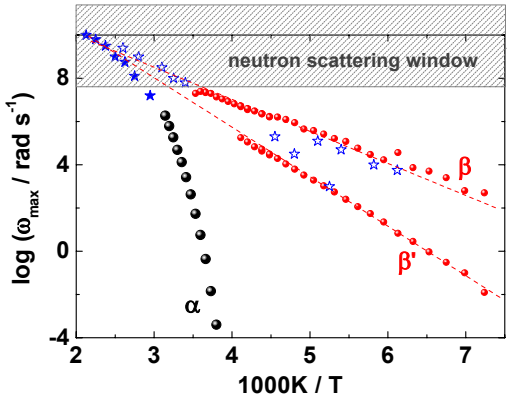

Temperature dependence of the maximum frequencies for the α and β relaxation for poly methylacrylate (PMA). The stars at higher frequencies correspond to data for the α process from Ref. [1]. Also included are data for the β process from the same reference (open stars). The neutron scattering (including NSE) region is marked.

From Figure 2 we observe no large effect between 300 and 350K in the temperature dependence of the scattering function. Note that the high frequency shape of the b process is in the backscattering window in this temperature range. The main part of the decreasing in the elastic intensity comes from temperature dependence in the Debye-Waller-Factor. One possible reason for the small effect is, that the spatial dimension of the β process is not muchly large. In other words, the corresponding intensity of the process is small, and therefore no effect is vissible in the raw data. At temperatures higher than 360K the the scattering function depends strongly from temperature, indicating a diffusion process . In this temperature range the α process becomes more and more relevant.

Presently we have not analyzed the spectra in detail. In future we have to fit the data with a folding of two scattering functions, one corresponding to the α and one to the β process, respectively, and this for all Q and temperatures. The elastic incoherent structure factor (EISF) than gives us information about the spastial range of the β process in PMA.

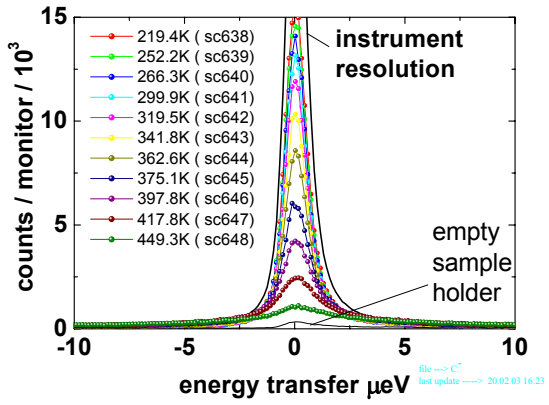

Raw data of the backscattering measurements on PMA (symbols). The lines correspond to the instrument resolution, and an empty sample holder scan.

References

[1] N.G. Mc Crum, B.E. Read and G. Williams, Anelastic and Dielectric Effects in Polymeric Solids (Dover, New York, 1967)

Institut für Festkörperforschung
Forschungszentrum Jülich GmbH
D-52425 Jülich

Experimental Report
of Neutron Scattering Experiments
at the FRJ-2 Reactor

Proposal number:	BSS-02-007		
Experiment title:	**Local dynamics of polyisobutylene- comparison with MD simulations**		
Dates of experiment:	27.05.02	Date of report:	17.02.2003
Experimental team: Names	Addresses		
Stefan Kahle	IFF, FZ-Jülich		
Local Contact:	S. Kahle		

Experimental report text body

(Please use 12 pt letters here !)

We present recent neutron scattering experiments (backscattering) of polyisobutylene (PIB). In order to focus the observations on the backbone dynamics in PIB a sample with protons at the methylene groups only and deuterons elsewhere (methyl groups) was investigated.

In the 17 days we measured the h2d6PIB sample at five temperatures (320, 369, 415, 461 and 503K). Further, for background correction, and resolution measurements we carried out an empty sample holder scan, and a resolution scan (sample at 4K), respectively. Additionally, to estimate the detector efficiency we carried out a vanadium scan. To get an overlap with the time window of the IN6 instrument (up to 70ps) we have used our backscattering instrument in the off-center configuration (65 ... 2000ps; compare with Figure1 right hand side), i.e. SiGe was used as monochromator. The Q-range covered by the BSS instrument was from 0.16 to 1.84$Å^{-1}$. The static structures factor of d6PIB and d8PIB (fully deuterated) are very different, i.e. it is not possible to subtract the background produced by deuterium by measuring a fully deuterated sample. Therefore, we measured only the d6PIB sample.Unfortunately, there were some inconsistencies in the temperature dependence of the elastic intensity. Possibly, this effect is due to from thermal expansion of the sample. Therefore, we have measured the sample a second time (at the same temperatures), but in this case we started from the lowest temperature.

Figure 1 shows the experimental results measured at the time of flight (IN6, left hand side top) and backscattering (BSS, left hand side bottom) instruments. The data were Fourier-transformed into the time domain and divided by the Fourier-transform of the instrument resolution ($S(Q,t) = FT\{S_{measured}(Q,\omega)\} / FT\{R(Q,\omega)\}$; see as an example the right hand side of Figure 1). Note that the discrepancy in intensity (of the order of 10%) between both measurements (IN6 and BSS) was corrected. From this figure we observe that a combination of these two experiments can cover a time range of 3 to 4 decades.

Further, there was also a good overlap in the Q-range between the two instruments. Six detector positions between 0.42 and 1.67Å^{-1} could be analyzed.

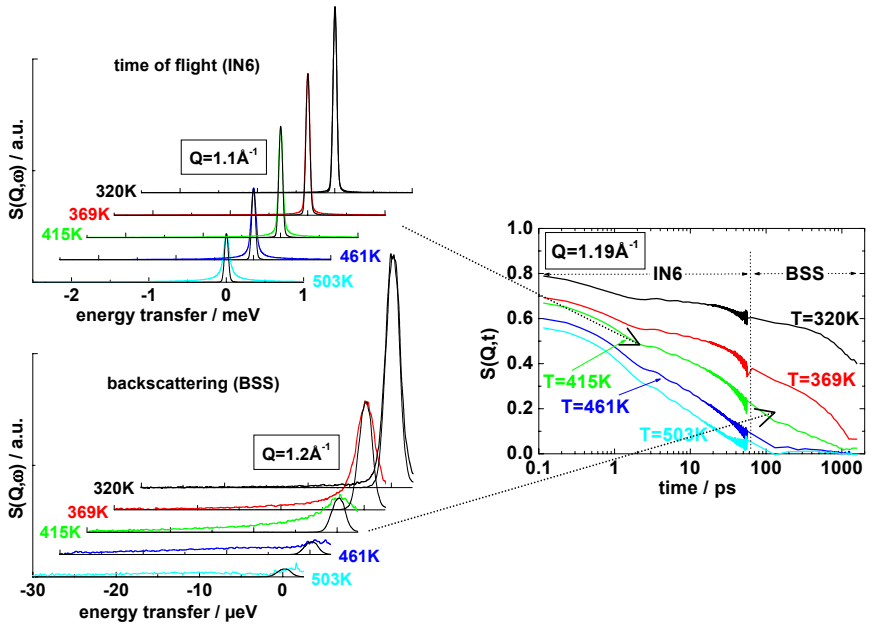

Figure 1. (left side) Experimental spectra measured with the IN6 instrument (above) and BSS (below) at different temperatures. To collect the two instruments the spectra were Fourier transformed into the time domain (right part).

To evaluate the neutron scattering data we pursued two paths: On the one hand – as predicted by the MD simulations – we fitted our spectra with two single exponential functions, and on the other hand the spectra where described by a single KWW function. Both strategies fit the data very well, however, we found that the elastic incoherent structure factor (EISF) of the t-t-jump process (the first path) is inconsistent with the theoretically expected EISF, i.e. the jump distance is too large. Furthermore, the EISF depends strongly on temperature, i.e. the quality of the jump process changes with temperature. (see Figure 2). Further, there is a distinct difference between the EISF from neutron scattering experiments, and simulations, respectively. Possibly, the temperature in the simulation is not correct. Note that a factor of 0.77 yield to comparable EISF.

The characteristic times of the tt- and tg-jump process (path one) corresponds to the jump rate of the two processes, respectively. In addition, the characteristic KWW- time (path two) shows the same temperature dependence as the WLF shift parameters from rheological experiments [1]. It is an open question whether the data can be analyzed by path one or two. The characteristic relaxation times favor path one, but the EISF path two. However, the EISF shows clearly a change in the quality of the dynamic process. This observation is far from any description for a local jump processes.

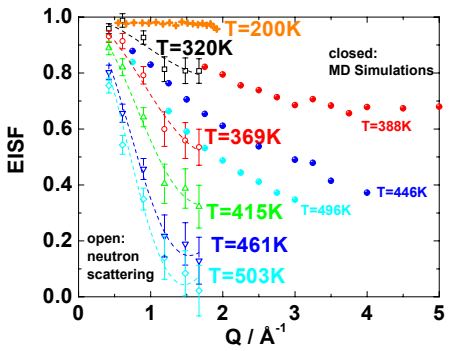

Figure 2. Q dependence of the elastic incoherent structure factor (EISF) at different temperatures. The open symbols correspond to the neutron scattering EISF, and the full symbols to the EISF from the MD simulations. Note that there is a large difference between experiment and simulations.

Institut für Festkörperforschung
Forschungszentrum Jülich GmbH
D-52425 Jülich

Experimental Report
of Neutron Scattering Experiments
at the FRJ-2 Reactor

Proposal number:	BSS-02-009		
Experiment title:	**Methyl group dynamics in methyl iodide clathrate**		
Dates of experiment:	12.7.02-14.7.02	Date of report:	27.2.03
Experimental team: Names	 Addresses		
M. Prager H. Grimm	Forschungszentrum Jülich Forschungszentrum Jülich		
Local Contact:	S.Kahle		

Experimental report text body

With the detection of large quantities of methane clathrates on the sea floor and the recent consideration of these materials as a possible future energy source („burning ice“) clathrates have attracted new scientific [1] and economic interest.

From the point of view of spectroscopy clathrates form an especially well defined matrix for the spectroscopy of rotationally almost free molecules [1,2]. The identity of the environments of the included guest molecules avoids disorder to a large extent. The clean spectra allow detailed analysis with respect to guest-host interaction [1], the character of rotational motion (e.g. rotation-translation-coupling [2]) and other characteristic details of the adsorption site.

Inclusion compounds involving methyl groups are so far only investigated in non-water host matrices like the calix-arenes [3]. Again, almost free methyl group rotation is found with coupling to a second degree of freedom which later was identified as rotation-translation coupling.

Clathrates were also investigated by other spectroscopic techniques as NMR. Beside of „classical“ clathrates as the one with tetrahydrofuran guests new clathrates were prepared in a thesis work of 1985. Among others methyl iodide clathrate was obtained by a new preparation technique which forced the two insoluble liquids to mix on a molecular level. The formation of a new compound, methyl iodide clathrate, was confirmed by the change of the melting point to +4degreeC. A comparison of the new material with pure methyl iodide by NMR relaxation studies showed that the methyl group in the clathrate is much less hindered than in the pure solid material. This makes the material interesting to be studied by neutron spectroscopy.

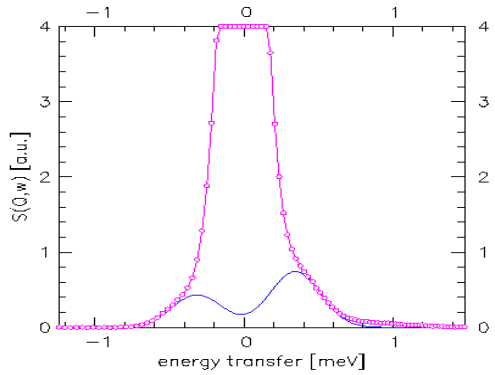

Figure 1: spectrum from the thermal TOF Spectrometer. Tunneling modes of methyl groups show energies around 0.36meV

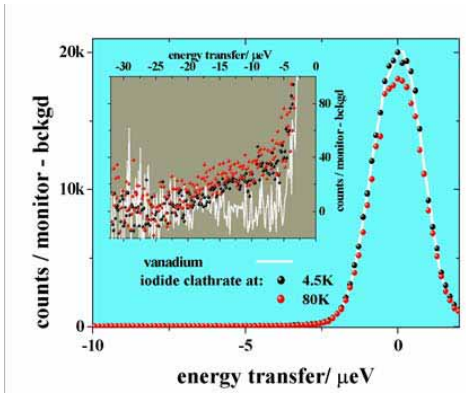

Figure 2: spectrum taken with the backscattering spectrometer. No low energy tunneling modes are found apart from a 'quasielastic' wing hardly outside the statistical error.

We have prepared the material by the technique described in ref. [4] and have confirmed the cubic II structure by neutron diffraction. The spectrum from SV29 (figure 1) shows a wing of inelastic intensity. The derived average tunnel splitting is 0.36meV. No transitions were observed in the μeV regime using the backscattering spectrometer (figure 2). This shows that the all interesting spectral features must be in the energy range between the two instruments.

A test experiment could be done in the meantime at the cold time-of-flight instrument NEAT at HMI. A spectrum with complex fine structure could be observed. Since methyl iodide occupies only the large cages of the cubic II structure, the different tunneling bands must be related to different adsorption sites. The work is going on.

[1] C.Gutt, W.Press, A. Hueller, J.S.Tse, H.Casalta, J. Chem. Phys. 114,4160(2001)
[2] P. Vorderwisch, A. Hueller, S. Hautecler, (2001)
[3] M. Prager, R. Caciuffo, G. Amoretti, C.J. Carlile, G. Coddens, F. Fillaux, O. Francescangeli, F. Ugozzoli, Mol. Phys. 81,609(1994)
[4] C.Albayrak, Dissertation, Aachen 1985

Institut für Festkörperforschung
Forschungszentrum Jülich GmbH
D-52425 Jülich

Experimental Report
of Neutron Scattering Experiments
at the FRJ-2 Reactor

Proposal number:	BSS-02-010 (continuation of BSS-02-002)		
Experiment title:	**Bound water on the surface of ionic micelles**		
Dates of experiment:	Within 24.10.-4.11.2002	Date of report:	08.03.03
Experimental team: Names	Addresses		
Vass, Szabolcs Gilányi Tíbor	Laboratory of Material Science KFKI Atomic Energy Research Institute 29-33 Konkoly-Thege út, 1121 Budapest, Hungary 1525 Budapest, P.O.Box 49, Hungary Department of Colloid Chemistry Loránd Eötvös University 1A Pázmány sétány, 1117 Budapest, Hungary 1518 Budapest 112, P.O.Box 32, Hungary		
Local Contact:	H. Grimm		

Experimental report text body

A recent SANS study revealed significant differences between the core radius R_c of ionic micelles and $R_0 = D_0/2$, the half-distance of their closest approach D_0. The difference was assumed to be explained in one or both of the following two ways: (i) Many experiments indicate that there is a so-called solvent structural term that must be included in the interaction potential. It arises because of the influence of a surface on adjacent solvent layers with decay length typically of order of 1.0 *nm* (Hunter, R.J.; *Foundations of Colloid Science*, Vols. 1 and 2, Clarendon Press, Oxford, 1989.). (ii) A too close approach of the micelles leads to the deformation of the local electric field. In case the double-layers frequently overlap, this deformation may induce energetically unfavorable changes in the core structure of the neighboring micelles, in particular in case of longer chains.

Molecules responsible for the solvent structural term should be bound to the surface of the micellar cores and, consequently, they are expected to move essentially slower than bulk solvent molecules. This is the basis of the proposed neutron backscattering measurments. In the previous experiment 0.07 mol/dm^3 H_2O solutions of sodium nonyl-, dodecyl- and hexadecyl sulphate have been studied at 40 °C. In the micellar solutions the experiments indicated the presence of H atoms whose translational diffusion coefficient is significantly less than that in the bulk water and, as expected, the diffusion coefficient decreased with the size of the micelles. The observed, positive, effect may stem from the H atoms of the core-forming alkyl chains or can be a contribution from elastic, small-angle, scattering. The fraction of H atoms in the core and from those in the bound water layer is calculated for 0.07 mol/dm^3 surfactant solutions and is plotted in Figure 1 for different thickness of the hypothetical bound-water layer.

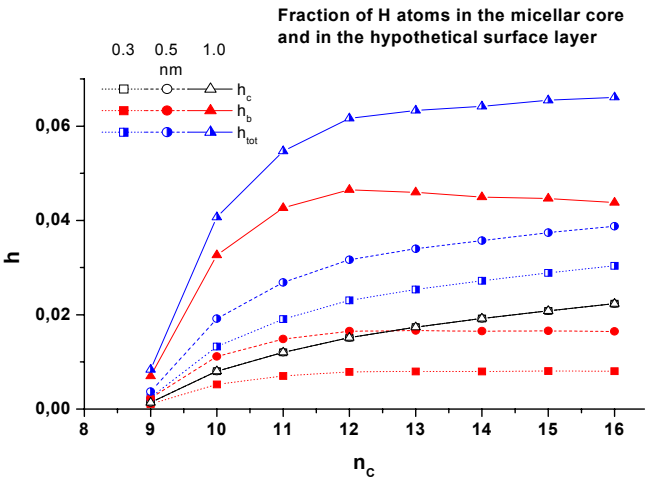

Figure 1. Fraction h_c (open symbols) of H atoms in the micellar core, h_b (full symbols) of those bound in the hypothetical layer formed around the core surface and their sum h_{tot}.(half-open symbols), as function of the number n_C of carbon atoms in the alkyl chain at 0.3, 0.5 and 1.0 nm layer thickness. An important consequence of the results is that the bound water-contribution are expected to be seen, provided core-effects can be detected.

The experiments have been done on H_2O, 0.07 mol/dm^3 solutions of (protonated) p-NaDDS in H_2O and D_2O, and (deuterated) d-NaDDS in H_2O; the interpretable results from the latter are plotted below in Figure 2. The d-NaDDS/H_2O curve at Q = 0.16 Å^{-1} in Fig. 2a indicates the presence of a strong elastic contribution from coherent scattering. The coherent-to-incoherent ratio for d-NaDDS/H_2O was found ~ 0.5, in good agreement with a guess made from SANS experiments, but in contradiction with model calculations.

The difference of the d-NaDDS/H_2O and H_2O curves could be described as a sum of an elastic- and a quasi-elastic component, details are given in Fig. 2b. The first (cyan line) is a multiple of the vanadium peak, the latter (olive line) resembles the water: its width is by ~30%, its area is by ~85% less than those of the bulk water (red line). Due to technical difficulties we were not able to gather similarly good quality data at higher Q's that should have been absolutely necessary for supporting this result. Thus we propose (i) to repeat the measurements with improved experimental conditions including the use of higher concentration d-NaDDS/H_2O solution and (ii) to make SANS experiments on the d-NaDDS/H_2O solutions to experimentally determine the Q-dependence of the elastic coherent contribution.

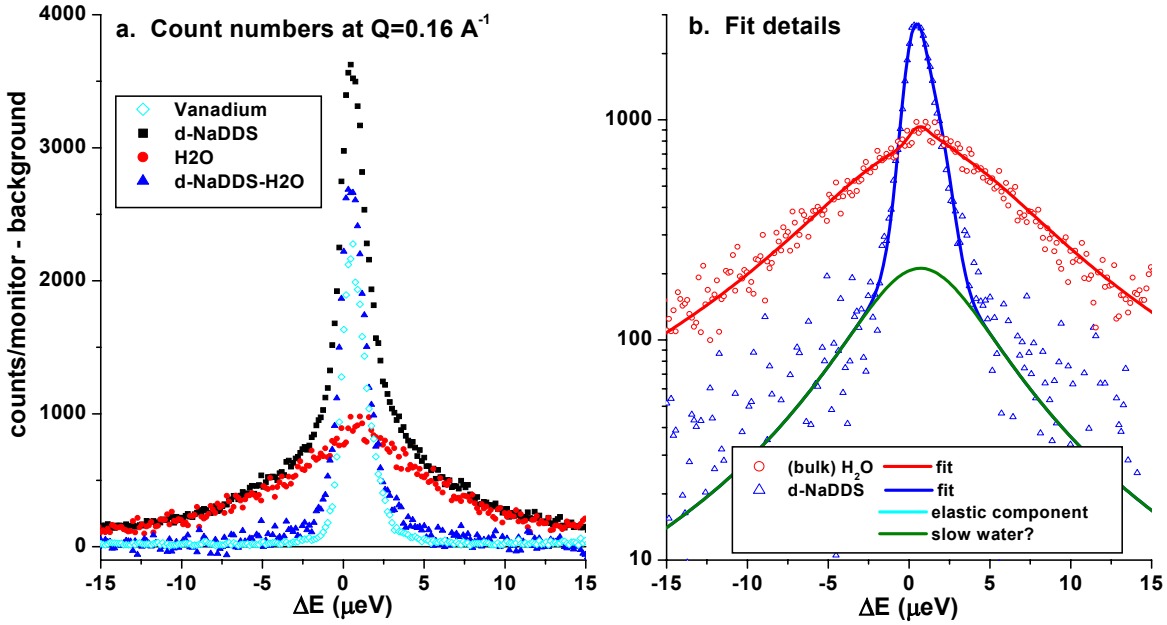

Figure 2. Interpretation of d-NaDDS results

Double Crystal Diffractometer (DKD)

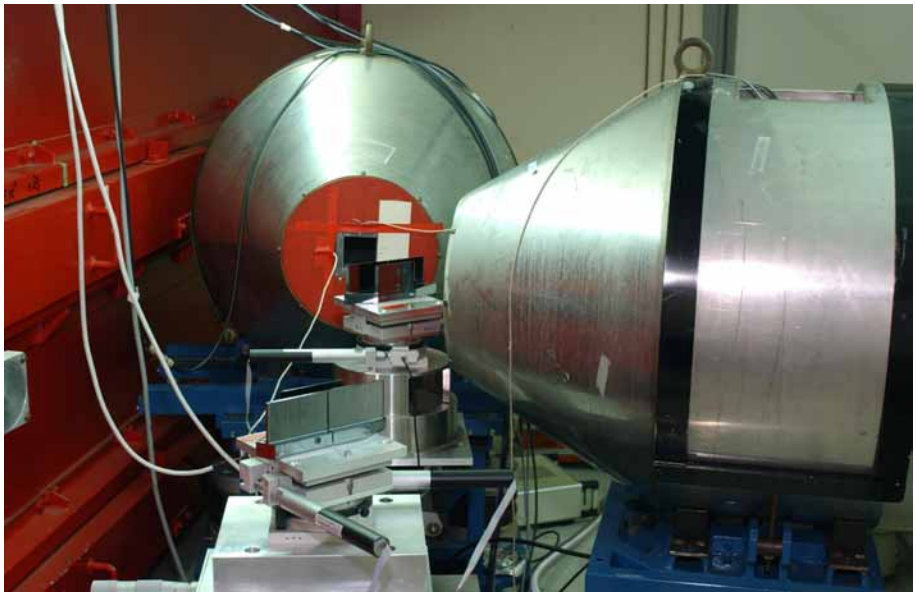

Instrument Parameters

Beam tube:	NLIIA straight guide cross section of guide 4.5 cm (height) × 3 cm (width)
Monochromator:	Si-crystal with coherent SiO_2 precipitates or graphite
Incoming beam ***- Cross section:*** ***- Sample size:***	 ≈ 10 cm^2 3 × 3 cm (max.)
Neutron flux at sample:	> 10^4 n/s (with graphite monochromator)
Momentum transfer range:	2×10^{-5} $Å^{-1} \leq Q \leq 10^{-3}$ $Å^{-1}$
Ancillary equipment:	heater device and pressure cell as for KWS1

Instrument Responsible

Dr. Dietmar Schwahn Tel. +49-(0)2461-61-6661 Email: d.schwahn@fz-juelich.de

Institut für Festkörperforschung
Forschungszentrum Jülich GmbH
D-52425 Jülich

Experimental Report
of Neutron Scattering Experiments
at the FRJ-2 Reactor

Proposal number:	**DKD-02-001**		
Experiment title:	**LONG- AND SHORT-RANGE SPATIAL INHOMOGENUITIES IN POROUS MATRICES OF VYCOR GLASS AND AEROGELS**		
Dates of experiment:	**10.9.2002-13.9.2002** **18.9.2002-20.9.2002** **23.09.2002-24.09.2002**	Date of report: 28 Feb. 2003	
Experimental team: Names	Addresses		
Melnichenko, Yuri B. Wignall, G.D.	Solid State Division ORNL P.O.Box 2008 Oak Ridge, TN 37831-6393		
Local Contact:	Dr. D. Schwahn		

Experimental report text body

Porous Vycor glass, aerogels and xerogels have been widely used for fundamental studies of transport, dynamic and critical phenomena in confined mixtures. However, information on the structure of these porous materials is usually restricted to nano- and mesoscopic scale, while there were several suggestions made in the iterature that much larger pores with the size of the order of microns may be present in these porous media. Evidently, the existence of such pores, if confirmed, should be taken into account for the interpretation of experimental data on the thermodynamic and dynamic properties of confined fluids.

Vycor porous glass is obtained from a borosilicate glass-forming melt which has undergone a phase separation, one of the two phases being removed by leaching. It is widely assumed that, as the result, a porous material with homogeneous pore diameters of 40 Å and the pore volume 28% is formed [2]. On the other hand, aerogels are ultra low density materials (with up to 98% of the void space) produced via sol-gel technology [8]. These porous systems do not possess a characteristic pore sizes, which can possibly span up to micrometer scale. So far, the structure of Vycor porous glass and aerogels has been investigated by neutron and X-ray small angle scattering in the range of scattering vectors $0.001\ Å^{-1} \le Q \le 0.2\ Å^{-1}$ [3-5] and it was suggested in our proposal to employ the ultra-small angle neutron scattering (USANS) technique in order to explore large voids, which should be visible in the USANS domain $Q << 0.001\ Å^{-1}$.

The experimental results obtained using Juelich DKD difractometer for two aerogels of different density as well as Vycor porous glass are shown in Fig 1 and Fig. 2, respectively.

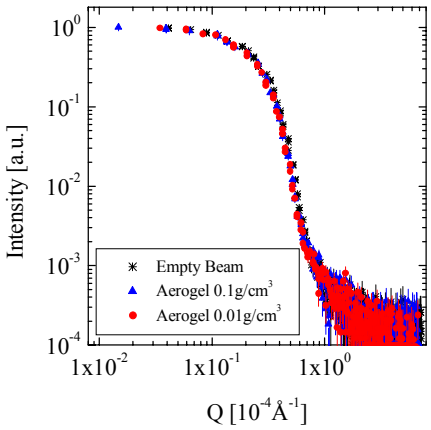

Fig. 1. USANS from aerogels.

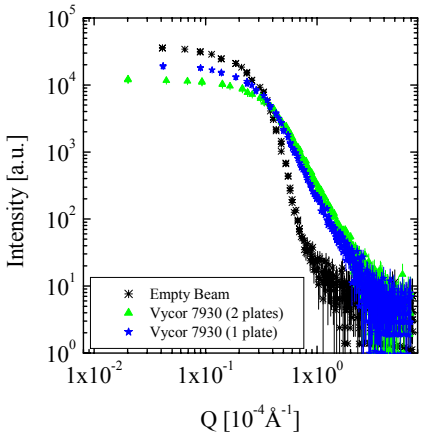

Fig. 2. USANS from Vycor porous glass.

As is seen, aerogels manifest no USANS scattering (Fig. 1), which is indicative of the absence of the micrometer size inhomogenuities in these systems. On the contrary, there exists a significant USANS signal coming from porous Vycor glass (Fig. 2). The intensity of scattering depends on the thickness of the material: it flattens out in the small Q region at different values of I(Q=0) and shifts in a parallel way with respect to incident intensity. The thorough analysis of the data obtained for aerogels is underway and will require resolution corrections along with conversion of experimental data obtained in a slit geometry to a „point" geometry. Interestingly, some conclusions can be already made by checking the exponent in the relation $I(Q) \sim Q^{-n}$ in the large-Q domain. In an „infinite slit" limit the Porod law $I(Q) \sim Q^{-4}$ translates into $I(Q) \sim Q^{-3}$. As is seen in Fig3, the function IQ^3 vs. Q levels off for the values of Q>0.0001, which implies that the scattering is coming from micrometer-level pores with sharp boundaries. Further analysis will include corrections for multiple scattering, and will allow for estimation of the pore sizes and volume fraction of big pores, the existence of which in Vycor has been demonstrated for the first time in this study [2].

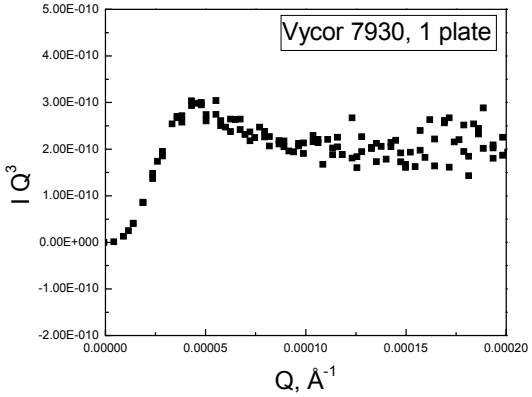

Fig.1. Analog of the Porod law for slit geometry. The figure demonstrates that USANS is coming from big pores in Vycor with sharp boundaries.

REFERENCES

1. Vycor Brand Porous Thirsty Glass 7930, Corning Technological Broshure, Corning Glass Works, Corning, NY 14830.
2. Melnichenko YB et al., J. Appl. Cryst., to be published.

Time-of-flight Spectrometer for Diffuse Neutron Scattering (DNS)

Instrument Parameters

Beam tube:	NL-1, straight neutron guide, 10 cm (height) × 7 cm (width)
Monochromator:	double focusing graphite, 6 crystals, each 5 × 4 × 0.2 cm^3
Wavelength:	3.3 Å < λ < 5.5 Å
Energy:	7.4 meV > $E_{initial}$ > 2.7 meV
Energy resolution:	0.9 meV > ΔE > 0.15 meV (FWHM, elastic)
Momentum transfer:	< 3.5 $Å^{-1}$ (elastic)
Vertical:	< 0.5 $Å^{-1}$ (elastic)
Polarizer:	focusing supermirror FeCoV/Ti:N
Transmission:	30 % to 50 % for correct spin
Sample position ***- Neutron flux:*** ***- Beam size:*** ***- Special sample*** ***- Environments:***	 (10^7... 3 × 10^6) n/cm^2s max. 6 cm (height) × 2 cm (width) split-coil magnet 5 tesla with dedicated cryostat, T > 2 K furnace T < 1600 °C, sample rotation inside
Detectors:	52(+12) ^{3}He-detectors (4 bar), solid angle: 0.3 srad
Angular range:	0° < 2Θ < 135°
Vertical:	2Θ < 15°
Distance to sample:	80 cm
Options for analysis ***- Time-of-flight:*** ***- Bragg:*** ***- Polarization:***	 disk chopper, duty cycle 0.05 104 graphite analyzers for E_{final} = 7.4 meV 12 detector unit with polarisation analysis; focusing, supermirrors FeCoV/Ti:N

Instrument Responsible

Dr. Werner Schweika Tel. +49-(0)-2461-61-6650 Email: w.schweika@fz-juelich.de
Dr. Yixi Su Tel. +49-(0)-2461-61-4786 Email: y.su@fz-juelich.de

Institut für Festkörperforschung
Forschungszentrum Jülich GmbH
D-52425 Jülich

Experimental Report
of Neutron Scattering Experiments
at the FRJ-2 Reactor

Proposal number:	DNS-02-001		
Experiment title:	**Nanoscale polaron-polaron correlation in perovskite CMR manganites**		
Dates of experiment:	24-01-2002	Date of report: 24-03-2003	
Experimental team: Names	Addresses		
Y. Su K. Istomin	IFF, Forschungszentrum Juelich GmbH		
Local Contact: W. Schweika	IFF, Forschungszentrum Juelich GmbH		

Experimental report text body

Short-range structural and magnetic correlations in the paramagnetic insulating (PI) regime of doped manganites compounds are believed to play a key role in the occurrence of Colossal Magnetoresistance (CMR). In a number of recent experimental investigations, short-range structural correlations were observed in the PI phase in $La_{1-x}Ca_xMnO_3$, $La_{2-x}Sr_{1+2x}Mn_2O_7$, $Pr_{1-x}Ca_xMnO_3$ and $Nd_{1-x}Sr_xMnO_3$. These correlations are interpreted as arising from nanoscale regions possessing charge/orbital ordering and associated lattice distortions. In this report, investigations on structural and magnetic correlations in several lightly doped $La_{1-x}Sr_xMnO_3$ (x~0.105, 0.115, 0.125) single crystals will be described. These single crystals were extensively characterized by electrical, magnetic and chemical methods, and are all exhibiting a ferromagnetic insulating (FI) ground state below charge/orbital ordering transition temperatures ($T_{CO/OO}$). The characteristic superstructures associated with charge/orbital ordering and lattice modulations can be observed by complementary synchrotron X-ray scattering techniques. These single crystals were measured at DNS, which is a diffuse neutron scattering spectrometer. The neutrons with wavelength at 3.3 Å were utilized throughout all measurements. Time-of-flight measurements and polarization analysis (PA) were undertaken at DNS, too. One of advantages with the DNS instruments is that a large reciprocal space can be measured in a short period, therefore, any short-range correlations would appear up as diffuse and broad scattering features around or between main Bragg reflections. Furthermore, these diffuse scattering due to structural or magnetic contributions can be separated by the PA method. Some preliminary results will be briefly discussed in the following sections.

1. Diffuse scattering around main Bragg reflections

Diffuse scattering from short-range structural and/or magnetic correlations were extensively searched in all 3 samples, as shown in Fig. 1 (a)-(c),

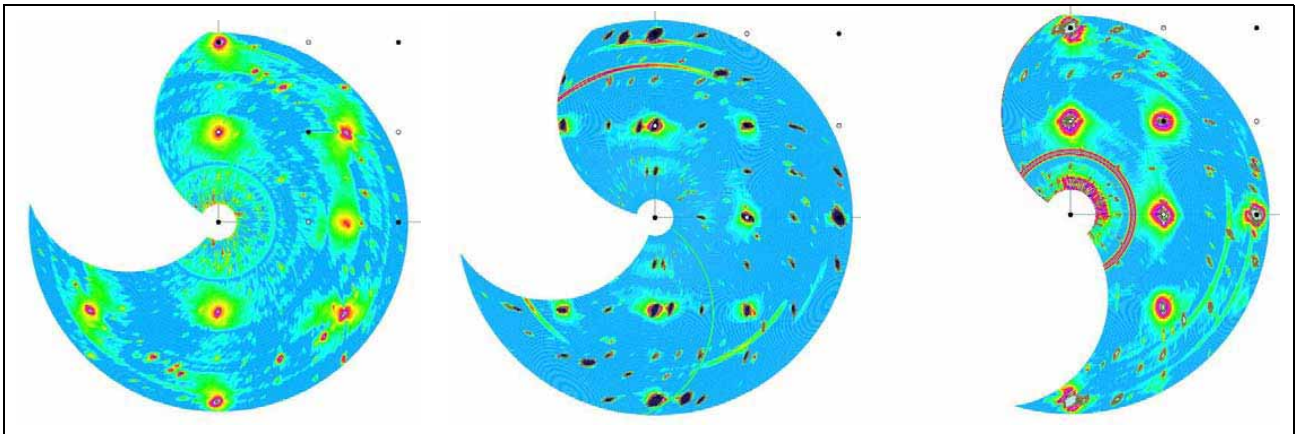

(a) $x \sim 0.125$ (b) $x \sim 0.105$ (c) $x \sim 0.115$

Fig. 1 2D reciprocal space plots at 250 K measures at DNS

It can be clearly shown that strong and anisotropic diffuse scattering can be observed around major Bragg reflections above the Curie temperature (T_C) in the paramagnetic phases. Careful measurements were also undertaken at possible charge/orbital ordering wavevector positions to search for the short range charge/orbital correlations, so far, no indications for such kind of correlations were made. The fact of that all three single crystals are intrinsically twinned, further complicated the data interpretation. The temperature dependence of diffuse scattering was measured as shown in Fig. 2,

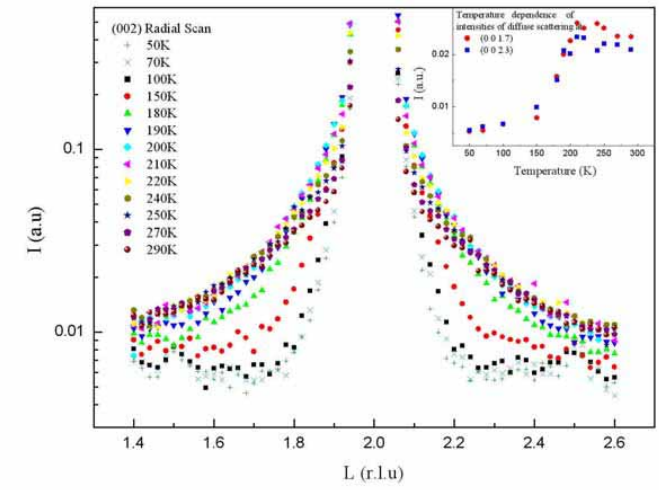

Fig. 2 Radial scans across (002) for the sample with $x \sim 0.125$ at different temperatures; intensities at (0 0 1.7) and (0 0 2.3) is shown in the inset

It can be indicated that the diffusing scattering slowly increases up to maximum when approaching T_C at around 210 K upon cooling, then decreases steeply below T_C, it become almost vanished below 150 K. This behavior is in reminiscence to a paramagnetic scattering, or short-range magnetic correlations.

2. Polarization analysis of neutron diffuse scattering

The *XYZ* - Polarization analysis (PA) was employed to identify the nature of the diffuse scattering observed around main Bragg reflections. The *XYZ*-PA provides full and unambiguous separation of magnetic, nuclear coherent and spin-incoherent cross sections on a multiple-detector instrument. Spin-flip and non-spin-flip cross

sections can be measured with the incident polarization alternatively in the *X, Y, Z* directions, therefore six cross sections in total will be obtained for separations. The separation rules have been developed as the following,

$$\frac{d^2\sigma}{d\Omega d\omega}_{paramagnetic} = 2(\frac{d^2\sigma}{d\Omega d\omega}^{SF}_{x} + \frac{d^2\sigma}{d\Omega d\omega}^{SF}_{y} - 2\frac{d^2\sigma}{d\Omega d\omega}^{SF}_{z}) = -2(\frac{d^2\sigma}{d\Omega d\omega}^{NSF}_{x} + \frac{d^2\sigma}{d\Omega d\omega}^{NSF}_{y} - 2\frac{d^2\sigma}{d\Omega d\omega}^{NSF}_{z})$$

$$\frac{d^2\sigma}{d\Omega d\omega}_{nuclear-coherent} = \frac{d^2\sigma}{d\Omega d\omega}^{NSF}_{z} - \frac{1}{2}\frac{d^2\sigma}{d\Omega d\omega}_{paramagnetic} - \frac{1}{3}\frac{d^2\sigma}{d\Omega d\omega}_{spin-incoherent}$$

$$\frac{d^2\sigma}{d\Omega d\omega}_{spin-incoherent} = \frac{3}{2}(3\frac{d^2\sigma}{d\Omega d\omega}^{SF}_{z} - \frac{d^2\sigma}{d\Omega d\omega}^{SF}_{x} - \frac{d^2\sigma}{d\Omega d\omega}^{SF}_{y})$$

The PA was made at several temperature around T_C, as shown in Fig. 3, and the depolarization of the neutron beam was also measured over temperatures as shown in Fig. 4,

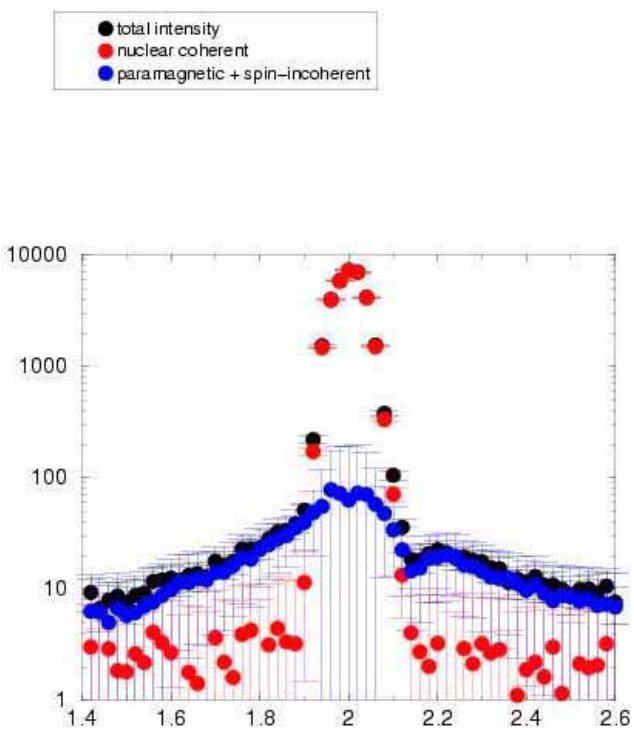

Fig. 3

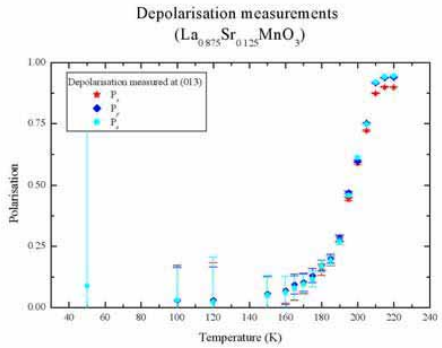

Fig. 4

These results clearly determined that the diffuse scattering observed at the PI range is dominated by the paramagnetic scattering. A comprehensive data treatment is in progress.

Institut für Festkörperforschung
Forschungszentrum Jülich GmbH
D-52425 Jülich

Experimental Report
of Neutron Scattering Experiments
at the FRJ-2 Reactor

Proposal number:	DNS-005		
Experiment title:	**A Diffuse Neutron Scattering Study of the Rattling Motion in Filled Skutterudites**		
Dates of experiment:	December 2002	Date of report:	January 2003
Experimental team: Names	Addresses		
Hermann Raphael P. Grandjean Fernande Long Gary J.	Bat B5 – Dept Phys – Universite de Liege – 4000 LIEGE – BELGIQUE “ “ University of Missouri Rolla		
Local Contact:	Dr W Schweika		

Experimental report text body

Experiment title: **A Diffuse Neutron Scattering Study of the Rattling Motion in Filled Skutterudites**

We proposed a direct study of the rattling motion of the atom in the antimony-iron cage. Indeed, the rattling of the filling atom has been described as a localized vibration, which should be responsible for the reduction in thermal conductivity. However, in view of the large open space in the antimony-iron cage, instead of harmonic vibrations, the dynamics of the filling atom could be determined by local jumps on preferred sites inside this cage. In this case a quasi-elastic scattering, determined by the atomic jump frequencies and distances, should be observable. Complementary, a Q-dependent variation of the elastic incoherent structure factor (EISF) would yield the Fourier Transform of the space of motion.

We have chosen to study $NdFe_4Sb_{12}$ because, in this compound, the contribution to the incoherent scattering signal from the neodymium is 85 %. The resolution of the DNS instrument is 0.2 to 1 meV and so it can readily be used to study processes on the picosecond time scale corresponding to activation energies smaller than 0.1 eV. Hence, we proposed a temperature dependent study over the full stability range of the compounds, i. e. from 10 to 1000 K, to study the elastic incoherent structure factor at different thermal energies in order to clarify the characteristics of the local dynamics, and in case of fast local jump diffusion processes to measure the thermal activation energy of the rattling process.

During the experimental period, we first measured the background on the sample holder designed for this project, a holder which proved to be adequate. Then we measured a room temperature TOF spectrum at 3.3 Å wavelength on $NdFe_4Sb_{12}$ that showed no broadening of the elastic lines, nor any variation in the EISF. We then proceeded to measure a 800 K spectrum, first at 3.3 Å then at 4.6 Å wavelength. These spectra didn't show any significant changes.

The experiment failed because the sample was not appropriately prepared. Because the sample was delivered with some delay shortly before the experiment, we could not do the usual characterization prior to the experiment. The problem of a substantial fraction of an undesired secondary phase became apparent after heating and evaporation of Sb. No conclusive results have been obtained with respect to the proposal so far. We plan to redo the experiment, when we shall have a well characterized, high purity sample.

A remaining part of the scheduled beam time was used for inelastic studies on $Sr_8Ga_{16}Ge_{30}$ with interesting results, which we shall describe in detail in a separate experimental report.

Institut für Festkörperforschung
Forschungszentrum Jülich GmbH
D-52425 Jülich

Experimental Report
of Neutron Scattering Experiments
at the FRJ-2 Reactor

Proposal number:	DNS-02-006	
Experiment title:	**Diffuse scattering and phonons in $Cu_{2-\delta}Se$**	
Dates of experiment:	25.-30.11.2002	Date of report: 12-Mar-03
Experimental team: Names	Addresses	
S.A. Danilkin	Hahn-Meitner-Institut, SF2 Glienicker Str. 100 D-14109 Berlin	
Local Contact:	W. Schweika	

Experimental report text body

In non-stoichiometric compounds $Cu_{2-\delta}Se$ ($0<\delta<0.25$) the temperature of superionic phase transition depends on composition and decreases with δ, so that $Cu_{1.8}Se$ has a structure of the high-temperature superionic α-phase at room temperature. The measurements of diffuse scattering in α-Cu_2Se by anomalous X-ray technique using synchrotron radiation reveal the strong correlation between thermal displacements of the Cu ions atoms [1]. The decrease of diffuse scattering intensity from α-Cu_2Se powder observed in $\Delta E \approx 0$ scans measured with triple-axis spectrometer in comparison with standard two-axis geometry of experiment shows that correlations among the thermal displacements are dynamic. Therefore the aim of the experiment with DNS spectrometer was to measure the inelastic scattering from $Cu_{2-\delta}Se$ single crystal and to obtain information about phonon contribution, its distribution in the reciprocal space and correlation with diffuse scattering.

The measurements with DNS spectrometer were performed on single crystal sample with composition $Cu_{1.85}Se$. At room temperature it has a structure of a high-temperature α-phase: anti-fluorite type cubic lattice of Se ions with Cu distributed over the interstitial sites. A crystal with lattice parameter 0.5755 nm and mosaic spread about 30′ was aligned with (01-1) as scattering plane. We used wavelength of incident neutrons of λ = 0.33 nm and measured Ω_s scans in inelastic mode of spectrometer.

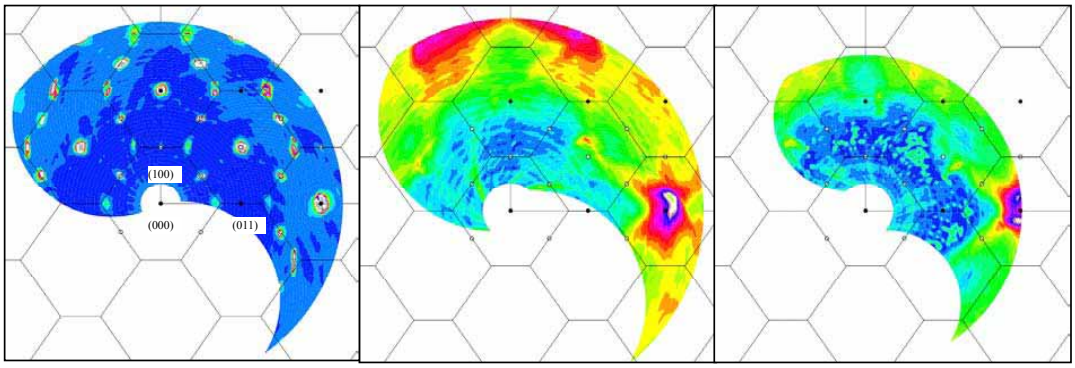

(100)

Fig.1 Intensity contours in (01-1) plane of α-$Cu_{1.85}Se$ at RT for elastic scattering (left) and for neutron energy transfer 3 meV (energy gain - middle, energy loss- right).

Elastic scattering map (Fig. 1) shows the superstructure spots in <111> direction which corresponds to modulated distribution of Cu ions with period $1/2d_{(000)-(011)}$. Such a structure was observed in Cu_2Se at RT in low-temperature β-phase [2]. In non-stoichiometric compound $Cu_{1.75}Se$ the ordering was only observed at temperatures below 170 K [3].

Inelastic scattering with annihilation of phonons is most intense in (022) and (311) Brillouin zones (BZ) (Fig. 1). The intensity contours are symmetric - extended along directions of high symmetry. In (022) BZ the elongation in [100] and [111] directions is clearly seen both in energy gain and energy loss spectra. In the measurements of elastic scattering on $Cu_{1.8}Se$ single crystal with neutron multidetector diffractometer E2 (HMI, Berlin) we observed the diffuse scattering along [111] direction. The present experiment shows that this diffuse scattering mainly inelastic and most probably comes from the low-energy phonon branches. The peculiarity of $Cu_{2-x}Se$ is the presence of the LE- modes in inelastic neutron scattering spectra on powder samples [1, 4]. These LE-modes are originated from the low-lying TA phonons, which in α-$Cu_{1.85}Se$ change the slope drastically at q>0.2-0.4 and became nearly flat at higher q having energy of about 4 meV [4]. The scattering processes involving these low-energy phonons appear as elongation of the intensity contours along [111] and [100] directions (Fig. 1). Note that in the measurements with triple-axis spectrometer the decrease of intensity of one-phonon peaks with increasing q was much stronger in direction [011] then in other directions of symmetry. This correlates with a sharp profile of (022) peak [011] direction (Fig. 1).

References:

[1] T. Sakuma, Bulletin of Electrochemistry 11 (1995) 57.

[2] Z. Vu?i?, O. Milat, V. Horvati?, Z. Ogorelec, Phys. Rev. B, **24** (1981) 5398.

[3] Y. Okada, T. Ohtani, Y. Yokota, Y. Tachibana, K. Morishige, J. Electron Microscopy, **49**(1) (2000) 25.

[4] S.A. Danilkin, A.N. Skomorokhov, A. Hoser, H. Fuess, V. Rajevac, N.N. Bickulova, Crystal structure and lattice dynamics of superionic copper selenide $Cu_{2-\delta}Se$, submitted to J. Alloys and Compounds, 2003.

Institut für Festkörperforschung
Forschungszentrum Jülich GmbH
D-52425 Jülich

Experimental Report of Neutron Scattering Experiments at the FRJ-2 Reactor

Proposal number:	DNS-007		
Experiment title:	A New Method for Vector Polarization Analysis Test on MnF_2		
Dates of experiment:	18.10.-2.11.02	Date of report:	11.03.03
Experimental team: Names:	Addresses:		
W. Schweika K.-U. Neumann	IFF, FZ-Jülich Dept. of Physics, Loughborough University		
Local contact:	—		

We report on first results of a new method for full polarization analysis using precessing neutron polarization.
The use of polarized neutrons and polarisation analysis of the scattered neutron intensity is a decisive tool to distinguish magnetic scattering from nuclear scattering contributions. The way how the scattering intensity depends on the scattering vector and in particular on the directions of the initial and final polarization provides a detailed description of magnetic properties on an atomistic scale. Therefore, as done in the well established xyz-method (Schärpf and Capellmann), for instance on multi-detector instruments DNS or D7 (at ILL), one may prepare the initial polarization in three orthogonal directions and analyse the scattering for non-spin-flip and spin-flip processes in the sample. However, this method does not provide in general a complete information. One only obtains the diagonal terms of the 3×3 polarisation matrix that is determined by the vectors of incident and final polarisation. If the polarisation, for instance, is turned by 90 degrees, spin-flip and non-spinflip scattering will be the same as if depolarisation would have occured.
A complete polarization analysis can be realized, if the sample is kept in a zero-field environment to avoid any additional precessions and changes of the polarization. Therefore, thin screening shields of mu-metal or super-conducting sheets (Cryopad) have been used, and since field changes at the boundaries are sudden enough, the initially (by a flipper) prepared polarization is maintained inside and can be analyzed using a secondary flipper. Restrictions of zero-field conditions are quite severe for the sample enviroment, and applications for time-of-flight machines and/or multi-detector instruments are practically impossible.

Recently it has been suggested by Schärpf, that one could analyze possible precessing polarization components of the scattered neutrons. Therefore an additional precession coil and $\pi/2$-flippers between sample and detectors would be required for the final analysis. Different to this original proposal, we tested a new method which uses a precessing polarization in the incident beam by operating the usual Flipper not in π but $\pi/2$ mode. This also allows to measure the off-diagonal elements of the polarisation matrix, since scattered neutrons with final non-precessing polarization are guided by the field to the detectors. However this method has decisive advantages, because it can be fulfilled independently of the energy transfer of the neutrons and it can be achieved simultaneously for all detectors covering a large range in scattering angles. Note that there are no additional equipments required compared to the standard xyz-method.
Our experiment demonstrates the feasibility by measuring the (100) Bragg reflection of the antiferromagnet MnF_2, with its **a** and **c**-axes in the scattering plane, see Fig. 1. This example considers a scattering process with a $\pi/2$-rotation in the scattering plane. The magnetic moments are aligned along the **c**-axis. Therefore, if the neutron polarization is precessing in the plane (yz), which is perpendicular to the applied field $\mathbf{B_x}$ pointing between the **a** and **c**-axes, upon a variation of the precession angle as a function of $\mathbf{B_x}$, oscillations of the Bragg scattering intensity can be observed. They result from a rotation of the polarization around the **c**-axis with transitions from a precessing to the non-precessing component of the neutron polarization. Maxima and minima occur if **P** points in $\mathbf{x}$ and $-\mathbf{x}$ direction, respectively, while **P** parallel to $\pm\mathbf{z}$ determines the points of zero curvature in figure 1.

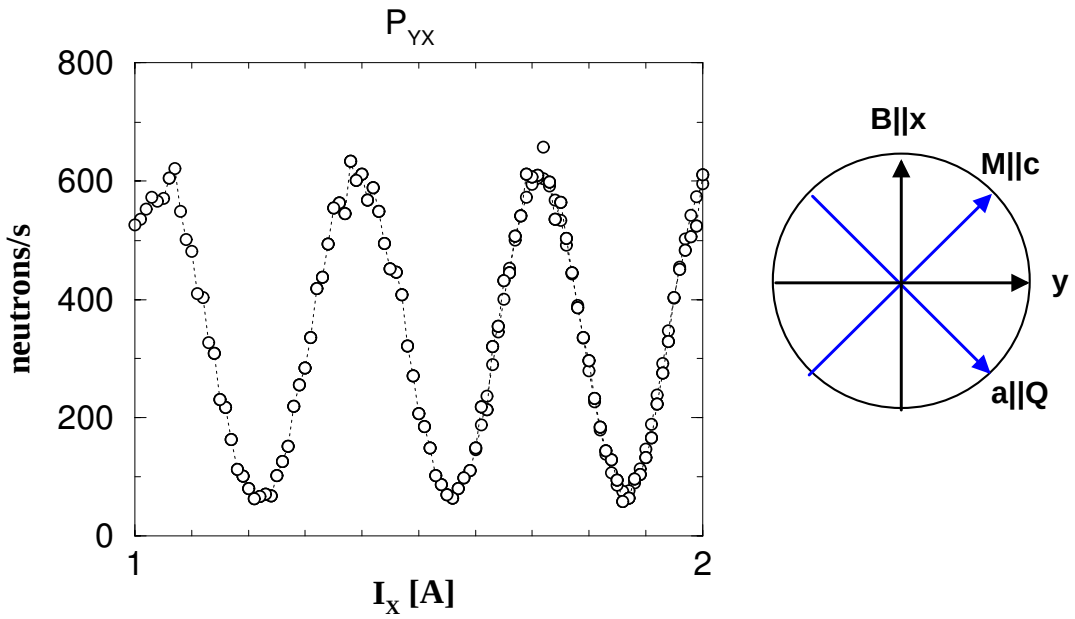

Fig.1 Measurement of an off-diagonal polarization element P_{yx} with the new technique of vector polarisation analysis of precessing neutron spins on the antiferromagnetic (100) Bragg peak of a MnF_2 single crystal.

Institut für Festkörperforschung
Forschungszentrum Jülich GmbH
D-52425 Jülich

Experimental Report
of Neutron Scattering Experiments
at the FRJ-2 Reactor

Proposal number:	DNS-02-008		
Experiment title:	Low Energy Charge Fluctuations in the Layered Manganite $La_{1.2}Sr_{1.8}Mn_2O_7$		
Dates of experiment:	17/02/03 up to 24/02/03	Date of report: 24/03/03	
Experimental team: Names	Addresses		
Werner SCHWEIKA Nadir ALIOUANE	Institut für Festkörperforschung, Forschungszentrum Jülich GmbH, D-52425 Jülich Hahn-Meitner-Institut, BENSC SF2, 100 Glienicker Str., Berlin D-14109		
Local Contact:	Werner Schweika		

Experimental report text body

$La_{1.2}Sr_{1.8}Mn_2O7$ is a layered magnetic manganite belonging to the Ruddlesden-Popper series $(La_x,Sr_{1-x})_{n+1}Mn_nO_{3n+1}$ with n=2 and x=0.4. It is well known that these compounds exhibit Colossal magneto resistance (CMR) properties [1], produced during the ferromagnetic-metal to the paramagnetic-insulator transition close to the Curie temperature (T_C). This transition is attributed to the competition between the magnetic double exchange [2] (producing the metallic-ferromagnetic states below T_C~125K) versus an electron-phonon coupling [3] via the Jan-teller active on Mn^{+3} ion (producing the insulator paramagnetic states above T_C). Recent inelastic neutron experiment [4,5] reveals strong anisotropic diffuse scattering rods elongated in the c direction. In this studies, the integrated intensity of these diffuse scattering is modulated and can be interpreted as the in-plane angle between spins in neighboring layers within the bilayer [5]. In addition to charge correlations that give rise to longitudinal pattern of displacement (which result to diffuse scattering at $\mathbf{q}_L$=(0.3,0,1) [6], one find diffuse reflections with propagation vector $\mathbf{q}_{CE}$=(1/4,1/4,0). This type of scattering is interesting because it suggests the same pattern of local displacements as those found for the long range charge and orbitally ordered state found at higher doping x=0.5. The most interesting aspect of these measurements however is that the scattering at $\mathbf{q}_{CE}$ is completely dynamic at high T, and localized around $\mathbf{q}_{CE}$. This suggest that at sufficiently high temperature, dynamic CE correlations are found with a dynamic correlation length of ~15Å, but then *freeze* upon cooling to a temperature T* ~ 310 K. This is indicated by a linear decrease of the quasielastic width for T>T*, a specral weight transfer from the quasielastic to the elastic and a non divergent coherence length. This glass transition (polaron glass to polaron liquid transition) suggests that the paramagnetic/insulating state arises from an inherent orbital frustration that inhibits the formation of a long range orbital- and charge-ordered state and a new at T*=310K[6].

In the scheme to better understand this features, we have performed formerly at DNS, an neutron time of flight experiments on a single crystal of $La_{1.2}Sr_{1.8}Mn_2O_7$ versus temperature around the (200) and in the (a,c) plan above the T* temperature (370K, 450K and 500K). The *TOF* data indicated holes in this anisotropic diffuse scattering rods <10l> direction.

The purpose of this experiment was to confirm weather the dynamic correlations are observed for the diffuse scattering at q=(0.3,0,1). Our measurements on DNS have shown that at $\mathbf{q}_L$=(0.3,0,1) the data is dominated by dynamic Huang scattering and no dynamic correlations with q=(0.3,0,1) are found.

The new measurements done at low temperature (from 80K up to room temperature) confirm this behavior. Indeed as one see the left side of the following figure (cut according to the E, *<10l>* direction of the reciprocal space) the holes appear due to the separation between different diffuse scattering condensing them and producing holes (the right side of the picture). We are still analyzing the data in a view to understand this intriguing behavior.

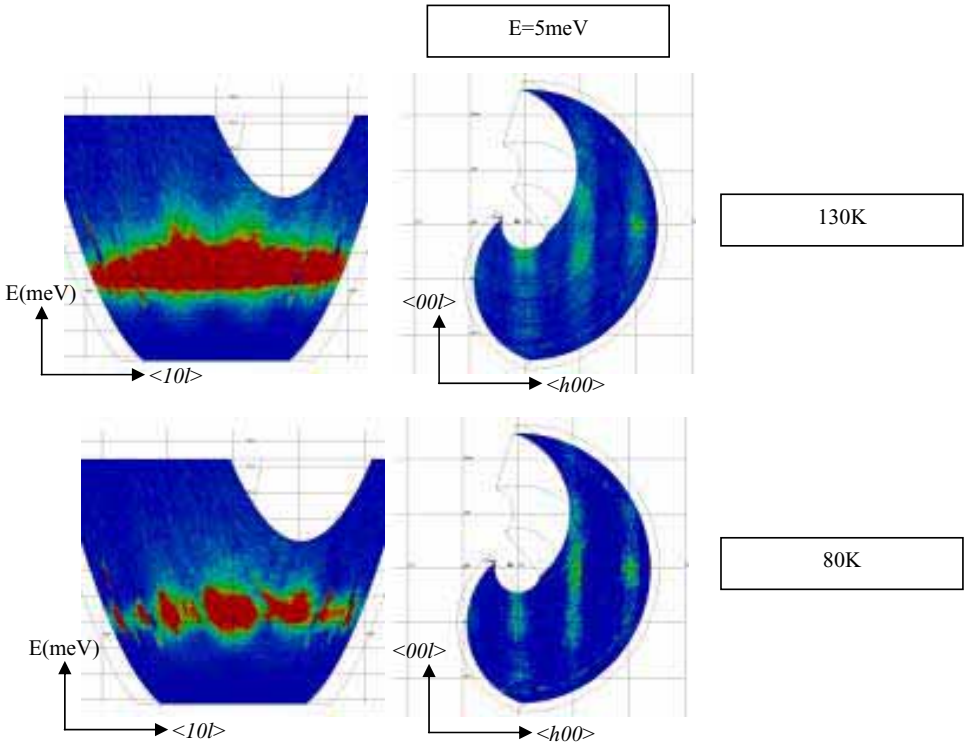

[1]. T. Kimura, Y. Tomioka, H. Kuwahara, A. Asamitsu, M. Tamura and Y. Tokura, Sciences **274**,1698 (1996)
[2]. C. Zener, Phys. Rev. **82**, 403 (1951); P. G. de Gennes, Phys. Rev. **118**, 141 (1960)
[3]. A. J. Millis, B. I. Shraiman and R. Mueller, Phys. Rev. Lett. **77**, 175(1996)
[4]. T. G. Perring, G. Aeppli, Y. Moritomo and Y,.Tokura, Phys. Rev. Lett. **78**, 3197 (1997)
[5]. R. Osborn, S. Rosenkranz, D. N. Argyriou, L. Vasiliu-Doloc, J. W. Lynn, S. K. Sinha, J. F. Mitchell, K. E. Gray and S. D. Bader, Phys. Rev. Lett. **81** (1998)
[6]. D. N. Argyriou, J. W. Lynn, S. Rosenkranz, R. Osborn, B. Campbell, J. F. Mitchell, U. Ruett, H. N. Bordallo, A. Wildes and C. D. Ling, Phys. Rev. Lett. **89** (2002)

Institut für Festkörperforschung
Forschungszentrum Jülich GmbH
D-52425 Jülich

Experimental Report
of Neutron Scattering Experiments
at the FRJ-2 Reactor

Proposal number:	UDS-01-012		
Experiment title:	**An Inelastic Neutron Scattering Study of the Phonon Density of States in Some Thermoelectric Materials**		
Dates of experiment:	June 2002	Date of report:	30.12.2002
Experimental team: Names	Addresses		
Hermann Raphael Grandjean Fernande Long Gary	*Department of Physics, B5, University of Liège, B-4000 Sart-Tilman, Belgium* *Department of Physics, B5, University of Liège, B-4000 Sart-Tilman, Belgium* *Department of Chemistry, University of Missouri-Rolla, Rolla, MO65409-0010*		
Local Contact:	Dr. W. Schweika		

Experimental report text body

There has recently been a renewed interest in the use of thermoelectric refrigerators both because of environmental concerns about the chlorofluorocarbons and for the use of waste heat to generate low-cost electric power. The resurgence of interest has also occurred because many new ternary compounds are now available for study, ternary compounds that were not investigated earlier. Further, experimental techniques, such as Mössbauer and x-ray absorption spectroscopy, x-ray inelastic nuclear resonant scattering, and neutron scattering, make possible a very detailed evaluation, on a microscopic level, of the intrinsic electronic and vibrational properties that lead to efficient thermoelectric materials. These techniques have the advantage of probing individual atoms or even specific electrons within thermoelectric materials. The combination of these developments provides an ideal framework for the design of new, more efficient, thermoelectric materials.

Among many semiconducting materials, the filled skutterudite compounds with formula $R_xFe_{4-y}Co_ySb_{12}$, where R is a rare-earth atom, or Tl, Ca, Sr, or Ba, have attracted much attention as good thermoelectric candidates. They meet the necessary requirements: a large number of atoms, 34, per unit-cell, a reasonable electric conductivity, and a low thermal conductivity. In $CoSb_3$, which crystallizes with the skutterudite structure, the R atoms are absent and in the filled skutterudite compounds[1] the R atoms are vibrating with large atomic mean-square displacement. The low thermal conductivity of the filled skutterudite is usually ascribed[2] to the "rattling" of the R atoms in their cubic cage.

We studied the phonon density of states of $CoSb_3$, $Tl_{0.8}Co_3FeSb_{12}$, $Tl_{0.8}Co_4SnSb_{11}$ and $Tl_{0.5}Co_{3.5}Fe_{0.5}Sb_{12}$, by inelastic neutron upscattering at 295 K on the DNS instrument. The results of this study are summarized in Fig.1, where the phonon density of states was modeled up to 10 meV by a Debye dependence in ω^2 for the unfilled $CoSb_3$ and the sum of this ω^2 dependence and a Gaussian mode attributed to an Einstein oscillator around 5 meV for the filled compounds[3]. Heat capacity measurements on $Tl_{0.8}Co_4SnSb_{11}$ and $CoSb_3$ confirm a contribution of an Einstein oscillator to the heat capacity of the filled compound[3].

The width of the Gaussian contribution to the density of states in $Tl_{0.8}Co_3FeSb_{12}$ is exactly equal to the instrumental resolution at that energy transfer. Hence, there is no significant hybridization with the acoustic phonons in this compound, whereas a broadening is clearly visible in $Tl_{0.8}Co_4SnSb_{11}$ which is an indication of hybridization.

Both the neutron scattering and heat capacity studies also confirm that $CoSb_3$ is an appropriate reference compound for thallium filled skutterudites, the lattice dynamics being close to that of the filled compounds, with the exception of a localized mode.

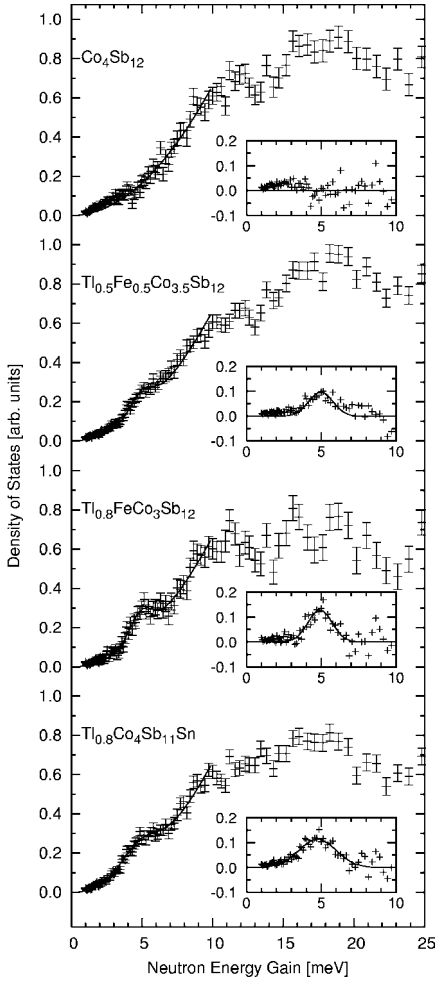

Fig. 1: 295 K density of states for the indicated compounds. The solid line is the result of the fit described in the text.
Insets: the difference between the measured density for the filled and unfilled compounds. The solid line is the Gaussian representing the localized vibrational mode.

[1] D. J. Braun and W. Jeitschko, *J. Less-Common Metals* **72**, 147 (1980).

[2] G. S. Nolas, G. A. Slack, D. T. Morelli, T. M. Tritt, and A. C. Ehrlich, *J. Appl. Phys.* **79**, 4002 (1996).

[3] R.P. Hermann, R. Jin, W. Schweika, F. Grandjean, D. Mandrus, G. J. Long, B.C. Sales, *submitted to Phys. Rev. Letters*, Dec. 2002.

Neutron Reflectometer with Polarization Analysis (HADAS)

Instrument Parameters

Monochromator:	(002) pyrolytic graphite double monochromator
Wavelength:	2 Å < λ < 6.5 Å, λ = 4.52 Å for reflectometry
Wavelength resolution:	1 %
Collimation:	0.1 mrad < ΔΘ < 10 mrad (unpolarized beam), 0.1 mrad < ΔΘ < 1.5 mrad (polarized beam)
Polarization analysis:	Stack of 30 double sided polarizing supermirrors (top m = 2.5, bottom m = 1.8) set up as divergent collimator
Detector:	2D position-sensitive scintillation detector, 80 mm diameter, resolution < 1.5 mm, at 1.6 m distance from the sample
Neutron flux at sample:	10^5 unpolarized neutrons /cm^{2}s with a collimation of ΔΘ = 2 mrad, 2×10^4 polarized neutrons /cm^{2}s with a collimation of ΔΘ = 1 mrad
Maximal beam size at sample:	50 mm × 10 mm (unpolarized), 20 mm × 10 mm (polarized with polarisation analysis)
Special sample environment:	Electromagnet 0.3 mT < $\mu_0 H$ < 1 T ; He flow cryostat 10 K < T < 300 K

Instrument Responsible

Dr. Ulrich Rücker Tel. +49-(0)-2461-61-6896 Email: u.ruecker@fz-juelich.de
Dr. Emmanuel Kentzinger Tel. +49-(0)-2461-61-3139 Email: e.kentzinger@fz-juelich.de

Institut für Festkörperforschung
Forschungszentrum Jülich GmbH
D-52425 Jülich

Experimental Report
of Neutron Scattering Experiments
at the FRJ-2 Reactor

Proposal number:	HAD-01-005		
Experiment title:	**Off-specular scattering of Polarized Neutrons on Epitaxial Fe / Cr / Fe (001) Trilayers exhibiting magnetoresistance**		
Dates of experiment:	29.5. – 5.6.2002	Date of report:	10.3.2003
Experimental team: Names	 Addresses		
D. Olligs U. Rücker E. Kentzinger	IFF-Elektronische Eigenschaften IFF-Streumethoden IFF-Streumethoden		
Local Contact:	U. Rücker		

Experimental report text body

Epitaxial Fe / Cr / Fe trilayers were grown by stopping the deposition of Fe and Cr at a reflection high-energy electron diffraction (RHEED) intensity maximum or minimum. Thus, a pair of identical samples was obtained that only differ (from the structural point of view) by their interface roughness with the nominal difference of ½ atomic Monolayer. This structural difference has been confirmed by X-ray reflectivity and offspecular scattering. The current-in-plane magnetoresistance (CIP-GMR) of such trilayers is found to be significantly enhanced in the samples with the rougher interfaces (half-integer number of Monolayers of the first layer).

We performed off-specular scattering of polarized neutrons on these samples to investigate, if the change of interface roughness implies a change in magnetic fluctuations at the Fe / Cr interfaces.

Fig. 1 shows the reflectivity and off-specular scattering from a sample with 14.5 ML lower Fe layer and 11 ML Cr interlayer, i.e. both interfaces are prepared at a RHEED oscillation minimum, i.e. with enhanced structural roughness.

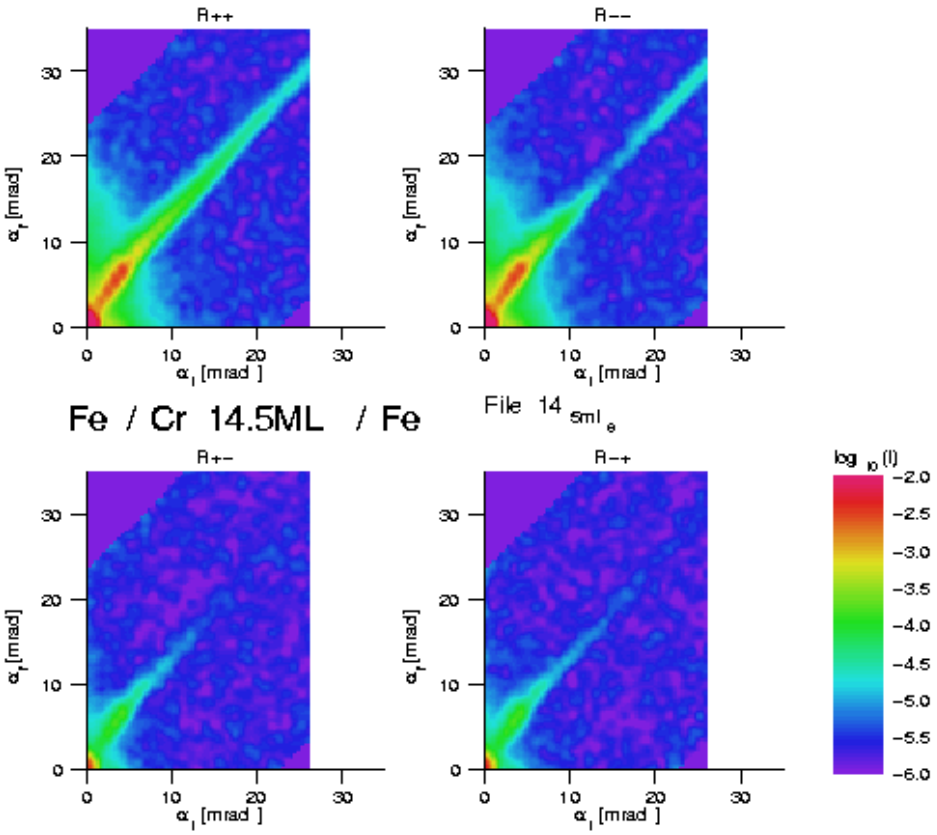

Fig.1: Reflectivity and diffuse scattering recorded from the sample with 14.5 ML thick lower Fe layer at small magnetic field, i.e. the magnetization of the two ferromagnetic films is aligned antiparallel.

One can easily observe the specular reflectivity, confirming the antiferromagnetic configuration with the thicker (top) Fe layer magnetized parallel to the applied field and the bottom Fe layer magnetized antiparallel to the field direction. But aside of that, no offspecular scattering is observed. That means, the interfaces are even with the enhanced roughness still too perfect to induce an off-specular signal visible in the dynamic range of HADAS. It turned out to be necessary, to produce a multilayer sample to enhance the sensitivity by increasing the number of interfaces contributing to scattering.

Institut für Festkörperforschung
Forschungszentrum Jülich GmbH
D-52425 Jülich

Experimental Report
of Neutron Scattering Experiments
at the FRJ-2 Reactor

Proposal number:	HAD-01-006		
Experiment title:	**Determination of the magnetic fluctuations in an Fe/Cr/Fe trilayer exhibiting a neutron resonance sate**		
Dates of experiment:	28.06. – 8.07.02	Date of report:	24.03.03
Experimental team: Names	Addresses		
E. Kentzinger U. Rücker B. Toperverg Th. Brückel	IFF, FZ-Jülich		
Local Contact:	U. Rücker		

Experimental report text body

We report on a measurement of off-specular polarized neutron scattering from an Fe/Cr/Fe trilayer inside which a second order neutron resonance has been excited, i.e. where the probability to find a neutron was maximized at both Fe/Cr interfaces. Simulating the data in the framework of the Distorted Wave Bon Approximation (DWBA) showed the presence of structural and magnetic fluctuations. Magnetic fluctuations in the vicinity of the Fe/Cr interfaces can be explained if one considers the anti-ferromagnetic structure of Cr and structural roughness.

In a trilayer structure exhibiting a square well in the variation of the neutron interaction potential as a function of depth, the probability to find a neutron at a certain depth can be strongly enhanced for an appropriate amplitude of the component of the incident wave vector perpendicular to the surface. This corresponds to the establishment of a stable stationary wave called resonance state.

We report on an experiment performed on an Fe/Cr/Fe trilayer from which we measured off-specular scattering of polarized neutrons with polarization analyzis on the HADAS instrument. The thicknesses were chosen to excite a second order resonance state for spin up neutrons, i.e. such that the probability to find a spin up neutron was maximum at both Fe/Cr interfaces (Fig.1).

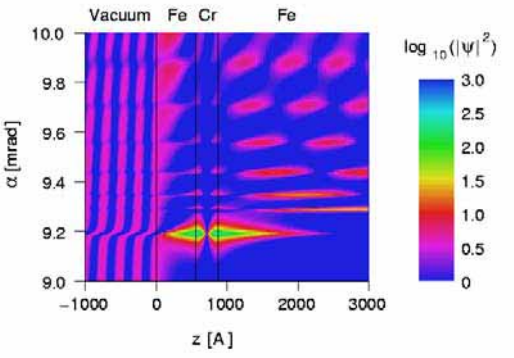

Fig.1: Simuation of the probability density for spin up neutrons in the saturated Fe/Cr/Fe trilayer considered in the text. α is the angle of incidence of the neutrons and z is the height below the surface.

In Fig. 2a the measured reflectivity and off-specular scattering from the trilayer considered in Fig. 1 is shown. The measurements were performed under an external field of 20 mT. α_i is the angle of incidence of the neutrons and α_f the outgoing angle. The reflectivity and diffuse scattering are strongly spin-polarized: the critical angles for total reflection for spin up and spin down neutrons are very different and close to the ones for saturated bulk Fe. The presence of a reflectivity signal ($\alpha_i=\alpha_f$) in the two spin-flip channels can be solely explained by the limited efficiencies of the polarizer and the analyzer. The presence of off-specular scattering shows that, on a length scale smaller than the projection on the sample surface of the coherence length of the neutron beam, structural and/or magnetic fluctuations exist. The diffuse scattering is mainly concentrated along the Yoneda wings for spin up and spin down neutrons and along lines for which the incident and/or the outgoing angles correspond to the angle where the excitation of a resonance for spin up neutrons is expected.

We simulated the data in the framework of the DWBA [2], considering structural roughness and magnetic fluctuations inside the almost saturated Fe layers, close to the Fe/Cr interfaces. The result of the simulations is given in Fig. 2b and compares very well with the data. From this procedure, we obtained the amplitudes and the characteristic length scales of the structural and magnetic fluctuations. However, the data did not permit us to discriminate between the two following models: 1) magnetic fluctuations only in the top-most Fe layer and 2) magnetic fluctuations in the top-most Fe layer and in a part of the bottom-most Fe layer, having a common interface with the Cr layer. A model with magnetic fluctuations in the whole thickness of the bottom-most Fe layer leads to simulations in strong disagreement with the data.

The presence of magnetic fluctuations close to the interfaces can be understood if one considers the anti-ferromagnetic structure of the Cr layer, the strong Fe/Cr coupling at the interfaces and the structural roughness. Structural steps at the Fe/Cr interfaces induce lateral magnetic frustrations in the Fe and Cr layers close to their interfaces. The magnetic energy induced by those frustrations can be minimized by the introduction of magnetic fluctuations in the body of the Fe and Cr layers, whose amplitudes decrease with the distance from the interfaces.

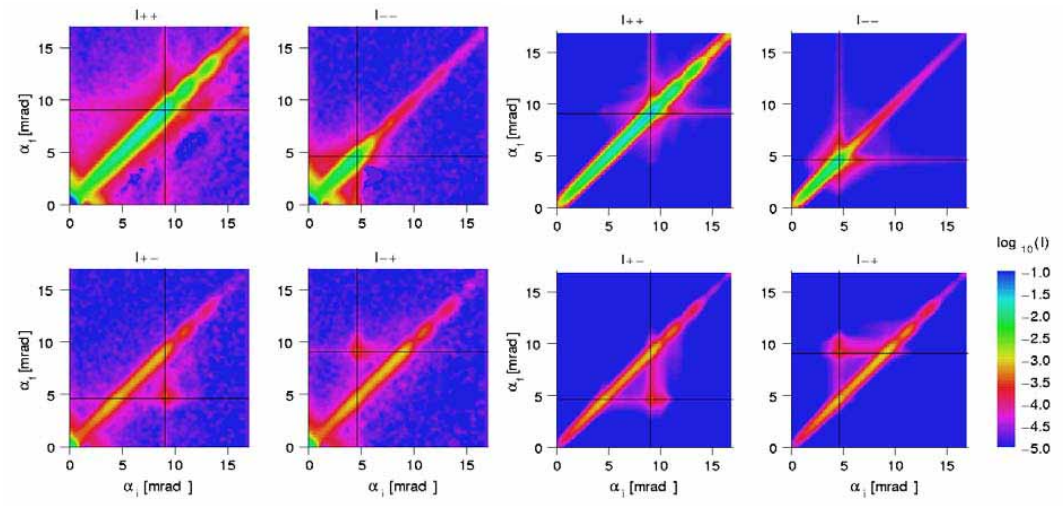

Fig.2a: Off-specular scattering of polarized neutrons from an Fe/Cr/Fe trilayer.

Fig.2b: Simulations of the data in Fig 2a. The model calculations were convoluted by the experimental resolution due to the limited collimation of the incident beam

References:

[1] E. Kentzinger, U. Rücker, B. Toperverg and T. Brückel, PNCMI'02, to be published in Physica B
[2] E. Kentzinger, U. Rücker and B.Toperverg, PNCMI'02, to be published in Physica B

Proposal number:	HAD-01-007		
Experiment title:	Diffuse scattering of polarized Neutrons from an [Er_5|Tb_{20}] multilayer		
Dates of experiment:	12.01 (10 days of -01.02 beamtime	Date of report:	27.2.03
Experimental team: Names:	Addresses:		
Jörg Voigt	intern		
Local contact:	Ulrich Rücker		

We report on the diffuse scattering of polarized neutrons from an [Er_5|Tb_{20}] multilayer. As known from wide angle neutron diffraction the sample exhibits a canted coupling of the ferromagnetic Terbium layers. As the momentum transfer in the small angle regime fits the characteristic length scale of the superlattice, the method of grazing incidence neutron scattering is perfectly suited for the study of magnetic correlations in our multilayer system.

The sample contains 120 bilayers of [Er_5|Tb_{20}], the subscripts denoting the number of mono-atomic layers. The sample is grown epitaxially on a sapphire substrate and a subsequent buffer layer, described in detail in [1]. We performed measurements of the diffuse scattering using the PSD of the HADAS reflectometer. The sample was cooled to 205 and 25 K, with a residual magnetic field of 10 G during cooling, using a Helium Flow cryostat. The diffuse scattering at 205 K are shown in figure. One Bragg sheet is seen, related to a thickness of 2 times the bilayer thicknes. Therefore the antiferromagnetic stacking of ferromagnetic terbium layers is present. Apparently the lateral size of the domains is rather small as the Bragg sheets are fairly broad. However, the data quality is quite bad, since the criostate was strongly absorbing, therefore we don't draw further conclusions. In a later experiment we measured the diffuse scattering from an [Er_{20}|Tb_{20}] with an optimized setup [2].

References

[1] J.Voigt, Diplomarbeit RWTH Aachen (2000)

[2] Experimental report for experiment HAD-02-007

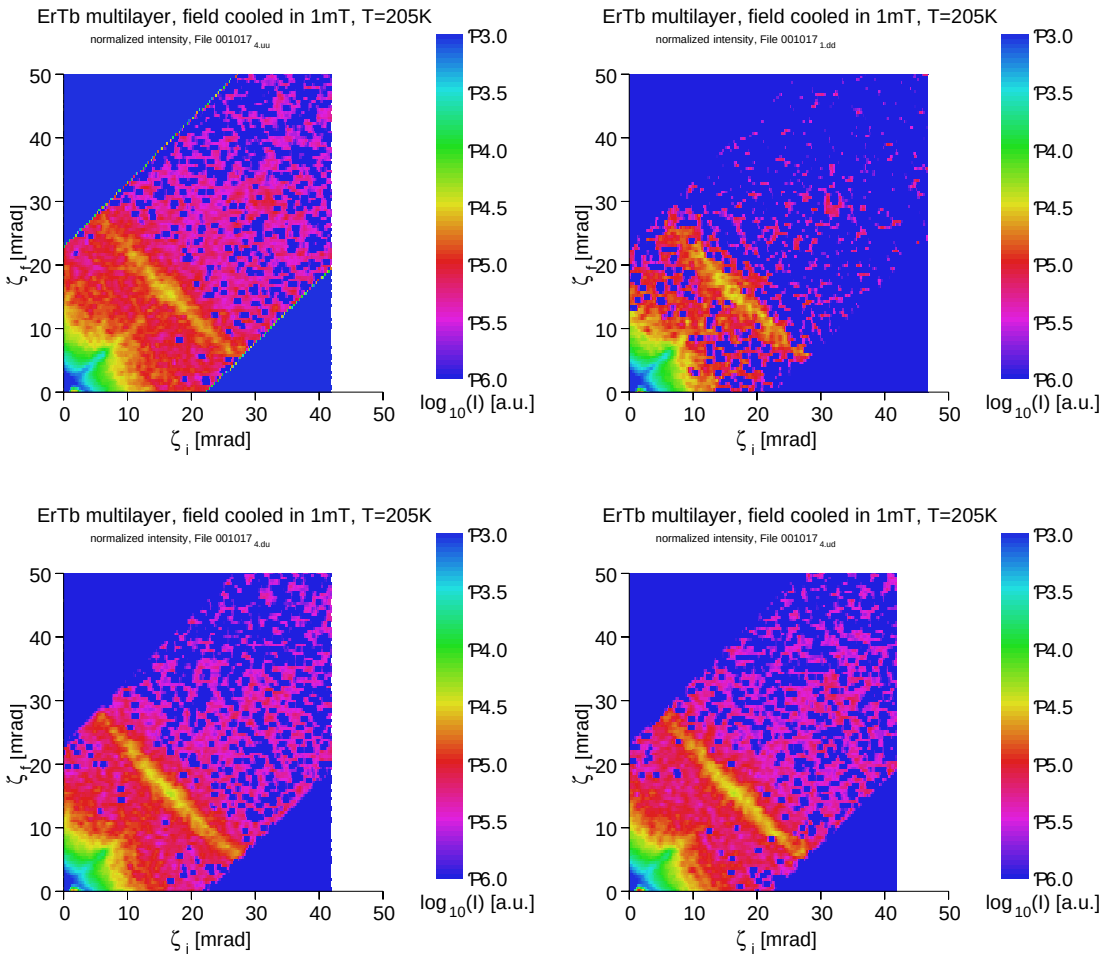

Fig.1: Diffuse scattering of the $[Er_5|Tb_{20}]$ sample cooled in a field of 10 G. One Bragg sheet, related to an antiferromagnetic stacking of ferromagnetic terbium layers, can be detected.

Institut für Festkörperforschung
Forschungszentrum Jülich GmbH
D-52425 Jülich

Experimental Report
of Neutron Scattering Experiments
at the FRJ-2 Reactor

Proposal number:	HAD-01-010		
Experiment title:	**Magnetic order in a (Co / Cu) $_{x20}$ superlattice**		
Dates of experiment:	14.-17.1. 2002	Date of report:	10.3.2003
Experimental team: Names	 Addresses		
W. Babik U. Rücker	IFF-Streumethoden		
Local Contact:	U. Rücker		

Experimental report text body

The sample is a Co / Cu superlattice with 20 periods based on a thick Cu buffer layer on a Si (001) substrate. The multilayer has a low crystal quality on a mesoscopic scale due to the large lattice mismatch between Cu and Si (001), but on a microscopic length scale (where island formation is predominant), the crystallinity is sufficient to investigate magnetic coupling phenomena.

MOKE measurements performed on this sample may suggest either ferromagnetic or 90° coupling.

Fig. 1 shows the polarized neutron reflectivity and offspecular scattering with polarization analysis. The multilayer Bragg peak is only observed for spin down. This is a clear indication for ferromagnetic alignment between the Co layer magnetizations, as the scattering length density of Cu and the sum of the nuclear and magnetic scattering length densities of Co are almost equal. I.e. in the case of magnetization parallel to the spin direction, the contrast between Co and Cu vanishes completely, what is observed.
Furthermore, no real spin flip signal is observed, indicating that no magnetization component perpendicular to the spin direction is present, what would be in the case of 90° coupling.

The sample has turned out to be perfectly suitable for a reflectivity experiment, the structure is so perfect, that the individual Laue oscillations between the total reflection edge and the superlattice Bragg peak have been observed (cf. Fig. 2). The scale of the disorder of the sample is different from the range observed by neutron reflectometry.

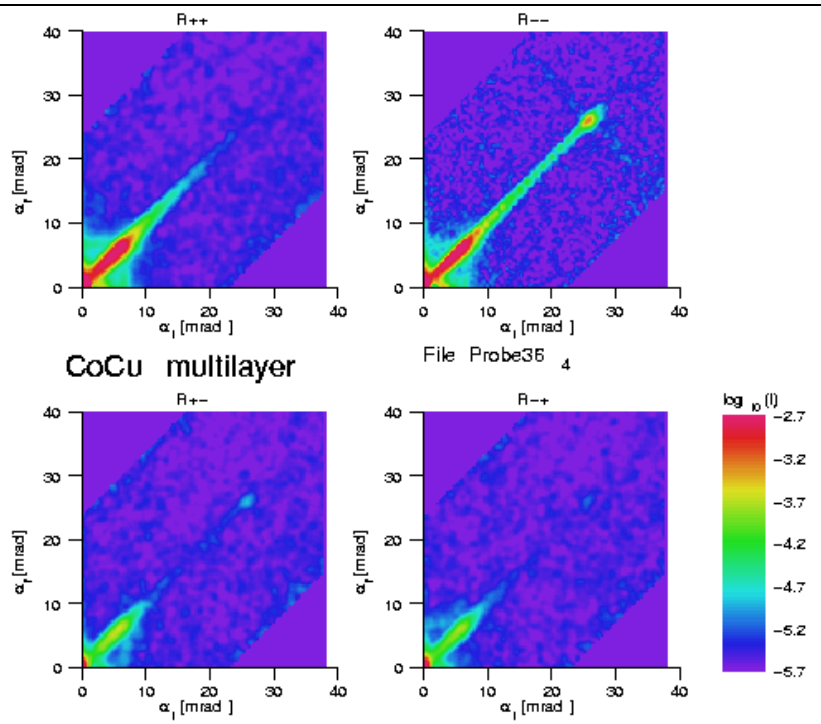

Fig. 1: Reflectivity and diffuse scattering measured with full polarization analysis. For spin up neutrons, the multilayer structure is invisible, while for spin down neutrons, the superlattice Bragg reflection is nicely visible. A little Bragg sheet through the superlattice Bragg is the only diffuse scattering visible, that is interpreted to come from structural roughness of the Co / Cu interfaces.
The spin-flip signal can completely be described as parasitic signal due to the finite polarization efficiency of polarizer and analyzer.

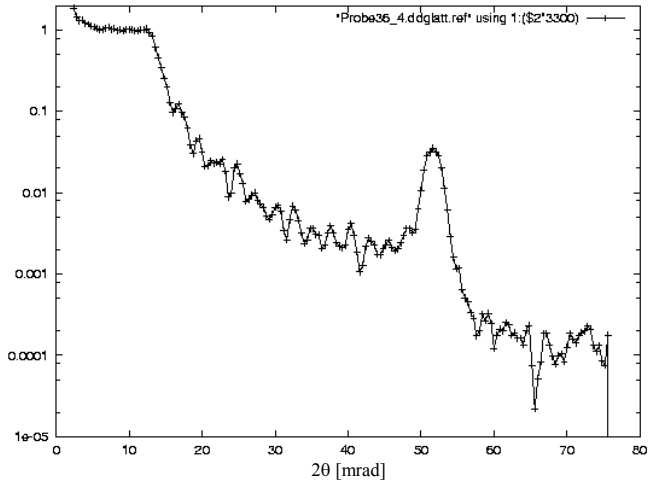

Fig. 2: Specular reflectivity with spin down (diagonal of the R-- figure above). The superlattice Bragg peak and the Laue oscillations between the Bragg peak and the total reflection edge are nicely observed.

Institut für Festkörperforschung
Forschungszentrum Jülich GmbH
D-52425 Jülich

Experimental Report
of Neutron Scattering Experiments
at the FRJ-2 Reactor

Proposal number:	HAD-02-001		
Experiment title:	**Quality control and improvement of neutron supermirrors**		
Dates of experiment:	see below	Date of report:	10.03.2003
Experimental team: Names	Addresses		
Andreas Knöpfler	S-DH Sputter-Dünnschichttechnik GmbH Hans-Bunte-Str. 8-10 D-69123 Heidelberg +49 6221 739441 knoepfler@s-dh.de		
Local Contact:	Dr. Ulrich Rücker		

Experimental report text body

0. Dates of experiment:

30.01.2002
27.02.2002
30.04.2002
08.07.2002
09.09.2002
29.10.2002
16.-17.12.2002

1. Introduction

Our company S-DH Sputter-Dünnschichttechnik Heidelberg is a supplier of supermirror-based neutron guides. After several years of development at the university of Heidelberg and production of a long ballistic supermirror guide for the ILL, Grenoble, the company was founded in 2000.
The neutron supermirrors are produced with magnetron sputtering technique. In order to maintain a high quality standard of neutron reflectivity in serial production of relatively large supermirrors (1000 x 200 mm^2) with different types of glass substrates and (for technical reasons) not perfectly constant sputtering conditions, periodical neutron reflectivity measurements are very important. Within the experiment HAD-02-001, the neutron reflectivity of about 200 supermirrors (most of them Ni/Ti supermirrors with m=2) has been measured.

2. Subject of investigation

The reflecting behavior of neutron supermirrors is characterized mainly by the critical angle of reflection and the reflectivity (ratio of intensities of reflected to incoming neutron beam) at this critical angle. Furthermore, the overall shape of the curve is of interest (a high and constant plateau up to the critical angle is desired).

Our supermirrors are float glass plates which are coated with Nickel/Titanium multilayer with typically about 100 single layers (for m=2 supermirrors). To achieve good neutron reflectivity it is very important that

- the glass substrate has low surface roughness (about several Å) and that it is very clean
- the produced multilayer does not have any impurities
- the single layers have dense structure and sharp interfaces with low roughness

3. Measurement results (examples):

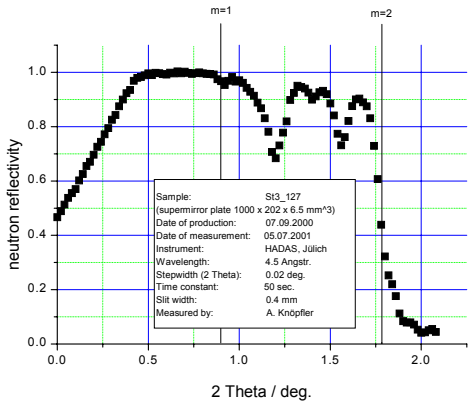

Fig 1: Sample St3-127

Fig. 1 shows a defective neutron reflectivity behavior: there are several layers missing in the supermirror structure due to instabilities in the sputtering plasma at low gas pressure

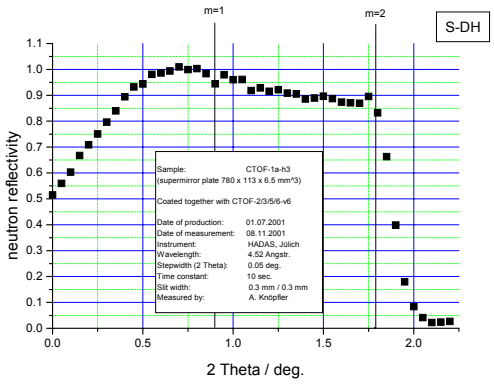

Fig. 2: Sample CTOF-1a-h3

Fig. 2: Non-ideal neutron reflectivity due to roughness of the glass substrate and the layer interfaces

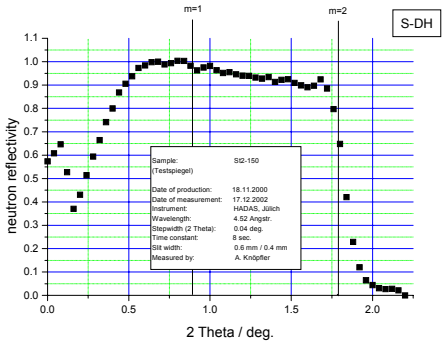

Fig. 3: Sample St2-150

Fig. 3: A supermirror that was produced two years ago has been measured again. There is no degradation in neutron reflectivity. The same test has been done with supermirrors that have been exposed to very high neutron flux.

4. Conclusions

With the investigation of a large number of neutron supermirrors further improvements in our production process have been achieved. We have produced neutron supermirrors on different types of glass as borated and non-borated float glass with different glass thicknesses and varying treatment before coating. We have found that it is very important the glass is being treated carefully. Due to the nature of the material the surface quality is varying from one 'batch' of glass to another.
Considering coating purity, some possible sources of contamination of the multilayer within the production process could be identified and eliminated.
Some important sputtering parameters have been optimized in order to achieve well-defined layer growth.

With the HADAS spectrometer, a reliable and effective instrument with capacity for a wide range of sample types has been made available to us. Because of the amount of measuring time, a great part of our supermirror production could be examined.

In conclusion, we were able to increase the reliability of our supermirror production and also to improve the standard of reflectivity of our mirrors. The quality of many supermirrors dedicated to operation in new neutron guides has been verified and documented. New neutron sources like FRM 2 and modernization of existing beam lines very much benefit from the use of supermirror neutron guides, as the intensity of the neutron beam available at the instruments can be improved considerably.

5. Acknowledgements

S-DH thanks the Institut für Festkörperforschung at Forschungszentrum Jülich GmbH for making this experiment possible and especially Ulrich Rücker for his qualified and friendly support that could hardly be found elsewhere.

Institut für Festkörperforschung
Forschungszentrum Jülich GmbH
D-52425 Jülich

Experimental Report
of Neutron Scattering Experiments
at the FRJ-2 Reactor

Proposal number:	HAD-02-002		
Experiment title:	Observation of the spin-flop transition in Fe/Cr multilayers		
Dates of experiment:	26.2.-11.3.02	Date of report: 6.3.03	
Experimental team: Names	Addresses		
H.J.Lauter V.Lauter-Pasyuk B.Toperverg M.Milyaev V.Ustinov	ILL, BP 156, F-38042 Grenoble Cedex 9 ILL, BP 156, F-38042 Grenoble Cedex 9 IFF, FZ-Jülich IMP, Ekaterinburg/Russia IMP, Ekaterinburg/Russia		
Local Contact:	U.Rücker		

Experimental report text body

The intention of the experiment was to investigate the supposed spin-flop transition in a magnetic uniaxial Fe/Cr multilayer (see insert in fig.1). The investigated multilayer with the composition $[Cr(12.4Å)/Fe(76Å)]_{x12}/Cr(83Å)$ was grown on a MgO(112) substrate with molecular beam epitaxy. The magnetic field is applied along the direction of the layer magnetic moments, which should be in zero field antiferromagnetically aligned. With increasing field it is expected that the layer magnetic moments turn 90^0 with respect to the field keeping the antiferromagnetic alignment.

The direction of the magnetization of each Fe layer in a Fe/Cr multilayer with uniaxial anisotropy was determined with polarized neutron reflectometry including polarization analysis on HADAS. The fit to the data of the four polarization combinations yielded the layer magnetization directions. The layer magnetization directions for 5 magnetic fields are displayed in fig.2. The value of the net magnetization, determined from the layer magnetization in fig.2, agree with the magnetization obtained from magnetometry VSM measurements shown in fig.1. Fig.2 exhibits that no spin-flop transition occurs in increasing the field from zero along the hysteresis curve. The vectors of the layer magnetization of the multilayer transit from an already perturbed antiferromagnetic alignment into a nearly ferromagnetic one with increasing magnetic field. In the transition region towards saturation the system consists of an antiferromagnetic-like aligned part and a ferromagnetic-like aligned part. The magnetization curve is characterized by the subsequent switching of the antiferromagnetic-like aligned bilayers into the nearly ferromagnetic-like aligned state. Via this mechanism the antiferromagnetic part of the multilayer reduces in favor of the ferromagnetically aligned part with increasing magnetic field.

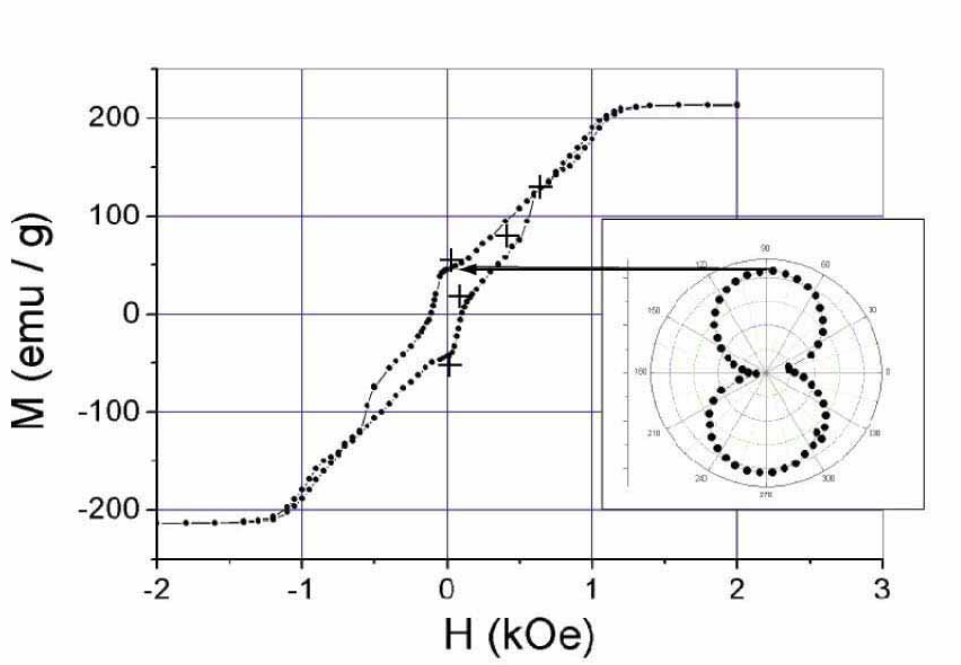

Fig.1: Magnetization curve of the Fe/Cr multilayer determined with VSM. The crosses indicate the magnetic field at which neutron reflectometry experiments were performed and what values of the net magnetization were obtained from the reflectivity data. The inset shows the uniaxial behavior of the sample measured at ~100G.

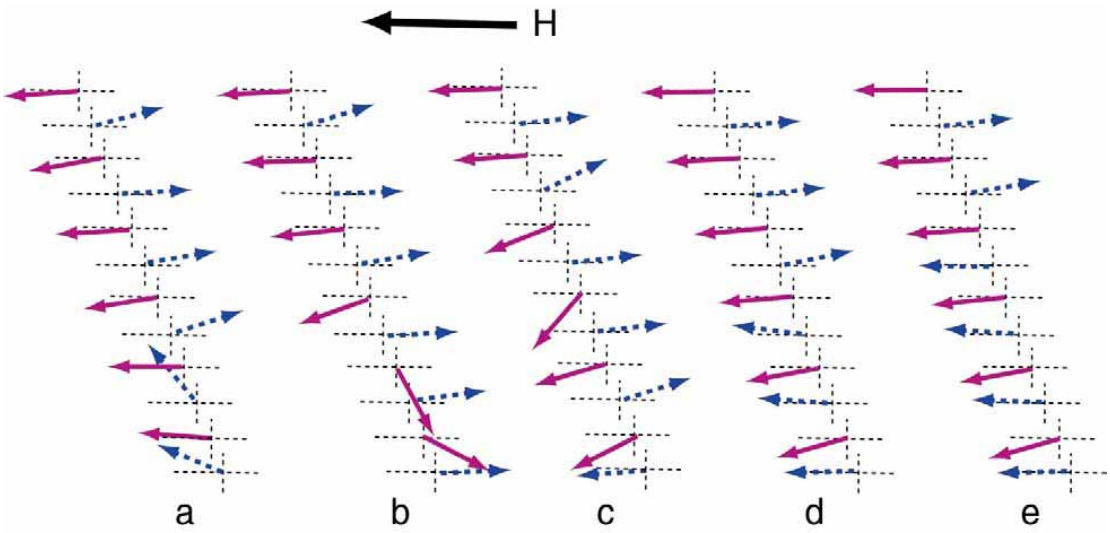

Fig.2: Configuration of the layer magnetization's at 5 magnetic fields a)H = 20 G (upper branch of hysteresis curve see fig.1), b) H = 14 G (in the remanent state on the lower branch of the magnetization curve), c) H = 90 G, d) H = 450 G and e) H = 680 G. The presentation of the layer magnetization's with full and broken arrows helps to identify couples of anitiferromagnetically coupled layers and their transition to the ferromagnetic-like alignment.

Institut für Festkörperforschung
Forschungszentrum Jülich GmbH
D-52425 Jülich

Experimental Report
of Neutron Scattering Experiments
at the FRJ-2 Reactor

Proposal number:	HAD-02-003		
Experiment title:	**Determination of the magnetic properties of a Fe / Cr multilayer**		
Dates of experiment:	17.1. – 21.1.2002 1.5. – 6.5.2002	Date of report:	26.3.2003
Experimental team: Names	Addresses		
N. Ziegenhagen U. Rücker E. Kentzinger B. Toperverg	IFF-Streumethoden FZ Jülich 52425 Jülich		
Local Contact:	U. Rücker		

Experimental report text body

As described in the following Experimental report HAD-02-004 (please regard the two as belonging together), reflectivity and diffuse scattering under grazing incidence of polarized neutrons with polarization analysis of the sample have been measured at different geometries, as there were $\mathbb{H}$ parallel and the beam perpendicular to the stripes, $\mathbb{H}$ perpendicular and the beam perpendicular to the stripes, $\mathbb{H}$ perpendicular to the stripes and the beam parallel to the stripes, and finally $\mathbb{H}$ perpendicular to stripes and the stripes almost parallel to the beam but moved by 10 degrees.

All measurements were taken at different outer magnetic field strengths, for example at saturation field and at a disappearing field. The saturation field strength had been detected before at various MOKE- measurements.

To have a possibility of comparison, also an unstructured sample has been measured at various fields.

Compared to this measurement, which is shown in figure 1 at an applied magnetic field of 10 mT, at the measurement of the structured sample a lot of diffuse scattering can be seen, that indicates domain formation within the sample. Compared to the unstructured sample, the diffuse scattering is enhanced by a factor of 3, and the extension away from the specular line is much longer, indicating a smaller domain size. The diffuse scattering is mainly concentrated in Bragg sheets around the half order specular peaks. This indicates a strong vertical correlation between the domain pattern in adjacent layers. So we observe columnar alternating domains throughout the complete multilayer stack.

Up to now, we have not yet found a suitable model to describe quantitatively the complete diffuse scattering observed. Nevertheless, we have found a description of the specular reflectivity, that reproduces the different peak width in non-spin-flip and spin-flip for the half order peaks.

They can be described assuming a structure, in that the component of the magnetization perpendicular to the stripes is alternating regularly while the magnetization component parallel to the stripes shows one phase shift between the 3rd and the 4th layer (counted from the top). With that structure, a net magnetization along the field is achieved without breaking too much the antiferromagnetic coupling.

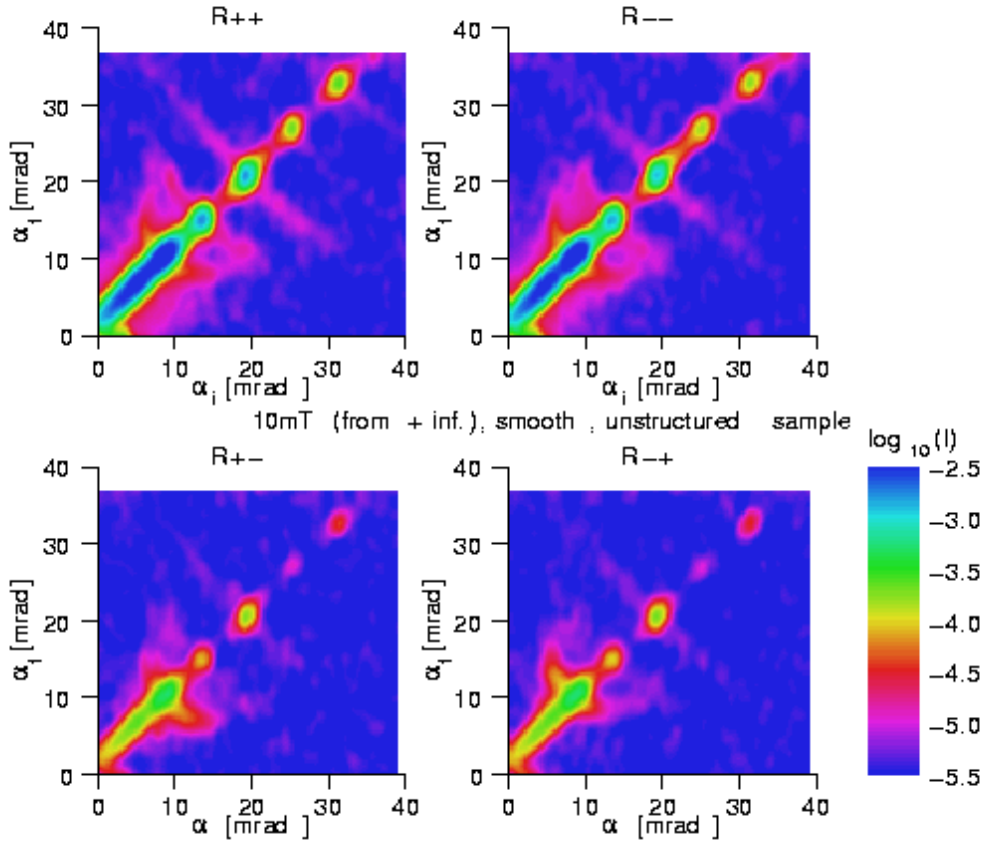

Fig. 1: Reflectivity and diffuse scattering under grazing incidence of polarized neutrons with polarization analysis as measured on the HADAS-reflectometer. The scattered intensity (on a logarithmic colour scale) is plotted against incident angle α_i and outgoing angle α_f of the polarized neutrons. The specular reflectivity ($\alpha_i = \alpha_f$) is shown on the main diagonal in each plot. The four polarization channels are R++ non-spin-flip with the neutron spin along the direction of the applied magnetic field, R-- non-spin-flip with the neutron spin antiparallel to the magnetic field direction and R+- and R-+ spin-flip with the incident neutron spin parallel or antiparallel to the magnetic field, respectively.

Institut für Festkörperforschung
Forschungszentrum Jülich GmbH
D-52425 Jülich

Experimental Report
of Neutron Scattering Experiments
at the FRJ-2 Reactor

Proposal number:	HAD-02-004		
Experiment title:	**Determination of the magnetic properties of a laterally structured Fe / Cr multilayer**		
Dates of experiment:	19.2. – 27.2., 26.3. – 4.4., 22.4. – 29.4., 6.5. – 13.5., 7.6. – 15.6. 2002	Date of report:	6.3.2003
Experimental team: Names	Addresses		
N. Ziegenhagen U. Rücker E. Kentzinger B. Toperverg	IFF-Streumethoden FZ Jülich 52425 Jülich		
Local Contact:	U. Rücker		

Experimental report text body

The surface layer of an Fe / Cr multilayer structure has been structured lithographically into stripes with 1 µm period. It serves as a model system for the investigation of the magnetic domain formation in layers with externally induced anisotropy due to the antiferromagnetic interlayer coupling between the structured layer and the individual unstructured layers.

The model system under investigation is shown in Fig. 1. It is basically an epitaxial Fe / Cr (001) multilayer structure with 11 periods prepared on 1500 Å Ag buffer on a GaAs (001) single crystal. The thickness of the Fe layers is 150 Å, and 11 Å of the Cr layers, yielding antiferromagnetic coupling between the neighboring Fe layers.

After deposition of the multilayer structure, the top Fe layer was patterned into stripes of 1 µm period using electron beam lithography and ion beam etching. The stripes are oriented parallel to the (100) easy magnetization axis of the Fe layers. Due to the magnetic interlayer coupling, the lateral structure of the top layer is coupled to the magnetization of the non-structured bottom layers.

For measuring the magnetization and the domain structure of layered structures, reflectometry and diffuse scattering of polarized neutrons is the method of choice, especially to access the buried magnetic layers.

A clear impression of the reflections of the surface and the layers has been gained by X-Ray Reflectometry, but the magnetic interactions can only be accessed by experiments with neutrons. Also, neutrons provide a much better contrast between Iron and Chromium than X-rays do.

Reflectivity and diffuse scattering under grazing incidence of polarized neutrons with polarization analysis have been measured at the HADAS reflectometer in the neutron guide hall ELLA at the Jülich research reactor FRJ-2 (DIDO) [2]. Fig. 2 shows the four different polarization channels, measured at $\mu_0 H$ = 9.5 mT, i.e. in an intermediate, complex magnetization state.

Reflectivity and diffuse scattering under grazing incidence of polarized neutrons with polarization analysis of the sample have been measured at different geometries, as there were ℍ parallel and the beam perpendicular to the stripes, ℍ perpendicular and the beam perpendicular to the stripes, ℍ perpendicular to the stripes and the beam parallel to the stripes, and finally ℍ perpendicular to stripes and the stripes almost parallel to the beam but moved by 10 degrees.

All measurements were taken at different outer magnetic field strengths, for example at saturation field and at a disappearing field. The saturation field strength had been detected before at various MOKE- measurements.

For the comparison between structured and unstructured sample, please cf. HAD-02-003.

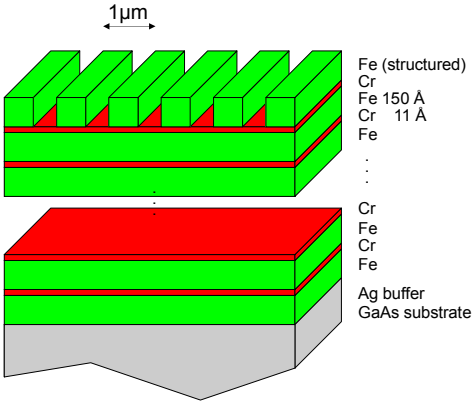

Fig. 1: Schematic picture of the sample under investigation. The Cr interlayer thickness of 11 Å yields strong antiferromagnetic coupling between neighboring Fe layers.

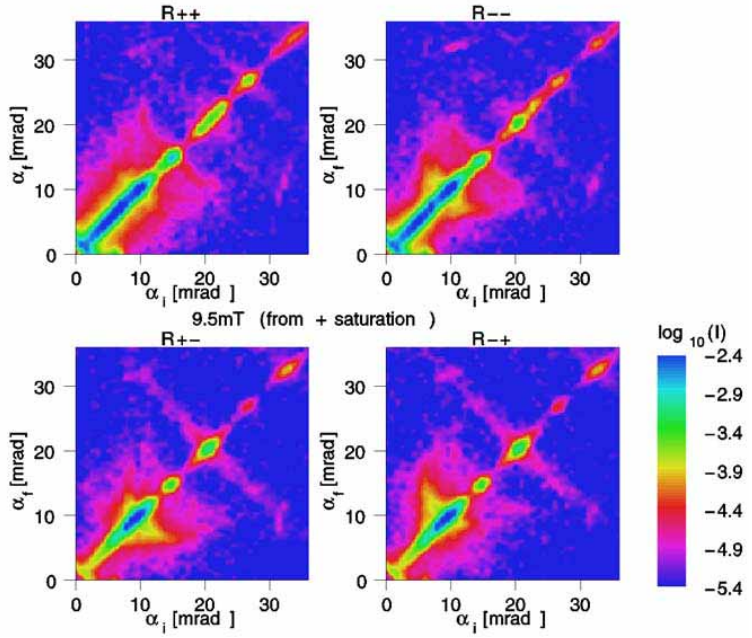

Fig. 2: Reflectivity and diffuse scattering under grazing incidence of polarized neutrons with polarization analysis as measured on the HADAS-reflectometer. The scattered intensity (on a logarithmic colour scale) is plotted against incident angle α_i and outgoing angle α_f of the polarized neutrons. The specular reflectivity ($\alpha_i = \alpha_f$) is shown on the main diagonal in each plot. The four polarization channels are R++ non-spin-flip with the neutron spin along the direction of the applied magnetic field, R-- non-spin-flip with the neutron spin antiparallel to the magnetic field direction and R+- and R-+ spin-flip with the incident neutron spin parallel or antiparallel to the magnetic field, respectively.

Institut für Festkörperforschung
Forschungszentrum Jülich GmbH
D-52425 Jülich

Experimental Report of Neutron Scattering Experiments at the FRJ-2 Reactor

Proposal number:	HAD-02-005		
Experiment title:	Characterization of neutron guide mirrors from FRM II		
Dates of experiment:	29.- 30. 04. 02	Date of report:	05.03.2003
Experimental team: Names	Addresses		
A. Fleischmann A. Urban	Technische Universität München ZWE FRM II Lichtenberg-Str.1 D – 85747 Garching		
Local Contact:	Dr. Rücker IFF, FZJ		

Experimental report text body

(Please use 12 pt letters here !)

The intension of the experiment was to determine the reflectivity of 21 samples from neutron super mirrors that have been produced for the construction of the neutron guides at the new high-flux neutron source FRM II. Within a period of 2 days the samples were measured at the spectrometer HADAS of the FZJ. All samples exhibited a reflectivity well above the expected values. This can seen in the figure 020417 where the reflectivity for a m=2.2 neutron super mirror is shown.

The measurement procedure was as follows:

1) The samples were adjusted on the mounting table according to their thickness using the established procedures.
2) The limits of the scanning angle range and the angular step width were set so that the measuring time for each point yields sufficient statistics.
3) The rocking curves were measured within an range of the scattering angle from 0.0° to 2.4° with a stepping width of 0.03°.
4) The data were collected and converted to diagrams.

The perfectly prepared spectrometer HADAS and the excellent support from the team of the FZJ enabled a fast and efficient accomplishment of the experiment. We take this opportunity to express our gratitude.

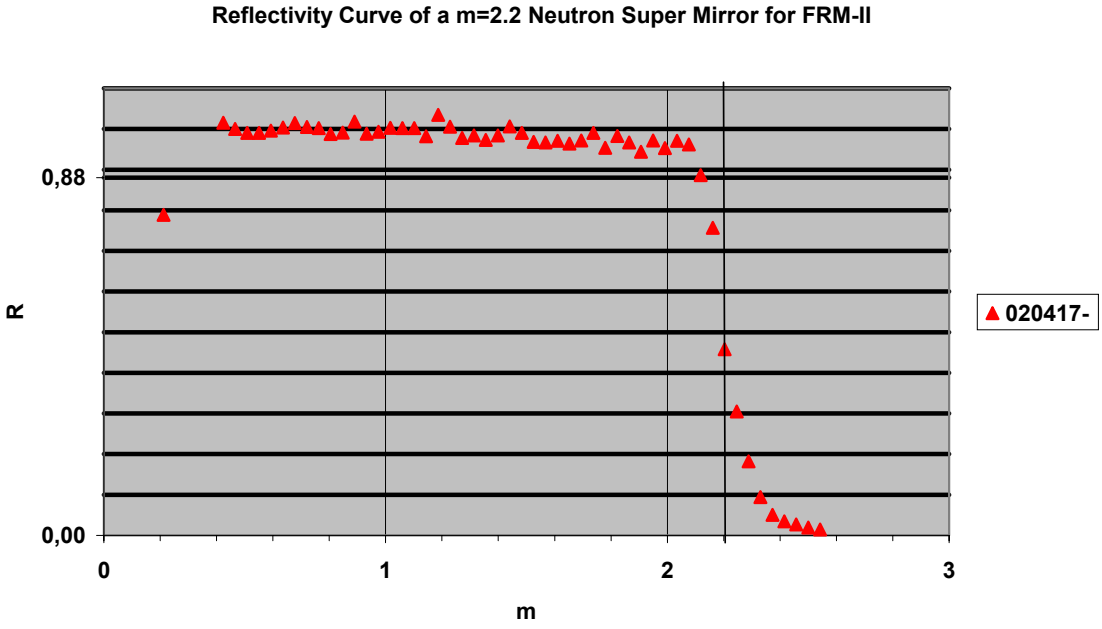
Reflectivity Curve of a m=2.2 Neutron Super Mirror for FRM-II
0,88
0,00
R
0
1
2
3
m
020417-

Proposal number:	HAD-02-007		
Experiment title:	Diffuse scattering of polarized Neutrons from an $[Er_{20}\|Tb_{20}]$ multilayer		
Dates of experiment:	22.10.02 (10 days of -28.11.02 beamtime	Date of report:	27.2.03
Experimental team: Names:	Addresses:		
Jörg Voigt	intern		
Local contact:	Ulrich Rücker		

We report on the diffuse scattering of polarized neutrons from an $[Er_{20}|Tb_{20}]$ multilayer as a function of the thermo-magnetic history. As known from wide angle neutron diffraction the sample exhibits an antiferromagnetic coupling of the ferromagnetic Terbium layers. As the momentum transfer in the small angle regime fits the characteristic length scale of the superlattice, the method of grazing incidence neutron scattering is perfectly suited for the study of magnetic correlations in our multilayer system.

The sample contains 80 bilayers of $[Er_{20}|Tb_{20}]$, the subscripts denoting the number of mono-atomic layers. The sample is grown epitaxiallyon a sapphire substrate and a subsequent buffer layer, described in detail in [1]. We performed measurements of the diffuse scattering using the PSD of the HADAS reflectometer. To saturate the magnetic order we cooled the sample to a temperature of 25 K, using an Helium Flow cryostat. The sample was cooled three times from room temperature to 25 K, first with an applied magnetic field of 250 G during cooling, then with the residual field of 3 G and last the sample was cooled in the magnetic field, but the field was switched off during the measurement. The diffuse scattering of the first and second case are shown in figure 1 and 2. As a qualitative interpretation we claim the coexistence of laterally small and large ferromagnetic domains, if the sample is cooled in a mediate external magnetic field. This order is stored, when the field is switched off after cooling. Cooling in a weak external field leads to the formation of antiferromagnetic and ferromagnetic stacking. We plan to model the diffuse scattering using the formalism described in [2].

References

[1] J.Voigt, Diplomarbeit RWTH Aachen (2000)

[2] E.Kentzinger, U.Rücker, B.P.Toperverg, to be published (2003)

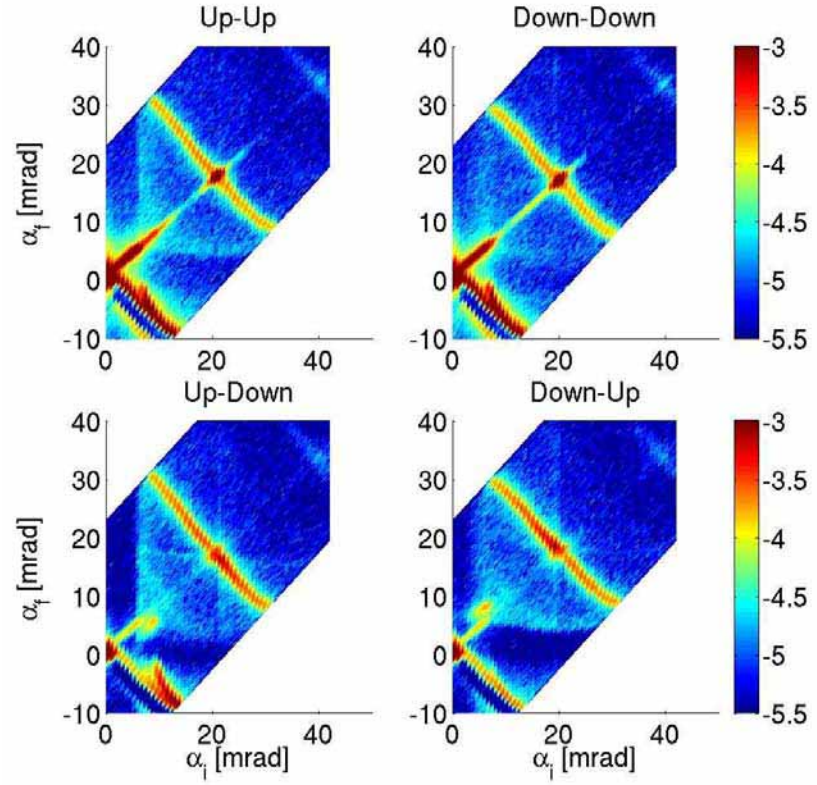

Fig.1: Diffuse scattering of the $[Er_{20}|Tb_{20}]$ sample cooled in a field of 250 G. In the nsf-channels the reflectivity shows peaks corresponding to large domains of ferromagnetic stacking with the magnetization parallel to the applied field. Extensive Bragg sheets point to coexistence of further small domains. The domains are vertically well correlated.

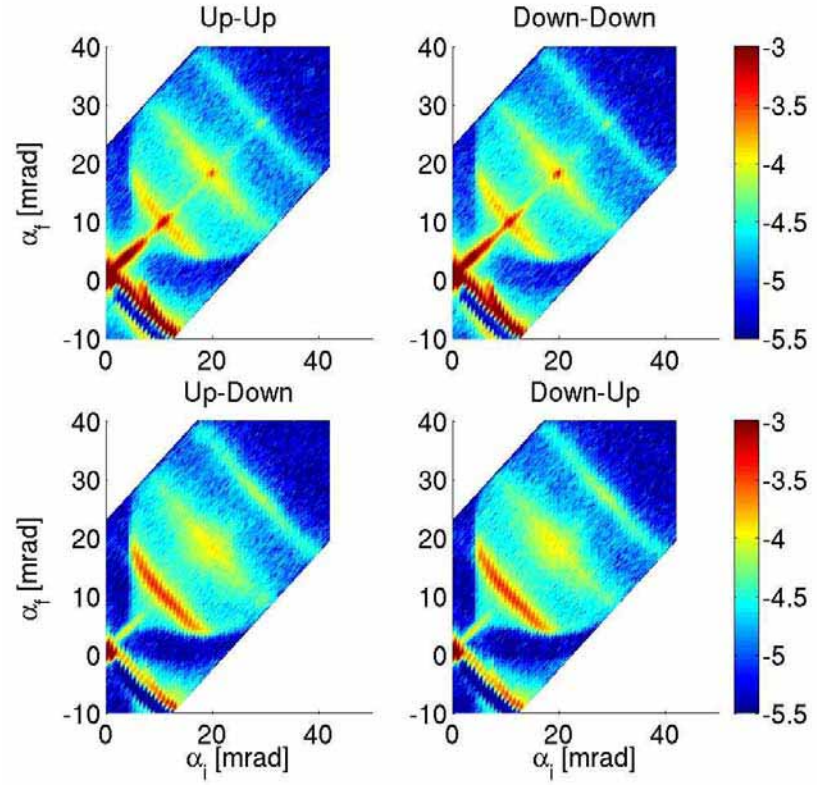

Fig.2: Diffuse scattering of the $[Er_{20}|Tb_{20}]$ sample cooled in a field of 3 G. Additional Bragg sheets appear due to an antiferromagnetic stacking of the Terbium layers. Apparently both types of magnetic domains coexist. The reflectivity in the spin-flip channels doesn't show any peak, therefore we suggest only small domains with the magnetic moments aligned perpendicular to the residual field. Vertical correlations are weaker, since the Bragg sheets are smeared out.

Institut für Festkörperforschung
Forschungszentrum Jülich GmbH
D-52425 Jülich

Experimental Report
of Neutron Scattering Experiments
at the FRJ-2 Reactor

Proposal number:	HAD-02-008		
Experiment title:	**Determination of the thickness of polymeric coatings on poly(vinylidenfluoride) films**		
Dates of experiment:	30.10.2002	Date of report:	8.3.2003
Experimental team: Names	 Addresses		
J. Salber U. Rücker	Deutsches Wollforschungsinstitut RWTH Aachen Veltmanplatz 8 D 52062 Aachen IFF-Streumethoden		
Local Contact:	U. Rücker		

Experimental report text body

We wanted to measure the effect of soaking the poly(acrylic acid) coating layer on a poly(vinylidenfluoride) foil by neutron reflectivity.

As the Polyvinyliden foil was far too much bent to use its surface for a reflectometry experiment, we have tried to glue it with double sided scotch tape on a Si wafer.
With this technique, at least a specular reflection was visible. But looking at the angular spread of the reflection compared to the (parasitic) reflection from the Si surface (see Fig. 1), it was immediately clear, that no successful experiment could be performed using this sample. The straightforward reflection was too weak and superimposed by the Si reflectivity, so that quantitative data analysis seemed to be impossible.

We decided to abort the experiment after 1 night of beamtime and to repeat it with an improved sample.
As it turned out to be difficult to coat a Si wafer directly with poly(vinylidenfluoride), this improvement took more than two months of experiments.

In the meantime (February 2003), the experiment has been repeated successfully.

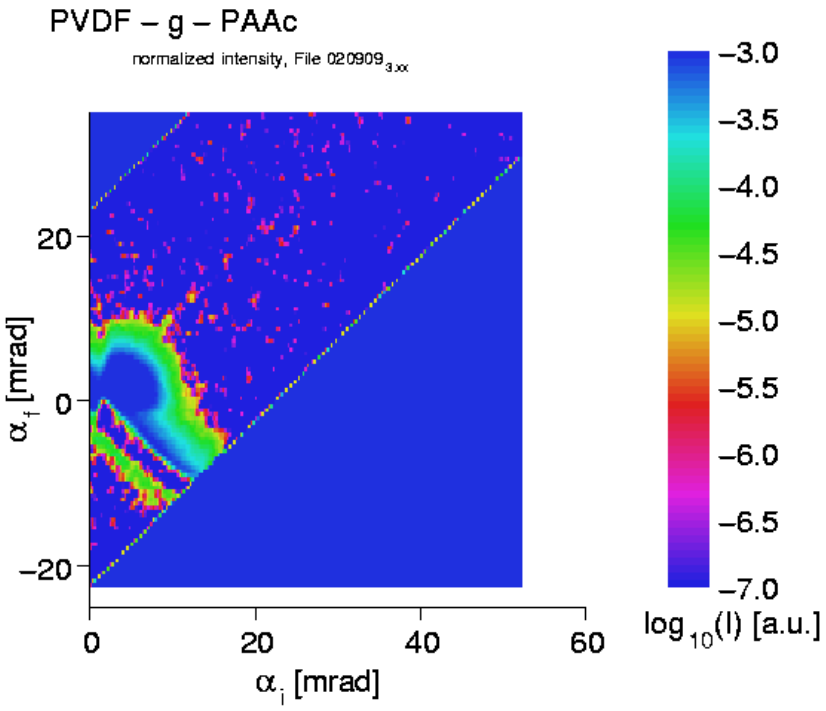

Fig.1 : Reflectivity and "diffuse scattering" pattern recorded from the dry PVDF-g-PAAc surface with the PVDF foil glued to a Si wafer. Only the broad reflectivity from the polymer and a tiny, sharp reflectivity line from the free Si wafer surface can be seen.

Institut für Festkörperforschung
Forschungszentrum Jülich GmbH
D-52425 Jülich

Experimental Report
of Neutron Scattering Experiments
at the FRJ-2 Reactor

Proposal number:	HAD-02-009		
Experiment title:	**Test von 10 A und 12 A Abzweigerelementen für NSE**		
Dates of experiment:	13.09.2002 26.09.2002	Date of report:	05.03.2003
Experimental team: Names	Addresses		
Monkenbusch, Michael Ralf Biehl	IFF, FZ-J IFF, FZ-J		
Local Contact:	U. Rücker		

Experimental report text body

Für die alternative Bestückung des polarisierenden Abzweigers am NSE mit Multilayerspiegeln mit Schichdicken, die für eine Nominalwellenlänge von 10 bzw. 12A ausgelegt sind, sind von P. Boeni bezogen worden. Die vormagnetisierten CoTi Multilayer wurden bezüglich Qualität und Magnetisierungsverhalten (Stichprobenartig) untersucht.
Die einzelnen Wafers (ca. 10cm x 5cm) wurden in einem Magnetfeld, welches entlang der langen Seite der Wafer orientiert war, vormagnetisiert. Anschließend wurden die Wafer in einem parallel zur Vormagnetisierung anliegenden Feld am HADAS Reflektometer vermessen. Die magnetische Feldstärke am Probenort wurde dazu an die im NSE Abzweiger herrschend Feldstärke mittels eines Spulenpaares angepasst (ca. 26 Gauss). Die interessanten Größen sind die Reflektivitäten für Spin-up und Spin-down als Funktion des Magnetfeldes und des Streuwinkels. Aufgrund der Vielzahl der zu untersuchenden Proben wurde auf die Variation der Feldstärke verzichtet und eine größere Stichprobe vermessen, da sich in den ersten Ergebnissen zeigte das es leichte Schwankungen in der Lage des Reflexionsmaximums gibt. In der Auswertung können weiterhin keine absoluten Reflektivitäten angegeben werden, da innerhalb einer Messung die absoluten Intensitätswerte für eine Reflektivität von 1 nicht erfasst wurden. Die Beurteilung der Reflektivität erfolgt aus diesem Grund anhand der auf die Monitorzählrate normierten Zählrate am Detektor. Die Detektorzählrate am Multidetektor wird innerhalb eines Fensters bestimmt, welches der Größe des einfallenden Strahls auf dem Detektor entspricht. Abbildung 1 zeigt die Messungen an den Superspiegeln für eine Wellenlänge von 10 A. Deutlich zu erkennen ist der verschobene Verlauf des Reflexionsmaximums.

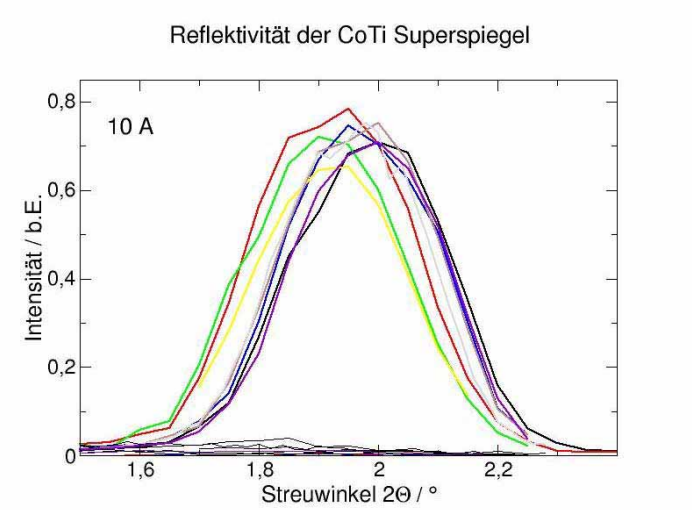

Abbildung 1 Relative Streuintensität der 10 A CoTi

Superspiegel bei Reflexion unter dem Streuwinkel 2Θ

Die Anpassung einer Gaussfunktion zeigt das die Peaklage zwischen 1,91° und 1,98° schwankt. Die Breite der Peaks liegt relativ konstant bei etwa 0,18°. Ebenso ist ersichtlich das die Reflektivitäten um 0,7 schwanken. Inwieweit diese Schwankung aus der Schichtstruktur der Co Ti Multilagen oder einer eventuell unvollständigen Vormagnetisierung resultieren konnte nur insoweit geklärt werden daß Wiederholungsmessungen die gleiche Peaklage und Peakposition liefern, die Intensitätsschwankungen vorhanden aber etwas kleiner sind. Die Vormagnetisierung und das Einbringen ins Probenmagnetfeld scheinen die Ursache der Schwankungen zu sein. Eine abschließende Beurteilung würde eine Vormagnetisierung am Probenort durch ein stärkeres Feld ermöglichen, was derzeit noch nicht möglich ist. Abbildung 2 zeigt die entsprechenden Messungen an einigen Superspiegeln für eine Wellenlänge von 12 A. Es zeigt sich hier im wesentlichen das gleiche Bild mit einer Verschiebung der Peaklagen zwischen 1,71° und 1,75° bei einer mittleren Breite von etwa 0,15°. Auch hier ist eine Schwankung im Intensitätsmaximum zu beobachten.
Insgesamt kann durch die Messung eine qualitative Auswahl und eine Einzelpositionierung der Superspiegel am geplanten neuen Abzweiger für das NSE durchgeführt werden.

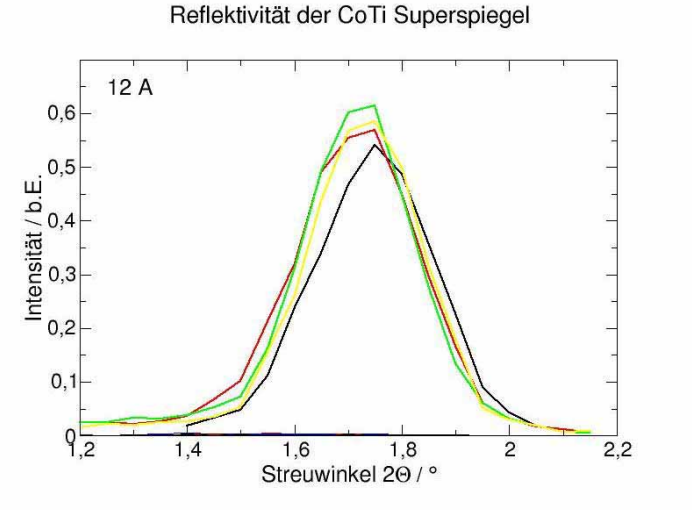

Abbildung 2 Relative Streuintensität der 12 A CoTi

Superspiegel bei Reflexion unter dem Streuwinkel 2Θ

Institut für Festkörperforschung
Forschungszentrum Jülich GmbH
D-52425 Jülich

Experimental Report
of Neutron Scattering Experiments
at the FRJ-2 Reactor

Proposal number:	HAD-02-010, UDS-02-001		
Experiment title:	Alignment of double focusing monochromators for Thermal Neutron Spectrometer/Diffractometer for Polarization Analysis (SV30)		
Dates of experiment:		Date of report: 6.03.2003	
Experimental team: Names	B. Schmitz, A. Ioffe, U Rü		
Local Contact:	U Rücker, A. Hoser		

Experimental report text body

The polarized neutron scattering is a powerful technique for condensed matter investigations and is successfully used both for structural and dynamical studies. However, the existing instruments are mostly operating with cold neutrons, where the problems of the beam polarization and analysis are effectively solved by modern supermirrors. In contrast to this, the use of supermirrors for the polarization and the polarization analysis of neutrons with energy E_n of about 100 meV is rather problematic. At present, the neutron spin filter based upon polarized ^{3}He is considered to be the most suitable mean to solve this problem.

These ideas are defining the construction of a new spectrometer for polarization analysis at the Research Center Jülich. The spectrometer is thought as a multiple purpose instrument, which can be used both as a diffractometer and a triple-axis spectrometer (Fig. 1). Therefore, it is equipped with two exchangeable detector modules, 5 and 9, which carry an analyzer unit with a single detector (or a multianalyzer unit with a multidetector, see details below) and a position sensitive detector, respectively. The polarization of the neutron beam will be performed by a flat ^{3}He - based wide band polarizer 6 that covers all the energy range of the incident neutron beam; similar neutron spin filters will be used as analyzers as well. Since the instrument will operate at a medium flux reactor, we use a double-focusing monochromator that allows for the gain in the neutron flux by the expenses of a modest relaxation in resolution. Actually, the instrument will be equipped with two monochromators, Cu (200) and PG(002), which can be elevated to the beam within a vacuum monochromator chamber. The size of the monochromators is (300 x 140) mm^2 and each of them consists of 15 x 7 adjustable crystals with the mosaicity of about 20'. Take off angles of the monochromators are fixed at 13º, 20.5º and 37.5º, so that that monochromatic neutron beams with energy 123 meV, 51 meV, 36 meV and 15 meV will be available.

The results of MC simulations by SIMRES98-ILL for a PG 002 monochromator are presented in Table 1. To obtain such a high gain, which actually amounts to the factor of 10, the monochromator crystals should be perfectly aligned. However, the outer surface of crystals is set off the Bragg planes by an angle of about 20-30'. Such an offset results in a significant spread of the images created by separate crystals in the focusing plane, thus increasing the size of the focal spot and decreasing the neutron flux density.

Horizontal	Vertical	Flux (n/cm²s)
R = ∞	R = ∞	$2 \cdot 10^7$
R = ∞	R = 0.5 m	$7 \cdot 10^7$
R = 2 m	R = ∞	$5 \cdot 10^7$
R = 2 m	R = 0.5 m	$18 \cdot 10^7$

Table 1. Flux at the sample position evaluated by SIMRES98-ILL for different settings of PG 002 monochromator, (E=14,6 meV, open collimation, no filters).

It was an aim of this experimental work to provide an alignment of neutron images created by separate crystals. The images have been recorded by a position sensitive detector placed in the focal point of the monochromator. To simplify the alignment procedure, optical images created by the reflection of the laser light from mirrors attached to outer surfaces of the Cu crystals or from partially reflecting outer surfaces of the PG crystals have been detected at a screen. Such reference points allowed us to carry out the alignment following optical marks; the final control was performed by a neutron image. The maximal shift of neutron images of size (25 x 25) mm^2 from the centre of the focal point amounted to the less then 5 mm, that corresponds to the angular deviation of about 5', which is well inside and much less than the mosaicity of the crystals (typically 20' – 30').

Because of requirements to the wavelength,, the alignment of Cu monochromator was carried out at the 2.3 Å neutron beam obtained from the monochromator of UNIDAS; the alignment of PG monochromator was carried out at the 3.5 Å neutron beam obtained from the monochromator of HADAS.

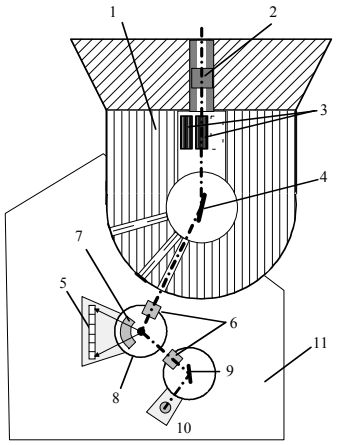

Fig. 1. Layout of a thermal neutron spectrometer/diffractometer for polarization analysis (SV30) at the research reactor FRJ-2: 1- monochromator shielding, 2- in-pile filter, 3 – remotely changeable collimators, 4 –double focusing monochromator, 5 – position –sensitive detector, 6 – flat ^{3}He neutron spin filters, 7 – banana-shaped ^{3}He neutron spin filter, 8 – sample , 9 – analyser assembly, 10– detector assembly, 11 – tanzboden

Institut für Festkörperforschung
Forschungszentrum Jülich GmbH
D-52425 Jülich

Experimental Report
of Neutron Scattering Experiments
at the FRJ-2 Reactor

Proposal number:	HAD-02-011		
Experiment title:	**Magnetic domain wall examination by neutron reflectometry in highly anisotropic thin layers**		
Dates of experiment:	2-12-2002 - 9-12-2002	Date of report:	8-3-2003
Experimental team: Names	Addresses		
V. Pierron-Bohnes M. Abes	IPCMS-GEMM BP43 23 rue du Loess F-67034 Strasbourg France idem		
Local Contact:	Ulrich Ruecker		

Experimental report text body

We have measured by neutron reflectometry a $Co_{57}Pt_{43}$ sample epitaxied on a (001)MgO substrate in order to get information on its domain wall structure. The sample was a partially ordered single crystal with [001] growth direction and easy magnetization axis (Fig 1). It was first demagnetized using 5 cycles of decreasing amplitude (from 1.8 T whereas its in plane coercive field is about 0.01 T) with the magnetic field in the [100] direction. MFM (magnetic force microscopy) showed irregular stripes along the [100] direction (Fig. 2) with a characteristic length around 0.3 µm.

The sample has been measured in this first magnetic state with a 8° angle between the [100] direction and the incident beam in order to bring the eventual Bragg peaks associated with the domain structure nearer to the origin of the reciprocal space. The spin polarization of the neutrons was along the [100] direction. Figure 3 shows the measured intensity in the (α_i, α_f) plane and figure 5 the intensity along the $\alpha_i = \alpha_f$ diagonal. The reflectivity oscillations associated with the thickness of the layer (50 nm) are clearly seen on the diagonal for R_{++}. There is no clear evidence of a Bragg peak showing that the coherence of the domain structure is not sufficient to observe it. The R_{++} and R_{--} measured intensities are identical and $R_{+-} = R_{-+}$ are non zero. Thus there is no component of the magnetization along [100] but a non zero component along [010]. As the stripes are in majority along the [100] direction this means that the domain walls are mainly of Bloch type and that the closure domains are very limited. Moreover, there is a significant R_{+-} intensity at the reflection critical angle ($\alpha_i = \alpha_f = 6$ mrad), meaning that there is a non zero average of the [010] magnetization component, this can originate from a too large amplitude of the last demagnetizing cycle.

After this first measurement, the sample was demagnetized using 25 cycles of decreasing amplitude (from 2 T) with the magnetic field in the [110] direction. The stripes structure observed by MFM was not qualitatively different and the reflectometry intensities were the same as in the following case.

Then the sample was demagnetized using 25 cycles of decreasing amplitude (from 2 T) with the magnetic field in the [100] direction. Figures 4,6,7 correspond to this magnetic state with different relative orientations of the spin polarization (H_G). We can see that the main changes compared to figures 3,5 are that the intensity at the critical angle is smaller than before in the H_G // [100] and very small in the other two configurations. The location of the diffuse intensity has changed (α_i = cste and α_f =cste) instead of ($\alpha_i + \alpha_f$ = cste).
These results show that the structure of the magnetic domains is very sensitive to the magnetic story of the sample. There is some interesting diffuse intensity present but its analysis is more complicate than expected and more experiments with well defined magnetic story is needed in order to understand quantitatively these observations.

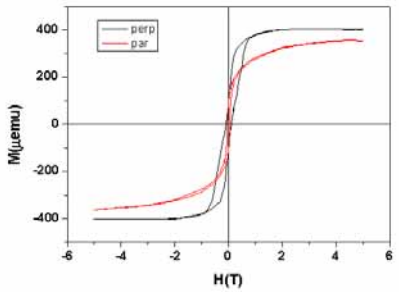

Fig. 1 : Magnetic cycles as measured using SQUID with magnetic field perpendicular or parallel to the film plane.

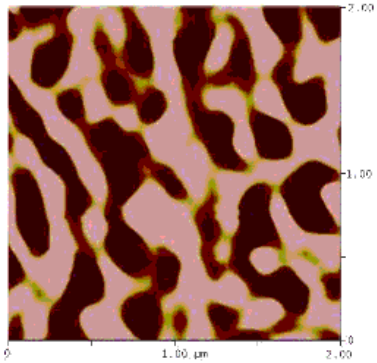

Fig. 2 : MFM image after the first demagnetization (vertical : [100] direction, horizontal : [010] direction).

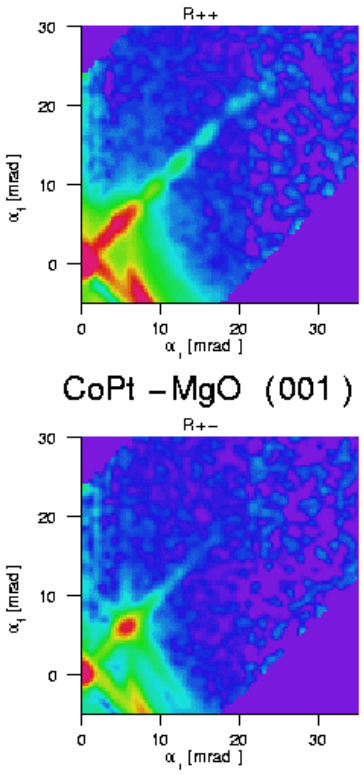

Fig. 3 : Neutron reflectometry map after the first demagnetization, H_G // [100].

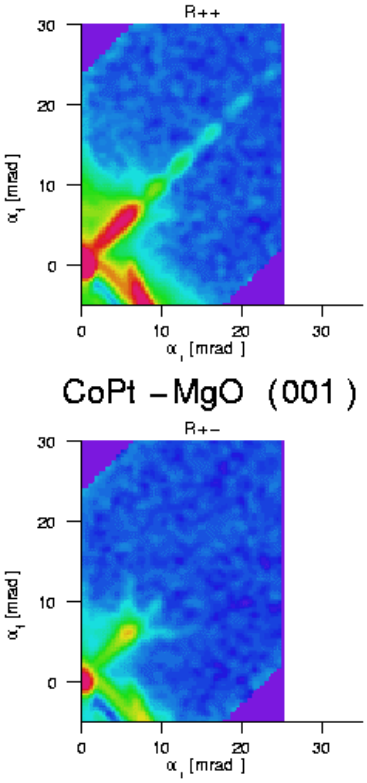

Fig. 4 : Neutron reflectometry map after the third demagnetization, H_G // [100].

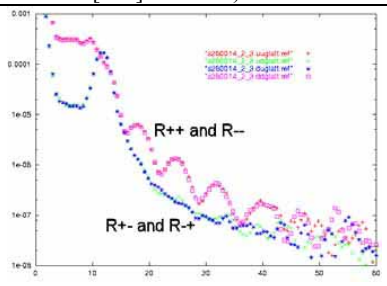

Fig.5 : Neutron reflectometry intensity for $\alpha_i = \alpha_f$ after the first demagnetization, H_G // [100].

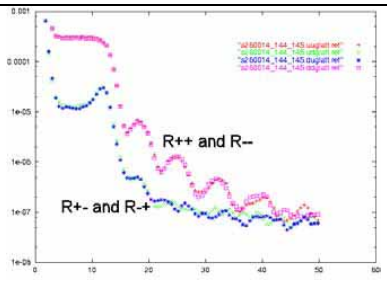

Fig.6 : Neutron reflectometry intensity for $\alpha_i = \alpha_f$ after the third demagnetization, H_G // [100].

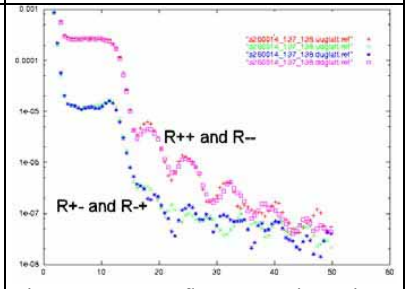

Fig.7 : Neutron reflectometry intensity for $\alpha_i = \alpha_f$ after the third demagnetization, H_G // [010] or [001].

Small Angle Neutron Scattering Instrument (KWS1)

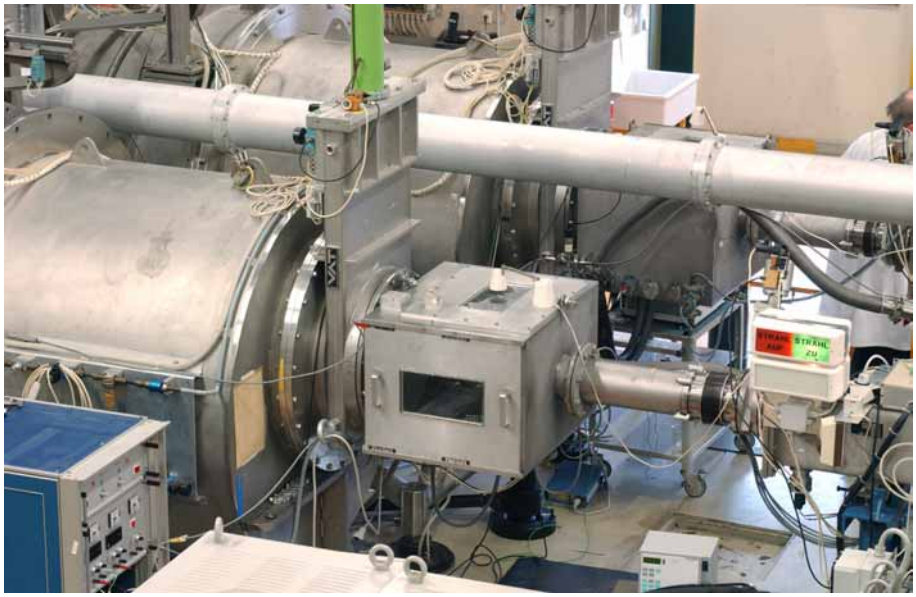

Instrument Parameters

Beam tube:	NLIIA straight guide; cross section: 4.5 cm (height) × 3 cm (width)
Monochromator:	velocity selector (DORNIER); $\Delta\lambda/\lambda = 0.2$
Incoming beam ***- Entrance aperture:*** ***- Sample aperture:***	 variable; suggested: 3 cm × 3 cm variable; suggested: 1 cm × 1 cm
Collimation:	length variable from 1 m to 20 m
Detector ***- Active area:*** ***- Scintillator:*** ***- Space resolution:*** ***- Max. pulse rate:*** ***- Detection probability:*** ***- γ-sensitivity:***	 60×60 cm^2 in 128×128 channels ^{6}Li-glass, 1 mm thickness 0.5×0.5 cm^2 ca. 1 MHz (τ_{dead} = 1 μsec) 95 % for λ = 7 Å 2×10^{-4} (1 MeV)
Neutron flux at sample:	2×10^5 ... 2×10^7 n/cm^2 s depending on collimation λ = 7 Å wavelength and entrance aperture 3×3 cm^2
Wavelength:	4.5 Å < λ < 15 Å
Momentum transfer range:	10^{-3} Å^{-1} < Q< 0.2 Å^{-1} optional $Q_{max} \cong 1$ Å^{-1}
Ancillary equipment:	automatic sample holder in vacuum and air; heating devices: –40 to 200°C; pressure cell: p = 1 ... 2000 bar / $T \approx$ –30 to 200°C; strain rigs and temperature control unit for quenched-elongational studies of melts (liquid N_2)

Instrument Responsible

Dr. Dietmar Schwahn	Tel. +49-(0)-2461-61-6661	Email: d.schwahn@fz-juelich.de
Dr. Wim Pyckhout-Hintzen	Tel. +49-(0)-2461-61-4681	Email: w.pyckhout@fz-juelich.de
Dr. Martine Heinrich	Tel. +49-(0)-2461-61-2868	Email: ma.heinrich@fz-juelich.de

Institut für Festkörperforschung
Forschungszentrum Jülich GmbH
D-52425 Jülich

Experimental Report
of Neutron Scattering Experiments
at the FRJ-2 Reactor

Proposal number:	KWI-01-011		
Experiment title:	**Cylindrical polyelectrolyte brushes**		
Dates of experiment:	18.1.-21.1.2002	Date of report:	24.2.2003
Experimental team: Names	Addresses		
Franziska Gröhn	Institut für Physikalische Chemie Universität Mainz Wedreweg11 55128 Mainz		
Local Contact:	Dr. Wim Pyckhout-Hintzen		

Experimental report text body

Polyelectrolytes, polymers that carry many charges along their backbone, are widely found in nature and applications and show special phenomena very different from uncharged polymers. Controverse discussion about physical chemical fundamentals explaining their behavior is ongoing since decades. Recent experimental results and modeling support earlier claims that an attractive interaction between macroions of the same charge exists and can yield ordered superstructures in aqueous solution. Structures may arise from mutual attractions mediated by counterions that are not uniformly distributed around macroions. However, many questions regarding the interaction of polyelectrolytes and counterions are unresolved which is in part due to the fact that classical flexible polyelectrolytes show a complex interplay of conformational effects and intermolecular interactions.

Therefore our goal is to use simple model systems with decreased degrees of flexibility that allow to study intermolecular interactions of polyelectrolytes.

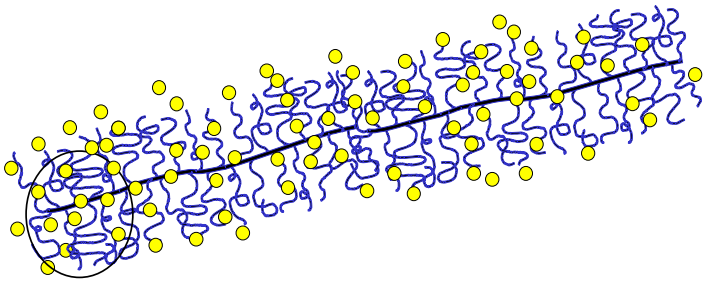

Figure1: Sketch of polyelectrolyte brush with counterions: the cross-section diameter does not depend on the type of counterion, but the intermolecular structures formed in solution strongly depend on the counterions.

In this experiment we have chosen cylindrical polyelectrolyte brushes as model system. Poly(styrene) brushes were prepared via polymerization of poly(macromonomers) and subsequently sufonated resulting in cylindrical poly(styrene sulfonate) brushes.

These polyelectrolyte brusehs were characterized in aqueous solution. SANS measurements were performed at 1.25m, 2m, 8m and 10m sample-detector distance using 1 or 2 mm quartz sample cells.

We have investigated poly(styrene sulfonate) brushes with H^+ and Cs^+ counterions. The SANS measurements allowed to characterize the cross section profile of the brushes which have a cross-sectional radius of gyration of 4.0 +/-0.3 nm, independent from the type of counterion.
At very low concentration the low q-behaviour of the scattering curve approximately shows a –1 slope in a double logarithmic I(q) vs q plot indicating the cylindrical structure.

At higher concentration an intermolecular structure factor peak is observed that can serve as measure for the interparticle distance. As known for other polyelectrolytes, the interparticle distance is smaller than for homogeneous distribution of the particles in solution, due to the formation of structured domains with higher concentration.
Interestingly, the interparticle distance is significantly different for the case of hydrogen and cesium counterions. This result shows that it is indeed an electrostatic force mediated by counterions that causes the structure formation which thus depends on the type of counterion.

Further, we have measured uncharged brushes in organic solvent for comparison, which allows to extract length as well as cross-section of the cylinders without disturbing effects due to electrostatic interaction.

Institut für Festkörperforschung
Forschungszentrum Jülich GmbH
D-52425 Jülich

Experimental Report of Neutron Scattering Experiments at the FRJ-2 Reactor

Proposal number:	KW 1-01-034		
Experiment title:	Structural modifications induced by classical surfactant addition on diblock copolymers in aqueous solution and at the silica-water interface		
Dates of experiment:	January 16-17, 2002 February 20 and 24, 2002	Date of report:	July 18, 2002
Experimental team: Names	Addresses		
Vangeyte, Patrick	Center for Education and Research on Macromolecules, University of Liège, Building B6a, B. 4000 Sart-Tilman, Belgium		
Leyh, Bernard	Laboratoire de Dynamique Moléculaire, University of Liège, Building B6c, B. 4000 Sart-Tilman, Belgium		
Jérôme, Robert	Center for Education and Research on Macromolecules, University of Liège, Building B6a, B. 4000 Sart-Tilman, Belgium		
Local Contact:	Heinrich, Martine		

Experimental report text body

Uncharged water-soluble polymers are known to interact with ionic surfactants in aqueous solutions. Polymer-surfactant mixtures are widely used in many application fields, such as detergency, cosmetics, painting, … requiring surface conditioning. It is therefore important to characterize their properties and to be able to tune their behaviour both in aqueous solutions and at the solid-liquid interface. The general purpose of this work is to unravel the behaviour of mixtures of two surfactants of different sizes, an amphiphilic water-soluble diblock copolymer and a classical surfactant, in water and at the silica-water interface. An anionic classical surfactant, sodium dodecyl sulfate (SDS), has been chosen. The diblock copolymers investigated consist of two blocks known for their biocompatibility, one of them being biodegradable. The hydrophilic part consists in a poly(ethylene oxide) block (PEO) whereas the hydrophobic one is a poly(κ-caprolactone) or a poly(ν-methyl-κ-caprolactone) block (PCL or PMeCL). The polymerization is well controlled, so that the polydispersity remains low and the hydrophilic/hydrophobic balance is controlled by the molar composition. Five copolymers were selected ; they are listed in Table 1.

Table 1. List of investigated copolymers

	M_n(PEO)/Daltons	M_n(PCL)/Daltons	M_w/M_n
PEO-b-PCL	5000	2200	1.14
PEO-b-PCL	5000	1850	1.16
PEO-b-PCL	5000	950	1.10
PEO-b-PCL	5000	350	1.10
PEO-b-PMeCL	5000	1500	1.12

Small angle neutron scattering is ideally suited for this study. It makes it possible to characterize auto-assembled structures in aqueous solution and it provides us with information on the different components of the system, using contrast variation. The experiments have been conducted on the KWS-1 instrument at a wavelength of 7 Å and in two momentum transfer ranges: 0.02 $Å^{-1}$Ωq Ω0.15 $Å^{-1}$ and 0.006 $Å^{-1}$Ωq Ω0.04 $Å^{-1}$.

This report is divided in two parts: (i) the study of the self-assembling properties of each individual copolymer in aqueous solution; (ii) the behaviour of the copolymers at the silica-water interface. As far as the

interaction with sodium dodecyl sulfate is concerned, additional experiments using deuterated SDS are needed, in order to perform contrast matching of either the copolymer or the surfactant.

1. Self-assembling of copolymers in aqueous solution

The very low critical micellar concentration of the copolymers considered here (cmc – 0.01 g/L) suggests that only micelles will be observed under our experimental conditions (concentration larger than 2 g/L). Two complementary approaches have been followed to infer information on the micellar structure.

(i) At concentrations as low as 2g/L, the intermicellar distance is large compared to the micellar radius, so that the SANS signal reduces to the micellar form factor. The experimental form factor has been fitted to an analytical formula developed for a dense spherical hydrophobic core, of radius equal to R, surrounded by a corona of hydrophilic rods of effective length equal to L [1]. The number of rods is equal to the aggregation number, N_{agg}. The polydispersity of the aggregation number has been taken into account in the fitting procedure. We observed that the z-average value of R, which corresponds to the micellar size giving the largest scattering signal, is nearly independent of the polydispersity.

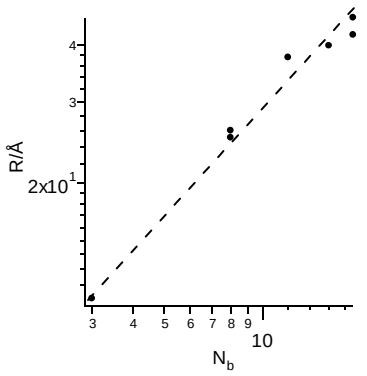

Fig.1. Core radius of copolymer micelles as a function of the polymerization degree (N_h) of the hydrophobic block

(ii) At higher concentrations, peaks resulting from the interference between waves scattered by different micelles, show up. Their location is related to the average intermicellar distance and thus to the concentration of micelles. The ratio of the copolymer and micelle concentrations is equal to the aggregation number, from which a core radius can be inferred, in the hypothesis of a dense hydrophobic core. Both procedures, (i) and (ii), are found to give similar results.

Figure 1 shows the evolution of the radius of the micellar core as a function of the polymerization degree, N_b, of the hydrophobic sequence. The following scaling relationships are found: $R \nabla N_b^{0.73}$, $N_{agg} \nabla N_b^{1.2}$ and $(R+L) \nabla N_b^{0.09}$. These results are compatible with scaling laws found in the literature [2,3]. The corona thickness lies in the 70-90Å range: this corresponds to a moderate PEO chain extension of about 25% of the contour length. Preliminary results using undeuterated SDS show that the PEO chains tend to stretch upon addition of ionic surfactant.

2. Behaviour at the silica-water interface

The copolymers mentioned in Table 1 have been investigated in the presence of silica at concentrations corresponding to complete saturation of the silica/water interface. The silica used is characterized by a pore size of 1250Å. It has been checked that the Porod regime is reached. We used a 60/40 w/w % D_2O/H_2O mixture in order to observe contrast matching between the solvent and silica. Figure 2 shows two example of the SANS data obtained under such conditions.

The scattered intensity, when plotted as q^4 I(q) versus q, shows interference patterns from which information can be extracted about the size of the adsorbed layers. From the position of the first maximum, global layer thicknesses in the 75-95 Å range are deduced. The situation investigated here is more complicated than the more conventional case of grafted polymers, because the presence of hydrophobic and hydrophilic blocks must be taken into account. A model introducing two sublayers needs to be developed to fully analyze the scattering data.

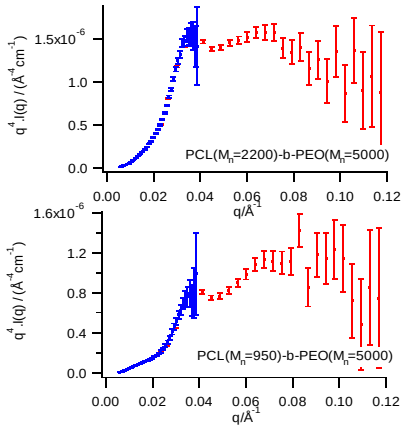

Fig. 2. Intensity scattered by an adsorbed layer of PCL-b-PEO copolymer at contrast match between silica and the solvent.

[1] B. Leyh, D. Fati, J.P. Gaspard and R. Jérôme, unpublished

[2] I.W. Hamley, The Physics of Block Copolymers, Oxford University Press, 1998

[3] R. Nagarajan and K. Ganesh, J. Chem. Phys. **90**, 5843 (1989)

Institut für Festkörperforschung
Forschungszentrum Jülich GmbH
D-52425 Jülich

Experimental Report
of Neutron Scattering Experiments
at the FRJ-2 Reactor

Proposal number:	KW1-01-901		
Experiment title:	**Trapping of water in sovramolecular biological aggregates: SANS study of the structural water in giant oligomeric proteins**		
Dates of experiment:		Date of report:	
Experimental team: Names	Addresses		
Dr.Romanzetti, Sandro Dr. Carsughi, Flavio Prof. Mariani, Paolo Dr. Spinozzi, Francesco	INFM Research Unit of Ancona,Via Brecce Bianche - 60131 Ancona – ITALY University of Ancona, Dibiaga, Via Brecce Bianche– 60131 Ancona - ITALY University of Ancona, Via Brecce Bianche– 60131 Ancona – ITALY University of Ancona, Via Brecce Bianche– 60131 Ancona - ITALY		
Local Contact:	Dr. Wim Pyckhout-Hintzen		

Experimental report text body

Introduction

The interaction of biological macromolecules with water has a fundamental role in their stabilization and function. Recently, comparing X-ray and neutron small angle scattering data (SAXS and SANS), it has been proved that for some small proteins the density of the water in the border layer is about 10% higher than the density of the bulk water [1,2]. Furthermore, protein aggregates have often the capability to confine water molecules from the bulk solvent into compartments which have low probability to interact with the bulk solvent. Being confined, such water molecules are expected to play a crucial role in stabilizing the tertiary and the quaternary structures. In order to have a better knowledge of these effects and to characterize the structure of the different conformations of Hemocyanin (Hc), a giant oligomeric protein isolated from the cephalopod *Octopus vulgaris* and responsible of oxygen transportation in several species of mollusc and arthropods, SANS measurements on the oxygenated and deoxygenated forms of the molecule have been performed.

Samples

Hemocyanins (Hcs) are giant oligomeric proteins with a molecular weight of some millions that transport oxygen in several species of molluscs and arthropods. Composed of five to eight different functional units, they can be considered as modular proteins able to assume a large number of spatial distributions ranging from a *loose state* to a *compact state* which is the responsible for their aggregation to native decameric structures with a hollow cylinder shape (Fig. 1). Furthermore, those conformations are strongly depending on the oxygenation state of the protein. Previous small angle scattering studies on the oxygenated and deoxygenated forms of the Hc indicated that upon binding of oxygen strong changes both in the form factor and in the intensity scattered at zero-angle occurred. Since no changes in the aggregation properties of the molecules were detected by biological analysis, it has been suggested that the conformational changes following oxygen affect the mobility and, hence, the density of water molecules occupying the central hole of the protein.

Experimental

Neutron scattering contrast variation approach is particularly suitable to establish the inner structure of a particle in solution and then in the present case to address on the quantification of the water contribution to the dimensions of the structural elements as well as to the scattering length density in terms of hydration shell and "bound water" [1,3,4]. SANS patterns have been measured at different D_2O content in order to distinguish the shape of the bound water from that of the protein inside the scattering volume for both the deoxygenated (Fig.2) and oxygenated forms (Fig.3). Successively, data have been analyzed with a Reverse Monte Carlo method, by taking into account the 3D structure of the 50 functional domains and moving their positional-orientational coordinates. Moreover the shape of the bound water has been described by a multipole expansion method. The aggregate point group symmetry is $D5$. A preliminary structure of the deoxy aggregate is shown in figure 4.

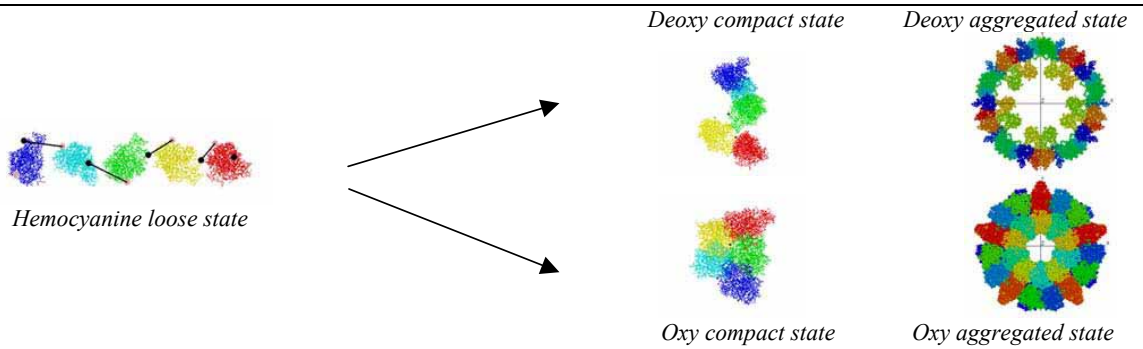

Fig. 1. Conformational changes model of the Hemocyanine protein depending on the oxygenation state

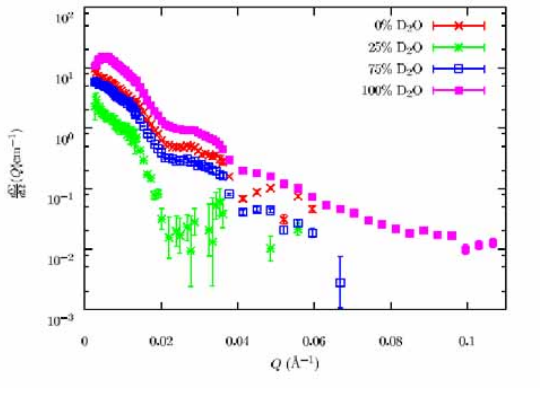

Fig. 2 SANS deoxygenated

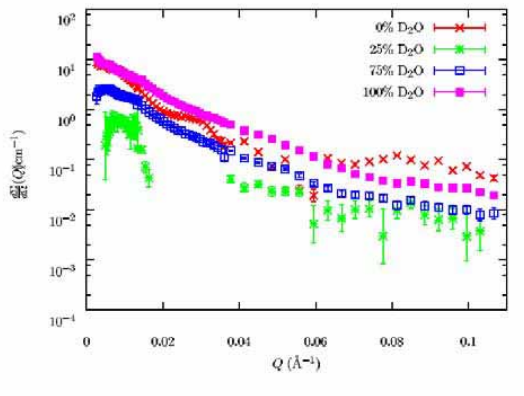

Fig. 3 SANS oxygenated

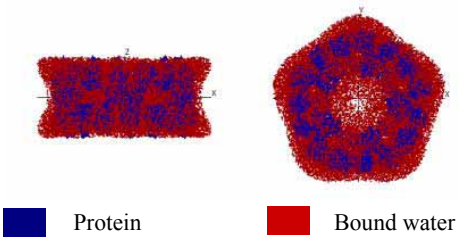

Fig.4 A preliminary structure of the deoxygenated aggregate

References

[1] Svergun, D., S. Richard, M.H.J. Koch, Z. Sayers, S. Kuprin and G. Zaccai. 1998. *Proc. Natl. Acad. Sci. USA*, 95, 2267

[2] Mariani, P., F. Carsughi, F. Spinozzi, S. Romanzetti, G. Meier, R. Casadio, C.M. Bergamini. 2000. *Biophys. J.*, 78, 3240

[3] Jacrot B., Rep. Prog. Phys., 39, 911 (1976)

[4] Ashton A. W. et al, J. Mol.. Bio. , 272, 408 (1997)

Institut für Festkörperforschung
Forschungszentrum Jülich GmbH
D-52425 Jülich

Experimental Report
of Neutron Scattering Experiments
at the FRJ-2 Reactor

Proposal number:	KW1-01-903		
Experiment title:	**LIVING POLYMERS FORMED BY THE SPONTANEOUS AGGREGATION OF DILAUROYLPHOSPHATIDYLNUCLEOSIDES**		
Dates of experiment:	06-08 March 2002	Date of report: 19/02/2003	
Experimental team: Names	Addresses		
Piero Baglioni Debora Berti	Department of Chemistry and CSGI, University of Florence Via della Lastruccia 3 Polo Scientifico, Sesto Fiorentino 50019-Firenze Italy		
Local Contacts:	Martine Heinrich, Wim Pyckhout-Hintzen		

Experimental report text body

INTRODUCTION

We have undertaken a structural study of supramolecular structures formed by the self-assembly of recently synthesized nucleolipids [see 1 for a review], that is double-chain phospholipids undergone to an enzymatic modification that transfers a nucleoside on the polar head.This work is motivated by the interest in the expression of molecular functions in self-organized systems, where the driving force of aggregation has a hydrophobic nature, which is the exclusion of hydrocarbon chains from the contact with aqueous medium. The molecular information (i.e. packing parameter and molecular recognition capacity) is amplified in the supramolecular arrangement and rules phase behavior. Their self-assembly can be fine-tuned by a proper choice of the alkyl chains of the lecithin in the synthetic step. But most important is the molecular information contained in the polar head, standing its biological relevance: like in nucleic acids its functionality is triggered by the macromolecular organization, in our case is the self-aggregation that makes possible base-base interactions. We have observed base-base interactions in bilayered closed vesicles and in micellar aggregates, notwithstanding the exposure of bases to aqueous environment that is a formidable competitor for H-bonding.
More recently our attention has been drawn to the study of semi-flexible wormlike aggregates, also called polymerlike micelles, formed by dilauroylphospholiponucleosides[2], DLPN, where N is adenosine or uridine.
DLPU micellar solutions have been characterized as a function of lipid volume fraction in a phosphate buffered solution, highlighting the crossing to a semidilute regime.
A combination of scattering techniques, namely SANS and SLS, allows in principle a complete characterization of the micelles, since accessible quantities are the global aggregate dimension (radius of gyration), the cylindrical cross section radius, the area per polar head, and the persistence length, directly proportional to the bending modulus of the rod. We can say that chemistry comes into play in the persistence length, because this quantity can vary by orders of magnitude in synthetic and natural polymers, depending on the chemical nature of the monomer. So the *local structure-mesoscopic structure* connection is contained in the persistence length.
Aim of the experiment was the evaluation of the intrinsic persistence length, correlated to the observed one by

($L_p=L_{p0}+L_{pel}$), where L_{pel} is the contribution arising from electrostatic repulsion; this term vanishes at sufficiently high ionic strength.

EXPERIMENTAL DETAILS, SANS RESULTS AND FUTURE PERSPECTIVES

Sample	$[NH_4Cl]$	κ^{-1}[Å]
a	0.10	10
b	0.18	7
c	0.25	6
d	0.50	4

Samples have been prepared by dissolving DLPU lipohylized powder in NH_4Cl solutions in D_2O at different ionic strengths. The surfactant concentration has been kept constant ($1x10^{-2}$ mol/l or 0.5% volume fraction). SANS spectra have been collected at room temperature for 4 different configurations (sample/detector distances and collimation) in order to exploit the available momentum transfer, that is $1.6x10^{-3}/0.24$ Å^{-1}.

For this surfactant volume fraction we have observed in D_2O (previous results) a strong intermicellar correlation peak and the spectrum is consistent with globular aggregates (axial ratio < 2) composed of 105 monomers. The decrease of Debye screening length causes a condensation of counterions on the micellar macroion. In this conditions, considering also the packing parameter of the surfactant, we expect that the formation of wormlike micelles is preferred over the presence of globular ones.

Figure 1 reports the spectra collected for samples a,b and d. The appeareance of a –1 scaling region in the log-log plot is the fingerprint of a cylindrical structure, and has been observed as a characteristic feature of polymerlike micelles that behave as semiflexible polymers in good solvents. A very convenient representation for such structures is the so-called Holtzer plot, shown in Figure 2 for samples a and c, where the rigid rod region is visualized as the zero slope portion.

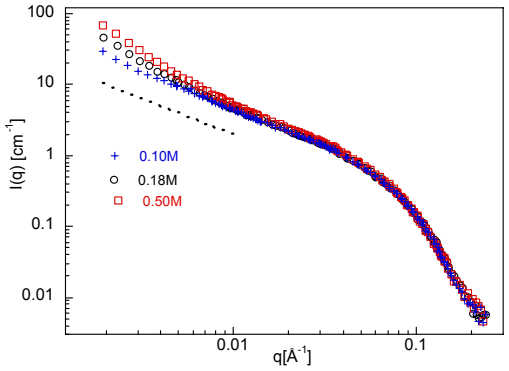

Figure 1

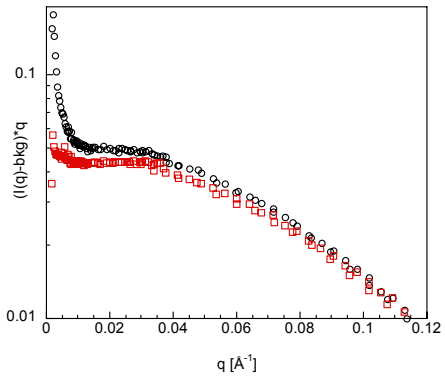

Figure 2

A very qualitative estimate of the persistence length can be done evaluating the scattering vector corresponding to the crossover between the rigid rod and the self-avoiding random-walk regime ($q^*L_p=1.9$); according to this coarse-grained analysis the persistence length goes from 211 to 135 Å as the ionic strength is increased.

According to the formalism of Skolnick and Fixman, the total persistence length can be written as the sum of intristic and electrostatic contribution, $L_p=L_{p0}+L_{pel}$; while the first contribution depends only on the chemical structure of the monomer, the second term is directly proportional to the Debye screening length.

Our preliminary results for the persistence length are reported in Figure 3, and the fit according to the Skolnick-Fixman model is the continuous line, which yields an intrinsic persistence length of 131 Å.

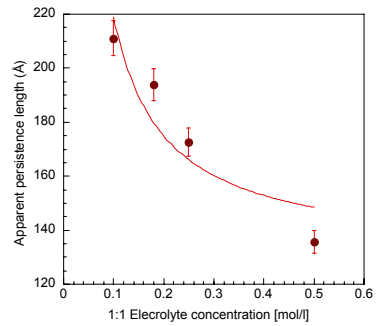

However the agreement is far from quantitative, and this is due to the non adequate estimate of persistence length.

We are currently testing on these spectra the approach developed by Pedersen and Schurtenberger, that allows to extract structural parameters through the determination of scattering functions of wormlike chain with and without excluded volume interactions thanks to Monte Carlo simulations. Preliminary results, yet to be confirmed, show the correct trend both for contour length and persistence length. This last parameter is found to be higher than that evaluated directly from the spectra, in agreement with usual values for polymerlike micelles.

[1] D. Berti, U. Keiderling, P.Baglioni, in Lipid and Lipid Polymer Systems, 2002, Nylander T, and Lindman, B. Editors, Springer Verlag: Heidelberg **[2]** Baldelli-Bombelli F., Berti D., Keiderling, U., Baglioni, P. J.Phys.Chem. B, 2002, 106, 11613-11621.

Institut für Festkörperforschung
Forschungszentrum Jülich GmbH
D-52425 Jülich

Experimental Report
of Neutron Scattering Experiments
at the FRJ-2 Reactor

Proposal number:	**KW1-02-001**		
Experiment title:	**LONG- AND SHORT-RANGE SPATIAL INHOMOGENUITIES IN POROUS MATRICES OF VYCOR GLASS AND AEROGELS**		
Dates of experiment:	**10.9.2002-13.9.2002** **18.9.2002-20.9.2002** **23.09.2002-24.09.2002**	Date of report: 28 Feb. 2003	
Experimental team: Names	Addresses		
Melnichenko, Yuri B. Wignall, G.D.	Solid State Division ORNL P.O.Box 2008 Oak Ridge, TN 37831-6393		
Local Contact:	Dr. D. Schwahn		

Experimental report text body

Porous Vycor glass, aerogels and xerogels have been widely used for fundamental studies of transport, dynamic and critical phenomena in confined mixtures. However, information on the structure of these porous materials is usually restricted to nano- and mesoscopic scale, while there were several suggestions made in the iterature that much larger pores with the size of the order of microns may be present in these porous media. Evidently, the existence of such pores, if confirmed, should be taken into account for the interpretation of experimental data on the thermodynamic and dynamic properties of confined fluids.

Vycor porous glass is obtained from a borosilicate glass-forming melt which has undergone a phase separation, one of the two phases being removed by leaching. It is widely assumed that, as the result, a porous material with homogeneous pore diameters of 40 Å and the pore volume 28% is formed [2]. On the other hand, aerogels are ultra low density materials (with up to 98% of the void space) produced via sol-gel technology [8]. These porous systems do not possess a characteristic pore sizes, which can possibly span up to micrometer scale. So far, the structure of Vycor porous glass and aerogels has been investigated by neutron and X-ray small angle scattering in the range of scattering vectors $0.001\ Å^{-1} \le Q \le 0.2\ Å^{-1}$ [3-5] and it was suggested in our proposal to employ the ultra-small angle neutron scattering (USANS) technique in order to explore large voids, which should be visible in the USANS domain $Q << 0.001\ Å^{-1}$.

The experimental results obtained using Juelich DKD difractometer for two aerogels of different density as well as Vycor porous glass are shown in Fig 1 and Fig. 2, respectively.

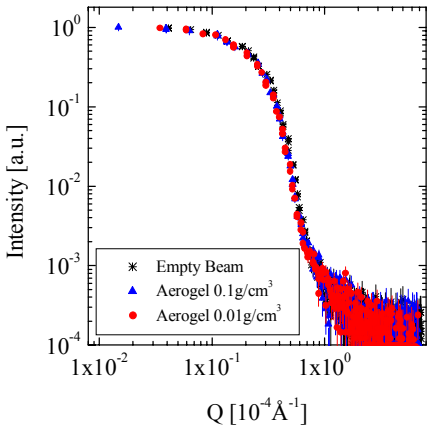

Fig. 1. USANS from aerogels.

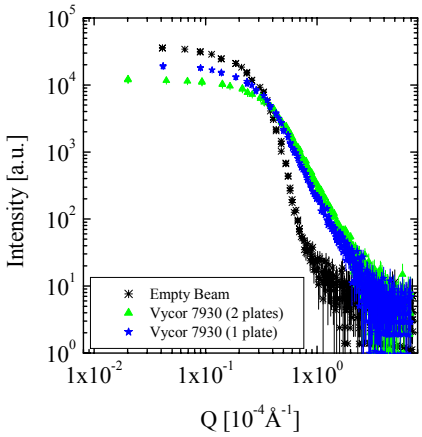

Fig. 2. USANS from Vycor porous glass.

As is seen, aerogels manifest no USANS scattering (Fig. 1), which is indicative of the absence of the micrometer size inhomogenuities in these systems. On the contrary, there exists a significant USANS signal coming from porous Vycor glass (Fig. 2). The intensity of scattering depends on the thickness of the material: it flattens out in the small Q region at different values of I(Q=0) and shifts in a parallel way with respect to incident intensity. The thorough analysis of the data obtained for aerogels is underway and will require resolution corrections along with conversion of experimental data obtained in a slit geometry to a „point" geometry. Interestingly, some conclusions can be already made by checking the exponent in the relation $I(Q) \sim Q^{-n}$ in the large-Q domain. In an „infinite slit" limit the Porod law $I(Q) \sim Q^{-4}$ translates into $I(Q) \sim Q^{-3}$. As is seen in Fig3, the function IQ^3 vs. Q levels off for the values of Q>0.0001, which implies that the scattering is coming from micrometer-level pores with sharp boundaries. Further analysis will include corrections for multiple scattering, and will allow for estimation of the pore sizes and volume fraction of big pores, the existence of which in Vycor has been demonstrated for the first time in this study [2].

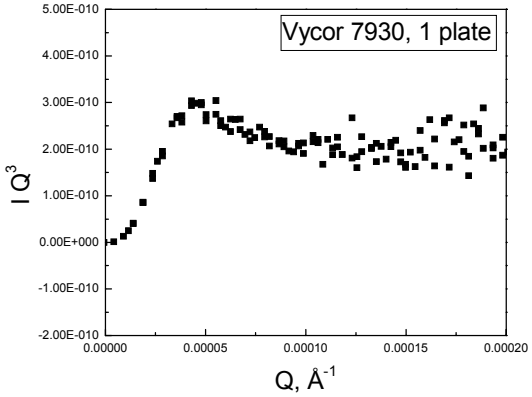

Fig.1. Analog of the Porod law for slit geometry. The figure demonstrates that USANS is coming from big pores in Vycor with sharp boundaries.

REFERENCES

1. Vycor Brand Porous Thirsty Glass 7930, Corning Technological Broshure, Corning Glass Works, Corning, NY 14830.
2. Melnichenko YB et al., J. Appl. Cryst., to be published.

Institut für Festkörperforschung
Forschungszentrum Jülich GmbH
D-52425 Jülich

Experimental Report
of Neutron Scattering Experiments
at the FRJ-2 Reactor

Proposal number:	KW1-02-002		
Experiment title:	**Miscibility of polypropylene blends vs. the tacticity distributions**		
Dates of experiment:	22.04. - 24.04. 2002 12.07. - 14.07.2002	Date of report:	24.02.2003
Experimental team: Names	Addresses		
A. Ramzi J. Pastoukhov	The Dutch Polymer Institute Eindhoven Polymer Laboratories Eindhoven University of Technology 5600 MB Eindhoven Niederlande		
Local Contact:	D. Schwahn		

Experimental report text body

The miscibility behaviour of semi-crystalline polymer blends has received attention in the literature during the past few years and the question of whether the polyolefin blends can exhibit any liquid-liquid phase separation in the melt has become somewhat very important. Most of the experimental evidence for any phase separation comes from indirect experiments in which rapidly quenched blend samples are studied in the solid state. It is known that the tacticity distribution of polypropylene (PP) strongly influences material properties through a variety of morphological factors such as crystallinity, lamellar structure, spherulitic macrostructure, and melting behaviour. Thus, the recent development of metallocene catalysts allows for the tailored production of new tacticity microstructures for polypropylenes of different properties. We are focusing in this project on polypropylene blends produced by metallocene and Ziegler-Natta catalysts with different tacticity distributions.

Small-Angle Neutron Scattering has been used to investigate the melt miscibility of PP blends via the contrast achieved by deuteration using KWS1 spectrometer at the research reactor FRJ2 at the Forschungszentrum Jülich GmbH. Various samples composed of a fraction ϕ of deuterated PP (D-PP) mixed with a fraction $(1-\phi)$ of hydrogenated PP (H-PP) have been measured. To cover a large Q range, the scattering patterns have been collected using three different spectrometer configurations: D=20m, C=20m; D=8m, C=8m; and D=2m, C=4m (D is the sample-detector distance and C is the collimation length) while the wavelength was kept constant (λ=7Å) corresponding then to three partially overlapping ranges of the scattering vector Q: 0.0023-0.015; 0.0057-0.038; and 0.024-0.15Å^{-1}, respectively.

We were investigating the effect of temperature on the miscibility behaviour in the melt state (above 170 ^{o}C). Different blends, prepared from deuterated isotactic PP (“D” iPP) and hydrogenated isotactoid PP (”H” isoPP), with various compositions have been measured.

Figure 1 shows the scattered intensity, in log-log representation, from the blend iPP(90%)/isoPP(10%) at four temperatures (170, 180, 190 and 200 ^{o}C). This blend clearly exhibits a Q^{-2} behaviour in the intermediate Q characteristic of random coil structures. Furthermore, the structure seems to represent an equilibrium state as it did not change even at higher temperature.

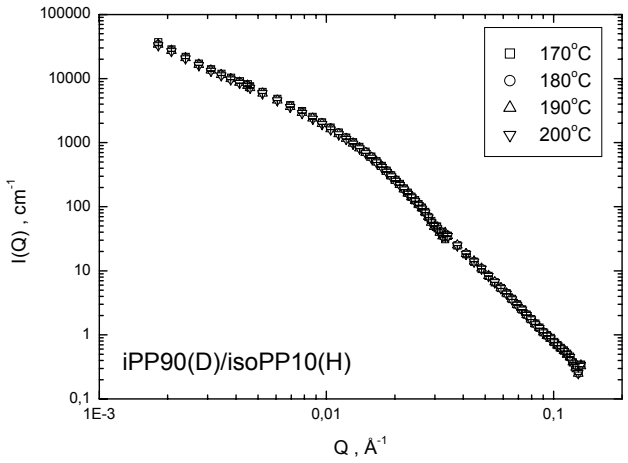

Figure 1. Scattering intensity from the blend iPP(90%)/isoPP(10%) at 170, 180, 190 and 200 °C.

As illustrated in figure 2, similar effect was observed for the same type of blend made from iPP(D)/isoPP(H) but with different composition 15%/85%(v/v). This indicates the stability of the Flory-Huggins χ parameter in melt state and its independent on temperature. No final conclusion can be drawn in this sense because of the limited measured samples. It is then very important to carry out systematic measurements for other blends made from other polymers with different compositions.

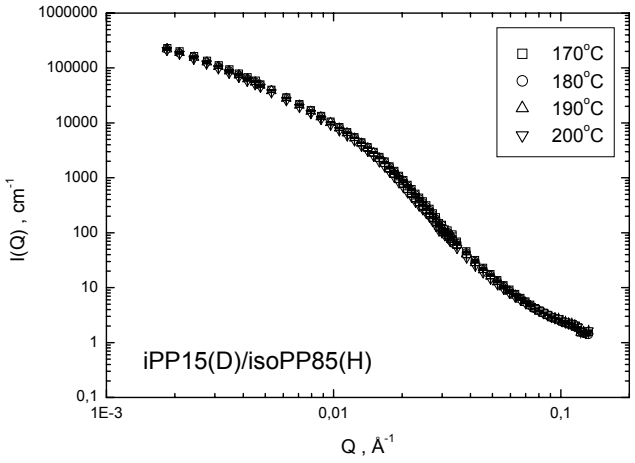

Figure 2. Scattering intensity from the blend iPP(15%)/isoPP(85%) at 170, 180, 190 and 200 °C

Institut für Festkörperforschung
Forschungszentrum Jülich GmbH
D-52425 Jülich

Experimental Report
of Neutron Scattering Experiments
at the FRJ-2 Reactor

Proposal number:	**KW1-02-003**		
Experiment title:	**Part II: relaxation study of deformed linear polymers in the quenched state**		
Dates of experiment:	**05.07.2002 – 08.07.2002**	Date of report:	**19.02.2003**
Experimental team: Names	Addresses		
Blanchard Ariane **Pyckhout-Hintzen Wim**	**IFF, Forschungszentrum Jülich**		
Local Contact:	**Wim Pyckhout-Hintzen**		

Experimental report text body

This study is part of a long term work on the relaxation mechanisms in step-strain elongated polymer melts. Most of the experiments were realized on linear polyisoprene chains prepared in a melt with a molecular mass of Mw ~ 220.000 g/mol. Since networks cannot relax (their topology is fixed by the crosslinks), their elongated structure shows an equilibrium state, which is especially interesting to use as a comparison with the non-linear case of a melt. During this beam time we worked with networks having different concentrations and elongated them to different rates (1,3 ;1,5 and 2).

The networks were prepared by means of vulcanisation of polyisoprene linear chains (Mw ~ 220.000 g/mol) at ~150°C. The study was carried out on three network concentrations: M_c~7783, M_c~6628 and M_c~8624.

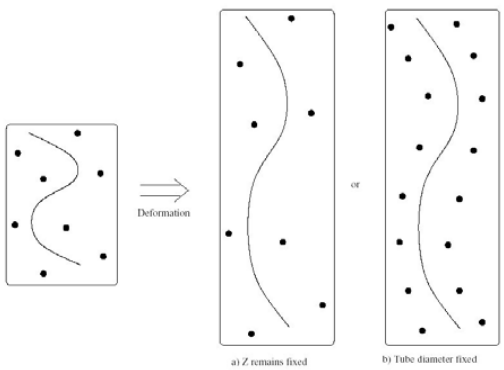

On the theoretical point of view, two cases are taken into account during the elongation of a sample (Fig.1). Either the number of entanglements remains constant (as represented on the left drawing) or the tube diameter remains constant, which implies an increase of the number of entanglements along the molecule. The first case is obtained in the elongation of a network whereas the second case corresponds to an elongated melt.

Fig. 1: the two theoretical cases for the entanglement repartition after an elongation

Experimental setup:

The samples were placed in home-built exensiometers and stretched to a factor of 1,3; 1,5 and 2. The three extensiometers were placed as depicted on Fig.2 on a mobile sample holder and were measured at C20D20, C8D8 and C4D2.

The main experimental problem was to fasten the networks to the extensiometers. Due to the high resistance of the polymers to an extension we had to glue them to the metallic frame. On the other hand, such networks are easily breakable and we lost some of the data because one sample broke before the end of the measurement.

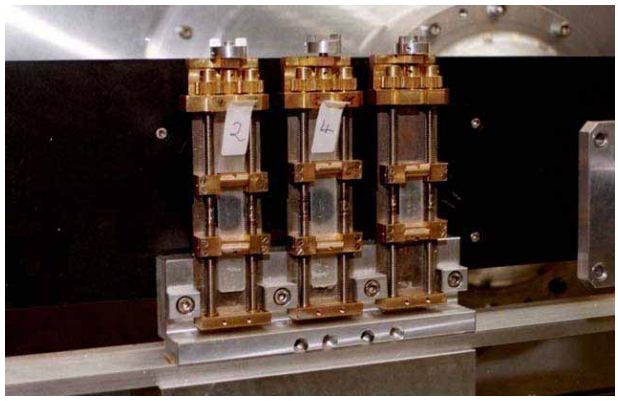

Fig.2: the extensiometers

SANS results and outlook:

Fig. 3 represents the scattering along the main detector axis.

- The blue curves are measured along the parallel direction to the stretch (below) and perpendicular to it (above).
- The black dots are a radial average of an isotropic measurement of the sample used as a reference.
- The red curves are fits obtained using the newest theoretical developments of E. Straube (Uni Halle-Wittenberg).

These fits deliver a tube diameter of 41 Å, which is in perfect agreement with former studies[1] performed on a similar system.

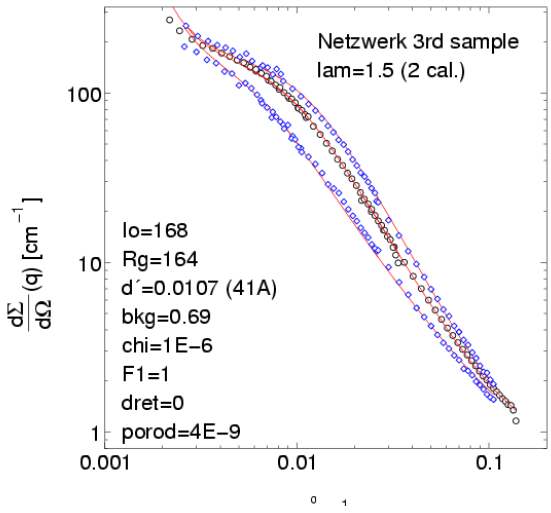

Fig.3: scattering of a network elongated by a factor of 1.5

The theory used to describe the data has been developped on a static tube-constrained structure factor. The same model is applicable to polymer melts under strain, the only difference being that the tube diameter in a deformed state is written as $d_\mu = d_0 * \lambda^\upsilon$, with $\upsilon=0$ for melts since the deformation is isotropic in all 3 directions, and $\upsilon=1/2$ in the case of networks. This facilitate of course the comparison of the data and in particular the high value of the tube diameter is noticeable. Under the same stretching conditions, it reaches 41 Å for a network, whereas for a melt we fit it about 24 Å.

In the future we will investigate a system of bimodal polymer blends, where the tube dilution is put forward due to the difference in chain lengths. We also plan to study the evolution of the tube diameter as a function of the temperature in elongated networks.

[1] S. Westermann, PhD Thesis, „Correlation of local deformation and chain dynamics in polymer networks“, Forschungszentrum Jülich, 1998

Institut für Festkörperforschung
Forschungszentrum Jülich GmbH
D-52425 Jülich

Experimental Report
of Neutron Scattering Experiments
at the FRJ-2 Reactor

Proposal number:	KW1-02-004 a		
Experiment title:	**Nucleation and crystal growth of calcium minerals in aqueous solution and at biomimetic interfaces; mineralization of $CaCO_3$ in the presence of Gold&DMAP and Ovalbumin**		
Dates of experiment:	2.4. – 3.4. 2002 4.4 - 5.4. 2002	Date of report:	18.02.2003
Experimental team: Names	Addresses		
M. Balz, W. Tremel	Johannes Gutenberg-Universität Mainz Institut für Anorganische Chemie und Analytische Chemie Becher Weg 24 D55099 Mainz		
Local Contact:	D. Schwahn		

Experimental report text body

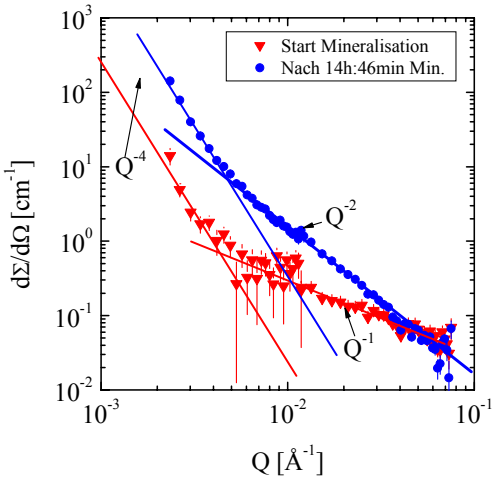

Figure 1: Scattering patterns before and after nearly 15 hours mineralization of $CaCO_3$ in the presence of 49mg/cm^3 gold & DMAP and 2.5mg/cm^3 Ovalbumin at T=30°C. Right from the beginning of mineralization one observes thin (<10Å) rod-like particles and after mineralization thin plates, as can be concluded from the Q^{-2} power law. The diameter of the rods appears comparable with the thickness of the plates as in both cases no deviations from the power laws at large Q are observed. For Q<0.005Å^{-1} one observes a Q^{-4} behavior. Quite surprisingly, no colloids are visible.

In figure 1 two scattering patterns are depicted showing the state of mioneralization before and after nearly 15 hours of $CaCO_3$ in an aqueous solution and in the presence of 49mg/cm^3 gold & DMAP and 2.5mg/cm^3 Ovalbumin at T=30°C. Already before the mineralization one observes scattering from thin (<10Å) rod-like particles indicated by the Q^{-1} power law at large Q. This means that the Ovalbumin already was denaturated probably from their interaction with the DMAP molecule.

After a 15h mineralization we observe the following: Again one observes a strong increase of large compact particles as concluded from the Porod constant. At large Q a Q^{-2} power law is observed which is related to thin platelet structure.

Figure 2 shows the time evolution of the mineralization process in more detail. On the left and right side the scattering patterns at large Q and the amplitudes P_1 and P_2 of the power laws are depicted, respectively. During the first 2.5 hours ones observes exclusively rods of nearly constant P_1, from 2.5 to 5.5 hours a gradual transition from rods to plates, and after that only plates with increasing volume fraction. The power laws are observed until the maximum Q of 0.08Å^{-1}, which means that the smaller distances of the rods and plates must be equal/less than 10Å. So, the mechanism of the mineralization seems to start at the rods and only grow in one direction. At the moment we do not understand this process.

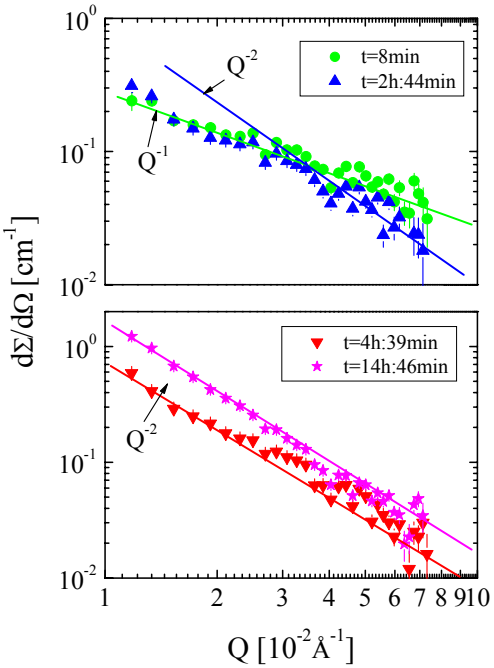

Figure 2: Links: Mineralisierung von $CaCO_3$ in Gegenwart von 49mg/cm^3 Gold &DMAP und 2.5mg/cm^3 Ovalbumin bei T=30°C. Man beobachtet gleich zu Beginn des Mineralisierungsprozesses dünne (<10Å) stäbchenförmige Teilchen, die nach knapp drei Stunden zu dünnen plättchenförmigen Strukturen (Q^{-2}) auswachsen. Im rechten Bild sind die entsprechenden Proportionalitätsgrößen P_1 und P_2 gegen Zeit aufgetragen. Zwischen 3 und 6 Stunden beobachtet man in dem gemessenen Q Fenster das Herauswachsen einer plattenförmigen Struktur aus Stäbchen und nach sechs Stunden ausschließlich platten-förmige Strukturen.

Institut für Festkörperforschung
Forschungszentrum Jülich GmbH
D-52425 Jülich

Experimental Report
of Neutron Scattering Experiments
at the FRJ-2 Reactor

Proposal number:	KW1-02-004 b		
Experiment title:	**Structure of Collagen in the Mineral Apatit - First SANS Experiments**		
Dates of experiment:	3.4. – 4.4. 2002	Date of report:	18.02.2003
Experimental team: Names	Addresses		
Frau Susanne Busch	Max-Planck-Institut für Chemische Physik fester Stoffe Nöthnitzer Strasse 40 D01187 Dresden		
Local Contact:	D. Schwahn		

Experimental report text body

These are first SANS test experiments in order to detect the organic collagen in the mineral apatit. Figure 1 shows two TEM micro graphs giving evidence of this organic structure.

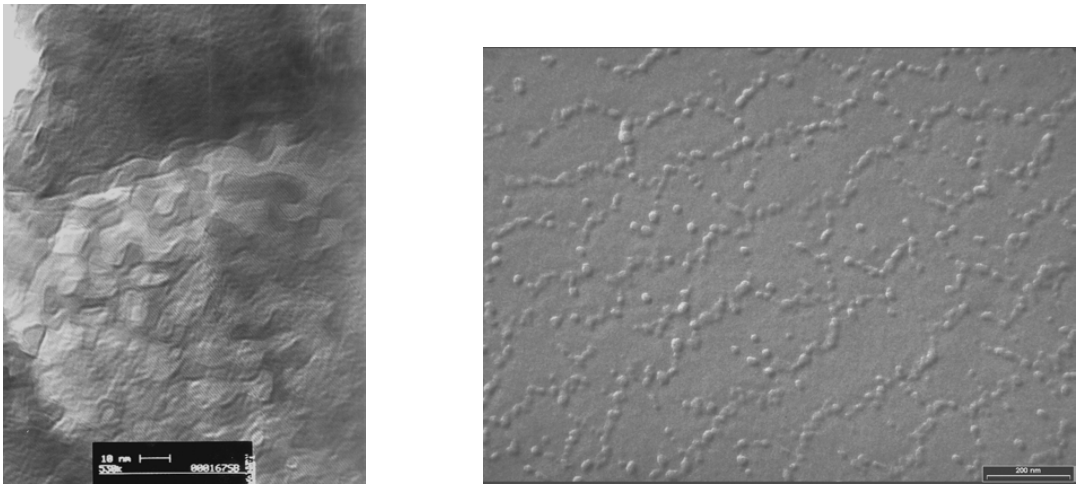

Figure 1: (left): TEM- micro graph of a fluorine apatit -collagen-composits; right: TEM-micrograph of a Pd/C-replica, of the organic component.

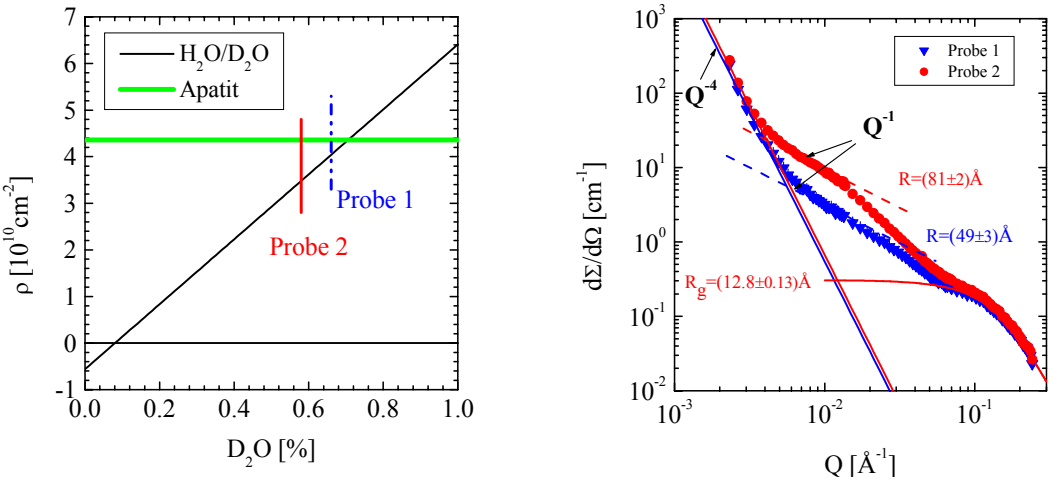

Figure 2: (left): coherent scattering length density ρ of apatit and D_2O/H_2O as a function of composition. (right): SANS scattering patterns of an apatit composite powder matched by two D_2O/H_2O mixtures of different composition as indicated.. Evaluations show that sample 1 has a smaller scattering contrast than sample 2 which becomes visible by the larger scattering of sample 2. At the intermediate Q scattering from rod-like structure with a diameter between 100 and 160Å which is quite consistent with the TEM results. At larger Q another type of particles with a diameter of 35Å becomes visible not seen with TEM.

A powder of an apatit composite was prepared in two different D_2O/H_2O mixtures. Sample 1 was better matched than sample 2. The scattering from sample 1 is therefore weaker. In both cases we observed scattering from three characteristically different particles. At small Q we observe the Q^{-4} power law of Porod's law. The scattering is probably caused by the surface of the apatit powder. At intermediate Q scattering from rod-like particles with diameter between 100 and 160Å becomes visible while at larger Q a further class of particles with a diameter of about 35Å. The comparison of SANS and TEM data show in both cases rod-like particles with comparable diameters and which represent the collagen matrix. The smaller particles could not yet be resolved from TEM.

Institut für Festkörperforschung
Forschungszentrum Jülich GmbH
D-52425 Jülich

Experimental Report
of Neutron Scattering Experiments
at the FRJ-2 Reactor

Proposal number:	KW1-02-005		
Experiment title:	**Reentrance phenomena in a ternary polymer blend dPB/PS/dPB-PS near the Lifshitz line**		
Dates of experiment:	25.01.02-28.01.02	Date of report:	19.02.03
Experimental team: Names	Addresses		
Vitaliy Pipich Dietmar Schwahn	IFF, FZ-Jülich, D-52425 Jülich		
Local Contact:	Dietmar Schwahn		

Experimental report text body

(Please use 12 pt letters here !)

Diblock copolymers dPB-PS act as surfactant in binary polymer blend PB/PS. Ternary polymer blends of two homopolymers with symmetric copolymers are ideal system for study of critical Lifshitz behavior. During this measurements two samples was studied by SANS: 6.6% and 7.5% of diblock copolymer content (B6.5 and B7.5). Sample B6.5 is at the left from the Lifshitz line, that means maximum of intensity of scattering cross-sections in disordered regime is at Q=0. On the other hand B7.5 sample is at the right from the Lifshitz line and scattering cross-sections have maximum at intermediate Q>0 range.

The neutron small angle diffraction experiments for B7.5 were performed at KWS1 facility in a Q range between $0.002<Q<0.04$ $Å^{-1}$ (20m and 8m detector position) in temperature range 160-33^{o}C. The data were corrected for scattering from empty cell and calibrated in absolute units by a Lupolen secondary standard. Above 90^{o}C scattering cross-sections have intermediate peak because homopolymers are locally ordered by diblockcopolymers. Due to fluctuation concentration below the Lifshitz line local order is disappearing and Q^{*} becomes 0. Below 60^{o}C ternary blend forms porous microemulsion structure with broad peak in low Q range and Q^{-4} dependence at high Q range.

Sample B6.5 demonstrates very interesting phenomena of reentrance criticality: above 80^{o}C and below 65^{o}C ternary blend is homogenous (reentrance one phase regime), and inside this temperature range sample demonstrates two phase demixing. Approaching to the Lifshitz line changes university class of critical behavior due to reducing the surface energy. No theoretical prediction of critical exponents near the Lifshitz line taking into account fluctuation of concentration is not available now. So SANS technique gives unique possibility to understand critical behavior near LL and to study approach to the double critical point for system in Lifshitz university class.

SANS measurements of B6.6 sample were performed at symmetric resolution conditions: 8m colimation and 8m detector distance near the upper critical point, and at asymmetric conditions neat lower critical point due to strong scattering: 20 m colimation and 8 m detector distance. Measurements were started at 160°C: sample was heated up to this temperature, stirred for homogeneity. Temperature stability of two heater thermostat in temperature range near critical point is 0.01K. Such high temperature stability allows to determine critical exponent near critical point very precisely. Scattering cross-sections were measurement in temperature range 160-79°C for 72 temperatures with step in temperature near the upper critical temperature 0.2K. At every temperature measurement was repeated 3 times to be sure then sample is in equilibrium.

Figure 1 shows the temperature dependence of the scattering cross-sections for B6.6 sample. At a first sight one can observe the strong increase of fluctuation concentration approach to the critical point. Analyze of data in Landau-Ginzburg approach shows strong Q^{-4} term in the structure factor. Existence of this term is consequence of non-Ising criticality near the Lifshitz line. Temperature dependence of the susceptibility for B3, B6.6 and B7.5% is shown at Figure 2. At the critical point the susceptibility S(0) diverges with scaling law $\tau^{-\gamma}$. Critical exponent of susceptibility are evaluated for above and below the double critical point.

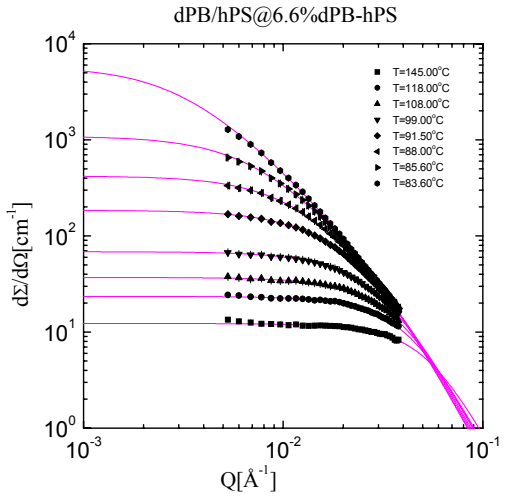

Fig. 1 – Scattering cross-sections from B6.6 above upper critical temperature.

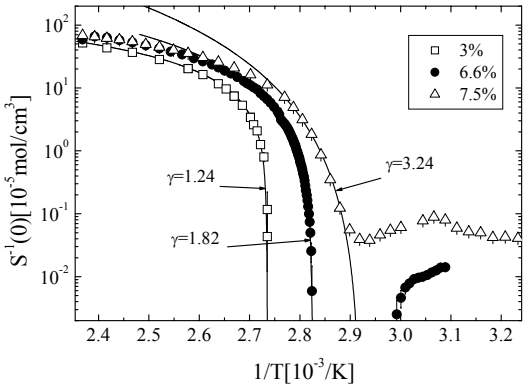

Fig. 2 – Data evaluated susceptibility of samples with 3%, 6.6% and 7.5% diblock content.

Institut für Festkörperforschung
Forschungszentrum Jülich GmbH
D-52425 Jülich

Experimental Report
of Neutron Scattering Experiments
at the FRJ-2 Reactor

Proposal number:	KW1-02-006		
Experiment title:	**Nucleation and crystal growth of calcium minerals in aqueous solution and at biomimetic interfaces; mineralization of $CaCO_3$ in the presence of malonic acid and gold& DMAP**		
Dates of experiment:	14.1. – 16.1. 2002 21.1 – 24.1. 2002	Date of report:	17.02.2003
Experimental team: Names	Addresses		
M. Balz, W. Tremel	Johannes Gutenberg-Universität Mainz Institut für Anorganische Chemie und Analytische Chemie Becher Weg 24 D55099 Mainz		
Local Contact:	D. Schwahn		

Experimental report text body

Mineralization of $CaCO_3$ in the Presence of Malonic Acid

The mineralization of $CaCO_3$ was studied in the presence of 1.3 mg/cm^3 malonic acid. The scattering patterns in figure 1 shows a Q^{-4} power law behavior over the whole Q-range for a time interval between 2 and 21 hours, as described by Porod's

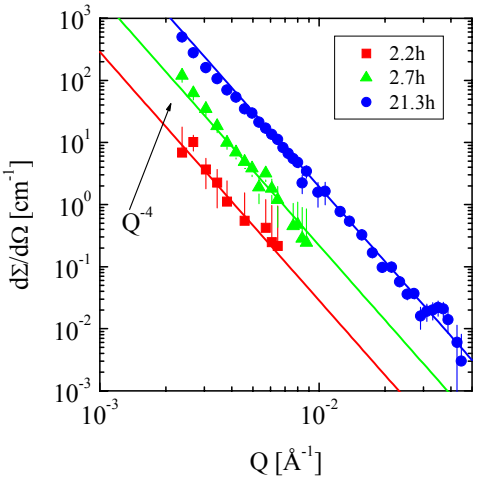

Figure 1: Mineralization of $CaCO_3$ in the presence of 1.3 mg/cm^3 malonic acid. After a time of mineralization of 2.2h the scattering patterns follow a Q^{-4} power law over the whole Q range. This means that large (> 1000Å) and compact minerals are formed.

law. In figures 2 the averaged intensity and the Porod constant has been depicted versus the time of mineralization. After an incubation time of slightly more than 2h a fast growth for nearly 2.5 h is observed which is then followed by a much slower growth rate. The dashed lines are a guide for the eye, their shape is described by a line first and then by a 2nd order power law. The same time behavior of both parameters shows

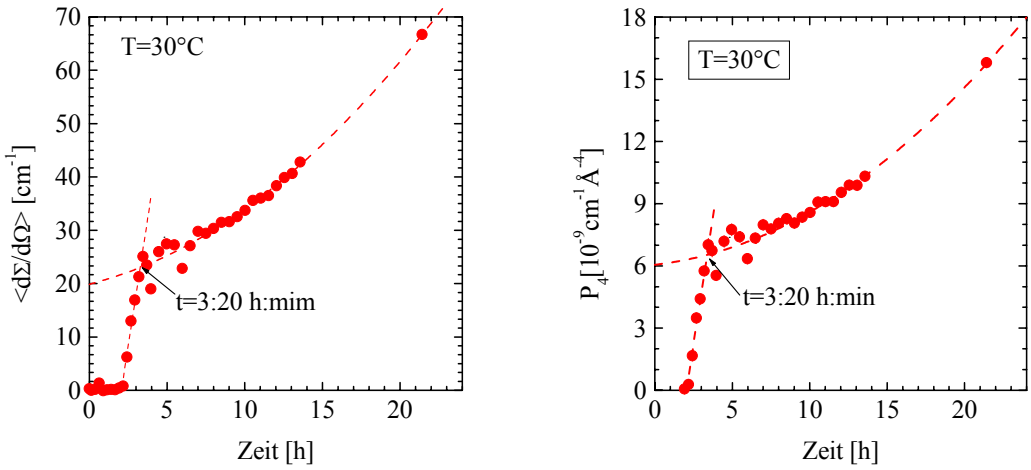

Figure 2: (left) over Q averaged intensity and (right) Porod's constant as a function of time. After an incubation time of slightly more than 2 hours a strong increase of intensity follows which after 3.33 hours increases more slowly but in a continuous manner. The dashed lines are a guide for the eye, their shape is described by a line first and then by a 2nd order power law. The same time behavior of both parameters shows that the scattering is solely determined from Porod's law. After an incubation time mineral particles larger than 1000Å are immediately formed. After 3.3 hours a strong change of the growth behavior is observed.

that the scattering is solely determined from Porod's law. So, after an incubation time mineral particles larger than 1000Å are immediately formed. After 3.3 hours a strong change to a much slower growth rate is observed. One

should mention here that the additive of malonic acid leads to large compact minerals quite in contrast to the homogeneous case described in the Proposal KW1-01-021. The observed changes of the growth rate is not yet understood. Probably is has to do with the amount of malonic acid.

Mineralization of $CaCO_3$ in the Presence of DMAP& Gold and Malonic Acid

Figure 3 shows the scattering patterns of start and end (14h) of the $CaCO_3$ mineralization in the presence of 49mg/cm^3 gold & DMAP and 1.3mg/cm^3 malonic acid at T=30°C. Only 5% of the gold colloids are visible, whose number density decreases only marginally during the process of 14h mineralization (see dashed lines).

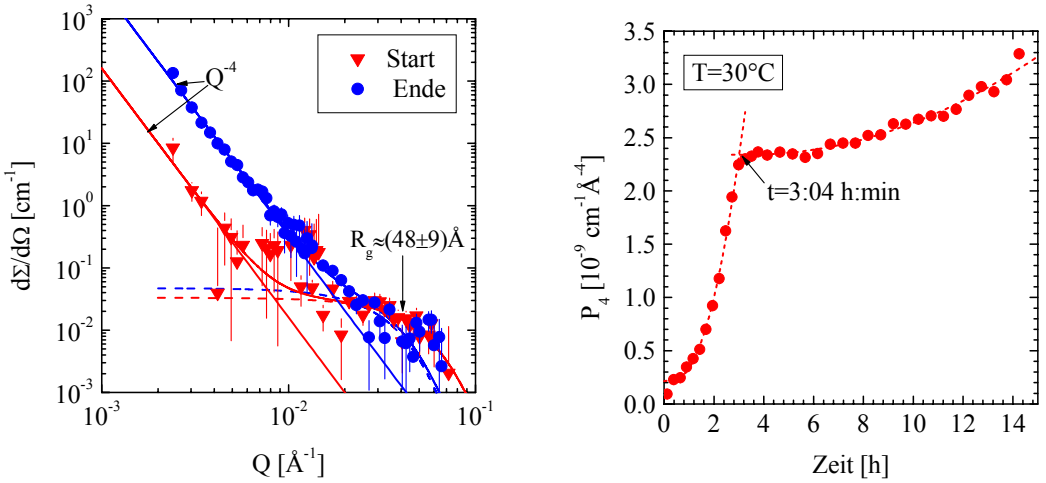

Figure 3: (left) Scattering patterns describing start and end (14h) of the mineralization of $CaCO_3$ in the presence of 49mg/cm^3 gold & DMAP and 1.3mg/cm^3 malonic acid at T=30°C. Only 5% of the gold colloids are visible, whose number density decreases only marginally during the process of 14h mineralization. Time evolution of the Porod constant in the right figure: P strongly increases during the first 3 hours and afterwards increases on a much slower rate. The shape of P_4 is very similar to the corresponding P_4 of the solution without colloids in figure 2. The size of P_4 and therefore the total surface of the $CaCO_3$ minerals is about 3 time less for the solution with the colloids in spite of the same concentration of malonic acid.

Time evolution of the Porod constant in the right figure: P_4 strongly increases during the first 3 hours and afterwards increases on a much slower rate. The shape of P_4 is very similar to the corresponding P_4 of the solution without colloids in figure 2. After about 3 hours the fast process is stopped and a transition to slower one is observed. On the other hand the size of P_4 and therefore the total surface of the $CaCO_3$ minerals increases from the beginning and the fast process has already been finished at a P_4=2.4 instead of 7 in units of 10^{-9} cm^{-1}Å^{-4}.

Institut für Festkörperforschung
Forschungszentrum Jülich GmbH
D-52425 Jülich

Experimental Report
of Neutron Scattering Experiments
at the FRJ-2 Reactor

Proposal number:	KW1-02-007		
Experiment title:	Charakterisierung von H/D-dotierten Metall/Oxid-Grenzflächen		
Dates of experiment:	19., 21. u. 23. Feb. 2002	Date of report:	16.09.2002
Experimental team: Names	Addresses		
C. Kluthe	Institut für Materialphysik Universität Göttingen Hospitalstr. 3-7 37073 Göttingen		
Local Contact:	Dr. Wim Pyckhout-Hintzen		

Experimental report text body

Die Absicht für unsere Messungen am KWS1 bestand darin, anhand des Modellsystems Cu_1At.%MgO herauszufinden, ob SANS benutzt werden kann um Information über die Segregation von Wasserstoff oder Deuterium an inneren Grenzflächen zu gewinnen.
Die SANS- Messungen der mit Wasserstoff, Deuterium und der H- freien Probe wurden alle an der gleichen Probe durchgeführt werden. Dies war erforderlich, um bei späterer Differenzbildung der zugehörigen Streuquerschnitte absolute Aussagen über den Einfluss des Wasserstoff auf $d\Sigma/d\Omega$ treffen zu können. Nur so wird gewährleistet, dass eine Änderung im Streuverhalten nicht durch Unterschiede in der Größenverteilung der Oxidteilchen unterschiedlicher Proben beeinflusst wird. Die Messung einer H- freien Cu- Probe mit MgO-Ausscheidungen zeigt im Bereich großer Q- Werte ein gutes Porod- Verhalten. Hieraus konnte die totale Grenzfläche der Oxidausscheidungen in der Cu- Probe zu $S = 2{,}32 \cdot 10^5$ cm^2/cm^3 bestimmt werden. Berücksichtigt man den Volumenbruchteil an MgO von $\nu = 0{,}02$ sowie die oktaedrische Form der Teilchen entspricht dies einem mittleren Teilchendurchmesser von $d = (8 \pm 1)$ nm.
Die Änderung in $d\Sigma/d\Omega$ durch H-Segregation an den Oxidteilchen lässt sich durch ein Kugel-Schale- Modell beschreiben. Der Normierte Streuquerschnitt einer Shell aus H oder D berechnet sich somit zu:

$$\left.\frac{d\Sigma}{d\Omega}\right|^{0}_{Shell\,H,D} = \frac{\left.\frac{d\Sigma}{d\Omega}\right|_{Kugel+Schale} - \left.\frac{d\Sigma}{d\Omega}\right|_{Kugel}}{\left.\frac{d\Sigma}{d\Omega}\right|_{Kugel}} = \frac{2\Delta\rho_3}{\Delta\rho_1}\frac{\delta R}{R} + \frac{\Delta\rho_3\left[\Delta\rho_3 \mp \Delta\rho_1\right]}{(\Delta\rho_1)^2} Q^2 \delta R^2 \quad , \qquad (1)$$

wobei $\Delta\rho_1 = -\ 0{,}57\cdot10^{12}$ cm^{-2} (Streukontrast: Ausscheidung – Matrix), δR die Dicke des segregierten Layers aus H oder D, R als Teilchenradius und $\Delta\rho_3$ als Streukontrast des Layers. $\Delta\rho_3$ und δR sind beide voneinander abhängig. Es ist daher geeigneter diese Parameter als Funktion der Belegungsdichte $\theta_H = \theta_D$ auszudrücken. Hierbei ist zu berücksichtigen, dass durch die Segregation von Wasserstoff an den Grenzflächen Kupfer-Atome mit Anteil θ_{Cu} von dieser verdrängt werden:

Für Wasserstoff: $\Delta\rho_3\cdot\delta R = \theta_H\cdot b_H - \theta_{Cu}\cdot b_{Cu}$ (b_H = -3,74 fm, b_{Cu} = 7,72 fm) (2)

Für Deuterium: $\Delta\rho_3\cdot\delta R = \theta_H\cdot b_D - \theta_{Cu}\cdot b_{Cu}$ (b_D = +6,67 fm, b_{Cu} = 7,72 fm) (3)

Für $\Theta_H \approx \Theta_{Cu}$ bedeutet dies eine geringe bzw. große Zunahme von $d\Sigma/d\Omega$ durch D bzw. H- Segregation an der M/O-Grenzfläche. Tatsächlich zeigten unsere Experimente eine Zunahme in $d\Sigma/d\Omega$ von 5% nach D-Beladung bzw. eine Zunahme von 12% nach H-Beladung der Probe. Zur Bestimmung von θ_H kann (1) für kleine Q somit umgeformt werden zu:

$$\left.\frac{d\Sigma}{d\Omega}\right|_{Shell\ H-D}^{0} \approx \frac{2\Theta_H\cdot(b_H - b_D)}{\Delta\rho_1\cdot R} \quad . \qquad (4)$$

Mittelung im Bereich 0,04 Å < q < 0,08 Å liefert $d\Sigma/d\Omega|_{Shell\_H\text{-}D} = (0{,}07 \pm 0{,}01)$. Nach (4) folgt somit für die H-Belegungsdichte: $\Theta_H = (8 \pm 3)\cdot10^{13}$ H/cm^2.

Man geht davon aus, das der Wasserstoff an der Grenzfläche durch Exzess- Sauerstoff gebunden wird. Die Belegungsdichte dieses überstöchiometrischen Sauerstoffs an den (111)-Grenzflächen des MgO entspricht etwa einer halben Monolage($\Theta_O = 6{,}5\cdot10^{14}$ O/cm^2). Nach dieser Vorstellung währen Werte mit $\Theta_H > \Theta_O$ nicht sinnvoll. Der bestimmte Wert der H-Belegungsdichte Θ_H beträgt ca. 12 % von Θ_O. Es besteht allerdings die Möglichkeit, das der Wert für Θ_H zu klein bestimmt wurde. Als mögliche Fehlerquellen unseres Experimentes müssen deshalb folgende Faktoren genannt werden:

(1) Durch die UHV- Glühung (bei T = 390°C) vor der H- Beladung der Proben ist ein Großteil des Exzess-O von den Grenzflächen desorbiert, was die Segregationsplätze des H reduziert.

(2) Das Deuterium konnte durch UHV- Glühung (bei T = 390°C) nicht vollständig von der M/O-Grenzfläche werden. Durch die anschließende Beladung mit H hat sich somit eine Mischung von segregierten D- und H-Atomen an der M/O- Grenzfläche eingestellt. Eine quantitative Auswertung nach Formel (2) wäre somit nicht korrekt.

Geht man davon aus, dass $\Theta_H = \Theta_{Cu}$ also, dass pro segregiertem H- Atom ein Cu- Atom von der Grenzfläche verdrängt wird, lässt sich die Belegungsdichte Θ_H auch ohne Verwendung der ev. fehlerbehafteten Streukurve der H- beladenen Probe bestimmen:

$$\left.\frac{d\Sigma}{d\Omega}\right|_{Shell\ D}^{0} = \frac{2\Theta_H\cdot(b_D - b_{Cu})}{\Delta\rho_1\cdot R} \qquad (5)$$

Mittelung im Bereich 0,04 Å < q < 0,08 Å liefert $d\Sigma/d\Omega|_{Shell\_D} = (0{,}05 \pm 0{,}01)$. Nach (5) ergibt dies somit eine H-Belegungsdichte von $\theta_H = (5 \pm 2)\cdot10^{14}$ cm^{-2}. Dieser Wert erscheint wesentlich realistischer als der nach Formel (4) bestimmte. Dies deutet darauf hin, dass das Deuterium durch UHV- Glühung nicht vollständig aus der Probe entfernt wurde. Durch die anschließende H- Beladung konnte sich somit nur eine Mischung segregierter D- und H- Atome an der M/O- Grenzfläche einstellen.

Institut für Festkörperforschung
Forschungszentrum Jülich GmbH
D-52425 Jülich

Experimental Report
of Neutron Scattering Experiments
at the FRJ-2 Reactor

Proposal number:	KW1–02-008		
Experiment title:	**Rodlike Aggregates formed by Poly-Para-Phenylenes in C_8E_4/Water Solution**		
Dates of experiment:	9.3-11.3.02	Date of report:	21.02.03
Experimental team: Names	Addresses		
Fuetterer, Tobias Hellweg, Thomas	TU Berlin, Stranski Laboratorium Sek. ER1, Ernst-Reuter-Haus Strasse des 17.Juni 112 D-10623 Berlin		
Local Contact:	Dr. W. Pyckhout-Hintzen		

Experimental report text body

Introduction:
In aqueous surfactant (C_8E_4) solutions the poly(paraphenylene) PPP-$C_{12}E_3$(12) forms elongated fiber aggregates with a contour length $L_c \approx 500$ nm and a diameter $d \approx 6$ nm in an excess of pure surfactant micelles (ref 1). As the polymer is insoluble in water in the absence of surfactant, it is inferred that these elongated structures represent composites of polymer and surfactant. Besides the particle shape characterization it is of interest to obtain information on the polymer-to-surfactant number ratio in these fiber aggregates. A SANS contrast-variation experiment can reveal information on this ratio. In the case of two different types of scattering particles the application of contrast-variation requires a sufficiently large difference in the scattering length density of the two different species contributing to the total scattering intensity. In neutron scattering experiments this is usually achieved by employing deuterated compounds. Hence, fully deuterated surfactant, d-C_8E_4, was used in the present study to generate the contrast difference between the micelles and fiber aggregates.
Furthermore, the deuterated surfactant micelles are nearly completely matched in pure D_2O, and the scattering intensity is due only to the fiber aggregates. The analysis of these data is presented in ref 2,3. In the following we focus on the contrast-variation experiments.

Experimental details:
We have measured 9 samples at 25°C with 2 wt % d-C_8E_4 and 0.2 wt % PPP in aqueous solutions with different H_2O/D_2O ratio covering a range of the mol fraction x_{D2O} from 0 to 1. And 1 sample with the pure d-C_8E_4 in D_2O. The wavelength was adjusted to 6 Å. For the detector-to-sample distances 1.25, 2, and 8 m were chosen. According to the institute standard procedure, the primary data were reduced and evaluated.

Results:

For given concentrations the total scattering intensity $I(q' = 0.1\ nm^{-1})$ of the fibers and the micelles is a function of the contrast $\Delta\sigma$, i.e. of the scattering length density of the solvent $\sigma_{solvent}(x_{D2O})$, and can be written as

$$I(x_{D_2O}) = \left(C_{Fib} \cdot \Delta\sigma^2_{Fib} \cdot P(q')_{Fib} + C_{Mic} \cdot \Delta\sigma^2_{Mic} \cdot P(q')_{Mic}\right) \cdot S(q')_{mix},$$

where x_{D2O} is the mole fraction of D_2O in the H_2O/D_2O solvent mixture, $\Delta\sigma = \sigma_{particle} - \sigma_{solvent}$, $C_{particle}$ is a concentration dependent factor, $P(q')_{particle}$ is the respective value of the form factor, and $S(q')_{mix}$ is the structure factor of the mixture (with the assumption that the particle interaction can be described by one structure factor $S(q')_{mix}$ for given concentrations c_{Fib} and c_{Mic}.). The scattering length density of the H_2O/D_2O solvent mixture can be calculated from the known mole fraction x_{D2O} and the scattering length densities of pure H_2O and D_2O. The scattering length density of the pure d-C_8E_4 micelles can also be calculated, and the x_{D2O}-independent factors $C_{particle}$, $P(q')_{particle}$, and $S(q')_{mix}$ can be condensed into a factor $C^*_{particle}$. The expression for $I(x_{D2O})$ then becomes

$$I(x_{D_2O}, q') = C^*_{Fib} \cdot (\sigma_{Fib} - \sigma_{solvent})^2 + C^*_{Mic} \cdot \Delta\sigma^2_{Mic}.$$

By fitting eq 15 to the scattering data for a wide mole fraction range x_{D2O} of the H_2O/D_2O solvent mixture, the parameters C^*_{Fib}, σ_{Fib}, and C^*_{Mic} can be determined. The result of such a fit is shown in Figure 1. It can be seen that the measured dependence of I on the contrast is described with good accuracy by this relation. The parameter C^*_{Mic} can be determined independently from the scattering intensity of d-C_8E_4 solutions in the absence of the polymer. On the assumption that $P(q')_{Mic}$ has the same value in the absence and presence of the polymer, and that $S(q')_{mix} \approx S(q')_{pure}$, the ratio of $C^*_{Mic,mix}$ to $C^*_{Mic,pure}$ yields the amount of dissolved surfactant which is incorporated in the fiber aggregates. From the data shown in Figure 10 and complementary data for d-C_8E_4 solutions without polymer, we derive a surfactant-to-polymer number ratio of 3 : 1, corresponding to a surfactant-to-polymer mass ratio of 1 : 4. However, the error limits of this determination are high, about 100%, due to the fact that only a small fraction of the surfactant is incorporated into the fiber aggregates. Accordingly, $C^*_{Mic,mix}$ and $C^*_{Mic,pure}$ differ by no more than 4% and the error in the determination of C^*_{Mic} is 2% (from the fit for $C^*_{Mic,mix}$ and from the measurement for $C^*_{Mic,pure}$).

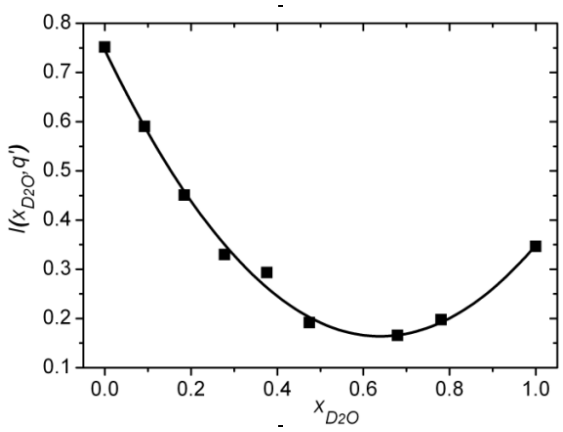

Figure 1. Total SANS intensity at q = 0.1 nm^{-1} as a function of the mole fraction x_{D2O} for a solution of 0.2 wt % PPP(12) and 2 wt % d-C_8E_4 in mixtures of H_2O and D_2O (symbols), and a fit according to eq 15 (line). The errors of I(q') are indicated by the size of the symbols.

References:

1. Fütterer, T.; Hellweg, T.; Findenegg, G. H.; Frahn, J.; Schlüter, A. D.; Böttcher, C. *Langmuir* **2003**, accepted, Intended Vol. *19*.
2. ACS book series *Mesoscale Phenomena in Fluid Systems*, Chapter: *Particle Characterization by Scattering Methods in Systems Containing Different Types of Aggregates*, in press.
3. Fütterer, T.; Hellweg, T.; Frahn, J.; Schlüter, A. D.; Findenegg, G. H., to be published.

Institut für Festkörperforschung
Forschungszentrum Jülich GmbH
D-52425 Jülich

Experimental Report
of Neutron Scattering Experiments
at the FRJ-2 Reactor

Proposal number:	KW1-02-009		
Experiment title:	Kinetics of nucleation of calcium carbonate		
Dates of experiment:	28. July - 01. February 2002 27. February - 02. March 2002	Date of report:	
Experimental team: Names	Addresses		
Hitoshi Endo Dietmar Schwahn	IFF, FZ-Juelich, D52425 Jülich IFF, FZ-Juelich, D52425 Jülich		
Local Contact:	Dietmar Schwahn		

Experimental report text body

We investigated calcium carbonate ($CaCO_3$) crystals which are influenced by double-hydrophilic block copolymer poly(ethylen glycol)-*block*-poly(methacrylic acid) (PEG-*b*-PMMA) with respect to their morphology and size [1].

We studied the kinetics of the reaction by means of time resolved SANS measurements, where a gas-liquid diffusion reaction was used to realize a slow reaction speed. We investigate the effect of the polymer concentration on the reaction through these experiments. To achieve a slow $CaCO_3$ crystallization, gas phase diffusion reaction, *i.e.*, ammonium-carbonate and aqueous solution with calcium ions and PEG-*b*-PMMA put together in a special chamber equipped with a thermostat, which was sealed from outer atmosphere. Ammonium-carbonate generates carbon dioxide gas in the chamber, and which very slowly reacts inside the aqueous solution. The obtained $CaCO_3$ particles were checked by optic microscopy, and the morphology for the time period of SANS experiments was identical as Ref. [1].

In Fig.1 the obtained SANS spectra with $CaCO_3$ contrast (the aqueous solution is H_2O) are shown. The sample was prepared with 0.1M $CaCl_2$ and 3wt% PEG-*b*-PMMA at 30°C and pH=7. Q^{-D} behavior was observed at the given reciprocal Q-range with 15 minutes time-resolution.

The curves were fitted with

$$I(Q) = A \cdot Q^{-D} + I_{incoh}$$

where A is a prefactor and I_{incoh} is a incoherent scattering intensity (constant). The obtained results of the time evolution of the index D in the equation are summed up in Fig. 2a, where the results of other PEG-*b*-PMMA concentrations are displayed together. At the lower polymer concentration, the index D immediately reaches

nearly 4, which is interfacial scattering (the Porod's low); on the other hand, at 3wt% of the polymer concentration, a gradual time-evolution from 2.5 to 4 is observed. Fig. 2b shows the mean intensity from the finite Q-range at 20m detector length. It is clear that higher concentration leads to a more rapid increase of intensity, and this is also a apparent evidence that the addition of the polymer strongly affects the reaction process.

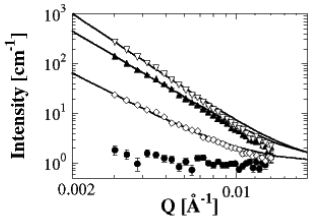

Figure 1
Time resolved SANS profiles at 20m detector length with 0.1M Ca^{2+} and 3wt% polymer concentration: after 0min (●), 60min (◇), 120min (▲), and 180min (▽), respectively. The corresponding fitting cureves are $D = 2.5$ for 60min, $D = 2.8$ for 120min, and $D = 3.2$ for 180min, respectively, with (13).

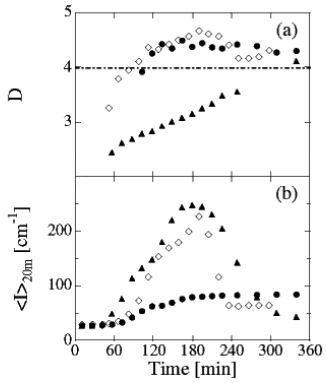

Figure 2
Effect of the polymer concentration on time evolution of (a) the index D in (13) and (b) the mean intensity at 20m detector length: 0.3wt% (■), 1wt% (◇) and 3wt% (△) respectively. Decreases of the intensities at the late reaction stage correspond to precipitation of $CaCO_3$ particles.

[1] H. Cölfen and L. Qi, *Chem. Eur. J.* 7, **106** (2001)

Institut für Festkörperforschung
Forschungszentrum Jülich GmbH
D-52425 Jülich

Experimental Report
of Neutron Scattering Experiments
at the FRJ-2 Reactor

Proposal number:	KW1-02-011		
Experiment title:	**Nucleation and crystal growth of calcium minerals in aqueous solution and at biomimetic interfaces; mineralization of $CaCO_3$ in the presence of the protein Ovalbumin**		
Dates of experiment:	25.2. – 27.1. 2002	Date of report:	17.02.2003
Experimental team: Names	Addresses		
M. Balz, W. Tremel	Johannes Gutenberg-Universität Mainz Institut für Anorganische Chemie und Analytische Chemie Becher Weg 24 D55099 Mainz		
Local Contact:	D. Schwahn		

Experimental report text body

We studied the mineralization of $CaCO_3$ in the presence of two concentrations (2.5 and 0.5 mg/cm^3) of the protein Ovalbumin. Figure 1 shows the scattering for the higher concentrated solvent at large Q during the first 3 hours. The scattering patterns of the first 1.5 hours can be described with Guinier's law. A radius of gyration of (22±0.8)Å is evaluated, which gives a radius of (28.6±1)Å for spherical particles. This number is in good

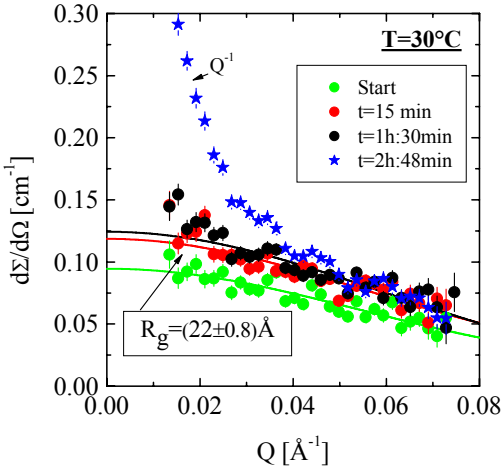

Figure 1: Scattering pattern from an aqueous solution of Ovalbumin during the first 3 hours of the mineralization process. During the first 1.5h the scattering is originated from globular structure with a radius of gyration which for spherical particles leads to a radius of R=(28.6±1)Å. This result is consistent with results given in literature. The increase of intensity is caused from an increase of the scattering contrast which might be originated from a complexation of Ca^{++} ions. After 1.5 hours the scattering behavior is changing. The scattering is continuously changing to a Q^{-1} behavior, which is observed in a "pure" form after nearly 3 hours. Such a scattering is caused from rod-like shape particles which a diameter less than 20Å. The time interval from 1.5 to 2:48 hours is correlated with the fast increase of the Porod constant in figure 3.

agreement with R≅25Å from X-ray measurements at the same protein. During the first 15 minutes the intensity is growing by about 20% relatively strong and followed by a relatively weak increase. During this period one observes a constant radius. After 1.5 hours a continuously transformation from a globular to a rod-like structure is observed which was finished after about 3 hours. The protein Ovalbumin changes its configuration;

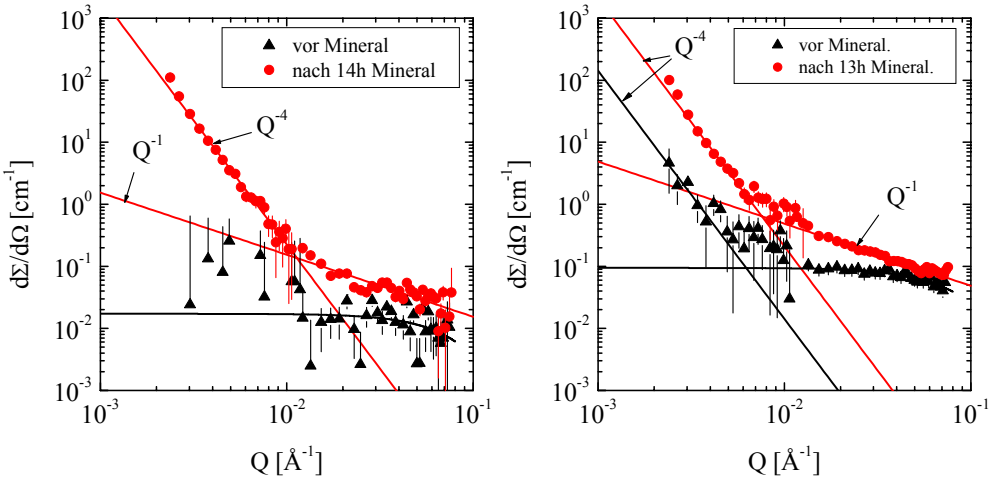

Figure 2: Scattering patterns before and after the mineralization of $CaCO_3$ in the presence of 0.5 mg/cm^3 (left) and 2.5 mg/cm^3 (right) malonic acid. Scattering is observed from the protein Ovalbumin before mineralization, while after a 13 respectively 14 hours duration of minelaization a Q^{-4} from large compact particles plus a Q^{-1} from rod-like structures of the denaturated Ovabumin becomes visible. These rods are extremely thin (<10Å), as no deviations are observed for Q larger than 0.08Å^{-1}.

probably, Ca^{2+} ions were absorbed by the protein leading to a larger scattering and finally to a denaturation, namely the defolding of a globular to a thin rod-like structure. Figure 2 shows the scattering the beginning and end of the mineralization of both samples. The Q^{-1} power law at large Q is clearly visible. At small Q the Q^{-4} behavior is an indication of large compact $CaCO_3$ particles. In figure 3 the Porod constants from these large particles have been depicted as a function of time for both samples. For the higher concentrated (2.5mg/cm^3) solvent of Ovalbumin three different processes are clearly distinguishable.

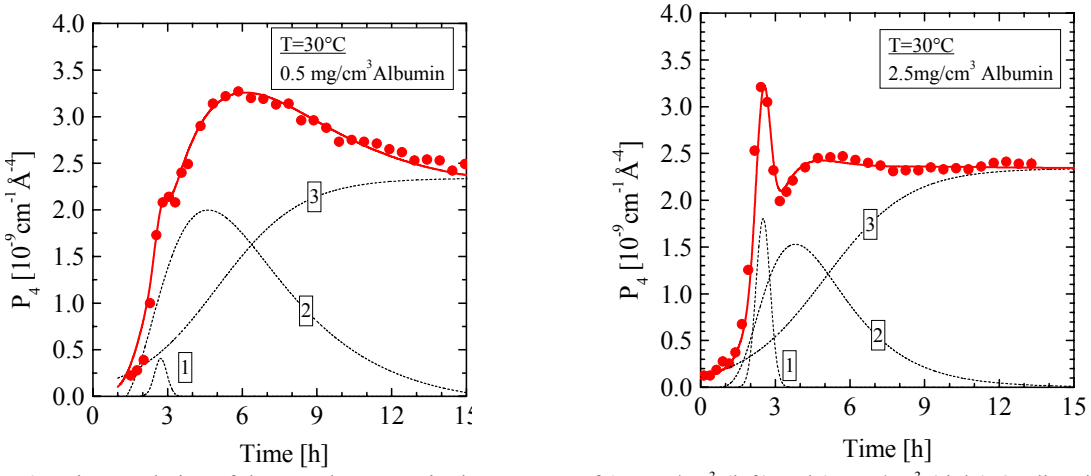

Figure 3: Time evolution of the Porod constant in the presence of 0.5 mg/cm^3 (left) and 2.5mg/cm^3 (right) Ovalbumin at T=30°C. Process "1" shows a relatively fast formation of particles, who after about 2.6 hours either dissolve or strongly coarsen into larger aggregates with the result of a decreasing total particle surface. Process "1" appears as a separate mineralization process strongly correlated with the concentration of Ovalbumin.

After about 1.5 hours the Porod constant strongly increases and shows after about 2.5 hours a pronounced peak maximum, decreases and increases again after 3 hours, approaches after 4 hours a weak maximum, in order to reach a constant number. The Ovalbumin solvent with the lower concentration of 0.5mg/cm^3 shows a qualitatively similar P_4. Again after 1.5 hours a strong increase is observed but with a weakly pronounced peak at about 2.5 hours and a further increase to new maximum at 6 hours. The three solid lines should demonstrate the time behavior of the single underlying processes. Process 3 is the same for both solvents while the amplitudes of the process 1 is proportional to the concentration of the Ovalbumin and Process 2 is about 30% weaker for the more concentrated solvent. In conclusion, a two-stage mineralization process is observed. The faster process "1" is correlated to the protein as it becomes active when the protein is unfolding.

Institut für Festkörperforschung
Forschungszentrum Jülich GmbH
D-52425 Jülich

Experimental Report
of Neutron Scattering Experiments
at the FRJ-2 Reactor

Proposal number:	KW1-02-012		
Experiment title:	**Study of microemulsion formation with temperature in block contrast.**		
Dates of experiment:	2.03.02-5.03.02	Date of report:	19.02.03
Experimental team: Names	Addresses		
Vitaliy Pipich Dietmar Schwahn Lutz Willner	IFF, FZ-Jülich, D-52425 Jülich		
Local Contact:	Dietmar Schwahn		

Experimental report text body

(Please use 12 pt letters here !)

We studied before microemultion channel of ternary polymer blend in bulk contrast: dPB/PS/dPB-PS, when homopolymers and one block in copolymers are visible by SANS. In order to understand role of diblock copolymers in this complex ternary system powerful matching instrument is suitable. The contrast between deuterated polybutadiene and deuterated polystyrene is vanishing small, therefor in ternary system dPB/dPS/dPS-PS only polystyrene blocks are visible for SANS. Three blends were explored by SANS: 7.4%, 7.9% and 8.6% of diblock content (C7.4, C7.9 and C8.6).

The neutron small angle diffraction experiments for were performed at KWS1 facility in a Q range between $0.002<Q<0.08 Å^{-1}$ (20m, 8m and 4m detector position) in temperature range 160-35^{o}C. Step in temperature is 10K above 100^{o}C and 5K below.

Figure 1 shows the temperature dependence of the scattering cross-sections for C8.6 sample. Above 90^{o}C the structure factor has maximum, and it disappears at the Lifshitz line because large scale fluctuation of concentration of homopolymers destroy near order of diblock copolymers. When temperature decrease from 90^{o}C to 85 ^{o}C forward scattering becomes by order of magnitude greater. Two possibility to describe it: diblock copolymers move to interface of fluctuation, or diblock copolymer prefer one type of fluctuation (polystyrene or polybutadiene). Q^{-2} dependence of scattering cross-section in low Q range says that interface (or film like) location of diblock more likely.

Simultaneously with strong increase of forward scattering and disappearing of peak Q^{-1} dependence at high Q range becomes clear. That means diblock copolymers are very stretched. Somewhere between 65^{o}C and 55^{o}C

Figure 2 demonstrates the temperature dependence of the scattering cross-section for C8.0 sample. Characteristic behavior of this sample stay the sampe as one of C8.6.

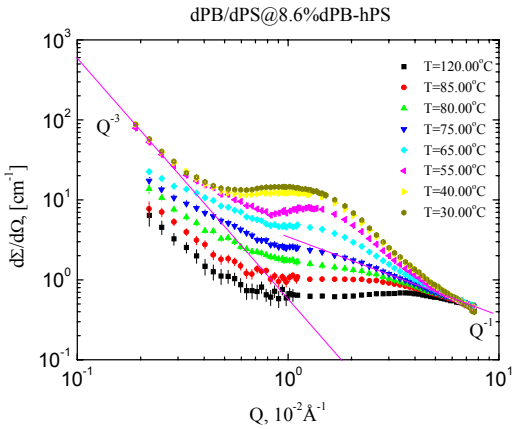

Fig. 1 – Scattering cross-sections from C8.6.

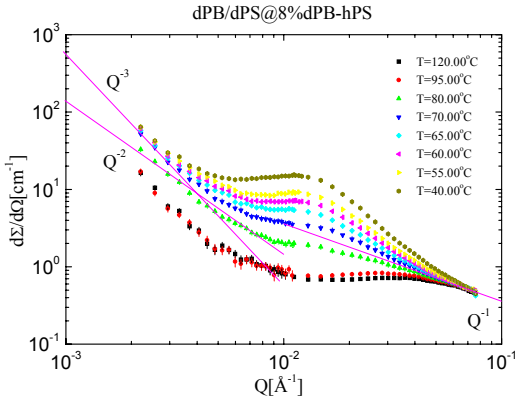

Fig. 2 – Scattering cross-sections from C8.0.

Institut für Festkörperforschung
Forschungszentrum Jülich GmbH
D-52425 Jülich

Experimental Report of Neutron Scattering Experiments at the FRJ-2 Reactor

Proposal number:	KW1-02-013		
Experiment title:	Comparative study of bone microstructure, and thickness dependence of the scattering patterns		
Dates of experiment:		Date of report:	27-03-2003
Experimental team: Names	Addresses		
A. Botti	INFM-Univ. Roma Tre, via della vasca navale, 84 00146 Roma (Italy)		
E. Bruner	Dip. Biologia Animale e dell'Uomo-Univ. La Sapienza, p.le A. Moro, 5 00185 Roma (Italy)		
G. Manzi	Dip. Biologia Animale e dell'Uomo-Univ. La Sapienza, p.le A. Moro, 5 00185 Roma (Italy)		
Local Contact:	Dr. Martine Heinrich		

Experimental report text body

The study of bone microstructure by small angle scattering is a relatively novel approach to find an answer to medical problems or in general to questions coming from the biological world. In these cases the osteological tissues are usually recent in time and do not show a relevant deterioration due to external agents such as cremation, bacterial action, or fossilization. On the other hand when the osteological tissues are ancient, the delicate task of reconstructing the evidence in an excavation site can take advantage from a quantitative, non–destructive way to correlate the microscopic structure of a bone to a species. Moreover the degree of fossilization as well as the type of fossilization could provide an extra parameter that can be used in the identification and linkage of the finds.
The measurements performed on KWS2 are the first attempt to extend on thicker samples the methodological approach used to analyse thin histological preparations.
Part of the samples were cut in series of growing thickness, to be compared with the original bone.
The samples were the cortical tissue of Homo sapiens and Bos taurus (fossil) cut in order to obtain flat fragments with Increasing thickness (d). From the averaged intensities of the 2D patterns it is possible to extract a measure, **T ,** of the smallest dimension of the hydroxyapaptite crystals and ξ, a parameter related to their shape and arrangement.

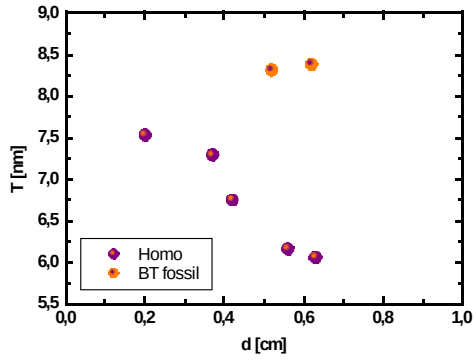

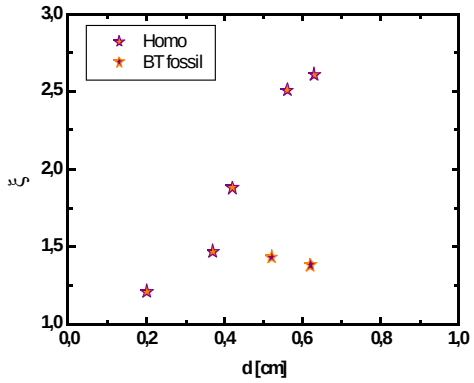

The increase of the thickness produces a decrease, possibly ascribable to multiple scattering, of **T** although the absolute values are affected by the uncertainties on the absolute calibration of the data.
The modest variation of d for the BT fossil, leaves T and ξ almost unchanged, but confirms the sensitivity of the approach also for fossilized thick samples.

Two long bones were measured: one (Homo sapiens) in the middle (thicker) and at the end (thinner), and the other one (Macaca) only in the middle. Choosing the thickness of Macaca bone as reference, in the direction parallel to bone axis it is possible to see a peak at about 0.01 $Å^{-1}$, which intensity increases with decreasing d. The Macaca peak is much higher than that extrapolated for Homo sapiens, suggesting the existence of a quantity which differs from species to species. In the direction perpendicular to the bone axis there is no evidence of peaks.
Both in the perpendicular and parallel direction the q^{-4} high q dependence is lost, for samples showing the peak at 0.01 $Å^{-1}$ in the 2D pattern.

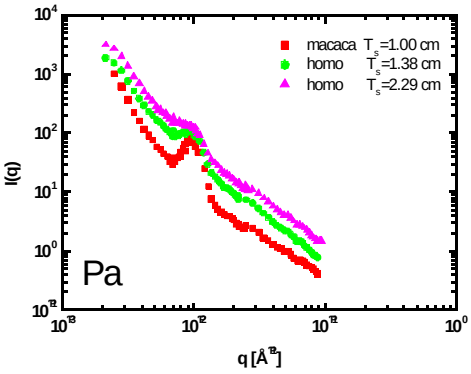

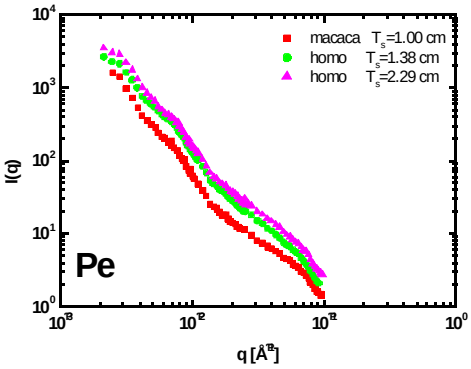

Institut für Festkörperforschung
Forschungszentrum Jülich GmbH
D-52425 Jülich

Experimental Report of Neutron Scattering Experiments at the FRJ-2 Reactor

Proposal number:	KW1-02-014		
Experiment title:	Characterisation of ancient pottery (VI-VIII century a. C.) from Rome, Miseno and Cuma (Italy).		
Dates of experiment:		Date of report:	06-03-2003
Experimental team: Names	Addresses		
Armida Sodo Alberto Botti	UdR INFM -Dip. di Fisica, Università dell'Aquila, Via Vetoio 67010 Coppito, L'Aquila, Italy UdR INFM -Dipartimento di Fisica "Amaldi", Università Roma Tre, Via della Vasca Navale, 84, 00146 Roma, Italy		
Local Contact:	Martine Heinrich		

Experimental report text body

The aim of this project was to characterise the ceramic production developed in the south of Italy during the V - XII century, selecting, as a first step, two different production classes: the "broad-line ceramic" and the transport amphorae.
The "broad line ceramic" represents an evolution of the common decorated ceramic of the late Roman age. The name comes from the decoration elements that were made by rags or paint brush. The interest in these medieval productions is based on the possibility of improving our knowledge on the commercial fluxes and the large-scale retail. This understanding could fill the lack of information on the trade routes between the factories and the end markets. Samples coming from Misenum (Naples), Cuma (Naples) and Rome have been investigated.
The Q range spanned from $1x10^{-1}$ Å^{-1} to $2x10^{-3}$ Å^{-1}. To avoid as much as possible multiple scattering effects, we chose λ=7.3 Å. The data could be referred to a fractal structure, and they have been fitted with a Beaucage empirical function, consisting in a power law and a Guinier-like function for the low-q range. In the following figure we report a typical data-set and the corresponding best fit.

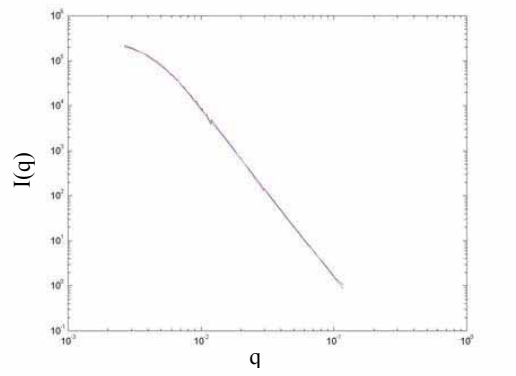

Because of the big uncertainties in the thickness and in the composition of the samples, the data were not absolutely calibrated and the prefactor of the Beaucage function was not considered as a useful parameter.

The same procedure has been applied to all the samples in order to obtain the radius of gyration (R_G) and the slope, or fractal dimension (d) for each of them.
The collected parameters were grouped in categories according the provenance and the age, while all different typology (e.g. amphorae, crockery and kiln wastes) have been gathered to increase the number of samples for each category.
The figures below report a possible trend of the sampled parameters as a function of the age.

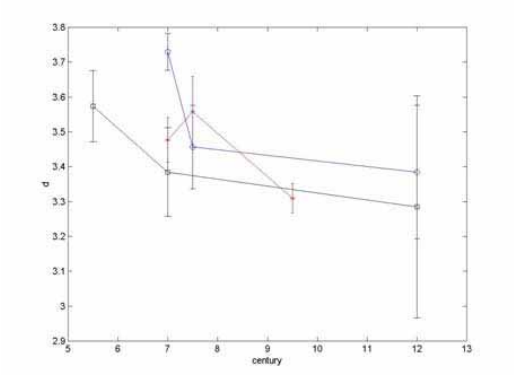

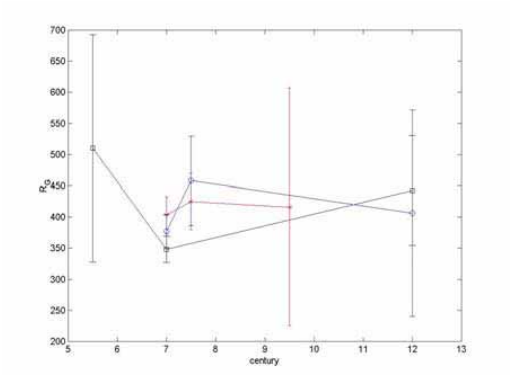

Although the error bars and the small number of the points force to inteprete the results with the due caution, it is possible to see a decrease of the value of the slope *d* depending on the century of production. Contrary, the size of the microscopic structures (e.g. pores or aggregates) presented in the samples seems not to vary significatively on the time.
For a correct and more sound interpretation of the data, and in order to correlate the microscopical features of earthwares to the production processes, it is necessary to perfom measurements on laboratory samples with defined and well known composition, thickness and cooking temperatures. A bigger and more differentiated collection of samples is also needed.
This will be certainly the object of future experiements.

Institut für Festkörperforschung
Forschungszentrum Jülich GmbH
D-52425 Jülich

Experimental Report
of Neutron Scattering Experiments
at the FRJ-2 Reactor

Proposal number:	KW1-02-015		
Experiment title:	Structure factor of partially deuterated PE-melt (II)		
Dates of experiment:	13.6-16.6.2002	Date of report:	6.3.2003
Experimental team: Names	Addresses		
H. Frielinghaus M. Zamponi	IFF, FZ Jülich IFF, FZ Jülich		
Local Contact:	H.Frielinghaus		

Experimental report text body

(Please use 12 pt letters here !)

A previous small angle scattering experiment on a 4k(d)-4k(h)-4k(d)-PE sample (see KW1-01-039) revealed a distinctive deviation from the expectation of the random phase approximation (RPA). To further investigate the discrepancy, additional measurements on 4k(d)-17k(h)-4k(d)-PE and 4k(h)-4k(d)-4k(h)-PE sample have been done. These samples are also used for neutron spin echo spectroscopy, where they are measured at a temperature of 509K.

At KWS2 measurements on 4 different samples with d-h-d resp. h-d-h labeling at two different temperatures (453K and 509K) have been performed. The experiments were done at a wavelength of 6Å, covering a q-range from 0.01Å^{-1} to 0.2Å^{-1}. Data were corrected for background and calibrated.

In fig.1 the structure factor for two 4k(d)-17k(h)-4k(d)-PE samples are shown. One sample consisted of the pure dhd-triblock, the second was a 20% mixture of the triblock in a corresponding 25k-d-PE matrix (as used for NSE). The data follow the RPA-prediction qualitatively, but again quantitative a distinctive deviation from the prediction can be observed at low q. The lines show the RPA expectation, where the unknown incoherent background is fitted.

A newly prepared 4k(d)-4k(h)-4k(d)-PE sample (100%) was remeasured. The data are comparable to the previous KWS1 experiment, the observed discrepancy persist. Now also a 4k(h)-4k(d)-4k(h)-PE sample (100%) was measured, which should display, after Babinet's theorem, the same scattering pattern as the dhd-sample, except for the different incoherent background level. As can be seen in fig. 2 this is not fulfilled. The structure factor of the hdh-sample correspond at low q not to the dhd-sample, it differs even more from the RPA-prediction. At low q there seems to be an additional contribution to the scattering spectrum.

All samples were first measured at a lower temperature of 453K, to see if deviations occur from chemical modifications due to the high temperature. As can be seen in fig. 3 and 4, there is no significant difference between the two measurements at different temperatures, the samples are all thermal stable.

The reason for the deviation at low q is still not clear, polydispersity might contribute to this effect. The q-range where the difference occur is not reached with NSE spectroscopy so that these spectra should not be falsified.

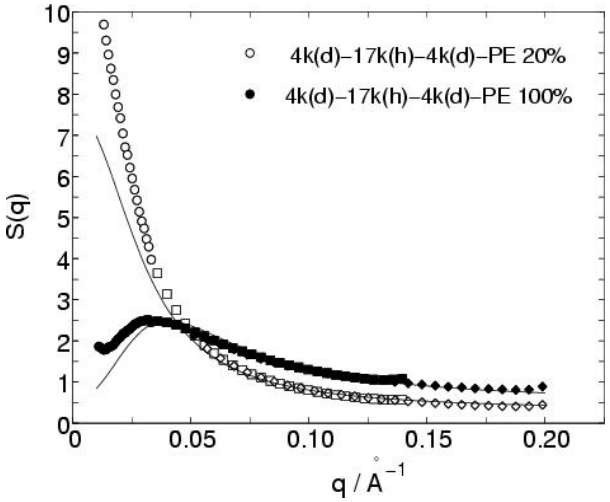

Fig. 1: Open symbols: 20% dhd-25k-PE, closed symbols: 100% dhd-25k-PE, lines: RPA, background fitted, T=509K.

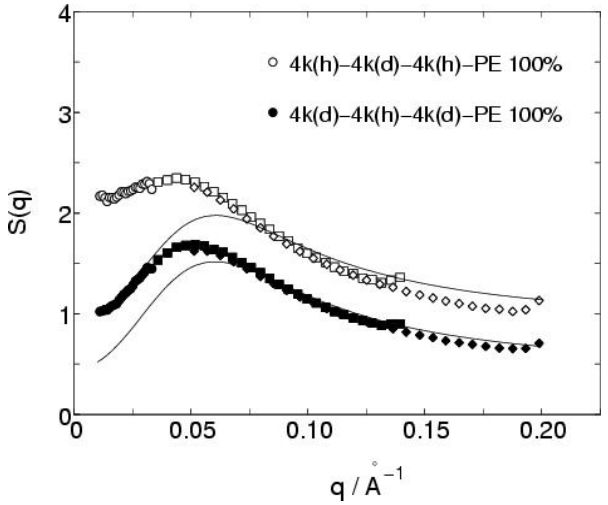

Fig. 2: Open symbols: 100% hdh-12k-PE, closed symbols: 100% dhd-12k-PE, lines: RPA, background fitted, T=509K.

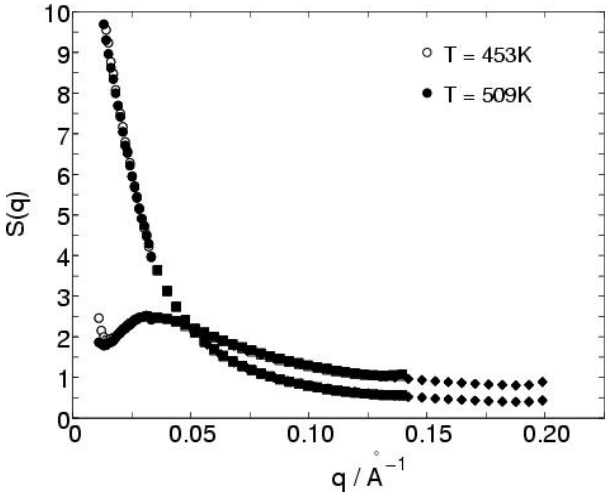

Fig. 3: Samples as in fig.1, for two different temperatures.

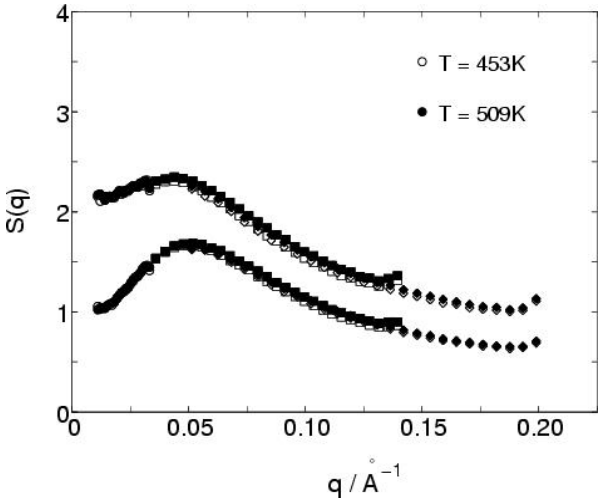

Fig. 4: Samples as in fig. 2, for two different temperatures.

Institut für Festkörperforschung
Forschungszentrum Jülich GmbH
D-52425 Jülich

Experimental Report
of Neutron Scattering Experiments
at the FRJ-2 Reactor

Proposal number:	KW1-02-016		
Experiment title:	**Texture and morphology of stones of archeological interest**		
Dates of experiment:	June 29-July 2 2002	Date of report:	February 25, 2003
Experimental team: Names	Addresses		
Fabrizio Lo Celso Roberto Triolo Alessandro Triolo	Dipartimento di Chimica Fisica "F. Accascina" Università degli Studi di Palermo viale delle Scienze, Parco d'Orleans II 90128, Palermo, Italy Istituto Processi Chimico-Fisici, Sezione di Messina - CNR Via La Farina 237, 98123 MESSINA, Italy		
Local Contact:	D. Schwahn, H. Frielinghaus		

Experimental report text body

Among the natural composites, there is a wide variety of stones used in buildings, monuments, statues and other objects of archaeological or cultural heritage interest. Sandstone, Limestone, Granite and Marble are the most common stones used for these purposes. Marbles may look very different as far as texture, color, mechanical and physical properties are concerned, mainly as consequence of their "formation history". Their morphology, in fact, is the result of the many small natural events occurring close to one another in time and in space and of a few large changes occurring in the same temporal or spatial region. The provenance of stone objects is of key importance to archaeology in so far as artistic, technological or commercial exchange patterns may be studied and correlated to historical events and social contacts between cultures. Among these, marble objects, white marble in particular, are considered the most valuable. Authentication of works of art in museums is also of great concern. Marble in general has similar physical and chemical properties. Although much has been accomplished in quantifying rock and mineral chemistry, grain size and trace elements, little effort has been made to quantify texture. One may expect that marbles with different geological history should show different texture and consequently different fractal properties. Although this does not describe the mechanism that produces the fractal scaling, it nonetheless helps sort out the description and analysis of crystal distributions, crystal morphology, crystal faces, crystal intergrowth, and zoning, all of them essential in characterising (fingerprinting) the material utilising a variety of analytical techniques. Neutron scattering is a most appropriate technique for measuring volume fractal properties because of a unique advantageous feature of the neutron-matter interaction: the high penetrability of neutrons. Complex natural composite materials like rocks are seen by neutrons as two-phase systems with a density contrast characteristic of an overall, average texture "signature". By combining Ultra and Small Angle Neutron Scattering data (USANS and SANS), it is possible to span 5 to 6 decades in momentum transfer, Q (length scale 100 microns to 10 nm), thus making it possible to probe the fractal nature of stones in an unambiguous way.

SANS measurements were performed at the KWSII instrument of the neutron scattering facility of Forschungszentrum Jülich (Germany). USANS experiments were performed at the neutron optical bench instrument S18 installed at the 58 MW high flux reactor at the Institut Laue-Langevin (Grenoble, France).

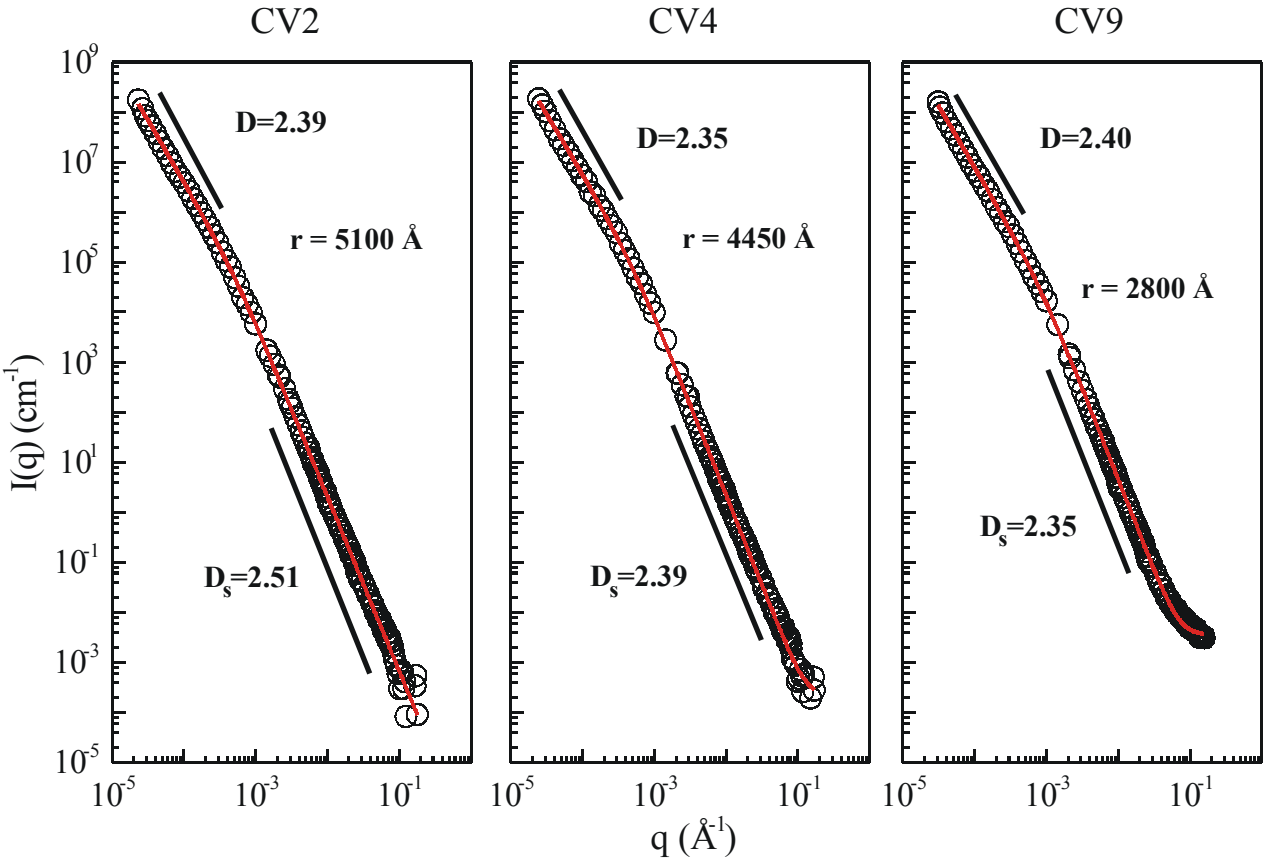

Figure 1. Combined USANS-SANS data (circles) and fit to the eq. 1 (solid line) for samples CV (Ornavasso, Piemonte Italy).

Figure 1 shows the combined USANS/SANS patterns for three different samples coming from the same location. Measurements performed have involved marbles coming from many different Italian and European sites. The scattering curve is matematically described by a hierachical model for a fractal aggregate, of radius **R**, formed by monodispersed primary particles of radius **r**. At very low q values the intensity is high and constant (the system cannot be resolved). For larger values of q the intensity drops (1/R) because aggregates of primary particles are being resolved, indeed it follows a power law characterized by the exponent **D** that indicates the fractal dimension or, in other words, the branching of the aggregate. Going towards larger q values it is possible to evaluate the radius **r** of the primary particles and then the intensity follows a power law with exponent **6-Ds**. **Ds** is related to the surface structure of the primary particles and its value must be between 2 and 3 (**Ds** = 2 is for smooth particles). The scattering intensity is expressed as follows:

$$\mathbf{I(q) \propto P(q,r,Ds)\cdot S(q,r,D,R)} \qquad (1)$$

$$\mathbf{P(q,r,Ds)} = \left(1+\frac{\sqrt{2}}{3}q^2r^2\right)^{\frac{Ds-6}{2}} \text{ and } \mathbf{S(q,r,D,R)} = 1+\frac{D\Gamma(D-1)}{qr^D}\left(1+\frac{1}{qR^2}\right)^{\frac{1-D}{2}}\sin\left[(D-1)\arctan(qR)\right]$$

Institut für Festkörperforschung
Forschungszentrum Jülich GmbH
D-52425 Jülich

Experimental Report
of Neutron Scattering Experiments
at the FRJ-2 Reactor

Proposal number:	KW1-02-017		
Experiment title:	**Mixtures of reverse pluronic copolymer and surfactants as controlled release drug delivery systems**		
Dates of experiment:	27.06.02 - 29.06.02	Date of report:	10.03.03
Experimental team: Names	Addresses		
Triolo, Roberto Lo Celso, Fabrizio Luigi Paduano	Dipartimento di Chimica Fisica Università degli Studi di Palermo viale delle Scienze, Parco d'Orleans II 90128, Palermo, Italy Chemistry Department University of Naples "Federico II" via Cinthia 80126 Napoli, Italy		
Local Contact:	H. Frielinghaus		

Experimental report text body

Hydrogels find increasing applications in controlled-release drug delivery systems such as transdermal patches and are useful as liquid formulations in oral and topical administration. [1,2] Gels are usually made with polymer that undergo a high degree of cross-linking upon increasing their concentration.[3] Active pharmaceutical substances are usually incorporated within the polymer matrix.[4] These formulations may contain some additives such as surfactants, that by increasing the extension of the hydrophobic domains in the system, allow a larger dissolution of hydrophobic drug compound. [5] Pluronic copolymers because of their low cost, biocompatibility and their chemical versatility, seem to be very suited for this purpose. In fact some of them (Pluronic® F-127 in combination with lecithin and isopropyl palmitate, named PLO gel) have been already used successfully as gelling agents. [6]

The aim of the project is addressed towards the structural investigation, by means of Small Angle Neutron Scattering (SANS) of a series of solutions of R-Pluronics ((PPO)n(PEO)m(PPO)n triblocks) with the purpose of tackling the following topics:
a) the influence of the Hydrophylic-Lipophylic Balance (HLB) in the copolymer is studied in binary water-Pluronic R systems in selected points of the T,C phase diagram. These investigation should lead to gain structural information on the agrregates and superaggregates that can be obtained.
b) the addition of surfactants of different nature (non-ionic and anionic, for example Pentaethylene glycol dodecyl ether, Sodium decylsulfate) to the aqueous Pluronic R systems should lead to the formation of a variety of aggregates and super aggregates with pluronic copolymers with structure and hydrohobicity that can be, in principle, modulated at will. [7] The final formulation should be formed by domains of different nature that should be suitable to host active principle of different nature.

SANS measurements performed at the "Forschungszentrum Jülich" have given a better understanding on a wide variety of structures in aqueous solution of the commercial polymer Pluronic 25R4 [8]. Different temperature and polymer concentration conditions have been investigated in order to estimate structural parameters of aggregates and superaggregates. Prelimary analisys have shown that at low concentration and temperature the polymer is basically dissolved as random coil. By increasing the concentration micellar like cluster are formed and solutions become turbid up to 30% wt. Above this concentration clear solution are obtained and the system is mainly formed by micelle network whose cores are constituted by the PPO tails while PEO chain bridges across different micelles. In the concentration range between 30 and 50% wt. a sticky hard spheres model has been successfully used to fit the experimental data. Raising the temperature in the intermediate concentration range leads to the formation of a more ordered system. A strong correlation peak is indeed observed and the above mentionned model still apply. Previous time resolved X-rays measurement are in agreement with the fact that ordered phase are formed as temperature increases. For temperatures higher than 60 °C lamellar phase occurs for polymer concentration above 30% wt. Furthermore when the concentration is the range of 50% wt. (40 °C) the cilyndrical hexagonal phase appears. Finally preliminary SANS measurements have been able to show an interaction between the polymer and the anionic surfactant, sodium decyl sulfate well below the critical micellar concentration of the surfactant. In particular the shape of the collected scattering profiles have suggested the presence of mixed micelles formed by the polymer and the surfactant even at quite low concentration of the solutes in the system. This a promising result for the aim of this research.

References

1) Peppas, N. A., Bures, P., Leobandung, W., Ichikawa, H. *Eur. J. Pharm. Biopharm.* (2000), 50(1), 27-46.
2) Bouhadir, K. H., Alsberg, E., Mooney, D. J. *Biomaterials* (2001), 22(19), 2625-2633.
3) S. H. Gehrke "Synthesis and Properties of Hydrogels Used for Drug Delivery," Transport in Pharmaceutical Sciences, G. Amidon and P.I. Lee, Eds., Marcel Dekker, New York, in press (1999).
4) Risbud, M. V., Hardikar, A. A., Bhat, S. V.; Bhonde, R. R. *J. Controlled Release* (2000), 68(1), 23-30.
5) Jeong, B., Choi, Y. K., Bae, Y. H.; Zentner, G., Kim, S. W. *J. Controlled Release* (1999), 62(1-2), 109-114.
[6] Morishita, M., Barichello, J. M., Takayama, K., Chiba, Y., Tokiwa, S., Nagai, T. *Int. J. Pharm.* (2001), 212(2), 289-293.
[7] Ashbaugh, Henry S., Piculell, Lennart, Lindman, Bjoern. *Langmuir* (2000), 16(6), 2529-2538.
[8] www.basf.com, Mortensen, K., *Macromolecules*; **1997**; *30*(3); 503-507

Institut für Festkörperforschung
Forschungszentrum Jülich GmbH
D-52425 Jülich

Experimental Report
of Neutron Scattering Experiments
at the FRJ-2 Reactor

Proposal number:	KW1-02-018		
Experiment title:	**Fractal patterns in biogenic platforms: the case of reefs built by *Dendropoma patraeum***		
Dates of experiment:	June 25-29 2002	Date of report:	February 25, 2003
Experimental team: Names	Addresses		
Fabrizio Lo Celso Roberto Triolo Alessandro Triolo	Dipartimento di Chimica Fisica "F. Accascina" Università degli Studi di Palermo viale delle Scienze, Parco d'Orleans II 90128, Palermo, Italy Istituto Processi Chimico-Fisici, Sezione di Messina - CNR Via La Farina 237, 98123 MESSINA, Italy		
Local Contact:	D. Schwahn, H. Frielinghaus, E. Kentzinger		

Experimental report text body

A typical feature of many tropical and temperate rocky shores is the development of biogenic platforms at tide level resulting from a massive overgrowth of the cylindrical shells of vermetid gastropods. In the Mediterranean area, the vermetid gastropod Dendropoma petraeum is the dominant reef building species along the lower midlittoral fringe. Preliminary observations on macroscopic samples suggested that vermetid growth follow a fractal pattern. The aim of the experiment is to investigate samples of the biogenic platforms coming from different zones. Indeed their growth mechanism, and therefore their structure, could be influenced by the different tidal impact on the reef. In order to reveal the fractal nature of the vermetid formations at mesoscopic and microscopic level, and to study how the different natural conditions may influence their growth, Small and Ultra Small Angle Neutron Scattering (SANS and USANS) seem to be the most appropriate techniques.
SANS and USANS measurements have been performed on a series of samples coming from different locations along the shoreline near Palermo (Sicily, Italy). Preliminary investigation by means of X rays diffraction and scanning electron microscopy have shown that vermetid shells are mainly constituted by calcium carbonate in the form of aragonite. Experimental data concerning both solid sample and powders have shown a power law dependence, indicating a porous structure. Samples are probably constituted by fractal aggregates at different length scales or, in other words, a network of fractal clusters formed by solid primary particles with a rough surface. Experiments have been also performed doing contrast matching of the solid matrix (calcium carbonate) with a mixture of D_2O and H_2O in order to obtain structural information on the porosity of the wet sample. When a solvent partially fills a pore network then scattering from the part of the network filled by the liquid is negligible and only the scattering from the porosity that is effectively close to the liquid will be measured. One contrast matching condition (D_2O/H_2O 70% vol.) has been measured and a network of fractal clusters has been observed (see fig.1) in the combined USANS/SANS pattern. Preliminary data treatment has been made by using a linear combination of two mass fractal terms.

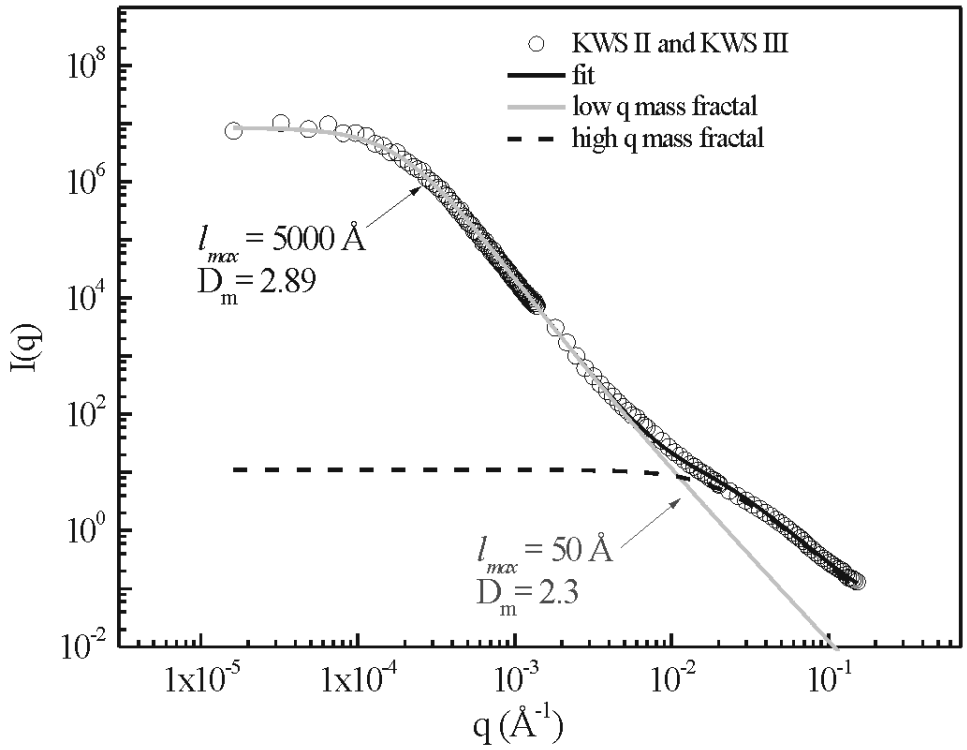

Figure 1

The scattering equation for mass fractals being:
$I(q)=q^{-1}\,\Gamma(\beta)\,l_{max}^{\beta}\,[1+(ql_{max})^2]^{-\beta/2}\sin[\beta \arctan(ql_{max})]$
where l_{max} is the upper cutoff limit, D_m is the mass fractal dimension and $\beta = D_m - 1$.

Institut für Festkörperforschung
Forschungszentrum Jülich GmbH
D-52425 Jülich

Experimental Report of Neutron Scattering Experiments at the FRJ-2 Reactor

Proposal number:	KW1-02-020		
Experiment title:	**Phase transformation of anatase TiO_2 induced by lithium intercalation**		
Dates of experiment:	7.05. – 8.05. 2002	Date of report:	17.03.2003
Experimental team: Names	Addresses		
Ad van Well M. Wagemaker	IRI, TU Delft, Mekelweg 15, 2629 JB Delft, Netherland IRI		
Local Contact:	D. Schwahn		

Experimental report text body

Samples
Li_xTiO_2 in hexane
aim: d/h hexane mixture, contrast matched with TiO_2
in practice:
- not sure about exact matching
- 2 of the 4 samples were dry (hexane evaporated)

sample 1: x = 0.35, dry
sample 2: x = 0.12, dry
sample 3: x = 0.07, wet
sample 4: x = 0.25, wet

Results

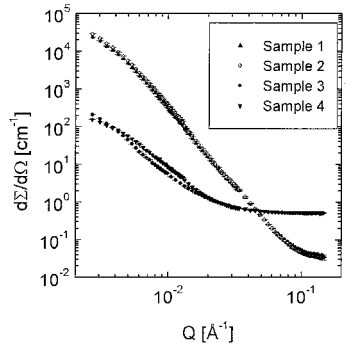

Fig 1 Corrected and normalised KWS1-data

Sample 1 and 2 in large Q-range more or less proportional to Q^{-4}
Sample 3 and 4 in large Q-range more or less proportional to Q^{-3}

Fits by Richard Heenan ('FISH')

Model:

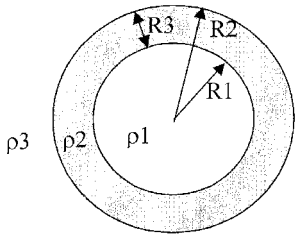

- Polydisperse spherical particles, radius R2, with log-normal distribution, with shell of constant thickness R3
- Interference modelled by hard-sphere S(Q)

Results:

		SAM1	SAM3 par. SAM1	SAM3 other minimum	SAM3 exact match	SAM4 par. SAM1	SAM4 'stronger S(Q)'
contrast							
ρ1-ρ2	10^{-4} nm^{-2}	0	0.33	1.11	0.33	0.27	0.27
ρ2-ρ3	10^{-4} nm^{-2}	2.6	-0.51	-0.81	-0.33	-0.35	-0.36
radii							
R3	nm	0	6.7	2.2	6.7	20.7	19.0
R2bar (log-normal)	nm	46.1	46.1	46.1	46.1	46.1	46.1
σ/R2 (log-normal)		0.30	0.30	0.30	0.30	0.30	0.30
hard sphere S(Q)							
R(HS)	nm	31.7	31.7	31.7	31.7	31.7	45.4
ϕ(HS)		0.167	0.167	0.167	0.167	0.167	0.237
SSE (quality of fit)		$3.87\ 10^5$	$1.29\ 10^4$	$3.86\ 10^4$	$1.19\ 10^6$	$8.59\ 10^4$	$5.65\ 10^4$
fit#		1a	3a	3b	3c	4a	4b

The log-normal distribution from the 'dry' fit is given in Fig.2
Some fit results are shown in Figs. 3-4.

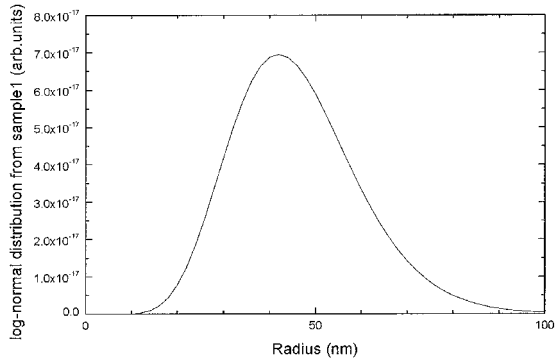

Fig.2 Log-normal distribution with Rbar = 46.1 nm and σ/R = 30%

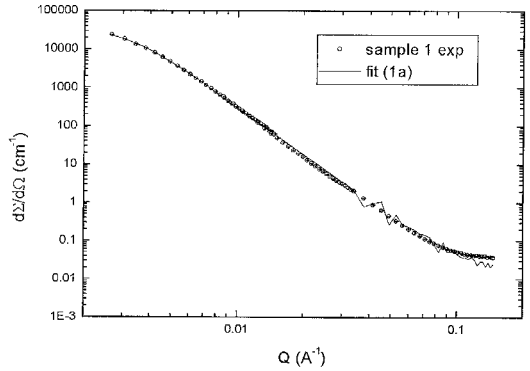

Fig 3. Sample 1: experiment (symbol) and fit # 1a (line)

Preliminary conclusions/remarks

Parameters from fits do not correspond to our expectations:
- The powder used are of μm size
- From X-ray diffraction line widths we expect 'domain sizes' of several tens of nm (e.g. for x = 0.25 $D_{anatase} \approx 30$ nm and $D_{titanate} \approx 65$ nm)

In the fits, a size distribution for P(Q) is used, while for S(Q) a mono-disperse system is assumed. Apparently, good fits can be obtained with unrealistic parameters → More parameters should be known independently.

Still uncertainties concerning absolute normalisation and degree of matching.

Following experiments:
- Series with different d/h combination in hexane to determine exact match point
- Determining (e.g. by weighing) powder volume fraction
- Dilute solution? (then only P(Q))

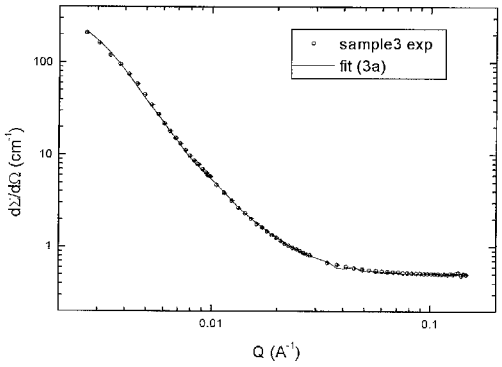

Fig.4 Sample 3: experiment (symbol) and fit 3a (line)

Institut für Festkörperforschung
Forschungszentrum Jülich GmbH
D-52425 Jülich

Experimental Report
of Neutron Scattering Experiments
at the FRJ-2 Reactor

Proposal number:	KW1-02-021		
Experiment title:	**Microscopic Deformation of Filler Particles in Rubber Under Uni-Axial Deformation**		
Dates of experiment:	25-28/04/2002	Date of report:	24/02/2003
Experimental team: Names	Addresses		
Volker URBAN Gabor BELINA	Oak Ridge National Laboratory PO Box 2008 MS6100 Oak Ridge TN 37831-6100, USA urbanvs@ornl.gov ESRF, BP 220, F-38043 Grenoble Cedex, France belina@esrf.fr		
Local Contact:	Wim Pyckhout-Hintzen		

Experimental report text body

We have studied model systems using small angle scattering techniques and have established a mean-field theory for comprehensive description of mechanical and scattering properties of non-filled polymer networks, filler model-systems (using block copolymers) and silica filled polymer networks[1,2]. To apply these theories to the industrial use we needed to study not only academic systems but also complex industrial samples.
The reinforcing filler in the studied rubber compound is a hard grade carbon black for rubber; its ASTM (American Standard of Testing Materials) number is N339. Its application is in the tyre treads, because this filler gives very good abrasion resistance to the rubber. The elastomer matrix is natural rubber.
The use of synchrotron X-ray radiation is very effective due to its high flux; it can be used to probe fast changes in microscopic structure. However, industrial rubber contains many additives beside the reinforcing filler, among which is ZnO. The electron density of Zn is very high compared to that of carbon and complementary measurements are needed to distinguish the scattering signal of the filler from background intensities of other additives. Small Angle Neutron Scattering is a perfect tool for this task, since for neutrons the scattering length density of Zn and carbon is similar and the concentration difference is so huge that the scattering contribution of Zn is negligible.
For the data analysis we used the unified fit approach developed by Beaucage[3,4], which can describe materials showing microstructural features on many length scales. Figure (1) presents the scattering curves from neutron and x-ray experiments and how the unified fit is applied. Among the additives of the industrial rubber there is ZnO_2 which gives a very strong signal in X-ray measurements, the scattering contribution of Zn is one order of magnitude stronger than that of the carbon. The scattering length density of Zn is similar to that of the filler and because of the small volume fraction of ZnO_2, it gives a negligible scattering contribution in SANS. In this way we are able to subtract the background that is produced by the matrix and the additives from the experimental measurements. The difference between the scattering length densities of the polymer matrix and the filler

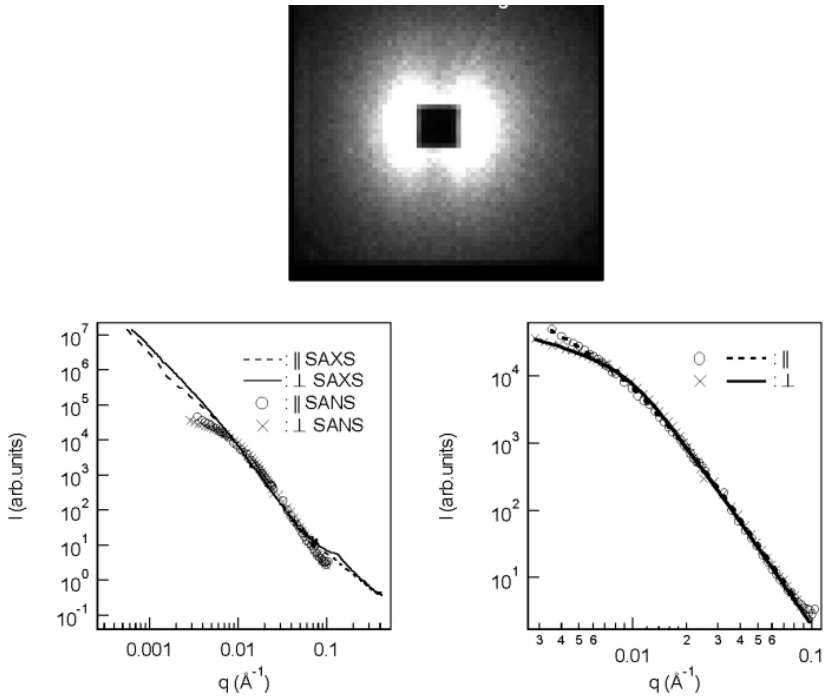

Figure 1. Two-dimensional image of SANS and scattering curves from SAXS and SANS. The solid lines and the x markers stand for the perpendicular direction, the dashed lines and open circles for the parallel. On the left graph the markers are SANS; lines are SAXS data sets, stretch ratio: $\lambda = 2.5$; carbon black filler concentration is 40 w/w% ($\phi = 0.22$ v/v). On the right graph lines are fits from the unified approach and symbols are SANS data sets of the same sample. The power law exponents for the low q part of the curves: $p_{\|} = -1.8$; $p_{\perp} = -1$; for the high q part: $p_{\|} = p_{\perp} = -3.8$; radius of gyration: $R_{g\|} = 181$Å; $R_{g\perp} = 187$Å

particles is much larger then the differences we get with X-rays. With SANS measurements we are able to look only at the filler without the surrounding material. From the SANS experiments it is clear that the scattering curves represent the carbon black filler even at low q, while for X-rays this is not true. The difference of the parallel and perpendicular direction comes from the difference in interparticle distances but not of the CB but of the ZnO.

For neutrons the difference is due to the structural changes in CB aggregates. The power law exponent at the carbon black primary particle level ($0.01 < q < 0.05$) is close to -3.8 for all of the samples. This can be explained by surface fractal model based on fairly rough particles, with surface fractal scaling extending over almost a decade in size. The final part of the SANS scattering curve is the beginning of the power law regime for the next structural level, which in this case is the aggregate. Care must be taken when analyzing the power law exponents from these parts of the scattering curves because they do not extend over a very large q range.

On the images of the stretched samples we detected orientations of the filler particles, similar to those of SAXS, but we are able to say with more certainty that they are only the result of the deformation of the carbon black filler network and not of the additives containing heavy elements. On the two dimensional images we saw "butterfly" patterns, which are usually attributed to inhomogeneous deformation in the range of the length scale corresponding to the scattering vector at the highest intensity of the pattern. The length scale of the deformation calculated from the scattering curves starts at approximately 20 nm, which corresponds to the CB aggregate level.

References:

[1] E. Straube, V. Urban, W. Pyckhout-Hintzen, D. Richter, C. J. Glinka, *Phys. Rev. Lett*. **1995**, *74*, 4464.
[2] S. Westermann, M.Kreitschmann, W. Pyckhout-Hintzen, D. Richter, E. Straube, *Physica B* **1997,** *234-236*, 306.
[3] G. Beaucage, *J. Appl. Cryst.* **1995**, *28*, 717.
[4] G. Beaucage, S. Rane, D. W. Schaefer, G. Long, D. Fischer, *J. of Polym. Sci. Part B.* **1999,** *37*, 1105.

Institut für Festkörperforschung
Forschungszentrum Jülich GmbH
D-52425 Jülich

Experimental Report
of Neutron Scattering Experiments
at the FRJ-2 Reactor

Proposal number:	KW1-02-022		
Experiment title:	**Film contrast measurements in a polymeric microemulsion**		
Dates of experiment:	9.09.02-12.09.02	Date of report:	19.02.03
Experimental team: Names	Addresses		
Vitaliy Pipich Dietmar Schwahn Lutz Willner	IFF, FZ-Jülich, D-52425 Jülich		
Local Contact:	Dietmar Schwahn		

Experimental report text body

(Please use 12 pt letters here !)

The binary system of two homopolymers polybutadiene (PB) and polystyrene (PS) mixed with symmetric diblock copolymers PB-PS had been studied by SANS in bulk and block contrasts. This system demonstrates a rich phase behavior due to different nature of critical phenomena in initial components. A microemulsion channel was detected for this system between 7% and 13% of diblock copolymer content in low temperature range. Reentrance one phase behavior was found between 6% and 7.2% of diblock volume fraction. Physical explanation for such behavior is still unclear. Therefor "film" contrast of system is seem to be useful to describe system.

In the present study we investigate by SANS the ternary system dPB/dPS/dPB-PB-dPS when only middle part of quasi-diblock copolymers is visible by neutrons. Matched part of triblock copolymers occupies roughly 5% of their volume. Deuteration of system usually influences on the phase diagram of the system. Therefor to compare behavior of system in different contrasts one should know the phase diagram in bulk and film contrast. Phase diagram in bulk contrast was revealed by SANS in previous measurements. Straight lines in Figure 1 depict the bulk phase diagram dPB/PS/dPB-PS. As since phase separation boundary is undetectable by neutrons due to weak scattering at small Q range for low triblock content samples line was determined by turbidity measurements. Deuteretion of polystyrene in the binary blend dPB/PS raises the critical solution temperature from 96^{o}C to 116^{o}C. The similar situation was found in another limit case: order-disorder transition temperature of quasi diblock copolymers dPB-PB-dPS is 20K above T_{ODT} of dPB-PS copolymers.

Though deuteration influences on critical parameters of initial systems strongly the microemulsion channel is detected at the same position for bulk and film contrasts.

The neutron small angle diffraction experiments for were performed at KWS2 facility in a Q range between $0.002<Q<0.2Å^{-1}$ (20m, 8m, 4m and 1.25m detector positions). The data were corrected for scattering from empty cell and calibrated in absolute units by a Lupolen secondary standard. Scattering cross-sections of 3%, 15%, and 100% "film-matched" diblock copolymers is received in temperature range 160-23°C. Film contrast measurements allow to detect disorder-order transition to lamellar phase for 15% and 100%. One can see clear indication of ordering transition for quasi diblocks dPB-PB-dPS on Figure 2. Above T_{ODT} copolymers shows peak which is independent from temperature at 0.068Å. Decrease of temperature from 90 to 86°C causes increase of intensity maximum position. Peak position in temperature range below ordering transition in film contrast is two times as large as in bulk contrast due to two times difference in periodicity of film and bulk samples. Peaks of sample above and below T_{ODT} have different nature. dPB-PS diblock copolymers demonstrate more smooth transition of intensity maximum position, but easy detectable one. A opposite situation for 15% bulk sample (dPB/PS/dPB-PS): continuous transition to ordered phase with second order peak formation.

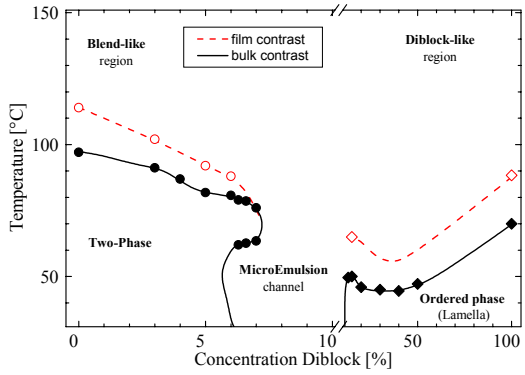

Fig. 1 – Phase diagrams of ternary system PB/PS/PB-PS in bulk and film contrast.

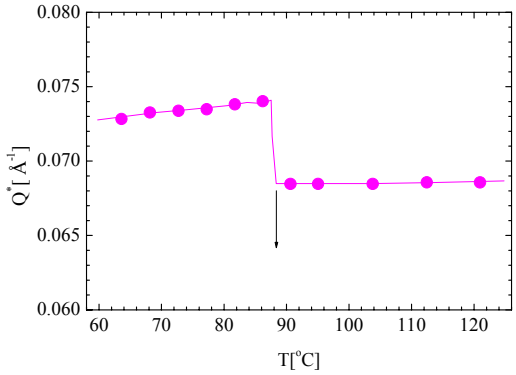

Fig. 2 – Temperature dependence of Q^*: triblock copolymers dPB-PB-dPS.

Institut für Festkörperforschung
Forschungszentrum Jülich GmbH
D-52425 Jülich

Experimental Report
of Neutron Scattering Experiments
at the FRJ-2 Reactor

Proposal number:	KW1--02-023		
Experiment title:	Kinetics of nucleation of calcium carbonate		
Dates of experiment:	30. March - 02. April 2002	Date of report:	
Experimental team: Names	Addresses		
Hitoshi Endo Dietmar Schwahn	IFF, FZ-Juelich, D52425 Jülich IFF, FZ-Juelich, D52425 Jülich		
Local Contact:	Dietmar Schwahn		

Experimental report text body

Calcium carbonate ($CaCO_3$) crystals which are influenced by double-hydrophilic block copolymer poly(ethylen glycol)-*block*-poly(methacrylic acid) (PEG-*b*-PMMA) with respect to their morphology and size [1] were investigated by means of SANS.

Last measurements, the kinetics of the reaction was studied by time resolved SANS measurements, where a gas-liquid diffusion reaction was used to realize a slow reaction speed. The obtained results with $CaCO_3$ contrast (the aqueous solution is H_2O) clearly showed that the addition of the polymer strongly affects the reaction process. The direct information about polymer can be obtained by performing same SANS experiments under the 'polymer contrast' where the scattering contrast of water is matched to that of $CaCO_3$, therefore the scattering arises from the polymer. The solution was prepared with 3wt% PEG-*b*-PMMA, 0.1M Ca^{2+} and pH ≈ 8.

In Fig. 1, the achieved scattering profiles are exhibiting. The profiles did not change after 4 hours from the reaction started; on the other hand, the profiles with the $CaCO_3$ contrast showed quite dramatic changes even after 2 hours. This result suggests that most of polymers do not take part in the reaction, which is consistent to the results obtained by pyrolysis measurements, which resulted that the polymer's concentration in $CaCO_3$ is roughly 6 wt% where the $CaCO_3$ crystals were prepared with the condition [Polymer]/[$CaCO_3$] = 0.3 – 0.9.

Therefore, to detect the signal of the polymer included by $CaCO_3$ crystals during the reaction, we concluded that a extreme condition is necessary, *e.g.*, 1wt% polymer solution with 3M Ca^{2+}, which is 30 times more concentrated compared to the current conditon.

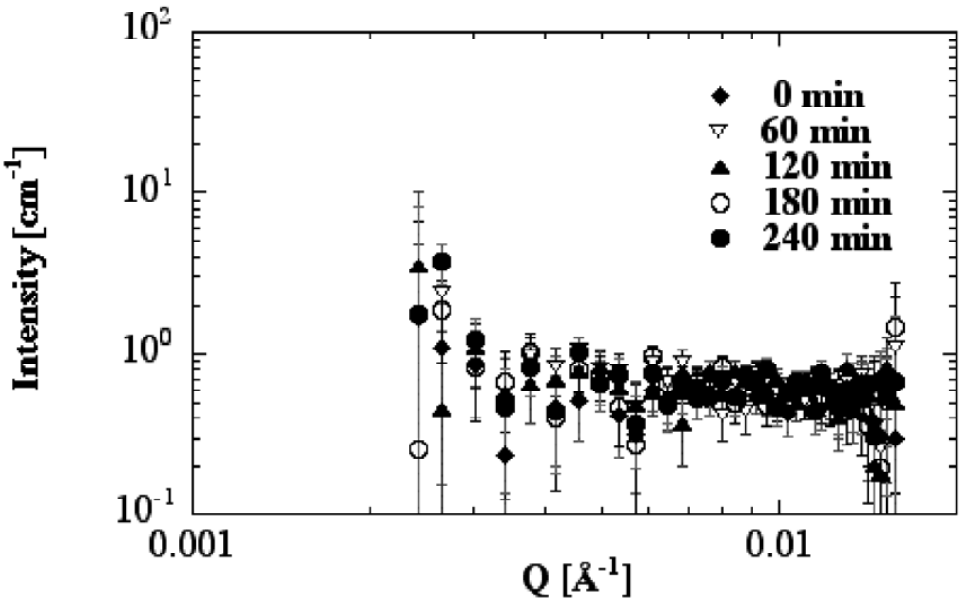

Figure 1. Time resolved SANS profiles at 20m detector length with 0.1M Ca^{2+} and 3 wt% concentration under the polymer contrast.

[1] H. Cölfen and L. Qi, *Chem. Eur. J.* 7, **106** (2001)

Institut für Festkörperforschung
Forschungszentrum Jülich GmbH
D-52425 Jülich

Experimental Report
of Neutron Scattering Experiments
at the FRJ-2 Reactor

Proposal number:	KW1-02-027		
Experiment title:	Interactions Between Carbon Nanotubes, Amphiphilic Polymers and Surfactants		
Dates of experiment:	27-30/10/2002	Date of report:	18/2/2003
Experimental team: Names	Addresses		
COHEN, Yachin DROR, Yael	Department of Chemical Engineering, Technion, Haifa, ISRAEL 32000 Department of Chemical Engineering, Technion, Haifa, ISRAEL 32000		
Local Contact:	Dr. Wim Pyckhout-Hintzen		

Experimental report text body

Background

Single-walled Carbon nanotubes (SWCNT) are exciting new materials. The main hindrance to processing SWCNT's for useful applications, such as high performance fibers or small-scale electric energy storage devices, is their strong tendency to self-aggregate. New methods of dispersion are being studied and developed. These include dispersion with surfactants and amhiphlic polymers. A new approach to stable dispersion of SWCNT's follows the ancient method of the "Pharaoh's Ink", using the natural polysaccharide Gum Arabic [GA]. GA is a complex natural polymer. It is prepared from the stems and branches of sub-Saharan *Acacia senegal* trees, and is a complex and variable mixture of arabinogalactan oligosaccharides, polysaccharides and glycoproteins,

Objectives

The objective of this project is to study the state of aggregation of single-walled carbon nanotubes (SWCNT) in aqueous dispersions formed by interactions with amphiphilic polymers. The specific objective of this experiment is to measure the small-angle neutron scattering with contrast variation of the solvent (H_2O/D_2O) to elucidate the complex microsctructure of the amphiphilic polymers and how they interact with the nanotube. As a preliminary objective we seek to study the microstructure of Gum Arabic)GA) in aqueous solution, to understand what structural attributes of this natural polymer give rise to its unique dispersion ability of carbon nanotubes.

Experimental

SANS experiments were carried out at KWS-1 at 2 and 8 m sample-detector distances. 2 exploratory runs were also carried out at 20 m. The main difficulty was the low scattering from the dispersions which required long measuring time. SWCNT, obtained from Carbolux Corp, were dispersed to concentration of 0.2 % (vol.) in aqueous solution of GA (5% vol.) assisted by ultra-sonication for 2 minutes. The solvent was mixed D_2O/H_2O at 100, 80 60 and 40 % (vol) D_2O compsitions.

Results
Preliminary analysis of the experimental data exhibited unexpected behavior in the studied .

Aqueous solutions of Gum Arabic (GA)
The SANS of 5% gum arabic in D_2O exhibits two maxima, as shown in Figure 1a. A broad maximum at about 20 Å spacing is interpreted as arising from the inner structure of GA micellar-like structure, whereas a sharper peak at about 40 Å spacing is interpreted as an inter-micellar peak due to electrostatic repulsion. Thus this unique polymer has a unique structure including possibly a hydrophobic core (glycoprotein), a swollen hydrophilic shell (arabinogalactan), and electrostatic outer shell. This is shown schematically in Figure 2. Contrast variation results in non-trivial changes to the SANS patterns. With 20% H_2O the intermicellar peak is not observed while the intra-micellar peak remains. 40% H_2O seems to match the dominant scattering entity.

Aqueous dispersions of single-walled carbon nanotubes and Gum Arabic
When nanotubes are present with GA only the 20 Å peak is observed. As in GA solutions, it seems to be matched out at about 40% H_2O. Moreover, significant increase in scattering at low angles is observed in the SWCNT/GA dispersions. This is due to the to the extended rod-like sstructure of the nanotubes which leads to q^{-1} behavior at low scattering vectors. Interstingly, the variation of intensity at low-angles with the solvent composition appears to go through a minimum, at increasing H_2O content. Current effort is aimed at elucidating the partial structure factors of the polymer and nanotubes from the contrast-variation series. Further studies are aimed at lower scattering angles and more solvent contrast variation.

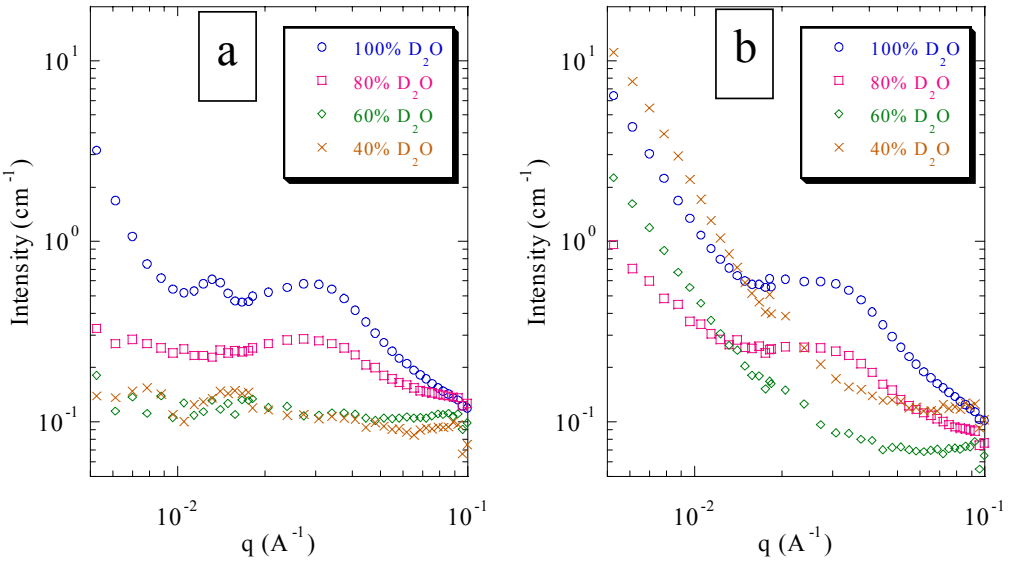

Figure 1: SANS patterns of (a) 5% GA and (b) 5% GA+0.2% SWCNT in different D_2O/ H_2O compositions

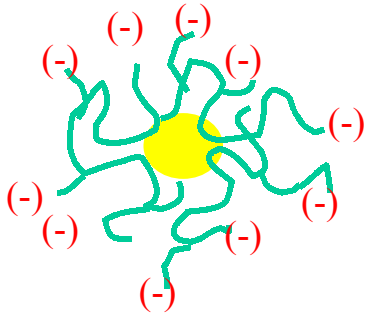

Figure 2: Schematic model for the structure of Gum Arabic in aqueous solution: a hydrophobic inner core surrounded by a highly branched hydrophillic polysaccharide shell, with chrged groups ned the ends of the branches.

Institut für Festkörperforschung
Forschungszentrum Jülich GmbH
D-52425 Jülich

Experimental Report
of Neutron Scattering Experiments
at the FRJ-2 Reactor

Proposal number:	KW1-02-030		
Experiment title:	**Stability of Silicon Complex Compounds in Water**		
Dates of experiment:	18.10. – 20.10. 2002	Date of report:	22.02.2003
Experimental team: Names	Addresses		
O. Seiler R. Tacke	Universität Würzburg Institut für Anorganische Chemie Am Hubland D97074 Würzburg		
Local Contact:	D. Schwahn		

Experimental report text body

The stability of two Silicon complex compounds in water were investigated with SANS. These were citric (1) and oxalic (2) acid whose structure has the following form

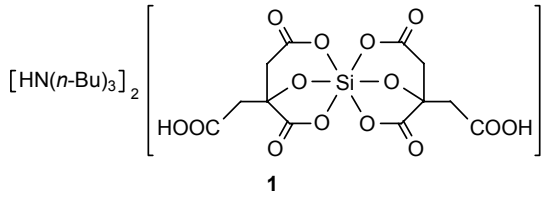

1

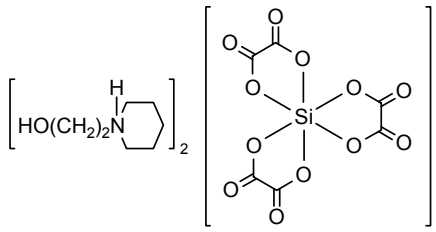

2

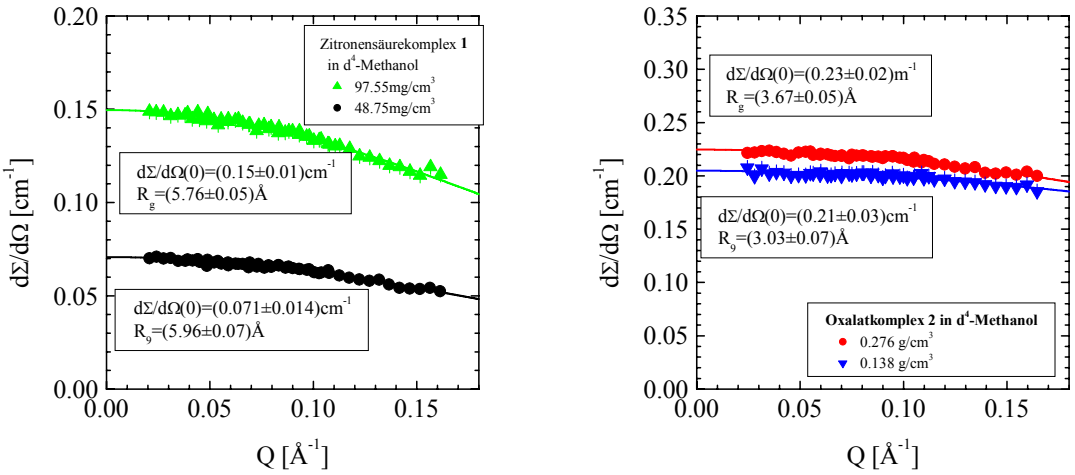

Figure 1: SANS scattering patterns in absolute units of 1 (left) and 2 (right) in a deuterated organic solvent with two concentrations. The molecules are stable in organic solvents.

Figure 1 shows the scattering patterns of both compounds in an organic solvent which can be analyzed by Guinier's law whose parameters are given in the figures. The oxalic acid molecule has a slightly smaller dimension than the citric acid complex.

The data in figure 2 and 3 show the experiments for the time evolution of the citric acid in D_2O. Figure 2 show the results at short times between 2.6 and 6.25 hours after mixing the acid with water. The data are described by Guinier's law, their parameters are plotted in the right figure versus time. Both parameters, namely the radius of gyration and the extrapolated scattering at Q=0 increase linearly with time. In this time regime appreciably smaller particle sizes are measured as a result from the destruction of the molecule by hydrolysis. After about 7 hours the intensity at small Q increases caused by formation of larger aggregates (probably silicic acid). These scattering patterns cannot be analyzed in terms of Guinier's law because of a broad size distribution.

.

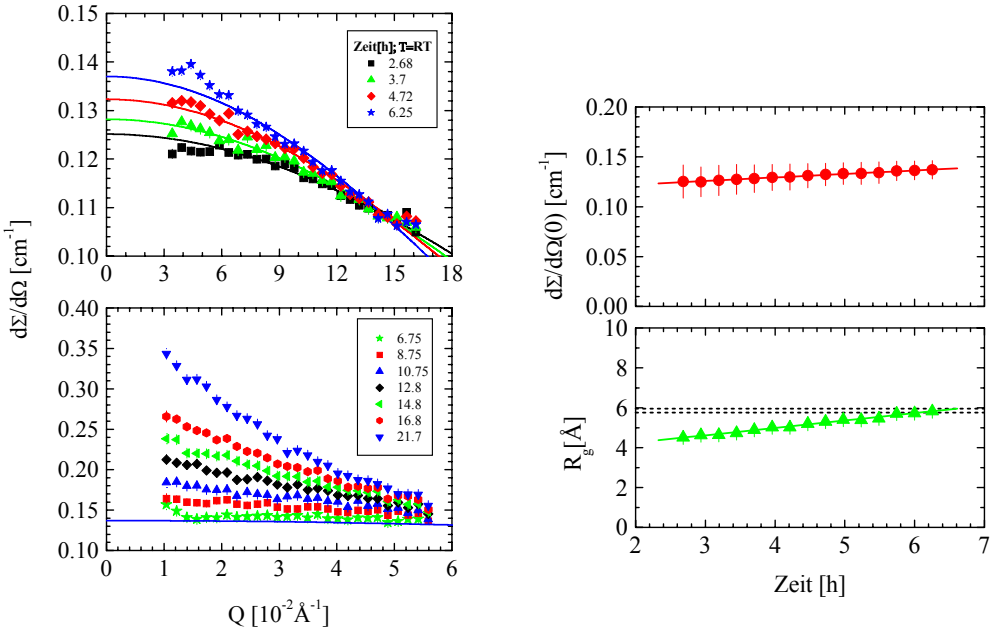

Figure 2: (Left) SANS patterns of an aqueous solution of 1 (c=48.75mg/cm^3) in D_2O at different times. The figures on the left side show the beginning of a sol-gel process. The figures on the right side show the size and scattering at Q=0 versus time. The size of the molecules first decreases as a result of the hydrolysis.

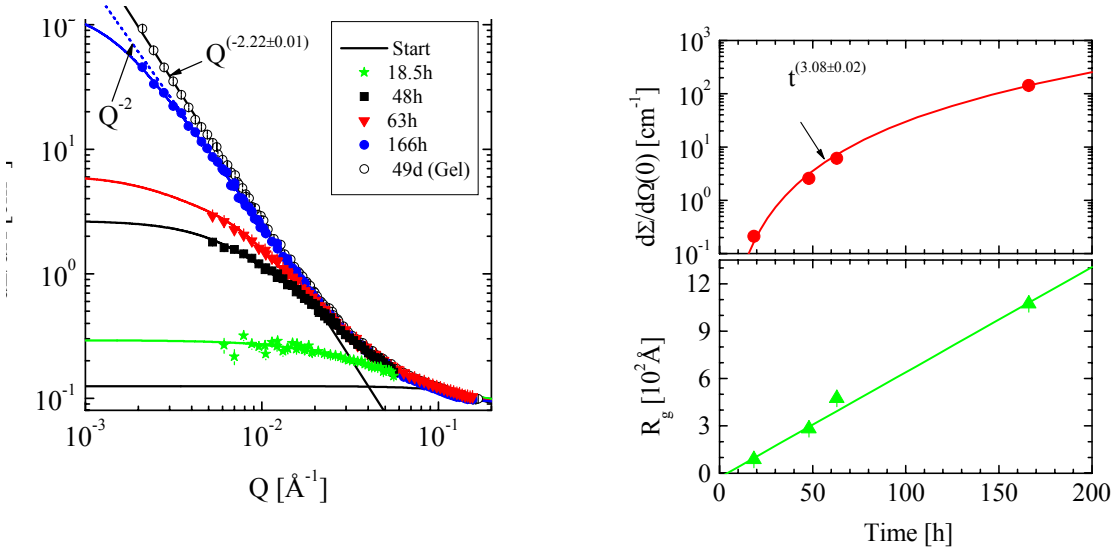

Figure 3:: (Left) SANS scattering patterns of 1 in D_2O for time larger than 18 hours. The scattered intensity steadily increases and seems to approach a limiting scattering pattern, for the larger Q earlier than for the smaller ones. The scattering curves are well described by an ansatz from Beaucage for mass fractals, as demonstrated by the solid lines. After 166h a Q^{-2} power law describes the intermediate Q range. the figure on the right side shows the time evolution of the extrapolated scattering at Q=0 and the radius of gyration.

The left side of figure 3 shows the scattering patterns measured between 18.5 and 49days. The solvent was a sol until 166h and became a gel in the mean time until 49 days. The scattering is well described by an ansatz from Beaucage for mass fractals with the upper limits at small and large Q determined by the total size of the aggregate and molecular size, respectively. Fit parameters are the extrapolated scattering at Q=0 and the radius of gyration as depicted versus time on the figures at the right side, and a microscopic length scale being less than 3 Å. This length is the reason for the deviations from the power law at $Q>0.05Å^{-1}$. Another parameter is a fractal dimensionality a, which continuously increases from a=1.2 (18.5h) to a=2 (166h). From the numbers of the dimensionality we conclude that the aggregates (Sole) first form more rod-like structures (a=1) and then grow to particles of more platelet shape (a=2). The radius of gyration gives the upper size of the fractal objects. The grow process in principle occurs by agglomeration of larger objects. This can be concluded from to observations: (1) The scattering pattern seem to approach a kind of equilibrium curve as observed for $Q>0.02$ $Å^{-1}$ and (2) the intensity at zero Q increases proportional to Rg^3. This means, that the volume fraction of the sol is constant with time.

On the other hand, the oxalic acid compounds do not show any tendency of sol formation within the time of investigations.

Institut für Festkörperforschung
Forschungszentrum Jülich GmbH
D-52425 Jülich

Experimental Report
of Neutron Scattering Experiments
at the FRJ-2 Reactor

Proposal number:	KW1-02-033		
Experiment title:	**Internal structure of new PNIPAM-copolymer microgels**		
Dates of experiment:	21.10.02 -22.10.02	Date of report:	5/12/02
Experimental team: Names	Addresses		
Thomas Hellweg, Sarah Höfl	Iwan-Stranski-Laboratorium Straße-des-17.Juni 112 10623 Berlin		
Local Contact:	Wim Pyckhout-Hintzen		

Experimental report text body

During the allocated beamtime several different types of PNIPAM-co-Poly(vinylacetic acid) microgels (with 1, 5, 10 and 15 mol% vinylacetic acid) were studied. The most remarkable property of PNIPAM based microgels is their so-called volume phase transition. Also the particles obtained by copolymerisation show this thermosensitive behavior (they show a reversible volume phase transition at about 32°C). The purpose of the SANS measurements performed on the KWS1 machine was the characterisation of the changes of the local network structure inside the new copolymer microgels. Therefore, the measurements were done between 25 and 35°C to learn about the changes occuring during the volume phase transition.
In Fig. 1 and 2 the obtained small angle scattering curves for PNIPAM-co-Poly(vinylacetic acid) with 1 mol% and 15 mol% comonomer are shown.

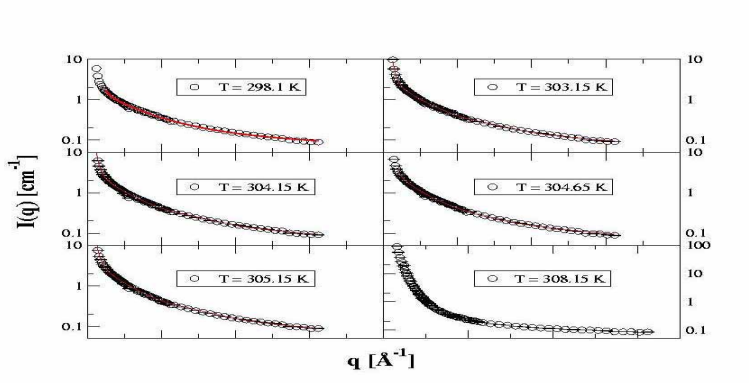

FIG 1: Temperatur-dependent SANS-curves of PNIPAM-co-Vinylpyridine(1 mol%). The black points are the measured values, the red line is the fit.

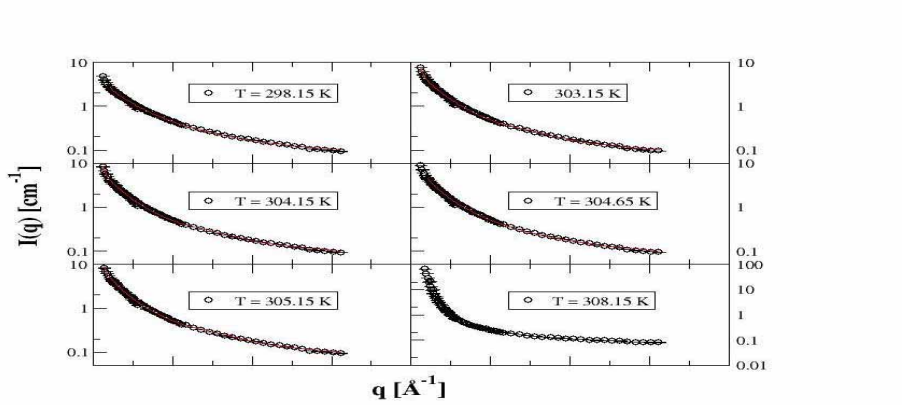

FIG 2: Temperatur-dependent SANS-curves of PNIPAM-co-Vinylpyridine(15 mol%). The black points are the measured values, the red line is the fit.

All data except the ones at the temperature of 35°C were fitted by a sum of a Porod function and an Ornstein-Zernickecontribution. This procedure was already succesfully applied before [1].
At a temperature over the volume phase transition temperature it is impossible to fit the values, because the network is collapsed. But for lower temperatures the Porod part at small q-values describes the surface scattering from the microgel spheres and the Ornstein-Zernicke-equation at high q-values the internal network structure.
For the microgel particles with 15 mol% Vinylacetic acid, this leads to a correlation length of 4.82 nm at 25°C that is growing up to 7.50 nm an 32°C. The scattering curves obtained for the other microgel samples show the same features as the ones shown in fig.1 and 2. Hence, these data were analysed using the same fitting function. For the other microgels one finds 1.23 nm to 2.83 nm (1 mol% vinyl acetic acid), 4.23 nm to 5.82 nm (5 mol% vinylacetic acid) and 4.80 nm to 6.46 nm (10 mol% vinylacetic acid).
These values show that the correlation length grows with the amount of comonomer inside the network and additionally with increasing sample temperature.
The reason for the growth of ξ with increasing vinylacetic acid content is presumeably the higher charge density in the network that occurs if more charged comonomer is added. This leads to an electrostatic repulsion and therefore to an increased mesh size. A similar behavior was observed for the also charged PNIPAM-co-acrylic acid microgels.
The growth of the correlation length with higher temperatures was also expected. In volume phase transitions of macro- and microgels a divergence of the intensity and the correlation length is usually observed.

The results of the experiments at the FZ Jülich are a major part of the diploma thesis of S. Höfl:

S. Höfl : ***Eigenschaften neuer Copolymer-Mikrogele*****, TU Berlin, Dezember 2002.**

1K. Kratz, A. Lapp, W. Eimer and Th. Hellweg, Coll. Sur. A, 197 (2002) 55

Small Angle Neutron Scattering Instrument (KWS2)

Instrument Parameters

Beam tube:	NLIIB bent guide, cross section: 4.5 cm (height) × 3 cm (width)
Monochromator:	velocity selector; $\Delta\lambda/\lambda$ = 10 %
Neutron flux at sample:	10^5 to 6 × 10^6 n/cm^2 s depending on collimation; for 20 MW reactor power λ = 7 Å wavelength and entrance aperture of 3 × 3 cm^2
Collimation:	variable apertures at 1 m, 2 m, 4 m, 8 m, 14 m, 18 m, 20 m distance from sample opening width variable 0.5 ... 4.5 cm vertical opening width variable 0.5 ... 3.0 cm horizontal
Beam size at sample:	typically 1 cm × 1 cm
Detector 1:	from end of 2003: Anger camera ^{3}He 2-dimensional detector with 50 × 50 cm^2 active area gas filling: ^{3}He (1 bar), ^{4}He (1 bar), CF_4 (1 bar) in detector volume; ^{4}He (3 bar) in buffer volume; space resolution 0.8 × 0.8 cm^2; dead time: 15µs max. count rate ≈ 7 kHz (10% dead time); background: ≈ 1Hz
Elastic Q-range:	$10^{-3} \le Q/Å^{-1} \le 0.3$ (typically $2 \times 10^{-3} \le Q/Å^{-1} \le 0.2$)
Sample environment:	evacuated sample chamber / open beam line cryofurnace 200 ... 500 K; shear cell of Searle type

Instrument Responsible

Dr. Henrich Frielinghaus Tel. +49-(0)-2461-61-5093 Email: h.frielinghaus@fz-juelich.de
Dr. Aurel Radulescu Tel. +49-(0)-2461-61-4685 Email: a.radulescu@fz-juelich.de

Institut für Festkörperforschung
Forschungszentrum Jülich GmbH
D-52425 Jülich

Experimental Report
of Neutron Scattering Experiments
at the FRJ-2 Reactor

Proposal number:	KW2-01-040		
Experiment title:	**SANS from highly Entangled Polymer Solutions Under Steady State Shear Flow**		
Dates of experiment:	30/03/02-03/04/02	Date of report:	26/02/03
Experimental team: Names	Addresses		
Nigel Clarke Mike Ries	Department of Chemistry, University of Durham, Durham, DH7 8UE Department of Physics, University of Leeds, Leeds, LS2 9JT		
Local Contact:	Henrich Frielinghaus		

Experimental report text body

(Please use 12 pt letters here !)

The last two years have seen very rapid and exciting growth in our understanding of the physics of entangled polymers in both equilibrium and under strain. For some 20 years now the tube model of Doi and Edwards has provided a good qualitative picture of polymer dynamics; for example, it has been particularly successful in explaining the strange properties of simple branched polymers. However, recent modifications that have included fluctuation modes within the entanglement tubes have shown that at least for monodisperse linear, star-branched, and H-branched polymers, the tube theory can also be quantitative in linear rheological response. In non-linear response more new physics comes into play – and in this case a direct structural probe is essential to accompany rheological data if the model is to be validated and extended in an appropriate way.

We have conducted a series of experiments on mixtures of deuterated polystyrene/hydrogenous polystyrene/di-octylphthalate (dPS/PS/DOP) using the Bohlin Couette shear cell. The molecular weight of the dPS and PS was ~3 million g/mol, and the total polystyrene concentration was 6%. Due to limitations of the rheometer, which is not well suited for samples with as a high a viscosity as our solution, it was only possible to apply relatively low shear rates to the sample. The critical parameter is the product of the polymer relaxation time, t, and the shear rate, $\dot{\gamma}$. We were only able to reach values of $\dot{\gamma}\tau \sim 1$. Structural changes of interest occur at values typically between $\dot{\gamma}\tau \sim 5$ and $\dot{\gamma}\tau \sim 100$. Despite this, we observed anisotropy in the scattering pattern, suggesting that the polymers are noticeably deformed, even at low shear rates. Such observations were made possible by the acessibility of very small scattering angles, and excellent statistics, on KWSII.

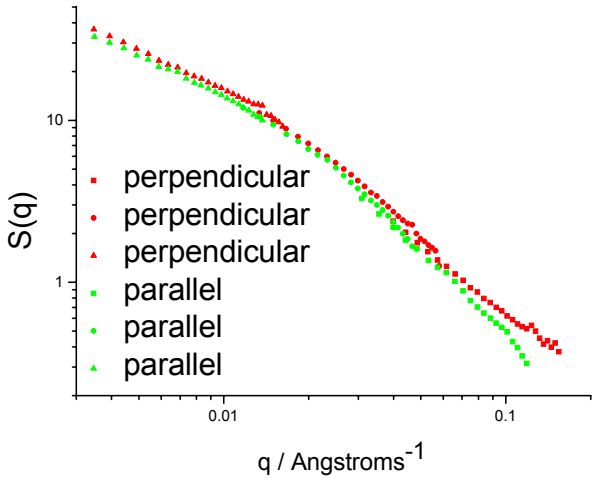

An example is shown in the above figure, where radial averages taken from the 2D scattering pattern have been calculated over 10 degrees either side of the direction perpendicular to the flow (vertical direction) and parallel to the flow (horizontal direction). It is clear that there is enhanced scattering in the direction perpendicular to the flow, suggesting that the chains have been stretched slightly parallel to the flow as can be anticipated. The above data reflects both the structure of individual chains (the single chain structure factor) and fluctuations in polymer concentration. In this experiment our interest is in extracting the former, in order determine the single chain scattering function it is necessary to combine the data with that taken from a solution in which the total polymer concentration is the same, but the ratio of deuterated to protonated polystyrene is different. Unfortunately, due to the problems encountered with the shear cell, the only two mixtures we studied had very similar ratios leading to statistically insignificant results.

This remains a challenging problem – the need for enough entanglements in the chain requires high molecular weights and reasonable concentrations. This results in solutions with high viscosities that are not well suited to being sheared in commercial rheometers.

Institut für Festkörperforschung
Forschungszentrum Jülich GmbH
D-52425 Jülich

Experimental Report
of Neutron Scattering Experiments
at the FRJ-2 Reactor

Proposal number:	KW2-02-001		
Experiment title:	**Bending rigidity of microemulsions with homopolymers and diblock copolymers – the cancellation of two opposite effects**		
Dates of experiment:	21.01.02 - 27.01.02	Date of report:	05.03.03
Experimental team: Names	Addresses		
Frielinghaus, Henrich Byelov, Dmytro Richter, Dieter	Institut für Festkörperforschung Forschungszentrum Jülich GmbH D-52425 Jülich Germany		
Local Contact:	Frielinghaus, Henrich		

Experimental report text body

After the polymer boosting effect has been established, which describes the increase of the efficiency of surfactants by amphiphilic diblock copolymers, the effect of homopolymers on microemulsions was found to decrease the efficiency. However, homopolymers could be useful to adjust the viscosity of the microemulsion and, therefore, we tried to superpose the two opposite polymer effects on the efficiency. It should be possible to find mixtures with constant efficiency but increased viscosity. SANS measurements should help to measure the bending rigidity of the surfactant layer in parallel to phase boundary determinations.

The studied microemulsions contain water (D_2O), the oil decane, and the non-ionic C_iE_j surfactant. On a microscopic level the surfactant forms an interfacial film, which separates the otherwise non-miscible water and oil. A minimum of surfactant is needed to solubilize the equal amounts of water and oil, i.e. to form a one-phase system. It was shown, that small amounts of the amphiphilic PEP-PEO block copolymer could decrease the minimum amount of surfactant, i.e. the efficiency was increased dramatically (boosting effect). On the other hand, the single homopolymers PEP and PEO were found to decrease the efficiency (10 times stronger than theoretically estimated by a theory of Eisenriegler). In this work the two opposite effects are tried to be superposed. Phase boundary determinations and SANS measurements were performed.

By SANS the bending rigidity of the surfactant layer could be determined. This was done in two steps: The measured intensity I(Q) was well described by the Teubner-Strey-Formula

$$I(Q) \sim \frac{8\pi\phi_O\phi_W / \xi}{((2\pi/d)^2 + \xi^{-2})^2 - 2((2\pi/d)^2 - \xi^{-2})Q^2 + Q^4}$$

The second step is the interpretation of the correlation length ξ and the domain size *d* by the gaussian random field model. The variables are connected by

$$k\xi = \frac{64}{5\sqrt{3}} \frac{\kappa_R}{k_B T} \Theta\left(\frac{\kappa_R}{k_B T}, \delta \frac{S}{V}\right)$$

and can be solved for the bending rigidity κ_R. The algebraic function Θ approaches 1 for large κ_R, which was assumed to be true for our case. This assumption was already attacked by several referees, but now is under discussion again since computer simulations were found to support the formula.

One example of bending rigidity measurements is shown in figure 1. Here simultaneously homopolymer and diblock copolymer was added to the microemulsion. The diblock copolymer addition leads to higher bending rigidities (shown) and the homopolymer addition leads to smaller κ_R (not shown). From the plot of figure 1 the strength of the influence of the diblock copolymer can be read off. The values compare well with former measurements without homopolymer, and are consistently slightly smaller (~30%) than theoretically predicted.

The phase boundary measurements are summarized in figure 2. Here one sees that the homopolymer addition leads to larger minimum surfactant contents (efficiency decreased), but the diblock copolymer decreases the minimum surfactant content (efficiency increased → boosting effect). From the practically chosen compositions one could predict which homopolymer amount corresponds to which diblock copolymer amount for a constant efficiency.

All in all, former measurements on "pure" systems containing one sort of polymer only are confirmed. One idea of the adjustment of the viscosity was shown. Further measurements could involve larger amounts of polymers, now.

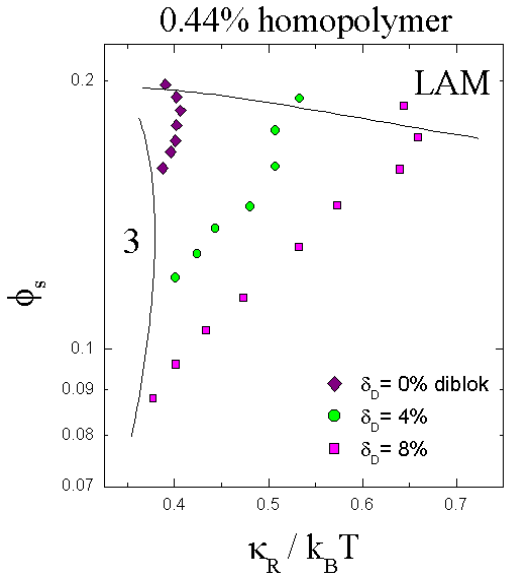

Figure 1: The surfactant content ϕ_S as a function of the by SANS measured bending rigidity κ_R. Here the diblock copolymer amount was varied (δ_D in units of the total surfactant), whereas the homopolymer amount was held constant.

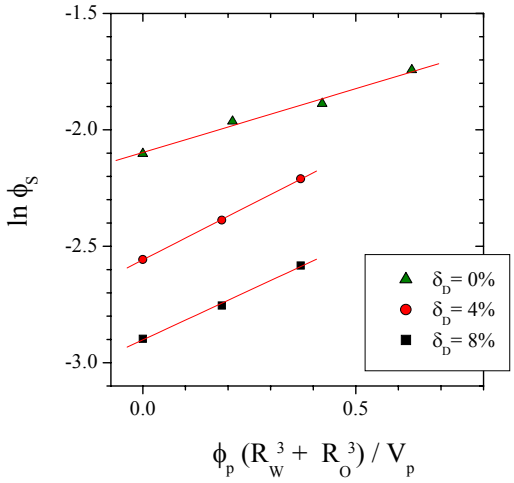

Figure 2: Here the minimum surfactant amount is shown as a function of the homopolymer amount ϕ_P. The x-axis is normalized by the end-to-end distance R_W and R_O of the two polymers (PEO and PEP) and the polymer volume V_P. Homopolymer addition leads to decreased efficiency, diblock copolymer to increased efficiency.

Institut für Festkörperforschung
Forschungszentrum Jülich GmbH
D-52425 Jülich

Experimental Report
of Neutron Scattering Experiments
at the FRJ-2 Reactor

Proposal number:	KW2-02-002		
Experiment title:	**The self-assembling behavior of the high molecular weight PEB-7 random copolymer (M_W=30000 g/mol) in decane investigated by SANS**		
Dates of experiment:	31.01.02-03.02.02	Date of report:	06.03.2003
Experimental team: Names	Addresses		
Aurel Radulescu Robert Stollenwerk	IFF, FZ-Jülich, D-52425 Jülich		
Local Contact:	Henrich Frielinghaus		

Experimental report text body

(Please use 12 pt letters here !)

The self-assembling behavior in decane dilute solution of a lower molecular weight poly(ethylene-butene) random copolymer PEB-7.5 (M_W=6 kg/mol) was earlier investigated with SANS [1]. The general tendencies shown by this system are: (i) the single chain regime is found only for a limited range at high temperatures; (ii) obviously, the aggregation starts at rather high temperatures (between 40°C and 60°C); this process shows a double evolution: first, the formation of large, compact aggregates takes place (distinguished by a pronounced Porod-like scattering) then, in parallel with the decrease of the Porod scattering the formation of a second kind of aggregates of a needle like shape (identified by a Q^{-1} power behavior at low Q) develops at low temperatures; (iv) a correlation peak evolves in the intermediate Q range below 30°C. Trying to understand better the origin of the correlation length, whether e.g. relates to the chain contour length, we checked by the present SANS investigation the self-assembling behavior of a higher MW random copolymer in dilute decane solutions. The PEB-n poly(ethylene-butene) random copolymers were synthesized by anionic polymerization [2] of butadiene with random alternation of 1,4- and 1,2- monomers. After hydrogenation the latter leads to the ethyl-side branches of the otherwise linear PE. The ethyl-side branches content “n” was about 7.5 per 100 backbone carbons while the final molecular weight was M_W=30 kg/mol. The neutron small angle diffraction experiments were performed at the KWSII SANS facility at the FRJ-2 research reactor in Jülich. In a Q range between $0.002Å^{-1}<Q<0.14Å^{-1}$. The data were corrected for the scattering from empty cell and solvent and then calibrated to absolute units by using a Lupolen secondary standard [3]. The polymer behavior was checked by measuring two solutions (with polymer volume fraction Φ_{pol}=0.6% and 1%) over a large temperature range, between the single coil and the aggregates regime (from 85°C to –20°C). The maximum contrast and the minimum incoherent background was achieved using fully protonated polymers in a fully deuterated solvent. Fig.1 displays a summary of the cross sections measured at different temperatures for the 1% polymer solution.

Generally, one can say that similar aggregation features were observed as in the case of lower M_W copolymer. The only difference is that they appear already at higher temperatures. A Zimm analysis performed for the single coil regime (at 85°C) provided a radius of gyration and a forward scattering of R_g=73.6Å and $d\Sigma(0)/d\Omega$=2.82 cm^{-1}, respectively, which are in good agreement with the expectation from the molecular characteristics of the polymers [4]. The dotted line in Fig.1 represents the theoretical description of the cross section by the single coil Beaucage form factor [5] inserting the parameters from the Zimm analysis. An analysis of the early stage of the self-aggregation in terms of the Porod constant was not possible because the SANS did not approach low enough Q values rendering a Q^{-4} power-law fit impossible. The correlation peak that again dominates the intermediate Q range is now less visible than in the case of the lower M_W polymer aggregates. The obtained correlation lengths ($2\pi/Q^*$) at –20°C are about 314Å and 216Å for the higher and lower M_W copolymers. No rule can be established between the correlation lengths obtained and the chain lengths of stretched copolymers which are of about 550Å and 2750Å for the lower and higher M_W copolymers respectively. Thus, the correlation which occurs below 30°C should have a different nature. Possibly it signifies a density modulation along the polymer needle.

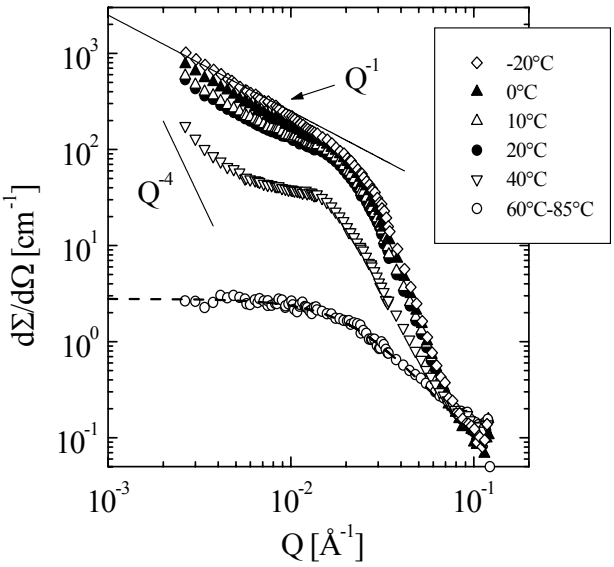

Fig. 1 – Scattering profiles from a solution of PEB-7.5 (M_W=30 kg/mol) in decane at a volume fraction of Φ_{pol}=1%

References:

[1] H.S.Ashbaugh et al., Macomolecules 35, 7044, 2002.
[2] M.Morton and L.J.Fetters, J.Rubber Chem.Technol. 48, 359, 1975.
[3] D.Schwahn et al., J.Chem.Phys. 93, 8383, 1990.
[4] L.J.Fetters et al., Macromolecules 27, 4639, 1994.
[5] G.Beaucage and D.W.Schaefer, J.Non-Crystalline Solids 172-174, 797, 1994.

Institut für Festkörperforschung
Forschungszentrum Jülich GmbH
D-52425 Jülich

Experimental Report of Neutron Scattering Experiments at the FRJ-2 Reactor

Proposal number:	KW2-02-003		
Experiment title:	Comparison of Q-Resolution between focussing mirror and pinhole SANS instruments		
Dates of experiment:	28.1.02	Date of report:10.3.03	
Experimental team: Names	Addresses		
J. Stellbrink	IFF-Neutronenstreuung, Forschungszentrum Jülich, D-52425 Jülich, Germany		
Local Contact:	A. Radulescu		

Experimental report text body

For testing the performance of the new focussing mirror SANS instrument KWS3 we investigated poly(methymethacrylate) (PMMA) colloids with R=776nm. In d-*cis*-decalin these colloids behave as a model colloidal solution (hard spheres). The form factor of the colloids, described by a solid sphere form factor, shows his first minimum at $Q_{min}R=4.49$ and therefore $Q_{min}=5.79\times10^{-4}$Å^{-1}, which fits exactly into the Q-Range of KWS3. For comparing the Q-resolution of KWS3 with those of a conventional pinhole SANS instruments the same solutions was also investigated at KWS2. Moreover, the same solutions have been characterised by static light scattering.

Investigating such large particles causes immediately problems arising from multiple scattering, not only when applying static light scattering, λ=5145Å, but also when using SANS. In particular at KWS3, where a wavelength of 12.7Å is used instead of 7Å at KWS2, see data shown in fig. 1.The sample with maximum contrast for SANS, i.e. protonated PMMA in d-*cis*-decalin ($\Delta\rho^2/N_A=6.34\times10^{-3}$mol/cm^4), shows just a power law dependence in I(Q), closed black squares (■). All details of the sphere form factor as seen by light scattering, open circles(○), with n_d=1.492(PMMA) and n_d=1.481(h-*cis*-decalin), are smeared out in the SANS data by the strong multiple scattering contributions (the transmission of this sample was only ≈2%). Therefore, one has either to decrease the path length, dilute the sample (to nearly infinite dilution), or one has to decrease the contrast. The used path length was already 1mm, so we applied the third possibility given by dissolving h-PMMA in h-*cis*-decalin ($\Delta\rho^2/N_A=6.98\times10^{-5}$mol/cm^4). This increases the transmission to ≈35%. Moreover one has to consider, that here the strong incoherent scattering from the protonated solvent contributes to the sample transmission (1mm h-cis –decalin has already a transmission of ≈50%). Under this contrast condition the first

and second minimum of the form factor appear in the KWS3 data, open red triangles (△).The depth of the minima in SANS data is deminished due to resolution effects arising from the used wavelength distribution of 9% (FWHM). The resolution becomes even worse in the KWS2 data, because here in addition q-smearing due to uncertainty in scattering angle θ is effective.

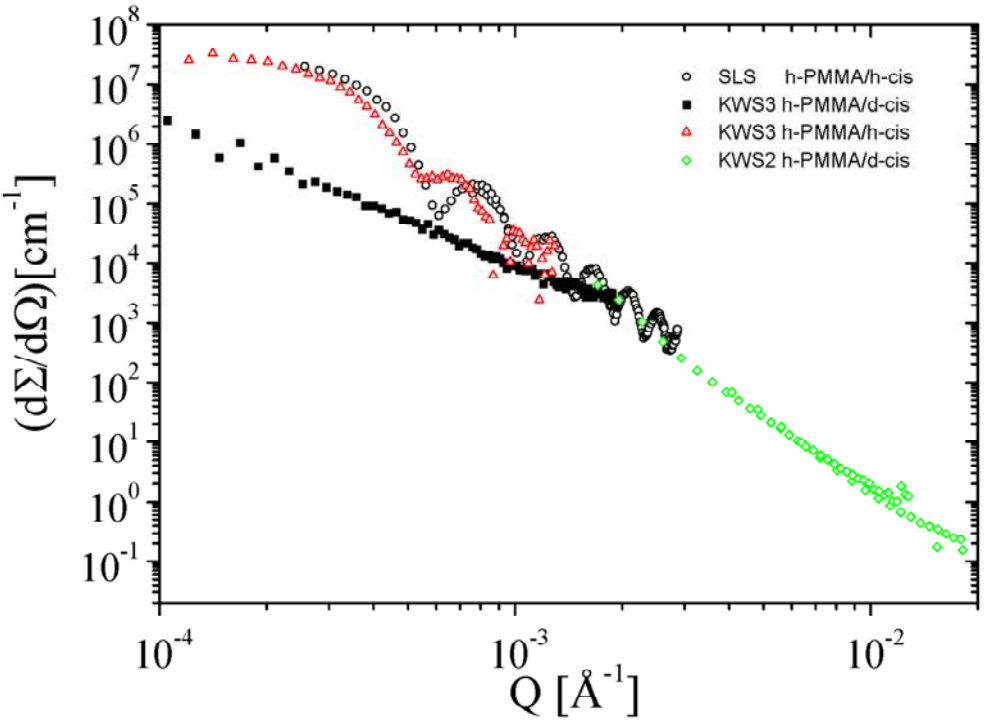

Figure 1: Intensity versus scattering vector Q of a 0.25% volume fraction solution of PMMA colloids in cis-decalin obtained from static light scattering (SLS), focussing mirror SANS (KWS3) and pinhole SANS (KWS2) using different contrasts, see text.

To summarize, these experiments have proven the expected Q-resolution for KWS3: A minimum Q-vector of 1.21×10^{-4} Å^{-1} was achieved. However, the above mentioned effects due to multiple scattering have limited data quality considerably. On the other hand, the need for a relatively low contrast to avoid multiple scattering opens the possibility to investigate sample without complicated deuteration or use of expensive deuterated solvents.

Institut für Festkörperforschung
Forschungszentrum Jülich GmbH
D-52425 Jülich

Experimental Report
of Neutron Scattering Experiments
at the FRJ-2 Reactor

Proposal number:	KW2-02-006		
Experiment title:	CRITICAL FLUCTUATIONS IN INDIVIDUAL FLUIDS CONFINED IN POROUS MEDIA		
Dates of experiment:	Sept. 12 – 15, 2002	Date of report: 10-28-2002	
Experimental team: Names	Addresses		
Y. B. Melnichenko G. D. Wignall D. R. Cole	Solid State Division ORNL P.O.Box 2008 Oak Ridge, TN 37831-6393		
Local Contact:	Dr. H. Frielinghaus		

Experimental report text body

ABSTRACT. The purpose of these experiments was to explore the effect of confinement imposed by a rigid network of aerogel on density fluctuations of carbon dioxide (CO_2) in the vicinity of liquid – gas critical point. During the September session we determined the structure of the aerogel, and studied the temperature variation of the correlation length of the density fluctuations (ξ) and intensity of scattering at zero angle I(0) of bulk and confined CO_2 at an off-critical average density ρ_C=0.597 g/cc. The results indicate that porous matrix of aerogel can reduce the amplitude of the density fluctuations and affect isothermal compressibility of confined fluid even at off-critical densities and length scales smaller than the correlation length of the aerogel $\xi_G \sim 70$ Å.

BLANK AEROGEL SANS from blank aerogel was measured over a wide range of scattering vectors 0.0025 < Q < 0.2 Å^{-1} (Fig.1). It is generally accepted that silica aerogels form mass fractal structures. We find that in the small- and intermediate Q-range I(Q) may be described by the function [1]:

$$I(Q) = \frac{I(0)}{[1+Q^2\xi_G^2]^{(D_f-1)/2}} \times \frac{\sin[(D_f-1)\tan^{-1}(Q\xi_G)]}{(D_f-1)Q\xi_G} \qquad (1)$$

where ξ_G is the gel correlation length and D_f is the fractal dimension. The dashed line in Fig.1 is the fit of Eq.1 to the data with the values of parameters $I(0)$=60 ± 1 cm^{-1}, D_f= 2.35 ± 0.15 and ξ_G = 70.6 ± 2.6 Å. The crossover to the Porod regime starts at Q ~ 0.08 Å (length scale 12 – 13 Å). The porosity (ϕ_p) and the surface area (S/V) of the aerogel determined from Porod law and the SANS invariant analysis are 96% and 275 m^2/g, respectively.

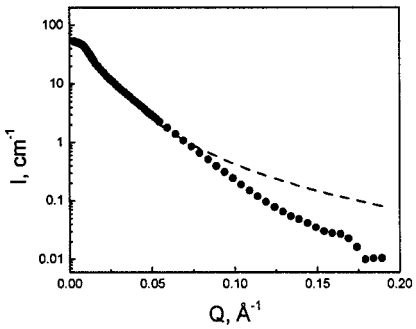

Fig. 1. Intensity of scattering from blank aerogel. The q^{-4} type of behavior, which corresponds to scattering from sharp interfaces is reached at length scales smaller than 8 Å (1/Q=0.13 Å) (from Porod law analysis).

BULK CO_2 The load parameters of the high pressure cell were T=35 C and P=1222 psi. I(Q) measured in the range 80 > T > 25 ^{O}C were fitted to O–Z structure factor to produce the correlation length ξ and I(0) at different temperatures shown in Figs 2 and 3.

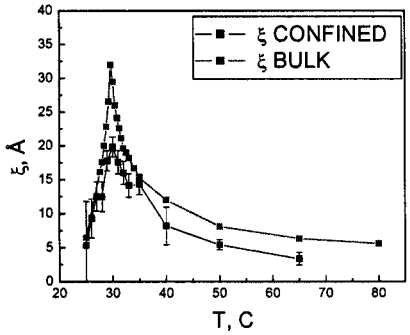

Fig.2. Temperature variation of ξ for bulk and confined CO_2.

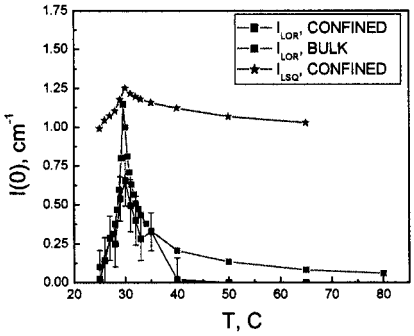

Fig.3. I_{LOR} for bulk and confined CO_2. The amplitude of the Lorentzian squared term is also shown (explanations in the text).

As is seen, although the values of both ξ and I(0) increase by about an order of magnitude as T → $T_{C,exp}$=29.4±0.02 C, the divergence of both parameters was not observed. The value of $T_{C,exp}$ is smaller than the literature value of T_C=31.1 ^{O}C. Using $T_{C,exp}$ for bulk CO_2 ($T_{C,expl}$ of the confined fluid turned out to be the same within experimental errors), it is possible to estimate the effective critical indices ν and γ for ξ and I(0), respectively. For $\xi = \xi_0|\tau|^{-\nu}$ and $I(0) = I_0|\tau|^{-\gamma}$ as a function of reduced temperature $\tau = \left|T - T_{C,\exp}\right| / T_{C,\exp}$ we obtain in the limit of τ→0: ν=0.27±0.01 and γ =0.43±0.01 (see Figs 4 and 5). The effective indices ν and γ are significantly smaller than the Ising model values ν=0.63 and γ=1.24.

The load pressure P=1222 psi which was supposed to generate the critical density of CO_2 ρ_C=0.468 g/cc was calculated using the SFE program obtained from Carbon Dioxide Center at University of North Carolina. It was later found that the program uses a simplified mean-field equation of states of CO_2 and thus generates erroneous pressures in the critical region. The correct value of pressure to generate the critical density in the cell at T=35 C, calculated using the state-of-the-art program NIST-12 is P=1171 psi. The actual density of CO_2 corresponding to P=1222 psi at T=35 C is 0.597 g/cc. Comparison with the literature data on the coexistence curve of CO_2 shows that the temperature of the liquid-gas phase separation at this density should be ~ 1.2 degree lower than the real critical liquid-gas temperature T_C=31.1 ^{O}C. The experimental $T_{C,exp}$=29.4±0.2 ^{O}C agrees with the anticipated value. The mismatch between the average and critical density of CO_2 explains why the "true" critical condition was not reached in the experiments.

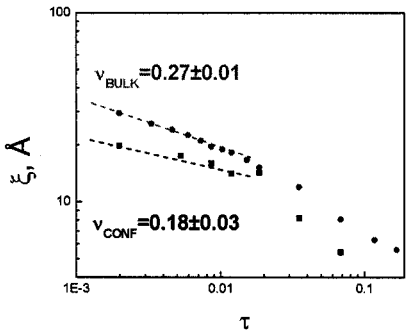

Fig.4. ξ vs. τ for bulk (●)and confined (■) CO_2 in log – log representation.

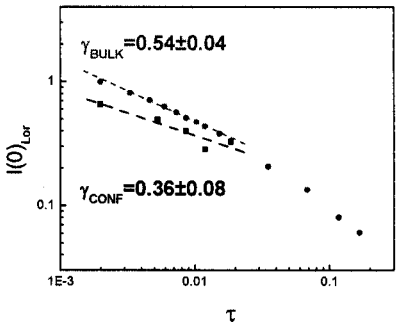

Fig.5. Amplitude of the Lorentzian for bulk (●) and confined (■) CO_2.

CONFINED CO_2 The high pressure cell containing an aerogel cylinder (Marketech, ρ=0.09 g/cc) was loaded at the same conditions as for bulk CO_2. Representative set of I(Q) is shown in Fig 6. The notable feature is the temperature variation of the intensity of scattering in the small Q-region below Q~0.3 Å which is characteristic of critical scattering. Although the absolute scattering intensity of bulk CO_2 is two orders of magnitude smaller than that from blank aerogel, the scattering from aerogel + CO_2 system is visibly temperature dependent.

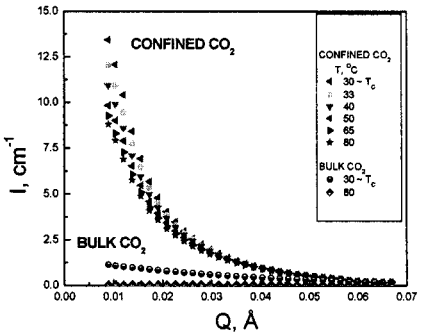

Fig.6. I(Q) for confined CO_2 taken at temperatures specified in the inset. For comparison, the intensity of scattering of bulk CO_2 at T=80 ^{O}C >> T_C (▲) and T=29.6 ^{O}C ~ T_C (◑) is also shown.

The data I(Q) for CO_2 confined in aerogel were fitted to the function, similar to that used in [2] to fit temperature variation of I(Q) from silica gel saturated with *binary solution* near liquid-liquid critical point:

$$I(Q,T) = \frac{I_{LOR}(T)}{1+Q^2\xi^2} + \frac{I_{LSQ}(T)}{(1+Q^2\xi^2)^2} I(Q,T=80)_{BGR} \qquad (2)$$

The first (Lorentzian) term in the right hand side of Eq. 2 is identical to O-Z structure factor. This term represents the scattering from critical fluctuations of CO_2 in pores. The second (Lorentzian squared) term arises from the static response of the system to the „random field" introduced by the aerogel network. Its amplitude I_{LSQ} is proportional to the „response function" α(Q,T), characterizing the response of the order parameter (density in this case) to the perturbing field imposed by the aerogel. I_{BGR} represents the "background" scattering which is I(Q) for CO_2 saturated aerogel at T=80 C >> T_C at which density fluctuations of the fluid are minimal (ξ ~ 5 Å and I(0) ~ 0.06 cm^{-1}, Fig. 6). The Eq.2 is similar to responses predicted by the RFIM for Ising antiferromagnets as well as for fluids in porous networks based on extensions of the RFIM [3]. The results of fitting the experimental data for confined CO_2 to Eq.2 are shown in Figs. 2 and 3. As is seen, the values of ξ and I(0) of confined CO_2 are systematically smaller than those of the bulk fluid. The temperature variation of the correlation length and isothermal compressibility with τ is weaker (compare the effective critical indices in Figs 4 and 5). Thus, even though the true critical condition was not reached in this experiment, there is an indication that the porous matrix of aerogel can affect the thermodynamics of confined fluid even on the length scales below the correlation length ξ_G of the gel. The difference between ξ of bulk and confined fluid should become more pronounced near the true critical liquid – gas demixing point of the confined fluid.

PRELIMINARY CONCLUSIONS:

1. The results demonstrate feasibility of experiments with confined individual fluids in SiO_2-based porous matrices. Despite the fact that the scattering intensity of aerogel exceeds that from CO_2 by about two orders of magnitude, the temperature variation of thermodynamic parameters of confined fluids can be extracted and explored.
2. The variation of ξ and I(0) of the confined fluid with τ is more retarded in compare to that in bulk. The ratio of ξ_{conf}/ξ_{bulk} is ~ 0.7, which is quite different from ξ of confined binary liquid solutions, where ξ_{conf} is the same as ξ_{bulk} [2].This effect should become more pronounced near the "true" critical temperature of confined fluids. Such experiments may be used for checking the predictions of RFIM, finite size scaling, and other theoretical approaches.
3. Both ξ and I(0) increase and than decrease below T_C, as in bulk. This behavior is also quite different from that observed in binary liquid solutions confined in Vycor [4] and/or aerogels [2], where fluctuations increase and that get pinned around T_C. Preliminary analysis suggests that we are dealing with the liquid-gas demixing when the liquid phase of CO_2 gets condensed on the strands of the aerogel. Back-of-the-envelope calculations show that liquid molecule condensate at T=25 C < T_C formed on the surface of the aerogel with S/V=275 m^2/g is a liquid film with the thickness of about four molecular diameters. The liquid-gas phase separation may become macroscopic at elevated densities, when the volume of the liquid phase is large enough to allow for macroscopic condensation. The crossover to macroscopic liquid-gas phase transition along with possible hysteresis effects may be explored in future experiments.

REFERENCES

1 T. Freltoft, J.K. Kjems, S. K. Sinha, Phys. Rev. B 33, 269 (1986).

2 B.J. Frisken, D. S. Cannell, M. Y. Lin, S. K. Sinha, Phys. Rev. E, 51, 5866 (1995).

3 P. G. de Gennes, J. Phys. Chem., 88, 6469 (1984).

4 M. Y. Lin et al., PRL, 72, 2207 (1994).

Institut für Festkörperforschung
Forschungszentrum Jülich GmbH
D-52425 Jülich

Experimental Report
of Neutron Scattering Experiments
at the FRJ-2 Reactor

Proposal number:	KW2-02-007		
Experiment title:	**Project "Shear induced brush deformation in polymer micelles" :** **PEP-PEO micelles in solutions of PEO oligomer /D_20 mixture**		
Dates of experiment:	07.03.02	Date of report:	09.03.03
Experimental team: Names	Addresses		
Philippe Carletto Silke Rathgeber Jan K.G. Dhont Dieter Richter Lutz Willner	Forschungszentrum Jülich GmbH Institut für Festkörperforschung – Weiche Materie D-52425 Jülich Forschungszentrum Jülich GmbH Institut für Festkörperforschung – Neutronenstreuung D-52425 Jülich		
Local Contact:	Henrich Frielinghaus		

Experimental report text body

The project focuses on the investigation of shear induced brush deformation of diblock copolymer micelles in solution with small angle neutron scattering.

The attractive van-der-Waals interaction between colloids can be screened by grafting or absorbing polymers onto the colloid surface. This leads to a stabilization of the colloidal suspension. Depending on the layer thickness, the solvent quality and the grafting density the interaction potential can be easily varied between hard-sphere interactions and the longer ranged (softer) potential of star polymers.
We are particularly interested into the phenomenon of "shear band formation" [1]. In various systems that contain mesoscopic entities, a hydrodynamic instability may be induced when a sufficiently strong shear flow is applied, leading to a stationary state where regions of different microstructure and/or shear-rates coexist. In a cylinder geometry, shear-banding leads to either band formation in the vorticity direction or along the gradient direction, depending on whether the stress as a function of the shear-rate is a multi-valued function or is of a van-der-Waals loop like form, respectively. Jan Vermant et al. [2] observed shear-band formation along the vorticity direction for a system of "hairy" colloids in a low viscosity solvent at high colloid concentration (40vol%). Neither the microstructure in the two phases nor the mechanism that leads to the phase separation are yet known. A possible explanation might be that the shear-induced polymer brush deformation may render the van-der-Waals attractions in certain directions unshielded, which could lead to a "thermodynamic instability". This instability is of thermodynamic nature, but is induced by shear-deformation of the brush. So the knowledge of how the polymer brush is deformed under the influence of applied shear is essential for the understanding of shear band formation.

Therefore the aim of this project is to measure the form factor of hairy colloids under shear with small angle neutron scattering.

As model system for hairy colloids we have chosen polyethylene-propylene-polyethyleneoxide (PEP-PEO) block copolymers micelles in water, with PEP as micellar core and PEO as corona. In figure 1 the SANS spectrum for a sheared PEP-PEO solution (c=1wt%) is plotted versus q (a) for the axes parallel || and (b) perpendicular ⊥ to the flow direction. The solid lines show the result of a fit with a model that was already successfully applied to the unperturbed micelles [3]. We derive for the ratio of the overall micelle radii parallel ($R_{\|}$) and perpendicular ($R_{\perp}$) to the flow direction: $R_{\|} / R_{\perp} = 1.10$ – the micelles are slightly elongated in flow direction.

The deformation of the micelle should only be visible in an insitu-rheological experiment if the longest internal relaxation rate γ, which is proportional to the viscosity of the solvent η, is of the order of the inverse of the applied shear rate. Therefore increasing the viscosity of the solvent, for example by adding PEO oligomer should lead to a stronger deformation of the brush. We used mixtures of 40wt% protonated PEO oligomer (Mw=600g/mole) and 60wt % D_2O for our shear experiment. At a temperature of 10°C the viscosity of the mixture is with η=17mPas significantly higher than that of pure water. In figure 2 the SANS spectrum for the sheared sample at a concentration of c=1wt% is plotted. The micelles formed in the oligmer- D_2O mixture are almost a factor two smaller than those formed in pure D_2O. However, a stronger deformation is not observed: $R_{\|} / R_{\perp}$ is with 1.15 of the same magnitude for both systems.

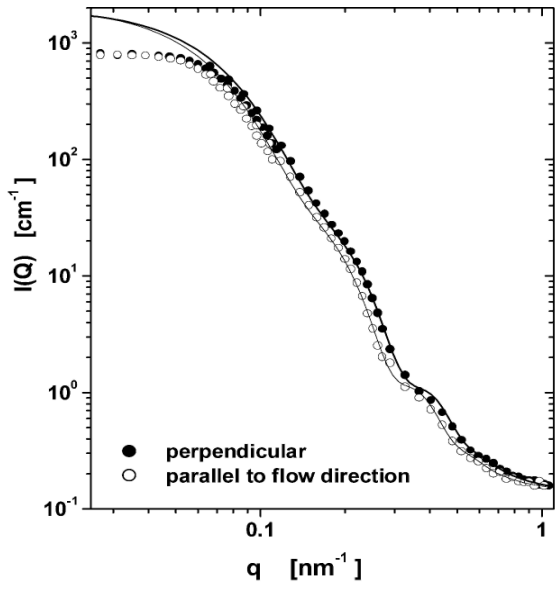

Fig. 1: SANS spectrum of a sheared PEP-PEO diblock-copolymer micelles in D_2O.

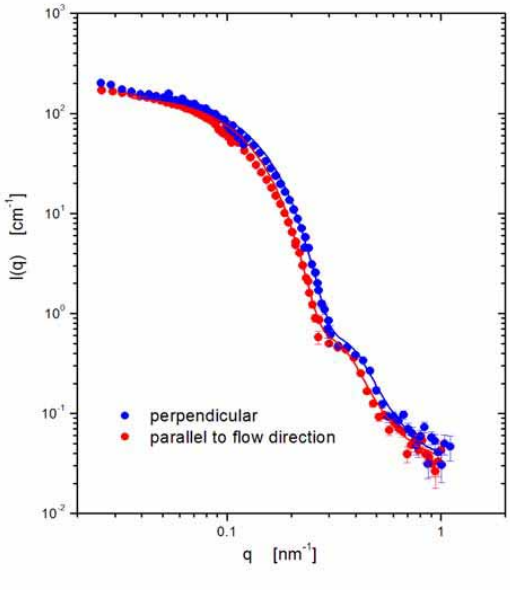

Fig. 2: SANS spectrum of a sheared PEP-PEO diblock-copolymer micelles solved in a mixture of 40wt% PEO oligomer and 60wt% D_2O.

References:

[1] J.K.G. Dhont, Phys. Rev. E 60 (1999) 8804.

[2] J. Vermant, J. Coll. Int. Sci. 211 (1999) 221.

[3] L. Willner, A. Poppe, J. Allgaier, M. Monkenbusch, P. Lindner and D. Richter, Europhys. Lett., 51 (2000) 628.

Institut für Festkörperforschung
Forschungszentrum Jülich GmbH
D-52425 Jülich

Experimental Report
of Neutron Scattering Experiments
at the FRJ-2 Reactor

Proposal number:	KW2-02-008		
Experiment title:	**Absoluteichung mit der „direct-beam“ Methode**		
Dates of experiment:	01.05.02 + 03.05.02	Date of report:	05.03.03
Experimental team: Names	Addresses		
Henrich Frielinghaus	Forschungszentrum Jülich GmbH IFF 52425 Jülich		
Local Contact:	Henrich Frielinghaus		

Experimental report text body

Die Einzigartigkeit von Neutronen liegt unter anderem in der Möglichkeit, Kleinwinkelstreudaten absolut zu eichen. Dazu bedarf es im allgemeinen eines Eichstandards. In Jülich wird hierfür eine 2mm dicke Lupolen-Platte verwendet, einem Polyethylen mit niedriger Dichte also geringer Kristallinität. Nach einem Besuch von G. Wignall jedoch wurde dieser Eichstandard in Frage gestellt. Darüber hinaus wurde Lupolen nur für 7Å Neutronen geeicht, und der weite Bereich zwischen 4.7Å und 13.5Å sollte ausgefüllt werden.

Eine ganz andere Methode, Kleinwinkelstreudaten absolut zu eichen, besteht darin, mit der Probe den Primärstrahl (direct beam) mitzumessen. Der Trick besteht darin, daß der Primärstrahl einfach die um die Transmission T der Probe abgeschwächte Primärintensität I_0 vor der Probe multipliziert mit der ausgeleuchteten Fläche A ist ($I_{primär} = I_0 \cdot A \cdot T$). Man muß nur einen geeigneten Abschwächer vor die Probe stellen, damit der gemessene Primärstrahl ein nicht zu starkes Signal auf dem Detektor bildet. Als Probe für diese Eichung wurde ein Diblock-Copolymer verwendet, weil das gelieferte Signal gering bei kleinen Streuvektoren Q ist, und ein deutlicher Interferenz-Peak (Debye-Scherrer-Ring) bei einem bestimmten $Q = 0.032 Å^{-1}$ auftritt.

Der differentielle makroskopische Streuquerschnitt $d\Sigma/d\Omega$ für das Diblock-Copolymer wird nun nach folgender Formel berechnet.

$$\frac{d\Sigma}{d\Omega} = \frac{\Delta I}{\Delta\Omega} \frac{1}{I_0 \cdot A \cdot d \cdot T}$$

Hierbei ist d die Dicke der Probe, ΔI die gemessene gestreute Intensität des Diblock-Copolymers, und $\Delta\Omega$ der Raumwinkel eines Detektor-Kanals.

Bei gleicher Konstellation (ohne Abschwächer, aber mit beam-stop) wird dann das Diblock-Copolymer nochmals vermessen. Den makroskopischen Streuquerschnitt hierfür kennt man ja jetzt. Dann wird im Vergleich hierzu bei gleicher Konstellation (aber kurzem Detektorabstand, 2m) das Lupolen vermessen. Die allseits bekannte Formel der Absoluteichung

$$\frac{d\Sigma}{d\Omega} = \frac{\Delta I}{\Delta\Omega}\frac{1}{d\cdot T}\frac{\mu_L}{\Delta I_L/\Delta\Omega}\left(\frac{D_P}{D_L}\right)^2$$

kann nun nach $\mu_L = d_L \cdot T_L \cdot d\Sigma/d\Omega$(von Lupolen) aufgelöst werden, da der makroskopische Streuquerschnitt links bekannt ist. Die nicht speziell indizierten Meßgrößen beziehen sich auf das Diblock-Copolymer ($d\Sigma/d\Omega$, $\Delta I/\Delta\Omega$, T, d), und mit L indizierten Meßgrößen beziehen sich auf das Lupolen. Das Verhältnis der Detektorabstände D_P/D_L bezieht den Raumwinkelunterschied für die unterschiedlichen Messungen des Diblock-Copolymers und des Lupolens mit ein. Eine Totzeitkorrektur wurde für alle Messungen gemacht.

Das für verschiedene Wellenlängen bestimmte μ_L ist in Abbildung 1 dargestellt. Man sieht, daß μ_L mit steigender Wellenlänge abnimmt. Dies spiegelt die höhere Streuwahrscheinlichkeit bei kleinen Wellenlängen wieder.

Erstaunlich ist, daß der von Schwahn angegebene Wert von $\mu_L = 0.0734$ für 7Å nach oben korrigiert werden muß auf 0.0804 (zumindest für die KWS-2). Der Grund könnte in der unterschiedlichen Empfindlichkeit auf inelastisch gestreute Neutronen beider Detektoren liegen (KWS-1 und KWS-2).

Zusammenfassend kann gesagt werden, daß die „Direct-Beam“ Methode eine sehr genaue Absoluteichung mit hoher Reproduzierbarkeit liefert.

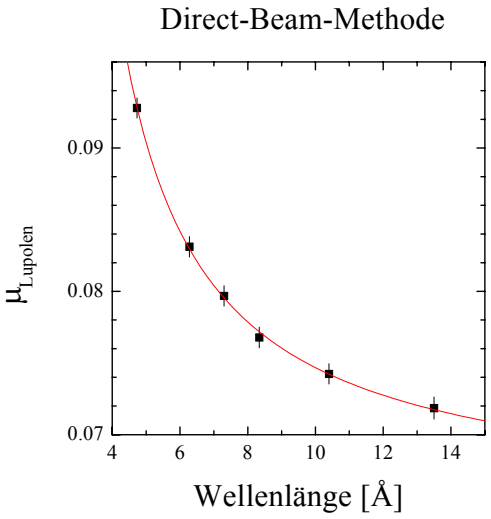

Abbildung 1: Die aus der „Direct-Beam“ Methode bestimmten μ_L.

Institut für Festkörperforschung
Forschungszentrum Jülich GmbH
D-52425 Jülich

Experimental Report
of Neutron Scattering Experiments
at the FRJ-2 Reactor

Proposal number:	KW2-02-009		
Experiment title:	**Polyisoprene: A feasibility study**		
Dates of experiment:	10.05.2002 – 12.05.2002	Date of report:	08.03.2003
Experimental team: Names	Addresses		
Ohl Michael Frielinghaus Henrich	Forschungszentrum Jülich GmbH, D - 52425 Jülich Forschungszentrum Jülich GmbH, D - 52425 Jülich		
Local Contact:	Henrich Frielinghaus		

Experimental report text body

Within this experiment Polyisoprene (PI) a glass forming polymer has been studied. PI with a glass transition temperature T_g =213K is in many aspects a rather particular polymer so people intend to interpret phenomena in this material as a peculiarity of Polyisobutylene and were motivated to study polyisoprene in the neighborhood of the first static structure factor peak and in the intermediate length scale. To obtain pure signals in the intermediate length scales PI has been investigated in this region at first by SANS before starting any dynamic measurements on those samples. The measurement of the small angle neutron scattering signal at first at KWS2 and in the second step at D22 should serve to confirm multiple scattering calculations for the correction of the multiple scattering signal which takes place in the low Q-region up to 0.5Å^{-1} and to check the samples quality. Additional NSE measurements at IN11 and IN15 have been performed after this experiment has been finished.

Measurements have been performed with fixed collimator-sample and detector-sample distances of about 2m and 1.4m at temperatures between 253K and 353K and wavelengths from 6 Å to 13 Å in a standard HELLMA sample container with a thickness of about d = 2mm and a samples molecular weight of about 100k. As “references” lupolene, boron carbide and an empty cell have been measured during the experiment, too.

In general and especially for not perfectly deuterated polymers the static structure factor sits on a relatively high background which relates partly to incoherent and partly to multiple scattering. In polyisobutylene (PIB) and in the intermediate Q - region the signal also can be assigned to the stress relaxation [1].

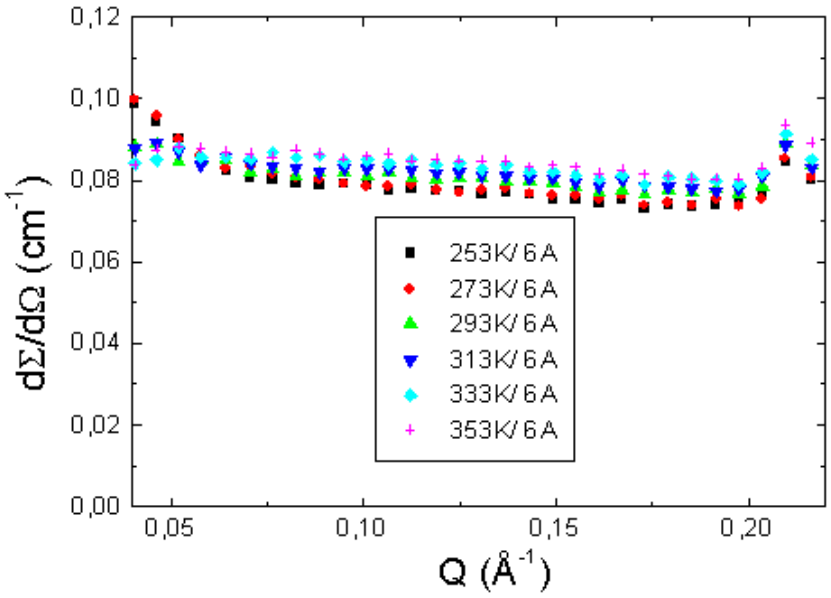

Fig. 1: Differential scattering cross section measured for deuterated PI by means of the small angle scattering instrument KWS2 at λ=6Å for different temperatures between 253K<T<353K.

However, here we observed a rather flat plateau for different wavelengths at low Q – values which are limited by the Q–values at Q=0.05Å^{-1} and Q=0.2Å^{-1}, respectively (see Fig. 1). With increasing temperature the plateau level of the differential cross section increases slightly. At this wavelength multiple scattering effects should be at a maximum level. In calculations we determined a ratio of 1/3 between the absolute value in the differential scattering cross section and the multiple scattering assuming a wavelength of about λ=6Å and a degree of deuteration of 97.7%. However no significant temperature dependencies of the plateau level have been observed beside the approximately linear dependence of the DWF.

Additionally, the small angle scattering signal has been measured for several wavelengths at room temperature. Whereas the scattering signal remains rather flat at 0.1Å^{-1}<Q<0.5Å^{-1} for wavelengths between 5Å and 20Å indicating that no further scattering contribution arises from impurities in the sample which gave hints to the high quality of the sample. Additional effects for plateau levels at different wavelengths as found for example for Polyisobutylene (PIB) were investigated, too in which a minimum of the wavelength dependent plateau level has been observed (see Ref. [1]).

Subsequently measurements at the NSE spectrometer IN11 and IN15 had been performed to observe the dynamical behavior over the whole accessible Q - range using the taking this sample into account. These new experiments also focused on the intermediate length scale dynamics showed that this almost unexplored area retains unexpected phenomena. For instance, in the NSE experiment on Polyisoprene the collective dynamics in the intermediate length scales and at the structure factor peak behaves quite similar in temperature and further experiments will be performed at the NSE spectrometer IN11 and IN15 within the next months to confirm unambiguously this bifurcation of the thermal behavior.

[1] B. Farago, A. Arbe, J. Colmenero, R. Faust, U. Buchenau and D. Richter, ”Intermediate Length Scale Dynamics of Polyisobutylene“, Phys. Rev. **E 65**, 051803 (2002).

Institut für Festkörperforschung
Forschungszentrum Jülich GmbH
D-52425 Jülich

Experimental Report
of Neutron Scattering Experiments
at the FRJ-2 Reactor

Proposal number:	KW2-02-010		
Experiment title:	Structure factor of star-like PEP-PEO block copolymer micelles		
Dates of experiment:	4.03.02-6.03.02	Date of report:	6.03.03
Experimental team: Names	Addresses		
Laurati, Marco Stellbrink, Jörg Willner, Lutz	IFF, FZ Juelich IFF, FZ Juelich IFF, FZ Juelich		
Local Contact:	H. Frielinghaus		

Experimental report text body

The investigation of the core-core structure factor of PEP1-PEO20 (the number denotes the molecular weight in kg/mol) star-like micelles was performed as a function of polymer concentration. In particular the concentration region around the overlap concentration c* (≈ 4%) has been investigated. We measured a concentration series of partially labeled micelles ranging from 2% to 8% polymer volume fraction in D_2O, a total of eight samples. The labeling was used to contrast match the PEO shell with the solvent, in order to observe the pure core-core scattering contributions.
At sufficiently low concentrations the scattered intensity results to be proportional to the product of the intramicellar structure factor (or form factor), P(Q), and the intermicellar structure factor, S(Q). Moreover at very low concentrations the intermicellar correlations can be neglected (S(Q)=1) and the intensity is only proportional to P(Q). To obtain S(Q) we divided out a SANS measurement of the micellar form factor, performed with a very dilute sample, 0.25% polymer volume fraction in D_2O. We should observe that since the core is constituted by PEP, a very rigid polymer chain, we assume that the core-contrast form factor is concentration indipendent.
All the measurements were performed at room temperature.

The measured intensities (fig.1) show a strong concentration dependence of the structure factor peak, with a discontinuous transition around the overlap concentration c*. A theoretically calculated phase diagram for star polymers predicts a liquid to solid phase transition at about c* [1]. Nevertheless recent improvements of the theory show that the ideal glass transition line runs parallel to the fluid-crystal coexistence line in the phase diagram and the fluid-crystalline phase transition should take place in a very narrow region around c* [2]. The structure factor peaks (fig.2) we obtained for polymer concentrations above c* are well below the value expected for a crystalline phase, namely 2.8 [3].

This should mean that we already entered the glass phase region. Macroscopically we observe a liquid phase to a metastable gel phase transition crossing the overlap concentration c*, in agreement with the SANS results.
The upturn that one can observe at low Q might result from the vicinity to a phase boundary (critical scattering), or from inhomogeneities in the gel. Further investigation is required.
A delicate point in the structure factor determination is the form factor division. Directly dividing out the experimental data might supply a "scattered" structure factor, which becomes difficult to compare with theory. The division of a model fitted form factor is in principle better. In our case considering a spherical compact core an hard sphere form factor should model properly the experimental data. We find instead that the assumption of a shell contribution, *i.e.* a core-shell model, is necessary to obtain a good fit of the measured form factor. Since a variation of the PEO scattering length density in solution can't be completely excluded, this could mean that pure D_2O is not exactly matching the shell scattering.
A very accurate contrast variation analysis is then needed in order to find the exact matching point of the shell. The structure factor peaks shown in fig.2 are obtained directly dividing out the experimental form factor.

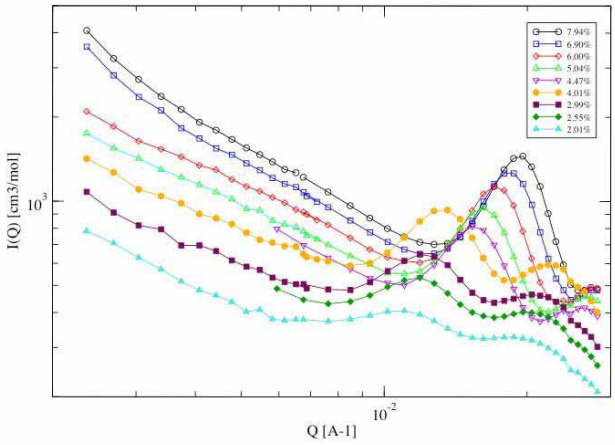

Figure 1 : SANS intensities (core-contrast) of PEP1-PEO20 micelles measured in the concentration range 2%-8%.

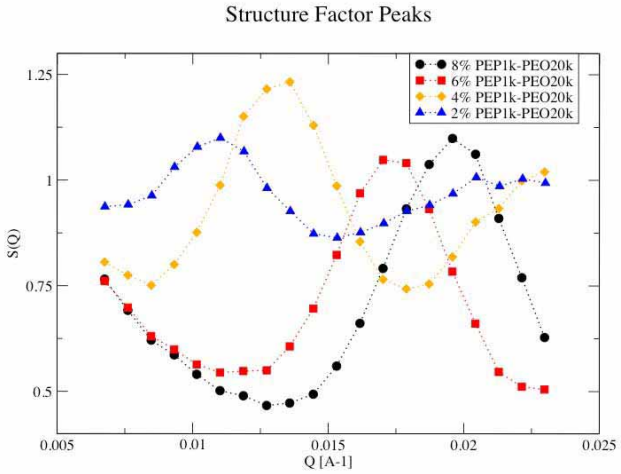

Figure 2 : Selected Structure Factor Peaks at different polymer volume fractions

1. M. Watzlawek, C.N. Likos, H. Löwen**,** *Phys. Rev. Letters,* **82**, 5289 (1999).
2. G. Foffi, F. Sciortino, P. Tartaglia, E. Zaccarelli, F. Lo Verso, L. Reatto, K.A. Dawson, C.N. Likos, In Press.
3. J.P. Hansen, L. Verlet, *Phys. Rev.*, **184**, 151 (1969).

Institut für Festkörperforschung
Forschungszentrum Jülich GmbH
D-52425 Jülich

Experimental Report
of Neutron Scattering Experiments
at the FRJ-2 Reactor

Proposal number:	KW2-02-011		
Experiment title:	Determination of form factors of h-PEP-1K-d,h-PEO-20K micelles in water and water/DMF mixtures by contrast variation experiments		
Dates of experiment:	6.06.02-7.06.02	Date of report:	6.03.03
Experimental team: Names	Addresses		
Willner, Lutz Laurati, Marco Stellbrink, Jörg Lund, Reidar	IFF, FZ Juelich IFF, FZ Juelich IFF, FZ Juelich IFF, FZ Juelich		
Local Contact:	H. Frielinghaus		

Experimental report text body

Star polymers have been intensively studied within our group during the last years as a new class of *ultra soft* colloids[1]. To avoid synthesis problems that occurr with high functionality star polymers, we recently started using PEP-1K-PEO-20K diblock copolymer micelles. For large block asymmetries these micelles behave as unimolecular star polymers and can be easily prepared in desired molecular weight and composition[2,3,4].

In the scheduled beam-time we started to perform a contrast variation analysis of the form factor of partially labeled PEP-1K-PEO-20K block copolymer micelles in water. The goal was obtaining the pure core contrast form factor, that is crucial to extract the core-core structure factors from concentrated samples. In detail we measured the form factor in three different contrasts; 0.25% polymer volume fraction samples in pure D_2O, 98% D_2O – 2% H_2O and 96% D_2O – 4% H_2O, together with solvents. We measured the samples at 2 and 8m detector distances and at room temperature, with a wavelength of 7 Å, in order to investigate the appropriate Q range. In fact with the selected solvents we are in the PEP core contrast region, and the core dimension is about 40 Å as obtained from previous measurements.

The form factors after correction for the experimental background and solvent subtraction are shown in fig.1. The intensity are normalized to the polymer volume fraction and the contrast, and multiplied by the Avogadro number. Since we were expecting a low scattering intensity resulting from the small amount of polymer we measured the samples for 150 minutes at 8m detector distances; the spectra show that the measurement time was not sufficient to obtain good statistics. It seems that the increasing content of H_2O reduces the upturn at low Q values, that should be due to a shell contribution. Anyhow the data are not good enough to be sufficiently confident. Further measurements performed for longer times are needed.

1. G.S. Grest, L.J. Fetters, J.S. Huang, D. Richter, *Adv. Chem. Phys.*, **94**, 67 (1996).
2. Poppe, L. Willner, J. Allgaier, , D. Richter, *Macromolecules*, **30**, 7462 (1997).
3. L. Willner, A. Poppe , J. Allgaier, M. Monkenbusch, P. Lindner, D. Richter, *Europhys. Lett.*, **51**, 628 (2000).
4. L. Willner, A. Poppe , J. Allgaier, M. Monkenbusch, D. Richter, *Europhys. Lett.*, **55**, 667 (2001).

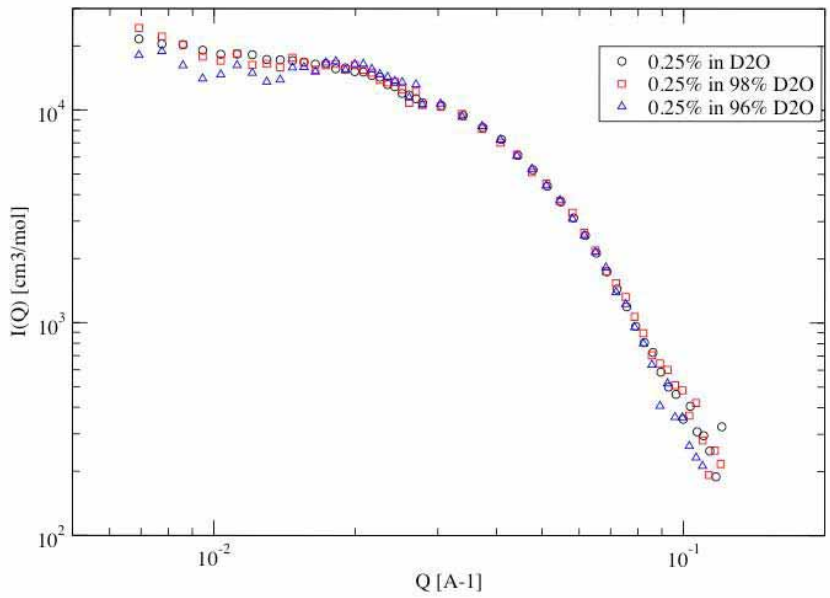

Institut für Festkörperforschung
Forschungszentrum Jülich GmbH
D-52425 Jülich

Experimental Report
of Neutron Scattering Experiments
at the FRJ-2 Reactor

Proposal number:	KW2-02-012		
Experiment title:	**Chain Exchange kinetics of Polymeric Micelles consisting of PEP-PEO in a DMF/Water Solvent Mixture**		
Dates of experiment:	02-05/06-02	Date of report: 05/03-03	
Experimental team: Names	Addresses		
Reidar Lund Dr. Lutz Willner Dr. Aurel Radelescu Prof. Dieter Richter	Forschungszentrum Jülich; IFF-Institut für Neutronenstreuung D-52425 Jülich		
Local Contact:	Henrich Frielingshaus		

Experimental report text body

A successful adaptation of the time resolved SANS technique to study micelle kinetics was carried out on a specific system. This project is a continuation of a project originally initiated by Willner et. al.[1] involving studies of chain exchange kinetics in polymeric micellar systems by time resolved SANS. The method is based upon mixing hydrogenated and deuterated polymer/micelle solutions and following the change in intensity by time resolved SANS. For details see ref. [1] The polymer we studied was PEP1-PEO20 (the numbers indicate the molecular weight in kg/mole). Firstly contrast variation measurements were performed yielding an optimal isotopic composition of H_2O/D_2O (optimal solvent scattering length density), i.e. the zero average scattering length density which can give the maximal contrast between the initial and final state in a kinetic measurement. This was necessary to have a sufficient time resolution in the kinetic measurement. As it came out this zero average solvent scattering length density slightly deviates from the one calculated theoretically. This may be due to uncertainties in molecular weight, density and the degree of deuteriation of the polymers etc. The issue is also complicated by formations of solvent shells (hydration layers) as described by Poppe et al. [2], however we found no indication of this and introduction of a "hydration factor", f, was not necessary to describe the data.

Furthermore, structural investigations, in the whole accessible Q-range, were carried out at both the fully deuterated polymer and its hydrogenated counterpart abbreviated dd-PEP_PEO and hh-PEP-PEO respectively. The scattering curve could be satisfactorily fitted to a core shell model with a star-like corona density profile. This gave important information of the structure characteristic, i.e. aggregation numbers, micelle radius, etc.

In water, we did not observe any chain exchange, i.e. no detectable change in intensity, even when the system was heated to high temperatures and after long times. This is possibly due to the high interface tension (≅ 51 mN/m) between the PEP- block and water. In order to increase the rate, we introduced a co-solvent,

, dimethylformamide DMF, which has a lower incompatibility for PEP and in addition will serve to break up the water structure leading to a reduced entropy penalty associated with the transfer of an unimer from a micelle to the bulk When the polymer was immersed in pure DMF we did not observe any aggregation. Thus by introducing different amounts of DMF, in water, we could tune the solvent quality and the aggregation properties (including the kinetics) of the polymers. The structural investigations of the dd-PEP-PEO and the hh-PEP-PEO. revealed that both the aggregation number and the micelle size decrease upon increasing amounts of DMF in an aqueous solution (See example in fig. 1.). After increasing the amounts of DMF up to a mole fraction (X_{DMF}) between 0.2 and 0.5, we found an appropriate kinetic time-window where measurements could be performed by time resolved SANS. We carried out kinetic measurements on the PEP1-PEO20 system in DMF/water at two compositions (X_{DMF} = 0.25 and 0.30) at four different temperatures. To reflect the chain kinetics, the square of the excess intensity due to the lack of homogeneity, i.e. $(I(t)-I_{oo})^{1/2}$, I(t) total integrated intensity, I_{oo} blend intensity, was plotted as a function of time (Some examples are displayed in fig 2.), we can see a decay in the reduced intensity which cannot be solid lines display fits of a two mode relaxation model (a sum of two exponentials). This model has previously been reported to well describe the relaxation behaviour in these kind of systems [2]. This give an indication that there are two processes of chain exchange occurring on a relatively well separated time scale. The fastest process has been assigned to a simple single chain expulsion/insertion mechanism but the explanation for the slow one remain less clear. However a close look at the data reveals that the fits are not completely satisfactorily. Deviations can be seen, especially prominent at longer times. However introducing a one or two stretched exponentials improves the fit but the physical explanation for the underlying mechanism becomes even more difficult. Additionally the fits get more unstabl

Fig. 1. Aggregation Number

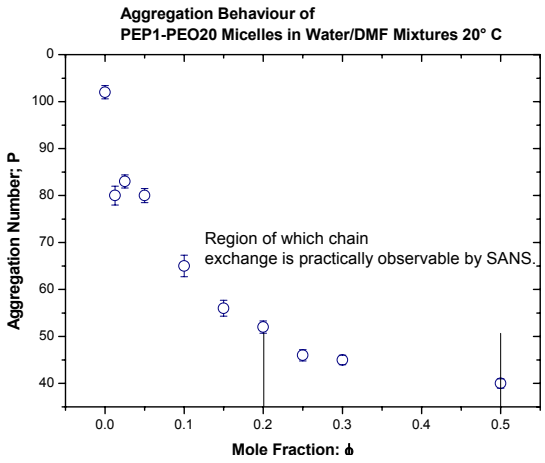

Fig. 2. Relaxation Behaviour

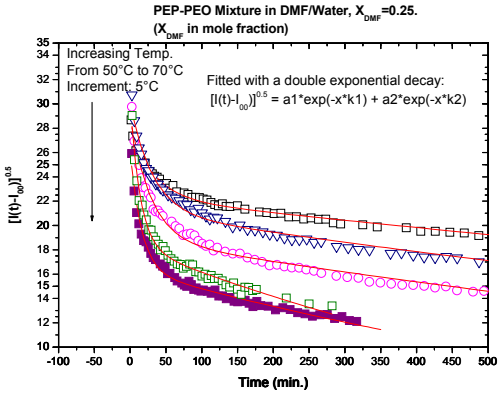

References:

1. Willner, L.; Poppe, A.; Allgaier, J.; Monkenbusch, M.; Richter, D. *Euro Phys. Lett.* **55**, (2001), 667

2. Poppe, A.; Willner, L.; Allgaier, J.; Stellbrink, J.; Richter, D. *Macromolecules* **30**, (1997), 7462

Institut für Festkörperforschung
Forschungszentrum Jülich GmbH
D-52425 Jülich

Experimental Report
of Neutron Scattering Experiments
at the FRJ-2 Reactor

Proposal number:	KW2-02-013		
Experiment title:	**Reaction-induced Phase Separation**		
Dates of experiment:	02/07/02 – 03/07/02	Date of report:	26/02/03
Experimental team: Names	Addresses		
Nigel Clarke Gordon Emmerson Chris Hill	Department of Chemistry, University of Durham, Durham, DH7 8UE ICI Strategic Technology, Wilton Centre, Middlesbrough TS90 8JE Department of Chemistry, University of Durham, Durham, DH7 8UE		
Local Contact:	Henrich Frielinghaus		

Experimental report text body

(Please use 12 pt letters here !)

We have studied mixtures of deuterated methylmethacrylate (d-MMA) and chlorosulphonated-polyethylene (CSPE). This is a simplified model system for commercial adhesives, utilised in the bonding of aluminium. By further mixing the blend with an initiator and accelerator the d-MMA undergoes free radical polymerisation. Such multi-component systems are initially homogenous, but the increase in molecular weight of the polymerising component results in phase separation, leading to a two-phase morphology. The type of morphology that develops, and the typical size scale associated with it, largely dictate the final properties of the adhesive.

Phase separation may occur by either spinodal decomposition or nucleation and growth. The former results in a co-continuous morphology, whilst the latter leads to a particulate morphology. Electron microscopy (both SEM and TEM) performed on the final, fully vitrified, material indicate a morphology with a typical length-scale of ~100nm. However, due to poor contrast, the exact nature of the morphology was unclear. Scattering techniques are ideal for complementing microscopy, and have the advantage that time resolved studies might be performed - in order to gain a complete understanding of the underlying process it is important to follow the dynamics of phase separation. Small-angle light scattering (SALS) is known to be an excellent method for following spinodal decomposition in particular; however, SALS is unsuitable for our MMA/CSPE samples due to the length-scales involved (indeed the samples remain transparent throughout the polymerisation process). We have previously performed SAXS experiments on a range of blends (with differing MMA/CSPE ratios). In all samples, some time into the polymerisation process, a shoulder, corresponding to length-scales of ~60nm, appeared which then grew in intensity.

However, there are two major problems that prevent detailed analysis of the X-ray data; firstly, X-rays initiate free radical polymerisation. Secondly, the main development in the scattering also occurred at values of *q* very close to the beam-stop, resulting in difficulties in extracting the scatter due to the sample from that due to the sample container (which has strong excess scattering at very low *q*). It was also not possible to quantify the dynamics of the phase separation due to variations between samples.

KWSII was found to be an excellent tool for probing the phase separation in these mixtures. The background on KWSII was negligible and the neutrons do not, of course, interfere with the chemical reactions. The intensity was such that we were able to perform dynamic experiments, by taking 'snapshots' of the scattering curves over a five minute period. We were able to firstly verify that the general trends observed in the SAXS experiments were real effects, but more importantly the SANS data has enabled us to undertake quantitative calculations. Phase separation manifested itself as a peak in the scattering curve, whose intensity increased with time. Whilst the breadth of the peak also increased with time, the position of the peak remained constant. This suggests that the average length-scale of the phase separation remains constant although the distribution of sizes broadens.

An example series of time-dependent scattering is shown below. Each successively higher peak represents scattering measurements at 5 minute intervals (with each measurement performed for 5 minutes). The quality of the data is excellent, with the appearance and growth of structures clear. In particular, the shoulder at higher q observed to appear at later times, is distinct and must be related to some physical phenomenon – we are in the process of understanding the physical origin of this feature.

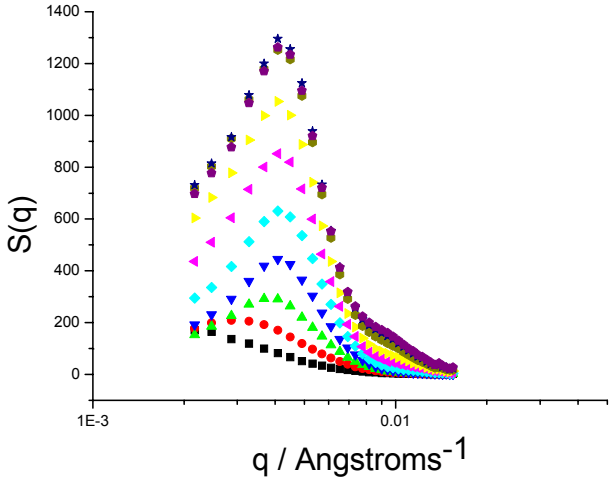

The data will be analysed in terms of phase separation theory, from which we will be able to determine growth rates and colective diffusion coefficients.

Institut für Festkörperforschung
Forschungszentrum Jülich GmbH
D-52425 Jülich

Experimental Report
of Neutron Scattering Experiments
at the FRJ-2 Reactor

Proposal number:	KW2-02-014		
Experiment title:	**WATER SOLUBLE LIQUID CRYSTALS: NEW RIGID SYNTHETIC POLYELECTROLYTE SOLUTIONS**		
Dates of experiment:	July 02	Date of report: 13/10/02	
Experimental team: Names	Addresses		
Mendes Eduardo Viale Sebastien	Polymer Materials and Engineering DCT-TUDelft Julianalaan 136 2628 BL Delft The Netherlands		
Local Contact:	Martine Heinrich		

Experimental report text body

Rigid rod molecules are extensively used in industry applications such as processing high strength fibers and composite materials. At the same time, they exhibit interesting physical properties that are appealing from a fundamental point of view. One of the most used molecules is the poly p-phenylene terephtalamide (PPTA), a rigid rod polymer used for high strength fiber manufacturing. The fiber spinning process takes place, however, in concentrated sulfuric acid, a solvent that is not environmental friendly. It also has a high boiling point, far above the degradation temperature of the polymer (180 ˚C), therefore, impossible to evaporate during processing.

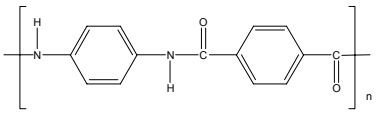

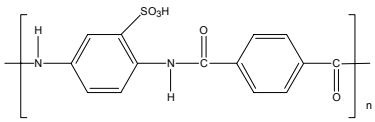

Figure 1. Structure of PPTA Structure of Sulfo PPTA

In order to ease PPTA processing, we are trying to make it water-soluble by introducing a sulfonic group (SO_3H) in the monomer motif. Sulfo poly p-phenylene terephtalamide, the ionic counter part of PPTA is shown in figure 1 together with the PPTA molecule. The introduction of the ionic group on the main-chain introduces electrostatic interactions in the system when the molecules are dispersed in aqueous medium. These interactions are long-ranged and, as it is well-know, they can induce soft order in the solutions leading to a scattering maximum observed in a Small Angle Neutron Scattering (SANS) spectrum.

The new polymerization route that we developed for SPPTA**,** uses LiCl as polymer chain solubilizer in a given step, leading to a naturally lithiated polymer. In aqueous solution, the role of Li^+ as a counter-ion is not the same as that played by H^+. *The aim of these experiments was to investigate the structure of these different polymer solutions at different polymer concentrations and* Li^+ *content.*

In figure 2, the scattering intensity as a functiuon of q (log-log scale) is plotted for a fixed polymer concentration and different Li^+ content. The scattering maximum observed for low lithium content is interpreted, as recalled above, as a correlation peak due to the interaction between neighbouring charged rods, while the upturn is attributed to aggregates that are probably present in the samples.

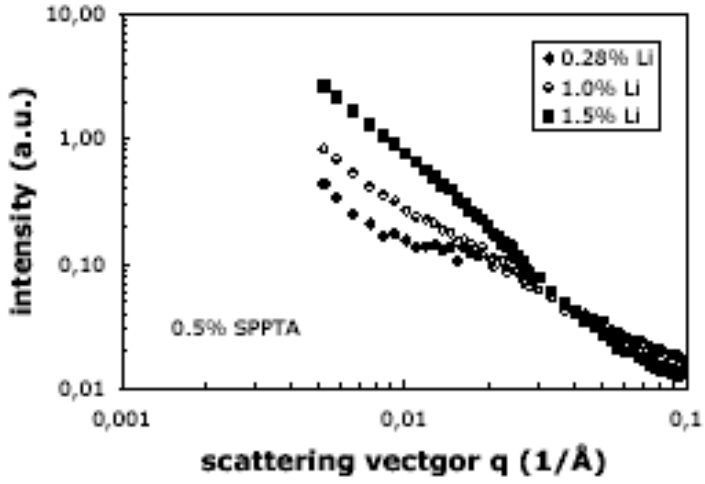

Figure 2 . Scattering intensity as a function of scattering vector for a 0.5% solution of the SPPTA in heavy water at 20°C. Different Li+ contents are displayed in Li w/w. 2% corresponds to 100 % at SO_3^- substituted.

As the proportion of the Li^+ counter-ion increases (see figure), the correlation maximum vanishes and at the same time, the upturn at very small angles increases. This indicates that the increase of Li counter-ions favours aggregration. This is probalby due to the fact that the repeting unit has only one sulfonted aromatic ring, the second ring is highly hydrophobic.

As a conclusion, we were able to bring into evidence the role of the Li^+ counter-ion as it replaces H^+ counter-ions. When their content is high enough, aggregation seems to occur. Also, as suggested by birefringence and alignment under shear, the aggregates have probably fibril shape, what could help to enhance alignment during fiber production in water, and therefore fiber strength.

These results have been presented at the SAS conference 2002, Venezia, and a paper has been sumitted to *Journal of Applied Crystalography*, as a proceeding.

Institut für Festkörperforschung
Forschungszentrum Jülich GmbH
D-52425 Jülich

Experimental Report
of Neutron Scattering Experiments
at the FRJ-2 Reactor

Proposal number:	KW2-02-015		
Experiment title:	Structure factor of partially deuterated PE-melt (II)		
Dates of experiment:	13.6-16.6.2002	Date of report:	6.3.2003
Experimental team: Names	Addresses		
H. Frielinghaus M. Zamponi	IFF, FZ Jülich IFF, FZ Jülich		
Local Contact:	H.Frielinghaus		

Experimental report text body

(Please use 12 pt letters here !)

A previous small angle scattering experiment on a 4k(d)-4k(h)-4k(d)-PE sample (see KW1-01-039) revealed a distinctive deviation from the expectation of the random phase approximation (RPA). To further investigate the discrepancy, additional measurements on 4k(d)-17k(h)-4k(d)-PE and 4k(h)-4k(d)-4k(h)-PE sample have been done. These samples are also used for neutron spin echo spectroscopy, where they are measured at a temperature of 509K.

At KWS2 measurements on 4 different samples with d-h-d resp. h-d-h labeling at two different temperatures (453K and 509K) have been performed. The experiments were done at a wavelength of 6Å, covering a q-range from 0.01Å^{-1} to 0.2Å^{-1}. Data were corrected for background and calibrated.

In fig.1 the structure factor for two 4k(d)-17k(h)-4k(d)-PE samples are shown. One sample consisted of the pure dhd-triblock, the second was a 20% mixture of the triblock in a corresponding 25k-d-PE matrix (as used for NSE). The data follow the RPA-prediction qualitatively, but again quantitative a distinctive deviation from the prediction can be observed at low q. The lines show the RPA expectation, where the unknown incoherent background is fitted.

A newly prepared 4k(d)-4k(h)-4k(d)-PE sample (100%) was remeasured. The data are comparable to the previous KWS1 experiment, the observed discrepancy persist. Now also a 4k(h)-4k(d)-4k(h)-PE sample (100%) was measured, which should display, after Babinet's theorem, the same scattering pattern as the dhd-sample, except for the different incoherent background level. As can be seen in fig. 2 this is not fulfilled. The structure factor of the hdh-sample correspond at low q not to the dhd-sample, it differs even more from the RPA-prediction. At low q there seems to be an additional contribution to the scattering spectrum.

All samples were first measured at a lower temperature of 453K, to see if deviations occur from chemical modifications due to the high temperature. As can be seen in fig. 3 and 4, there is no significant difference between the two measurements at different temperatures, the samples are all thermal stable.

The reason for the deviation at low q is still not clear, polydispersity might contribute to this effect. The q-range where the difference occur is not reached with NSE spectroscopy so that these spectra should not be falsified.

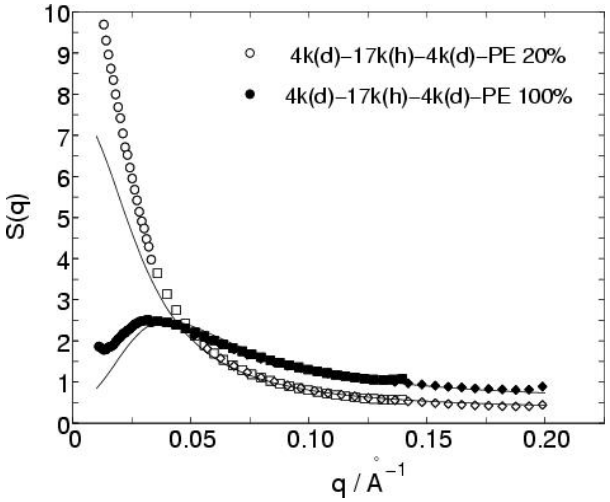

Fig. 1: Open symbols: 20% dhd-25k-PE, closed symbols: 100% dhd-25k-PE, lines: RPA, background fitted, T=509K.

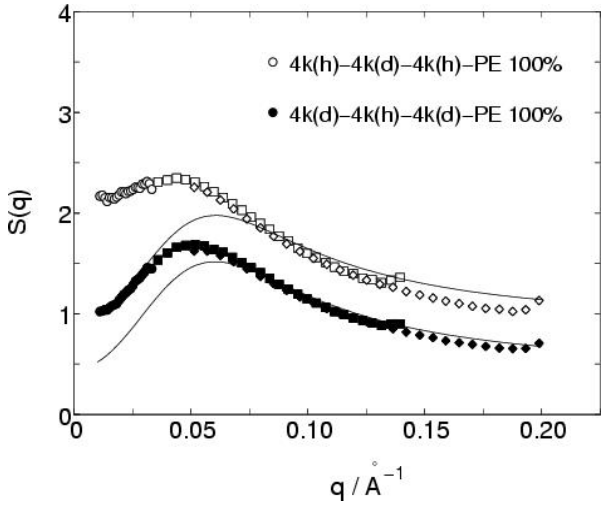

Fig. 2: Open symbols: 100% hdh-12k-PE, closed symbols: 100% dhd-12k-PE, lines: RPA, background fitted, T=509K.

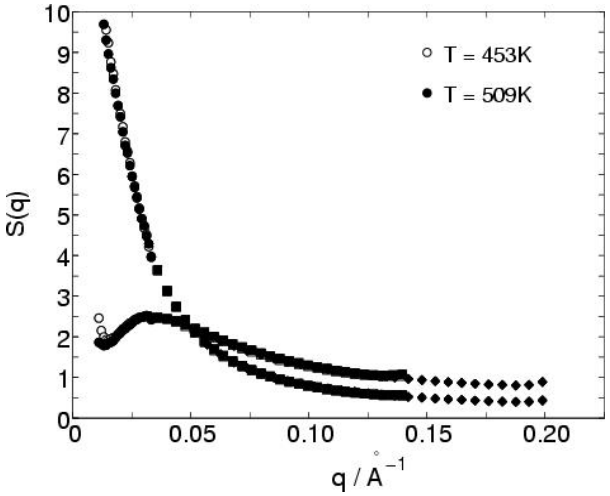

Fig. 3: Samples as in fig.1, for two different temperatures.

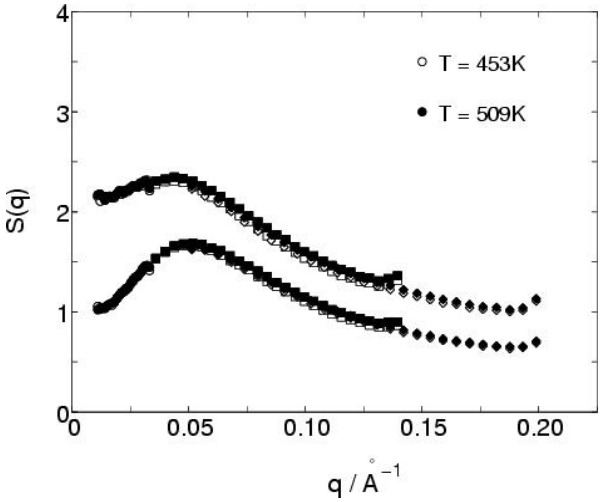

Fig. 4: Samples as in fig. 2, for two different temperatures.

Institut für Festkörperforschung
Forschungszentrum Jülich GmbH
D-52425 Jülich

Experimental Report
of Neutron Scattering Experiments
at the FRJ-2 Reactor

Proposal number:	KW2-02-017		
Experiment title:	Time resolved SANS experiments during "living" anionic polymerisation		
Dates of experiment:	Jun. 07-11, 2002	Date of report:	19-06-02
Experimental team: Names	Addresses		
A. Niu J. Stellbrink J. Allgaier L. Willner D. Richter L. J. Fetters	IFF-Neutronenstreuung, Forschungszentrum Juelich, D-52425 Juelich IFF-Neutronenstreuung, Forschungszentrum Juelich, D-52425 Juelich IFF-Neutronenstreuung, Forschungszentrum Juelich, D-52425 Juelich IFF-Neutronenstreuung, Forschungszentrum Juelich, D-52425 Juelich IFF-Neutronenstreuung, Forschungszentrum Juelich, D-52425 Juelich Department of Chemical Engineering, Cornell University, Ithaca, NY 14584, USA		
Local Contact:	A.Niu: a.niu@fz-juelich.de, 02461-612258		

Experimental report text body

Lithium based living anionic polymerization is an established method for preparing well-defined model polymers. Howeverthe anionic polymerization of dienes and styrene in non-polar solvents based on organolithium compounds is now recognized to be a more complicated operation than that presented as the "textbook explanation", has been of long term academic and commercial interest. This kind of anionic polymerization proceeds by chain initiation and propagation steps only, these two steps overlap during much of the total polymerization process depend on the rates of initiation propagation. However, the question of the mechanism through which the chain growth event takes place is not resolved. A key question is the aggregation behavior of the organolithium head groups. In particular the detailed structure of these intermediate aggregates is still under discussion.

In addition we followed by time resolved SANS experiments the changes in aggregation state and structure of intermediate species formed in the course of living anionic polymerization. We found in the very early reaction stages, there are large scale aggregates (Figure 1).

Figure 2 is the SANS data we measured the propagation stage of the anionic polymerization of butadiene in D-heptane. If we assume the aggregation state is constant and aggregation number is 4, the propagation rate constant caculated from SANS data is 1.26×10^{-4} min^{-1}.

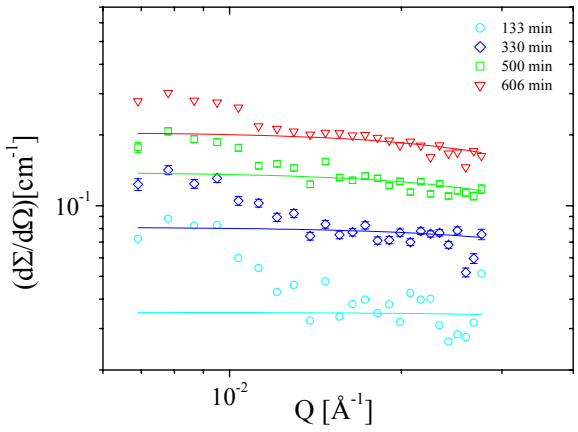

Figure 1: SANS data of the initiation stage of the butadiene anionic polymerization in d-heptane at 8°C.

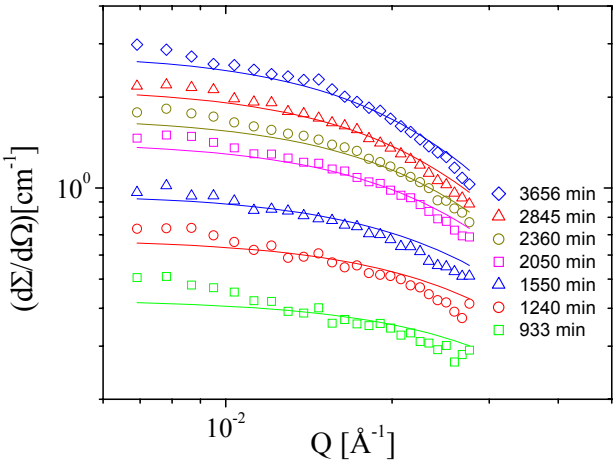

Figure 2: SANS data of the propagation stage of the butadiene anionic polymerization in d-heptane at 8°C.

Institut für Festkörperforschung
Forschungszentrum Jülich GmbH
D-52425 Jülich

Experimental Report
of Neutron Scattering Experiments
at the FRJ-2 Reactor

Proposal number:	**KW2-02-018**		
Experiment title:	Characterisation of Hyperbranched Polyglycerols with small angle neutron scattering		
Dates of experiment:		Date of report:	17/12/2002
Experimental team: Names	Addresses		
Soddemann, Matthias Maksimova, Tatiana Richtering, Walter	Institut für Physikalische Chemie Christian Albrechts Universität Kiel Olshausenstrasse 40 D-24098 Kiel Phone: 0431/880-2831 Fax: 0431/880-2830 E-mail: Richtering@email.uni-kiel.de Matthias.Soddemann@makro.uni-freiburg.de maksimova@phc.uni-kiel.de		
Local Contact:	Silke Rathgeber		

Experimental report text body

Well-defined structures of nanometer-dimensions are subject to intense research efforts. From a fundamental perspective, the transition from the properties of molecular entities to those of the bulk occurs in this size range. In view of potential applications, such materials are of interest with regard to *e.g.* catalysis or microelectronics. However, a rational control of structure formation and of functional properties on this length scale remain key challenges.

Controlling the molecular architecture of dendrimers is crucial for their intended use in applications such as drug delivery, biocides, gene transfer, catalyst supports and processing aids.[1-3] The molecular conformation in solution, which controls efficacy in such applications, has been the subject of theory and experiment.[4]

As a novel approach, the research proposed here investigates shape and size of easily accessible hyperbranched polymers. Only recently, a one-step synthesis allowing for a convenient access to hyperbranched polyglycerols of controlled, narrow molecular weight distributions ($M_w/M_n < 1.7$) was found.[5]

Hyperbranched polymers are generally composed of dendritic (D), linear (L) and terminal (T) units, see scheme.

It has been show that most of the hyperbranched polymers possess some of the unique properties exhibit dendritic macromolecules, such as low visvosity, good solubility, and multifunktionality[6,7].

In order to analyse the correlation between the nanostructure of hyperbranched polymer and it function as a scaffold for further syntheses we carried out neutron scattering experiments.

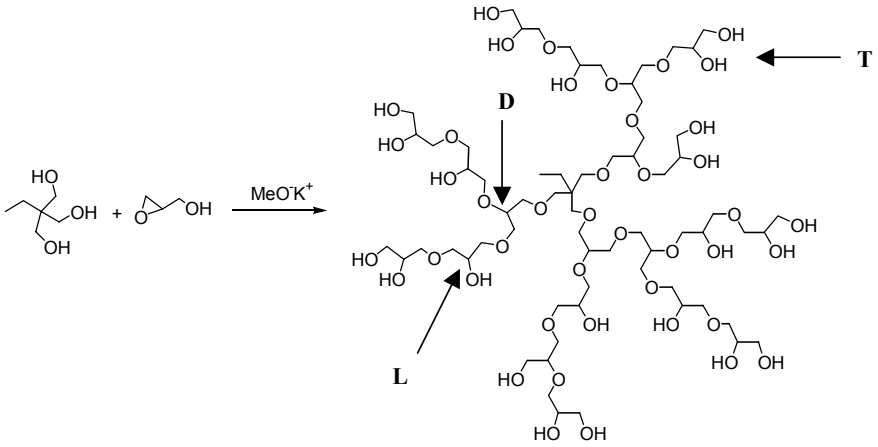

We investigated polyglycerols of different molecular weights (M_n= 2500-30000 g/mol), each with by concentration in 1 and 2 wt.-%. As solvent we used D_2O. The neutron wavelength was 6.28 Å with 10% of wave length resolution. The range of scattering vectors ($0.005 < q < 0.25$ Å^{-1}) was obtained using five sample-to-detector distances (1.4– 14 m). The samples were measured at 25°C in quartz cuvettes with a path length of 2 mm.

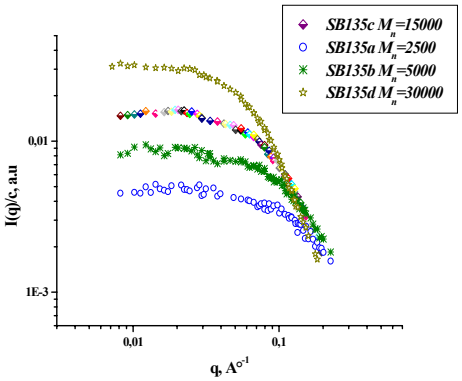

Figure 1. Scattering curves of hyperbranched polyglycerols for different molecular weights in D_2O; concentration of solutions 1 wt.% (11.1 g/l), T=25±1°C.

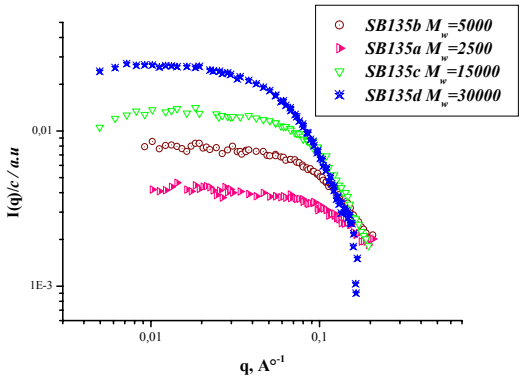

Figure 2. Scattering curves of hyperbranched polyglycerols for different molecular weights in D_2O; concentration of solutions 2 wt.% (22.1 g/l), T=25±1°C.

Figure 1 and 2 show the q dependence of measured neutron scattering intensity divided by concentration of hyperbranched polyglycerols in D_2O solutions. At all curves there are at low q a typical Guinier behavior originating from the overall size of polymers. The sizes (radius of Gyration (R_G)) of polymers were obtained from the Guinier approximation eq. 1. applied to the computed SANS spectra.

$$I(q) = I_0 \cdot e^{-\frac{1}{3} \cdot q^2 \cdot \langle s^2 \rangle}, \quad R_G = \sqrt{\langle s^2 \rangle} \qquad (1),$$

where I(q) is the scattered intensity, q – the wavevector, defined as $q=(4\pi/\lambda)\sin(\theta/2)$, with λ the wave length of the incident beam and θ the scattering angle; $\langle s^2 \rangle$ is average size of particles (polymer).

The calculated radius of Gyration (R_G) via eq. 1. for amphiphilic hyperbranched polyglycerols with different molecular weights (M_n= 2500-30000 g/mol %) are given in Table 1. As can be directly seen, R_G depend on the molecular weight. We were obtained that R_G increase with increase of molecular weight of hyperbranched polyglycerols .

Table 1. *Radius of Gyration R_G for the polyglycerols obtained from applications of the Guinier approximation to the simulated SANS curves*

Sample	*M_n of polyglycerol*	*Solvent*	*R_G (Guinier)*	
			C=11.1 g/l	*C=22.099 g/l*
SB135a	2500	D_2O	-	0.95 nm
SB135b	5000	D_2O	1.03 nm	1,15 nm
SB135c	15000	D_2O	1.38 nm	1.35 nm
SB135d	30000	D_2O	2.2 nm	2.2 nm

References:

1 Bosman, A..; Janssen, H.M.; Meijer, E.W. *Chem. Rev.* **1999**, *99*, 1655
2 Hawker, C.J. *Curr. Opinion. Colloid Interface Sci.* **1999**, *4,* 117
3 Newkome, G.R.; He, E.; Moorefield, C.N. *Chem.Rev.* **1999**, *99*, 1689
4 Tande, B.M.; Wagner, N.J.; Mackay, M.E.; Hawker, C.J.; Jeong, M. *Macromolecules* **2001**, *34* 8550
5 Sunder, A.; Hanselmann, R.; Frey, H.; Mülhaupt, R. *Macromolecules* **1999**, *32*, 4240.
6 Gelade, E.T.F.; Goderis, B.; de Koster, C.G.; Meijerink, N.; van Benthem, R.A.T.M.; Fokkens, R.; Nibbering, N.M.M.; Mortensen, K. *Macromolecules* **2001**, *34*, 3552
7 Jikei, M.; Kakimoto, M. *Prog. Polym. Sci.* **2001**, *26*, 1233

Institut für Festkörperforschung
Forschungszentrum Jülich GmbH
D-52425 Jülich

Experimental Report
of Neutron Scattering Experiments
at the FRJ-2 Reactor

Proposal number:	KW2-02-019		
Experiment title:	**Concentration dependent swelling of blockcopolymer micells**		
Dates of experiment:	24.-25. 06. 2002	Date of report	10. 03. 2003
Experimental team: Names	Adresses		
Gerhard Meier	IFF „weiche Materie“/FZ-Juelich, D-52425 Juelich		
Local Contact:	Henrich Frielinghaus		

Experimental report text body

(Please use 12 pt letters here !)

We have measured 4 different concentrations of block copolymer micelles consisting of PBMA-b-PCMEA block copolymers in d-toluene. The concentrations were 0.0005 , 0.0092 , 0.0313 and 0.141 g/ccm resp. The first concentration is much below the overlap concentration , the next one is just about and the latter two ones are clearly above c*. Data was due to restrictions in beam time taken only at 2 and 8 meter detector distance. For the lowest c clearly the typical intensity variations for ie. a sphere form factor are visible. It is roughly possible to scale all curves with regard to intensity by the concentration. Then a structure peak evolves for the two highest concentration which shifts with c according to our expectations. In the figure we show raw data (that means intensity in cm^{-1} calibrated against Lupolen and Q in $Å^{-1}$ after radial average) not scaled with c in order not to confuse the plot, where obviously for the two higher concentrations a maximum in the scattering curve appears. For the second lowest c being about c*,a maximum at the lowest Q edge is visible We find for the two higher concentrations that the maxima of the peaks shift by a factor of 1.6 while varying c by a factor of 4.5 For the second lowest concentration a similar estimation gives a consistent result taking the limitations of the Q-range into account. Since we speculated that a peculiar dynamic finding (see proposal where results from dynamic light scattering are reported) may be due to a structural anomaly , we would have expected a kink in a plot relating the interparticel distance d with the concentration via $c^{1/3}$. The higher concentrations in our SANS experiment were taken above and below this concentration related to the dynamic anomaly. As obviously $4.5^{1/3}$ is in very good approximation 1.6, the variation of d with c , any structural reasons for the kink wise variation of the diffusion coefficient with c can be ruled out.

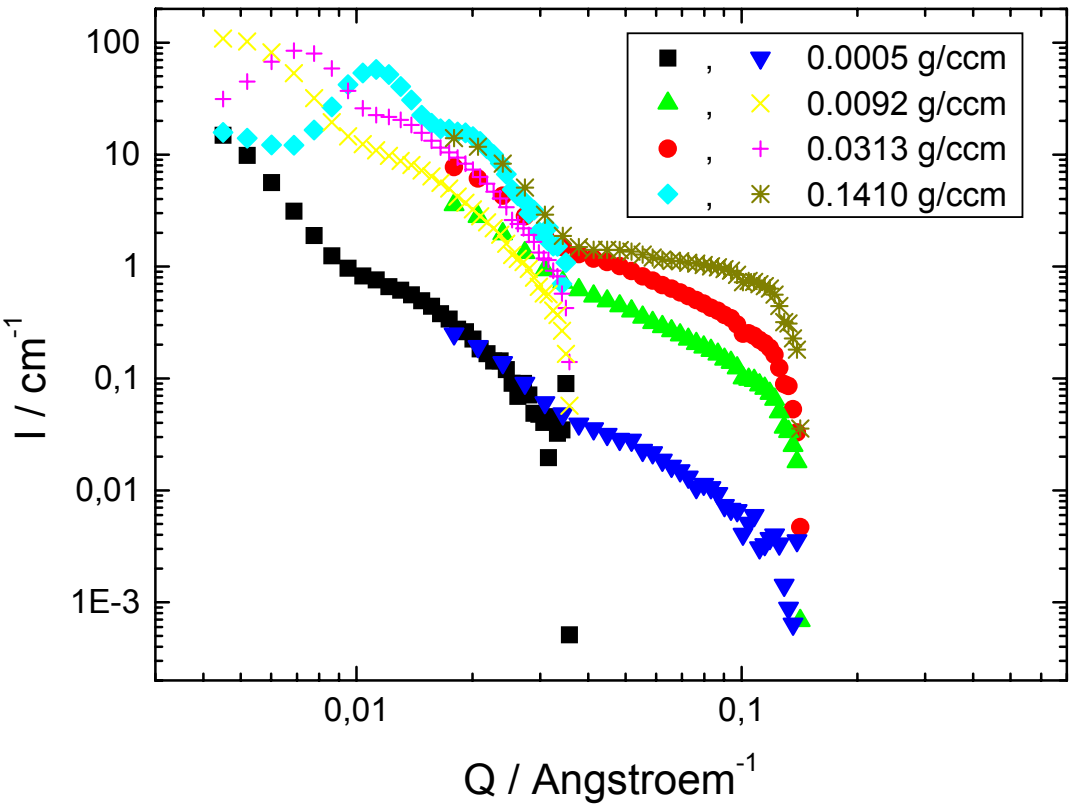
100
10
1
0,1
0,01
1E-3
I / cm-1
0,01
0,1
Q / Angstroem-1
0.0005 g/ccm
0.0092 g/ccm
0.0313 g/ccm
0.1410 g/ccm

Institut für Festkörperforschung
Forschungszentrum Jülich GmbH
D-52425 Jülich

Experimental Report
of Neutron Scattering Experiments
at the FRJ-2 Reactor

Proposal number:	KW2-02-020		
Experiment title:	**Self-assembly in solution of lower M_W poly(s-propylene)(polyethylene-propylene) diblock copolymer and poly(s-propylene) homopolymer**		
Dates of experiment:	31.05.02-01.06.02	Date of report:	06.03.2003
Experimental team: Names	Addresses		
Aurel Radulescu Robert Stollenwerk	IFF, FZ-Jülich, D-52425 Jülich		
Local Contact:	Henrich Frielinghaus		

Experimental report text body

(Please use 12 pt letters here !)

A recent publication [1] has announced that near-monodisperse poly(co-olefin) diblocks can be prepared from olefin monomers allowing the synthesis in a direct fashion of polyolefin chains that are possible via the two-step anionic routes. Such as diblocks consisting of a sydiotactic-polypropylene segment tied to an amorphous poly(ethylene-propylene) block (sPP-PEP) have been investigated by SANS in parallel with the syndiotactic-polypropylene homopolymer (sPP) in order to get a first insight about the self-assembling characteristics of these materials in dilute hydrocarbon solution. The sPP homopolymer has a molecular weight of M_W=61400 g mol^{-1} while the diblock copolymer has a total molecular weight M_W=47000 g mol^{-1} with the sPP block of M_W=22300 g mol^{-1}. Solutions of 0.5% polymer volume fraction were prepared in decane. Since the melting point of the sPP is around 147°C a very wide temperature range was investigated, between the single coil (at 160°C) and the aggregation regime (below 0°C). The SANS measurements were performed at KWSII spectrometer set-up at the FRJ-2 reactor in Jülich. Using a neutron wavelength of 7Å and three sample-to-detector distances a Q range between 0.002$Å^{-1}$ and 0.14$Å^{-1}$ could be investigated. The data were corrected for the scattering from empty cell and solvent and then calibrated in absolute units by using a Lupolen secondary standard [2]. Working with fully protonated polymers the maximum contrast and the minimum incoherent background were achieved by choosing fully deuterated solvent (d-22). sPP and PEP have practically the same scattering length density thus the only contrast is between them and solvent while no contrast occurs between the two blocks. Figure 1 displays scattering profiles at different temperatures from 0.5% sPP homopolymer solution. At 160°C all polymers are dissolved and stay as single coils. The analysis of the single chain properties performed in terms of the Zimm approximation yields a radius of gyration of about 99.8Å. The polymer has a little tendency to self-assemble at around 60°C but the process is developed massively below this temperature. Already at 40°C the scattering intensity shows an increasing with about 3 orders of magnitude. The morphology of the polymer aggregates is easily identified from the well revealed Q^{-2} behavior

of the intensity, characteristic for scattering from platelets. The scattering patterns practically coincide for all temperatures below 40°C proving that almost all polymers might be involved in the rapid self-assembling even at the beginning of the process. The forward scattering (giving the scattering volume) and the platelet thickness (about 57Å) have been evaluated using the 2-d Guinier approximation [3]. Supposing compact platelets from the obtained $d\Sigma(0)/d\Omega$ one gets that indeed, almost all polymers are inside the platelets even at 40°C.
Figure 2 shows the scattering patterns from the 0.5% sPP-PEP diblock solution at different temperatures between the single coil and the aggregates regime. The spectra indicate a much more complex morphology of the self-assembled objects. The features revealed for different Q ranges prove a multi-level structure showing at least two characteristic sizes. At low Q the well-revealed Q^{-1} power law indicates the larger structure of a needle-like shape. However, the decrease of the intensity towards higher Q is too sharp in order to show the form factor details of the 1-d objects. Thus, a possible local increase of the intensity due to interparticle correlation might be taken into account. At intermediate Q also a power law behavior ($d\Sigma/d\Omega \sim Q^{-2}$) could be tentatively identified. This would relate to a smaller platelet-like structure possibly as a sublevel of the larger aggregates or as a separate entity. These first observations prove the complex self-assembling behavior of the sPP-PEP diblock copolymer in dilute solution and lead to the conclusion that partially deuterated copolymers are of a strong interest in order to identify separately the conformation of both blocks inside the aggregates.

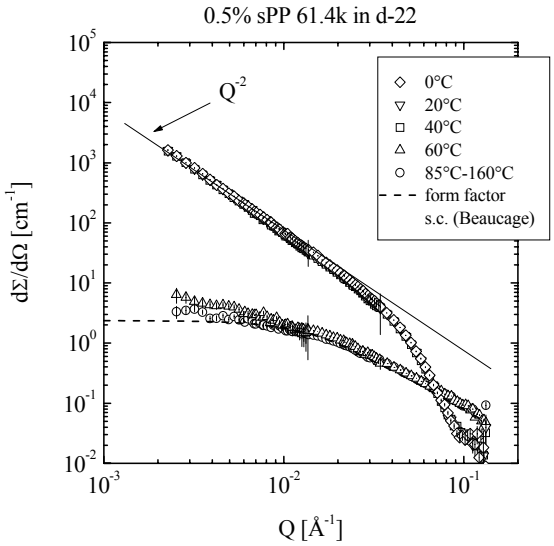

Fig. 1 - The scattering patterns from the 0.5% sPP solution at different temperatures

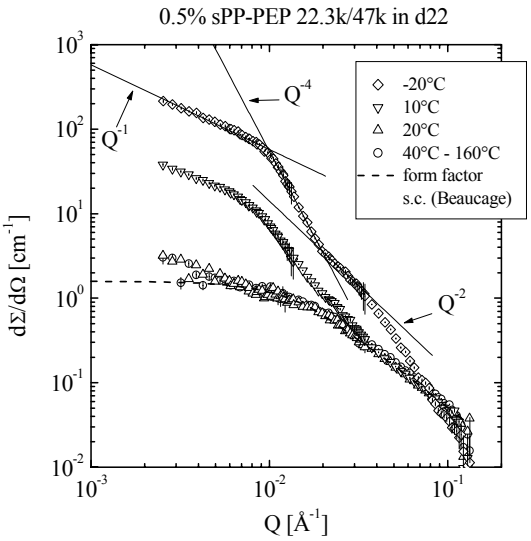

Fig. 2 – The scattering patterns from the 0.5% sPP-PEP solution at different temperatures for both blocks visible

References

[1] J.Tian et al., J.Am.Chem.Soc. 123, 5134, 2001.
[2] D.Schwahn et al., J.Chem.Phys. 93, 8383, 1990.
[3] D.Schwahn et al., Macromolecules 35, 861, 2002.

Institut für Festkörperforschung
Forschungszentrum Jülich GmbH
D-52425 Jülich

Experimental Report
of Neutron Scattering Experiments
at the FRJ-2 Reactor

Proposal number:	KW2-02-021		
Experiment title:	**The self-assembling behavior of the three-armed star copolymers PS(PE-PEP)$_2$ in selective solvents investigated by SANS (I)**		
Dates of experiment:	01.06.02-03.06.02	Date of report:	06.03.2003
Experimental team: Names	Addresses		
Aurel Radulescu Robert Stollenwerk	IFF, FZ-Jülich, D-52425 Jülich		
Local Contact:	Henrich Frielinghaus		

Experimental report text body

(Please use 12 pt letters here !)

Association of block copolymers in selective solvents (solvent for one type of block and a nonsolvent for the other type of block) may produce various structures ranging from nano- to microscopic dimensions. While micellization of diblock and triblock copolymers has been intensively studied both in selective organic solvents and aqueous media [1] micellization and related association phenomena in solutions of star-shaped copolymers have been studied only a little. The aggregation of polyethylene-poly(ethylene-propylene) (PE-PEP) block copolymers dissolved in decane was studied by SANS recently [2]. The system was found to have a very low critical micelle concentration. At the concentrations studied all polymers are precipitated in lamellar micelles with a crystalline PE core and a corona of PEP hairs. The influence of polymer architecture on the micelle formation was checked also by SANS applied on miktoarm star polymers with a functionality of the centre ≤ 4 (PE_nPEP_m, n,m =1,2 with m+n=3,4) [3]. Like in the case of PE-PEP diblocks the SANS patterns show the signature of lamellar micelles (inner PE lamella separated from the solvent by solvated amorphous PEP brushes). New miktoarm stars were prepared as asymmetric three-armed star copolymers where one arm is polystyrene and the other two are PE-PEP diblocks with one end of the PE segment attached to the center of the star and the other to the PEP. By SANS we obtained first information about the structures formed by this fully protonated star polymer in selective solvents as a function of temperature. Two polymers have been studied having the molecular weight as follows: PS 16000 and 43000 g mol^{-1}, each PE 12000 and 20000 g mol^{-1} and each PEP 12000 and 20000 g mol^{-1}. The solvents were decane and toluene in accordance with the main aim of the study: to find out what type of architectures are formed with these asymmetric stars under the conditions where PS retains its single coil behavior over the complete temperature range (using the aromatic solvent) and when it forms micelles (in decane). The aromatic solvent at around 80°C should lead to single coil behavior prior to cooling. The self-assembly event involving the PE segments may be partially frustrated due to the soluble PS.

In decane cooling will lead to self-assembly of the PE component (below 60°C) and will allow PS micelles to be formed. Thus, the decane case represents a dual self-assembly event process: the PE crystallization along with the progressive insolubility of the PS component as temperature is lowered. Also in this case the crystallization induced self-assembly may undergo some frustration as a consequence of the PS micelle formation. Only fully protonated polymer have been investigated in this first part of the study. The possible contrast conditions for an useful structural investigation allowed only the PE-PEP arm visible for the PS arm matched with the mixed deuterated-protonated solvent. For both solvents the protonated content was very high, of about 92% and 75% for toluene and decane, respectively. The SANS measurements were performed at KWSII spectrometer set-up at the FRJ-2 reactor in Jülich. Using a neutron wavelength of 7Å and three sample-to-detector distances a Q range between 0.002Å^{-1} and 0.14Å^{-1} could be investigated. The data were corrected for the scattering from empty cell and solvent and then calibrated in absolute units by using a Lupolen secondary standard [4]. Due to the high incoherent background an evaluation of the single coil behavior was not possible, the measured signal being very poor after correction of the raw data. Figure 1 shows the scattering patterns from both decane and toluene solutions of the higher M_W polymer captured at 0°C. One can see that a general Q^{-1} power law behavior at low Q was obtained proving formation of 1-dimensional aggregates. Qualitatively, these morphology is similar with that shown by the PE-PEP star copolymers having the crystalline block tied to the center of star too [5]. The influence of the solvent on the general aggregation behavior of the present investigated star copolymers might be related to the presence of a correlation peak just below 0.01Å^{-1} in the case of aromatic solvent. Tentatively, this correlation could be related to an association of the 1-d objects via the entanglement of PS arms which are soluble in this case over the whole temperature range while in decane PS assembles too, possibly inside the objects already defined by the PE-PEP arms at higher temperatures.

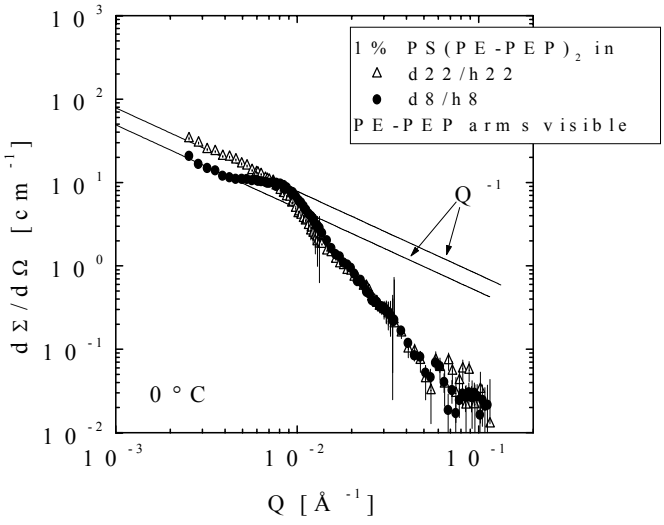

References

[1] C.Tsitsilianis et al., Langmuir, 16, 6868, 2000 and references herein.
[2] D.Richter et al., Macromolecules 30, 1053, 1997.
[3] A.Ramzi et al., Macromolecules, 30, 7171, 1997.
[4] D.Schwahn et al., J.Phys.Chem. 93, 9393, 1990.
[5] D.Schwahn et al., Macromolecules 35, 861, 2002.

Institut für Festkörperforschung
Forschungszentrum Jülich GmbH
D-52425 Jülich

Experimental Report
of Neutron Scattering Experiments
at the FRJ-2 Reactor

Proposal number:	KW2-02-022		
Experiment title:	**Characterisation of PEP-PEO Polymeric Micelles in DMF/Water Solvent Mixtures**		
Dates of experiment:	25-02-02-03/02	Date of report: 26-02-03	
Experimental team: Names	Addresses		
Reidar Lund Dr. Lutz Willner Dr. Aurel Radelescu Prof. Dieter Richter	Forschungszentrum Jülich; IFF-Institut für Neutronenstreuung D-52425 Jülich		
Local Contact:	Henrich Frielingshaus		

Experimental report text body

In this experimental project we will like to continue the investigation of the properties of starlike polymeric micelles formed by highly assymmetric PEP-PEO block copolymers. Earlier we have performed experiments on a system consisting of PEP1-PEO20 polymers (the numbers indicate the molecular weight of the blocks (in Da, kg/mole)) in a solvent mixture of dimethylformamide (DMF) and water. The main purpose for these investigations is to unravel some of the dynamical properties of polymeric micelles. By mixing equal amounts of two differently labelled polymers, it is possible to follow the chain exchange in these micelles by monitoring the change in intensity by SANS [for a more detailed description see ref. 1 and 2.]. However, as we have previously reported [2], no chain exchange is observed in pure water for the PEP1-PEO20 micelles. The purpose of the introduction of DMF was to tune the dynamical properties of the micelles by increasing the solvent quality for the insoluble block, PEP. We found that at DMF contents corresponding to a mole fraction in the range between 0.2 and 0.5, chain exchange occur on a time scale practically accessible by SANS. From the static measurements we found that the tuning of the kinetic properties was accompanied by change in the micellar structural parameters, i.e. we found a decrease in both the micelle radius and the aggregation number upon increasing the DMF content. In order to further corroborate the observed trend we decided to perform more measurements on new compositions as well as repeat some of the old measurements in full contrast. The results are given below in figure 1. where the aggregation numbers obtained from a core-shell fit of the scattering curves of h-PEP1-hPEO20 and the d-PEP1-dPEO20 are shown:

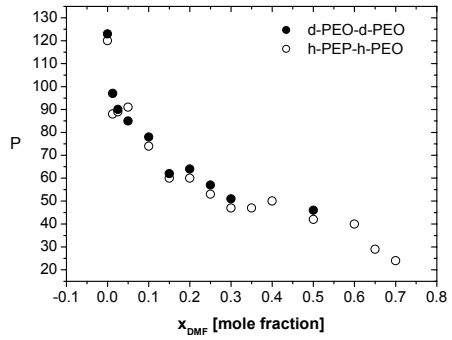

Figure 1. Aggreagation number as a function of DMF.

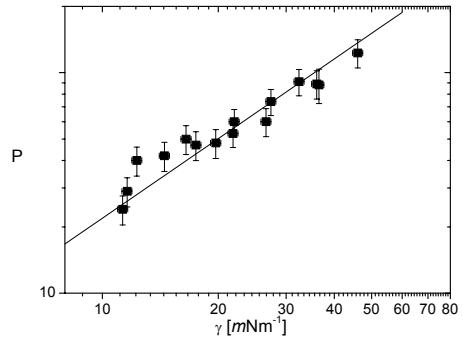

Figure 2. Aggregation Number vs. Interfacial Tension

In figure 2. we correlate this with the corresponding interfacial tensions exhibited by the insoluble block PEP1k in the same mixtures. The solid line is due to Halperin[1] and is thus in good agreement with the data, especially at high P. At lower P the deviation may come from the limitations in the simple scaling model.

References:

1. A. Halperin, *Macromolecules* **20** (1987) 2943

Institut für Festkörperforschung
Forschungszentrum Jülich GmbH
D-52425 Jülich

Experimental Report
of Neutron Scattering Experiments
at the FRJ-2 Reactor

Proposal number:	KW2-02-023		
Experiment title:	Segmental Mobility in Clusters of Aggregated Cellulose-Derivative Chains		
Dates of experiment:	23.11.02	Date of report:	09.03.03
Experimental team: Names	Addresses		
Rathgeber, Silke Burchard, Walther	Forschungszentrum Jülich GmbH Institut für Festkörperforschung – Weiche Materie D-52425 Jülich Universität Freiburg Institut für Makromolekulare Chemie D- 79104 Freiburg		
Local Contact:	Michael Monkenbusch		

Experimental report text body

Cellulose is a biological chain molecule abundantly found in plants. The fibrous material is semi-crystalline and insoluble in water and common organic solvents. Water solubility is obtained when the chains are partially derivatized, i.e. not all hydroxyl groups of the chain are substituted. In contrast to most synthetic chain molecules these cellulose derivatives do not dissolve molecularly, but the dissolution process stops at a colloidal level [1]. This unusual behavior is suppose to originate from an uneven derivatization along the chain. The amorphous regions of the fiber become preferably derivatized while the crystalline regions remain mainly unaffected by the chemical reagents.

Structure and dynamic properties of these colloidal particles were extensively studied by static and dynamic light scattering and small-angle neutron scattering. As sketched in figure 2 a *fringed micellar* structure was deduced, in which *f* chains are side-by-side aligned thus forming a quasi-crystalline short stem with coronas of dangling chains at the two ends of the stem [2]. The scattering spectra for one sample (c=2wt%) and fit curves derived from the fringed micelle model are also shown. The translational mobility of these clusters was measured as a function of concentration by dynamic light scattering. Because of the large radii of gyration (R_g ≈ 250 nm) also internal modes of motion has been partially detected. For $qR_g > 4$ a characteristic asymptotic behaviour has been observed that appears to be characteristic for Zimm-Rouse modes (i.e. relaxations under the influence of hydrodynamic interactions). However the plateau height of Γ/q^3, Γ is the first cumulant of the field (or intermediate) time correlation function, turned out to be considerably smaller than predicted by the Zimm theory for flexible linear chains. Furthermore, the plateau height, which is a measure of internal flexibility, sharply decreases with increasing concentration and approaches hard sphere behavior when the overlap concentration is largely exceeded. Figure 3 summarizes these findings which suggest that at high concentrations the segment mobility of the dangling chains become fully suppressed.

With the neutron spin-echo experiment we focused on the relaxation dynamics of the dangling ends as a function of the cellulose concentration. Preliminary experiments were performed on samples at concentrations below and above the overlap concentration which is about 3% in D_2O. The obtained relaxation rates are plotted in figure 3 as a function of the scattering vector. We expected a slowing-down of the segmental relaxations when the concentration is increased beyond the overlap concentration. However, we found an additional fast relaxation process at low q values which is unaffected by changing the concentration beyond the overlap concentration. The origin of this extra fast relaxation process is not understood yet.

To rule out that the effect is just an artifact due to *disturbing effects of the primary beam* we repeated a test experiment with a beam stop before the analyzer for one sample (c=5wt%). The new results are shown in figure 2 by the hollow, red circles. The results confirm the existence of an extra fast relaxation process showing up at small q values. For the future more thorough investigations of this q range with neuron spin-echo spectroscopy for various cellulose concentrations are planned.

References:

[1] L. Schulz et al. in: *Cellulose Derivatives; Modification, Characterization and Nanostructures* (Eds. T.J. Heinze, W.G. Glasser) *ACS Symposium Series* **688** (1998) 218.

[2] W. Burchard and H. J. Vogel, Comput. Theor. Polym. Sci. **10** (2000) 133.

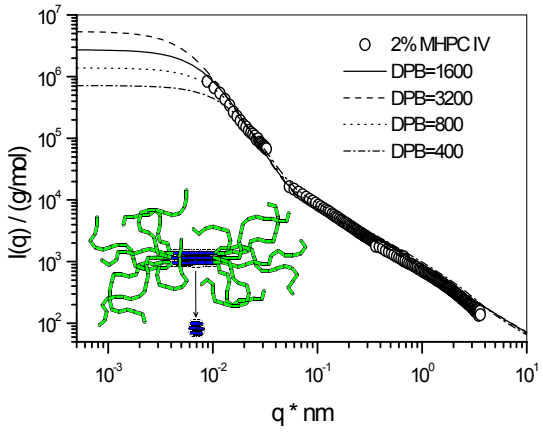

Fig. 1: Scattering spectra obtained from static light scattering and SANS experiments. The full line represents the best fit with the fringed micelle model; the dotted lines correspond to results calculated for various dangling chain length.

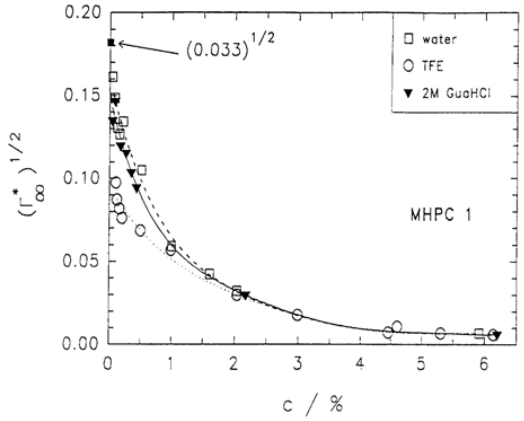

Fig. 2: Concentration dependence of the asymptotic plateau of $\Gamma/q^3 \equiv \Gamma^*(\infty)$ at large $qR_g \geq 4$ for MHPC in different solvents. The plateau height is a measure of segment mobility. A decrease indicates a hindered motion. For hard spheres the plateau height becomes zero.

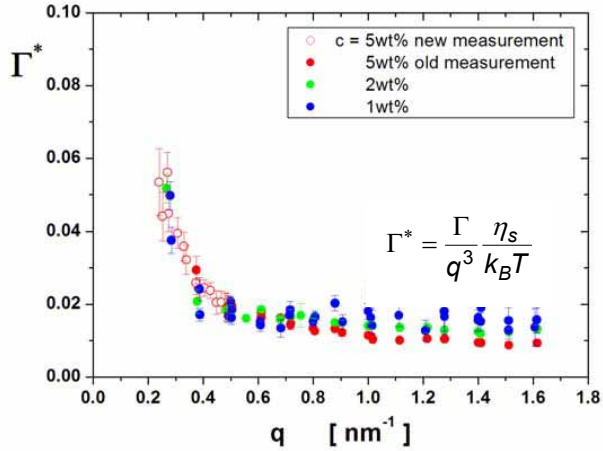

Fig. 3: Normalized relaxation rates obtained for cellulose in heavy water solution at various concentrations.

Institut für Festkörperforschung
Forschungszentrum Jülich GmbH
D-52425 Jülich

Experimental Report of Neutron Scattering Experiments at the FRJ-2 Reactor

Proposal number:	KW2-02-024		
Experiment title:	Zero average contrast measurement for h/d mixtures of PEP-PEO micelles in D2O/H2O solvent		
Dates of experiment:	11.06.02	Date of report:	19.02.03
Experimental team: Names	 Addresses		
Silke Rathgeber Philippe Carletto Jan K.G. Dhont Dieter Richter Lutz Willner	Forschungszentrum Jülich GmbH Institut für Festkörperforschung – Weiche Materie D-52425 Jülich Forschungszentrum Jülich GmbH Institut für Festkörperforschung – Neutronenstreuung D-52425 Jülich		
Local Contact:	Henrich Frielinghaus		

Experimental report text body

The project focuses on the investigation of shear induced brush deformation of diblock copolymer micelles in solution with small angle neutron scattering.

The attractive van-der-Waals interaction between colloids can be screened by grafting or absorbing polymers onto the colloidal surface. This leads to a stabilization of the colloidal suspension. Depending on the layer thickness, the solvent quality and the grafting density the interaction potential can be easily varied between hard-sphere interactions and the longer ranged (softer) potential of star polymers.
We are particularly interested into the phenomenon of “shear band formation” [1]. In various systems that contain mesoscopic entities, a hydrodynamic instability may be induced when a sufficiently strong shear flow is applied, leading to a stationary state where regions of different microstructure and/or shear rates coexist. In a cylinder geometry, shear-banding leads to either band formation in the vorticity direction or along the gradient direction, depending on whether the stress as a function of the shear-rate is a multi-valued function or is of a van-der-Waals loop like form, respectively. Jan Vermant et al. [2] observed shear-band formation along the vorticity direction for a system of “hairy” colloids in a low viscosity solvent at high colloid concentration (40vol%). Neither the microstructure in the two phases nor the mechanism that leads to the phase separation are yet known. A possible explanation might be that the shear-induced polymer brush deformation may render the van-der-Waals attractions in certain directions unshielded, which could lead to a “thermodynamic instability”. This instability is of thermodynamic nature, but is induced by shear deformation of the brush. So the knowledge of how the polymer brush is deformed under the influence of applied shear is essential for the understanding of shear-band formation. Not only the deformation induced directly by the flow field but also the role of inter-particle interaction is of great importance.

Therefore the aim of this project is to measure the form factor of hairy colloids under shear with small angle neutron scattering over a broad concentration range. In order to measure the polymer form factor at higher concentrations an experiment under zero average contrast (ZAC) conditions can be used [3]. In mixtures of analogous protonated and deuterated polymers the scattering length density of the solvent can be adjusted in such a way that all inter-particle contributions to the scattering are eliminated and only the single-particle scattering, i.e. the form factor, remains. Theoretically the matching conditions for h/d PEP-PEO in H_2O/D_2O are given by: 24.5 vol% h-PEP-PEO/ 75.5 vol% d-PEP-PEO in 13.1 vol% H_2O/ 86.9 vol% D_2O. As found in previous experiments the PEO contrast differs strongly from the theoretical one because of the densification of the water molecules in the hydration shell [4]. For this reason we had to proof the zero average contrast conditions experimentally.

This was done by dissolving the protonated and deuterated diblock-copolymers in benzene which is a good solvent for both blocks. The polymer has been subsequently dried and redissolved in H_2O/D_2O mixtures with various compositions. The procedure should lead to a random distribution of deuterated and protonated polymers in the micelles. The best result in terms of suppression of the scattering for $q \rightarrow 0$ has been obtained for: 18vol% H_2O/ 82vol% D_2O, a composition quiet close to the theoretical one.

References:

[1] J.K.G. Dhont, Phys. Rev. E **60** (1999) 8804.

[2] J. Vermant, J. Coll. Int. Sci. **211** (1999) 221.

[3] L. Willner, O. Jucknischke, D. Richter, J. Roovers, L.-L. Zhou, P.M. Toporowski, L.J. Fetters, J.S. Huang, M.Y. Lin, and N. Hadjichristidis, Macromolecules **27** (1994) 3821.

[4] Andreas Poppe, Thesis, „ Selbstassoziation amphiphiler Blockcopolymere in Wasser: Strukturuntersuchungen und Untersuchungen zur Kinetik der Mizellbildung", Münster, 1998.

Institut für Festkörperforschung
Forschungszentrum Jülich GmbH
D-52425 Jülich

Experimental Report of Neutron Scattering Experiments at the FRJ-2 Reactor

Proposal number:	KW2-02-025		
Experiment title:	Time resolved SANS experiments during "living" anionic polymerization: II. characterization of the final products		
Dates of experiment:	Jun. 25-27, 2002	Date of report:	19-02-03
Experimental team: Names	Addresses		
A. Niu	IFF-Neutronenstreuung, Forschungszentrum Juelich, D-52425 Juelich		
J. Stellbrink	IFF-Neutronenstreuung, Forschungszentrum Juelich, D-52425 Juelich		
J. Allgaier	IFF-Neutronenstreuung, Forschungszentrum Juelich, D-52425 Juelich		
L. Willner	IFF-Neutronenstreuung, Forschungszentrum Juelich, D-52425 Juelich		
D. Richter	IFF-Neutronenstreuung, Forschungszentrum Juelich, D-52425 Juelich		
L. J. Fetters	Department of Chemical Engineering, Cornell University, Ithaca, NY 14584, USA		
Local Contact:	A.Niu: a.niu@fz-juelich.de, 02461-612258		

Experimental report text body

This experiment is the continuing of experiment KW2-02-17, In order to understand the aggregation behavior of the living polybutadiene chain, we have to terminate the living chain and characterize it by SANS experiment.

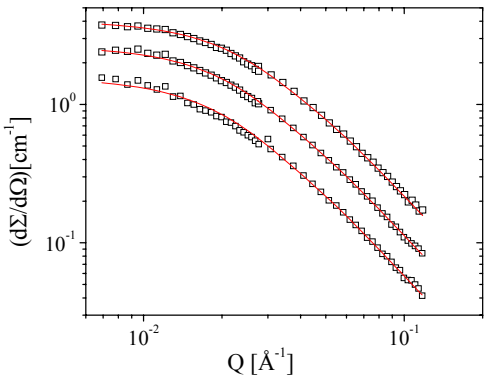

Figure 1: SANS data of the terminated solution of polybutadiene

Terminated chain solution from the reactor was diluted to three concentrations: 1.17%, 2.33% qnd 4.65%, the results of Beaucage fitting is as follows:

M_w= 2.54x10^4±0.01g/mole, R_g= 80±2Å, p=2.00, A_2=3.69X10^{-4}±0.03cm^{3}mol/g^2

Institut für Festkörperforschung
Forschungszentrum Jülich GmbH
D-52425 Jülich

Experimental Report
of Neutron Scattering Experiments
at the FRJ-2 Reactor

Proposal number:	KW2-02-026		
Experiment title:	**Characterization of length scales such as persistence length and radius of gyration of a cationic surfactant system that forms wormlike micelles.**		
Dates of experiment:	04/12/02-06/12/02	Date of report:	09/02/03
Experimental team: Names	Addresses		
Terence Cosgrove Vania Croce	University of Bristol. School of chemistry. Cantock's close. Bristol. BS8 1TS UK		
Local Contact:	A. Radulescu		

Experimental report text body

In this experiment we investigated the effect of solution concentration, added salt and temperature on the micellar system formed by aqueous solution of erucyl bis(hydroxyethyl) methyl ammonium chloride. This surfactant system can self-assembly into long, flexible wormlike micelles, in the presence of salt, and the entanglement of these micelles into a transient network imparts useful physical properties, as seen by *Raghavan et al* [1]. The interest in these systems is the marked increase in viscosity that appears on adding salt, which above a higher salt concentration (>6wt%) then reduces again. The effects are also strongly temperature dependent**.** The surfactant solutions have gel-like behaviour at room temperature and become Maxwellian, as the temperature is increased. Small-angle neutron scattering is a technique that enables us to correlate these bulk rheology measurements with the nanoscale structure being formed in solution.
The results obtained from this experiment are presented in the following figures. Figure 1A shows the scattering intensity (*I(Q)*) as a function of surfactant concentration. This data was fitted to a core-shell model that indicates the presence of spherical micelles with an inner radius of 29 Å and an outer radius of 35 Å. It can be seen that as the surfactant concentration is increased the distance between micelles, defined as $d=2\pi/Q^*$, decreases and the structure factor increases revealing the presence of strong interactions between micelles. In Figure 1B, the effect of added salt on this system can be seen. Adding salt to the system screens the interactions between the micelles and promotes uniaxial growth. Thus, a transition from spherical micelles to wormlike micelles occurs and the structure peak disappears.
Figure 2A shows *I(Q)* as a function of surfactant concentration with 6wt% of KCl and the insert shows the *I(Q)* as a function of salt concentration for different surfactant concentrations. Figure 2B shows the dependence of *I(Q)* on temperature for difference surfactant concentrations with 6wt% of KCl and the variation of *I(Q)* with salt for three temperatures (insert). It can be seen that at low *Q* values differences in *I(Q)* can be observed, reflecting the increase in contour length of the micellar worms and the increase in the number of persistence lengths per worm as the surfactant concentration is increased or the temperature is reduced.

On the other hand, at high values of *Q*, all the scattering curves superimpose each other suggesting that the local micellar structure of the wormlike micelles does not change with addition of salt. This is due to the fact that micellar growth occurs in a one dimensional fashion along the contour and leaves the cylindrical cross section unaltered, and due to the strong screening of intermicellar interactions on local length scales. Fitting the high Q regime to a Kratky-Porod wormlike chain model give a radius of gyration of the cross-section of 20 Å. From the inserts, the dependence of *I(Q)* on added salt is shown. As the concentration of salt is increased the scattering intensity increases reflecting micellar growth [2-4].

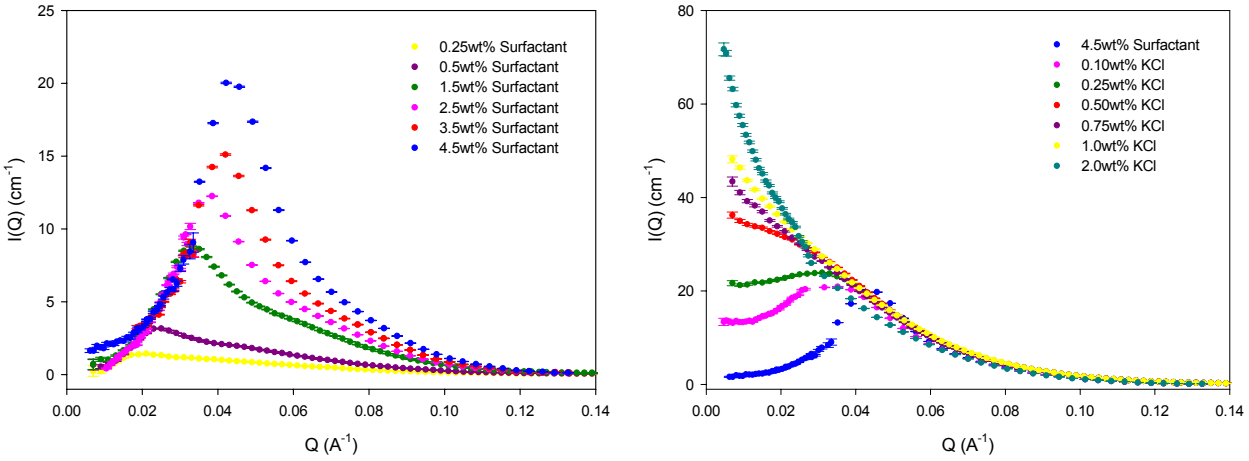

Figure 1: (A) Scattering intensity as a function of surfactant concentration at 25°C. (B) Scattering intensity as a function of salt content at a fixed surfactant concentration of 4.5wt%.

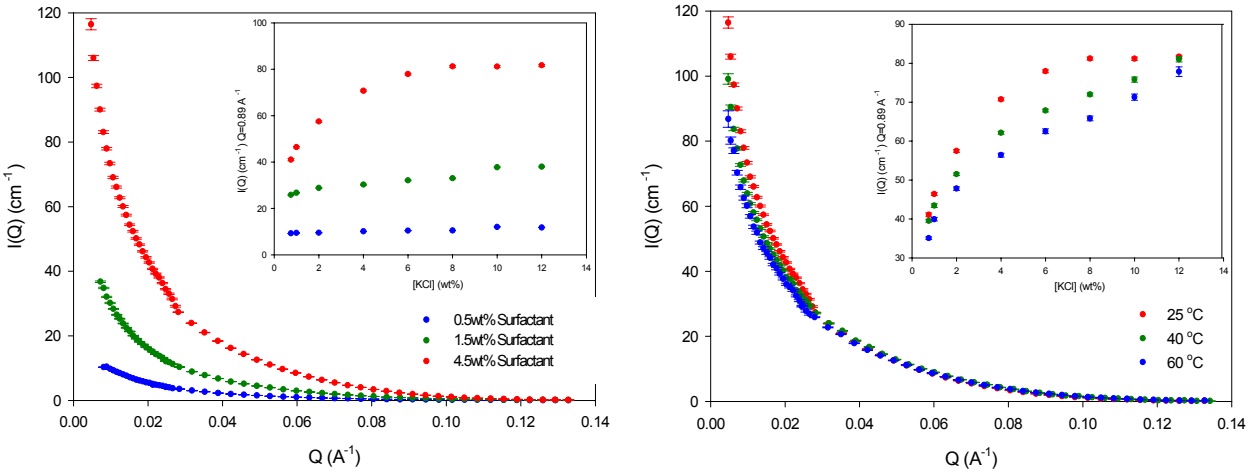

Figure 2: (A) Scattering intensity as a function of surfactant concentration with 6wt% of KCl (fixed). Insert: Scattering intensity as a function of salt concentration for different surfactant concentrations. (B) Scattering intensity as a function of temperature with 6wt% of KCl (fixed). Insert: Scattering intensity as a function of salt concentration for different temperatures

In conclusion, it can be said that the increase in viscosity is due to the formation of wormlike micelles and the decrease due to changes in the properties of the saturated network.. The strong dependence of the viscosity on temperature is a concequence of the decrease in countor length of the micelles which was reflected by the SANS experiment.

References

[1] Raghavan, S.R.; Kaler, E.W., Langmuir. **17**. 2001. 300.
[2] Cappelaere, E.; Cressely, R., Colloid Polym Sci. **276**. 1998. 1050.
[3] Magid, L. J.; Li, Z., Langmuir. **16**. 2000. 10028.
[4]Stradner, A.; Glatter, O.; Schurtenberger, P., Langmuir. **16**. 2000. 5354

Institut für Festkörperforschung
Forschungszentrum Jülich GmbH
D-52425 Jülich

Experimental Report
of Neutron Scattering Experiments
at the FRJ-2 Reactor

Proposal number:	KW2-02-029		
Experiment title:	**Film contrast measurements in a polymeric microemulsion**		
Dates of experiment:	30.11.02-3.12.02	Date of report:	19.02.03
Experimental team: Names	Addresses		
Vitaliy Pipich Dietmar Schwahn Lutz Willner	IFF, FZ-Jülich, D-52425 Jülich		
Local Contact:	Dietmar Schwahn		

Experimental report text body

(Please use 12 pt letters here !)

The binary system of two homopolymers polybutadiene (PB) and polystyrene (PS) mixed with symmetric diblock copolymers PB-PS had been studied by SANS in bulk and block contrasts. This system demonstrates a rich phase behavior due to different nature of critical phenomena in initial components. A microemulsion channel was detected for this system between 7% and 13% of diblock copolymer content in low temperature range. Reentrance one phase behavior was found between 6% and 7.2% of diblock volume fraction. Physical explanation for such behavior is still unclear. Therefor "film" contrast of system is seem to be useul to describe system.

In the present study we investigate by SANS the ternary system dPB/dPS/dPB-PB-dPS when only middle part of quasi-diblock copolymers is visible by neutrons. Matched part of triblock copolymers occupies roughly 5% of their volume.

The neutron small angle diffraction experiments for were performed at KWS2 facility in a Q range between $0.002<Q<0.2Å^{-1}$ (20m, 8m, 4m and 1.25m detector positions). The data were corrected for scattering from empty cell and calibrated in absolute units by a Lupolen secondary standard. Scattering cross-sections of 7% and 10% "film-matched" diblock copolymers is received in temperature range 160-23^{o}C.

Both samples show high momentum transfer peak. The peak position is temperature independent, but the the peak intensity decreases with cooling. This is because stretching of diblockcopolymers. Figure 1 contents structure factors of 7% sample at high Q range. Cross-sections of 10% sample for a few temperatures is shown at Figure 2. Scattering cross-sections in low Q range at high temperatures (160-60^{o}C) almost do not change. In temperature range 60-40^{o}C intensity of intermediate part of the scattering cross-section increases. It looks like formation of droplets with the radius approximately 70Å.

Below 45°C sharp increase of forward scattering one can see at Figure 2 for 10% sample. Formation of interconnected microemulsion structure is the reason of such behavior. The Q^{-2} power behavior of the scattering intensity in intermediate range at 35°C is another indication of film's formation. A crossover of the power behavior from Q^{-2} to Q^{-3} (10%, 35°C) reveals that system has at larger scale porous structure. Further the decrease of temperature to 23°C leads to formation of large scale droplets with radius 200Å. At low temperature ternary polymer system demonstrates bicontinuous-droplet microemulsion transition with temperature. It seems to be the formation of droplet microemulsion leads to complex reentrance phase behavior of system in a vicinity of the Lifshitz line.

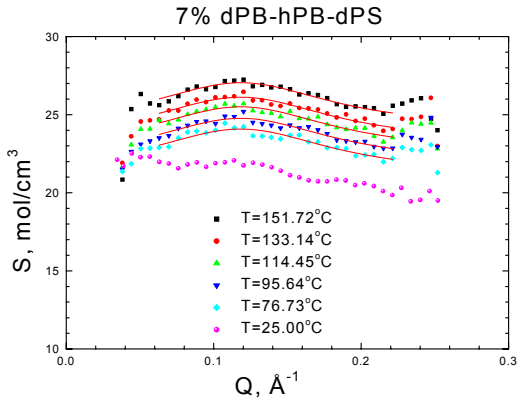

Fig. 1 – Temperature dependence of the structure factor of 7% sample in high Q range.

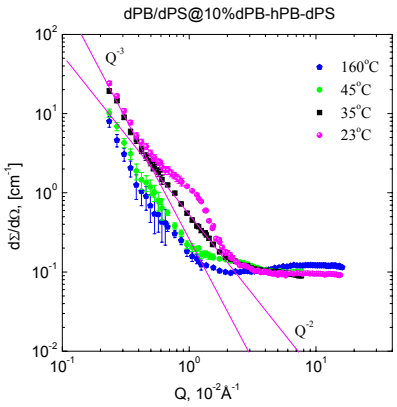

v

Fig. 2 – Scattering cross-sections of 10% sample.

Institut für Festkörperforschung
Forschungszentrum Jülich GmbH
D-52425 Jülich

Experimental Report
of Neutron Scattering Experiments
at the FRJ-2 Reactor

Proposal number:	KW2-02-030		
Experiment title:	**Effizienzsteigerung von Tensiden in Tröpfchen-Mikroemulsionen – Bestimmung der Strukturen mit dem neuen Tensid $C_{12}E_5$**		
Dates of experiment:	23.09.02 - 26.09.02	Date of report:	06.03.03
Experimental team: Names	Addresses		
Dmytro Byelov Henrich Frielinghaus	Forschungszentrum Jülich GmbH Institut für Festkörperforschung Postfach 1913 D-52425 Jülich		
Local Contact:	Henrich Frielinghaus		

Experimental report text body

Die bisherigen Studien umfassen die Effizienzsteigerung *eines* Tensids in Tröpfchen-Mikroemulsionen, nämlich die des $C_{10}E_4$. Hierin wurden ausführlich verschiedene Polymere zur Effizienzsteigerung getestet, die sich im Molekulargewicht und im Blocklängenverhältnis unterscheiden. Alle Polymere haben dieselbe chemische Struktur PEP_X-PEO_Y, wobei X und Y das Molekulargewicht in kg/mol angeben. Das PEP_5-PEO_2 scheint sich nicht besonders gut für eine Effizienzsteigerung zu eignen, wohingegen alle anderen Polymere PEP_5-PEO_5, PEP_{15}-PEO_5, PEP_{22}-PEO_{22}, PEP_{22}-PEO_4 sich sehr gut eignen. Es zeigte sich mittels SANS-Untersuchungen, daß für die maximale Ölkonzentration sich die Struktur der Öltröpfchen ändert. Für die Tröpfchen ohne Polymer bzw. mit dem schwach wirkenden PEP_5-PEO_2 ist die Struktur zylinderförmig. Dahingegen wird unter dem Einfluß der stark effizienzsteigernden Polymere eine eher kugelförmige Tröpfchenstruktur beobachtet. Diese Strukturen sollten nun mittels der Transmissions-Elektronen-Mikroskopie (TEM) überprüft werden. Da aber die gebildeten Strukturen für TEM etwas zu klein sind, muß nun ein von vorne herein etwas effizienteres Tensid $C_{12}E_5$ verwendet werden, welches größere Strukturen erlaubt. Nun wollen wir bereits mit SANS die gebildeten Strukturen dieses Tensids charakterisieren, bevor eine kleine Auswahl an Proben mit der TEM untersucht werden soll. Darüberhinaus ist es auch interessant, ob die Effizienzsteigerung an einem anderen Tensid anders wirkt.

Nach den bisherigen Studien wurde die Effizienzsteigerung für alle Polymere nach dem Phasendiagramm bewertet (Abb. 1). Für ein festes Tensid-zu-Wasser-Verhältnis (und auch Polymer-zu-Tensid-Verhältnis) gibt man nach und nach kleine Mengen an Öl (Dekan) hinzu. Für jede Ölmenge wird die untere und obere Phasengrenze des Einphasengebietes (1) bestimmt. Bei tiefen Temperaturen gibt es eine Öl-Excess-Phase (2-Phasigkeit: $\underline{2}$), bei hohen Temperaturen eine Wasser-Excess-Phase ($\overline{2}$). Für die maximal lösliche Menge an Öl treffen sich diese beiden Temperaturen.

Die bisherigen SANS-Messungen wurden nun für eine feste Ölmenge (4%vol) bei der niedrigsten und höchsten Temperatur im Einphasengebiet durchgeführt. Die beobachteten Strukturen zeigten sich unbeeinträchtigt von der Polymerzugabe. Bei tiefen Temperaturen findet man ein kugelförmiges Tröpfchen, bei hohen Temperaturen wurden zylinderförmige Strukturen beobachtet. Ein weiterer Meßpunkt der SANS-Untersuchungen war die maximale Ölkonzentration. Während man ohne Polymer bzw. mit schwach wirkendem Polymer auch hier zylinderförmige Strukturen beobachtet, sind die gebildeten Strukturen mit den stark effizienzsteigernden Polymeren eher kugelförmig. An der maximalen Ölkonzentration scheint sich also die entropische Feder (d.h. das Polymer) Platz zu schaffen, indem kugelförmige Tröpfchen bevorzugt werden.

Dieses Verhalten wird nun weitestgehend auch für das neue Tensid $C_{12}E_5$ bestätigt. Die Strukturen für eine feste Ölmenge (3%) waren ebenfalls kugelförmige und zylinderförmige Tröpfchen für niedrige/hohe Temperaturen (Abb. 2). Leider sprechen die Daten für die hohen Temperaturen nicht mehr für das Auftreten reiner Zylinderstrukturen, sondern andere Tröpfchen mit nicht unbedingt eindeutiger Struktur koexistieren. Diese mögliche Koexistenz erschwert ebenfalls die Interpretation bei maximaler Ölkonzentration, doch kann man hier den generellen Trend zu kugelförmigen Tröpfchen unabhängig von der Polymerbeigabe feststellen. Hierin scheint sich das Tensid $C_{12}E_5$ vom vorherigen $C_{10}E_4$ zu unterscheiden.

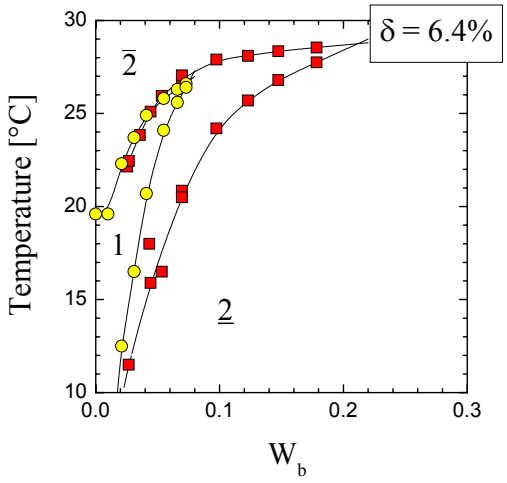

Abbildung 1: Phasendiagramm Temperatur gegen Ölkonzentration W_b (in Volumenbruchteilen) für eine feste Tensid/Wasser-Menge (4%vol). Einmal gezeigt ist das Phasendiagramm ohne Polymer (O) und einmal mit dem Polymer PEP_{22}-PEO_4 (□) bei einem Verhältnis Polymer/Tensid von 6.4%vol. Das Einphasengebiet ist mit 1 gekennzeichnet, das Zweiphasengebiet mit einer Öl-Excess-Phase mit 2, und mit einer Wasser-Excess-Phase mit $\bar{2}$.

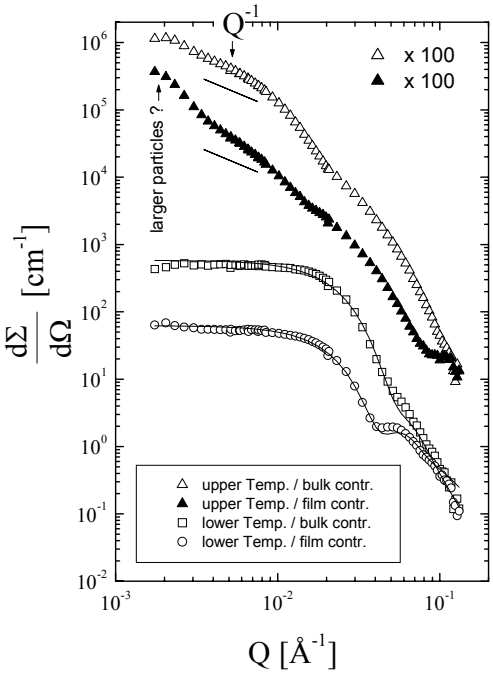

Abbildung 2: SANS-Streukurven einer Mikroemulsion aus Wasser (D_2O), dem Öl Oktan, dem Tensid $C_{12}E_5$ und dem Polymer PEP_{22}-PEO_4. Während man bei tiefen Temperaturen (□,○) kugelförmige Tröpfchen beobachtet, sind bei hohen Temperaturen (△,▲) die Tröpfchen zylinderförmig. Allerdings koexistieren hier wahrscheinlich zwei Strukturen.

Institut für Festkörperforschung
Forschungszentrum Jülich GmbH
D-52425 Jülich

Experimental Report
of Neutron Scattering Experiments
at the FRJ-2 Reactor

Proposal number:	KW2-02-031		
Experiment title:	Structural Order in Polymer Colloids (under Shear)		
Dates of experiment:	20.09.02	Date of report:	19.02.03
Experimental team: Names	Addresses		
Silke Rathgeber Axel Müller Mingfu Zhang	Forschungszentrum Jülich GmbH Institut für Festkörperforschung – Weiche Materie D-52425 Jülich Universität Bayreuth Makromolekulare Chemie II Universitätsstr. 30; NW II D-95440 Bayreuth		
Local Contact:	Silke Rathgeber		

Experimental report text body

We consider bottle-brush or comb-like polymers as macromolecules where relatively long side chains are densely grafted to a backbone in a regular manner. The interest in cylindrical comb polymer brushes is related to the possibility to form stiff cylindrical, shape persistent structures based exclusively on the intra-molecular excluded volume interaction. In melts of bottlebrush polymers thermotropic transitions between isotropic, nematic and smectic phases have been found [1].

The comb diblock copolymers consist of a poly(ethyl methacrylate) backbone to which poly(acrylic acid)-poly(n-butyl acrylate) diblock copolymers are densely grafted. The comb polymer has a core-shell structure where the poly(acrylic acid) and the poly(n-butyl acrylate) build the core and the shell, respectively. In a first experiment the combs have been dissolved in mixtures of deuterated methanol and chloroform. Chloroform is supposed to be a good solvent for the shell polymer (bad solvent for the core polymer) and methanol should be a good solvent for the core polymer (bad solvent for the shell polymer) [2]. In Fig. 1 the form factors obtained from SANS for three different solvent compositions are shown: (1) 75vol% MEOD/25vol% $CDCl_3$, (2) 62.5vol% MEOD/37.5vol% $CDCl_3$, and (3) 50vol% MEOD/50vol%$CDCl_3$. Fig. 2 shows the corresponding cross section form factors $P_{CS}(q)$ which can be approximately obtained from the overall form factor using the relation $P_{CS}(q)= P(q)q^{1/\nu}$, where ν is the fractality of the whole bottle-brush. The equation only holds if the contour length of the bottle-brush polymer is much larger then its thickness. In this case the scattering contributions of the overall shape and that of the cross section density profile are well separated in q-space. Studies on similar samples have shown that the bottle-brushes can be seen as worm-like chains on large length scales and ν equals approximately 0.588 as expected for a self avoiding random walk.

As can be seen from Fig. 2 the cross section form factor is nearly unaffected by increasing the methanol content from 50vol% to 62.5vol% but significant changes occur for the sample with 75vol% methanol. Unfortunately the comb polymer could neither be solved in solutions with methanol contents higher than about 85vol% methanol nor in solutions with chloroform contents higher than about 75vol%, even so the latter is supposed to be a good solvent for the outer shell polymer.

Outlook:

The main aim of this preliminary experiment are insitu-rheological measurements to investigate the alignment of these soft, anisotropic polymer colloids in shear flow. Shear induced transitions to nematic phases might be observed at high polymer concentrations.

References:

[1] Shibaev VP, Barmatov EB, Tao YJ, Richardson R, Polymer Science Series A, 2000, 42, 1086.

[2] Polymer Handbook, 4th Ed., Eds. J. Brandrup, E.H. Immergut, and E.A. Grulke, John Wiley & Sons, 1999.

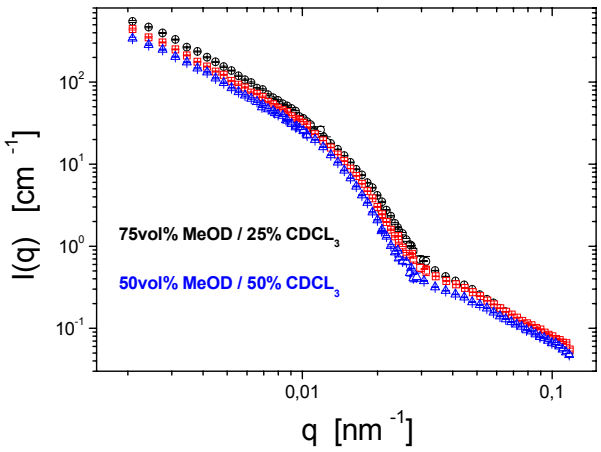

Fig.1: Form factors of diblock copolymer bottle-brushes measured with SANS for various methanol/ chloroform compositions.

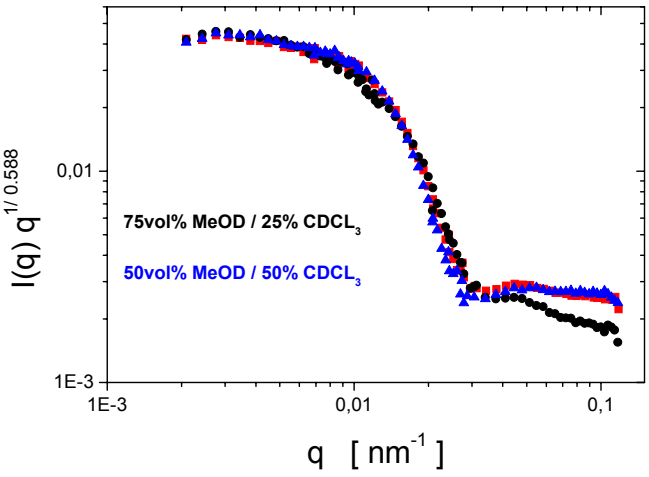

Fig.2: Cross section form factors obtained from the form factors shown in fig. 1.

Institut für Festkörperforschung
Forschungszentrum Jülich GmbH
D-52425 Jülich

Experimental Report
of Neutron Scattering Experiments
at the FRJ-2 Reactor

Proposal number:	KW2-02-032		
Experiment title:	**The M_W and volume fraction dependence of the self-assembly in solution of syndiotactic polypropylene (sPP) and poly(ethylene-propylene) (PEP) polymers**		
Dates of experiment:	17.09.02-18.09.02	Date of report:	06.03.2003
Experimental team: Names	Addresses		
Aurel Radulescu Robert Stollenwerk	IFF, FZ-Jülich, D-52425 Jülich		
Local Contact:	Henrich Frielinghaus		

Experimental report text body

(Please use 12 pt letters here !)

Previous SANS investigations [1,2] of the temperature behavior of syndiotactic-polypropylene-poly(ethylene-propylene) (sPP-PEP) diblock copolymers in dilute solution have shown that these systems yield by self-assembling complex morphologies formed by multi-level structures: very large one-dimensional aggregates possibly made by association of smaller two-dimensional objects. The sizes of these structures vary as depending on the polymer molecular weight: the higher the molecular weight the larger the formed structures are. On the other side, the sPP homopolymer self-assembles from dilute solution by forming thin compact platelets of a thickness of about 57Å. In order to improve the knowledge about the self-assembly behavior of these diblock copolymers (how the structural characteristics of the aggregates vary with the molecular characteristics of the component blocks) we investigated here by SANS the correspondent homopolymers to the constituent blocks of the copolymer: (i) the self-assembling behavior of the sPP homopolymer in dilute solution for different molecular weights and polymer concentrations and (ii) the temperature behavior of the high M_W PEP homopolymer in low hydrocarbons. The temperature behavior of three sPP homopolymers with M_W of about 43400 g mol^{-1}, 61400 g mol^{-1} and 85000 g mol^{-1} has been studied in decane solutions for 0.5% and 1% polymer volume fractions. Since the melting point of the sPP is around 147°C a very wide temperature range was investigated, between the single coil (at 160°C) and the aggregation regime (below 0°C). The behavior of a PEP homopolymer with M_W of about 192000 g mol^{-1} was also checked in a decane solution for 1% polymer volume fraction at temperatures between 85°C and 0°C. The SANS measurements were performed at KWSII spectrometer set-up at the FRJ-2 reactor in Jülich. Using a neutron wavelength of 7Å and three sample-to-detector distances a Q range between 0.002$Å^{-1}$ and 0.14$Å^{-1}$ could be covered. The data were corrected for the scattering from empty cell and solvent and then calibrated in absolute units by using a Lupolen secondary standard [3]. Working with fully protonated polymers the maximum contrast and the minimum incoherent background were achieved by choosing fully deuterated solvent (d-22).

Figure 1a and b show the scattering cross sections of different sPP solutions measured at room temperature. One can observe that the scattering patterns from solutions of different M_W polymers at the same polymer volume fraction coincide while those from solutions with different polymer volume fractions are shifted only by a factor depending on the concentrations ratio. All scattering curves prove the formation of thin platelet-like aggregates. Data analysis in terms of the 2-dimensional Guinier approximation [4] gives a constant platelet thickness of about 57Å and proves that platelets are compact objects including almost all polymers.

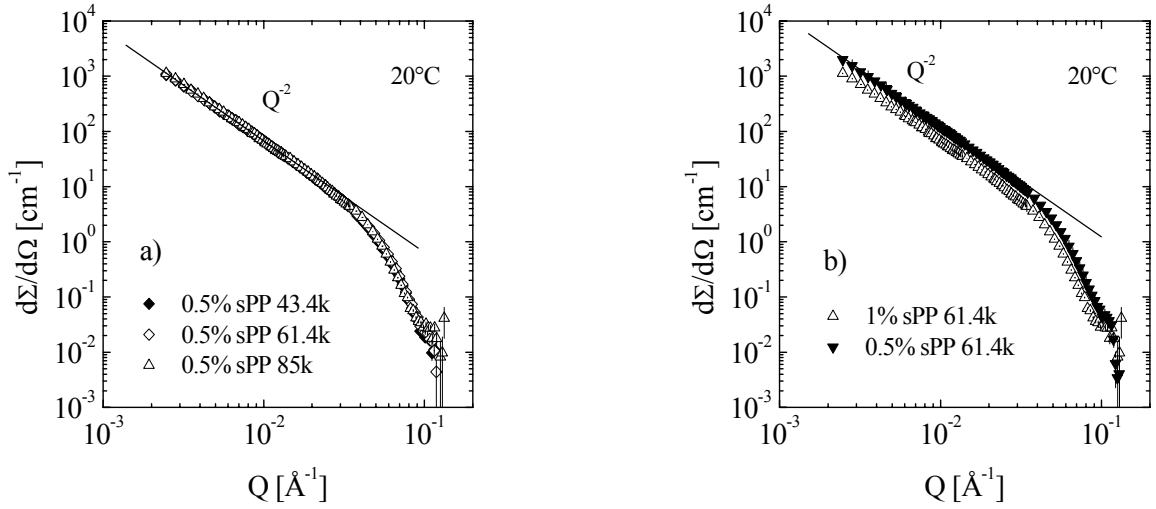

Fig.1 – Scattering from sPP homopolymer solutions at room temperature for different M_W polymers (a) and different polymer contents (b)

Figure 2 shows the scattering patterns from the PEP solution for a 0.5% polymer volume fraction. For the whole temperature range investigated the high M_W PEP stays in single coil regime and does not show any aggregation tendency. An analysis of the single chain properties in terms of the Zimm approximation yields a radius of gyration of about 220Å and a forward scattering that is in a good agreement with the molecular characteristics of the polymer [5].

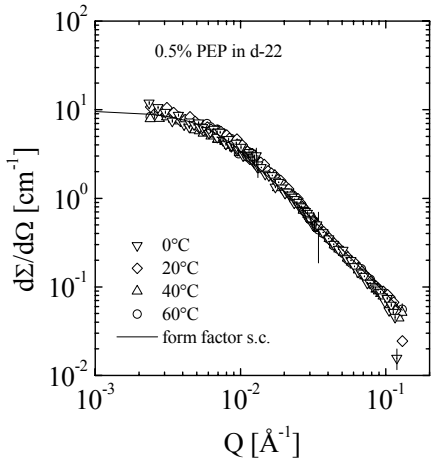

Fig. 2 –Scattering from a PEP solution at different temperatures

References

[1] proposal KW2-01-37, IFF, FZ Jülich
[2] proposal KW2-02-20, IFF, FZ Jülich
[3] D.Schwahn et al., J.Phys.Chem. 93, 8383, 1990.
[4] D.Schwahn et al., Macromolecules 35, 861, 2002.
[5] L.J.Fetters et al., Macromolecules 27, 4639, 1994.

Institut für Festkörperforschung
Forschungszentrum Jülich GmbH
D-52425 Jülich

Experimental Report of Neutron Scattering Experiments at the FRJ-2 Reactor

Proposal number:	KW2-02-033		
Experiment title:	Core contrast form factor of PEP-PEO block copolymer micelles obtained by contrast variation.		
Dates of experiment:	18.09.02-19.09.02	Date of report:	6.03.03
Experimental team: Names	 Addresses		
Laurati, Marco Stellbrink, Jörg Willner, Lutz Lund, Reidar	IFF, FZ Juelich IFF, FZ Juelich IFF, FZ Juelich IFF, FZ Juelich		
Local Contact:	H. Frielinghaus		

Experimental report text body

In recently performed measurements (03/02) we found that the core-contrast condition for PEP1-PEO20 star-like micelles is not completely achieved in pure D_2O, as we expected. This is probably due to a variation of the PEO density in solution.
In the present session of measurements we investigated the shell matching condition of the PEP1-PEO20 diblock copolymer micelles using contrast variation.
In detail we measured the micellar form factor in five different contrasts. Very dilute samples, 0.25% polymer volume fraction, were measured in pure D_2O, 99% D_2O – 1% H_2O, 98% D_2O – 2% H_2O, 97% D_2O – 3% H_2O and 96% D_2O – 4% H_2O. The measurements were performed at 2 and 8m detector distances and at room temperature. Due to the low intensity resulting from the small polymer concentration we measured each sample for three hours at 8m detector distance, in order to obtain good statistics. Due to the very long time required we could not measure the samples at 20m detector distance.

The form factors measured in D_2O solvent and 99% D_2O – 1% H_2O solvent are shown in fig.1. The intensity are normalized by the polymer volume fraction. As one can notice it is not straightforward to say which solvent is better matching the shell scattering since both spectra are flat at low Q values, condition that should be achieved if no shell contributions are present. The decreasing value of the intensity in the limit of $Q \rightarrow 0$ is in agreement with theory predictions.
On the other hand one can clearly see that increasing the H_2O content over 2% makes the shell contribution visible at low Q, as shown in the form factor spectra measured in 98% D_2O – 2% H_2O solvent and 97% D_2O – 3% H_2O solvent (fig.2).
The shell matching solvent seems then to be somewhere in between pure D_2O and 99% D_2O – 1% H_2O.

Further investigation of this narrow region has no sense since is becoming comparable with the uncertainty in the known purity of D_2O.

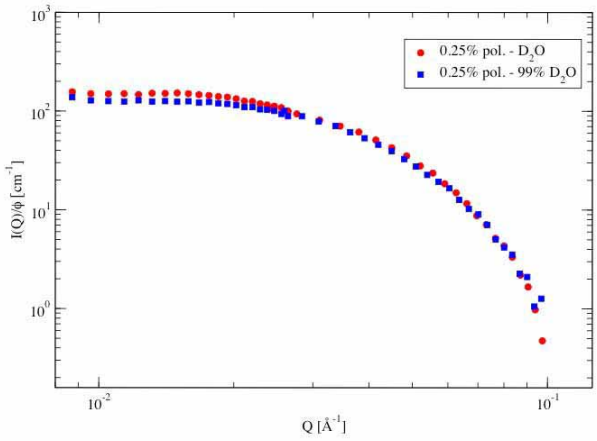

Figure 1 : Form Factor measured in D2O and 99% D2O

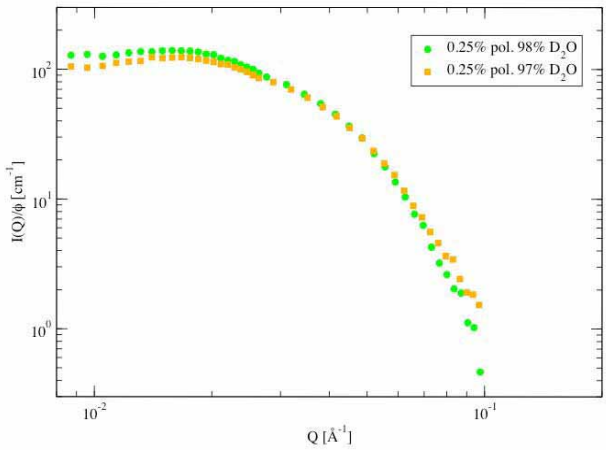

Figure 2 : Form Factor measured in 98% D_2O and 97% D_2O

1. H. Endo et al., *Phys. Rev. Lett.*, **85**, 102 (2000).

An alternative way of extracting the pure core-core contribution is that of directly calculating the partial scattering functions, following the method elaborated by Endo et al. [1]. The coherent scattering cross section can be written (incompressible systems) as: $I(Q) = \sum_{i,j} (\rho_i-\rho_0)(\rho_j-\rho_0)S_{ij}(Q)$ where ρ_i, ρ_j are the scattering length densities of the components and ρ_0 that of the solvent (taken as reference). Measuring intensities at different contrasts provides the relation between the vector of intensities and that of the partial structure factors: $\mathbf{I} = \mathbf{AS}$ where A is the matrix of the contrasts. The generalized inverse of the A matrix can be calculated using the singular value decomposition (SVD). Once calculated that matrix allows the determination of partial structure factors.

We tried to apply this method to our data: with the measured contrast we have a good spanning of the core contrast region, so we obtained a good evaluation of the core-core partial scattering function. On the other hand the shell and cross terms need additional measurements in the shell contrast and intermediate contrast regions to be evaluated.

Institut für Festkörperforschung
Forschungszentrum Jülich GmbH
D-52425 Jülich

Experimental Report
of Neutron Scattering Experiments
at the FRJ-2 Reactor

Proposal number:	KW2-02-034		
Experiment title:	Time resolved SANS experiments during "living" anionic polymerisation: III. The initiation period		
Dates of experiment:	Nov. 02-05, 2002	Date of report:	19-02-03
Experimental team: Names	Addresses		
A. Niu J. Stellbrink J. Allgaier L. Willner D. Richter L. J. Fetters	IFF-Neutronenstreuung, Forschungszentrum Juelich, D-52425 Juelich IFF-Neutronenstreuung, Forschungszentrum Juelich, D-52425 Juelich IFF-Neutronenstreuung, Forschungszentrum Juelich, D-52425 Juelich IFF-Neutronenstreuung, Forschungszentrum Juelich, D-52425 Juelich IFF-Neutronenstreuung, Forschungszentrum Juelich, D-52425 Juelich Department of Chemical Engineering, Cornell University, Ithaca, NY 14584, USA		
Local Contact:	A.Niu: a.niu@fz-juelich.de, 02461-612258		

Experimental report text body

Living anionic polymerization of dienes and styrene in non-polar solvents based on organolithium compounds is now recognized to be a more complicated operation than that presented as the "textbook explanation", has been of long term academic and commercial interest. This kind of anionic polymerization proceeds by chain initiation and propagation steps only, these two steps overlap during much of the total polymerization process

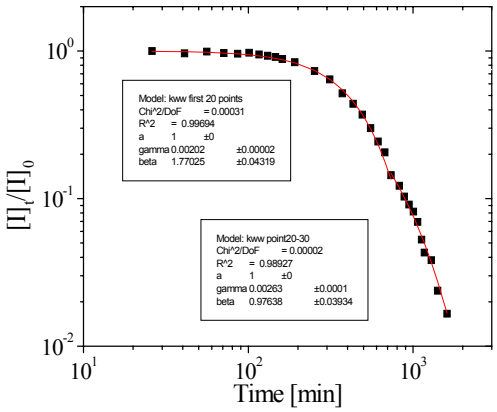

Figure 1 Time dependence of initiator concentration

depend on the rates of initiation propagation, produces polymers with controlled molar mass, architecture, and narrow molar mass distribution. However, the question of the mechanism through which the chain growth event takes place is not resolved. A key question is the aggregation behavior of the organolithium head groups. NMR data show that the initiation occurs over quite a long time range where chain growth is already quite important. In the initiation stage, both initiator and monomer concentration decay with a streched exponential (Fig. 1). Figure 2 is the SANS data we measured at low Q range during the initiation stage of the anionic polymerization of butadiene in D-heptane. It clearly shows that there are large scale aggregates in this system.

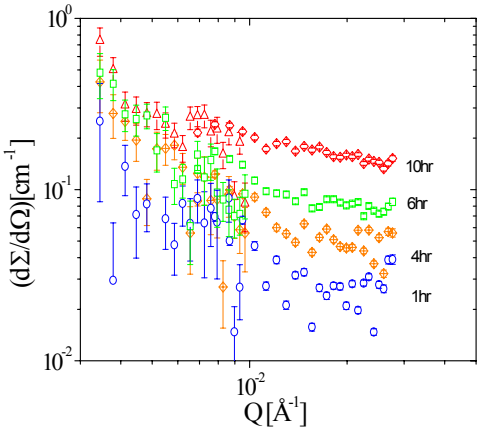

Figure 2 SANS data obtained duing the initiation period at low Q range.

Institut für Festkörperforschung
Forschungszentrum Jülich GmbH
D-52425 Jülich

Experimental Report
of Neutron Scattering Experiments
at the FRJ-2 Reactor

Proposal number:	KW2-02-035		
Experiment title:	**Structure of h-PB-d-PS Micelles in Decane**		
Dates of experiment:	22-23/09-02	Date of report: 26/02-03	
Experimental team: Names	Addresses		
Reidar Lund Dr. Lutz Willner Dr. Aurel Radelescu Prof. Dieter Richter	Forschungszentrum Jülich; IFF-Institut für Neutronenstreuung D-52425 Jülich		
Local Contact:			

Experimental report text body

In previous experiments we have studied the structure and kinetics of PEP-PEO block copolymer micelles in water/DMF Mixtures. We have revealed several interesting things, ie. the association behaviour as a function of the solvent quality and correlated this to the surface tension. We also observed that upon increasing DMF content, the PEO chains apparently shrinked and above a certain DMF content a macroscopic phase separation was observed at room temperature.
In order to further elucidate the behaviour of PEO in aqueous solutions containing DMF, we decided to measure the second virial coefficient, A_2, as a function of DMF content. We originally decided to measure: the structure of h-PB-d-PS Micelles in decane, however to complement and finish our last topic we decided to measure PEO homopolymer instead.
Starting with Light Scattering, we discovered that this was very difficult due to very low contrast between PEO and DMF. The refractive indices of PEO and DMF are 1.48 and 1.43 respectively. Test experiments during the beamtime showed that the experiment was readily done using SANS and isotopic solvent mixtures. However due to a reactor break down, we were only able to use ca. 24 hours of the beamtime. During the time we measured PEO in pure DMF system and rechecked some of our previous measurements of PEP1-PEO20k micelles in water/DMF. The PEO homopolymer measurements[see fig 1] revealed that PEO in DMF at 30°C are in a marginally good solvent, A_2 was of the order of 2E-3 mole*cm^3/g^2. We continued the experiment in Proposal: KW2-02-037

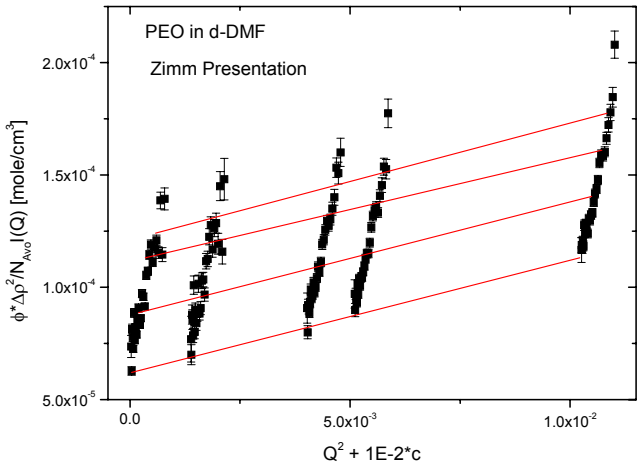

Fig. 1 Zimm Plot of PEO in d-DMF at 30°C. Radius of Gyration, R_G~ 58 Å

Institut für Festkörperforschung
Forschungszentrum Jülich GmbH
D-52425 Jülich

Experimental Report
of Neutron Scattering Experiments
at the FRJ-2 Reactor

Proposal number:	KW2-02-036		
Experiment title:	**Investigation of DMAP phase behavior**		
Dates of experiment:	10.12. – 12.12. 2002	Date of report:	23.02.2003
Experimental team: Names	Addresses		
D. Schwahn	IFF-FZJ		
Local Contact:	D. Schwahn		

Experimental report text body

From investigation of mineralization of $CaCO_3$ in the presence of gold colloids and DMAP and 0.1 M $CaCl_2$ in aqueous solutions we got the suspicion that DMAP in the concentration range of 30 mg/cm^3 forms aggregates. We therefore performed an independent experiment. Figure 1 shows the scattering patterns of a $CaCl_2$ aqueous solution without and with the addition of 30mg/cm^3 DMAP in D_2O and H_2O. The scattering at small Q seems to be originated from the $CaCl_2$ while DMAP seems to be in solution. In figure 3 concentrations of DMAP are depicted. The scattering seems to be roughly proportional to the concentration.

From these results we cannot conclude any aggregation effect of the DMAP molecules. One reason might be that the $CaCl_2$ we used was not clean enough. So our earlier results from which we speculated aggregated DMAP seems to be mysterious so that we need more investigations.

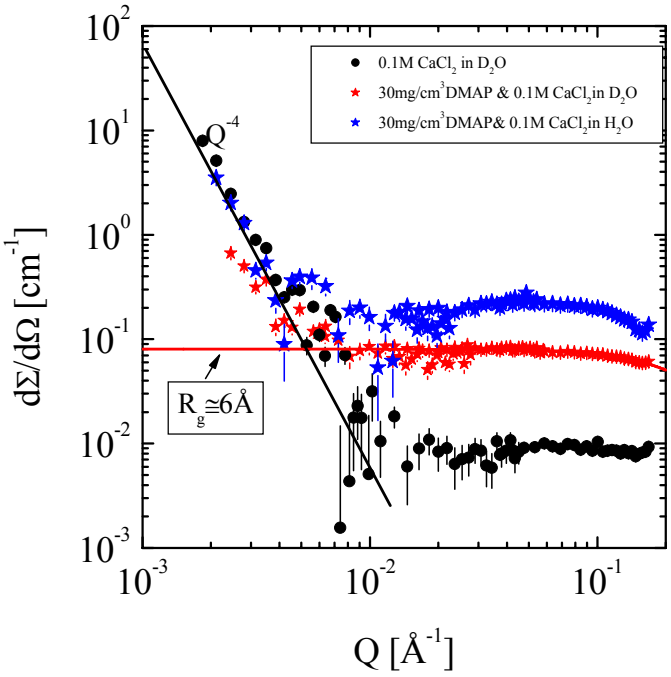

Figure 1: Aqueous solution of 0.1M $CaCl_2$ without and with 30mg/cm^3 DMAP in D_2= and H_2O. There are large aggregates as well as scattering from the small molecules

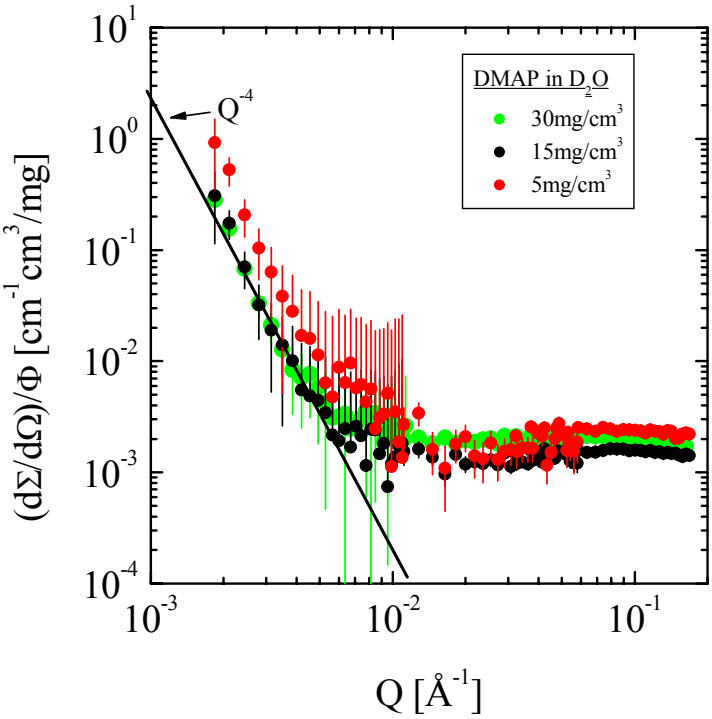

Figure 2: DMAP in water at different concentrations. The intensity is roughly proportional to the DMAP concentration.

Institut für Festkörperforschung
Forschungszentrum Jülich GmbH
D-52425 Jülich

Experimental Report
of Neutron Scattering Experiments
at the FRJ-2 Reactor

Proposal number:	KW2-02-037		
Experiment title:	**Determination of the Second Virial Coefficient in of PEO in Solvent Mixtures consisting of DMF and Water**		
Dates of experiment:	23-25/10-02	Date of report: 04/03-03	
Experimental team: Names	Addresses		
Reidar Lund Dr. Lutz Willner Dr. Aurel Radelescu Prof. Dieter Richter	Forschungszentrum Jülich; IFF- Institut für Neutronenstreuung D-52425 Jülich		
Local Contact:			

Experimental report text body

In the last proposal experiment (proposal nr. KW2-02-035) we started to measure the second virial coefficient, A_2, og PEO homopolymer as a function of DMF content. Starting with Light Scattering, we discovered that this was very difficult due to very low contrast between PEO and DMF. The refractive indices of PEO and DMF are 1.48 and 1.43 respectively. Test experiments during the previous beamtime(Prop.nr. KWS2-02-035) showed that the experiment was readily done using SANS and isotopic solvent mixtures. However due to a reactor break down, we were only able to use ca. 24 hours of the beamtime. This experiment was therefore to complete the earlier measurements.

Figure 1 shows the obtained results:

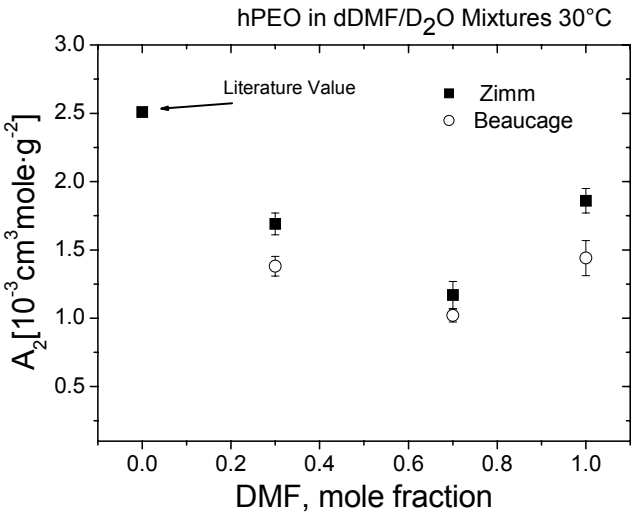

Fig. 1 The second virial coefficient, A2, in different DMF/Water mixtures.

If we compare these results to the apparent shrinking of the micellar corona observed from earlier measurements we obtain a good correlation as best illustrated in the following plot(the line correspond to the predicted power law by Wijmans and Zhulina [1]):

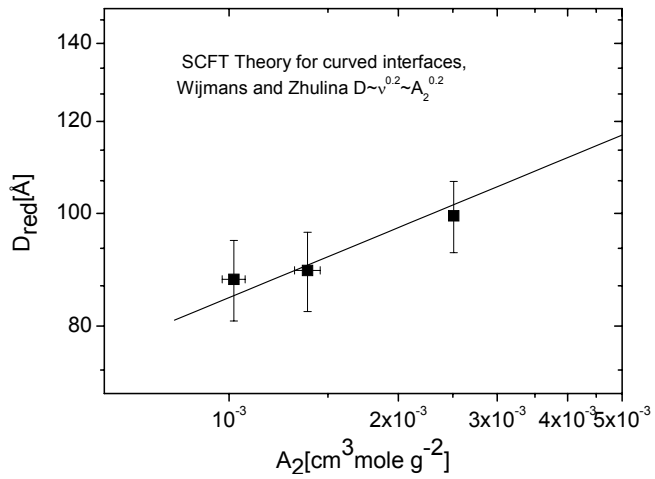

References

[1] C.M. Wijmans and E.B. Zhulina *Macromolecules* **26** (1993) 7214.

Institut für Festkörperforschung
Forschungszentrum Jülich GmbH
D-52425 Jülich

Experimental Report
of Neutron Scattering Experiments
at the FRJ-2 Reactor

Proposal number:	KW2-02-039		
Experiment title:	**Domänengrößenbestimmung in einer bikontinuierlichen Mikroemulsion für Patentanmeldung eines Polymerboosters**		
Dates of experiment:	03.12.02	Date of report:	06.03.03
Experimental team: Names	Addresses		
Frielinghaus, Henrich Allgaier, Jürgen	Institut für Festkörperforschung Forschungszentrum Jülich GmbH D-52425 Jülich Germany		
Local Contact:	Frielinghaus, Henrich		

Experimental report text body

In dieser Meßzeit wurde routinemäßig die Domänengröße von bikontinuierlichen Mikroemulsionen untersucht. Hierbei sollte die Anwendbarkeit eines PBO6-PEO6 Diblock-Copolymers als Effizienz-Booster in silikonöl-haltigen Mikroemulsionen demonstriert werden. Es wurde gezeigt, daß die Domänengröße mit zunehmender Polymerkonzentration zunimmt, was wie erwartet die Anwendbarkeit demonstriert.

Die Mikroemulsionen wurden aus Siloxan (Silikonöl), (schwerem) Wasser, Tensid und ggf. amphiphilen Diblock-Kopolymer hergestellt. In der Vorbereitung wurde durch Messung des Phasendiagramms die minimal nötige Menge an Tensid bestimmt, die nötig ist, um eine einphasige Mikroemulsion zu erreichen (Fisch-schwanzpunkt). Die drei optimalen einphasigen Proben mit Polymer-Anteilen von $\delta = 0$, 5% und 10% bezogen auf die Gesamttensidmenge zeigen bereits, daß sich mit zunehmendem Polymergehalt die benötigte Tensid-konzentration verringert. Diese optimalen Proben wurden nun mit der Neutronenkleinwinkelstreuung vermessen.

Die gemessenen Kleinwinkelstreuspektren werden mit der theoretischen Streukurve von Teubner und Strey beschrieben, um die Domänengröße d und die Korrelationslänge ξ zu erhalten:

$$I(Q) \sim \frac{8\pi\phi_O\phi_W / \xi}{((2\pi/d)^2 + \xi^{-2})^2 - 2((2\pi/d)^2 - \xi^{-2})Q^2 + Q^4}$$

Die Anwendbarkeit dieser Formel ist in Abbildung 1 demonstriert. Man sieht, daß die Peakform für alle Polymerkonzentrationen durch die theoretische Formel wiedergegeben wird. Die aus der Kurvenanpassung erhaltenen Parameter sind in Abbildung 2 wiedergegeben.

Wie erwartet erhöht sich die Domänengröße d mit steigendem Polymergehalt. Die Korrelationslänge ξ verhält sich analog und beträgt in etwa die Hälfte der Domänengröße. Damit wurde in dieser Routinemessung erfolgreich demonstriert, daß mit steigendem Polymergehalt sich die Effizienz einhergehend mit der Domänengröße erhöht. Diese Ergebnisse können nun für die Patentanmeldung des PBO6-PEO6 Polymers genutzt werden.

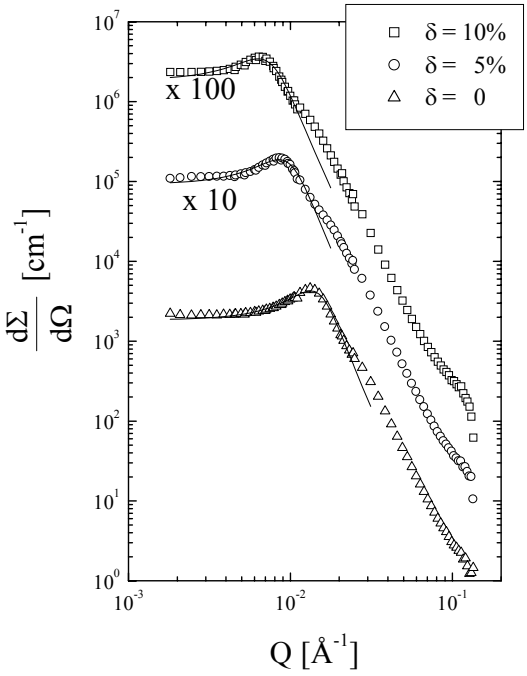

Abbildung 1: Die Streukurven als Funktion des Streuvektors Q für verschiedenen Polymergehalt. Die durchgezogenen Linien sind angepaßte Kurven der Teubner-Strey Theorie.

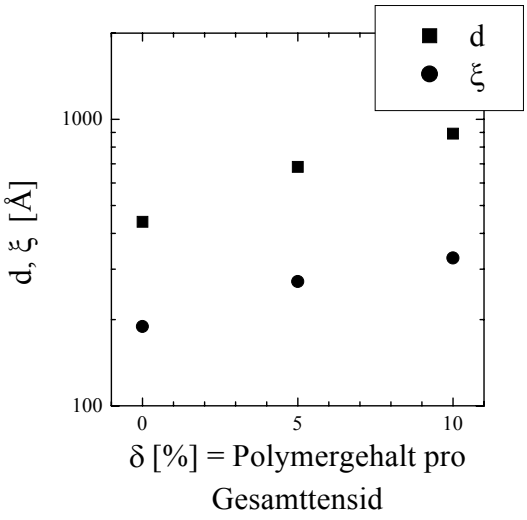

Abbildung 2: Die Domänengröße d und die Korrelationslänge ξ als Funktion der Polymerkonzentration.

Institut für Festkörperforschung
Forschungszentrum Jülich GmbH
D-52425 Jülich

Experimental Report
of Neutron Scattering Experiments
at the FRJ-2 Reactor

Proposal number:	KW2-02-040		
Experiment title:	Partial structure factors of PEP-PEO star-like micelles obtained by contrast variation		
Dates of experiment:	13.12.02-15.12.02	Date of report:	6.03.03
Experimental team: Names	 Addresses		
Laurati, Marco Stellbrink, Jörg Willner, Lutz Lund, Reidar	IFF, FZ Juelich IFF, FZ Juelich IFF, FZ Juelich IFF, FZ Juelich		
Local Contact:	H. Frielinghaus		

Experimental report text body

In recently performed measurements (09/02) we started a detailed contrast variation analysis of the form factor of PEP1k-PEO20k star-like micelles, in order to extract the different partial scattering functions using the method elaborated by Endo et al.
In the present measurements session we extended our contrast variation analysis in the shell contrast and intermediate contrast region, in order to obtain a good estimation of the shell-shell and core-shell partial scattering functions.
In detail we measured the form factor (very dilute sample, 0.25% polymer volume fraction) in shell contrast, 70% D_2O- 30% H_2O, and in 99% D_2O – 1% H_2O for comparison with previous measurements. Measurements were performed at both 2 and 8m detector distances and at room temperature.

The additional measurements let us obtain reasonable partial scattering functions (see fig.1) with good reconstructions of the initial scattering intensity. The relatively poor quality of the shell and intermediate contrast measurements in the high Q region is due to the strong incoherent background of H_2O. This also affects the quality of the shell-shell and core-shell partial scattering functions obtained. The problem can be solved using a partially labeled PEP core for the shell and intermediate contrast measurements, in order to use solvents with a high percentage of D_2O. This polymer has to be synthesized yet.

We also investigated the effect of temperature to the micellar dimension. We measured the shell contrast form factor at room temperature and at 70 °C. As we expected the shell is shrinking due to the decreasing quality of the solvent (Fig. 2). In particular assuming a star-like profile ($\propto r^{-4/3}$) for the shell we obtained a micellar radius of 250 Å at room temperature and of 200 Å at 70 °C, as fitting results.

Finally we also measured a 5% polymer volume fraction sample in 99% D_2O – 1% H_2O solvent at room temperature and at 70 °C. The measurement at room temperature was repeated after cooling down and no differences in the spectra were found. The measurement at 70 °C was also performed a second time after several hours producing the same result. Dividing out the corresponding form factor we derived the core-core structure factors (Fig. 3). In agreement with our previous structure factor measurements the sample seems to be in a meta stable gel phase and the temperature does not seem to drastically modify the structure. In fact one can only observe a slight relaxation of the system.

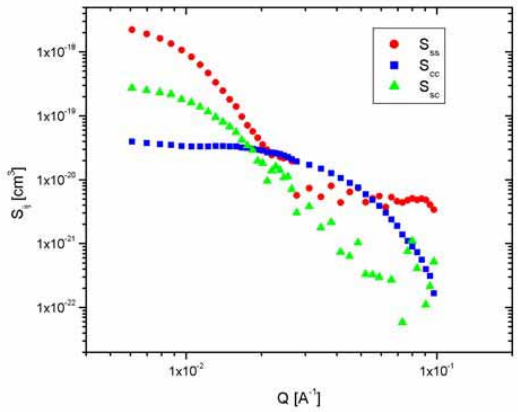

Figure 1 : Partial scattering functions obtained from SVD.

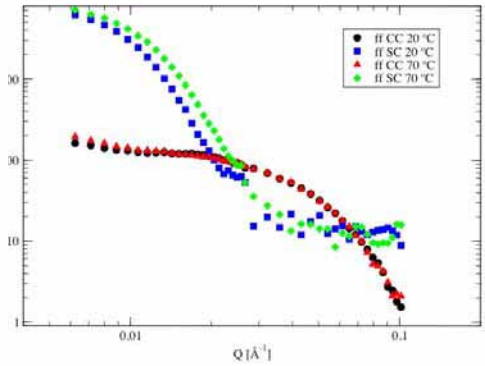

Figure 2 : Shell contrast form factor measured at 20 ºC and 70 ºC.

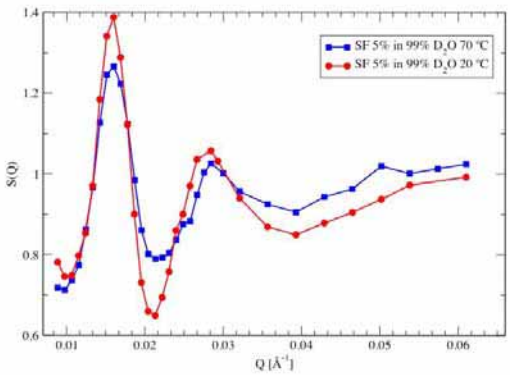

Figure 3 : Core-Core Structure Factor (5% polymer volume fraction) measured at 20 ºC and 70 ºC.

Institut für Festkörperforschung
Forschungszentrum Jülich GmbH
D-52425 Jülich

Experimental Report of Neutron Scattering Experiments at the FRJ-2 Reactor

Proposal number:	KW2-02-041		
Experiment title:	Time resolved SANS experiments during "living" anionic polymerisation: IV. Characterisation of the terminated samples		
Dates of experiment:	Nov. 17-24, 2003	Date of report:	19-02-03
Experimental team: Names	Addresses		
A. Niu J. Stellbrink J. Allgaier L. Willner D. Richter L. J. Fetters	IFF-Neutronenstreuung, Forschungszentrum Juelich, D-52425 Juelich IFF-Neutronenstreuung, Forschungszentrum Juelich, D-52425 Juelich IFF-Neutronenstreuung, Forschungszentrum Juelich, D-52425 Juelich IFF-Neutronenstreuung, Forschungszentrum Juelich, D-52425 Juelich IFF-Neutronenstreuung, Forschungszentrum Juelich, D-52425 Juelich Department of Chemical Engineering, Cornell University, Ithaca, NY 14584, USA		
Local Contact:	A.Niu: a.niu@fz-juelich.de, 02461-612258		

Experimental report text body

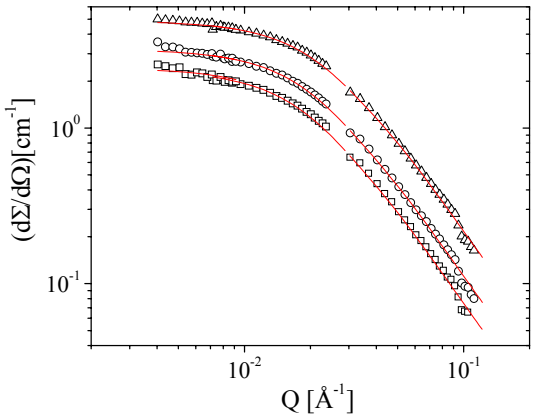

This experiment is the complement of experiment KW2-02-034 to characterize the terminated polybutadiene chain by SANS experiment. The living polymer sample was used in the experiment KW2-02-034 was terminated by d-methanol in this experiment.

The above figure is the SANS data of the terminated chain of polybutadiene fitted with beaucage theory as P=2,

we got :

Mw = 31.3Kg/mole

Rg = 8.9 nm

A2 = 3.13×-4cm3mol/g2

The SANS results were compared with the characterizations of terminated polybutadiene by GPC, NMR and SANS methods, the results from different methods match each other very well. The details are as follows:

	M_n g/mol	M_w (g/mol)	R_g (Å)	$A_2 x 10^4$ ($cm^3 mol/g^2$)	M_w/M_n
GPC(SANS cell)	32.0K	33.0K	85.3		1.034
GPC(reactor)	31.9K	32.3K	88.1		1.011
NMR 400MHZ	31.5K				
SANS		31.3K	89	3.13(±0.03)	

Focusing-Mirror High-Resolution Small Angle Scattering Instrument and Reflectometer (KWS-3)

Instrument Parameters

Wavelength:	$\lambda = (12.7 \pm 0.6)$ Å (9% FWHM)
Entrance aperture:	$r_E = 1$ to 10 mm
Wave vector resolution given by the opening of the entrance aperture:	$\Delta Q = k\, r_E / L \qquad (k = 2\pi/\lambda)$
Scattering wave vector range:	$10^{-4} \le Q \le 2 \times 10^{-3}$ Å^{-1} $10^{-4} \le Q_z \le 0.08$ Å^{-1} in reflectometry mode
Neutron intensity at sample position is proportional to the surface of the entrance aperture:	$I = 180$ n/s per mm^2 entrance aperture; for a wave vector resolution of 10^{-4} Å^{-1} (2×2 mm^2 entrance slit aperture) the intensity is therefore 720 n/s
Cross section of beam at sample position:	10 cm wide, 2 cm high
Detector:	Position sensitive detector, 8 cm diameter, 1.5 × 1.5 mm resolution

Instrument Responsible

Dr. Emmanuel Kentzinger	Tel. +49-(0)-2461-61-3139	Email: e.kentzinger@fz-juelich.de
Ludwig Dohmen	Tel. +49-(0)-2461-61-3479	Email: l.dohmen@fz-juelich.de
Dr. Jörg Stellbrink	Tel. +49-(0)-2461-61-6683	Email: j.stellbrink@fz-juelich.de

Institut für Festkörperforschung
Forschungszentrum Jülich GmbH
D-52425 Jülich

Experimental Report
of Neutron Scattering Experiments
at the FRJ-2 Reactor

Proposal number:	KW3-01-901		
Experiment title:	Ordering and istabilities in ferrofluids		
Dates of experiment:		Date of report:	03.03.03
Experimental team: Names	Addresses		
Gordeev Gennady Vorobiev Alexei Toperverg Boris	Petersburg Nuclear Physics Institute, Gatchina, 188350 St. Petersburg, Russia. Max-Planck-Institut für Metallforschung, Heisenbergstr. 3, D-70569 Stuttgart. Forschungszentrum Jülich Institut für Festkörperforschung, IFF-8		
Local Contact:	Kentzinger Emmanuel		

Experimental report text body

Ferrofluids (FF) are stable colloidal suspensions of fine (usually 10 nm in diameter) single domain magnetic particles coated with a nonmagnetic molecular surfactant shell. External magnetic field tends to order dipolar moments parallel to each other. Parallel orientation promotes chaining of particles along the field and increases repulsion between chains in the plane perpendicular to the field. On the other hand, thermal motion of particles tends to destroy field-induced structuring reducing a length of chains as well as their lifetime. Depending on ferrofluid concentration, magnetic field strength, temperature, nature of surfactants and solvents some other types of the ordered structures may appear: (anti)-ferromagnetic, spin-glass-like, or fractal objects.

We have accomplished high resolution SANS experiment aiming to provide a direct evidence of the FF long-range ordering and to deliver a set of parameters quantifying ordered state. Such an information is highly requested in view of both theoretical and practical applications interests. Investigations of bulk FFs self-organization on micro- and nano-scopic scale is only possible employing high resolution neutron scattering technique. This is due to the fact that an interpretation of widely employed macroscopic measurements is not straightforward, while FFs are not transparent and optical methods have limited range of application for this purpose.

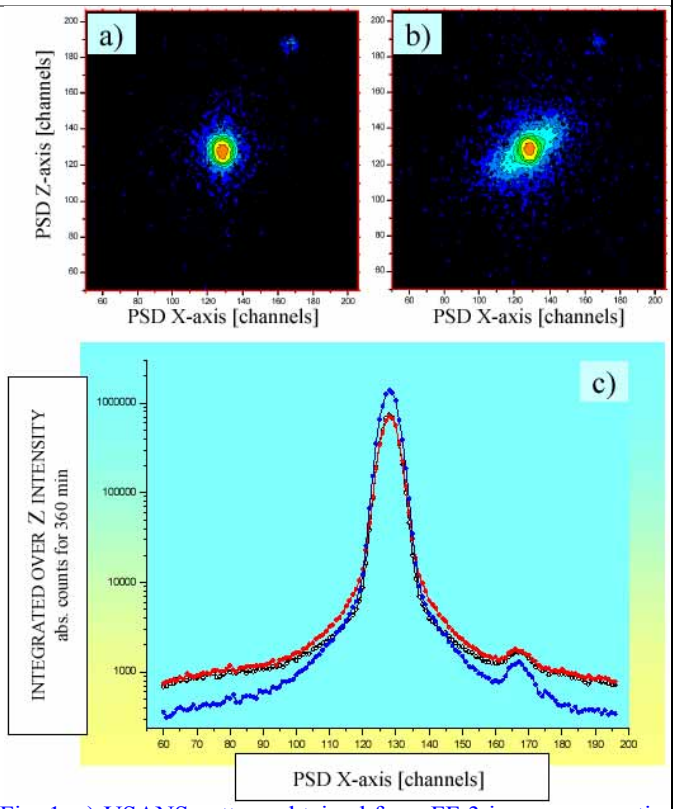

Fig. 1. a) USANS pattern obtained from FF-3 in zero magnetic fields; b) scattering from FF-3 in the field $H_{\|}$= 114 Oe applied parallel to the incoming beam; c) the curves obtained after the integration of 2D scattering patterns along PSD Z-axis: blue – D_2O (I_{IB} - incoming beam shape-function), black – FF-3 at $H_{\|}$=0 Oe (I_{ZF}), red – FF-3 at $H_{\|}$=114 Oe (I_{FI}). A peak between channels 160 and 170 is an artifact due to the PSD defect.

The samples were put in a cell 110 mm wide, 40 mm high and 1 mm thick, the longest edges being perpendicular to the incident beam. External fields were applied either parallel to the incident beam ($H_{\|}$), or at the angle α (up to 90°) to its direction.

The main result can be formulated as follows:

1. In the parallel (to the neutron beam) fields the nanoparticles form the chain-like structure extended over a characteristic size, which along one direction is about one order of magnitude higher than the mean diameter of the particles (Fig.1b). This leads to the appearing of the second scale on the 1D scattering pattern (Fig.1c), while the only one length scale is present at zero field. In the latter case the difference between the incoming beam intensity (I_{IB}) and the intensity I_{ZF} scattered from FF is well described by the scattering on uncorrelated single particles. The scattered intensity is seen as broad wings extended over a whole q-range available for PSD. When the external field applied an extra scattering I_{FI} appears in the region very close to the direct beam, which corresponds to the scattering on very large objects.
2. The particle ordering is better pronounced as higher external fields.
3. On the 2D patterns (Fig.1b) the scattered intensity I_{FI} is visible as an asymmetric halo around the direct beam. The halo has an elliptical shape with the long axis parallel to the longest diagonal of the sample container. The scattering intensity distribution along the short axis of ellipse is the same as at zero field, hence the scatters have the size of a single particle along this direction. These two facts reveal the shape and spatial orientation of the field induced structures – the chains of particles are displayed parallel to the longest diagonal of the sample container. The reason of such configuration is that along this direction the whole sample body has a minimal demagnetization factor and consequently a maximal magnetic induction.
4. The chaining effect is time dependent – the scattering from the big structure appears in the first moment after the field switched on and disappears after about 2 hours of measurements at the same conditions.
5. The ordering process depends on the particle's size and on their concentration.
6. The effect is smaller for sample with higher concentration (comparing FF-3 and FF-5).
7. The ordering is much less pronounced if the external field is not parallel to the neutron beam.

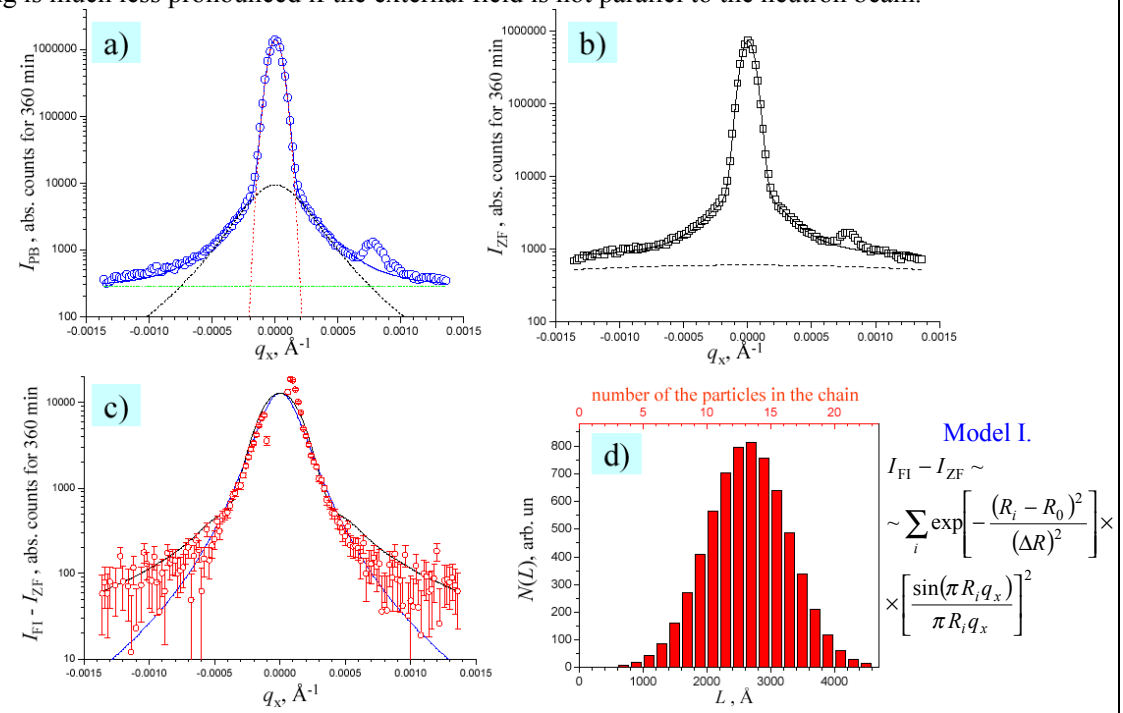

Fig. 2. USANS 1D data simulation. a) Incoming beam (resolution function) I_{IB} is well described (blue line) as a sum of Gaussian (red), Lorentzian squared (black) and constant background (green). b) FF-3 at $H_{\|}$=0 Oe: experimental data I_{ZF} (squares), simulation result (solid line) obtained as a sum of reduced I_{IB} and scattering on single particles with a form-factor $\sim 1/(4q_x + r^{-2})^2$ (dash line) with the particle mean size r =(100±10) Å. c) Red points – field induced scattering (I_{FI}-I_{ZF}) (see Fig.1c), black line – simulations of the difference (I_{FI}-I_{ZF}) due to scattering on a set of thin rods with the length L distributed according to normal law [Model I], blue line – simulation of the difference (I_{FI}-I_{ZF}) for scattering on monodisperse objects with smeared edges, i.e. with form-factor $\sim 1/(4q_x + R^{-2})^2$, where the characteristic size R =(2300±100) Å [Model II]. d) The distribution of L in Å (bottom X-axis) and in number of particles (top X-axis) according to Model I.

Neutron Spin Echo Spectrometer (NSE)

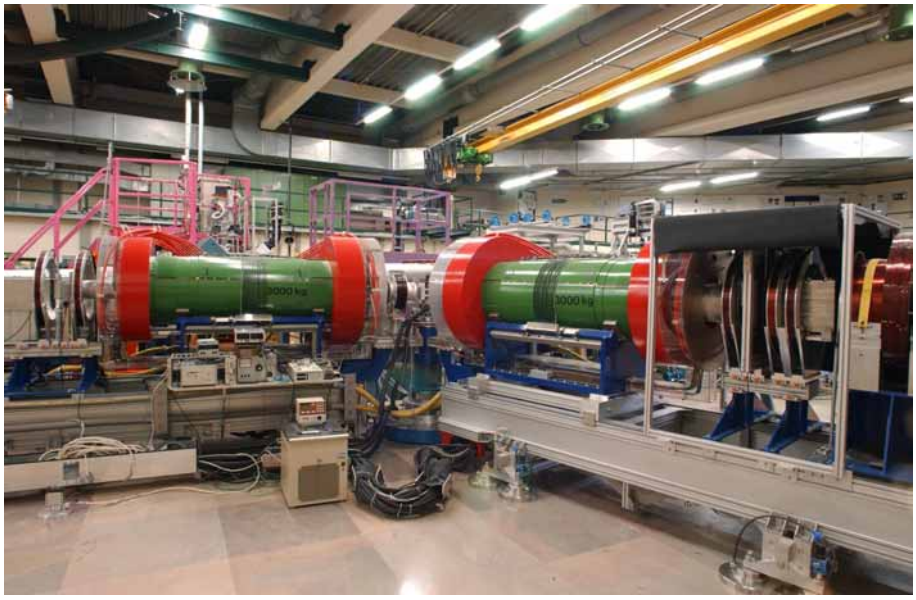

Instrument Parameters

Beam tube:	NLIIB curved guide
Monochromators:	polarizing multilayer mirror (FeGe) velocity selector (DORNIER) $\Delta\lambda/\lambda = 0.1$ (or 0.2)
Incoming beam ***- Cross section of guide:*** ***- Sample size:***	 4.5 cm (height) × 3 cm (width) 4 cm × 4 cm (max.)
Collimation:	by source and sample size or wire collimators 0.5° × 0.5°
Polarised neutron flux at sample (λ = 8 Å):	8×10^5 n/cm^2 s (natural collimation)
Wavelength range:	$\lambda = (8 \pm 2)$ Å, alternative mirror (6 ± 2) Å
Momentum transfer range:	0.01 ... 1.5 Å^{-1}
Fourier time range (in STD set-up):	0.04 ... 48 ns
Max. field integral:	0.5 Tm
Analyzer:	30 × 30 cm^2 CoTi supermirror Venetian blind
Detector:	32 × 32 1cm^2 cells ^{3}He multidetector

Instrument Responsible

Dr. Michael Monkenbusch Tel. +49-(0)-2461-61-4314 Email: m.monkenbusch@fz-juelich.de
Dr. Ralf Biehl Tel. +49-(0)-2461-61-4685 Email: ra.biehl@fz-juelich.de

Institut für Festkörperforschung
Forschungszentrum Jülich GmbH
D-52425 Jülich

Experimental Report
of Neutron Scattering Experiments
at the FRJ-2 Reactor

Proposal number:	NSE-01-010		
Experiment title:	**Elastic Scattering Component on Dynamically Asymmetric Polymer Blend**		
Dates of experiment:	Scheduled in the first half of April of 2002	Date of report: 8th/March/2003	
Experimental team: Names	Koizumi Satoshi Addresses: Tokai, Naka-gun, Ibaraki-ken, 319-1195 Japan		
Local Contact:	M. Monkenbusch		

Experimental report text body

(Please use 12 pt letters here !)

In order to determine dynamical asymmetry enhanced by temperature, we have done neutron spin echo (NSE) measurements on the polymer blend of deuterated polystyrene (DPS)/ protonated poly (vinyl methyl ether) (PVME). This blend is characteristic to show large difference of glass transition temperatures (Tg) of PS and PVME, which are 100 ^{o}C and –20 ^{o}C, respectively. Due to large difference of Tg's, we expect a crossover behavior from dynamical symmetry to asymmetry as temperature decreases in single phase (the LCST phase with a phase boundary at round 120 ^{o}C). By dynamical measurements with NSE, we expect to observe the elastic scattering component (the elastic plateau in a decay curve) due to slower fluctuating DPS rich region. Data evaluations are under development.

So far we studied the DPS/PVME mixture by small-angle neutron scattering (Macromolecules, 1996, 29, 2440-2448). We observed anomalous phase behaviors; the small-angle scattering is more suppressed than expected by a mean field random phase approximation with an interaction parameter χ determined in the dynamically symmetric single phase. Recently, we further investigated this mixture under shear flow and found abnormal butterfly scattering due to shear-induced phase separation or a dynamical coupling between stress and diffusion. Along this observation, the key word is again the dynamical asymmetry due to large difference of Tg's. In the conference paper of sas2006, which will be soon published, we discussed these two findings of anomalous suppression at a quiescence state and abnormal butterfly scattering under shear as related to a gel-like limit in a mixture with dynamical asymmetry, where rheological relaxation is much slower than concentration fluctuations (Figure 1 shows this situation).

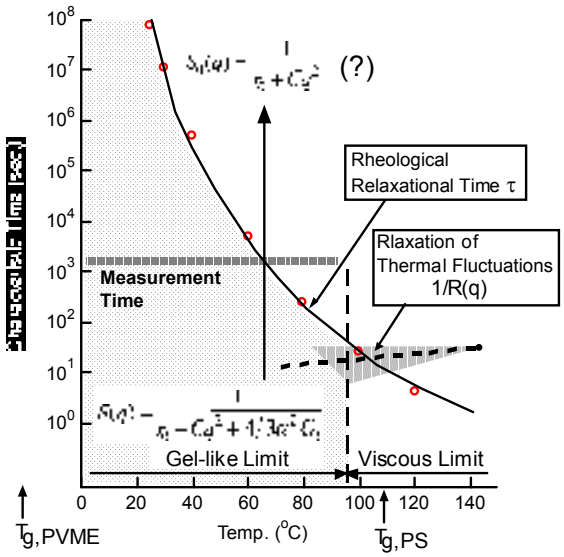

Figure 1 Crossover from a viscous to a gel-like limits as temperature decreases. This figure will be appeared as figure 7 of the conference paper of sas2006.

Institut für Festkörperforschung
Forschungszentrum Jülich GmbH
D-52425 Jülich

Experimental Report
of Neutron Scattering Experiments
at the FRJ-2 Reactor

Proposal number:	NSE-01-901		
Experiment title:	How far are protons moving in Polyisobutylene in order to achieve the structural relaxation?		
Dates of experiment:	18/02/2002 – 6/03/2002	Date of report: 21/05/2002	
Experimental team: Names	Addresses		
Juan Colmenero Arantxa Arbe Dieter Richter Michael Monkenbusch	Dpto. de Física de Materiales, UPV/EHU, Apdo. 1072, 20080 San Sebastian, SPAIN Unidad de Física de Materiales, CSIC-UPV/EHU, “ , “ , “ IFF, FZJ, Jülich, Germany “ , “ , “ , “		
Local Contact:	Michael Monkenbusch		

Experimental report text body

The aim of this experiment was to extend towards low temperatures the study of the self motion in a polyisobutylene (PIB) melt at Q-values below the first structure factor peak Q_{max}. By using the NSE intrument we wanted to determine the temperature dependence of the characteristic time for the self motion of the protons as well as that of the structural time ϑ_ξ (ϑ_ξ is defined as the characteristic time for the decay of the pair correlation function at Q_{max}). This would allow us to establish whether or not the spatial extend of the proton motion in the timescale of the structural relaxation continuously increases with decreasing temperature, as a recent experiment [1] seems to indicate.

The incoherent scattering was measured on a fully protonated sample at two different Q-values (0.4 and 0.7 $Å^{-1}$) and two temperatures, 320 K and 280 K; the structural relaxation was investigated on the fully deuterated sample at 320 K, 300 K and 280 K. In Figure 1 (a) as an example the incoherent scattering function is displyed for 0.7 $Å^{-1}$ and the two temperatures investigated. The solid lines correspond to fitting Kohlrausch-Williams-Watts functions $\exp[-(t/\vartheta)^\eta]$ (η fixed to the value 0.55). At 320 K, the Q-dependence of the times corresponding to the decay of the self correlation function agree with that expected in the framework of the Gassian approximation, $\vartheta_{inc} \nabla Q^{-2/\eta}$, as it was observed for higher temperatures in the same sample [1].

Technical problems resulted in a poorer instrumental resolution that prevented to determine the time scales for 300 K and 280 K with accuracy. A magnetic field generated in the new cryostat used in this experiment produced

strong distortions in the measurements. This is evident from Figure 1 (b), where the results obtained in this experiment for the deuterated sample at 300 K and Q_{max} are directly compared with previous ones . The structural relaxation time deduced now is much slower, as can be seen in Figure 2. Thus the results obtained in these measurements are not very reliable, at least at the conditions where the decay of the scattering function is not very strong.

From the results obtained we cannot conclude whether the activation energy of the self motion is lower than that of the structural relaxation. Due to the problems above mentioned it is not possible to extract quantitative information about an increase with temperature of the mean squared displacement at the structural time for temperatures below 320 K.

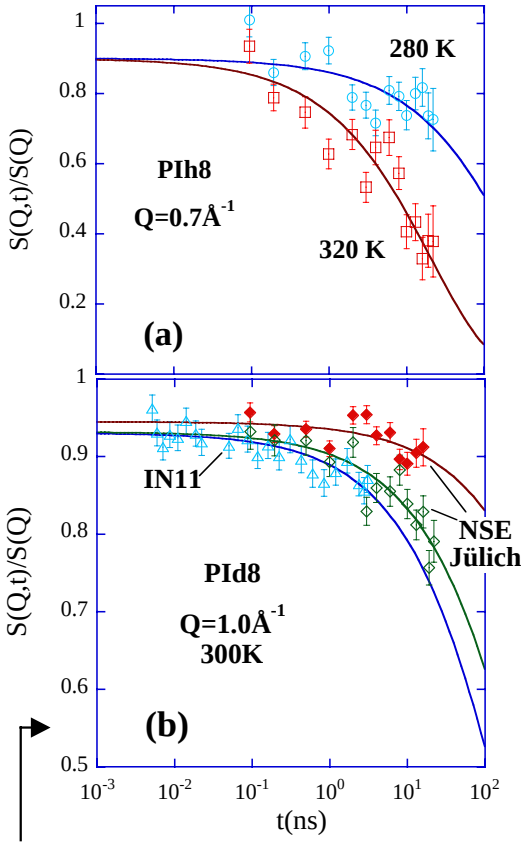

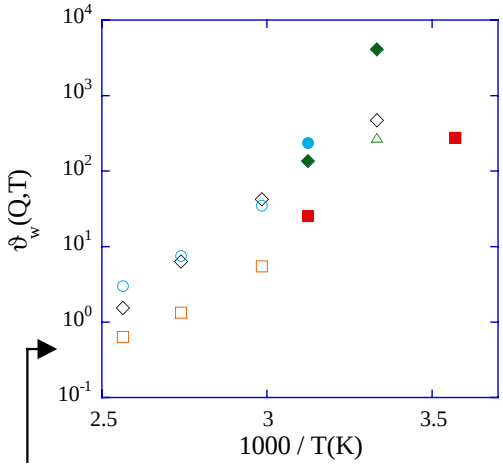

Figure 2: Temperature dependence of the characteristic times corresponding to incoherent scattering [Q = 0.4 Å^{-1} (●,○); 0.7 Å^{-1} (■,□)] and to coherent scattering at Q_{max} (◆,◇,△). Solid symbols indicate results obtained from this experiment; empty symbols correspond to previous measurements: ○ and □ to IN11C [1], △ to IN11 [2], and ◇ to the NSE Jülich instrument.

Figure 1: NSE spectra obtained in this experiment from (a) the fully protonated sample at 320 K (□) and 280 K (○) for 0.7 Å^{-1} and (b) the fully deuterated sample at 300K and Q_{max} = 1.0 Å^{-1} (◆). In (b) the data are compared with previous results obtained by the same instrument (◇) and by the IN11 spectrometer at the ILL (△) at the same Q and T [2]. Solid lines are KWW fitting curves.

REFERENCES

[1] B. Farago, A. Arbe, J. Colmenero, U. Buchenau and D. Richter, Physical Review E (in press)

[2] D. Richter, A. Arbe, J. Colmenero, M. Monkenbusch, B. Farago and R. Faust, Macromolecules **31**, 1133 (1998)

Institut für Festkörperforschung
Forschungszentrum Jülich GmbH
D-52425 Jülich

Experimental Report
of Neutron Scattering Experiments
at the FRJ-2 Reactor

Proposal number:	NSE-01-902		
Experiment title:	Limits to the Zimm dynamics in PVE related to torsional barriers		
Dates of experiment:	26/04/2002 – 04/05/2002	Date of report: 21/05/2002	
Experimental team: Names	Addresses		
Juan Colmenero Arantxa Arbe Dieter Richter Michael Monkenbusch	Dpto. de Física de Materiales, UPV/EHU, Apdo. 1072, 20080 San Sebastian, SPAIN Unidad de Física de Materiales, CSIC-UPV/EHU, “ , “ , “ IFF, FZJ, Jülich, Germany “ , “ , “ , “		
Local Contact:	Michael Monkenbusch		

Experimental report text body

Like in the case of other polymers, the dynamic chain structure factor of Poly(vinyl ethylene) (PVE) in the melt shows deviations from Rouse behavior at large Q-values. However, in PVE such deviations are already detected at unusually small Q-values. The aim of this experiment was to identify the limiting mechanism of the Zimm dynamics in PVE at short length scales. This will allow us to unravel the nature of the local processes behind the strong deviations from Rouse behavior observed in the melt. For doing this, an analogous approach to that used in a previous study [1] is used. In that work, the nature of the mechanism limiting the universal dynamics in polyisobutylene (PIB) was deciphered by comparing its behavior in solution with the dynamics of a solution of poly(dimethylsiloxane) (PDMS) in the same conditions (toluene). PDMS is a highly flexible polymer with almost no internal barriers. Measuring now a dilute solution of protonated PVE in deuterated toluene in identical conditions to that of the PDMS/toluene solution and using the PDMS data [1] as reference we want to determine the origin of the limiting mechanism of the Zimm dynamics in PVE.

The dynamic chain structure factor of PVE in solution has been investigated at 250, 300, 327, and 378 K at Q-values in the range $0.05 \leq Q \leq 0.35$ Å-1. We note that the main interest of this experiment was to look for deviations from the Zimm dynamics that would manifest at high Q-values. In such a Q-range, the measurements resulted to be strongly affected by both, the incoherent contribution of the polymer chains and the total scattering from the solvent and sample holder. For this reason, careful measurements on the background and the resolution function were performed, especially at high Q-values.

Figure 1 displays some of the obtained results in order to show the good quality of the data. A first phenomenological description of the curves in terms of a single exponential exp[-Γt] (solid lines in Fig. 1) delivers the Q-dependence of the decay rate Γ represented in Figure 2 as full squares. For $Q \geq 0.15$ Å^{-1}, the deviations from the Q^2 dependence of Γ characteristic for diffusion at low Q-values indicate the contribution of the internal modes of the chain to the dynamics. We realize that this contribution is clearly weaker in this case than that observed for PDMS, and comparable to that found for PIB, both in an identical solution. This observation implies that a similar internal friction has to be present in PVE and PIB that slows down the purely entropic dynamics as it is displayed by PDMS. We note that the value of the C-C torsional barriers is quite the same for PIB and PVE (about 3.5 Kcal/mol) [1,2], and much higher that that of the skeletal bonds in PDMS [1]. Thus, also the dynamics of PVE chains in solution seems to be affected by the intrachain viscosity due to the local conformational transitions as previously reported for PIB [1]. Future work will be devoted to try to describe the single chain dynamic structure factor of PVE in solution taking into account the rigidity of the chains as well as this internal friction mechanism by using the model proposed by Allegra et al [3] as done in [1] for PIB.

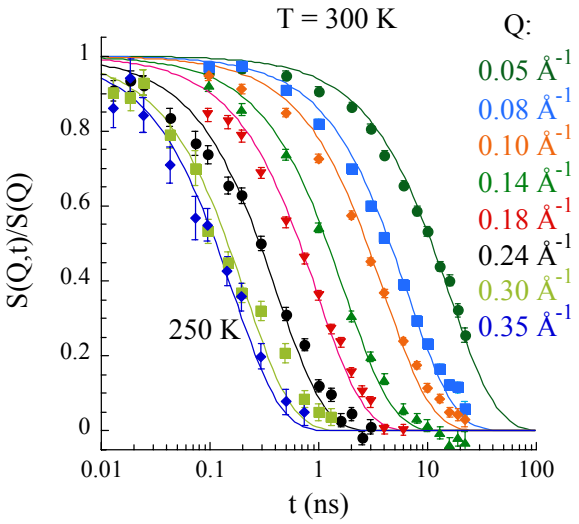

Figure 1: Time evolution of the single chain dynamic structure factor of PVE in toluene solution at 300 K. The corresponding Q-values are indicated (top to bottom). Solid lines show exponential functions with prefactor 1.

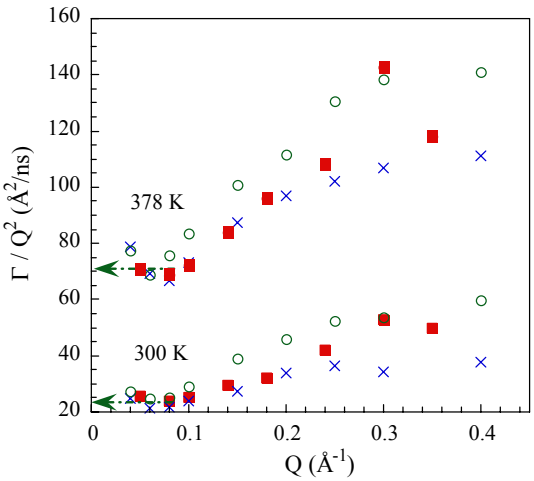

Figure 2: Q-dependence of the decay rate Γ divided by Q^2 for PVE (■), PDMS (O), and PIB (×) in solution at the two temperatures indicated. The dashed arrows show the values obtained by DLS for PDMS [1].

REFERENCES:

[1] A. Arbe, M. Monkenbusch, J. Stellbrink, D. Richter, B. Farago, K. Almdal and R. Faust, Macromolecules **34**, 1281 (2001)

[2] W. Zhu and M. D. Ediger, Macromolecules **28**, 7549 (1995)

[3] G. Allegra and F. Ganazzoli, in Advances in Chemical Physics; I. Prigogine, S. A. Rice (eds); Wiley: New York, 1989, Vol. 75, p. 265.

Institut für Festkörperforschung
Forschungszentrum Jülich GmbH
D-52425 Jülich

Experimental Report
of Neutron Scattering Experiments
at the FRJ-2 Reactor

Proposal number:	**NSE-02-001**		
Experiment title:	**Norbornene-polymers in solution: do they form stiff and frozen coils ? II:fractionated samples**		
Dates of experiment:	17.102-25.1.02	Date of report:6.3.02	
Experimental team: Names	,.; Greiner, A.; Richter,D. Addresses		
Yoon, Do Yeung Monkenbusch, M. Fetters, L. Greiner, A. Richter, D.	Department of Chemistry, Seoul National University, Seoul 151-742, Korea IFF, FZ-Jülich Cornell University, USA Univ. Marburg IFF, FZ-Jülich		
Local Contact:	M. Monkenbusch		

Experimental report text body

(Please use 12 pt letters here !)
Norbornene polymers had been synthesised by A. Greiner in Marburg in three variations:

- Poly(norbornene) , Mn=750 Kg/mol, Mw=1100 Kg/mol Mn/Mw=1.48, soluble in chlorobenzene
- Poly(5-norbornene-2-propane), Mn=110- Kg/mol, Mw=190 Kg/mol, Mn/Mw=1.74 , soluble in THF,chloroform,toluene and chlorobenzene
- Poly(5-norbornene-2-hexane), Mn=90 Kg/mol, Mw=180 Kg/mol, Mw/Mn=4, soluble in THF,chloroform,toluene and chlorobenzene

Only the latter two with side groups propane or hexane could be measured since they are soluble in THF or toluene which are available in the required deuterated form.
Own GPC measurements (L.Fetters, L.Willner) have shown that their molecular weights are rather Mw=400Kg/mol and 600 Kg/mol respectively with **large polydisperity indices** Mw/Mn=2 resp. 4.
Previous measurements of the concentration dependence of the viscosity of solution of these polymers (Yoon) have shown that they behave rather like a suspension of solid spheres than a solution of flexible polymers.
It has been inferred that these polymers are frozen coils, i.e. the barriers to change an actual coil conformation into any other are prohibtively high. If this were true these polymers would be the first example for such an behavior
The spin-echo technique is now suited to measure the inner coil dynamics which should be frozen or at least considerably slowed down compared to the standard Zimm dynamics of flexible polymer chains.
For an immediate model free comparison with a standard Zimm dynamics a solution in the same solvent of a flexible linear polymer of comparable molecular weight has also been measured.

In a previous experiment (NSE proposal 01-008) the polymers as received, i.e. with high polydispersities have been investigated at a concentration of 1% to avoid mutual overlap of the coils but still preserve enough scattering intensity. Clear deviation from the Zimm dynamics expected for a linear polymer (green data points in the right figure below are for linear PI) had been found.

.

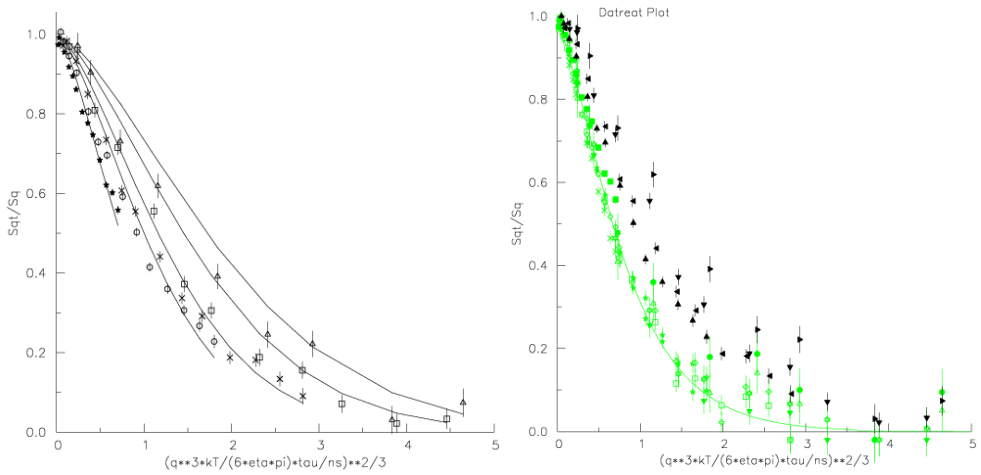

However, since the molecular weight distribution of the norbornenes is broad and contains a short chain tail with fast center-of-mass diffusion a full quantitative analysis of the present data is difficult. In the experiment reported here fractionated polymer samples where the short molecular weights were removed were investigated. Besides the 1% also a lower concentration (0.5%) has been used to quantify possible overlap effects.

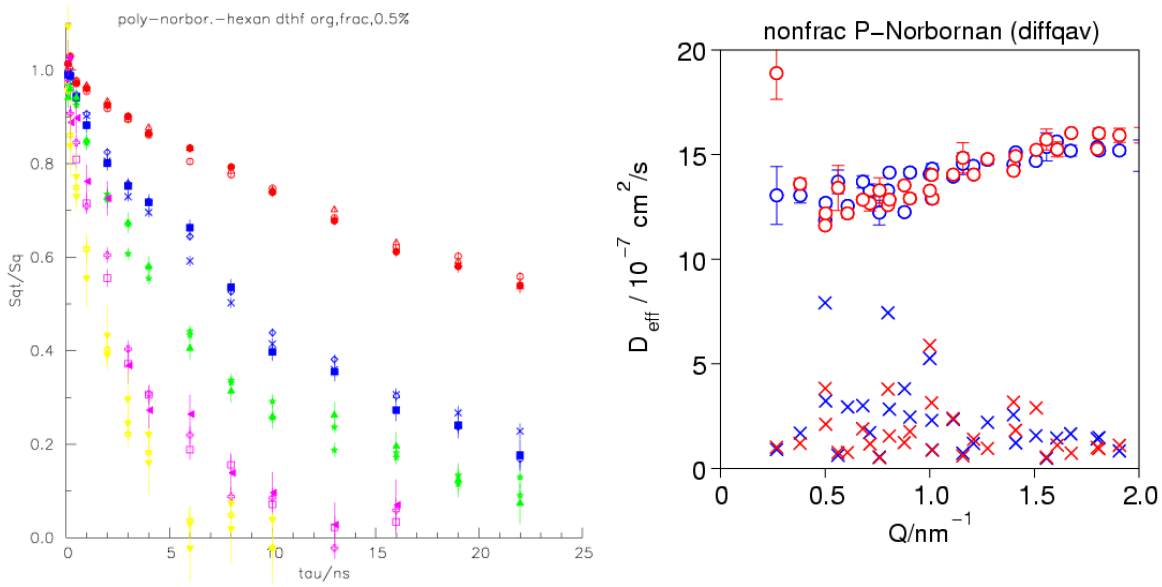

The figures above illustrate the results of the check fractionated vs. non-fractionated polymers, as can be seen from the left figure the S(Q,t)/S(Q) data show only marginal differences virtually within the error bars. By these comparisons it has been verified that the polydispersity does not affect the results as well the 1% concentration could be classified as sufficiently dilute. The right figure shows the effective diffusion constant extracted from the spin-echo curves (**circles**) red and blue symbols represent fractionated and nonfractionated samples. It is clearly visible that the fractionation has virtual no effect on the results (the lowest Q-point is not very reliable!). The effective diffusion constant is close to Q independent and not proportional to Q as expected for a flexible chain with Zimm-dynamics. The slight trend in D(Q), however, indicates some residual but strongly reduced chain flexibility. MD-simulations to further rationalize the results are under way (Yoon).

Institut für Festkörperforschung
Forschungszentrum Jülich GmbH
D-52425 Jülich

Experimental Report
of Neutron Scattering Experiments
at the FRJ-2 Reactor

Proposal number:	NSE--02-002		
Experiment title:	Small Angle Polarized Neutron Scattering Study		
Dates of experiment:	15. Sep. - 17. Sep. 2002	Date of report: 10. March 2003	
Experimental team: Names	Addresses		
Hitoshi Endo	IFF, FZ-Juelich, D52425 Jülich		
Local Contact:	Michael Monkenbusch		

Experimental report text body

We performed small angle polarized neutron scattering measurements to separate the elastic scattering intensities into the coherent component and the incoherent component. The separation can be done experimentally with polarized neutron scattering experiments to measure spin-flip and non-spin-flip scattering. This measurement may be extremely important when the observed intensity is quite low, since in such a case, the high-Q slope is typically affected by the background (mainly contributed by incoherent scattering) subtraction.

We have studied the role of block copolymer additives for calcium carbonate ($CaCO_3$) crystallization [1] by small angle neutron scattering experiments, and we have known that the determination of the incoherent scattering level affects significantly the high-Q slope of the polymer scattering. This high-Q slope gives the direct aspect of the polymer chain in $CaCO_3$ crystals, namely, Q^{-D} for collapsed chains ($D < 2$), Gaussian chains ($D = 2$), swollen chains ($D = 5/3$), and so on. Therefore the experimental determination of the high-Q slope is quite meaningful and the polarized neutron scattering analysis can only allow us to give this opportunity.

The experiments were performed at the neutron spin-echo spectrometer NSE at research center Jülich, since this is only the possibility to perform the small angle polarized neutron scattering experiments.

In Fig.1, the obtained result from $CaCO_3$ with H_2O aqueous solvent is exhibited. It is clearly shown that the incoherent component (♦) is constant, on the other hand, the coherent component (◦) dominated $CaCO_3$ elastic scattering shows Q^{-4} behavior, which is interfacial scattering. This result shows the feasibility of this kind of experiments, and as a next step, we want to perform the same experiments under the polymer contrast, where the water is matched to the scattering contrast of $CaCO_3$, so that the observed scattering intensity arises from the polymer.

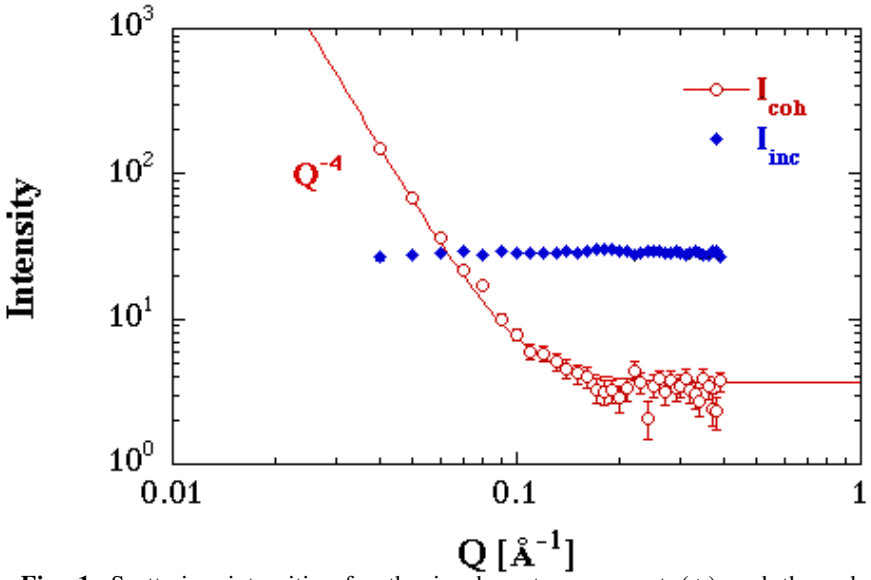

Fig. 1. Scattering intensities for the incoherent component (♦) and the coherent component (○) from $CaCO_3$ particles separated by polarized neutron analyses.

[1] H. Cölfen and L. Qi, *Chem. Eur. J.* 7, **106** (2001)

Institut für Festkörperforschung
Forschungszentrum Jülich GmbH
D-52425 Jülich

Experimental Report
of Neutron Scattering Experiments
at the FRJ-2 Reactor

Proposal number:	NSE-02-005		
Experiment title:	Dynamics of bottle-brush macromolecules		
Dates of experiment:	24.06.02	Date of report:	11.03.03
Experimental team: Names	Addresses		
Silke Rathgeber Tadeusz Pakula Krzysztof Matyjaszewski	Forschungszentrum Jülich GmbH Institut für Festkörperforschung – Weiche Materie D-52425 Jülich Max-Planck-Institut für Polymerforschung Ackermannweg 10 55128 Mainz Carnegie Mellon University Department of Chemistry Pittsburgh, PA 14213, USA		
Local Contact:	Michael Monkenbusch		

Experimental report text body

We investigated the (internal) dynamics of bottle-brush macromolecules in dilute solutions with neutron spin-echo (NSE) spectroscopy.
We consider here bottle-brush or comb-like polymers as macromolecules where relatively long side chains are densely grafted to a backbone in a regular manner (see fig.1). The interest in cylindrical comb polymer brushes is related to the possibility to form stiff cylindrical shape persistent structures based exclusively on the intra-molecular excluded volume interaction. In fig. 2 the SANS results of a bottle-brush macromolecule is shown. For high grafting densities and long backbones (if compared to the side chain length) the overall shape of a bottle-brush macromolecule can be well described by a flexible cylinder with a fast decaying radial density profile. The power-law scattering at higher q-values ($q>0.5nm^{-1}$) corresponds to the scattering originating from the internal loose, polymeric structure (blob scattering, stemming predominantly from the side chains) whereas the lower q-region reveals information about the overall shape of the macromolecule. The solid line in fig.2 shows the scattering curve calculated from such a model.
The samples under investigation consist of a 2-(bromopropionicacid) ethoxy methacrylate p(BPEM) backbone with poly(b-butyl) acrylate p(nBA) side chains. They have been synthesized via controlled growth of the side chains from a linear polymeric macroinitiator using atom transfer radical polymerization (ATRP) as described in [1]. Solutions were prepared in toluene that is known from SANS experiments to be a good solvent for p(nBA) as well as for p(BPEM). As reference we also performed NSE measurements on the linear backbone macromolecule p(BPEM) and a p(nBA) homopolymer corresponding to the side chains of the bottle-brush polymer.

At small q vectors ($q<0.5nm^{-1}$) we are sensitive to the overall shape of the bottlebrush macromolecule. The form factor can be described by $P(q)=P_{fc}(q)\times P_{cs}(q)$ where $P_{fc}(q)$ is the form factor of a flexible cylinder (self - avoiding random walk like a worm-like chain) and $P_{cs}(q)$ is the square of the two-dimensional Fourier transform of the radial density profile. Therefore we might be sensitive to collective modes of the side chains which can lead to a slowing down of the reduced relaxation rates similar to the case of high-functionality star polymers or/and to fluctuations of the overall "worm-like" macromolecule.

The NSE spectra were fitted using the Zimm model for each q-value separately. From the single fits the length scale dependent relaxation times t_R can be obtained. In fig. 3 the product $t_R \times q^3$, that should be constant for Zimm relaxation is plotted as a function of the scattering vector. Whether the slow relaxation seen at small q values is related to center-of-mass diffusion D or to shape fluctuations of the bottle-brush macromolecule has to be double-checked by determining D by dynamic light scattering independently.

References:

[1] K.L. Beers et al., Macromolecules **31** (1998) 9413.
[2] M. Saariaho, Macromolecules **32** (1999) 4439.

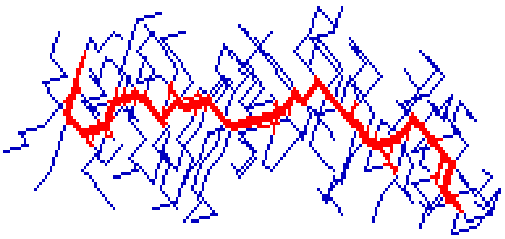

Fig. 1: Schematic structure of a bottle-brush macromolecule.

Fig. 2: SANS spectrum of a bottle-brush macromolecule.

Fehler! Keine gültige Verknüpfung.

Fig. 3: Relaxation times t_R normalized for Zimm relaxation as a function of the

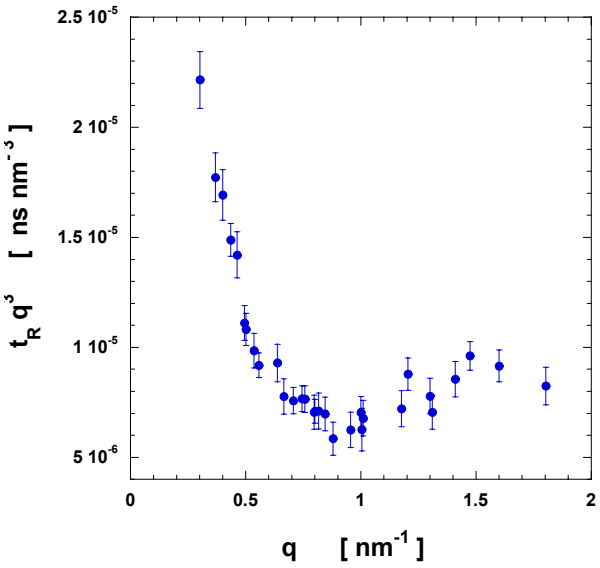

Institut für Festkörperforschung
Forschungszentrum Jülich GmbH
D-52425 Jülich

Experimental Report
of Neutron Scattering Experiments
at the FRJ-2 Reactor

Proposal number:	NSE-02-006, KW2-02-028		
Experiment title:	**Neutron Spin-Echo Study of Dynamics of Hydrophobically Modified Polymer-Doped Surfactant Bilayers**		
Dates of experiment:	Sept. 2002	Date of report:	Mar.6th, 2003
Experimental team: Names	Addresses		
Lal, Jyotsana	IPNS, Argonne National Lab., Argonne, IL-60439, USA		
Hu, Xuesong	IPNS, Argonne National Lab., Argonne, IL-60439, USA		
Prud'homme, Robert, K.	Dept. of Chemical Engineering, Princeton University, Princeton, NJ 08544, USA		
Biehl, Ralf	Institut für Festkörperforschung, Forschungszentrum Jülich GmbH, D-52425 Jülich		
Monkenbusch, Michael	Institut für Festkörperforschung, Forschungszentrum Jülich GmbH, D-52425 Jülich		
Local Contact:	Dr. Michael Monkenbusch		

Experimental report text body

Surfactant layers are very soft and fluctuating. The elastic constant $\kappa_c \sim k_B T$. It is very hard to stabilize these layer by introducing high molecular weight homopolymers, because of high entropic cost on polymer conformation but a few percentage of hydrophobic groups along the backbone helps in the introduction of high molecular weight polymer within bilayers. We try to extend the previous study of dynamics of oriented bilayers containing hydrophobically modified polymers by neutron spin-echo spectroscopy (NSE).[1] This time we studied bare membranes with no polymer and hmPEG6kDp13 in 20% membrane volume fraction. We want to examine in more details the crossover point from fast to slow dynamics as function of polymer coverage.

Experiments:

Samples and Materials:

The surfactant lamellar phase consists of the nonionic surfactant penta(ethylene glycol) dodecyl ether ($C_{12}E_5$; >99%, Nikko Chemical Co. Ltd., Tokyo) and 1-hexanol(>99%, Fluka), used as received. The $C_{12}E_5$/hexanol molar ration in all of our samples is fixed at 1:1.43, the solvent phase is 0.1M $NaCl_{(D2O)}$. The total molecular weights *Mw* and *Mn* of hmPEG13 are 112*kg/mol* and 78 *kg/mol* respectively. We use the SANS instrument in Juelich to check for alignment of the sample.

Results and Discussion:

Bare Membrane: The dynamics of the membrane systems was investigated by NSE spectroscopy. Zilman et al.[2] consider an ensemble of membrane plaquettes at random orientations and calculated the effect of membrane undulations and model their statistics by bending energy and standard hydrodynamic dispersion law. They predict a stretched exponential relaxation in the form of

$$S(\vec{q},t) \cong S(\vec{q}) e^{-(\Gamma_q t)^{2/3}}$$

where $S(\vec{q})$ is the static structure factor and Γ_q is the relaxation rate.

[1] Yang, B.-S., et al. *Langmuir* **2002**, *18*, 6-13
[2] Zilman, A.G.;Granek,R. *Phys. Rev. Lett.* **1996**, *77*, 4788-4791

Figure 1 shows the normalized dynamic structure factor *S(q,t)/S(q,0)* for the bare membrane samples ($\phi = 0.1$, 0.2 and $\phi = 0.3$). Both of our bare membrane systems exhibit a relaxation behavior that cannot be fitted by a single exponential but is well fitted by this stretched exponential. The $\phi = 0.1$ sample relaxes faster than $\phi = 0.2$, the $\phi = 0.2$ sample relaxes faster than $\phi = 0.3$, for the whole $\vec{q}$ range, example at one fixed q=0.14Å^{-1} is shown in Figure 1.

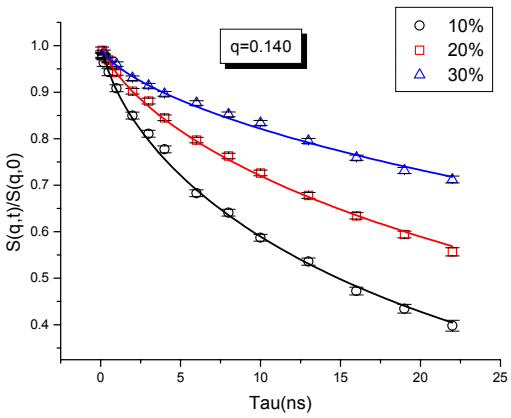

Figure 1

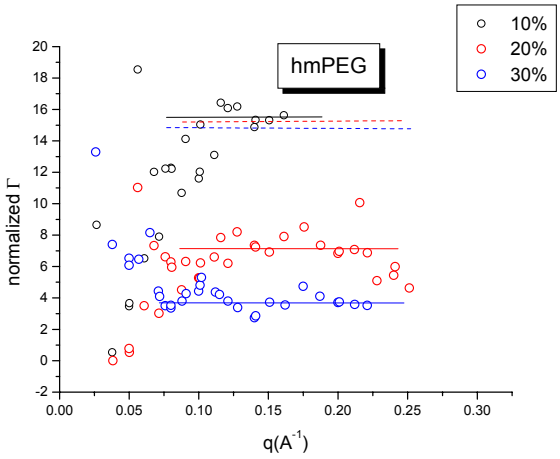

Figure 2

Figure 2 shows the q dependence of the normalized relaxation rate $\overline{\Gamma}_q = S(q)\Gamma_q / q^3$ for the bare membranes(10%, 20% and 30%). The normalized relaxation rate $\overline{\Gamma}_q$ is almost independent of q beyond the lamellar peak, with average values shown in solid lines. The dash lines show the normalized results $\overline{\Gamma}'_q = S(q)\Gamma_q d / q^3$, where d is the interlamellar spacing. So unlike the prediction of Zilman and Granek where at $qd>>1$ we should recover the behavior of single membrane there still seems to be a dependence on the distance d between membrane. This can be seen well in Fig. 2 after we multiply normalized $\overline{\Gamma}_q$ by d for 20% and 30% respectively. Both curves will superimpose on 10% data of normalized $\overline{\Gamma}_q'$ at large q. This implies that even at these q values, we are not sensitive via $\overline{\Gamma}_q$ to κ_c, bending elastic constant of a single membrane, but to bulk splay elastic constant κ of a stack of membranes where $\kappa = \kappa_c/d$.

Polymer-Doped Membrane: In Figure 3 we illustrate the dependence on the surface coverage σ of the ratio of the average normalized relaxation rate $\overline{\Gamma}_{q,avg}$ above $q = 0.1$Å^{-1} to that of the corresponding bare membranes for hmPEG doped membranes at 20% and 30%(old data). The relaxation rate depends subtly on the surface-coverage of polymer, slowing down at high surface coverage and increasing slightly at low coverage, relative to the bare membranes. The crossover at low membrane coverage is well defined and repeatable, which needs further theoretical work.

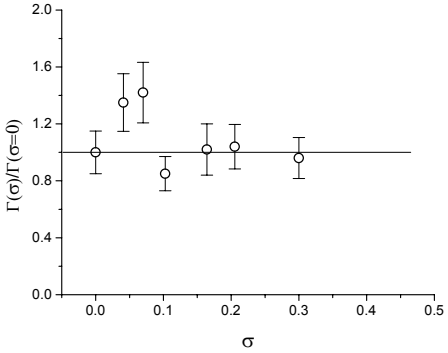

Figure 3

Institut für Festkörperforschung
Forschungszentrum Jülich GmbH
D-52425 Jülich

Experimental Report of Neutron Scattering Experiments at the FRJ-2 Reactor

Proposal number:	NSE-02-009		
Experiment title:	Transition from Rouse to reptation dynamics		
Dates of experiment:	26.9.2002-28.9.2002	Date of report:	5.3.2003
Experimental team: Names	Addresses		
M. Monkenbusch M. Zamponi	IFF, FZ Jülich IFF, FZ Jülich		
Local Contact:	M. Monkenbusch		

Experimental report text body

(Please use 12 pt letters here !)

Long chain polymers in the melt entangle each other and restrict their motion by forming topological constraints. By successive shortening of the matrix length a loss of confinement due to constraint release can be observed. In the limit of low matrix molecular weight one expect the transition to pure Rouse motion.

A previous NSE measurement of 5% protonated 36kg/mol PE in 2kg/mol deuterated PE showed that the dynamic in this limit is indeed Rouse-like, but the fitted Rouse-rate was much too small. The 5% concentration of the long chains correspond to the overlap–concentration so that the long chains themselves do not form topological constraints. Now NSE spectroscopy on only 2.5% of protonated 36kg/mol PE in a 2kg/mol deuterated matrix has been performed, to check if the observed deviation stems from the chosen concentration.

The measurements were done at a temperature of 509K with a wavelength of 8Å, covering a q-range from 0.05 $Å^{-1}$ to 0.115$Å^{-1}$. Data were corrected for resolution and background, the background was estimated from a sample of fully deuterated 2kg/mol matrix.

In fig. 1 the resulting dynamic structure factor is depicted in comparison to the previous measurement of 5% long chain PE in 2kg/mol-d-PE. No significant difference could be observed. In the accessible time range, both data sets lie close together, a fit with the Rouse model leads to a similar, too small Rouse rate.
So the deviation from pure Rouse behaviour does not depend on the concentration of the long chains, the concentration of 5% is low enough. Although the matrix length of 2kg/mol corresponds to only one entanglement length, this length seems to lead to the observed discrepancy. To further investigate this, a measurement with an even shorter matrix length will be performed.

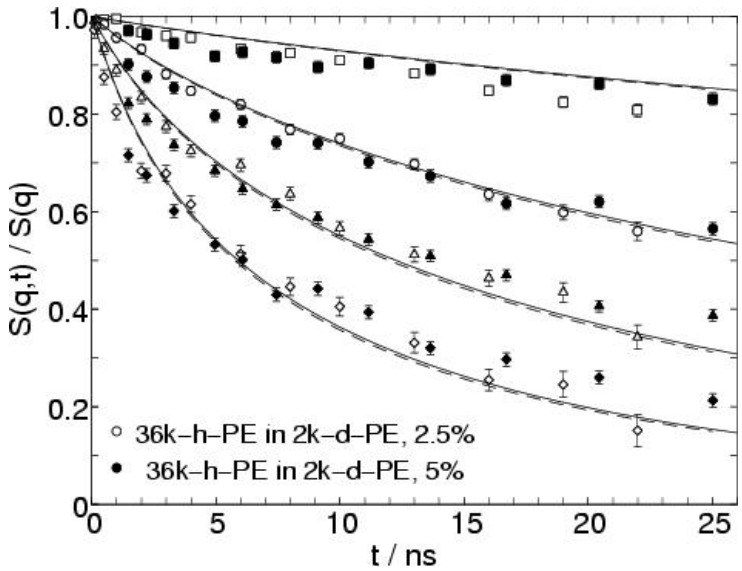

fig. 1: Open symbols: 2.5% 36k-h-PE in 2k-d-PE, NSE, FZJ.
Closed symbols: 5% 36k-h-PE in 2k-d-PE, IN15, ILL.
Lines: fit with Rouse-model. Q-values (in $Å^{-1}$): squares 0.05, circles 0.077, triangles up 0.096, diamonds 0.115.

Institut für Festkörperforschung
Forschungszentrum Jülich GmbH
D-52425 Jülich

Experimental Report
of Neutron Scattering Experiments
at the FRJ-2 Reactor

Proposal number:	NSE-02-010		
Experiment title:	Precise determination of the Q-dependence of incoherent scattering in poly(vinyl ethylene): the intermediate length scales region		
Dates of experiment:	25/11/2002-09/12/2002	Date of report: 29/01/2003	
Experimental team: Names	Addresses		
Juan Colmenero Arantxa Arbe Dieter Richter Michael Monkenbusch	Dpto. de Física de Materiales, UPV/EHU, Apdo. 1072, 20080 San Sebastian, SPAIN Unidad de Física de Materiales, CSIC-UPV/EHU, “ , “ , “ IFF, FZJ, Jülich, Germany “ , “ , “ , “		
Local Contact:	Michael Monkenbusch		

Experimental report text body

The aim of this experiment was to accurately determine the Q-dependence of the intermediate scattering function of poly(vinyl ethylene) (PVE) in the intermediate scale regime, i.e., at length scales of several times the intermolecular distances. The ultimate goal was to fully characterise the crossover from the entropy driven dynamics towards the α-relaxation governing the decay of the interchain correlations, which is universal for glass forming systems. This study has also allowed us to fill the experimental gap between previous NSE measurements on the single chain dynamic structure factor and on the self motion of the protons in this polymer.

The intermediate scattering function corresponding to the protons in the fully protonated PVE sample was measured by the Jülich NSE at 418 K and momentum transfers of Q = 0.1, 0.15, 0.20, 0.30 and 0.40 $Å^{-1}$. Long measuring times were employed (about 1 day per spectrum), specially for the lowest Q-values. Careful measurements were also performed to determine the background and the resolution function. The good quality of these experimental results, that can be appreciated in Fig. 1, has allowed us to determine with high accuracy the shape of the decay (β parameter of the Kohlrausch-Williams-Watts function, β=0.5) and the characteristic time as a function of Q. The resulting time scales are displayed in Fig. 2 together with those deduced for incoherent scattering from an independent previous study of the single chain dynamic structure on PVE. The agreement between both kinds of results is strinkingly good.

We realize that in this case, as β=0.5, the same Q-dependence (Q^{-4}) is expected for the characteristic time in the Rouse region at small Q-values [1] and in the glassy region approaching the intermolecular distances [2]. However, from Fig. 2 it is evident that the crossover from Rouse to glassy behavior does not take place continuously, but a clear step develops at about 0.12 $Å^{-1}$ in the Q-dependence of the characteristic time for self motion. Such a step is the signature of the transition from entropy driven dynamics to the glass behavior at shorter length scales.

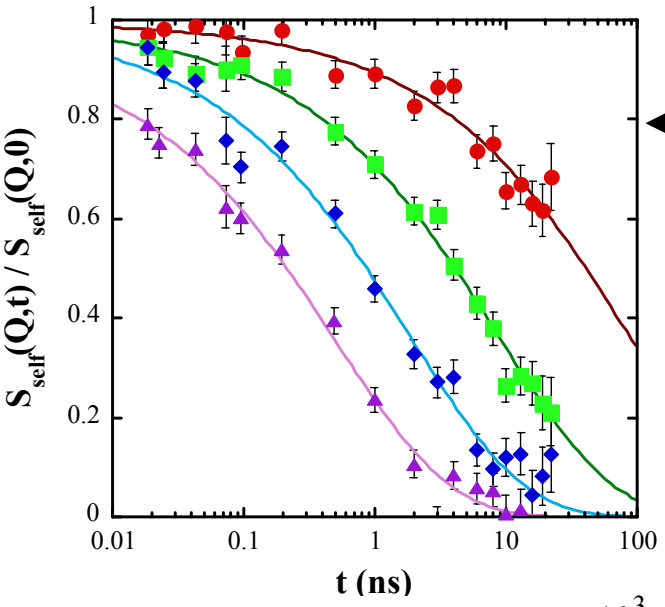

Figure 1: Self correlation function of the protons measured by the Jülich NSE spectrometer on the PVE protonated sample at 418 K and 0.1, 0.2, 0.3 and 0.4 $Å^{-1}$ (top to bottom). Solid lines are descriptions in terms of stretched exponential functions with β = 0.5.

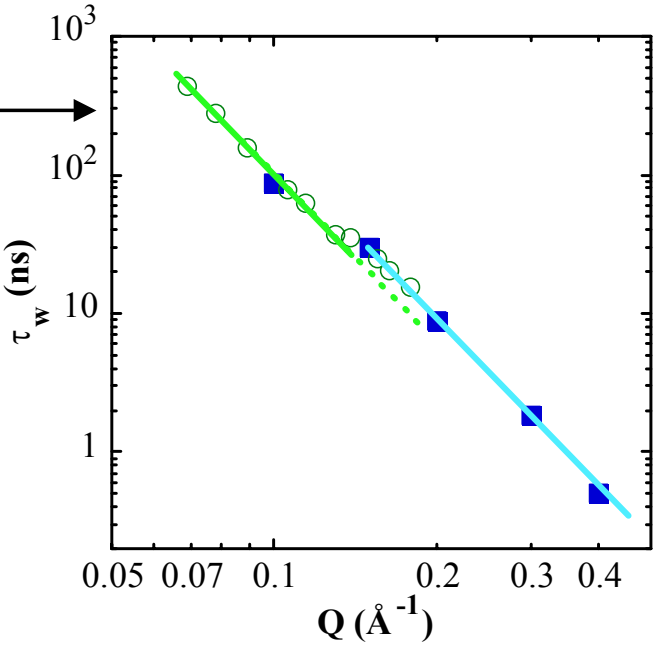

Figure 2: Q-dependence of the characteristic time corresponding to the self motion directly measured by the Jülich NSE spectrometer on the protonated sample (■) and obtained from the description of the single chain dynamic structure factor in terms of the Rouse model (O). The straight lines show the Q^{-4} dependencies expected for the Rouse and for the glassy regions.

REFERENCES

[1] See, e.g., M. Doi and S. F. Edwards, *The Theory of Polymer Dynamics* (Clarendon Press, Oxford, 1986)

[2] J. Colmenero, A. Alegría, A. Arbe and B. Frick, Phys. Rev. Lett. 69, 478 (1992).

Institut für Festkörperforschung
Forschungszentrum Jülich GmbH
D-52425 Jülich

Experimental Report
of Neutron Scattering Experiments
at the FRJ-2 Reactor

Proposal number:	NSE-02-008		
Experiment title:	Bending elasticity of mixed block copolymer surfactant films		
Dates of experiment:	29.10. – 03.11.02	Date of report:	10.02.03
Experimental team: Names	Addresses		
Egger, Holger Hellweg, Thomas Findenegg, Gerhard H.	Stranski-Laboratorium TU Berlin Straße des 17. Juni 112 10623 Berlin		
Local Contact:	Monkenbusch, Michael		

Experimental report text body

The structuring processes in amphiphilic systems are determined by the contribution of the curvature energy of the interfacial film to the total free energy. This contribution is quantified by the Helfrich equation [1], where the two elastic constants κ (bending modulus) and $\bar{\kappa}$ (Gaussian modulus) are characteristic values for the amphiphilic film. They describe the elastic properties of the film. Therefore dynamic methods like Neutron-Spinecho (NSE) are suitable to determine these dynamic quantities.
Since measurements of the elastic properties of films and membranes based on amphiphilic block copolymers are rare, we investigated a complex microemulsion consisting of a triblock copolymer of the type poly(ethylene oxide)-poyl(propylene oxide)- poly(ethylene oxide) in *o*-xylene and water, were the addition of the ionic surfactant n-octyltrimethyl-ammoniumbromide induces a phase transition into a lamellar phase. In the Helfrich equation the part with the Gaussian modulus vanishes for the lamellar phase. Therefore the elasticity is only related to the bending modulus κ. Hence our NSE-investigations focus on the lamellar phase where two series of measurements with different surfactant content are performed. The measurements were done at room temperature on an orientated lamellar phase, which means that the neutron beam was parallel to the amphiphilic layers.

Fig. 1 shows the NSE-relaxation curves for the two different surfactant concentrations at different scattering vectors q. The left part shows the curves with a weight fraction of C_8TAB of wt = 0.095, the right part the ones with the higher surfactant content of wt = 0.12. The first qualitative result is that the relaxation time decreases with increasing amount of surfactant, which means that added surfactant reduces the flexibility of the layers. This is in good agreement with X-ray scattering results [2], where it is possible to correlate the peak width with the elasticity of the layer.

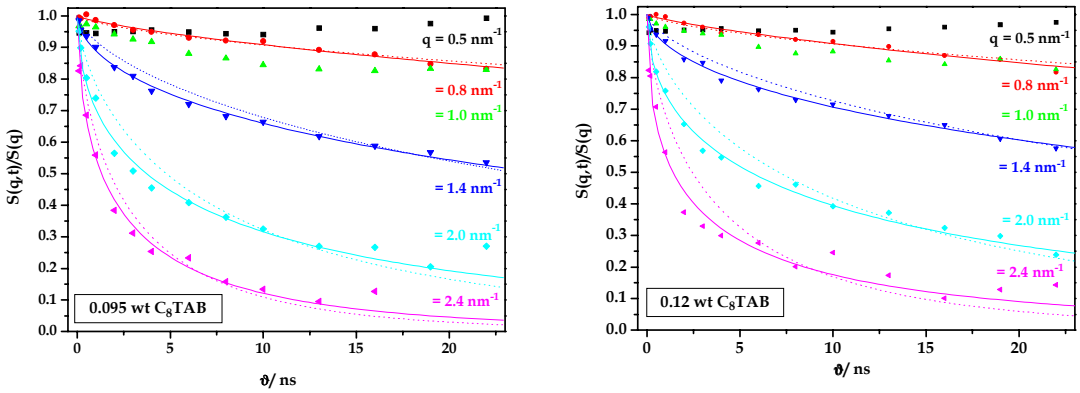

Fig. 1: NSE-Scattering curves of the lamellar phase of the system $PEO_{37}PPO_{58}$ PEO_{37} / xylene / water / C_8TAB for two different surfactant concentration. left: wt C_8TAB = 0.095, right: wt C_8TAB = 0.12.

Moreover, the curves are fitted with a single stretched exponential function.

$$S(q,t)/S(q)| \exp(-(t/\tau)^{\beta})$$

The curves at 0.5 and 1 nm^{-1} are not fitted because these q-values correspond to the position of the Bragg-peaks of the lamellar phase. Around the structure factor maximum the relaxation time of the curves is raised (de Gennes-narrowing), consequently no reliable fit result can be obtained . The dotted lines are fits with a fixed exponent of $\eta = 2/3$ according to the theory of Granek and Zilman [3]. They proposed this exponent for large q-values, where single membrane dynamics is responsible for the scattering behavior.

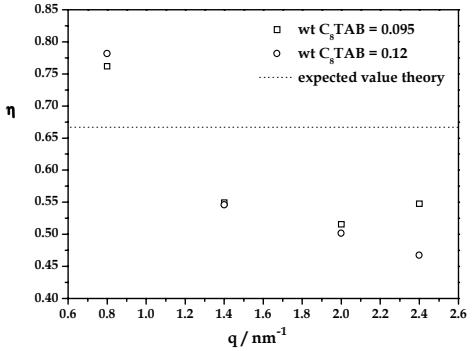

Fig. 2: Exponent plotted as function of q of a stretched exponential fit. The dotted line is the expected value of the theory of Zilman and Granek.

However the fits describe the curves only insufficiently. Additionally, fits with free exponents are shown (solid lines). This leads to a better description of the data. The resulting exponents are plotted in fig. 2. For both series systematic deviation from the predicted exponent (dotted line) can be observed. To obtain a more complete image of these complex self-assembled systems more experiments are necessary. On the basis of the present results it is not yet possible to draw final conclusions.

References: [1] W. Helfrich, Z. Naturforschung 28c, 693 (1973).
[2] H. Egger, T. Hellweg, G. H. Findenegg, to be published.
[3] A. G. Zilman, R. Granek, Phys. Rev. Lett. 77, 4788 (1996).

Institut für Festkörperforschung
Forschungszentrum Jülich GmbH
D-52425 Jülich

Experimental Report
of Neutron Scattering Experiments
at the FRJ-2 Reactor

Proposal number:	**NSE-02-003**		
Experiment title:	Investigation of the self correlation of α and β process of poly methylacrylate		
Dates of experiment:	June 2002	Date of report:	03.03.2003
Experimental team: Names	Addresses		
Stefan Kahle	IFF, FZ-Jülich		
Local Contact:	M. Monkenbusch		

Experimental report text body

(Please use 12 pt letters here !)

In the 20 days we have measured partially deuterated polybutadiene (the methine groups carry protons, and deuterons elsewhere – d4h2 PB) at different *Q*'s and temperatures (*T=210K*: *Q=0.4*, *0.6*, *0.8*, *1.0*,and *1.4 Å*$^{-1}$; *T=250K*: *Q=0.4*, *0.6*, *0.8*,and *1.4 Å*$^{-1}$). Due to the variation in scattering length along the polymer chain with this sample essentially we observe the double bond/double bond correlation. To cover a large time range, we have used the "shorty" option of the instrument. Due to protons, the d4h2 PB sample have a very large incoherent background. Therefore, we have a strong loss in the spin polarization, and the difference of spin up and spin down is very, i.e. the spin echo amplitude is very small, and therefore the experiment becomes very time consuming.

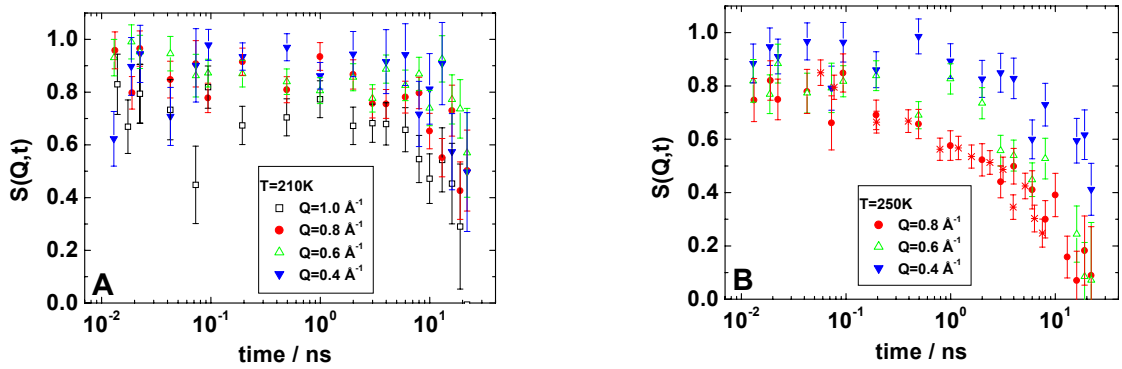

Figure 1 Neutron spin echo data measured at different Q (see legends) and temperatures (210 K (A) and 250K (B). Also included is a spectrum from previous experiments at *T=250K* and *Q=0.8 Å*$^{-1}$ (x in part B).

Figure 1 shows NSE spectra measured at T=210 (A) and 250K(B). Due to the large incoherent intensity, in this Q range the d4h2 PB sample scatters mainly incoherent. The quality of the spectra is poor especially for the T=210K measurement, but note that the time spend for each scan was about two days.
Nevertheless, we have evaluated the data to get the characteristic times. First, we have fitted our spectra with a single KWW function:

$$S(Q,t) = A(Q)\{\exp[-(t/\tau(Q))^{\beta}]\}. \qquad (1)$$

Figure 2 (open symbols) shows the fit-results. We observe the familiar behavior.
Of course, the sample scatters both coherently and incoherntly in a significant manner. Therefore, we have also fitted the spectra with:

$$S(Q,t) = A(Q)\cdot\left\{A_{coh}(Q)\{\exp[-(t/\tau_{coh}(Q))^{\beta}]\} + A_{inc}(Q)\{\exp[-(t/\tau_{inc}(Q))^{\beta}]\}\right\}. \qquad (2)$$

The parameter A_{coh} and A_{inc} was taken from former diffraction measurements, and incoherent times was taken from backscattering experiments. The fitresults are also included in figure 2. At Q=*0.6, 0.8 Å^{-1}* and *1.0 Å^{-1}* we get acceptable results for the coherent times, τ_{coh}, i.e. τ_{coh} is in the expected order of magnitude. However, at Q=*0.4*, τ_{coh} seems to be too low. Note that at this Q the coherent intensity is about eight times smaller than the incoherent one.

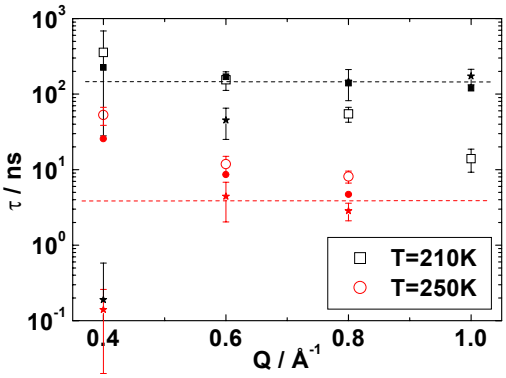

Figure 2 Q dependence of characteristic times for T=210 and 250K. The open symbols correspond to results from a single KWW fit, the filled symbols to the incoherent times taken from backscattering experiments. The stars correspond to the coherent times obtained by fitting eq.2.

Résumé: Due to the high incoherent background, the measurement is very difficult, and time consuming, respectively. It seems to get acceptable results we have to spend more time for each scan.

Publications

In the following section publications of the years 2002 to now resulting from experiments at the Jülich research reactor FRJ-2 are listed. The list is based on the response of experimentalists and therefore not complete. A total of 286 journal publications was reported to us, in addition 109 invited talks, 111 conference presentations, 11 reactor-related publications, and 37 theses. We thank the users for this great support!

A database research (ISI web of science, keywords “Jülich” and “neutrons”) resulted in 96 journal publications in 2000 and 93 in 2001. Therefore we assume that the compilation here is complete to more than 60%.

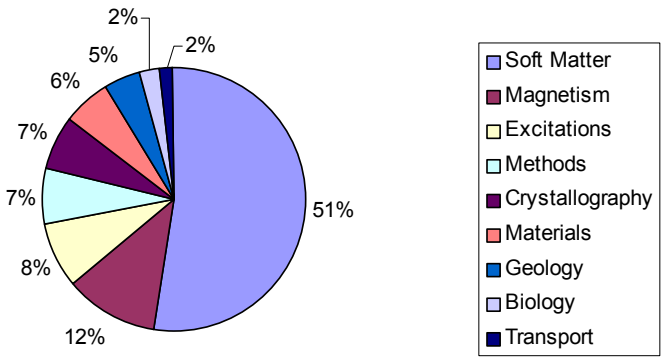

Distribution of topics of journal publications of the years 1998–now.

The figure above represents the breakdown of the journal publication number by topics. Although the categories are slightly different here, the similarity with Fig. 3 of the introduction shows that the distribution of topics is about the same in the scientific output as in the experiments performed. Again the focus is on soft matter. Notably, there is a considerable fraction of methodical publications showing that the work at FRJ-2 has also contributed largely to the development of neutron scattering techniques.

Neutron Instruments and Methods

Publications

Villa,M, Baron,M, Hainbuchner,M, Jericha,E, Leiner,V, Schwahn,D, Seidl,E, Stahn,J, Rauch,H
Optimization of a Crystal Design for a Bonse-Hart Camera
J. Appl. Cryst (in press)

Ioffe,A, Conrad,H, Zeiske,T, Mueller,R, Küssel,E, Masalovich,S, Schlapp,M, Schmitz,B, Brückel,T
A new thermal neutron spectrometer/diffractometer for polarization analysis (SV30) at the research reactor FRJ-2
Applied Physics A **74**, 107 (2002)

Massalovitch,S, Ioffe,A, Küssel,E, Schlapp,M, Brückel,Th
Development of Image Plate Based Neutron Detector
International Workshop on Position-Sensitive Neutron Detectors - Status and Perspectives, ISSN 1433-559 **2**, 569 (2002)

Massalovitch,S, Ioffe,A, Küssel,E, Schlapp,M, vonSeggern,H, Brückel,Th
Development of neutron image plate for low-flux measurements
Appl. Physics A [Suppl.] **74**, S118 (2002)

Schlapp,M, vonSeggern,H, Massalovich,S, Ioffe,A, Conrad,H, Brueckel,T
Materials for neutron image plates with low γ-sensitivity
Appl. Phys. A **74 [Suppl.]**, 109-111 (2002)

Brückel, Th, Heger,G, Richter,D, Zorn, R (Ed.)
5th laboratory course neutron scattering
Schriften des Forschungszentrums Jülich, Materie und Material, Vol. 9 (2001)

Kemmerling,G, Engels,R, Bussmann,N, Clemens,U, Heiderich,M, Reinartz,R, Rongen H, Schelten J, Schwahn D, Zwoll K
A new two-dimensional scitillation detector system for small angle neutron scattering
Transactions on Nuclear Science **48**, 1114 (2001)

Plakhty,VP, Schweika,W, Brückel,Th, Kulda,J, Gavrilov,SV, Regnault,L-P, Visser, D
Chiral criticality in helimagnet Ho studied by polarized neutron scattering
Phys. Rev. B **64**, 100402(R) (2001)

Rücker,U, Bergs,W, Alefeld,B, Kentzinger,E, Brückel,Th
Polarization analysis for the 2D position-sensitive detector of the HADAS reflectometer
Physica B **297**, 140 (2001)

Schweika,W, Böni,P
The Instrument DNS: Polarization Analysis for Diffuse Neutron Scattering
Physica B **297**, 155-159 (2001)

Zeitelhack,K
Eurisys ^{3}He-proportional Counters squashed series
Internal Report 29-05-01; Technische Universität München (2001)

Brückel,Th, Heger,G, Richter, D (Ed.)
Neutron scattering: lectures
Schriften des Forschungszentrums Jülich, Materie und Material, Vol. 5 (2000)

Alefeld,B, Dohmen,L, Richter,D, Brueckel,T
Space technology from X-ray telescopes for focusing SANS and reflectometry
Physica B **276-278**, 52 (2000)

Alefeld,B, Dohmen,L, Richter,D, Brueckel,T
X-ray space technology for focusing small-angle neutron scattering and neutron reflectometry
Physica B **283**, 330 (2000)

Borbely,S, Heiderich,M, Schwahn,D, Seidl,E
Resolution of the USANS diffractometer at the FRJ-2 reactor in Jülich
Physica B **276-278**, 138-139 (2000)

Kemner,E, Schepper,IM, Schmets,AJM, Grimm,H
Model independent determination of the elastic incoherent structure factor in neutron scattering experiments
Nucl. Instr. and Methods B **160**, 544 (2000)

Prager,M
The thermal time-of-flight spectrometer SV29 at FZ Jülich: focusing in space and time
Physica B **283**, 376 (2000)

Rücker,U, Alefeld,B, Bergs,W, Kentzinger,E, Brückel,Th
The new polarized neutron reflectometer in Jülich
Physica B **276-278**, 95 (2000)

Rücker,U, Alefeld,B, Kentzinger,E, Brückel,Th
Monochromator design for the HADAS reflectometer in Jülich
Physica B **283**, 422 (2000)

Montes,H, Monkenbusch,M, Willner,L, Rathgeber,S, Fetters,L, Richter,D
Neutron Spin-Echo Investigation of the Concentration Fluctuation Dynamics in Melts of Diblock-Copolymers
J. Chem. Phys. **110**, 10188 (1999)

Wroblewski,T, Jansen,E, Schäfer,W, Skowronek,R
Neutron imaging of bulk poly-crystalline materials
Nucl. Instrum. Methods in Phys. Research A **423**, 428 (1999)

Engels,R, Jansen,E, Reinartz,R, Reinhart,P, Schäfer,W, Schelten,J
Realisation of a small-size high resolution linear neutron scintillation detector
IEEE Transactions on Nuclear Science **45**, 502 (1998)

Invited Talks

Kahle,S
High Resolution Inelastic Neutron Scattering Spectroscopy
Joint ICTP-INFM School and Workshop on Spectroscopy Investigation of the Collect (Trieste) (2002)

Kentzinger,E
KWS-3, the new Focusing Mirror SANS Instrument at Juelich
6th ESS- Scientific Advisory Commitee Meeting (Bochum, Germany) (2002)

Kentzinger,E
First Experiments on the Focusing-Mirror USANS Diffractometer KWS-3
European Users Meeting Juelich Neutrons For Europe (Kerkrade, NL) (2002)

Prager,M
Status and Experience with the time-focusing thermal TOF-spectrometer SV29 at Jülich
Paul-Scherrer-Institut (Villigen, CH) (2002)

Schweika,W
Time of Flight and Polarization Analysis for Diffuse Neutron Scattering
Polarized Neutrons in Condensed Matter Investigations 2002 (Jülich) (2002)

Alefeld,B
Space technology from X-ray telescopes for focusing SANS and reflectometry
ECNS (Budapest) (1999)

Conference Presentations

Alefeld,B, Conrad,H, Dohmen,L, Ioffe,A, Kentzinger,E, Küssel,E, Prager,M, Rücker,U, Brückel,Th
Instrument Modernisation Program at the FRJ-2 Reactor
ESS European Conference (Bonn) Poster (2002)

Dohmen,L, Alefeld,B, Kentzinger,E, Ruecker,U, Stellbrink,J, Ioffe,A, Springer,T, Richter,D, Brueckel,T, Drochner,M, Engels,R, Kleines,H, Suxdorf,F, Zwoll,K
A High Resolution Small Angle Scattering Instrument and Reflectometer with Focusing Mirror (KWS3) at Juelich
Deutsche Neutronenstreutagung & ESS Meeting (Bonn) Poster (2002)

Massalovitch,S, Ioffe,A, Küssel,E, Brückel,Th, Schlapp,M, vonSeggern,H
The optimization of neutron image plate detector with low gamma-sensitivity
ESS-Konferenz (Bonn) Poster (2002)

Mueller,R, Chang,LJ, Appelt,St, Haesing,W, Horriar-Esser,Ch, Ioffe,A, Brückel, Th
Progress in the production of polarised ^{3}He in Jülich
Workshop on Polarised Neutrons in Condensed Matter Investigations (FZJ, Jülich) Poster (2002)

Schäfer,W, Jansen,E, Skowronek,R, Kirfel,A
Recent examples of scientific projects using the University of Bonn powder diffractometer SV7-a in Jülich
Deutsche Neutronenstreutagung 2002 and The European Spallation Source (Bonn) Poster (2002)

Ioffe,A, Conrad,H, Zeiske,Th, Mueller,R, Küssel,E, Masalovich,S, Schlapp,M, Schmitz,B, Brückel,Th
A New Thermal Neutron Spectrometer/Diffractometer for Polarization Analysis (SV30) at the research reactor FRJ-2
ICNS 2001 (München) Poster (2001)

Ioffe,A, Conrad,H, Zeiske,Th, Mueller,R, Küssel,E, Masalovich,S, Schlapp,M, Schmitz,B, Brückel,Th
Spektrometer SV30 für Polarisationsanalyse mit thermischen Neutronen am Forschungsreaktor FRJ-2
Deutsche Neutronenstreutagung (Jülich) Poster (2001)

Kirfel,A, Schäfer,W
Forschung mit Neutronen in den Außenstellen des Mineralogisch-Petrologischen Instituts der Universität Bonn in Jülich und England
BMBF-Veranstaltung Förderschwerpunkt Kondensierte Materie (Bonn) Talk (2001)

Monkenbusch,M, Mihailescu,M, Allgaier,J, Richter,D, Jakobs,B, Sottmann,T
Interface Dynamics in Bicontinuous Microemulsions Investigated by Neutron Spin Echo Spectroscopy
ACS Conference COLLOIDS2001 (Pittsburgh) Talk (2001)

Mueller,R, Brückel,Th, Horriar-Esser,Ch
Entwicklung einer Anlage zur Herstellung von kernspin-polarisiertem ^{3}He am Forschungszentrum Jülich
Deutsche Neutronenstreutagung (FZJ, Jülich) Poster (2001)

Rücker,U, Bergs,W, Alefeld,B, Kentzinger,E, Brückel,Th
The new neutron reflectometer with polarization analysis in Jülich
Deutsche Neutronenstreutagung (Jülich) Poster (2001)

Rücker,U, Bergs,W, Kentzinger,E, Brückel,Th
Polarization Analysis for a neutron reflectometer with 2D position sensitive detector
European Neutron Polarization Initiative (Jülich) Talk (2001)

Rücker,U, Kentzinger,E, Bergs,W, Alefeld,B, Brückel,Th
The new reflectometer with polarization analysis in Jülich
ICNS 2001 (Munich) Poster (2001)

Crystallography

Publications

Halevy,I, Salhov,S, Kimmel,G, Atzmony,U, Pereira,LCJ, Goncalves,AP, Schäfer,W
High-pressure studies of a $ThMn_{12}$-type actinide compound: UFe_5Al_7
Journal of Physics: Condensed Matter **14**, 11189 (2002)

Schäfer,W, Kirfel,A
Neutron powder diffraction study on the thermal expansion of cuprite
Applied Physics A **74**, 1010 (2002)

Sosnowska,I, Schäfer,W, Kockelmann,W, Barbier,B, Andersen,KA, Troyanchuk,IO
Crystal structure and spiral magnetic ordering of $BiFeO_3$ doped with manganese
Applied Physics A **74**, 1040 (2002)

Kockelmann,W, Schäfer,W, Kirfel,A, Klapper,H, Euler,H
Hydrogen positions in KCo-, CsCo-, CsNi-, and CsCu-Tutton's Salt type compounds determined by neutron powder diffraction
Materials Science Forum **378-381**, 274 (2001)

Schäfer,W, Halevy,I
Neutron powder diffraction on iron-rich rare earth-iron-aluminium intermetallics RFe_7Al_5 (R = Tb, Dy, Ho, Er)
Material Science Forum **378-381**, 414 (2001)

Sosnowska,I, Schäfer,W, Kockelmann,W, Troyanchuk,IO
Neutron diffraction studies of crystal and magnetic structure of $BiMn_xFe_{1-x}O_3$ solid solutions
Materials Science Forum **378-381**, 616 (2001)

Alefeld,B, Dohmen,L, Heidemann,A
GaAs as a backscattering crystal
Physica B **283**, 299 (2000)

Kotsanidis,PA, Schäfer,W
Neutron diffraction study of $RPtGe_2$ (R = Dy, Ho) compounds
Physica B **276-278**, 576 (2000)

Kümmerle,EA, Güthoff,F, Schweika,W, Heger,G
Single-crystal neutron diffraction investigations on the phase transitions in $CeO_{1.800}$ and $CeO_{1.765}$
Journal of Solid State Chemistry **153**, 218 (2000)

Schäfer,W, Barbier,B, Halevy,I
$ThMn_{12}$-type magnetic $ErFe_7Al_5$ and non-magnetic YFe_7Al_5 studied by X-ray and neutron diffraction
J. Alloys Compounds **303**, 270 (2000)

Schäfer,W, Kockelmann,W, Halevy,I, Gal,J
Structural and magnetic ordering in rare earth - iron - aluminium intermetallics studied by neutron powder diffraction
Material Science Forum **321-324**, 670 (2000)

Schäfer,W, Kockelmann,W, Kirfel,A, Potzel,W, Burghart,FJ, Kalvius,GM, Martin,A, Kaczmarek,WA, Campbell,SJ
Structural and magnetic variations of $ZnFe_2O_4$ spinels - neutron powder diffraction studies
Material Science Forum **312**, 802 (2000)

Sosnowska,I, Schäfer,W, Troyanchuk,IO
Investigations of crystal and magnetic structure of $BiMn_{0.2}Fe_{0.8}O_3$
Physica B **276-278**, 576 (2000)

Kümmerle,EA, Heger,G
The Structures of C-$Ce_2O_{3+\delta}$ Ce_7O_{12}, and $Ce_{11}O_{20}$
Journal of Solid State Chemistry **147**, 485-500 (1999)

Wickleder,MS, Schäfer,W
Synthesis and structure of anhydrous rare-earth perchlorates $M(ClO_4)_3$ (M=La, Ce, Er, Y): Derivatives of the UCl_3 type of structure
Zeitschrift für anorganische und allgemeine Chemie **625**, 309 (1999)

Kirfel,A, Klapper,H, Schäfer,W, Schwabenländer,F
The crystal structure of Tutton's salt type $K_2[Co(H_2O)_6](SO_4)_2$. A combined X-ray and neutron study
Zeitschrift für Kristallographie **213**, 456 (1998)

Schweika,W
Disordered Alloys, Diffuse Scattering and Monte Carlo Simulations
in G. Höhler (Ed.): Springer Tracts in Modern Physics Vol. 141, Springer, Heidelberg, (1998)

Schäfer,W, Kockelmann,W, Jansen,E, Fredo,S, Gal,J
Structural characteristics of rare earth (R) ternary magnetic intermetallics RFe_xAl_{12-x} with iron concentrations x = 6
Material Science Forum **278-281**, 542 (1998)

Waibel,B, Schwahn,D, Magerl,A
Reflectivity of sound-excited crystals measured on a double crystal diffractometer
Physica B **241-243**, 183-185 (1998)

Conference Presentations

Schäfer,W, Kirfel,A
On the unusual negative thermal expansion of cuprite
Deutsche Neutronenstreutagung 2002 and The European Spallation Source (Bonn) Poster (2002)

Schäfer,W, Kirfel,A
Neutronenbeugung zum thermischen Verhalten von Cuprit
10. Jahrestagung der Deutschen Gesellschaft für Kristallographie (Kiel) Poster (2002)

Bieniok,A, Bertoldi,C, Schäfer,W, Heger,G, Amthauer,G
Strukturelle Untersuchungen an einem natürlichen Chamosit
79. Jahrestagung der Deutschen Mineralogischen Gesellschaft (Potsdam) Poster (2001)

Sauerwald,F, Wacker,K, Buck,P, Schäfer,W
Neutronenbeugungsuntersuchungen (Rietveld) an Spinellmischkristallen $MnFe_2O_{4+\delta}$
9. Jahrestagung der Deutschen Gesellschaft für Kristallographie (Bayreuth) Talk (2001)

Schweika,W, Shramchenko,N, Caudron,R, Bellissent,R, Widom,M
Phason disorder in icosahedral AlPdMn quasicrystals
International Conference on Neutron Scattering (München) Poster (2001)

Schweika,W, Shramchenko,N, Caudron,R, Bellissent,R, Widom,M
Phason disorder in icosahedral AlPdMn quasicrystals
Deutsche Neutronenstreutagung (Jülich) Poster (2001)

Schäfer,W, Kirfel,A
Neutron powder diffraction study on the thermal expansion of cuprite
ICNS 2001 (Munich) Poster (2001)

Excitations

Publications

Elter,P, Eckold,G, Caspary,D, Güthoff,F, Hoser,A
Time-evolution of phonon spectra during decomposition in $Ag_xNa_{1-x}Br$ ionic crystals
Appl. Phys. A **74 [Suppl 1]**, 1169-1171 (2002)

Hoelzel,M, Danilkin,SA, Hoser,A, Ehrenberg,H, Wieder,T, Fuess,H
Phonon dispersion in austenitic stainless steel $Fe_{18}Cr_{12}Ni_2Mo$
Appl. Phys. A **74 [Suppl 1]**, 1013-1015 (2002)

Prager,M, Grimm,H, Parker,SF, Lechner,R, Desmedt,A, McGrady,S, Koglin,E
Methyl group rotation in trimethyl aluminum
J.Phys.: Cond. Matter **14**, 1833 (2002)

Prager,M, Schiebel,P, Combet,J
Rotational tunnelling and disorder in 4-iodo-toluene
Chem. Phys. **276**, 69 (2002)

Prager,M, Schiebel,P, Grimm,H
Dipolar interaction in $(NH_{3.6}D_{0.4})_2PtCl_6$
Appl. Phys. A **74 [Suppl.]**, 1363 (2002)

Prager,M, Schiebel,P, Grimm,H
Rotational Tunelling of NH_4 and NH_3D and dipolar interaction in $(NH_{3.6}D_{0.4})_2PtCl_6$
J. Chem. Phys. **116**, 10338 (2002)

Schweika,W, Maleyev,SV, Brückel,Th, Plakhty,VP, Regnault,L-P
Longitudinal spin fluctuations in the antiferromganet MnF_2 studied by polarized neutron scattering
Europhys. Lett. **60**, 446 (2002)

Danilkin,SA, Fuess,H, Wieder,T, Hoser,A
Phonon dispersion and elastic constants in Fe-Cr-Mn-Ni austenitic steel
Journal of Materials Science **36 (4)**, 811-814 (2001)

Eckold,G
Kinetics of decomposition in ionic solids: neutron scattering study of the system AgBr-NaBr
Journal of Physics-Condensed Matter **13 (2)**, 217-240 (2001)

Kirstein,O, Prager,M, Combet,J, Johnson,MR
Ammonia group rotation in $Zn(NH_3)_4I_2$
Molecular Physics Report **31**, 47 (2001)

Köbler,U, Hoser,A, Englich,J, Snezhko,A, Kawakami,M, Beyss,M, Fischer, K
On the failure of the Bloch-Kubo-Dyson spin wave theory
Phys. Soc. Jpn. **70 (10)**, 3089-3097 (2001)

Köbler,U, Hoser,A, Kawakami,M, Abens,S
Observation of a spin wave exponent of 5/2 in the uniaxial antiferromagnet MnF_2
Physica B **307 (1-4)**, 175-183 (2001)

Gibhardt,H, Eckold,G, Güthoff,F
Kinetics of the stress induced phase transitions in quartz by real-time neutron scattering
Physica B **276-278**, 240-241 (2000)

Lee,SA, Grimm,H, Pohle,W, Scheiding,W, vanDamm,L, Song,Z, Levitt, M H, Korolev, N, Szabo, A, Rupprecht, A
NaDNA-bipyridil-(ethylenediamine)platinum(II) complex: Structure in oriented wet-spin films and fibers
Physical Review E **62 (5)**, 7044-7058 (2000)

Prager,M, Grimm,H, Parker,SF, McGrady,S
Rotational potentials of bridging and terminal methyl groups in trimethylaluminum dimers
Physica B **276-278**, 250 (2000)

Gibhardt,H, Eckold,G
Kristalle unter wechselndem Stress
Spektrum, Universität Göttingen (ISSN 0945-3512) **2**, 8 (1999)

Güthoff,F, Ohl,M, Reehuis,M, Loidl,A
Phase transitions and relaxation dynamics in $(NH_4I)_x(KI)_{1-x}$ mixed crystals
Physica B **266 (4)**, 310-320 (1999)

Prager,M, Schiebel,P, Johnson,M
Deuteration induced Phase Transition in an Ammonium-Perovskite
DIM-Newsletter **12**, 10 (1999)

Prager,M, Schiebel,P, Johnson,M, Grimm,H, Hagdorn,H, Prandl,W, Lalowicz,Z
Isotope effect and phase transitions in ammoniumhexachloropalladate studied by neutron tunnelling spectroscopy
J.Phys.: Condens. Matter **11**, 5341 (1999)

Bödecker,P, Hucht,A, Schreyer,A, Borchers,J, Güthoff,F, Zabel,H
Reorientation of Spin Density Waves in Cr(001) Filmes induced by Fe(001) Cap Layers
Phys. Rev. Lett. **81**, 914 (1998)

Eckold,G, Hagen,M, Steigenberger,U
Kinetics of phase transitions in modulated ferroelectrics: Time-resolved neutron diffraction from Rb_2ZnCl_4
Phase Transitions **67**, 219-245 (1998)

Eckstein,GA, Eckold,G, Schmidt,W, Steiner,HJ, Lutz,HD
Dynamics of lithium ions in spinel-type $^7Li_2MnCl_4$
Solid State Ionics **111**, 283-287 (1998)

Schwalowsky,L, Vinnichenko,V, Baranov,A, Bismayer,U, Merinov,B, Eckold,G
Protonic conductivity and ferroelastic instability in triammonium hydrogen disulphate: A dielectric and neutron diffraction study
J. Phys. Cond. Matter **10**, 3019 (1998)

Invited Talks

Prager,M
Rotational potentials studied by spectroscopy and relaxation
6th International Conference on Quasielastic Neutron Scattering (Potsdam) (2002)

Prager,M
Rotational tunnelling: from simple to complex systems
HMI (Berlin) (2001)

Prager,M, Schiebel,P, Combet,J
Rotational tunnelling and disorder of 4-iodo-toluene
Quantum Atomic and Molecular Tunnelling 2001 (Nottingham UK) (2001)

Gratz,E
Phonon dispersion in the orthorhombic YCu_2 and $NdCu_2$ compounds
University of South Illinois (1999)

Conference Presentations

Caspary,D, Elter,P, Eckold,G, Schmidt,W
Time-evolution of phonon spectra during decomposition in ionic crystals
ESS Conference (Bonn) Poster (2002)

Danilkin,S, Skomorohov,A, Hoser,A, Fuess,H, Bickulova,NN, Rajevac,V
Lattice dynamics of superionic conductor $Cu_{2-\delta}Se$
ESS Conference (Bonn) Poster (2002)

Danilkin,SA, Skomorokhov,AN, Rajevac,V, Fuess,H, Hoser,A, Bickulova,NN
Crystal structure and lattice dynamics of superionic conductor $Cu_{2-x}Se$
5th International Conference Solid State Chemistry 2002 (Bratislava, Slovakia) Poster (2002)

Hense,K, Gratz,E, Lindbaum,A, Nowotny,H, Hoser,A, Güthoff,F, Klenke, J
Lattice Dynamics in YCu_2
ESS Conference (Bonn) Poster (2002)

Caspary,D, Elter,P, Eckold,G
Zeitaufgelöste Phononen während der Entmischung in den Ionenkrsitallsystemen AgBr-NaBr und AgCl-NaCl
Deutsche Neutronenstreutagung (Jülich) Poster (2001)

Elter,P, Eckold,G, Caspary,D, Güthoff,F, Hoser,A
Time-evolution of phonon spectra during decomposition in $Ag_xNa_{1-x}Br$ ionic crystals
ICNS Conference (München) Poster (2001)

Hense,K, Gratz,E, Nowotny,H, Hoser,A, Güthoff,F
Lattice Dynamics in the orthorhomibic compound YCu_2
Deutsche Neutronenstreutagung (Jülich) Poster (2001)

Hoelzel,M, Danilkin,SA, Hoser,A, Ehrenberg,H, Wieder,T, Fuess,H
Phonon dispersion in austenitic stainless steel $Fe_{18}Cr_{12}Ni_2Mo$
ICNS Conference (München) Poster (2001)

Hölzel,M, Danilkin,S, Hoser,A, Wieder,T, Fuess,H
Phonon dispersion in nitrogen doped austenitic steels
Deutsche Neutronenstreutagung (Jülich) Poster (2001)

Magnetism

Publications

Kalvius,GM, Noakes,DR, Wäppling,R, Grosse,G, Schäfer,W, Kockelmann,W, Yakinthos,JK, Kotsanidis,PA
Spin dynamics and spin order in frustrated $TbCo_xNi_{1-x}C_2$
Physica B **326**, 465 (in press)

Kalvius,GM, Wagner,FE, Noakes,DR, Schreier,E, Wäppling,R, Zimmermann,U, Schäfer,W, Kockelmann,W, Halevy,I, Gal,J
Magnetic behaviour of YFe_xAl_{12-x}
Physica B **326**, 460 (in press)

Kentzinger,E, Ruecker,U, Toperverg,B
Simulations of off-specular scattering of polarized neutrons from laterally patterned magnetic multilayers
Physica B (in press)

Kentzinger,E, Ruecker,U, Toperverg,B, Brueckel,Th
Determination of the magnetic fluctuations in an Fe/Cr/Fe trilayer exhibiting a neutron resonance state
Physica B (in press)

Lauter,HJ, Lauter-Pasyuk,V, Toperverg,BP, Rücker,U, Milyaev,M, Romashev,L, Krinitsyna,T, Ustinov,V
Layer magnetization evolution in an Fe / Cr multilayer with uniaxial anisotropy
Physica B (in press)

Schäfer,W, Buschow,KHJ
Neutron Diffraction Study on Intermetallic Er_5Mg_{24} and Tm_5Mg_{24}
Materials Science Forum (in press)

Siouris,IM, Semitelou,IP, Yakinthos,JK, Schäfer,W
Presence of a spin glass state in antiferromagnetic Tb_2CuIn_3
Materials Science Forum (in press)

Ziegenhagen,N, Rücker,U, Kentzinger,E, Lehmann,R, vanderHart,A, Toperverg,B, Brückel, Th
Magnetic Properties of Laterally Structured Fe/Cr Multilayers
Physica B (in press)

Brückel, Th.; Schweika, W. (Ed.)
Polarised neutron scattering: lectures
Schriften des Forschungszentrums Jülich, Materie und Material, Vol. 12 (2002)

Köbler,U, Hoser,A, Fischer,K, Beyss,M
The impact of fourth-order exchange interactions on the thermal variation of the order parameter
Appl. Phys. A **74 [Suppl 1]**, s604 (2002)

Papathanasiou,GF, Kotsanidis,PA, Yakinthos,JK, Schäfer,W
The two antiferromagnetic phases of $TbPtGe_2$
J. Alloys and Compounds **343**, 26 (2002)

Rücker,U, Kentzinger,E, Toperverg,B, Ott,F, Brückel,Th
Layer-by-Layer magnetometry on polarizing supermirrors
Applied Physics A **74**, 607 (2002)

Voigt,J, Kentzinger,E, Rücker,U, Schmidt,W, Ohl,M, Hupfeld,D, Brückel,Th
Interlayer coupling in [Er/Tb] superlattices
Appl. Phys. A [Suppl.] **74**, 1517 - 1519 (2002)

Voigt,J, Rücker,U, Nerger,S, Kentzinger,E, Hupfeld,D, Schmidt,W, Brückel,Th
Structural and magnetic properties of [Er/Tb] superlattices
Journal of Magnetism and Magnetic Materials **240**, 559 - 561 (2002)

Kalvius,GM, Wagner,FE, Schreier,E, Wäppling,R, Noakes,DR, Zimmermann,U, Schäfer,W, Kockelmann,W, Halevy,I, Gal,J
The magnetism of frustrated RFe_6Al_6 compounds studied by μSR and Mössbauer
Hyperfine Interactions **136/137**, 269 (2001)

Plakhty,VP, Maleyev,SV, Kulda,J, Visser,ED, Wosnitza,J, Moskvin,EV, Brückel, Th, Kremer, K
Spin chirality and polarised neutron scattering
Physica B **297**, 60 - 66 (2001)

Siouris,IM, Semitelou,IP, Yakinthos,JK, Arons,RR, Schäfer,W
Competing ferro- and antiferromagnetism in R_2CuIn_3 (R=Tb, Ho, Er) intermetallics studied by neutron diffraction and magnetization measurements
J. Magn. Magn. Mater **226**, 1128 (2001)

Burghart,FJ, Potzel,W, Kalvius,GM, Schreier,E, Grosse,G, Noakes,DP, Schäfer,W, Kockelmann,W, Campball,SJ, Kaczmarek,WA, Martin,A, Krause,MK
Magnetism of crystalline and nanostructured $ZnFe_2O_4$
Physica B **289-290**, 286 (2000)

Kalvius,GM, Noakes,DR, Grosse,G, Schäfer,W, Kockelmann,W, Fredo,S, Halevy,I, Gal,J
Magnets frustrated by competing exchange ($TbFe_6Al_6$ and $ErFe_6Al_6$)
Physica B **289-290**, 225 (2000)

Kentzinger,E, Rücker,U, Caliebe,W, Goerigk,G, Werges,F, Nerger,S, Voigt, J, Schmidt, W, Alefeld, B, Fermon, C, Brückel, Th
Structural and magnetic characterization of Fe/δ-Mn thin films
Physica B **276 - 278**, 586 - 587 (2000)

Potzel,W, Schäfer,W, Kalvius,GM
Nanocrystalline oxide Zinc materials studied by the Mössbauer effect, μSR and neutron diffraction
Hyperfine Interactions **130**, 241 (2000)

Siouris,IM, Semitelou,IP, Yakinthos,JK, Schäfer,W, Arons,RR
Magnetic structure of Tb_2CuIn_3
J. Alloys Compounds **314**, 1 (2000)

Siouris,J, Semitelou,JP, Yakinthos,JK, Schäfer,W
Structure and magnetic states of R_2AgIn_3 (R = Pr, Nd, Tb, Ho, Er) intermetallics
Physica B **276-278**, 582 (2000)

Brückel,Th, Kentzinger,E
Streumethoden zur Untersuchung von Dünnschichtsystemen
in: Schriften des Forschungszentrums Jülich, Materie und Material, Vol. 2, B3.1 (1999)

Brückel,Th, Kentzinger,E
Streuung unter streifendem Einfall
in: Neutronenpraktikum, 7-1 (1999)

Papathanasiou,G, Kotsanidis,PA, Yakinthos,JK, Schäfer,W
Canted antiferromagnetic structure of $HoPtGe_2$
J. Alloys and Compounds **290**, 17 (1999)

Semitelou,JP, Siouris,J, Yakinthos,JK, Schäfer,W, Schmitt,S
Antiferromagnetic intermetallic Tb_2AgIn_3
J. Alloys and Compounds **283**, 12 (1999)

Hauer,B, Hempelmann,R, Udovic,TJ, Rush,JJ, Jansen,E, Kockelmann,W, Schäfer,W, Richter,D
Neutron-scattering studies on the vibrational excitations and the structure of ordered niobium hydrides: The epsilon-phase
Phys. Rev. B **57**, 11115 (1998)

Kockelmann,W, Schäfer,W, Yakinthos,JK, Kotsanidis,PA
Crossover from ferromagnetic $RCoC_2$ to antiferromagnetic $RNiC_2$ (R = rare earth) investigated on mixed $Tb(Co,Ni)C_2$
J. Magn. Magn. Mater. **177-181**, 792 (1998)

Papathanassiou,GF, Kotsanidis,PA, Yakinthos,JK, Schäfer,W
Amplitude sine modulated magnetic structures of $DyPtGe_2$
Zeitschrift für Kristallographie **213**, 22 (1998)

Schäfer,W, Kockelmann,W, Fredo,S, Gal,J
Neutron diffraction studies of ferrimagnetic RFe_6Al_6 (R=Tb, Ho, Er) intermetallics
J. Magn. Magn. Mater. **177**, 808 (1998)

Invited Talks

Brückel,Th
The Colorful Palette of Magnetism: Resonant Magnetic X-Ray Scattering
Kolloquium (Max-Planck-Institut, Stuttgart) (2002)

Brückel,Th
Von korrelierten Elektronen zu komplexen Legierungen: Festkörperforschung am IFF
HGF-Workshop Kondensierte Materie (FZJ, Jülich) (2002)

Brückel,Th
FZJ @ MuCAT: Examples for Research Activities
APS User Science Seminar (Argonne, USA) (2002)

Lauter,HJ, Lauter-Pasyuk,V, Toperverg,B, Rücker,U, Romashev,L, Milyaev,M, Ustinov,V
Spin-flop transition in Fe / Cr multilayers
Polarized Neutrons in Condensed Matter investigations (Jülich) (2002)

Toperverg,B
Diffuse neutron scattering on multilayers
XXXVI PNPI Winter School Condensed State Physics (Gatchina (RU)) (2002)

Toperverg,B
Neutron scattering at grazing incidence
Workshop RNIKS-2002 (Gatchina(RU)) (2002)

Toperverg,B
Supermatrix formalism to model off-specular neutron scattering
The 7th International Conference on Surface X-Ray and Neutron Scattering (Lake Tahoe, CA) (2002)

Toperverg,B
Theoretical interpretation and quantitativ analysis of data on reflectometry and off-specular scattering
Workshop Neutron Reflection: Progress in the Study of Interfaces (Grenoble) (2002)

Toperverg,B
Theoretical interpretation of off-specular polarized neutron scattering from nanocomposite films
International Workshop on Nanocomposites: Materials, Neutrons and Data Interpretation (Argonne) (2002)

Toperverg,B
Lateral magnetic patterns in thin films and layered superstructures: polarized neutron off-specular scattering
Seminar Ruhr-Universität Bochum (Bochum) (2002)

Toperverg,B
Neutron scattering at grazing incidence
IPNS / SNS Seminar (Argonne) (2002)

Toperverg,B
Polarized neutron reflection and off-specular scattering
GKSS-Seminar (Geesthacht) (2002)

Ziegenhagen,N, Rücker,U, Kentzinger,E, Toperverg,B, Brückel,Th, Lehmann,R, van der Hart,A
Magnetic Properties of Laterally structured Fe/Cr Multilayers
Polarized Neutrons for Condensed Matter Investigations (Jülich) (2002)

Kentzinger,E
Reflectivity and off-specular scattering of neutrons from magnetic thin films
Deutschen Neutronenstreutagung 2001 (Juelich) (2001)

Toperverg,B
Grazing Incidence Scattering with Polarized Neutrons: Examples and Applications
ANL Seminar (Argonne) (2001)

Toperverg,B
Off-specular polarized neutron scattering from magnetic fluctuations in thin films and multilayers
ICNS 2001 (Munich) (2001)

Toperverg,B
Polarized Neutron Off-specular Scattering from Magnetic Fluctuations in Films and Multilayers
NIST Seminar (Gaithersburg) (2001)

Brückel,Th
Magnetism in a new light: Applications of resonant and non-resonant magnetic x-ray diffraction
Seminar of the Solid State Physics Group (Ames Laboratory, USA) (2000)

Brückel,Th
Magnetic Scattering: Synchrotron X-rays versus Neutrons
Workshop Magnetism with Synchrotron Radiation and Neutrons (HMI, Berlin) (1999)

Brückel,Th
Komplementäre Anwendung von Neutronen- und Synchrotronröntgenstreuung bei Untersuchungen des Festkörpermagnetismus
Physikalisches Kolloquium (RWTH Aachen) (1999)

Brückel,Th
Komplementarität von Neutronen- und Synchrotronröntgenstreuung in der Festkörperforschung
Kolloquium Physikalische Institute (Technische Universität Dresden) (1999)

Conference Presentations

Kalvius,GM, Noakes,DR, Wäppling,R, Schäfer,W, Kockelmann,W, Yakinthos,JK, Kotsanidis,PA
Spin dynamics and spin disorder in frustrated $TbCo_xNi_{1-x}C_2$
9th Intern. Conference on Muon Spin Rotation/Relexation/Resonance (Williamsburg, Virginia) Talk (2002)

Kalvius,GM, Wagner,FE, Noakes,DR, Schreier,E, Wäppling,R, Zimmermann,U, Schäfer,W, Kockelmann,W, Halevy,I, Gal,J
Magnetic behavior of YFe_xAl_{12-x}
9th Intern. Conference on Muon Spin Rotation/Relexation/Resonance (Williamsburg, Virginia) Talk (2002)

Kentzinger,E, Ruecker,U, Toperverg,B, Brueckel,T
Determination of the magnetic fluctuations in an Fe/Cr/Fe trilayer exhibiting a neutron resonance state
Polarized Neutrons for Condensed Matter Investigations (Juelich) Poster (2002)

Kentzinger,E, Toperverg,B, Rücker,U, Brückel,Th
Simulation of Reflectivity and Off-Specular Scattering of Polarised Neutrons from Laterally Patterned Magnetic Multilayers
Workshop on Polarised Neutrons in Condensed Matter Investigations (FZJ, Jülich) Poster (2002)

Köbler,U, Hoser,A, Bos,J, Schäfer,W, Mueller,R, Fischer,K
On the thermodynamic universality classes of Heisenberg type magnets
Deutsche Neutronenstreutagung 2002 and The European Spallation Source (Bonn) Poster (2002)

Lemmens,P, Choi,KY, Güntherodt,G, Kageyama,H, Hiroi,Z, Schäfer,W, Geibel,C, Brenig,W, Gros,C, Valentini,R, Millet,P, Törnroos,KW, Johnsson,M, Mila,F
From singlet to Néel State - a substitution study on the spin tetrahedra system $Cu_2Te_2O_5(Br_{1-x}Cl_x)_2$
DPG Frühjahrstagung (Regensburg) Talk (2002)

Rücker,U, Kentzinger,E, Toperverg,B, Ziegenhagen,N, Brückel,Th
Off-specular scattering from magnetic structures measured with full polarization analysis using HADAS@DIDO, Jülich
REFILL-Workshop (Grenoble) Poster (2002)

Rücker,U, Toperverg,B, Kentzinger,E, Brückel,Th
Resonant states in a ferromagnetic quantum well for neutrons
ESS-Konferenz (Bonn) Poster (2002)

Schäfer,W, Buschow,KHJ
Neutron diffraction on intermetallic Er_5Mg_{24} and Tm_5Mg_{24}
8th European Powder Diffraction Conference (Uppsala) Poster (2002)

Siouris,IM, Schäfer,W
Coexistence of spin glass states in the antiferromagnetic $Tb_2(Ag,In)_3$ and $Tb_2(Cu,In)_3$ systems
Deutsche Neutronenstreutagung 2002 and The European Spallation Source (Bonn) Poster (2002)

Siouris,IM, Semitelou,IP, Yakinthos,JK, Schäfer,W
Presence of a spinglass state in antiferromagnetic Tb_2CuIn_3
8th European Powder Diffraction Conference (Uppsala) Poster (2002)

Su,Y, Istomin,K, Schweika,W, Fattah,A, Foucart,P, Meuffels,P, Brueckel Th
Polarization analysis of diffuse neutron scattering in lightly doped $La_{1-x}Sr_xMnO_3$
European Conference ESS (Bonn, Germany) Poster (2002)

Su,Y, Schweika,W, Istomin,K, Fattah,A, Foucart,P, Brueckel,Th
Investigation of lightly doped $La_{1-x}Sr_xMnO_3$ single crystals with polarized neutrons and synchrotron X-rays
Polarized Neutrons in Condensed Matter Investigations (PNCMI) (Juelich, Germany) Poster (2002)

Voigt,J, Kentzinger,E
Untersuchung magnetischer Übergitter mit Neutronen und Synchrotronröntgenstrahlung
Workshop Magnetismus und Streumethoden (Jülich) Talk (2002)

Voigt,J, Kentzinger,E, Rücker,U, Schweika,W, Brückel,Th
Magnetic Structures and Phase Transitions in Er/Tb Superlattices
ESS-Konferenz (Bonn) Poster (2002)

Ziegenhagen,N, Rücker,U, Kentzinger,E, Lehmann,R, vanderHart,A, Toperverg,B, Brückel, Th
Magnetic Properties of Laterally Structured Fe/Cr Multilayers
ESS-Konferenz (Bonn) Poster (2002)

Köbler,U, Hoser,A, Fischer,K, Beyss,M
The impact of fourth-order exchange interactions on the thermal variation of the order parameter
ICNS Conference (München) Poster (2001)
Köbler,U, Hoser,A, Kawakami,M
Beobachtung eines Bloch Exponent von 5/2 am Antiferromagneten MnF_2 mit S=5/2 and axialer Austauschanisotropie
Deutsche Neutronenstreutagung (Jülich) Poster (2001)

Massalovitch,S, Ioffe,A, Küssel,E, Schlapp,M, Brückel,Th
Development of the large-area 2D neutron detector based on the imaging plate
Deutsche Neutronenstreutagung (FZJ, Jülich) Poster (2001)

Massalovitch,S, Ioffe,A, Küssel,E, Schlapp,M, vonSeggern,H, Brückel,Th
Development of neutron image plate for low flux measurements
ICNS-Konferenz (München) Poster (2001)

Rücker,U
Untersuchung lateral strukturierter magnetischer Vielfachschichten
Workshop Magnetismus und Streumethoden, HMI (Berlin) Talk (2001)

Rücker,U, Kentzinger,E, Brückel,Th
Spin-split diffuse scattering under grazing incidence from polarizing supermirrors
Deutsche Neutronenstreutagung (Jülich) Poster (2001)

Rücker,U, Kentzinger,E, Toperverg,B, Ott,F, Brückel,Th
Spindependent diffuse scattering from polarizing supermirrors
ICNS 2001 (Munich) Poster (2001)

Schlapp,M, vonSeggern,H, Massalovitch,S, Ioffe,A, Conrad,H, Brückel,Th
Materials for neutron image plates with low gamma sensitivity
ICNS-Konferenz (München) Poster (2001)

Siouris,I, Semitelou,JP, Yakinthos,JK, Schäfer,W, Arons,RR
Structure and magnetic Structure states of the rare earth intermetallics R_2AgIn_3 and R_2CuIn_3
Deutsche Neutronenstreutagung (Jülich) Poster (2001)

Sosnowska,I, Kockelmann,W, Schäfer,W, Barbier,B, Troyanchuk,IO
Influence of Mn doping on the crystal structure and magnetic order of $BiFeO_3$ - preliminary powder diffraction results
9. Jahrestagung der Deutschen Gesellschaft für Kristallographie (Bayreuth) Poster (2001)

Sosnowska,I, Kockelmann,W, Schäfer,W, Troyanchuk,IO
Influence of Mn doping on the crystal structure and magnetic order of $BiFeO_3$
Deutsche Neutronenstreutagung (Jülich) Poster (2001)

Sosnowska,I, Schäfer,W, Kockelmann,W, Barbier,B, Andersen,KA, Troyanchuk,IO
Crystal structure and spiral magnetic ordering of $BiFeO_3$ doped with manganese
ICNS 2001 (Munich) Poster (2001)

Toperverg,B, Kentzinger,E, Rücker,U, Brückel,Th
Specular reflection and off-specular scattering of polarized neutrons from magnetic multilayers
Deutsche Neutronenstreutagung (FZJ, Jülich) Poster (2001)

Voigt,J, Kentzinger,E, Rücker,U, Schweika,W, Brückel,Th, Schmidt,W, Ohl, M Hupfeld, D
Proximity effects in Er/Tb superlattices: How Neutrons and X-Rays complement each other
International Conference on Neutron Scattering (München) Poster (2001)

Voigt,J, Schmidt,W, Ohl,M, Brückel,Th
Magnetische Ordnung in Erbium/Terbium-Schichtsystemen
Deutsche Neutronenstreutagung (FZJ, Jülich) Poster (2001)

Soft Condensed Matter, Liquids, Glasses

Publications

Dhont,JKG, Lettinga,MP, Dogic,Z, Lenstra,TAJ, Wang,H, Rathgeber,S, Carletto P, Willner L, Frielinghaus H, Lindner P
Shear-banding and microstructures of colloids in shear flow
Faraday Discuss. **123**, 157 (in press)

Endo,H, Cölfen,H, Schwahn,D
Analysis of Polymer Templates in Calcium Carbonate - SANS Investigation Applying Contrast Variation
J. Appl. Cryst. (in press)

Keiper,JS, Simhan,R, DeSimone,JM, Lynn,GW, Wignall,GD, Melnichenko,YB
Self-assembly of phosphate fluorosurfactants in carbon dioxide
(in press)

Melnichenko,YB, Wignall,GD, Schwahn,D
Universal Behavior of Polymers in Blends, Solutions and Supercritical Mixtures and Implications for the Validity of the random Phase Approximation
Fluid Phase Equilibria (in press)

Mendes,O, Viale,S, Santin,O, Heinrich,M, Picken,SJ
A small-angle neutron scattering investigation of rigid polyelectrolytes under shear
J. Appl Cryst (in press)

Pipich,V, Schwahn,D, Willner,L
Observation of a Double Critical Point and Lifshitz Line in an A/BA-B three component Homopolymer/Diblock Copolymer Mixture
J. Appl. Cryst (in press)

Radulescu,A, Schwahn,D, Richter,D, Fetters,LJ
Co-crystallization of Poly(ethylene-butene) Copolymers and Paraffin Molecules in Decane Solution studied by SANS
J. Appl. Cryst. (in press)

Richter,D
Viscoelasticity and microscopic motion in dense polymer systems
Diffusion in Condensed Matter, 2. Auflage, Eds. P. Heitjans and J. Kärger (in press)

Schwahn,D
Small Angle Neutron Scattering in Polymer Blends
in George P. Simon (Ed.): Polymer Characterization Techniques and their Applications to Blends, ACS Books, (in press)

Arbe,A, Colmenero,J, Alvarez,F, Monkenbusch,M, Richter,D, Farago,B, Frick,B
On the Nature of the non-Gaussianity in the alpha-Relaxation of Glass Forming Polyisopren
Physical Review Letters **89**, 245701 (2002)

Arbe,A, Colmenero,J, Richter,D
Polymer dynamics by dielectric spectroscopy and neutron scattering - a comparison
in Broadband Dielectric Spectroscopy, Eds. F. Kremer & A. Schönhals, ISBN 3-540-43407-0 (2002)

Arbe,A, Moral,A, Alegria,A, Colmenero,J, Pyckhout-Hintzen,W, Richter,D, Farago,B
Heterogeneous Structure of Poly(vinyl chloride) as the Origin of Anomalous Dynamical Behavior
Journal of Chemical Physics **117**, 1336 (2002)

Ashbaugh,HS, Radulescu,A, Prud'homme,RK, Schwahn,D, Richter,D, Fetters,LJ
Interaction of paraffin wax gels with random crystalline/amorphous hydrocarbon copolymers
Macromolecules **35**, 7044 (2002)

Botti,A, Pyckhout-Hintzen,W, Richter,D, Straube,E
Filled elastomers: polymer chain and filler characterization by a SANS-SAXS approach
Physica A **304**, 230-234 (2002)

Botti,A, Pyckhout-Hintzen,W, Richter,D, Straube,E
An in situ rheological and SANS investigation of the crosslinking reaction of polyisoprene and dicumyl peroxide
Acta Rheologica **41**, 475 (2002)

DeSimone,JM, Keiper,JS, Simhan,R, Wignall,GD, Melnichenko,YB, Frielinghaus,H
New phosphate fluorosurfactants for carbon dioxide
J. Am. Chem. Soc. **124**, 1834 (2002)

Endo,H, Allgaier,J, Mihailescu,M, Monkenbusch,M, Gompper,G, Richter,D, Jakobs,B, Sottmann,T, Strey,R
Amphiphilic block copolymers as efficiency boosters in microemulsions: A SANS investigation of the role of polymers
Appl. Phys. A **74**, 392-395 (2002)

Fytas,G,Nothofer,G,Scherf,U,Vlassopolous,D, Meier,G
Structure and Dynamics of Nondilute Polyfluorene Solutions
Macromolecules **35**, 481-488 (2002)

Farago,B, Arbe,A, Colmenero,J, Faust,R, Buchenau,U, Richter,D
Intermediate Length Scale Dynamics of Polyisobutylene
Physical Review E **65**, 051803 (2002)

Fetters,LJ, Lohse,DJ, Garcia-Franco,C, Brant,P, Richter,D
Prediction of melt state polyolefin rheological properties: the unsuspected role of the average molecular weight per backbone bond
Macromolecules **35**, 10096-10101 (2002)

Frielinghaus,H, Schwahn,D, Willner,L, Freed,KF
Small Angle Neutron Scattering Studies of a Polybutadiene/Polystyrene Blend with Small Additions of Ortho-di-Chlorine-Benzene for varying Temperatures and Pressures Fields; Part II: Phase Boundaries and Flory-Huggins Parameter
J. Chem. Phys. **116,** 2241 (2002)

Gohr,K, Schaertl,W, Willner,L, Pyckhout-Hintzen,W
SANS investigatons of PS-PB block copolymer micelles in a short chain PB homopolymer matrix
Macromolecules **35**, 9110 (2002)

Hardy,C, Bates,FS, Kim,MH, Wignall,GD
Model ABC Triblock Copolymers and Blends Near the Order-Disorder Transition
Macromolecules **35**, 3189 (2002)

Heinrich,M, Pyckhout-Hintzen,W, Allgaier,A, Richter,D, Straube,E, Read,DJ, McLeish,TCB, Groves,D, Blackwell,RJ, Wiedenmann,A
Arm relaxation in deformed H-polymers in elongational flow by SANS
Macromolecules **35**, 6650-6664 (2002)

Heinrich,M, Pyckhout-Hintzen,W, Richter,D, Straube,E, Wiedenmann,A
Relaxation of entangled model H-shaped polymers: a SANS investigation
Applied Physics A **74,** S380-S382 (2002)

Iatrou,H, Hadjichristidis,N, Meier,G, Frielinghaus,H, Monkenbusch,M
Synthesis and Characterization of Model Cyclic Block Copolymers of Styrene and Butadiene. Comparison of the Aggregation Phenomena in Selective Solvents with Linear Diblock and Triblock Analogues
Macromolecules **35**, 5426 (2002)

Jeng,U, Lin,T-L, Hu,Y, Chang,T-S, Canteenwala,T, Chiang,L-Y, H Frielinghaus
Study on Aqueous Mixtures of Fullerene-Based Star Ionomers and Sodium Dodecyl Sulfate
J. Phys. Chem. A **106**, 12209-12213 (2002)

Kahle,S, Willner,L, Monkenbusch,M, Richter,D, Arbe,A, Colmenero,J, Frick,B
Neutron Scattering on Partially Deuterated Polybutadiene
Applied Physics A **74**, 371 (2002)

Kawabata,Y, Nagao,M, Seto,H, Komura,S, Takeda,T, Schwahn,D
Neutron Spin Echo Studies on the Effects of Temperature and Pressure in a Ternary Microemulsion.
Applied Physics **74 [Suppl.]**, S534 (2002)

Keiper,JS, Simhan,R, DeSimone,JM, Wignall,GD, Melnichenko,YB, Frielinghaus,H
New Phosphate Fluorosurfactants for Carbon Dioxide
J. Am. Chem. Soc. **124**, 1834 (2002)

Koizumi,S, Monkenbusch,M, Richter,D, Schwahn,D, Farago,B, Annaka,M
Frozen Concentration Fluctuations in a Poly(N-isopropyl acrylamide) Gel Studied by Neutron Spin Echo and Neutron Small-angle Sacttering
Applied Physics A [Suppl.] **74**, S399 (2002)

Koizumi,S, Monkenbusch,M, Richter,D, Schwahn,D, Farago,B, Annaka,M
Observation of Concentration Fluctuations in Polymer Gels Performed by Neutron Spin Echo
Journal of Neutron Research **10**, 155 (2002)

Krishnamoorti,R, Graesseley,WW, Zirkel,A, Richter,D, Hadjirchristidis,N, Fetters,LJ, Lohse,DJ
Melt state polymer chain dimensions as a function of temperature
J. Polymer Science **B40**, 1768-1776 (2002)

Melnichenko,YB, Wignall,GD, Schwahn,D
Universal Aspects of Macromolecules in Polymer Blends, Solutions, and Supercritical Mixtures
Phys. Rev E **65**, 061802 (2002)

Menge,H, Pyckhout-Hintzen,W, Meier,G, Straube,E
Butadiene rubbers: Topological constraints and microscopic deformations by mechanical and small angle neutron scattering investigation
Polymer Bulletin **48**, 183 (2002)

Mihailescu,M, Monkenbusch,M, Allgaier,J, Frielinghaus,H, Richter,D, Jakobs,B, Sottmann,T
Neutron scattering study on the structure and dynamics of oriented lamellar phase microemulsions
Phys. Rev. E **66**, 041504-1 (2002)

Montes,H, Monkenbusch,M, Willner,L, Rathgeber,S, Richter,D, Fetters,LJ, Farago B
Direct observation of domain wall excitations in symmetric diblock copolymer melts at and above the order-disorder transition
Europhys. Lett. **58**, 389 (2002)

Moral,A, Arbe,A, Alegria,A, Colmenero,J, Pyckhout-Hintzen,W, Richter,D, Farago B, Frick B
Heterogenous structure of poly(vinylchloride) as the origin of anomalous dynamical behaviour
J. Chem Phys. **117**, 1336 (2002)

Pipich,V, Schwahn,D, Willner,L
Complex phase behaviour near the Lifshitz line in a ternary polymer blend
Applied Physics A **74**, S345 (2002)

Radulescu,A, Schwahn,D, Fetters,L, Richter,D
Crystallization of paraffin in decane in the presence of PEB-7 ethylene-butene random copolymers
Applied Physics A **74**, S411 (2002)

Rathgeber,S, Monkenbusch,M, Kreitschmann,M, Urban,V, Brulet,A
Dynamics of Star-burst Dendrimers in Solution in Relation to their Structural Properties
J. Chem. Phys. **117**, 4047 (2002)

Richter,D, Monkenbusch,M, Willner,L, Wischnewski,A, Arbe,A, Colmenero,J
Experimental Aspects of Polymer Dynamics
Polymer International **51**, 1211 (2002)

Schwahn,D, Frielinghaus,H, Willner,L
Small Angle Neutron Scattering Studies of a Polybutadiene/Polystyrene Blend with small Additions of Ortho-di-Chlorine-Benzene for varying Temperatures and Pressures Fields; Part I: Mean Field to 3D-Ising Crossover Behavior.
J. Chem. Phys. **116,** 2229 (2002)

Schwahn,D, Richter,D, Lin,M, Fetters,LJ
The Co-crystallisation of a Poly(ethylene-butene) Random Copolymer with C_{24} in n-Decane
Macromolecules **35**, 3762 (2002)

Schwahn,D, Richter,D, Wright,PJ, Symon,C, Fetters,LJ
Self-Assembling Behavior in Decane Solution of Potential Wax Crystal Nucleators Based on Poly(co-olefins)
Macromolecules **35**, 861 (2002)

Schwahn,D, Willner,L
Phase behaviour of binary polybutadiene copolymer mixtures as an examle of weakly interacting polymers
Applied Physics A **74**, S358 (2002)

Schwahn,D, Willner,L
Phase Behavior and Flory-Huggins Parameter of Binary Polybutadiene Copolymer Mixture of different Vinyl Content and Molar Volume
Macromolecules **35,** 239 (2002)

Senapati,S, Keiper,JS, DeSimone,JM, Wignall,GD, Melnichenko,YB, Frielinghaus,H, Berkowitz, ML
Structure of Phosphate Fluorosurfactant Based Reverse Micelles in Supercritical Carbon Dioxide
Langmuir **18**, 7371 (2002)

Stellbrink,J, Allgaier,J, Richter,D, Moussaid,A, Schofield,AB, Poon,WCK, Pusey,PN, Lindner,P, Dzubiella,J, Likos,CN, Löwen,H
Partial structure factors in star/polymer colloid mixtures
Appl. Phys. A **74** [Suppl], 355 (2002)

Stellbrink,J, Allgaier,J, Willner,L, Richter,D, Slawecki,T, Fetters,LJ
Real time SANS study on head group self-assembly for lithium based anionic polymerisations
Polymer **43**, 7101-7109 (2002)

Stiakakis,E, Vlassopoulos,D, Likos,CN, Roovers,J, Meier,G
Polymer-mediated melting in ultrasoft colloidal gels
Physical Review Letters **89**, 208-302 (2002)

Stiakakis,E, Vlassopoulos,D, Loppinet,B, Roovers,J, Meier,G
Kinetic arrest of crowded soft spheres in solvents of varying quality
Physical Review E **66**, 051804 (2002)

Vass,S, Haimer,K, Meier,G, Klapper,M, Borbely,S
Small-angle neutron scattering study of poly(methyl methacrylate-sodium acrylate-methyl methacrylate) triblock copolymers in aqeous solution
Colloid Polym Sci **280**, 245-253 (2002)

Volkmer,D, Bredenkötter,B, Tellenbröker,J, Kögerler,P, Kurt,DG, Lehmann,P, Schnablegger H, Schwahn D, Piepenbrink M, Krebs B
Structure and Properties of the Dendron-Encapsulated Polyoxometalate $(C_{52}H_{60}NO_{12})12[(Mn(H_2O))_3(SbW_9O_{33})_2]$, a First Generation Dendrozyme
J. Am.Chem. Soc. **124**, 10489 (2002)

Yang,BS, Lal,J, Mihailescu,M, Monkenbusch,M, Richter,D, Huang,JS, Kohn J,Russel WB, Prud'homme RK
Neutron spin-echo study of dynamics of hydrophobically modified polymer-doped surfactant bilayers
Langmuir **18**, 6 (2002)

Dzubiella,J, Jusufi,A, Likos,CN, vonFerber,C, Löwen,H, Stellbrink,J, Allgaier,J, Richter,D, Schofield,AB, Smith,PA, Poon,WCK, Pusey,PN
Effect of amphiphilic block copolymers on the structure and phase behavior of oil–water-surfactant mixtures
Phys. Rev. E **64**, 010401-1 (2001)

Edelmann,K, Janich,M, Hoinkis,E, Pyckhout-Hintzen,W, Hoering,S
The aggregation behaviour of Poly(ethylene oxide)-Poly(methyl methacrylate) diblock copolymers in organic solvents
Macromol. Chem. Phys **202**, 1638 (2001)

Endo,H, Mihailescu,M, Monkenbusch,M, Allgaier,J, Gompper,G, Richter,D, Jakobs,B, Sottmann,T, Strey,R, Grillo,I
Effect of amphiphilic block copolymers on the structure and phase behavior of oil-water surfactant mixtures
J. Chem. Phys. **115**, 580 (2001)

Endo,H, Mihailescu,M, Monkenbusch,M, Allgaier,J, Gompper,G, Richter,D, Jakobs,B, Sottmann,T, Strey,R
Effect of amphiphilic block copolymers on the structure and phase behaviour of oil-water surfactant mixtures
J. Chem. Physics **115**, 1 (2001)

Erhardt,R, Boeker,A, Zettl,H, Pyckhout-Hintzen,W, Kaya,H, Krausch,G, Abetz,V, Mueller,A
Janus Micelles
Macromolecules **34**, 1069 (2001)

Frielinghaus,H, Schwahn,D, Dudowicz,J, Foreman,JKW, Freed,K
Application of the LCT to describe the Temperature, Pressure, and Microstructure Dependent Small Angle Neutron Scattering Experiments on Polybutadiene/ Polystyrene Blends
J. Chem. Phys. **114**, 5016 (2001)

Frielinghaus,H, Schwahn,D, Willner,L
Blends of Polybutadiene with different Vinyl Contents and Polystyrene studied with Small Angle Neutron Scattering in varying Temperature and Pressure Fields
Macromolecules **34,** 1751 (2001)

Gompper,G, Endo,H, Mihailescu,M, Allgaier,J, Monkenbusch,M, Richter,D, Jakobs,B, Sottmann,T, Strey,R
Measuring bending rigidity and spatial renormalization in bicontinuous microemulsions
Europhys. Lett. **56**, 683 (2001)

Gompper,G, Richter,D, Strey,R
Amphiphilic block copolymers in oil-water-surfactant mixtures: Efficiency boosting, structure, phase behavior and mechanism
J. of Physics: Condensed Matter **13**, 9055 (2001)

Götz,H, Ewen,B, Maschke, U, Meier,G, Monkenbusch,M
Neutron Scattering Investigations on the Statics and Dynamics of Polydimethyl- and Polyethylmethylsiloxane Melts
Macromol.Chem.Phys. **202**, 3334-3341 (2001)

Koizumi,S, Monkenbusch,M, Richter,D, Schwahn,D, Annaka,M
Frozen Concentration Fluctuations of a Poly (N-isopropyl aclyamide) Gel Decomposed by Neutron Spin Echo
J. Phys. Soc. Jpn. **70 Suppl. A**, 320-322 (2001)

Moreno,AJ, Alegria,A., Colmenero,J, Prager,M, Grimm,H, Frick,B
Methyl group dynamics in glassy toluene: a neutron scattering study
Journal of Chemical Physics **115**, 8958 (2001)

Melnichenko,Y, Wignall,GD, Schwahn,D
Universal Behavior of Polymer Molecules in Blends, Solutions, and Supercritical Fluids
Polymeric Materials **85** (2001)

Mihailescu,M, Monkenbusch,M, Endo,H, Allgaier,J, Gompper,G, Stellbrink,J, Richter D, Jakobs B, Sottmann T, Farago B
Dynamics of bicontinuous microemulsion phases with and without amphiphilic block-copolymers
J. Chem. Phys **115**, 9563 (2001)

Prabhu,VM, Muthukumar,M, Wignall,GD, Melnichenko,YB
Dimensions of Polyelectrolyte Chains and Concentration Fluctuations in Semidilute Solutions of Sodium-Polystyrene Sulphonate as Measured by Small Angle Neutron Scattering
Polymer **42**, 8935 (2001)

Richter,D
Neutrons in soft condensed matter
Conf. Proceedings ILL Millennium Symposium & European User Meeting (2001)

Richter,D, Monkenbusch,M, Arbe,A, Colmenero,J, Kahle,S, Colmenero,J
Neutron Scattering and the Glass Transition in Polymers: Present Status and Future Opportunities
Journal of Non-Crystalline Solids **287**, 286-296 (2001)

Schwahn,D, Frielinghaus,H, Mortensen,K, Almdal,K
Abnormal Pressure Dependence of the Order-Disorder Phase Boundary in (PEE;PEP)-PDMS Binary Polymer Blends and Diblock Copolymers
Macromolecules **34,** 1694 (2001)

Schwahn,D, Willner,L
Phase Behavior of Binary Polybutadiene Copolymer Mixtures with different Vinyl Content as an Example of a Blend of Weak Interacting Polymers
Polymeric Materials **85** (2001)

Smith,GD, Paul,W, Monkenbusch,M, Richter,D
On the non-Gaussianity of chain motion in unentangled polymer melts
J. Chem. Phys. **114**, 4285 (2001)

Westermann,S, Pyckhout-Hintzen,W, Richter,D, Straube,E, Egelhaaf,S, May,R
On the length scale dependence of microscopic strain by SANS
Macromolecules **34**, 2186 (2001)

Wignall,GD, Alamo,RG, Mandelkern,L, Schwahn,D
SANS Studies of Liquid-Liquid Phase Separation in Heterogeneous and Metallocene-based Linear Low Density Polyethylenes
Macromolecules **34**, 8160 (2001)

Willner,L, Poppe,A, Allgaier,J, Monkenbusch,M, Richter,D
Time-resolved SANS for the determination of unimer exchange kinetics in block copolymer micelles
Europhys. Lett. **55**, 667-673 (2001)

Abbas,B, Schwahn,D, Willner,L
Concentrated Diblock Copolymer Solutions in a Pressure Field
Physica B **276-278**, 377-378 (2000)

Allgaier,J, Stellbrink,J, Poppe,A, Willner,L, Richter,D
PEP-PEO block copolymers as a model system for micellisation in aqueous solution
ACS Symp. Ser. **765**, 21 (2000)

Botti,A, Pyckhout-Hintzen,W, Richter,D, Straube,E, Urban,V, Kohlbrecher,J
Chain deformation in filled elastomers: a SANS approach
Physica B **276-278**, 371-372 (2000)

Casagrande,M, Heldmann,C, Pawelzik,U, Meier,G, Stamm, M
Influence of Composition on the Interdiffusion of Poly(vinylacetate) Latex Particles
Progr. Colloid Polym.Sci. **115**, 128-133 (2000)

Endo,H, Allgaier,J, Gompper,G, Jakobs,B, Monkenbusch,M, Richter,D, Sottmann,T, Strey,R
Membrane decoration by amphiphilic block copolymers in bicontinuous microemulsions
Phys. Rev. Lett. **85**, 102 (2000)

Goetz,H, Maschke,U, Wagner,T, Rosenauer,C, Martin,K, Ritz,S, Ewen, B
Comparison of Different Methods for the Determination of the Molecular Mass and Molecular Mass Distribution of Poly(ethylmethylsiloxane)
Macromol. Chem. Phys. **201**, 1311 (2000)

Hoffmann,S, Willner,L, Richter,D, Arbe,A, Colmenero,J, Farago,B
On the Origin of Dynamic Heterogeneities in Miscible Polymer Blends - A Quasielastic Neutron Scattering Study
Physical Review Letters **85**, 772 (2000)

Koizumi,S, Annaka,M, Borbely,S, Schwahn,D
Fractal Structures of a Poly(N-Isopropylacrylamide) Gel studied by Small-Angle Neutron Scattering over a Q-range from 10^5 to $0.1Å^{-1}$
Physica B **276-278**, 367-368 (2000)

Kurth,DG, Lehmann,P, Volkmer,D, Müller,A, Schwahn,D
Biologically-inspired polyoxometalate-surfactant composite materials. Investigations on the structures of discrete surfactant-encapsulated clusters, monolayers, and Langmuir-Blodgett films of $DODA_{40}(NH_4)_2[(H_2O)_nMo_{132}O_{372}(CH_3CO_2)_{30}(H_2O)_{72}]$
J. Chem. Soc., Dalton Trans. 3989 (2000)

Leube,W, Monkenbusch,M, Schneiders,D, Richter,D, Adamson,D, Fetters,LJ, Dounis,P, Lovegrove,R
Wax crystal modification for fuel oils by self aggregating partially crystllizable hydrocarbon blockcopolymers
Energy and Fuels **14**, 419 (2000)

Lohse,DJ, Fetters,LJ, Richter,D
The prediction of polyolefin melt state rheological properties
Exxon Report (2000)

Mariani,P, Carsughi,F, Spinozzi,F, Romanzetti,S, Meier,G, Casadio,R, Begamini,C
Ligand-induced conformational changes in tissue transglutaminase: monte carlo analysis of small-angle scattering data
Biophysical journal **78**, 3240 (2000)

Matsuoka,H, Yamamoto,Y, Nakano,M, Endo,H, Yamaoka,H, Zorn,R, Monkenbusch,M, Richter,D, Seto,H, Kawabata,Y, Nagao,M
Neutron Spin Echo Study of the Dynamics of Polymer Micelle in Aqueous Solution
Langmuir **16**, 9177 (2000)

Meier,G, Pawelzik,U, Schweika,W, Kockelmann,W
The Static Structure Factor S(Q) of Partially Deuterated Ethyl- and Hexylmethacrylate
Physica B **276-278**, 369 (2000)

Monkenbusch,M, Schneiders,D, Richter,D, Willner,L, Leube,W, Fetters,LJ, Huang,JS, Lin,M
Aggregation behaviour of PE-PEP copolymers and the winterization of diesel fuel
Physica B **276-278**, 941 (2000)

Mortensen,K, Schwahn,D, Frielinghaus,H, Almdal,K
Lifshitz Critical Line in the Ternary Mixture of Homopolymer Blend and Diblock Copolymer, studied by Small-Angle Neutron Scattering
J. Appl. Cryst. **33**, 686 (2000)

Pyckhout-Hintzen,W, Westermann,S, Botti,A, Richter,E, Straube,E
Chain deformation in unfilled and filled polymer networks: a SANS approach
Notizario Neutroni e Luce di Sincrotone **5**, 34 (2000)

Richter,D
Neutron scattering in polymer physics
Physica B **276-278**, 22 (2000)

Richter,D
Polymer dynamics by neutron spin echo spectroscopy
Article in Scattering in Polymeric and Colloidal Systems, Eds. Wyn Brown and Kell Mortensen ISBN 90-5699-260-0, 535 (2000)

Richter,D, Monkenbusch,M, Pyckhout-Hintzen,W, Arbe,A, Colmenero,J
Response to comment on From Rouse dynamics to local relaxation: A neutron spin echo on polyisobutylene melts
J. Chem. Phys. **113**, 11398 (2000)

Schwahn,D
Ginzburg Number and Phase Behavior of Binary Polymer Blends in Pressure Fields
Macromol. Symp. **149**, 43 (2000)

Schwahn,D, Mortensen,K
Thermal Composition Fluctuations in Polymer Blends Studied with Small Angle Neutron Scattering
in W. Brown and K. Mortensen (Ed.): Scattering in Polymeric and Colloidal Systems, Gordon and Breach Publishers, Chapter 8 (2000)

Schwahn,D, Mortensen,K, Frielinghaus,H, Almdal,K
3D-Ising and Lifshitz Critical Behavior in a Mixture of a Polymer Blend and a Corresponding Diblock Copolymer
Physica B **276-278**, 353 (2000)

Schwahn,D, Mortensen,K, Frielinghaus,H, Almdal,K, Kielhorn,L
Thermal Composition Fluctuations near the Isotropic Lifshitz Critical Point in a Ternary Mixture of a Homopolymer Blend and Diblock Copolymer
J. Chem. Phys. **112**, 5454-5472 (2000)

Smith,GD, Paul,W, Monkenbusch,M, Richter,D
A comparison of neutron scattering studies and computer simulations of polymer melts
Chem. Phys. **261**, 61 (2000)

Stellbrink,J, Allgaier,J, Monkenbusch,M, Richter,D, Lang,A, Likos,CN, Watzlawek M, Löwen H, Ehlers G, Schleger P
Neither Gaussian coils nor hard spheres: star polymers seen as ultra soft colloids
Prog. Colloid Polymer Sci. **115**, 88 (2000)

Westermann,S, Willner,L, Richter,D, Fetters,LJ
The evaluation of polyethylene chain dimensions as a function of concentration in nonodecane
Macromolecular Chemistry + Physics **201**, 500-504 (2000)

Willner,L, Poppe,A, Allgaier,J, Lindner,P, Richter,D
Micellarization of amphiphilic diblockcopolymers in water: shape transition and meanfield to scaling cross over
Europhysics Letter **51**, 628 (2000)

Arbe,A, Alegria,A, Colmenero,J, Hoffmann,S, Willner,L, Richter,D
Segmental Dynamics in Poly(vinylethylene)/Polyisoprene Miscible Blends Revisited. A Neutron Scattering and Broad Band Dielectric Spectroscopy Investigation
Macromolecules **32**, 7572 (1999)

Arbe,A, Colmenero,J, Monkenbusch,M, Richter,D
Arbe et al. reply
Phys. Rev. Lett. **82**, 1336 (1999)

Carlsson,P, Zorn,R, Andersson,D, Farago,B, Richter,D, Torrell,LM, Boerjesson,L, Jacobsson,P
The segmental dynamics of a polymer electrolyte investigated by neutron spin echo technique
The American Inst. of Physics **I-56396-811-8/99**, 607 (1999)

Casadio,R, Polverini,E, Mariani,P, Spinozzi,F, Carsughi,F, Fontana,A, Polverino de Laureto P, Matteucci G, Bergamini C
The structural basis for the regulation of tissue transglutaminase by calcium ions
Eur. J. Biochem. **262**, 672 (1999)

Cendoya,I, Alegria,A, Alberdi,JM, Colmenero,J, Grimm,H, Richter,D, Frick,B
Effect of blending on the PVME dynamics - a comparative study by means of dielectric, NMR and QENS spectroscopies
Macromolecules **32**, 4065 (1999)

Colmenero,J, Arbe,A, Alegria,A, Monkenbusch,M, Richter,D
On the origin of the non-exponential behavior of the alpha- relaxation in glass forming polymers: incoherent neutron scattering and dielectric relaxation results
J. Phys. Condensed Matter **11**, A363 (1999)

Dreja,M, Pyckhout-Hintzen,W, Tieke,B, Mays,H
Cationic Gemina surfactant with oligo(oxyethylene) spacer groups and their in the polymerization of styrene in ternary microemulsion
Langmuir **15**, 391 (1999)

Eilhard,J, Zirkel,A, Tschop,W, Hahn,O, Kremer,K, Schärpf,O, Richter,D, Buchenau,U
Spatial correlations in polycarbonates: neutron scattering and simulation
J. Chemical Physics **110**, 1819 (1999)

Fetters,LJ, Wheeler,LM, Xenidou,M, Richter,D
Modification potential for ShellvisTM star polymers
Exxon Research and Engineering Company; Proprietary Information, CR.17BU.99 (1999)

Gorski,N, Kalus,J, Schwahn,D
The Pressure Dependence of the Chemical Potential of Tretradecyldimethylaminoxid Micelles in D_2O - A SANS Study
Langmuir **15,** 8080-8085 (1999)

Gorsky,N, Kalus,J, Meier,G, Schwahn,D
The Temperature Dependence of the Chemical Potential of Tretradecyldimethylaminoxid Micelles in D_2O - A SANS Study
Langmuir **15**, 3476-3482 (1999)

Hasegawa,H, Sakamoto,N, Takeno,H, Jinnai,H, Hashimoto,T, Schwahn,D, Frielinghaus, H, Janssen, S, Imai, M, Mortensen, K
SANS Studies on Phase Behavior of Block Copolymers
J. Phys. Chem. Solids **60**, 1307-1312 (1999)

Jakobs,B, Sottmann,T, Strey,R, Allgaier,J, Willner,L, Richter,D
Amphiphilic block copolymers as efficiency boosters for microemulsions
Langmuir **15**, 6707 (1999)

Leube,W, Monkenbusch,M, Schneiders,D, Richter,D, Dounis,P, Lovergrove,R, Fetters,LJ, Symon,C
Wax-crystal modification in fuel oil by selfaggregation partially crystallizable hydro-carbon blockcoplymers
Exxon Company Report CR.1A.99 (1999)

Montes,H, Monkenbusch,M, Willner,L, Rathgeber,S, Richter,D, Fettters,LJ, Farago B
Direct Observation of Domain Wall Excitations in Symmetric Diblock Copolymer Melts at and above the Order Disorder Transition
J. Chem. Phys. **110**, 10171 (1999)

Nakano,M, Matsuoka,H, Yamaoka,H, Poppe,A, Richter,D
Sphere to rod transition of micelles formed by amphiphilic diblock copolymers of vinyl ethers in aqueous solution
Macromolecules **32**, 697 (1999)

Richter,D, Monkenbusch,M, Allgaier,J, Arbe,A, Colmenero,J, Farago,B, Cheol,B
From Rouse Dynamics to Local Relaxation - a Neutron Spin Echo Study on Polyisobutylene Melts
Journal of Chemical Physics **111**, 6107 (1999)

Richter,D, Monkenbusch,M, Arbe,A, Colmenero,J, Farago,B, Faust,R
Space Time Observation of the alpha-Process in Polymers by Quasielastic Neutron Scattering
Journal of Physics: Condensed Matter **11**, A297 (1999)

Richter,D, Monkenbusch,M, Farago,B, Schleger,P, Montes,H
Large scale motions in dense polymer systems
AIP Conference Proceedings, St Petersburg **469**, 587 (1999)

Schwahn,D, Mortensen,K, Frielinghaus,H, Almdal,K
Crossover from 3d-Ising to Isotope Lifshitz Critical Behavior in a Mixture of a Homopolymer Blend and Diblock Copolymer
Phys. Rev. Lett. **82,** 5056 (1999)

Seto,H, Kato,T, Monkenbusch,M, Takeda,T, Kawabata,Y, Nagao,M, Okuhara, D, Imai, M, Komura, S
Collective motions of a network of wormlike micelles
Journal of Physics and Chemistry of Solids **60**, 1371 (1999)

Smith,GD, Paul,W, Monkenbusch,M, Willner,L, Richter,D, Qiu,XH, Ediger MD
Molecular dynamics of a 1,4-polybutadiene melt. Comparison of experiment and simulation
Macromolecules **32**, 8857 (1999)

Stellbrink,J, Willner,L, Richter,D, Lindner,P, Fetters,LJ, Huang,JS
Self-assembling behavior of living butadienyllihium head-groups in benzene
Macromolecules **32**, 5321 (1999)

Westermann,S, Kreitschmann,M, Pyckhout-Hintzen,W, Richter,D, Straube,E, Farago,B, Goerigk,G
Matrix chain deformation in reinforced networks: a SANS approach
Macromolecules **32**, 5793 (1999)

Westermann,S, Pyckhout-Hintzen,W, Thyagarajan,P, Wosniak,D, Richter,D, Straube,E
A SANS study on thermal degradation kinetics in Polyisoprene networks
in P. Thyagarajan, F. Trouw, B. Marzec, C-K Loong (Ed.): Mat. Res. Using cold neutons at pulsed neutron sources, World Scientific Publ., Singapore, 210 (1999)

Allgaier,J, Stellbrink,J, Poppe,A, Willner,L, Richter,D
PEP-PEO block copolymers: Synthesis and micellar properties
Abs. papers ACS **216**, 258 (1998)

Arbe,A, Colmenero,J, Frick,B, Monkenbusch,M, Richter,D
Investigation of the dielectric beta-process in polyisobutylene by incoherent quasielastic neutron scattering
Macromolecules **31**, 4926 (1998)

Arbe,A, Colmenero,J, Monkenbusch,M, Richter,D
Dynamics in Glass-Forming Polymers: Homogeneous versus Heterogeneous Scenario
Physical Review Letters **81**, 590 (1998)

Dreja,M, Pyckhout-Hintzen,W, Tieke,B
Copolymerization behaviour and structure of styrene and polymerizable surfactants in three-component cationic microemulsion
Macromolecules **31**, 272 (1998)

Dux,Ch, Musa,S, Reus,V, Versmold,H, Schwahn,D, Lindner,P
Small Angle Neutron Scattering Experiments from Colloidal Dispersions at Rest and under Sheared Conditions
J. Chem. Phys. **109,** 2556-2561 (1998)

Frielinghaus,H, Abbas,B, Schwahn,D, Willner,L
Temperature and Pressure dependent Composition Fluctuations in a Polybutadiene/Polystyrene Polymer Blend and Diblock Copolymer
Europhys. Lett. **44 (5)**, 606-612 (1998)

Frielinghaus,H, Schwahn,D, Willner,L, Springer,T
Thermal Composition Fluctuations in Binary Homopolymer Mixtures as a Function of Pressure and Temperature
Physica B **241-243**, 1022-1024 (1998)

Goecking,KD, Monkenbusch,M
Neutron scattering investigation of a macroscopic single crystal of a lyotropic L_α phase
Europhys. Lett. **43**, 135 (1998)

Likos,CN, Löwen,H, Poppe,A, Willner,L, Roovers,J, Cubitt,B, Richter,D
Ordering phenomena of star polymer solutions approaching the Xi-state
Phys. Rev. E **58**, 6299 (1998)

Likos,CN, Löwen,H, Watzlawek,M, Abbas,A, Jucknischke,O, Allgaier,J, Richter,D
Star polymers viewed as ultra soft colloidal particles
Phys. Rev. Lett. **80**, 4450 (1998)

Nakano,N, Matsuoka,H, Yamaoka,H, Poppe,A, Richter,D
Micellization of Vinyl-Ether Amphiphilic Block Copolymers by Small Angle Neutron Scattering
Physica B **241-243**, 1038 (1998)

Richter,D
Visoelasticity and microscopic motion in dense polymer systems
Review article in Diffusion in Condensed Matter, Eds. J. Kärger, P. Heitjans, R. Haberlandt **ISBN 3-528-06910-4**, 176 (1998)

Richter,D, Arbe,A, Colmenero,J, Monkenbusch,M, Farago,B, Faust,R
Molecular Motions in Polyisobutylene: A Neutron Spin Echo and Dielectric Investigation
Macromolecules **31**, 1133 (1998)

Richter,D, Monkenbusch,M, Arbe,A, Colmenero,J, Farago,B
Dynamic Structure Factors due to Relaxation Processes in Glass Forming Polymers
Physica B **241-243**, 1005 (1998)

Schwahn,D, Frielinghaus,H, Mortensen,K, Almdal,K
Pressure Dependence of the Order-Disorder Transition in several Diblock Copolymers studied with SANS
Physica B **241-243**, 1029-1031 (1998)

Stellbrink,J, Abbas,B, Allgaier,J, Richter,D, Likos,CN, Löwen,H, Watzlawek M
Structure and dynamics of star polymers
Prog. Colloid Polymer Sci. **110**, 25 (1998)

Stellbrink,J, Willner,L, Jucknischke,O, Richter,D, Lindner,P, Fetters,LJ, Huang,JS
Self-assembling behavior of living polymers
Macromolecules **31**, 4189 (1998)

Westermann,S, Urban,V, Pyckhout-Hintzen,W, Richter,D, Straube,E
Comment on Lozenge contour plots in scattering from polymer networks
Phys. Rev. Lett. **80**, 5449 (1998)

Invited Talks

Clarke,N
Self Assembled Polymer Composites
High Polymer Conference (Devon, UK) (2002)

Colmenero,J
Atomic self motions and the alpha-relaxation in glass forming polymers. MD-simulations and quasielastic neutron scattering results
Juelich Soft Matter Days (Kerkrade) (2002)

Colmenero,J
Self motion and the alpha-relaxation in glass-forming polymers. Neutron Scattering Results
American Conference on Neutron Scattering (Knoxville, USA) (2002)

Kahle,S
Untersuchung der lokalen Relaxation von Polymeren mittels Neutronenstreuung
6. Labortreffen Relaxationsdynamik (Halle) (2002)

Kahle,S
Segmental Dynamics in Polyisobutylene: Comparison between Neutron Scattering and Computer Simulations
7. Labortreffen Relaxationsdynamik (Rostock) (2002)

Kahle,S
Local Dynamics in Polymers
Joint ICTP-INFM School and Workshop on Spectroscopic Investigation of the Dynamics in Disordered Systems (Trieste) (2002)

Melnichenko,YB
SANS studies of isotopically labelled polymers
Gordon Conf. on Isotopes in Biological and Chemical Sci. (Ventura, California, USA) (2002)

Melnichenko,YB
Universal aspects of macromolecules in small molecule and polymeric solvents
Mid-Atlantic Conf. on Thermodynamics (College Park, Maryland, USA) (2002)

Melnichenko,YB, Wignall,GD, Schwahn,D
On the validity of the random phase approximation in weakly and strongly interacting polymer blends
Int. Conf. on Small-Angle Neutron Scattering (Venice, Italy) (2002)

Melnichenko,YB, Wignall,GD, Schwahn,D
Universal aspects of macromolecules in polymer blends, solutions and supercritical mixtures and implications for the validity of the random phase approximation
Europ. Conf. on THermodynamic Properties (London, UK) (2002)

Monkenbusch,M, Mihailescu,M, Endo,H, Allgaier,J, Gompper,G, Stellbrink,J, Richter D, Jakobs B, Sottmann T, Farago B
Dynamics of Microemulsions from Neutron Spin-Echo Experiments
6th international Conference on Quasielastic Neutron Scattering QENS2002 (Potsdam) (2002)

Richter,D
Neutrons in soft matter science
Seminar (Fa. ExxonMobil) (2002)

Richter,D
Wax control by self-assembling polymers - a science approach
6th Int. Symp. on the Science and Technology of Polymer Assembly (Kyoto) (2002)

Richter,D
Polymer dynamics from large to small scales
XII. International Conference on Small Angle Scattering (SAS) (Venice) (2002)

Richter,D
Polymer dynamics from large to small scales
American Conference on Neutron Scattering (ACNS) (Knoxville) (2002)

Schwahn,D
Methode der Kleinwinkelstreuung mit Neutronen zur Untersuchung nano- und mesoskopischer Strukturen
Institut für Anorganische und Analytische Chemie, Johannes-Gutenberg-Universität (Mainz) (2002)

Kanaya,T, Monkenbusch,M, Watanabe,H, Nagao,M, Richter,D, Kaji,K
Dynamics of Polymer Micelles Studied by Neutron Spin Echo Technique - Breathing Mode or Zimm Mode
International Symposium Organized by ICR, Kyoto University (Uji, Kyoto, Japan) (2002)

Erhardt,R, Boeker,A, Zettl,H, Kaya,H, Pyckhout-Hintzen,W, Krausch,G, Abetz,V, Mueller,A
Superstructures of janus micelles
ACS 221:56-PMSE,Part2 (USA, 2001)

Frielinghaus,H, Byelov,D, Allgaier,J, Richter,D, Sottmann,T, Strey,R
Mikroemulsionen mit Polymerbeigaben untersucht mit Neutronenkleinwinkelstreuung
Kolloquium der physikalischen Chemie der Uni-Münster (Uni-Münster) (2001)

Frielinghaus,H, Byelov,D, Endo,H, Allgaier,J, Stellbrink,J, Richter,D, Jakobs B, Sottmann T, Strey R
Polymer boosting effect in the Droplet Phase Studied by Small Angle Neutron Scattering
Jülich Soft Matter Days (Kerkrade) (2001)

Kahle,S
Dynamic Neutron Scattering on Partially Deuterated Polybutadiene
4th Int. Discussion Meeting on Relaxations in Complex Systems (Heraklion) (2001)

Richter,D
Soft condensed matter
OECD Workshop on Large Facilities for Studying the Structure and Dynamics of Matter (Kopenhagen) (2001)

Richter,D
Neutrons in soft condensed matter
Colloquium (Univ. Bayreuth) (2001)

Richter,D
Neutrons in soft condensed matter
ILL Millennium Symposium (ILL Grenoble) (2001)

Richter,D
Wax crystal modification by Random copolymers of the PEB-n type
Seminar (Univ. of Princeton) (2001)

Richter,D
Experimental aspects of polymer dynamics
Conf. on Polymers in the Third Millennium (Montpellier) (2001)

Schwahn,D
Scattering Experiments Relevant for Polymer Research at the Neutron Guide Laboratory of the Jülich Research Center
222nd ACS National Meeting (Chicago) (2001)

Wischnewski,A
Kettendynamik in Polymerschmelzen: Grenzen des Reptationsmodells
Deutsche Neutronenstreutagung (Juelich, Germany) (2001)

Wischnewski,A, Monkenbusch,M, Willner,L, Richter,D, Farago,B, Ehlers,G, Schleger,P
NSE spectroscopy on reptating polymers
IDMRCS (Kreta) (2001)

Kahle,S
Neutron Scattering and Partial Structure Factor
Glasuebergangstreffen SFB418 (Berlin) (2000)

Monkenbusch,M, Richter,D, Wischnewski,A, Willner,L, Farago,B, Ehlers,G, Schleger P, Montes H, Fetters LJ
Dynamics of Homo- and Blockcopolymer Melts -- Recent Advances from Neutron Spin Echo-
The Nagoya COE-RCMS Conference on Materials Science and Nanotechnology (Nagoya) (2000)

Richter,D
The role of amphiphilic polymers in emulsification boosting in oil water microemulsion – a SANS and NSE study
Colloquium at the MPI für Kolloid- und Grenzflächenforschung (Potsdam) (2000)

Richter,D
The role of amphiphilic polymers in emulsification boosting in oil-water microemulsions
Conf. on Scattering Studies of Mesoscopic Scale Structure and Dynamics in Soft Matter (Messina/Italy) (2000)

Richter,D
Neutron scattering in polymer physics – recent highlights
Summer School Recent developments in neutron scattering (Les Houches/France) (2000)

Richter,D
Amphiphilic polymers as amphiphilicity boosters in microemulsion systems
219th ACS Conference (San Francisco) (2000)

Richter,D
Neutron scattering and the glass transition in polymers – Present status and future opportunities
VI Int. Workshop on Non Crystalline Solids (Bilbao) (2000)

Richter,D
Neutron scattering and the glass transition in polymers – Present status and future opportunities
Workshop "Future perspectives for understanding the unsolved problem of the glass-transition by neutron scattering and computer simulation" (San Sebastian) (2000)

Richter,D
Neutron spin echo
Workshop on Neutron Scattering in Soft Matter (Lungtan/Taiwan) (2000)

Richter,D
Polymer dynamics from local to the global scale
Workshop on "Neutron Scattering in Soft Matter" (Lungtan/Taiwan) (2000)

Richter,D
Dynamics of homo- and blockcopolymer melts – recent advances from neutron spin echo
APS March Meeting (Minneapolis) (2000)

Schwahn,D
Investigations of Polymer Blends with SANS
The Dutch Polymer Institute (Eindhoven) (2000)

Schwahn,D, Frielinghaus,H, Abbas,B, Willner,L
Temperature and Pressure Dependent Composition Fluctuations in a d-PB/PS Polymer Blend and Diblock Copolymer
2000 March Meeting of the American Physical Society (Minneapolis) (2000)

Wischnewski,A
Reptation in polymer melts - What's new ?
EPS-CMD18 (Montreux, Switzerland) (2000)
Kahle,S
Vergleich zwischen inkohaerenter Neutronenstreuung und dielektrischer Spektroskopie am Polyvinylacetat
Glasuebergangstreffen SFB418 (Rostock) (1999)

Richter,D
Neutronenstreuung in der Polymerphysik
Physikkolloquium (ETH Zürich) (1999)

Richter,D
Neutronen in der Polymerphysik
Chemisches Kolloquium (Univ. Köln) (1999)

Richter,D
Neutron scattering in polymer physics
2nd European Conference on Neutron Scattering (Budapest) (1999)

Richter,D
Neutron scattering in chemistry - chances and perspectives
IUPAC Conference (Berlin) (1999)

Richter,D
Neutron scattering on soft condensed matter
Colloquium (ETH Zürich) (1999)

Richter,D
Neutron scattering in polymer physics
2nd Spanish Symposium on Neutron Scattering (Oviedo/Spain) (1999)

Richter,D
Neutronenstreuung in der Polymerdynamik
Colloquium (Univ. Essen) (1999)

Richter,D
Random copolymers as wax crystal modifiers
Colloquium (Fa. Exxon, Annandale/USA) (1999)

Richter,D
Struktur und Dynamik von Polymeren
Colloquium (Fa. Bayer Leverkusen) (1999)

Richter,D
Neutronenspinechountersuchungen zur Dynamik von Polyisobutylen
Glasübergangstreffen (Rostock) (1999)

Richter,D
Dynamik von Polymeren
Colloquium at the University (Goettingen) (1999)

Richter,D, Monkenbusch,M, Montes,H
Neutron Spin Echo Spectroscopy on Large Scale Motions in Dense Polymer Systems - Recent Advances
3rd Int. Symposium Molecular Mobility and Order in Polymer Systems (St. Petersburg) (1999)

Schwahn,D
Phase Behaviour of a Ternary Symmetric Homopolymer/Homopolymer/Diblock Copolymer Blend studied with SANS
Department of Polymer Engineering (Brooklyn) (1999)

Schwahn,D
Phase Behaviour of a Ternary Symmetric Homopolymer/Homopolymer/Diblock Copolymer Blend studied with SANS
NIST (Washington) (1999)

Schwahn,D
Phase Behaviour of a Ternary Symmetric Homopolymer/Homopolymer/Diblock Copolymer Blend studied with SANS
Department of Polymer Engineering, University of Akron (Akron (USA)) (1999)

Schwahn,D
Phase Behaviour of Binary Polymer Blends in Pressure Fields and with small additions of a third component
European Conference on Polymer Blends (Mainz) (1999)

Schwahn,D
Crossover from 3d-Ising to Isotropic Lifshitz Critical Behaviour
APS Centennial Meeting (Atlanta) (1999)

Schwahn,D
Effect of Thermal Composition FLuctuations in a Critical Polymer Blend Mixed with a Diblock Copolymer
ORNL - Neutron Scattering Group of the Solid State Division (Oak Ridge) (1999)

Wischnewski,A
Reptation in polyethylene-melys with different molecular melts
ECNS (Budapest, Hungary) (1999)

Hasegawa,H, Sakamoto,N, Takeno,H, Jinnai,H, Hashimoto,T, Schwahn,D, Abbas, B, Frielinghaus, H, Janssen, S, Imai, M, Nagao, M, Mortensen, K
Phase Transitions of Block Copolymers
The 7th ISSP International Symposium: Frontiers in Neutron Scattering Research (Institute for Solid State Physics, The University of Tokyo, Tokyo, Japan) (1998)

Richter,D
Polymer dynamics at short and long scales
Colloquium (Univ. Kyoto) (1998)

Richter,D
Neutron Scattering in polymer research
7th ISSP International Symposium on the Frontier in Neutron Scattering Research (Tokio) (1998)

Richter,D
Polymer in solutions and bulk dynamics
Fourth European School on: Scattering Methods applied to soft condensed matter (Planneralm/Austria) (1998)

Richter,D
Polymer dynamics at short and long scales
Int. Symposium on neutron scattering and soft condensed matter (Ede Wageningen (The Netherlands)) (1998)

Richter,D
Space time observation of the alpha-process in polymers
II. Workshop on Non Equilibrium Phenomena in Supercooled Fluids, Glasses and Amorphous Materials (Pisa) (1998)

Richter,D
Polymer dynamics at short and long scales
Annual meeting of the Swedish Neutron Scattering Society (Göteborg) (1998)

Richter,D, Monkenbusch,M, Farago,B, Schleger,P, Montes,H
Large scale motions in dense polymer systems
Slow Dynamics in Complex Systems, 8th Tohwa University International Symposium (Fukuoka) (1998)

Schwahn,D
Characterization of Polymers with SANS
Association of Chemists (Miscolc (HU)) (1998)

Schwahn,D
Theory of Small Angle Scattering and Studies in Polymer Blends
Institute of Materials Science of the University of Miskolc (Miscolc (HU)) (1998)

Schwahn,D
Effect of thermal composition fluctuations in polymer blends and diblock copolymers
Research Institute for Solid State Physics, Hungarian Academy of Science (Budapest) (1998)

Schwahn,D
The Effect of high pressure fields on thermal composition fluctuations in polymer blends and diblock copolymers
National Laboratory Los Alamos (Los Alamos, New Mexico) (1998)

Schwahn,D
The Effect of Thermal Composition Fluctuations on the Thermodynamics of Polymer Blends
PMSE Symposium on Thermodynamics of Polymer Blends (Dallas, TX) (1998)

Conference Presentations

Blanchard,A, Pyckhout-Hintzen,W, Heinrich,M, Straube,E, Willner,L, Richter,D
Relaxation mechanisms in a streched linear polymer melt studied by SANS
Jülich Soft Matter Days (Kerkrade, NL) Poster (2002)

Byelov,D, Frielinghaus,H, Allgaier,J, Richter,D
SANS studies of bicontinuous microemulsions with homopolymer and diblock copolymer additions
Jülich Soft Matter Days 2002 (Kerkrade) Poster (2002)

Frielinghaus,H, Byelov,D, Allgaier,J, Richter,D
Small angle neutron scattering studies of microemulsions in the droplet phase with polymer as an efficiency booster
Jülich Soft Matter Days 2002 (Kerkrade) Poster (2002)

Heinrich,M, Pyckhout-Hintzen,W, Allgaier,J, Richter,D, Straube,E, Wiedenmann,A
Relaxation dynamics of entangled branched polymers investigated by SANS
Jülich Soft Matter Days 2002 (Kerkrade (NL)) Poster (2002)

Heinrich,M, Pyckhout-Hintzen,W, Richter,D, Straube,E, Wiedenmann,A
Time evolution of strain relaxation in a model-branched H-polymer by SANS
Deutsche Neutronenstreutagung 2002 (Bonn) Poster (2002)

Heinrich,M, Pyckhout-Hintzen,W, Richter,D, Straube,E, Wiedenmann,A
Time evolution of strain relaxation in a model-branched H-polymer by SANS
SAS2002 (Venezia (I)) Talk (2002)

Kahle,S, Monkenbusch,M, Richter,D, Ryckaert,JP, Koza,M
Local Dynamics in Polymers
ESS European Conference (Bonn) Poster (2002)

Kahle,S, Monkenbusch,M, Ryckaert,JP, Karatasos,K, Koza,M
Segmental Dynamics in Polyisobutylene: Comparison between Neutron Scattering and Computer Simulations
Juelich Soft Matter Days (Kerkrade) Poster (2002)

Lund,R, Willner,L, Monkenbusch,M, Radulescu,D, Richter,
Tuning of chain exchange kinetics and structure in PEP-PEO block copolymer micelles
Juelich Soft Matter Days (Kerkrade, The Netherlands) Poster (2002)

Lund,R, Willner,L, Radulescu,A, Richter,D
Tuning of chain exchange kinetics and structure in PEP-PEO block copolymer micelles
International Meetings: ESS European Conference, The European Spallation Source- Satellite Meetings 16-17 May 2002 (Bonn, Germany) Poster (2002)

Monkenbusch,M
Segmental dynamics and confinement in polymer melts
Jülich Soft Matter Days 2002 (Kerkrade) Talk (2002)

Monkenbusch,M, Mihailescu,M, Allgaier,J, Richter,D, Jakobs,B, Sottmann,T, Yang BS, Prud'homme RK, Lal J
Neutron Spin Echo Study on the Modification of Surfactant Membrane Properties Due to Polymer Addition
American Conference on Neutron Scattering ACNS 23-27.6. 2002 (Knoxville) Talk (2002)

Niu,A, Stellbrink,J, Allgaier,J, Willner,L, Richter,D, Fetters,LJ
Real-time SANS and 1H-NMR studies during "living" anionic polymerisation of Butadiene in hydrocarbon media
ESS European Conference (Bonn, Germany) Poster (2002)

Niu,A, Stellbrink,J, Allgaier,J, Willner,L, Richter,D, Fetters,LJ
Real-time SANS and 1H-NMR studies during "living" anionic polymerisation of Butadiene in hydrocarbon media
Soft Matter Days 2002 (Kerkrade, Holland) Poster (2002)

Radulescu,A, Schwahn,D, Richter,D, Fetters,LJ
Co-crystallization of poly(ethylene-butene) copolymers and paraffin molecules in decane studied with SANS
Small Angle Scattering Conference SAS2002 (Venice, Italy) Poster (2002)

Rathgeber,S, Pakula,T, Wilk,A, Matyjaszewski,K
Regular branched Macromolecules: Structure of Bottlebrush Polymers in Solution
XII International Conference on Small-Angle Scattering (Venice, Italy) Talk (2002)

Byelov,D, Frielinghaus,H, Endo,H, Allgaier,J, Richter,D
Polymer anti boosting. A small angle neutron scattering study of the bicontinuous microemulsion.
Jülich Soft Matter Days 2001 (Kerkrade) Poster (2001)

Byelov,D, Frielinghaus,H, Endo,H, Allgaier,J, Richter,D
Polymer anti boosting. A small angle neutron scattering study of the bicontinuous microemulsion
Int. Summerschool Fundamental Problems in Statistical Physics X (Odenthal-Altenberg) Poster (2001)

Frielinghaus,H, Endo,H, Allgaier,J, Richter,D, Jakobs,B, Sottmann,T, Strey R
Polymer boosting effect in der Tröpfchenphase - eine Studie mit Neutronenkleinwinkelstreuung
Würzburger Tagung Fortschritte für Wasch- und Reinigungsmittel (Würzburg) Poster (2001)

Heinrich,M, Pyckhout-Hintzen,W, Richter,D, Straube,E, Wiedenmann,A
Relaxation of entangled model H-shaped polymers: a SANS investigation
ICNS 2001 (München) Poster (2001)

Heinrich,M, Pyckhout-Hintzen,W, Richter,D, Straube,E, Wiedenmann,A
SANS investigations of relaxation dynamics of entangled model H-polymers
Deutsche Neutronenstreutagung 2001 (Jülich (D)) Poster (2001)

Kahle,S, Willner,L, Monkenbusch,M, Richter,D, Arbe,A, Colmenero,J, Frick,B
Dynamic Neutron Scattering on Partially Deuterated Polybutadiene
International Conference on Neutron Scattering (Muenchen) Poster (2001)

Kahle,S, Willner,L, Monkenbusch,M, Richter,D, Arbe,A, Colmenero,J, Frick,B
Dynamic Neutron Scattering on Partially Deuterated Polybutadiene
ILL Millennium Symposium (Grenoble) Poster (2001)

Kahle,S, Willner,L, Monkenbusch,M, Richter,D, Arbe,A, Colmenero,J, Frick,B
Dynamische Neutronenstreuung an partiell deuteriertem Polybutadien
Deutsche Neutronenstreutagung (Juelich) Poster (2001)

Melnichenko,YB, Wignall,GD, Schwahn,D
Universal aspects of macromolecules in polymer blends, solutions, and supercritical mixtures, and implications for the validity of the RPA
222nd ACS National Meeting (Chicago, Illinois, USA) Talk (2001)

Mihailescu,M, Allgaier,J, Monkenbusch,M, Richter,D
Dynamics of bicontinuous phase microemulsions with amphiphilic block-copolymer
Deutsche Neutronenstreutagung (Jülich) Poster (2001)

Mihailescu,M, Allgaier,J, Monkenbusch,M, Richter,D
Structural and dynamical investigation of mixed amphiphilic membranes. A combined SANS-NSE study
ICNS (Munich) Poster (2001)

Schwahn,D
Phase Behaviour of Binary Polybutadiene Copolymer Mixtures as an Example of Weakly Interacting Polymers
Jülich Soft Matter Days (Kerkrade (NL)) Talk (2001)

Schwahn,D
Phase Behaviour of Binary Polybutadiene Copolymer Mixtures as an Example of Weakly Interacting Polymers
ICNS 2001 (Munich) Talk (2001)

Schwahn,D
Phase Behaviour of weakly interacting binary Polybutadiene Copolymer mixtures with different Vinyl Content
222nd ACS National Meeting (Chicago) Talk (2001)

Wischnewski,A, Willner,L, Monkenbusch,M, Richter,D, Farago,B, Ehlers,G, Schleger,P
Constraints of motion in polymer melts: coherent and incoherent scattering analyzed by NSE
ICNS (Munich, Germany) Talk (2001)

Transport Processes

Publications

Skripov,AV, Soloninin,AV, Sibirtsev,DS, Buzlukov,AL, Stepanov,AP, Balbach,JJ, Conradi M S, Barnes R G, Hempelmann R
^{45}Sc NMR and high-resolution quasielastic neutron scattering studies of localized H(D) motion in alpha-$ScH_x(D_x)$
Phys. Rev. B **66**, 054306 (2002)

Dzheparov,F, Gul'ko,A, Heitjans,P, L'vov,D, Schirmer,A, Shestopal,V, Stepanov
Spin dynamics and beta-NMR after polarized neutrons capture
Physica B **297**, 288-292 (2001)

Skripov,AV, Combet,J, Grimm,H, Hempelmann,R, Kozhanov,VN
Quasielastic neutron scattering study of H motion in the hydrogen-stabilized C15-type phases $HfTi_2H_x$ and $ZrTi_2H_x$
J. Phys.: Condens. Matter **12**, 3313 (2000)

Skripov,AV, Pionke,M, Randl,O, Hempelmann,R
Quasielastic neutron scattering study of hydrogen motion in
J. Phys.: Condens. Matter **11**, 1489 (1999)

Stockmeyer,R
Diffusive motion of water molecules in harmotome studied by neutron scattering
Berichte der Bunsen-Gesellschaft
Physical Chemistry Chemical Physics
102, 623-628 (1998)

Biology

Publications

Schwahn,D, Balz,M, Bartz,M, Fomenko,A, Tremel,W
Nucleation and Growth of $CaCO_3$ Minerals on Biomimetic Templates studied by Small Angle Neutron Scattering
J. Appl. Cryst. (in press)

Grimm,H, Sokolov,AP, Dianoux,AJ
Relaxation dynamics in dry and humid DNA
Applied Physics A **74**, S1248 (2002)

Sokolov,AP, Grimm,H, Kisliuk,A, Dianoux,AJ
Slow Relaxation Process in DNA
J.Biological Physics **27**, 313 (2002)

Sokolov,AP, Grimm,H, Kisliuk,A, Dianoux,AJ
Slow relaxation process in DNA at different levels of hydration
J. Biol. Phys. **27**, 313 (2001)

Winter,R, Czeslik,C
Pressure effects on the structure of lyotropic lipid mesophases and model biomembrane systems
Zeitschrift für Kristallographie **215**, 454-474 (2000)

Johnson,MR, Prager,M, Grimm,H, Neumann,MA, Kearley,GJ, Wilson,CC
Methyl group dynamics in paracetamol and acetanilide: probing the static properties of intermolecular hydrogen bonds formed by peptide groups
Chem. Phys. **244**, 49 (1999)

Winter,R, Gabke,A, Czeslik,C, Pfeifer,P
Power-law fluctuations in phase-separated lipid membranes
Physical Review E **60**, 7354-7359 (1999)

Invited Talks

Schwahn,D
Grundlagen der Neutronenbeugung im Kleinwinkelbereich
Workshop Grundlegende Aspekte der Biomineralisation (Bochum) (2002)

Conference Presentations

Schwahn,D
Nucleation and Growth of $CaCO_3$ Minerals on Biomimetic Templates studied by SANS
XII International Conference on Small-Angle Scattering (Venice) Talk (2002)

Schwahn,D
Untersuchungen zur Keimbildung und dem Kristallwachstum von $CaCO_3$ in wäßriger Lösung an biomimetisch strukturierten Grenzflächen
1. Bereichskolloquium Prinzipien der Biomineralisation (Bonn-Röttgen) Talk (2002)

Geology, Archaeology

Publications

Pleuger,J, Hundenborn,R, Kremer,K, Babinka,S, Jansen,E, Froitzheim,N
Structural evolution of the Adula nappe, Misox zone, and Tambo nappe in the San Bernardino area: Constraints for the exhumation of the Adula eclogites
in: Mitteilungen der Österreichischen Geologischen Gesellschaft -Sonderband über die Alpen-, Österreichische Geologische Gesellschaft (in press)

Siemes,H, Klingenberg,B, Rybacki,E, Naumann,M, Schäfer,W, Jansen,E, Rosière,CA
Texture, microstructure, and strength of hematite ores experimentally deformed in the temperature range 600° to 1100°C and at strain rates between 10^{-4} and 10^{-6} s^{-1}
J. Structural Geology (in press)

Artioli,G, Kockelmann,W, Magerl,A, Mezei,F, Rinaldi,R, Schäfer,W, Schofield,PF, Zoppi,M
Cultural Heritage: Artefacts and Materials
in D. Richter (Ed.): The ESS-Project, New Science and Technology for the 21st Century, Vol.II, ESS Council, 6-47 (2002)

Pleuger,J, Jansen,E, Schäfer,W, Oesterling,N, Froitzheim,N
Neutron texture study of natural gneiss mylonites affected by two phases of deformation
Applied Physics A **74**, 1058 (2002)

Rinaldi,R, Artioli,G, Dove,MT, Schäfer,W, Schofield,PF, Winkler,B
Mineral Sciences, Earth Sciences, Environment and Cultural Heritage
in D. Richter (Ed.): The ESS-Project, New Science and Technology for the 21st Century, Vol. II, ESS Council, 4-89 (2002)

Schäfer,W
Neutron diffraction applied to geological texture and residual stress analysis
European Journal of Mineralogy **14**, 263 (2002)

Froitzheim,N, Pleuger,J, Hundenborn,R, Kremer,K, Babinka,S, Jansen,E
Constraints on the exhumation of the Adula nappe (Part 1): A top-north mega-shear zone in the roof of the nappe
Geol. Paläont. Mitt. Innsbruck **25**, 90 (2001)

Rinaldi,R, Artioli,G, Dove,MT, Schäfer,W, Schofield,PF, Winkler,B
Neutron Scattering in Mineral Science, Earth Science, and related fields with the European Spallation Source
in D. Richter (Ed.): Progress Report: ESS-SAC/ENSA Workshop on Scientific Trends in Condensed Matter, Engelberg, Schweiz, 91 (2001)

Siemes,H, Klingenberg,B, Jansen,E, Schäfer,W, Dresen,G, Rybacki,E, Naumann,M
Textures of experimentally deformed hematite ores with magnetite and wuestite
in: Electronic Proceedings (CD-ROM) of the 2001 Annual Conference of the International Association for Mathematical Geology, Cancun, Mexico, (2001)

Jansen,E, Bauer,W, Schäfer,W
Neutron diffraction pole figures of geological anorthosite textures
Physica B **276-278**, 948 (2000)

Jansen,E, Schäfer,W, Kirfel,A
The Jülich neutron diffractometer and data processing in rock texture investigation
Journal of Structural Geology **22**, 1559 (2000)

Siemes,H, Rosière,CA, Hackspacher,P, Schäfer,W, Jansen,E
Defocussing correction of X-ray pole figures by means of neutron pole figure measurements
Textures and Microstructures **34**, 55 (2000)

Ghildilay,H, Jansen,E, Kirfel,A
Volume texture of a deformed quartite observed with U-stage microscopy and neutron diffractometry
Textures and Microstructures **31**, 239 (1999)

Conference Presentations

Froitzheim,N, Nagel,Th, Pleuger,J, Hundenborn,R, Jansen,E
Zwei Subduktionszonen und der Aufstieg der Adula-Eklogite
9. Symposium Tektonik - Strukturgeologie - Kristallingeologie (Erlangen) Talk (2002)

Kurz,W, Froitzheim,N, Jansen,E, Schäfer,W
Neutron texture study of eclogite rocks from the Alps
ESS European Conference (Bonn) Poster (2002)

Rinaldi,R, Artioli,G, Kockelmann,W, Schäfer,W, Schofield,PF, Zoppi,M, Magerl,A
Cultural Heritage: Artefacts and Materials
Scientific and Technological Challenges in the 21st Century (Dourdan (F)) Talk (2002)

Schäfer,W
Rock textures studied by neutron diffraction at SV7-b
ESS-SAC-Workshop Earth Science (Cambridge (UK)) Talk (2002)

Schäfer,W, Jansen,E, Kirfel,A, Kurz,W, Froitzheim,N
Chances and challenges of rock texture investigations by neutron diffraction
XIX Congress and General Assembly of the International Union of Crystallography (Genf) Poster (2002)

Schäfer,W, Jansen,E, Skowronek,R, Kirfel,A
Rock texture investigations on the University of Bonn diffractometer SV7-b in Jülich
Deutsche Neutronenstreutagung 2002 and The European Spallation Source (Bonn) Poster (2002)

Froitzheim,N, Pleuger,J, Hundenborn,R, Kremer,K, Babinka,S, Jansen,E
Constraints on the exhumation of the Adula nappe (Part 1): A top-north mega-shear zone in the roof of the nappe
5th Workshop of Alpine Geological Studies (Obergurgl (A)) Talk (2001)

Pleuger,J, Jansen,E, Schäfer,W, Oesterling,N, Froitzheim,N
Neutron texture study of natural gneiss mylonites affected by two phases of deformation
ICNS 2001 (Munich) Poster (2001)

Rinaldi,R, Artioli,G, Dove,MT, Schäfer,W, Schofield,PF, Winkler,B
Comparative texture studies of complex systems, time evolution of rock texture; phase and texture analysis of archaeological materials
Scientific Trends in Condensed Matter Research and Instrumentation Opportunities (Engelberg (CH)) Talk (2001)

Siemes,H, Klingenberg,B, Jansen,E, Schäfer,W
Texturuntersuchungen mit Neutronen an experimentell verformten Hämatiterzen mit Magnetit und Wüstit
9. Jahrestagung der Deutschen Gesellschaft für Kristallographie (Bayreuth) Poster (2001)

Siemes,H, Klingenberg,B, Jansen,E, Schäfer,W, Dresen,G, Rybacki,E, Naumann,M
Textures of experimentally deformed hematite ores with magnetite and wuestite
IAMG2001 (Cancun (Mexico)) Poster (2001)

Siemes,H, Klingenberg,B, Jansen,E, Schäfer,W, Dresen,G, Rybacki,E, Naumann,M
Texturen experimentell verformter Hämatiterze mit Magnetit und Wüstit
Deutsche Neutronenstreutagung (Jülich) Poster (2001)

Materials Science, Engineering

Publications

Hermann,RP, Jin,R, Schweika,W, Mandrus,D, Sales,BC, Long,G, Grandjean F
Einstein Oscillator in Thallium Filled Antimony Skutterudites
Phys. Rev. Lett. (in press)

Jansen,E, Schäfer,W, Kirfel,A, Palacios,J
On the Development of Copper Textures – Neutron Diffraction Control over a Period of 12 Years
Materials Science Forum (in press)

Jansen,E, Kyek,A, Schäfer,W, Schwertmann,I
The structure of 6-line ferrihydrite
Applied Physics A **74**, 1004 (2002)

Caspary,D, Eckold,G, Guethoff,F, Pyckhout-Hintzen,W
Kinetics of decomposition in ionic solids II: neutron scattering study of the system AgCl-NaCl
J. Phys.: Condens. Matter **13**, 11521 (2001)

Jansen,E, Schäfer,W, Kirfel,A, Neuroth,M
Neutron texture investigation on electrolytic $Li_2CO_3/KLiCO_3$ of a molten carbonate fuel cell
Materials Science Forum **378**, 718 (2001)

Maxelon,M, Pundt,A, Pyckhout-Hintzen,W
Small angle neutron scattering of hydrogen segregation at dislocations in palladium
Scripta Mater **44**, 817 (2001)

Maxelon,M, Pundt,A, Pyckhout-Hintzen,W, Barker,J, Kirchheim,R
Interactions of hydrogen and deuterium with dislocations in palladium as observed by small angle neutron scattering
Acta Materialia **49**, 2625 (2001)

Schäfer,W
Texture in Materials and Earth Sciences
in Th. Brückel, G. Heger, D. Richter (Ed.): Neutron Scattering -Lectures-, Schriften des Forschungszentrums Jülich, Matter and Materials, Vol.9, p. 18.1 (2001)

Sosnowska,I, Przenioslo,R, Schäfer,W, Kockelmann,W, Hempelmann,R, Wysocki,K
Possible deuterium positions in the high temperature deuterated proton conductor $Ba_3Ca_{1+y}Nb_{2-y}O_{9-\delta}$ + x D_2O studied by neutron and X-ray powder diffraction
J. Alloys and Compunds **328**, 226 (2001)

Remhof,A, Song,G, Labergerie,D, Isidorsson,J, Schreyer,A, Güthoff,F, Hartwig, J, Zabel, H
On the structure of epitaxial YH_x films
Journal of Alloys and Compounds, Conference International Symposium on Metal-Hydrogen Systems, Fundamentals and Applications (MH2000) **276**, 330-332 (2000)

Schäfer,W
Texture in Materials and Earth Sciences
in Th. Brückel, G. Heger, D. Richter (Ed.): Neutron Scattering - Lectures (Matter and Materials, Vol.5), Forschungszentrum Jülich, 18.1-18.17 (2000)

Schäfer,W, Jansen,E, Kockelmann,W, Alker,A, Kirfel,A, Seitz,D, Grönefeld,M
Variations of microstructure and texture of permanent magnetic Alnico alloys
Physica B **276-278**, 866 (2000)

Sosnowska,I, Schäfer,W, Przenioslo,R, Lind,K, Hempelmann,R
Neutron diffraction studies of the $Ba_3Ca_{1+y}Nb_{2-y}O_{9-\delta}$ high temperature proton conductor
Physica B **276-278**, 864 (2000)

Remhof,A, Song,G, Sutter,C, Schreyer,A, Siebrecht,R, Zabel,H, Güthoff, F, Windgasse, J
Hydrogen and deuterium in epitaxial Y(0001) films: Structural properties and isotope exchange
Physical Review B-Condensed Matter **59 (10)**, 6689-6699 (1999)

Alker,A, Jansen,E, Schäfer,W, Kirfel,A, Seitz,D, Grönefeld,M
Neutron diffraction applied to the study of microstructure and texture of magnetic Alnico materials
Material Science Forum **278-281**, 514 (1998)

Jansen,E, Schäfer,W, Kirfel,A, Palacios,J
On the longtime stability of a copper rolling texture as analysed from neutron diffraction pole figures
Material Science Forum **278-281**, 502 (1998)

Schweika,W, Pionke,M
Neutron Scattering and Monte Carlo Studies of Disorder in Oxides
in M. F. Thorpe and S. Billinge (Ed.): Local Structure from Diffraction / Fundamental Materials Science Series, Plenum Press, New York, p. 85-100 (1998)

Conference Presentations

Jansen,E, Kyek,A, Schäfer,W, Schwertmann,U
Neutronenbeugung an nanokristallinem Ferrihydrit
10. Jahrestagung der Deutschen Gesellschaft für Kristallographie (Kiel) Poster (2002)

Jansen,E, Schäfer,W, Kirfel,A, Palacios,J
On the development of copper textures - neutron diffraction control over a period of 12 years
8th European Powder Diffraction Conference (Uppsala) Poster (2002)

Jansen,E, Schäfer,W, Kirfel,A, Palacios,J
Copper textures periodically monitored over twelve years
Deutsche Neutronenstreutagung 2002 and The European Spallation Source (Bonn) Poster (2002)

Zotov,N, Schäfer,W, Jansen,E, Kockelmann,W, Deleplane,R
Neutron diffraction studies of glasses in the Collaborative Research Project SFB 408 Bonn, Germany
Deutsche Neutronenstreutagung 2002 and The European Spallation Source (Bonn) Poster (2002)

Jansen,E, Kyek,A, Schäfer,W, Schwertmann,U
The structure of 6-line ferrihydrite
ICNS 2001 (Munich) Poster (2001)

Schäfer,W, Jansen,E, Kirfel,A, Neuroth,M
Textur des $Li_2CO_3/KLiCO_3$-Elektrolytmaterials in Schmelzkarbonat-Brennstoffzellen
Deutsche Neutronenstreutagung (Jülich) Talk (2001)

Reactor

Damm,G, Nabbi,R
Status of HEU-LEU conversion of FRJ-2
Proceedings of the 24th International RERTR-Meeting
Bariloche, Argentina (2002)

Nabbi,R, Wolters,J
Ein Verfahren zur genauen Bestimmung von Brennelementleistungen am FRJ-2
Jahrestagung Kerntechnik 2002, Deutsches Atomforum
Stuttgart (2002)

Nabbi,R, Wolters,J, Damm,G
Characteristic differences of LEU and HEU core at the German FRJ-2 research reactor
6th International Topical Meeting on Research Reactor Fuel Management
Ghent, Belgium (2002)

Nabbi,R, Wolters,J, Damm,G
Effect of Geometric Heterogeneity on Neutron Capture Rate in Absorber Blades
ANS 2002 Annual Meeting,
Hollywood, Florida USA (2002)

Esser,F, Hansen,G, Wolters,J
Auslegung und Inbetriebnahme einer Anlage zur Erzeugung von Radiopharma im FRJ-2 des Forschungszentrums Jülich
Tagungsbericht Jahrestagung Kerntechnik 2001
Dresden, Deutsches Atomforum, Bonn (2001)

Nabbi,R, Wolters,J
Coupling MCNP and a Depletion Code for Detailed Neutronic Analysis and Optimum Core Management at the German FRJ-2 Research Reactor
Intern. Meeting on: Math. Methods for Nuclear Applications
Salt Lake, USA (2001)

Nabbi,R, Wolters,J
Ein MCNP-Modell für FRJ-2 zur Erhöhung der Betriebssicherheit und der Brennstoffnutzung
Tagungsbericht der Jahrestagung Kerntechnik 2001
Dresden, Deutsches Atomforum, Bonn (2001)

Nabbi,R, Wolters,J
Investigation of Radiation Damage in the Aluminium Structures of the German FRJ-2 Research Reactor
Proceedings of 8th Meeting of the International Group on Research Reactor IGORR-8,
München (2001)

Nabbi,R, Thamm,G, Wolters,J
A Sophisticated Computational Method for HEU-LEU Conversion of the German FRJ-2 Research Reactor Using MCNP
23 th Intern. RERTR-Meeting
Las Vegas, USA (2000)

Nabbi,R, Wolters,J
Application of MCNP for the Criticality Analysis of the German FRJ-2 Research Reactor
ENS 4th Intern. Topical Meetg. On Research Reactor Fuel Management, RRFM 2000
Colmar, Frankreich (2000)

Nabbi,R, Wolters,J
Analysis of the Criticality State of the German FRJ-2 Research Reactor Using MCNP4B
Proc. of the VI. Intern. Conf. on Nucl. Criticality Safety, Bd. I
Versailles, Frankreich (1999)

Theses

Caspary,D
Zeitaufgelöste inelastische Neutronenstreuung an entmischenden Silber-Natriumchlorid-Einkristallen
Dr. rer. nat. (Physical Chemistry), Physikalische Chemie, Universität Göttingen
(2002, *Excitations*)

Elisbihani,K
Gammadiffraktometrie zur Untersuchung der ferroelektrischen Lock-In Phasenumwandlung in Rb_2ZnCl_4
Dr. rer. nat. (Physical Chemistry), Physikalische Chemie, Universität Göttingen
(2002, *Excitations*)

Günther,A
Magnetische Anisotropie gebänderter Eisenerze und deren Beziehung zu kristallographischen Vorzugsorientierungen
Dr. rer. nat. (Geology), Mathematisch-Naturwissenschaftliche Fakultät, Technische Universität Clausthal
(2002, *Geology, Archaeology*)

Hense,K
CEF-Phonon interaction in the orhtorhombic compound $NdCu_2$
Dr. rer. nat. (Physics), TU Wien
(2002, *Excitations*)

Hill,C
Curing and Morphology of Adhesives
M.Sc. (Polymer Science), Department of Chemistry, University of Durham
(2002, *Soft condensed matter, Liquids, Glasses*)

Istomin,K
Interplay between Charge, Spin and Orbital Ordering in $La_{1-x}Sr_xMnO_3$ Manganites
Dr. rer. nat. (Physics), Fakultät für Mathematik, Informatik und Naturwissenschaften der RWTH Aachen
(2002, *Magnetic structures*)

Kaya,H
Mizellbildung amphiphiler Blockcopolymere in wässriger Lösung
Dr. rer. nat. (Physics), Mathematisch-Naturwissenschaftliche Fakultät der Westfälischen Wilhelms-Universität Münster
(2002, *Soft condensed matter, Liquids, Glasses*)

Mattauch,S
Untersuchung der strukturellen Phasenübergänge und Domänenbildung in den ferroischen Modellsubstanzen RbH_2PO_4 und RbD_2PO_4
Dr. rer nat. (Crystallography), Fakultät Bergbau, Hüttenwesen und Geowissenschaften,RWTH-Aachen
(2002, *Neutron instruments and methods*)

Papathanassiou,G
Magnetic properties of $RPtGe_2$ compounds studied by neutron diffraction
Dr. (Physics), Department of Electrical and Computer Engineering, Democritos University of Thrace, Greece
(2002, *Magnetic structures*)

Ziegenhagen,N
Einfluss lateraler Oberflächenstrukturen auf die Eigenschaften von Fe/Cr-Schichtsystemen
Diploma (Physics), Fakultät für Mathematik, Informatik und Naturwissenschaften, RWTH Aachen
(2002, *Magnetic structures*)

Botti,A
Microscopic Deformations in Filled Networks
Dr. rer. nat. (Physical Chemistry), Mathematisch-Naturwissenschaftliche Fakultät der Westfälischen Wilhelms-Universität Münster
(2001, *Soft condensed matter, Liquids, Glasses*)

Endo,H
Small Angle Neutron Scattering Investigation on the Emulsification Efficiency of Amphiphilic Block Copolymer in Microemulsions
Dr. rer. nat. (Chemistry), Mathematisch-Naturwissenschaftliche Fakultät der Westfälischen Wilhelms-Universität Münster
(2001, *Soft condensed matter, Liquids, Glasses*)

Erhardt,R
Janus-Mizellen
Dr. rer. nat. (Chemistry), University of Bayreuth
(2001, *Soft condensed matter, Liquids, Glasses*)

Hundenborn,R
Entstehung, Metamorphose und Deformation der basischen und ultrabasischen Gesteine in der Adula-Decke und der Misoxer-Zone, unter besonderer Berücksichtigung der Adula-Eklogite
Dipl.-Geol. (Geology), Geologisches Institut, Universität Bonn
(2001, *Geology, Archaeology*)

Kowald,T
Jakobsit - Einfluss der Materialsynthese auf die elektrischen und magnetischen Eigenschaften
Dipl.-Mineraloge (Mineralogy), Fachbereich Geowissenschaften, Philipps-Universität Marburg
(2001, *Crystallography*)

Meents,A
Kombinierte Strukturuntersuchungen der Tuttonsalze $(NH_4)_2(M \times 6H_2O)(SeO_4)_2$ (M = Mn,Co und Zn) mittels Röntgen- und Neutronenbeugung
Dipl. Min. (Mineralogy), Mineralogisch-Petrologisches Institut, Universität Bonn
(2001, *Crystallography*)

Meven,M
Entwicklung eines hochauflösenden Röntgen-Einkristalldiffraktometers und Strukturuntersuchungen an $La_{2-x}Sr_xCuO_{4-}$ Einkristallen.
Dr. rer nat (Crystallography), Fakultät für Bergbau, Hüttenwesen und Geowissenschaften RWTH-Aachen
(2001, *Crystallography*)

Mihailescu,M
A study of the structural and dynamical properties of microemulsions with amphiphilic block-copolymers
Dr. rer. nat. (Physical Chemistry), Mathematisch-Naturwissenschaftliche Fakultät der Westfälischen Wilhelms-Universität Münster
(2001, *Soft condensed matter, Liquids, Glasses*)

Moreno,A
Estudio mediante tecnicas de dispersion de neutrones de la dinamica rotacional de grupos metilo en vidrios polimericos y de bajo peso molecular
Dr (Physics), Universidad del Pais Vasco (UPV/EHU)
(2001, *Soft condensed matter, Liquids, Glasses*)

Pleuger,J
Strukturgeologische Untersuchungen in der Adula-Decke, Misoxer Zone und Tambodecke am Passo del San Bernardino
Dipl. Geol. (Geology), Geologisches Institut, Universität Bonn
(2001, *Geology, Archaeology*)

Abbas,Basil
Untersuchung des Phasenverhaltens von Diblock Copolymeren mit und ohne Beimischung von Lösungsmittel und Homopolymeren in externen Druckfeldern
Dr. rer. nat. (Physical Chemistry), Mathematisch-Naturwissenschaftliche Fakultät der Westfälischen Wilhelms-Universität Münster
(2000, *Soft condensed matter, Liquids, Glasses*)

Gastreich,M
Stoffliche Natur und metamorphe Entwicklung eines Orthopyroxen-Sillimanit-Gneis der Umba-Kolvitsa-Suturzone
Dipl. Geol. (Geology), Mineralogisch-Petrologisches Institut, Universität
(2000, *Geology, Archaeology*)

Hoffmann,S
Untersuchungen zum Ursprung des heterogenen Verhaltens der molekularen Dynamik in Polymermischungen
Dr. rer. nat. (Chemistry), Mathematisch-Naturwissenschaftliche Fakultät der Westfälischen Wilhelms-Universität Münster
(2000, *Soft condensed matter, Liquids, Glasses*)

Maxelon,M
Segregation von Wasserstoff und Deuterium an Versetzungen in Palladium
Dr. rer. nat. (Physics), Georg-August-Universität Göttingen, Mathematisch-naturwissenschaftliche Fakultäten
(2000, *Materials science, Engineering*)

Moral,A
Dinamica en poli(cloruro de vinilo): Estudio mediante tecnicas de espectroscopia dielectrica y dispersion de neutrones y revision critica de antecedentes
Dr (Physics), Universidad del Pais Vasco (UPV/EHU)
(2000, *Soft condensed matter, Liquids, Glasses*)

Scherf,Ch
Strukturelle Phasenübergänge und Zwillingsdomänen des Kaliumlithiumsulfats und verwandter Sulfate
Dr. rer nat (Crystallography), Fakultät für Bergbau, hüttenwesen und Geowissenschaften RTWH-Aachen
(2000, *Crystallography*)

Burghart,FJ
Untersuchung der magnetischen Eigenschaften des Spinells $ZnFe_2O_4$ in kristallinen und nanostrukturierten Modifikationen
Dr. rer. nat. (Physics), Fakultät für Physik, Technische Universität München
(1999, *Materials science, Engineering*)

Cendoya,I
Estudio de la dinamica del poli(vinil metil eter) en mezclas con poliestireno. Un estudio comparativo mediante espectroscopia dielectrica, resonancia magnetica nuclear y dispersion cuasielastica de neutrones
Dr. (Physics), Universidad del Pais Vasco (UPV/EHU)
(1999, *Soft condensed matter, Liquids, Glasses*)

Elter,P
Zeitaufgelöste Röntgen- und Neutronenstreuung während der Entmischung im System AgBr-CuBr
Diplomarbeit (Physical Chemistry), Institut für Physikalische Chemie, Universität Göttingen
(1999, *Excitations*)

Goetz,H
Chemistry
Dr. rer. nat. (Struktur und Dynamik in niedermolekularen Polymermischungen), University of Mainz
(1999, *Soft condensed matter, Liquids, Glasses*)

Hense,K
Gitterdynamik in der orthorhombischen Verbindung YCu_2
Diplomarbeit (Physical Chemistry), Wien
(1999, *Excitations*)

Caspary,D
Untersuchung zur spinodalen Entmischung im System AgCl-NaCl mit zeitaufgelöster Neutronenkleinwinkelstreuung
Diplomarbeit (Physical Chemistry), Institut für Physikalische Chemie, Universität Göttingen
(1998, *Excitations*)

Frielinghaus,H
Thermische Fluktuationen der Zusammensetzung in der Polymermischung Polybutadien/Polystyrol mit unterschiedlichen Mikrostrukturen im externen Druckfeld
Dr. rer. nat. (Physics), Mathematisch-Naturwissenschaftliche Fakultät der RWTH Aachen
(1998, *Soft condensed matter, Liquids, Glasses*)

Gibhardt,H
Kinetik der druckinduzierten Phasenumwandlung in Quarz
Dr. rer. nat. (Physical Chemistry), Institut für Physikalische Chemie, Universität Göttingen
(1998, *Excitations*)

Kümmerle,EA
Sauerstoffleerstellen-Ordnung in CeO_y - Neutronenstreuuntersuchungen an Einkristallen
Dr. rer nat. (Crystallography), Fakultät Bergbau, Hüttenwesen und Geowissenschaften,RWTH-Aachen
(1998, *Crystallography*)

Poppe,A
Selbstassoziation amphiphiler Blockcopolymere in Wasser: Strukturuntersuchungen und Untersuchungen zur Kinetik der Mizellbildung
Dr. rer. nat. (Physical Chemistry), Mathematisch-Naturwissenschaftliche Fakultät der Westfälischen Wilhelms-Universität Münster
(1998, *Soft condensed matter, Liquids, Glasses*)

Westermann,S
Correlation of local deformation and chain dynamics in polymer networks
Dr. rer. nat (Physics), University of Münster
(1998, *Soft condensed matter, Liquids, Glasses*)

User Access

The majority of neutron scattering experiments at the research reactor FRJ-2 is carried out by external user groups. We strive to support such groups optimally during the preparation, execution, and evaluation of their experiments.

For this purpose the User Office (neutron@fz-juelich.de) was established which supports the experimenters logistically. It guides the users through security clearance and radiation safety procedures to obtain free access to the experimental area. The User Office also arranges accommodation for the visit to Jülich and conducts the reimbursement of travel expenses where possible.

Each experiment (external and internal) requires a proposal, a two-page description of the experimental objectives. Up-to-date proposal forms can be found on the web site www.neutronscattering.de together with advice how to fill them. Although most of the information about instrumentation is available on the web site it is recommended that users get into contact with the responsible staff of the instrument they wish to use to assure feasibility of their project. It is also mandatory to write reports for each experiment performed.

Each instrument of our suite (or combinations) may be requested by external proposals. Nevertheless, there may be different beam time quota allocated to external users due to the different demand of the individual instruments.

In many cases we can offer travel support to users doing experiments at FRJ-2. German university users can be supported. Non-German users from the European Union and associated states can be funded by the European Commission access programme “Jülich Neutrons for Europe”. In both cases the support in general covers the travel expenses and subsistence costs of two scientists for the experiment.

General proposals will be reviewed internally and can be submitted at any time. EU access proposals are reviewed by an international panel. They have to be submitted for three deadlines per year. The deadlines are announced by advertisements in Neutron News and by an e-mail newsletter for which prospective users can sign up at our web site. Depending on the evaluation of the panel a proposal may be accepted, postponed for reconsideration in the next round, or rejected. In the case of acceptance EU support will be applied for. Postponed proposals may be carried out without funding or the proposers can wait for a more favorable decision in the next round.

Cover Picture:

View of the external neutron guide hall ELLA. The reactor with its cold source is behind the rear wall. Neutron guides emerge to the front and provide various instruments with cold neutrons. Visible are the neutron spin echo spectrometer NSE (green/red on the left), the small angle cameras KWS-1 and 2 (vacuum tanks in the front), ultra-small angle scattering KWS-3 (middle cylindrical tube), β-NMR (pink scaffold on the right), and the reflectometer HADAS (in front of the latter).